

Tissue specific damage control leading to disease tolerance in african green monkey SIV infection

Philippe Rascle

▶ **To cite this version:**

Philippe Rascle. Tissue specific damage control leading to disease tolerance in african green monkey SIV infection. Human health and pathology. Université Paris Cité, 2020. English. ⟨NNT : 2020UNIP7262⟩. ⟨tel-05094093⟩

HAL Id: tel-05094093

https://theses.hal.science/tel-05094093v1

Submitted on 2 Jun 2025

HAL is a multi-disciplinary open access archive for the deposit and dissemination of scientific research documents, whether they are published or not. The documents may come from teaching and research institutions in France or abroad, or from public or private research centers.

L'archive ouverte pluridisciplinaire **HAL**, est destinée au dépôt et à la diffusion de documents scientifiques de niveau recherche, publiés ou non, émanant des établissements d'enseignement et de recherche français ou étrangers, des laboratoires publics ou privés.



HAL Authorization

Université de Paris

Ecole doctorale BioSPC ED562

HIV : Inflammation et Persistance

TISSUE SPECIFIC DAMAGE CONTROL LEADING TO DISEASE TOLERANCE IN AFRICAN GREEN MONKEY SIV INFECTION

Par Philippe RASCLE

Thèse de doctorat d'Infectiologie

Dirigée par Michaela MÜLLER-TRUTWIN

Présentée et soutenue publiquement le 29 Septembre 2020

Devant un jury composé de :

- CECCALDI Pierre-Emmanuel, Professeur d'université, Université de Paris, Président du jury
- SCARLATTI Gabriella, IRCCS, PR, Rapporteur,
- VIEILLARD Vincent, UPMC, DR (HDR), Rapporteur
- SERETI Irini, National Institute of Allergy and Infectious Diseases, M.H.S., Examinatrice
- BEIGNON Anne-Sophie, Université de Paris Saclay – Paris Sud 11, DR (HDR), Examinatrice
- MÜLLER TRUTWIN Michaela, Institut Pasteur, PR, Directrice de thèse
- HUOT Nicolas, Institut Pasteur, Doctorat, Invité

Except where otherwise noted, this is work licensed under
https://creativecommons.org/licenses/by-nc-nd/3.0/fr/

Titre : REPONSE TISSULAIRE SPÉCIFIQUE CHEZ LE SINGE VERT D'AFRIQUE PERMETTANT LE CONTRÔLE DE L'INFECTION SIV.

Résumé :

Le VIH persiste dans des cellules réservoirs et sanctuaires anatomiques, tels que les lymphocytes T auxiliaires folliculaires (T_{FH}) dans les follicules des cellules B des ganglions lymphatiques pendant le traitement antirétroviral. Cette persistance virale est associée à plusieurs dérégulations immunitaires telles que l'inflammation chronique résiduelle, l'hypergammaglobulinémie et la désorganisation du réseau cellulaire dendritique du follicule. À l'aide de modèles animaux, nous recherchons des mécanismes de protection contre ces dérégulations. L'infection par SIVmac chez le macaque (*Macaca fascicularis*, *Macaca mulatatta*, MAC) récapitule la physiopathologie de l'infection par le VIH-1 chez l'homme. En revanche, l'infection à SIVagm chez le singe vert africain (*Chlorocebus sabaeus*, AGM) n'est pas pathogène. Les AGM infectés par le SIVagm sont dépourvues d'inflammation chronique, malgré une forte virémie persistante. SIVagm se réplique dans l'intestin, où il n'y a pas de lésion tissulaire. Contrairement à l'intestin, la réplication du SIVagm est fortement contrôlée dans les ganglions lymphatiques.

Nous avons découvert que les cellules tueuses naturelles (Natural Killer, NK) sont responsables de ce contrôle viral dans les ganglions lymphatiques lors d'une infection à SIVagm. Les cellules NK peuvent entrer dans les follicules des cellules B par induction de l'expression CXCR5 et contrôler l'infection par SIVagm dans les cellules T_{FH}. Nous avons montré que de grandes quantités d'IL-15 sont présentées par les cellules dendritiques des follicules, ce qui permet la survie des cellules NK dans les follicules.

Suite à cette observation, il nous a semblé important d'étudier le mécanisme permettant aux cellules NK d'acquérir la capacité de migrer dans les follicules. Nous avons recherché des facteurs pouvant induire l'expression de CXCR5 sur les cellules NK. Par immunohistochimie, nous avons observé la présence de cellules NK dans les follicules uniquement lorsque les cellules B proliféraient fortement. Nous avons entrepris des co-cultures de cellules NK avec des cellules B autologues et observé une augmentation significative de CXCR5 sur les cellules NK. Cette augmentation n'a été observée qu'en condition « transwell ». Le surnageant des co-cultures seul induisait CXCR5 sur les cellules NK. Une analyse de profilage transcriptionnel des cellules CXCR5 + NK a révélé l'expression de *bcl-6* et d'*IL6R*. Nous avons montré que l'IL-6 induisait l'expression de CXCR5 sur les cellules NK d'AGM et d'humains. Nous avons en outre démontré des foyers d'expression d'ARNm *d'IL-6* dans les zones interfolliculaires des ganglions lymphatiques dans une infection à SIVagm.

Ensuite, nous avons analysé comment les cellules NK contrôlent la réplication du SIVagm dans les ganglions lymphatiques. Nous avons identifié des peptides dérivés de SIV ENV qui se lient au CMH-E. Nous avons démontré que les cellules NK d'animaux non infectés ont une forte activité restreinte au CMH-E en présence du peptide SIVagm ENV, tandis que le peptide SIVmac ENV présenté par le CMH-E inhibait les cellules NK. Les cellules NK collectées après une infection au SIVagm ont montré une capacité améliorée d'activité restreinte du CMH-E envers les peptides ENV SIV, tandis que celle des macaques infectés par le SIVmac a diminué. Des analyses phénotypiques et transcriptionnelles ont démontré que les cellules NK dans le ganglion de l'AGM infecté par SIVagm présentaient un profil adaptatif et se sont différenciées en de cellules effecteurs cytotoxiques puissants contrairement aux cellules NK

dans une infection par SIVmac qui présentaient un profil moins differencié et pro-inflammatoire (IFN-g).
Nous avons ensuite soulevé la question de savoir comment l'AGM protège les tissus intestinaux malgré l'absence de contrôle viral efficace. Nous avons démontré que les cellules NK migraient dans les ganglions lymphatiques mésentériques. Par analyse des tissus par microscopie confocale et cytométrie de flux *ex vivo*, nous avons détecté une préservation des IgA dans l'intestin lors d'une infection à SIVagm tandis que l'IgA était massivement perdue dans la lumière intestinale après une infection par SIVmac. Les niveaux en cellules CXCR5+ NK dans les ganglions lymphatiques mésentériques étaient corrélés aux niveaux d'IgA. La préservation des IgA intestinales pourrait apporter une contribution importante à la protection de la barrière intestinale lors d'une infection à SIVagm. Nous avons également identifié l'expansion des cellules NKG2A+CD8+ T dans l'intestin au cours d'une infection à SIVagm, tandis que les cellules NK étaient diminuées.
Notre étude fournit de nouveaux mécanismes participant à la protection efficace des tissus lors d'une infection à SIVagm chez l'hôte naturel et qui pourraient être intéressants également dans le cadre d'autres maladies inflammatoires ou infectieuses.

Mots clefs : SIV, VIH, Hôte naturel, Cellule NK, CXCR5, IL-6, CMH-E, Cellule B, IgA, Cellule T CD8+ NKG2A+, ganglion, intestin

Title: TISSUE SPECIFIC DAMAGE CONTROL LEADING TO DISEASE TOLERANCE IN AFRICAN GREEN MONKEY SIV INFECTION.

Abstract:

HIV persists in reservoir cells and anatomical sanctuaries, such as follicular helper T cells (T_{FH}) within the B cell follicles of lymph nodes during antiretroviral therapy. This viral persistence is associated with several immune deregulations such as residual chronic inflammation, hypergammaglobulinemia and disorganization of the follicle dendritic cell network. Using animal models, we are looking for protective mechanisms against these deregulations. SIVmac infection in the macaque (*Macaca fascicularis*, *Macaca mulatatta*, MAC) recapitulates the pathophysiology of HIV-1 infection in humans. In contrast, SIVagm infection in the African green monkey (*Chlorocebus sabaeus*, AGM) is non-pathogenic. SIVagm-infected AGM lack chronic inflammation, despite strong persistent viremia. SIVagm replicates in the intestine, where there is no tissue damage. In contrast to the intestine, SIVagm replication is strongly controlled in lymph nodes.

We have found that Natural Killer (NK) cells are responsible for this viral control in lymph nodes during SIVagm infection. NK cells entered B cell follicles through induction of CXCR5 expression and controlled SIVagm infection in T_{FH} cells. We showed that large amounts of IL-15 are presented by follicle dendritic cells which allows the survival of NK cells in the follicles.

Following this observation, it seemed important to us to study the mechanism allowing NK cells to acquire the capacity to migrate into follicles. We searched for factors that can induce CXCR5 expression on NK cells. By immunohistochemistry, we observed the presence of NK cells in follicles only when the B cells were strongly proliferating. We undertook co-cultures of NK cells with autologous B cells and observed a significant increase in CXCR5 on NK cells. This increase was observed only in transwell condition. The supernatant of the co-cultures alone induced CXCR5 on NK cells. A transcriptional profiling analysis of CXCR5+ NK cells revealed bcl-6 and IL6R expression. We showed that IL-6 induced the expression of CXCR5 on NK cells from AGM and humans. We furthermore demonstrated clusters of IL-6 mRNA expression in the interfollicular areas of the lymph nodes in SIVagm infection.

Next, we analysed how NK cells control SIVagm replication in lymph nodes. We identified peptides derived from SIV ENV that bind to MHC-E. We demonstrated that NK cells from uninfected animals have a strong MHC-E restricted activity in presence of the SIVagm ENV peptide, while the SIVmac ENV peptide presented by MHC-E inhibited NK cells. NK cells collected after SIVagm infection showed an improved capacity of MHC-E restricted activity toward the SIV ENV peptides, while that from SIVmac-infected macaques decreased. Phenotypical and transcriptional analyses demonstrated that NK cells in LN of SIVagm-infected AGM show an adaptive profile and differentiate toward strong cytotoxic effectors in contrast to NK cells in SIVmac infection which displayed a pro-inflammatory (IFN-g) profile.

We subsequently raised the question how AGM protect intestinal tissues despite the lack of efficient viral control. We demonstrated that NK cells migrated into mesenteric lymph nodes. By analysis of tissues by confocal microscopy and ex vivo flow cytometry, we detected a

preservation of IgA in the intestine during SIVagm infection while IgA was massively lost in the intestinal lumen after SIVmac infection. CXCR5+ NK cells in the mesenteric lymph nodes were correlated with IgA levels. The preservation of intestinal IgA could make an important contribution to the protection of the intestinal barrier during SIVagm infection. We also identified the expansion of NKG2A+CD8+ T cells in the intestine during SIVagm infection, while NK cells were diminished.

Our study provides novel mechanisms participating to the efficient tissue protection during SIVagm infection in the natural host and which could be interesting also in the context of other inflammatory or infectious diseases.

Keywords: SIV, HIV, Natural Host, NK cell, CXCR5, IL-6, MHC-E, B cell, IgA, NKG2A+ CD8+ T cell, lymph node, intestine

ACKNOWLEDGEMENTS

Je tiens à remercier toutes les personnes qui ont contribué à la réalisation de ce travail.

Je tiens notamment à remercier les membres du jury, Pierre Emmanuel CECCALDI, Irini SERETI, Vincent VIEILLARD, Gabriella SCARLATTI, Anne-Sophie BEIGNON, Nicolas HUOT et Michaela MÜLLER-TRUTWIN ; pour le suivi et pour le temps qu'ils ont accordé à ces travaux.

Je tiens également à remercier toutes les personnes qui m'ont aidé à murir personnellement et/ou professionnellement durant ces toutes ces années de thèse au laboratoire. Ainsi donc, je remercie tout d'abord Michaela, Nicolas et Béatrice pour leur aide et encadrement durant cette thèse. Merci de votre soutien et conseils qui m'ont aidé à avancer.

À l'unité Hiper : Merci Marie pour ton aide, ton implication et nos discussions du quotidien. Je tiens à remercier Asier, Brigitte, Amal, Aurelio, Federico, Anaïs, Valérie, Caroline et Caroline ; pour soit leur aide et/ou pour leurs simplicités et leurs sourires. Merci aux anciennes personnes du laboratoire ; Annie, Anastassia, José Carlos et Mathieu ; qui m'ont également aidé dans ce projet de thèse.

Je remercie l'équipe d'IDMIT / CEA pour avoir pris soin des animaux et leur aide précieuse dans ces travaux. Je remercie nos les collaborateurs Hugo, Cyril et les personnes à la plateforme microscopie tel que Jean-Yves, Leslie ou Julien qui ont beaucoup contribuer à la concrétisation de ce travail.

Merci à tous mes amis et principalement, Jérémy, Fabio, Benoit, Benjamin, Loïc, Kévin, Robin, Maxime, Antoine, Virgil, Thibaut, Nicolas, Marianne, Inès ; qui ont été là derrière moi à me soutenir et/ou à me changer les idées quand c'était nécessaire.

Merci à ma famille pour leur soutien, et particulièrement envers mes parents qui ont toujours fait en sorte de me faciliter au maximum la vie pour que je puisse me concentrer sur mes études sans la venue d'autres stress extérieurs.

Merci à Maggie qui m'a également beaucoup aidé à surmonter le stress de la thèse.

Merci à toi Aurélia, ma femme, qui était là depuis le début. Merci pour ton soutien et ton engagement à mes côtés.

TABLE OF CONTENTS

Acknowledgments …… 6

Illustration table …… 10

Abbreviations …… 11

PART I. INTRODUCTION…… 13

CHAPTER 1: HUMAN IMMUNODEFICIENCY VIRUS (HIV) INFECTION …… 13

1.1 GLOBAL SITUATION …… 13

1.2 NATURAL HISTORY OF THE INFECTION AND PROGRESSION PHENOTYPES..13

CHAPTER 2: NON-HUMAN PRIMATE MODELS FOR HIV …… 15

2.1 PATHOGENIC SIV INFECTION …… 16

2.2. INSIGHTS THANKS TO NON-HUMAN PRIMATE MODELS …… 17

2.3. NON-PATHOGENIC SIV INFECTION …… 18

CHAPTER 3: CHRONIC IMMUNE ACTIVATION …… 20

3.1 CELLULAR SOURCES OF CHRONIC IMMUNE ACTIVATION …… 20

3.2 MECHANISMS OF CHRONIC IMMUNE ACTIVATION SUSTAINMENT …… 21

CHAPTER 4: VIRAL RESERVOIRS …… 23

4.1. TISSUE VIRAL RESERVOIRS …… 23

4.2. CELLULAR VIRAL RESERVOIRS …… 24

CHAPTER 5 : TISSUE DAMAGES …… 28

5.1. LYMPH NODES …… 29

5.1.1. ARCHITECTURE …… 29

5.1.1.1. MEDULLA …… 29

5.1.1.2. PARACORTEX …… 29

5.1.1.3. INTERFOLLICULAR ZONE …… 29

5.1.1.4. B CELL FOLLICLES …… 30

5.1.2. VIRAL REPLICATION PROFILES IN LYMPH NODES DURING HIV/SIV INFECTIONS …… 31

5.1.3. TISSUE DAMAGE IN LYMPH NODES DURING HIV/SIV INFECTIONS …… 31

5.2: INTESTINAL MUCOSA …… 33

5.2.1 ARCHITECTURE …… 33

5.2.1.1 INTESTINAL EPITHELIAL BARRIER ……..…… 33

5.2.1.2 INTESTINAL MUCOSA HOMEOSTASIS ……..…… 34

5.2.1.3 GUT ASSOCIATED LYMPHOID TISSUE (GALT) ……...…… 35

5.2.2. VIRAL REPLICATION PROFILES IN THE INTESTINE DURING HIV/SIV INFECTIONS ……..…… 36

5.2.3 INTESTINAL TISSUE DAMAGE IN HIV/SIV INFECTIONS ……..…… 36

5.2.3.1 DISRUPTION OF THE EPITHELIAL BARRIER …… 37

5.2.3.2 DISRUPTION OF THE LYMPHOID FOLLICLES ……..…… 39

CHAPTER 6: B CELLS AND NK CELLS IMMUNE RESPONSES IN TISSUES FROM HIV/SIV INFECTION ……..……..…… 39

6.1. B CELLS IN HUMAN AND NON-HUMAN PRIMATES …… 40

6.1.1. MUCOSAL B CELLS ……..…… 41

6.1.2. B CELLS IN HIV/SIV INFECTION …… 41

6.2. NK CELLS ……...…… 43

6.2.1. NK CELLS IN TISSUES ……..…… 44

6.2.2. NK CELLS IN HIV/SIV INFECTIONS ……..…… 45

6.3. NKG2A+ CD8+ T CELLS ……..…… 48

6.3.1. NKG2A+ CD8 T CELLS FUNCTIONS ……..…… 48

6.3.2. NKG2A+ CD8 T CELLS IN HIV/SIV INFECTIONS …… 49

PART II. HYPOTHESES and OBJECTIVES ……..…… 51

PART III: RESULTS ……...…… 52

1. NK cells migrate into and control SIV replication in lymph node follicles in African green monkeys ……..…… 53

2. Identification of a soluble factor inducing CXCR5 expression on NK cells …….…… 92

3. Expansion of terminally differentiated adaptive NK cells in lymph nodes of SIV-infected natural hosts associates with enhanced MHC-E restricted activity ……..… 125

4. Non-Human Primate Determinants of NK Cells in Tissues at steady-state and during SIV infection …… 181

5. NK cell profiles and IgA responses in mesenteric lymph nodes during SIV infections….208

6. Tissue profiles of NKG2a/c+CD8+ T cells in SIV infections ……..…… 238

PART IV. Discussion ……..…… 268

PART V. General conclusions and Perspectives ……..…… 285

PART VI. References (Introduction & Discussion) ……..…… 287

Part VII: Appendices …… 332
Part VII: Substantial Summary ……362

ILLUSTRATION TABLE

Figure 1. Physiopathology of untreated HIV-1 infection.
Figure 2. Non-human primate models for the study of HIV infection.
Figure 3. Different disease outcomes based on host-virus interactions.
Figure 4. Variation in the main virological and immunological markers of HIV/SIV infection.
Figure 5. Host and viral determinants determine the disease progression rate.
Figure 6. Potential mechanisms of chronic immune activation.
Figure 7. Structure of the intestinal mucosa in small and large intestine.
Figure 8. Schematic representation of pathological changes underlying intestinal epithelial barrier disruption during HIV/SIV infection.
Figure 9. Multiple facets of NK cell in HIV-1 infection. (A) Cytotoxic NK cells response to via favoring of activator signals or downregulation of inhibitor signals. (B) Cytokine NK cells production, like IL-22 or β-chemokines. (C) Crosstalk mechanism between immature DC and NK cell. NK cells indirect impact on humoral response, via Tfh potential elimination.
Figure 10. The NKG2A$^+$ CD8$^+$ T cells (also named innate CD8$^+$ T cells) characterize in humans. The different receptors and transcription factors are represented, as defining this new unique population. This CD8$^+$ T cell population in humans are susceptible to several cytokines such as IL-12, IL-18, IL-15 or IL-4.

Table 1. Examples of major contributions of MAC model to the HIV/AIDS research.
Table 2. HIV/SIV replication in different tissues.
Table 3. Tissues with detectable HIV or SIV upon suppressive ART.
Table 4. Major similarities and differences between HIV/SIVmac infections and SIV infections in natural hosts at the level of lymph nodes (LNs).
Table 5. Abnormalities in HIV infection impacting B-cell function.

ABBREVIATIONS

ADCC: Antibody-dependent cell-mediated cytotoxicity

APC: Antigen Presenting cell

AGM: African Green Monkey

AIDS: Acquired Immunodeficiency Syndrome

ART: antiretroviral therapy

B_{AM}: Activated Memory B cell

BCF: B cell follicle

BCR: B cell receptor

B_{RM}: Resting Memory B cell

B_{TLM}: Tissue-like Memory B cell

CCR: C-C chemokine receptor

CD: Cluster differentiation

CXCR: C-X-C chemokine receptor

DC: Dendritic cell

DNA: Deoxyribonucleic acid

FAE: Follicle-associated epithelium

FDC: Follicular dendritic cells

FRC: Fibroblastic Reticular Cell

GALT: Gut-associated lymphoid tissue

GC: Germinal Center

GP: Glycoprotein (120, 140, 160)

HEV: High Endothelial Venule

HIC: HIV controller

HIV: Human immunodeficiency virus

HLA: Human leukocyte antigen

HSP: Heat shock Protein

IA: Immune Activation

IEC: Intraepithelial cell

IFN: Interferon (alpha, gamma)

I-FABP: Intestinal fatty-acid binding protein

Ig: Immunoglobulin (A, G, M, D)

IL: Interleukin (-6, 15, -21,…)

ILC: Innate Lymphoid Cells

ILF: Isolated Lymphoid follicle

ISG: IFN-stimulated gene

LN: Lymph node

LP: Lamina Propria

LPS: Lipopolysaccharide

Nab: Neutralizing antibodies

NHP: Non-human primate

NK: Natural Killer

NKT: Natural Killer T cell

Mφ: Macrophage

MAC: Macaque

MAIT: Mucosal associated invariant T cell

M cell: Microfold cell

mLN: mesenteric LN

MND: Mandrill

MHC: Major histocompatibility complex

Mo: Monocyte

PB: Peripheral Blood

pDC: plasmacytoid dendritic cell

PLWH: People living with HIV

PP: Peyer's patch

PreP: pre-exposure prophylaxis

PMPA: 9-[2-(phosphomethoxy)propyl]-adenine

PTC: Post treatment controller

PTM: Pig-tailed macaque

RM: Rhesus macaque

RNA: Ribonucleic acid

SED: Subepithelial dome

SHIV: Simian-human immunodeficiency virus

SIgA: Secretory IgA

SIV: Simian immunodeficiency virus

SLT: Secondary Lymphoid Tissue

SM: Sooty Mangabey

T_{CM}: Central memory CD4+ T cells

TCR: T cell receptor

T_{FH}: T follicular helper

TGF-beta: transforming growth factor beta

Th: Helper T cell

TNF-alpha: Tumor necrosis factors alpha

T_{reg}: Regulatory CD4+ T cells

VL: Viral Load

VNP: Viremic non-progressors

CHAPTER 1: HUMAN IMMUNODEFICIENCY VIRUS (HIV) INFECTION

1.1 GLOBAL SITUATION

HIV/AIDS remains one of the worlds´ most important public health challenges, having claimed more than 35 million lives so far. Currently, according to the World Health Organization, there are 37 million people living with the Human Immunodeficiency Virus (HIV-1) around the world. Moreover, only in 2018, 1.7 million individuals become newly infected and nearly a 770 thousand died from HIV-related causes globally. Importantly, HIV remains the major cause of death in women between the age of 15 and 49 years worldwide (who.int/hiv/data/en/).

Since 1996, HIV infection can be efficiently treated. The development and evolution of antiretroviral treatment (ART) dramatically increased the life expectancy and life-quality of patients, transforming the HIV infection from a fatal diagnosis to a chronic condition (Paiardini and Müller-Trutwin, 2013). However, it was estimated that in 2018, 23.3 million people received ART; representing only 62% of the total infected individuals (who.int/hiv/data/en/). The delay, either in the diagnosis or in the treatment, compromises the medical care of the infection and associated malignances. This situation also increases the risk of spreading the virus. Of note, the stigma and prejudice around the infection still impact the will of people for being diagnosed and/or treated.

Moreover, age-related diseases are often increased among treated individuals. This is the case for the People Living With HIV (PLWH) who did not initiated their treatment in primary infection but only several years after HIV diagnosis, which unfortunately still represents the majority of cases. In France, the estimated delay between HIV infection and HIV diagnosis is 3 years. Non-AIDS morbidities, such as cardiovascular events, metabolic complications (diabetes) and cancers (e.g. lymphoma) represent a medical issue (Deeks and Phillips, 2009). The chronic inflammatory state associated with HIV infection, as well as potential toxicity of long-term treatment and lifestyle account for the potential causes of such non-AIDS co-morbidities (Paiardini and Müller-Trutwin, 2013).

1.2 NATURAL HISTORY OF THE INFECTION AND PROGRESSION PHENOTYPES

HIV transmission occurs by sexual contact of mucosal surfaces, by mother-to-child exposure and by inoculation with contaminated blood. The cell targets of the virus comprise predominantly $CD4^+$ T lymphocytes, Dendritic cells (DC) and Macrophages (Mφ) (Barton et al., 2016).

In general, the course of the untreated infection is divided in: acute, chronic asymptomatic phase and AIDS (Fig. 1). Typically, during the acute phase, a burst of viral replication and a pronounced decline

of CD4$^+$ T cells are observed. The viral load (VL) is afterwards stabilized (set point) and the level at which such equilibrium appears in the course of infection has been associated with the subsequent rate of progression towards AIDS (Geskus et al., 2007).

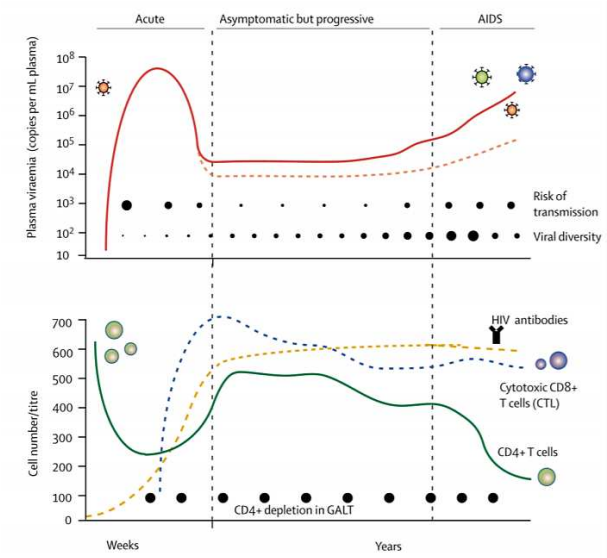


Figure 1. Physiopathology of untreated HIV-1 infection
The infection progresses from acute to a chronic/asymptomatic stage. In the absence of treatment, AIDS arises. Relevant events along the infection course, occurring on the virus (top) and on the immune system (bottom) are shown. Image come from (Simon et al., 2006).

Based on viral load set-points and CD4$^+$ T cell counts progression, HIV-infected individuals can be categorized into different progression phenotypes (Casado et al., 2010):

- Rapid progressors: AIDS or AIDS-related signs appear within 3 years after seroconversion.
- Progressors: In the absence of ART, the disease symptoms appear within 10 years after seroconversion. Most of the patients belong to this category.
- Viremic non-progressors (VNP): CD4$^+$ T cells are maintained to high levels and the symptoms of a progressive disease are delayed beyond 10 years after seroconversion, despite the fact that the viremia remains elevated (≥2000 copies/mL).
- HIV controllers (HIC): As for VNP, the symptomatic phase is delayed more than 10 years after seroconversion. HIV controllers display a long-term control of viremia (below 400 HIV RNA copies/mL in French cohorts). Below 0.5% of PLWH are controllers (Lambotte et al., 2005) (Sáez-Cirión et al., 2007).
- Post-treatment controllers (PTC): there are rare individuals, who demonstrate sustained virologic suppression for a prolonged period of time after treatment interruption. However, PTC are difficult to be clearly defined, some studies considered virologic rebound to be a plasma viral load above 50 HIV-1 RNA copies/ml after treatment interruption, while others used a threshold of 400 HIV-1 RNA copies/ml or 1,000 HIV-1 RNA copies/ml. Moreover, the duration of viral control after treatment interruption differed between studies and ranged from a median of 6 months to more than 2 years. Also, some studies considered the loss of control as two consecutive viral loads above 50 HIV-1 RNA copies/ml, while others considered one to four consecutive viral loads higher than 400 HIV-1 RNA copies/ml to be defined as loss of PTC profile (Etemad et al., 2019).

CHAPTER 2: NON-HUMAN PRIMATE MODELS FOR HIV

After the discovery of HIV, a related virus was isolated from captive macaques (MAC) named Simian Immunodeficiency Virus (SIVmac) (Letvin et al., 1983). Nowadays, it is known that HIV and SIVmac arose from cross-species transmission of viruses that naturally infect African nonhuman primates (Fig. 2).

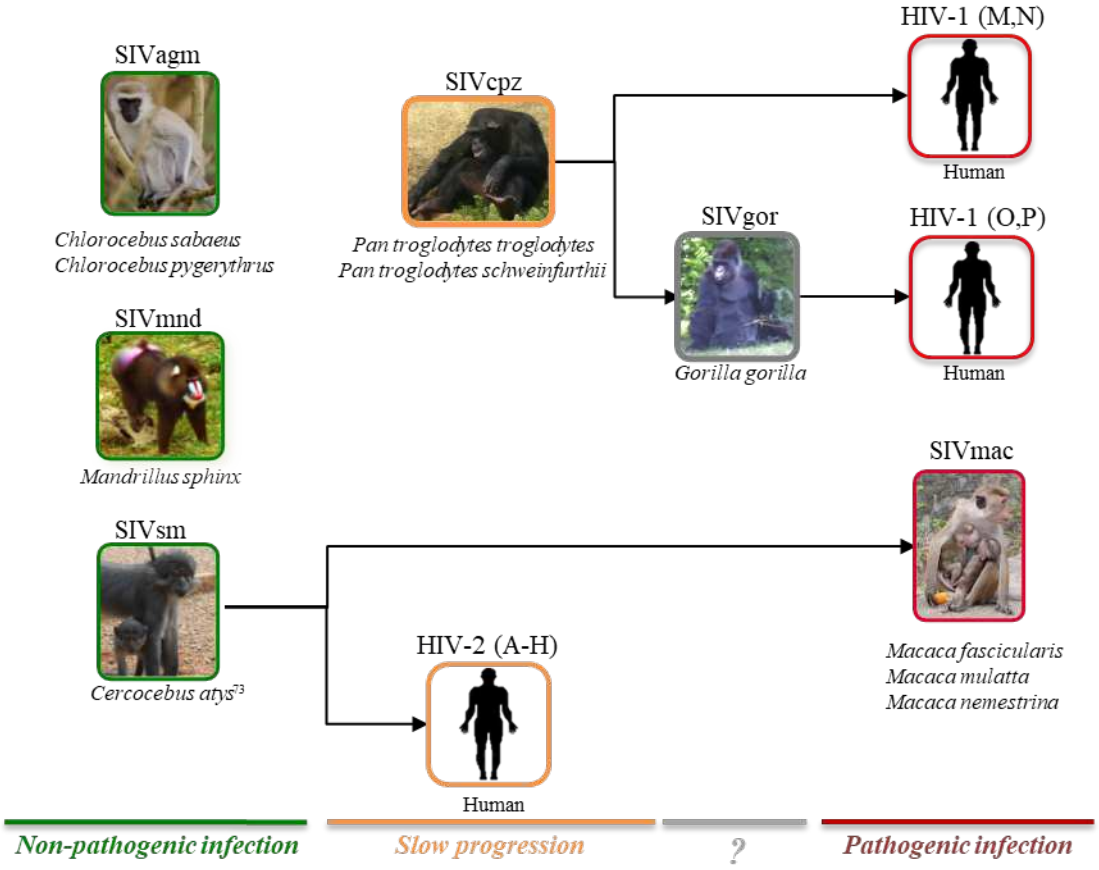


Figure 2. Non-human primate models for the study of HIV infection
Non-human primates can be divided into pathogenic (macaques) and non-pathogenic (sooty mangabeys, mandrills and African Green Monkeys) models for HIV research. The two most common African monkey species used (African green monkeys and sooty mangabeys) are represented here. The figure depicts the ancestral relationship between the HIV and SIV viruses and the type of infection caused by them (Garcia-Tellez et al., 2016).

Cross-species transmissions demonstrated that the outcome of the infection depends on a combination of both, viral and host determinants (Fig. 3). Thus, the same SIV strain can cause opposite outcomes of infection, depending of the host species. For example, the SIVsmm9, which is non-pathogenic in the original host (sooty mangabeys) causes AIDS in macaques. SIVagm.sab9218 is virologically controlled in rhesus macaques (RM) while it induces AIDS in pigtail macaques. Moreover, not all SIV strains induce AIDS in macaques, i.e. SIVagm.ver155 infection in Pigtailed macaques is

asymptomatic; while SIVagm-ver90 and SIVagm.sab9218 infections induce AIDS in pigtailed macaques (Fig. 3).

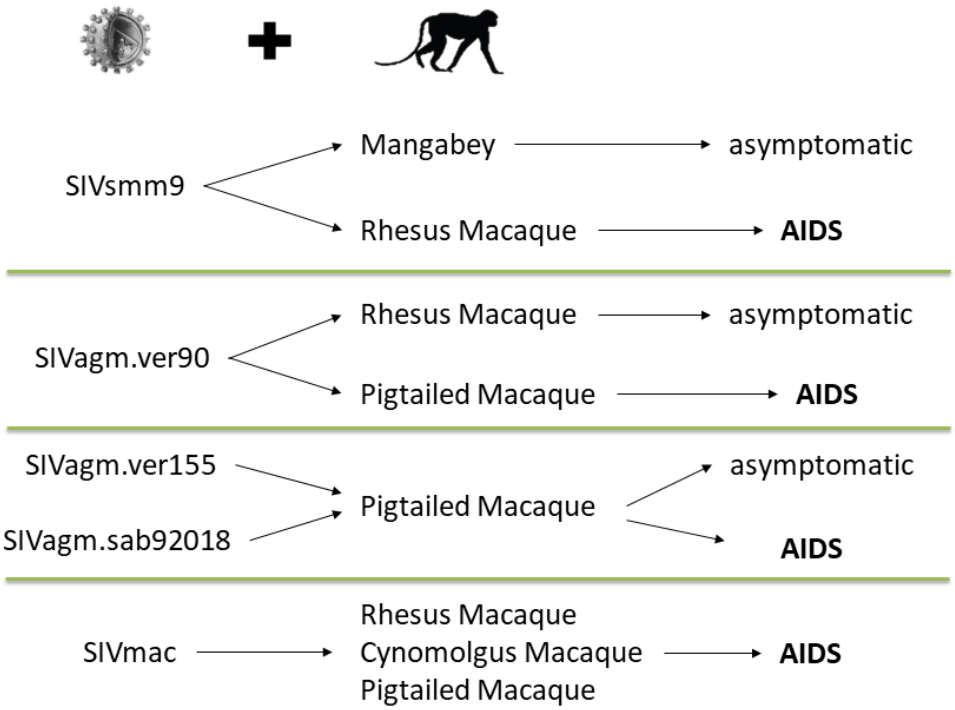


Figure 3. Different disease outcomes based on host-virus interactions
The presence or absence of progression depends on both, viral and host factors. Host and viral determinants interact which each other and a combination of both governs the outcome of infection (Garcia-Tellez et al., 2016).

2.1 PATHOGENIC SIV INFECTION

SIV infects the same cells than HIV-1 and triggers similar physiopathology and immune responses that we observed with HIV-1 in humans (Fig.4). The SIVmac infection mirrors the course of HIV-1, in shorter time. Notably, SIVmac-infected macaques display a sustained immune activation (IA), exactly as HIV-1 infected progressors do. Moreover, SIVmac-infected monkeys can recapitulate all the progression phenotypes observed in humans. In this regard and similarly to HIC, SIV controller status in monkeys is often associated with the MHC haplotype (Aarnink et al., 2011). Therefore, SIVmac-infected macaques became a suitable model for studying the pathogenesis of HIV-1 infection.

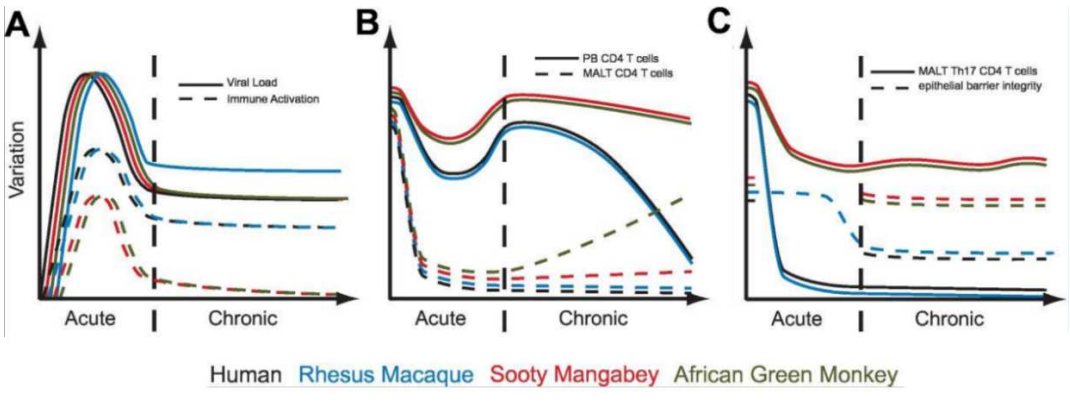


Figure 4. Variation in the main virological and immunological markers of HIV/SIV infection.
Infection features are shown for humans (black), Rhesus macaques (blue) and two natural hosts (red and green) during the acute and the chronic phases of HIV/SIV infection. Image taken from (Brenchley and Paiardini, 2011).

The most frequently used primate models are Indian and Chinese rhesus macaques (RM, *Macaca mulatta*), pigtailed macaques (PTM, *Macaca nemestrina)* as well as cynomolgus macaques (CM, *Macaca fascicularis*) infected by the molecular clone SIVmac239 or the viral isolate SIVmac251. Of note, the most rapid disease progression is generally observed in Indian RM infected with SIVmac239 (Fig. 5).

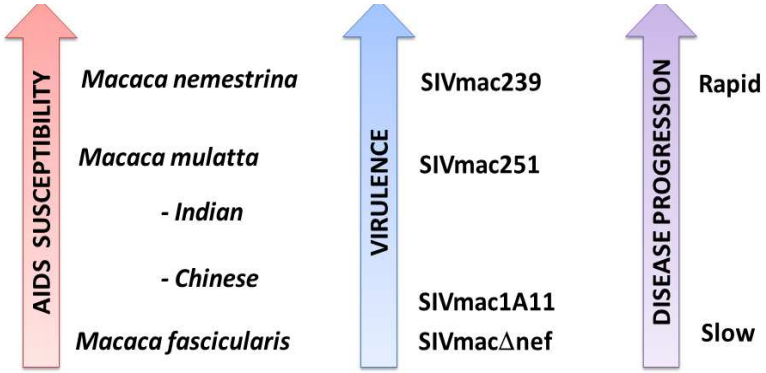


Figure 5. Host and viral determinants determine the disease progression rate
The progression of the disease depends on the intrinsic susceptibility of each species to develop AIDS and on the virulence of the SIV strain used (Garcia-Tellez et al., 2016).

2.2. INSIGHTS THANKS TO NON-HUMAN PRIMATE MODELS

The exhaustive study of early immune responses or the investigation of the mechanisms associated with the viral control in human tissues are difficult in terms of availability of samples and control of parameters. Also, viral challenges to prove the efficacy of novel eventually risky preventive strategies needs relevant models. That is why the use of animal models, particularly of non-human primates (NHP) in the case of HIV research, are of outstanding help (Garcia-Tellez et al., 2016). Non-human primate models have during the last 35 years revealed major insights into virus-host interactions in tissues. They have contributed to the understanding of HIV pathogenesis as well as to the improvement of therapeutic interventions and vaccine research. More recently, the development of more sophisticated humanized mice models is also contributing to HIV research. Some examples of the contributions of nonhuman primate models are explained as follows. For example, the study on the early phases in the SIV infections have shown that virus-host interactions already in acute infection determine the progression profiles (Levy, 2011) (Whitney et al., 2014) (Jacquelin et al., 2009) (Hatziioannou et al., 2014).These studies therefore contributed to the current recommendation to treat PLWH as early as possible and underlines that cohorts of acute HIV infection are of outmost importance for HIV research (Stacey et al., 2009) (Ananworanich et al., 2017) (Ndung'u et al., 2018). NHP models have also produced knowledge about how the virus penetrates mucosal barriers and establishes persistent infections (Martinelli et al., 2014) (Zhang et al., 1999) (Reynolds et al., 2005)

(Stieh et al., 2016). They lead to the co-discovery of cellular restriction factors of HIV-1 (Ltd, 2004). They provided key elements for our understanding on HIV pathogenesis. For example, rhesus MAC infected with SIVmac239 provided the proof of the extremely rapid and massive $CD4^+$ T cell depletion in the gut (Mattapallil et al., 2005) (Veazey et al., 1998) (Veazey and Lackner, 2017). Studies realized in macaques showed that the establishment of viral reservoirs occurs extremely rapidly, before 3 days post-infection (Whitney et al., 2014). Moreover, only animal models can be challenged experimentally to test a new preventive method against HIV. Efforts to develop anti-retroviral drugs in macaques enhanced indeed the development of Tenofovir (PMPA) and pre-exposure prophylaxis (PreP) (Tsai et al., 1995) (García-Lerma et al., 2010). Macaque models provided the proof of concept that neutralizing antibodies protect against infection (Parsons et al., 2018) (Zolla-Pazner et al., 2019). Other examples of relevant discoveries obtained with the MAC model are summarized in Table 1.

Table 1. Examples of major contributions of MAC model to the HIV/AIDS research (Parsons et al., 2018)**.**

- Discovery of initial founder populations of infected cells in tissues
- $CD8^+$ T cell response: too little and too late in mucosa to clear infection
- Short window of opportunity to prevent infection
- $CD8^+$ T cells response: impact on viral setpoint
- Events in acute infection determine disease progression
- Rapid and dramatic depletion of $CD4^+$ T cells in intestine
- Nef viral protein: necessary for high viral load
- Loss of central memory T cells (T_{CM}) associated with disease progression
- Trafficking of regulatory T cells (T_{reg}), plasmacytoid DC (pDC) and natural killer (NK) cells to the intestine
- Co-discovery of cellular factors restricting HIV-1 replication and demonstration that TRIM5a alleles restrict viral replication *in vivo*
- Proof of concept that neutralizing antibodies (Nabs) can protect against infection
- Contribution to the development of PreP
- NK cells can control a viral reservoir in secondary lymphoid tissues during chronic infection (Huot et al., 2017)
- *In vivo* reservoir study, by SIV imaging in all lymphoid and non-lymphoid tissues during ART

2.3. NON-PATHOGENIC SIV INFECTION

At the opposite to macaques, African NHP are carrying SIV in their natural habitat. So far, more than 40 African-NHP species carrying their species-specific SIV have been detected in the wild.

It was observed that Sooty Mangabeys (SM), mandrills (MND), and African Green Monkeys (AGM), so called natural-hosts, upon SIV-infection display high viremia but do not progress to AIDS. During the chronic phase, the virus continues replicating to high levels, in most cases at around 10^3-10^6 SIV RNA copies/ml of plasma (Pandrea et al., 2006).
During the acute phase of infection there is a strong decrease of $CD4^+$ T lymphocytes in blood and intestinal mucosa. However, circulating $CD4^+$ T cells recover rapidly. In the chronic phase of infection, the $CD4^+$ T cells in the gut remain low in SM, while they are progressively and partially recovered in AGMs. In contrast to HIV infection in humans and SIVmac infection in MAC, the Th_{17} cells in the gut are preserved in AGMs (Pandrea et al., 2007).

To explain the lack of disease progression in SIV-natural host, several hypotheses are proposed in the literature:

- **Rapid control of immune activation.** As observed in pathogenic HIV/SIV infections, SIVagm and SIVsm (from SM) trigger a potent type I-interferon (IFN) production. Nevertheless, it was shown that this response is rapidly controlled in AGM (Jacquelin et al., 2014)**.** Indeed, it has been consistently observed that after the acute phase, the IA is controlled and returns close to pre-infection levels by the end of chronic infection in natural hosts (Jacquelin et al., 2014) (Bosinger et al., 2009). There is a particular rapid control of immune activation, including of IFN-stimulated gene (ISG) expression, in secondary lymphoid tissues (SLT). Lymph nodes (LNs) are characterized by a lack of lymphadenopathy and a lack of fibrosis. The FDC network in LNs remains intact in contrast to HIV-1 and SIVmac infections (Huot et al., 2018).
- **Low infection of central memory $CD4^+$ T cells.** A lower frequency of T_{CM} infection has been reported. It has been suggested that this lower rate of T_{CM} infection is associated with a low expression of CCR5. Indeed, a reduced expression of this co-receptor has been reported in natural hosts in T_{CM} and pDC (Chahroudi et al., 2012) (Paiardini et al., 2011) (Jochems et al., 2015a). However, SIVsm and SIVagm are non-strictly dependent of CCR5 to infect $CD4^+$ T cells, as they also effectively use GRP15 (Bob) and CXCR6 (Farzan et al., 1997) (Wetzel et al., 2017).
- **Nef-mediated TCR downregulation.** In natural hosts, the CD3-TCR receptor is downregulated by the action of the SIV-Nef protein. This might limit the immune activation during the infection (Joas et al., 2018) (Schindler et al., 2006). Such capacity was lost in HIV-1. However, it has been shown that AGMs infected with SIVagm clones coding for SIVmac Nef, do not downregulate CD3 and still do not display chronic immune activation and do not progress to AIDS (Joas et al., 2018).
- **Homeostatic process of $CD4^+$ T cells**. A functional homeostatic replenishment process seems to act in AGMs and SMs (Chahroudi et al., 2012).
- **Th_{17} maintenance**. The Th_{17} cells are maintained in the gut for unknown reasons, which could positively contribute to maintain the intestinal barrier integrity (Brenchley et al., 2008).
- **Early monocyte responses**: Monocytes from AGMs SIV infected rapidly activate the regenerative wound healing mechanisms in mucosal tissues via fibronectin production and TGF-beta signature (Barrenas et al., 2019).

It is not excluded, that the lack of progression in natural hosts might be explained by synergistic or simultaneous mechanisms, with some of them that are still not fully understood.

The control of chronic immune activation in natural hosts, which is one of the most striking difference between pathogenic and non-pathogenic SIV infection, has not been fully explained. Some of potential mechanisms behind such phenomenon, and which are not mutually exclusive, are:

- **Preservation of the intestinal epithelial barrier.** In the absence of gut damage, microbial translocation would not be exacerbated and therefore immune activation would be limited (Chahroudi et al., 2012).
- **Control of the viral replication in secondary lymphoid organs.** LNs and spleen in the natural hosts are characterized by a rapid control of the virus and no or rare follicular accumulation of virus (Diop et al., 2000) (Martinot et al., 2013).
- **Different sensing and triggering of antiviral innate responses.** The IFN-type I-mediated responses have been extensively studied in natural hosts (Jacquelin et al., 2009). Plasmacytoid dendritic cells (pDCs) from natural hosts are the main producers of IFN-α as in HIV infection (Harris et al., 2010) (Jochems et al., 2015b) (Jochems et al., 2015a). They rapidly home to LNs during acute infection and have a strong capacity to produce IFN-α, similar as to HIV and SIVmac infections (Diop et al., 2008) (Jacquelin et al., 2009) (Jacquelin et al., 2014). However, there differences in the kinetics and quality of the response that are not well understood. For instance, IFN-α production is stronger at early time points (day 1 and 2 p.i.) in SIVagm than SIVmac infection. Also, SIVmac infection at day 1 p.i. is characterized by the up-regulation of an inhibitor (NLRX1) of ISGs coding for antiviral restriction factors (Barouch et al., 2016) while the expression of these restriction factors is strongly up-regulated in SIVagm infection (Jacquelin et al., 2009). Studies in the natural hosts suggest, that ISGs in acute infection are induced by IFN-α and in the chronic phase by IFN-γ (Jacquelin et al., 2009). Other inflammation pathways such as the inflammasome, IFN-γ or IL-6 pathways are less explored in natural hosts of SIV and also need further attention in the future (C Kornfeld et al., 2005) (Keating et al., 2016).

Thus, natural hosts represent excellent models to depict mechanisms of protection against tissue damage. However, more studies are needed to decipher the mechanisms that intervene in the resolution of systemic immune activation in SM and AGM. Such data would allow the development of novel strategies to control HIV associated non-AIDS comorbidities and mortality in PLWH under ART, and might by highly useful as well for a better understanding of the regulation and impact of the early anti-viral innate immune responses.

CHAPTER 3: CHRONIC IMMUNE ACTIVATION

3.1 CELLULAR SOURCES OF CHRONIC IMMUNE ACTIVATION

Only few cellular sources of inflammatory mediators have been fully defined. Some reports have shown that T cells are the major source of the pro-inflammatory chemokine IP-10, while others

reported myeloid cells as the major source of IP-10 during HIV/SIV infections (Peperzak et al., 2013) (Ploquin et al., 2016) (Qin et al., 2010) (Simmons et al., 2013). The type of cellular source might differ depending of the tissue analyzed. $CD8^+$ T regulatory cells seems to be the most important producers of TGF-β in the LN (Huang et al., 2018). pDCs are the predominant type I-IFN source in acute infection (Jacquelin et al., 2009) (Huot et al., 2016) while monocytes, DCs and Mφ seem to be important in the production of IL-1 cytokines, IL-6 (Shive et al., 2012), TNF-α, and IFN-γ (Echebli et al., 2018). Finally, stromal fibroblasts, monocytes and DCs seem to be a major source of IL-15 (Perera et al., 2012).

Intestinal mucosa and LNs are predominant sites where the immune activation is sustained. In addition, it has been observed that the expression of homing receptors changes during HIV-1 infection, and therefore the distribution of cells to the tissues. Some reports showed an infiltration of $CD8^+$ T cells into the brain (Gray et al., 2013); of Treg, NK, Mφ and pDCs into the gut (Swan et al., 2016) (Reeves et al., 2012); of Mφ into the lung, of pDCs into the spleen (Nascimbeni et al., 2009) and an expansion of T follicular helper cells (T_{FH}) in the LN (Velu et al., 2018) (Onabajo and Mattapallil, 2013). Such changes in the cellular environment can shape the cytokine milieu in each compartment and therefore contribute differently to the chronic IA.

3.2 MECHANISMS OF CHRONIC IMMUNE ACTIVATION SUSTAINMENT

The molecular mechanisms through which HIV-1 induces and sustains immune activation have not been entirely understood. Most likely there does not exist a single and unique mechanism, but a synergistic action of molecular pathways that contributes to the inflammation. The contribution of each of the different processes might also according to the individual and the phase of infection (Paiardini and Müller-Trutwin, 2013).

Potential mechanisms that might cause and sustain the immune activation include (Fig. 6):

- **Pro-inflammatory responses:** One of the earliest antiviral responses is the induction of potent inflammatory mediators such as IFN-I. These cytokines stimulate the expression of ISGs, which code for proteins that limit the infection (Crosse et al., 2018) (Schoggins, 2014) (Sandler et al., 2014), and for chemokines that stimulate cell recruitment of other pro-inflammatory and anti-viral cells (NK cells, B cells, T cells) but also of cellular targets for HIV ($CD4^+$ T cells) (Jacquelin et al., 2009) (Jacquelin et al., 2014). Such cell trafficking amplifies the inflammatory response (Huot et al., 2016) (Hasegawa et al., 2009). Other pro-inflammatory molecules such as IL-15, TNF-α, IL-6, IL-1β and IL-18 can contribute to the sustained inflammation (Jacquelin et al., 2014). IL-1β and IL-18 production are the result of inflammasome activation (Barouch et al., 2016). Other molecules might be produced as consequence of subsequent persistent lymphocyte activation (IFN-γ).
- **HIV replication:** Viral proteins can also modulate immune activation. Some examples comprise the accessory proteins (Nef, Tat and Env) which have been reported to trigger directly cell activation. The Nef protein, for example, appears to be important in the activation of $CD4^+$ T cells by eventually prompting its susceptibility to stimulation (Schindler et al., 2006) (Joas et al., 2018). This could contribute to residual IA in ART-treated PLWH with non-detectable virus in the blood (Hunt et al., 2003). In untreated patients, the level of

inflammation and pathological disorders are not related with viral load in the brain. The immune activation is correlated with $CD4^+$ T cell decline more closely than viral load (Deeks et al., 2004).

- **Defective homeostasis of $CD4^+$ T cell populations:** HIV/SIV infection affects many $CD4^+$ T cells subsets (Gordon et al., 2010). The Th_{17} subpopulation in the gut is among the first and most strongly depleted immune cell population (Brenchley et al., 2008). This cell subset produces IL-17 and IL-22. Such interleukins serve to recruit other cell types to the areas of infection, to promote epithelial regeneration, to promote IgA+ B cells by direct IL-21 secretion and contact stimulation with B cells and to induce the production of antibacterial defensins (Wacleche et al., 2017). Th_{17} cells are present at significantly lower frequencies in the gastrointestinal tract of acutely and chronically HIV/SIV-infected individuals compared with natural hosts. T_{CM} are predominant in LN and also strongly affected by HIV/SIV infections. They are longer-lived, self-renewing and contribute to the replenishment of other $CD4^+$ T subsets. T_{CM} represents the most important reservoir for the virus which might in part explain their loss (Price et al., 2004). The deep loss of these subsets might affect the proliferation and homeostasis of T cells in general. ART fails to restore the intestinal damage and to restore CD4+ T cell counts (Okoye and Picker, 2013) (Ciccone et al., 2010). Another importantly affected population of T lymphocytes is constituted by T_{reg}. During HIV/SIVmac infection, an imbalance between this cell population and Th_{17} cells occurs, which could affect the immune activation levels (Valverde-Villegas et al., 2015).
- **Innate Lymphoid cells (ILCs):** A study showed that ILCs are depleted and enter in apoptosis with similar kinetics as CD4+ T cells in blood compartment during HIV/SIV infection. Among ILC, ILC3 population has effector function similar to Th17. Indeed, ILC3s are producer of IL-17/IL-22, source of preservation of epithelial barrier in intestine (Domingues and Hepworth, 2020). However, it was showed that ILC3, more precisely the ILC3-NKp44+ subpopulation, was depleted in intestine during SIV pathologic infection (Li et al., 2014a) (Mudd et al., 2018). Moreover, NKp44+ ILC3s from mLN correlated with marker of bacteria translocation level in plasma (Mudd et al., 2018).
- **Microbial translocation:** The mechanisms that cause the loss of epithelial integrity are not fully understood. There are reports where the severity of Th_{17} and NKp44+ ILC3 loss correlates with microbial translocation (Mudd et al., 2018) (Pallikkuth et al., 2013). Moreover, it was shown that the cell structure of the epithelial barrier changes during SIV infection, with modification of cell adhesion molecule expression (Benson et al., 2010). Other studies suggest that sustained TNF-α production causes the apoptosis of intestinal epithelial cells (Cumont et al., 2008). Whatsoever the underlying mechanism is, the resulting loss of the epithelial barrier integrity causes a sustained systemic exposure to microbial products (Ponte et al., 2016).

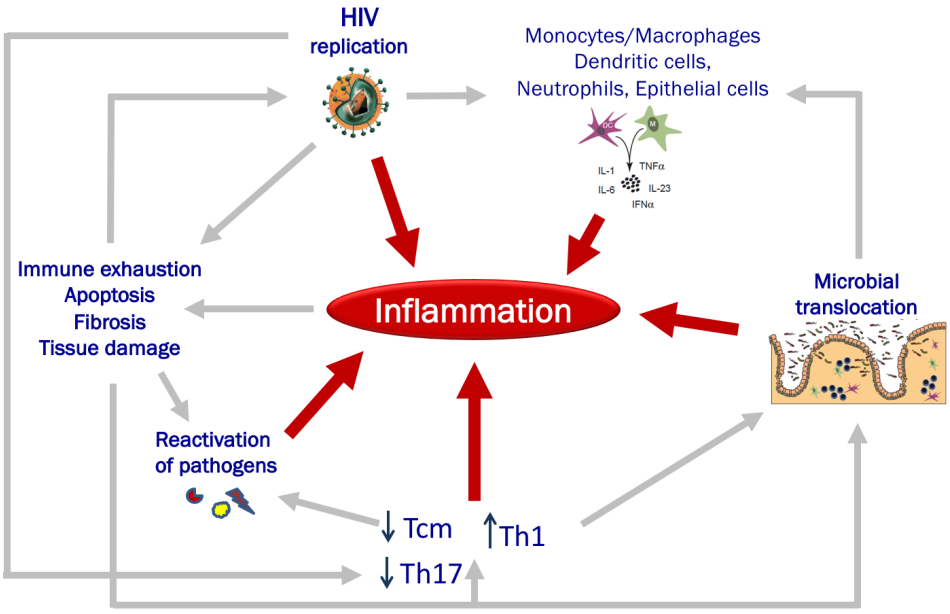


Figure 6. Potential mechanisms of chronic immune activation.
Several factors might act synergistically to the sustained immune activation present in pathogenic HIV/SIV infections. Adapted from Deekt et al (IAS) and (Paiardini and Müller-Trutwin, 2013).

ART initiated during early acute HIV infection is associated with less local and systemic immune activation (DaFonseca et al., 2015) (Schuetz et al., 2014) (Jiri Mestecky et al., 2015). ART initiated during acute HIV infection has indeed multiple benefits. For example, it restricts the size of the HIV reservoirs as compared to PLWH who initiated ART in chronic infection (Jiri Mestecky et al., 2015); it prevents the loss of mucosal Th17 cells (Schuetz et al., 2014); and is also associated with the preservation of follicle structure (Kök et al., 2015).

CHAPTER 4: VIRAL RESERVOIRS

As mentioned above, ART is not curative and treatment interruption usually leads to a viral rebound. HIV persists in viral reservoirs during ART. The viral reservoir is defined by cell types or anatomical sites of viral replication which persist for a prolonged period and constitutes the source of the virus that rebounds (Bachmann et al., 2019) (Henrich et al., 2017) (Jiri Mestecky et al., 2015) (Estes et al., 2017). The source of the viral rebound after ART interruption in PLWH is a matter of intensive research.

4.1. TISSUE VIRAL RESERVOIRS

Using next-generation-sequencing technology, a study in PLWH reported that multiple tissues contribute to the reservoir (Rothenberger et al., 2015). The majority of the long-lived latent HIV-1 reservoir is established near the time of ART initiation (Abrahams et al., 2019). *In vivo* imaging analyses of SIVmac-infected macaques currently investigate the dynamics of viral replication and persistence in all tissues during and after ART treatment (Santangelo et al., 2015) (Estes et al., 2017).

A large quantitative study demonstrated the presence of HIV/SIV DNA in nearly all tissues (Estes et al., 2017) (Table 2, Table 3). They showed in HIV/SIV infection that before ART the majority of SIV_{RNA} were in LNs (35.9%) and intestine (62.3%) in NHP. After ART in NHP, the majority of SIV_{RNA} were in intestine (98%), LNs (0.83%) and lung (0.73%) in NHP. Regarding SIV_{DNA}, no difference was observed in LNs and intestine before and after ART. Both in HIV and SIV infections, the viral load decreased more significantly in LNs that in gut with ART. Thus, in PLWH before ART, cell-associated HIV_{DNA} in LNs corresponded to 6.2×10^7 vDNA+ (viral DNA +) cells/g and declined to 2.7×10^5 vDNA+ cells/g after ART. In the intestine, cell-associated HIV_{DNA} in PLWH corresponded to 3.2×10^5 vDNA+ cells/g before ART and 2.7×10^5 vDNA+ cells/g after ART (Estes et al., 2017).

The major contributor to the SIV DNA during ART was thus intestine. The tissue, where residual viral replication *in situ* was the most clearly detected were LN (Estes et al., 2017). ART drugs level present in LNs and gut seem to be lower than in blood (Fletcher et al., 2014). In addition, a study found persistent SIV replication in the chronic phase in elite controllers inside B cell follicles despite the presence of potent antiviral CD8+ T cell activity (Fukazawa et al., 2015). It was shown that Tfh cells constitute an important source of persistent replication-competent virus even in PLWH with ART (Aid et al., 2018). Since B cell follicles represent a structure devoid of CD8+ T cells, they constitute an immune sanctuary allowing residual low-level replication in LNs despite efficient ART.

Additionally, HIV/SIV vDNA and vRNA is present in multiple tissues, including brain, liver, bone marrow, reproductive tissues and adipose tissues (Table 2). Even if contributing less to the overall size altogether these tissues might represent sites with unique immunological and pharmacological sanctuary characteristics that promote HIV/SIV persistence.

4.2. CELLULAR VIRAL RESERVOIRS

In HIV/SIV infection CD4+ T cells are the preferential viral targets. Naive CD4+ T cells are generally highly resistant to HIV infection and HIV susceptibility increases with activation and differentiation. In PLWH, central and transitional memory CD4+ T cells in the blood are major reservoirs of HIV (Chomont et al., 2009) (Jiri Mestecky et al., 2015). In the intestine, effector CD4+ T cells are frequent and might contribute more than in the blood to the viral reservoir. Of note, a recent study reported that the metabolic program determines even more strongly the susceptibility of the CD4+ T cell to HIV/SIV infection than the differentiation state of the cell (Valle-Casuso et al., 2019).

CD4+ T cells also divide in distinct functional subsets depending on the tissue. For example, Th17 and Th22 cells are mostly present in the gut, while T_{FH} cells are located inside B cell follicles of SLT. Th17 and T_{FH} cells have been shown to be highly susceptible to HIV/SIV infection and to support active viral replication (Yelina Alvarez et al., 2013) (Perreau et al., 2013) (Table 2). Paradoxically, Th17 cells in the gut are lost during HIV/SIV infection, while T_{FH} cells expand in LNs, in particular the Th1 T_{FH} cells (Velu et al., 2018).

Other viral targets are DCs and monocyte/macrophages. Dendritic cells in mucosa might belong to the first target cells of HIV and are able, like Trojan horses, to transport HIV/SIV to draining LNs. Only

two studies, one in HIV-1 and one in SIVagm infection, quantified pDC infection in tissues. They both showed high level of viral DNA in LN pDCs (Jochems et al., 2015a).

HIV_{DNA} was reported in bronchoalveolar lavage (Wong et al., 2019) and in central nervous system microglia (Wallet et al., 2019). HIV_{DNA} and HIV_{RNA} can be detected in CD163+CD68+ macrophages in the gut (Vásquez et al., 2019) (Allers et al., 2014) (Clayton et al., 2017). $SHIV_{RNA}$ was also detected in macrophages from liver (Igarashi et al., 2001). Whether macrophages are a viral reservoir or not has been a matter of debate (Calantone et al., 2014) (Clayton et al., 2017). Recent data clearly confirmed their role in HIV/SIV persistence. Studies in humanized mice have shown that macrophages sustain HIV replication in vivo independently of T cells (Honeycutt et al., 2016). HIV-1 persists in urethral macrophages of patients under suppressive antiretroviral therapy (Ganor et al., 2019).
Other types of cells have also been described as rare target for HIV, such as astrocytes. It has to be clarified in future studies which cells are relevant for viral persistence and/or the viral rebound.

It is however difficult to distinguish between cells that are infected or show traces of viral DNA or RNA and those that would be relevant as source of viral rebound. In addition, cells that carry HIV in the latent form without production of viral proteins are invisible to the immune system and also difficult to target and analyze. Several studies tried to define markers of the latently infected cells in ART-treated PLWH. Some of the proposed markers are listed below:

- **Immune checkpoint molecules (PD-1, TIGIT and LAG-3):** Memory CD4+ T cells which co-expressing these three markers were enriched for HIV_{DNA} (Fromentin et al., 2016). PD-1 positive cells in LNs also are preferentially infected (Banga et al., 2016).
- **CTLA-4:** CD4+ T cells in the T zone of LNs and expressing CTLA-4 have been shown to be preferentially infected (McGary et al., 2017).
- **CD2:** This receptor, involved in the interaction with APC, was strongly expressed on the surface of CD4+ T cells containing higher HIV_{DNA} copies than total CD4+ T cells. However, the HIV_{DNA} enrichment level observed was modest (Iglesias-Ussel et al., 2013).
- **CD30:** It was shown that CD4+ T cells expressing CD30 are enriched in cell-associated HIV_{RNA}. Yet, this enrichment was not reproduced in all studies and this population was not enriched for HIV_{DNA} (Hogan et al., 2018) (Wang et al., 2018).
- **CD20dim:** CD20dim expressing CD4+ T cells were shown as enriched population for HIV_{RNA}. However, the level enrichment was also only modest (Serra-Peinado et al., 2019).
- **CD32a:** CD32a is the low-affinity receptor for the IgG-Fc fragment highly expressed by myeloid cells. This receptor was proposed as a marker of the latent CD4+ T cell HIV reservoir (Descours et al., 2017). In contrast to most other candidate markers, CD32a shows high enrichment of HIV_{DNA} in CD4+ T cells in several studies (Darcis et al., 2020). However, no study could clearly reproduce CD32a as a marker of latently infected cells. Several studies rather showed that CD32+CD4+ T cells present an enrichment in cell-associated of HIV_{RNA} (Abdel-Mohsen et al., 2018) (Badia et al., 2018). CD32+ CD4+ T cells might be a marker for cells that are infected with transcriptionally active HIV.

Table 2. HIV/SIV replication in different tissues. The tissues are listed in alphabetical order.

Tissue	HIV/SIV replication
Adipose tissue	• Detection of viral DNA in $CD4^+$ T and $CD14^+$ cells in ART-treated patients indicating HIV infection of CD4+ T cells and macrophages (Couturier et al., 2015). Replication-competent HIV has been detected in the CD4+ T cells.
Bone marrow	• HIV-DNA in the bone marrow of ART-treated patients, suggesting that certain types of hematopoietic progenitors might constitute HIV-1 reservoirs (Wong and Yukl, 2016). • $CD34^+$ or $CD133^+$ cells have been suggested as HIV-1 reservoirs (Wong and Yukl, 2016) (Bordoni et al., 2015).
Brain	• HIV/SIV replication detected in microglial/macrophage lineage cells, multinucleated giant cell and also $CD4^+$ T cells (Wallet et al., 2019) (Abreu et al., 2019a).
Genital tract	• HIV has been found in $CD4^+$ T cells, Mφ and as free particles in the genital tract (Karris and Smith, 2011). • HIV/SIV replication takes place in both, $CD4^+$ T cells and Mφ in early stages of the infection (Tortorec et al., 2008). • HIV reservoir cells are found in semen (Chéret et al., 2017).
Gut	• The majority of the gut T-lymphocytes show an activated phenotype ($CD45RO^+$) which is associated with a high HIV/SIV infection rate (Karris and Smith, 2011). • Th17 cells are a major target of HIV • Upon infection, activated Mφ tend to accumulate in the gut which increases the proportion of infection targets and of pro-inflammatory cytokine production (Cassol et al., 2015).
Liver	• HIV/SIV has been probed to infect $CD4^+$ T cells and Kupffer cells (Blackard et al., 2011) (Gueye et al., 2004). • In macaques, Kupffer cells seem to support the active replication of SIVmac when $CD4^+$ T cells are depleted (Igarashi et al., 2001).
Lung and Bronchoalveolar lavage	• Macrophages (Mφ) are the predominant HIV -infected cells in the alveolar space (Cribbs et al., 2014). In lung mucosa, the virus has been found in $CD4^+$ T cells and Mφ (Abreu et al., 2019b).
Lymph nodes (LN)	• $CD4^+$ T cells are highly abundant, particularly memory T cells, which are productively infected by HIV/SIV in LN (DiNapoli et al., 2017). • T_{FH} cells in B cell follicles are major targets for HIV. • HIV/SIV can also be found as free particles trapped by follicular dendritic cells, where they remain infectious (Huot et al., 2018). • Tissue resident macrophages of the LN have been shown to be infected by SIVmac (DiNapoli et al., 2017).

	• SIV RNA detected in pDCs from LN (Jochems et al., 2015a).
Spleen	• As in LN, T_{FH} cells act as an important replication target for HIV and SIV (Vaccari and Franchini, 2018). • SIV RNA and DNA was detected in splenic pDCs (Jochems et al., 2015a).
Vaginal mucosa	• $CD4^+$ T cells are highly infected by SIV and particularly Th17 population (Veazey et al., 2003) (Stieh et al., 2016).

Under ART, HIV/SIV-DNA can still be found in most anatomical compartments (Estes et al., 2017). The Table 3 shows the tissues where HIV/SIV genomes have been detected in treated individuals (humans and/or macaques). Our understanding of the HIV/SIV-replication dynamic and establishment of viral reservoirs is though far from being complete (Barton et al., 2016).

Table 3. Tissues with detectable HIV or SIV upon suppressive ART.

Tissue	HIV/SIV/SHIV-DNA	HIV/SIV/SHIV-RNA	Protein/Antigen	*In vivo* imaging
Lymph nodes	X	X (SHIV, SIV)	X	X
Spleen	X (SHIV, SIV)	X (SHIV, SIV)		X
Bone marrow	X			
Thymus		+/- (1 of 6 SHIV-infected macaques)		
Liver	X (macrophages)	X (low SHIV, SIV)		X
Gut	X	X (SHIV, SIV)	X (macrophages)	X
Nervous system	X	X (brain, CSF) (SHIV, SIV)		
Lung	X	X (SHIV, SIV)		X
Heart		X (low SIV)		X
Kidney	X	X (low SIV)		X
Male reproductive tract	X (SIV)	X (SIV; human genital secretions)		X
Female reproductive tract	X (genital secretions)	X (genital secretions)		
Placenta	X (mast cells)			
Breast and breast milk	X	X	X	
Adipose tissue	X	X		

The original table was taken from (Wong and Yukl, 2016). The information was supplemented with data from (McGary et al., 2017) (Gueye et al., 2004) (Estes et al., 2017) (Santangelo et al., 2015).

CHAPTER 5: TISSUE DAMAGES

Chronic HIV infection if not treated induces a chronic inflammation and tissue damage. There was a hope that treatment initiated very early in HIV infection could prevent such tissue damage. However, most infections are still diagnosed in chronic infection and thus treatment cannot be initiated early enough in these cases. Moreover, even in early treated PLWH, some immunological and anatomic deteriorations persisting in tissues have been observed. It is important to understand what causes these deteriorations in tissues and how to prevent or repair them. We will focus in the following chapters on the intestine and the secondary lymphoid organs. Indeed, as described above, cells in the intestine are a major target for HIV and given the very large size of this organ, the intestine contains massive numbers of infected cells representing the major anatomical reservoir in PLWH under ART. Lymph nodes in addition show continuous signs of residual replication despite long-term efficient ART.

5.1. LYMPH NODES

5.1.1. ARCHITECTURE

Lymph nodes are composed of three major regions: medulla, paracortex and cortex (composed of interfollicular zone and B cell follicles). The normal LN is surrounded by sinuses and sometimes fat. Lymph nodes have as function to monitor the dangers and to educate adaptive immune responses. Lymph nodes collect the different antigens from tissues by the lymph. For example, cervical lymph nodes drain brain, mesenteric lymph nodes drain intestine, inguinal lymph nodes drain legs and genitals, etc... (Haley, 2017) (von Andrian and Mempel, 2003). Lymph flows from the subcapsular sinuses, through the medullary sinuses into the LN.

5.1.1.1. MEDULLA

Efferent lymph vessels take their origins in and around of the medulla (Haley, 2017) (von Andrian and Mempel, 2003). In this region resident Mφ, long-lived plasma cells, natural killer (NK) cells and memory T cells are present (von Andrian and Mempel, 2003) (Fang et al., 2017) (Bajénoff et al., 2006).

5.1.1.2. PARACORTEX

Paracortex (or T zone) is in majority composed of T cells and dendritic cells (DCs), but monocytes, Mφ, plasmacytoid DCs, NK cells and ILCs can also be found here (von Andrian and Mempel, 2003) (Fang et al., 2017) (Bajénoff et al., 2006) (Sozzani et al., 2010) (Wong et al., 2018) (Withers, 2016). There are two ways to enter into the paracortex. One way is by afferent lymph vessels particularly used by DCs but also lymphocytes. The second way is by high endothelial venules (HEVs). They provide the primary point of entry for naive T and B lymphocytes, pDCs and NK cells from the systemic circulation. The afferent vessels are distributed in the subcapsular sinus which is in contact with the paracortex. High endothelial venules (HEVs) are localized directly inside the paracortex. Subcapsular sinus and HEVs are delimited with paracortex fibroblastic reticular cell (FRC) layers. Networks of FRCs form wide corridors along cell migration and survival factors (Rodda et al., 2018). CCL21 and CCL19 are recognized by CCR7 and CCR8 respectively, and lead the control of migration and retention of cells toward the Paracortex (Rodda et al., 2018). The paracortex is the main area where mature DCs meet naive T cells, to activate and differentiate T cells according to the microenvironment (von Andrian and Mempel, 2003) (Fang et al., 2017) (Bajénoff et al., 2006).

5.1.1.3. INTERFOLLICULAR ZONE

The interfollicular zone is the area present between paracortex and cortex in lymph nodes. This region is an important region for the differentiation of T_{FH} cells. Indeed, once naïve $CD4^+$ T cells have encountered DCs in the paracortex, some of them will differentiate into pre-CD4+ T follicular cells (pre-T_{FH}) depending of specific cytokines in the microenvironment. This differentiation is led by two steps. First the activation pathway, principally induced by contact with DCs in the paracortex between the following receptor/ligand combinations: CD4-TCR/p:MHC-II; CD28/CD80-CD86; CD40L/CD40 and IL-2R/IL2. Second, the differentiation pathway, principally induced by cytokines: IL-21, IL-6 and

IL-27 secreted by the DC (Rao, 2018) (Eivazi et al., 2016) (Suh, 2014). At this moment pre-T_{FH} cells are able to express CXCR5 which is necessary for migration of these cells into the interfollicular region of LN where they can encounter activated B cells (Rao, 2018) (Eivazi et al., 2016) (Suh, 2014). During this contact, both cell types exchange different activation signals by ICOS/ICOSL; CD28/CD80-CD86; TCR/MHC-II; CD40L/CD40; IL-21/IL-21R. That leads to finish the differentiation of pre-T_{FH} cells into T_{FH} cells with further up-regulation of CXCR5 and loss of CCR7 expression enabling them to leave the interfollicular zone and to migrate toward CXCL13, the CXCR5 ligand, present in B cell follicles.

5.1.1.4. B CELL FOLLICLES

B cell follicles (BCF) in SLT are the center for the education of humoral responses. B cell follicles contain B cells, T_{FH} cells and follicular Dendritic cells (FDCs). In some cases, other cells have been detected such as CD8+ T regulatory cells and ILCs (Perdomo-Celis et al., 2017) (Withers, 2016) (Wang et al., 2011) (Bordet et al., 2019). The B cell follicles are composed of three major zones. The mantle is the outer region and is composed in majority of naive B cells ($CD20^+$; $CD27^-$; IgD^+; IgM^+) which wait their activation. Indeed, after B cell activation by capture of antigen via BCR signal, B cell downregulate CXCR5 and upregulate CCR7. Thus, the activated B cells leave the mantle zone and migrate into the interfollicular zone to meet pre-T_{FH} cells. This mutual activation leads B cells to either (i) migrate into extrafollicular zones, proliferate and become short-lived plasma cells, or (2) upregulate CXCR5 and lose CCR7 allowing migration into BCF and formation of germinal centers (GC). The GCs contain a dark and a light zone. The dark zone is principally composed of B cells becoming centroblasts ($CD20^+$; $CD27^-$; $IgD^{+/-}$; IgM^+) which proliferate with a high rate of point mutations on the IgH locus during cell division, also known as somatic hypermutation. The centroblasts continue their differentiation into centrocytes ($CD20^+$; $CD27^-$; IgD^-; IgM^-), which migrate into the light zone of GCs. In the light zone, the centrocytes are selected by FDCs and T_{FH} cells. According to the affinity of centrocytes with antigen presented by FDCs and survival signals induced by T_{FH} cells, if these parameters receipted by centrocytes are not enough, the centrocytes can (i) enter into apoptosis or (2) go back into the dark zone to improve their affinity for the antigen by the somatic hypermutation mechanism. However, if centrocytes display enough affinity to antigen presented by FDCs and receipt enough survival signal, centrocytes differentiate into memory B cells ($CD20^+$; $CD27^+$; IgD^-) or plasmablasts ($CD20^{dim}$; $CD27^{high}$; IgD^-), according to the signal delivery. In the same moment and according to signal delivery during the differentiation of centrocytes, these cells undergoes immunoglobulin class switched recombination allowing to express IgA, IgG and/or IgE on their surfaces to release adapted humoral response. Then, plasmablasts finish their differentiation into plasma cells ($CD20^-$; $CD27^{high}$; IgD^-) which will be responsible of antibody secretion in inflammatory tissues and at the systemic level (Wang and Müschen, 2018) (Bagnara et al., 2015) (McHeyzer-Williams et al., 2012) (Cyster and Allen, 2019). There are many different signals that are important for induction of GC. Recent studies reported important contributions by NKT cells, ILC3, $CD8^+$ T regulatory cells and subcapsular sinus macrophages (Perdomo-Celis et al., 2017) (Withers, 2016) (Wang et al., 2011) (Gaya et al., 2018) (Louie and Liao, 2019).

5.1.2. VIRAL REPLICATION PROFILES IN LYMPH NODES DURING HIV/SIV INFECTIONS

During the acute phase of infection, productively infected cells are found essentially in the paracortex of LN (Chakrabarti et al., 1994) (Brocca-Cofano et al., 2017). Only after the viral peak, by the end of the acute phase and in chronic infection, viral production is also found inside BCF, where the virus replicates within T_{FH} cells. In the chronic phase, in the absence of ART, T_{FH} cells become the major replicating cell in LN. Paradoxically, T_{FH} cells even expand in chronic HIV infection despite being a target for HIV. There is a selective increase of CXCR3+ T_{FH} cells in GC. $CXCR3^+$ GC- T_{FH} cells expressed higher levels of ICOS, CCR5 and α4β7, contained more copies of SIV DNA compared to $CXCR3^-$ GC-T_{FH} cells (Velu et al., 2016). CXCR3+ T_{FH} cells thus seem to be highly susceptible to HIV infection. These data demonstrate that chronic HIV infection promotes expansion of GC-T_{FH} cells, which are phenotypically and functionally distinct from conventional GC-T_{FH} cells and could contribute to viral reservoirs. In addition, virus is trapped within the follicles by FDCs where it remains infectious for 9 months or more (Huot et al., 2018). Under ART and in HIC, virus replication is well controlled in the T zone. However, low-level viral replication can persist in the T_{FH} cells of BCFs (Fukazawa et al., 2015) (Banga et al., 2016).

Strikingly, SIV infection in the natural hosts is characterized by similar viral replication patterns in the acute phase until the time of peak viremia, but then display a strongly controlled viral replication in the T zone during chronic infection (Diop et al., 2000) (Table 4). Moreover, the BCFs in natural hosts are characterized by an absence of viral replication and a frequent lack of FDC deposition of virus leading to the absence of virus RNA detection in BCF (Gueye et al., 2004) (Diop et al., 2000) (Huot et al., 2018) (Brocca-Cofano et al., 2017) (Martinot et al., 2013). T_{FH} cells in LN do not expand in contrast to HIV-1/SIVmac infections (Brocca-Cofano et al., 2017).

5.1.3. TISSUE DAMAGE IN LYMPH NODES DURING HIV/SIV INFECTIONS

The disruption of LN structure starts already in primary HIV infection. Collagen deposition has been demonstrated to occur in acute HIV infection (Schacker et al., 2002) (Zeng et al., 2012). Persistent collagen deposition leads to fibrosis (Estes, 2013a) (Estes et al., 2015). It has been shown in the macaque model that the infiltrating Treg cells are the major producers of TGF-β which induces the collagen deposition (Estes, 2013a) (Estes et al., 2008). The fibrosis damages LN architecture and dysregulation of immune responses. For instance, it reduces the access of CD4+ T cells to IL-7 inside the LN. It was shown in the macaque model, that the level of CD4+ T cell apoptosis during primary infection in the LN is predictive of the disease progression (Hodge et al., 2011) (Mogensen et al., 2010). Most of the CD4+ T cells dying by apoptosis are not infected (Février et al., 2011) (Saeidi et al., 2018).

In chronic HIV infection in the absence of ART, B follicles lose their structure, in part because of the loss of FDC network and because of hypergammaglobulinemia with hyperplastic germinal centers (Poultsidi et al., 2018) (Petrovas et al., 2012). There are important alterations of the T_{FH} cells with aberrant expansion in HIV and SIV infections. A rapid depletion of CCR6+ T_{FH} ($T_{FH}1$) cells and selective increase of CXCR3+ T_{FH} cells was observed in LN (Velu et al., 2018) (Velu et al., 2016). CXCR3+ T_{FH} cells are Th1 T_{FH} cells ($T_{FH}1$). They produce IFN-γ which favorizes the

hypergammaglobulinemia. Immunohistochemistry analysis demonstrated indeed an accumulation of IFN-γ^+ $CD4^+$ T cells within the hyperplastic follicles during chronic SIV infection (Velu et al., 2016).

The mLNs are located along the gut and drain the small and the large intestine. In mLNs, it was noticed that high level of cellular activation was measured in chronically SIVmac infection. It was also observed that high level of viral replication in mLNs (Scharko et al., 1996) (Cumont et al., 2007). It was reported that mLNs represented the main anatomical SIV_{DNA} reservoirs in the acute phase of SIVmac infection. In mLNs the Th17/T_{reg} ratio is altered with enrichment of T_{reg}. Also, the results showed a correlation between TGF-β production and fibrosis marker (collagen) in mLNs (Yero et al., 2019). Moreover, after ART interruption, observed SIV_{DNA} and SIV_{RNA} detection was observed in mLNs from SIVmac infection (Rabezanahary et al., 2020). Study also showed that early ARV initiation failed to decrease the levels of total T_{reg} and immune activation in mLNs (Yero et al., 2019).

Such damage effects on LN function and architecture are reduced by ART but the tissue does not recover entirely. Lymph node immune activation was higher in PLWH with ART than in uninfected people (Hong et al., 2017) (Paiardini and Müller-Trutwin, 2013). The level of activation, turnover, and/or cell death in T cells, B cells and monocytes is increased in PLWH with ART (Hong et al., 2017) (Hasegawa et al., 2009) (Walker and McMichael, 2012). Moreover, there are only little differences in PLWH with ART compared to untreated PLWH concerning fibrosis. For this reason, current trials try to combine ART treatment with an antifibrotic drug to try to resolve this issue (Estes et al., 2015).

In SIVagm infection, there are no structural damages in LN (Table 4). There is no loss of the FDC network, no hypergammaglobulinemia or hyperplastic germinal centers and no fibrosis (Huot et al., 2018).

LNs		**Natural host (African green monkeys, sooty mangabeys)**	**Non-natural host (human/macaque)**
Viral replication in LN (17, 12, 34)	Acute phase	High	High
	Chronic phase	**Low**	**High**
Inflammation	Acute phase	**Rapid**	**Strong**
	Chronic phase	**No**	**Yes**
	IFN-a	High in acute infection	High in acute infection
	Interferon-stimulated gene	High in acute infection	**High in acute and chronic infection**
	TGF-β and collagen deposition	**No**	**Yes**
LN architecture	Lymphadenopathia	**No**	**Yes**
	Follicular dendritic cell network	**Preserved**	**Lost**
	Fibrosis	**No**	**Yes**
Location of SIV-infected cells	T cell zone	Yes	Yes
	B cell follicles	**Rare/absent**	**Yes**
	Virus trapping	**Rare/absent**	**Yes**
SIV-infected cells	$CD4^+$ T_{CM}	**Low**	**High**
	T_{CM} PD-1^+CTLA4^+	nd	Yes
	T_{FH}	**Rare/absent**	**High**
	Plasmacytoid dendritic cell	Yes	Yes
	macrophage	Yes	Yes
Antiviral immune responses	HIV/SIV-specific T cell responses	Weak	Variable (strong in Elite controllers)
	Follicular $CD8^+$ T cells	nd	Yes (rare)
	Follicular NK cells	**Yes**	Yes (rare)
	bNAb	nd	Yes (rare)

The green and red colors highlight, respectively, major differences between SIV infection in natural hosts and HIV/SIV infections in non-natural hosts.

Table 4: Major similarities and differences between HIV/SIVmac infections and SIV infections in natural hosts at the level of lymph nodes (LNs). The original table was taken from (Huot et al., 2018).

5.2: INTESTINAL MUCOSA

5.2.1 ARCHITECTURE

The intestine contains more immune cells than any other organ. The intestinal mucosa is formed by three different layers of tissue: muscularis mucosae, lamina propria (LP) and epithelium. Besides, it is covered by a thin layer of mucine which regulates the interaction of the tissue with nutrients and inhabitant bacteria.

5.2.1.1 INTESTINAL EPITHELIAL BARRIER

The intestinal barrier is composed by simple columnar epithelial cells that line the luminal surface of the small and large intestines. These cells are tightly joint to avoid the split-out of the content and the pass-in of pathogens, forming a barrier. The epithelium is constantly renewed (every 4-5 days) from stem cells that resides in the crypts (de Santa Barbara et al., 2003). When needed, these cells might differentiate into seven different types: enterocytes, goblet cells, enteroendocrine cells, Paneth cells, microfold cells (M cells), cup cells and tuft cells (Kandasamy et al., 2014) (de Santa Barbara et al., 2003) (Peterson and Artis, 2014) (Fig. 7). The integrity of the barrier depends on a fine equilibrium between the apoptosis rate and the differentiation speed of the progenitors, as well as of the maintenance of the tight junctions.

The two main functions of the epithelial barrier are i) metabolic, by the absorption of nutrients and ii) immunologic, defending the body against harmful agents. The accomplishment of these functions relay on its structure, the cellular composition, the junctional elements and the physicochemical processes (active transport, passive permeability, synthesis and secretion of bioactive components) (Kandasamy et al., 2014).

Each type of intestinal epithelial cell (IEC) contributes differently to the performance of the barrier:

- **Enterocytes:** Most predominant cell type (80%). Specialized in absorption of nutrients. In the apical side, they have microvilli which augments their functional surface. They express immunoglobulin receptors, glucose and galactose transporters on their membrane (Kandasamy et al., 2014) (de Santa Barbara et al., 2003).
- **M cells:** Participants in the immune response. Due to their structure, microfolds and a pocket-like compartment, these cells can engulf pathogens and present their antigens to DCs, B and T cells (de Santa Barbara et al., 2003) (Ohno, 2016).
- **Goblet cells:** They also participate in the immune responses. These cells are specialized in the secretion of antimicrobial peptides such as mucin, trefoil peptides, resistin-like proteins and Fcγ binding protein (Kandasamy et al., 2014) (de Santa Barbara et al., 2003).
- **Paneth cells:** Opposite to other IEC, Paneth cells reside in the crypts and not in the villi and are exclusively found in small intestine. They serve as a protective niche for stem cells and participate in the production of defensins, cathelicidins, lysozyme C, phospholipase A2 and Ang4 in response to microbial invasion. Some trophic factors like TNF-α, Wnt3 and DII4 are also secreted by these cells (de Santa Barbara et al., 2003) (Bevins and Salzman, 2011). The secretion of all these molecules contributes to the immune defense, causes inflammation,

attracts other cells and improves the differentiation and recruitment of stem cells to promote the healing process.

- **Tuft cells**: Also known as "brush cells", they are less characterized. It is known that in mice tuft cells participate in the regulation of inflammatory processes by their cyclooxygenase activity and the production of prostaglandins (Ting and Moltke, 2019).

There are also lymphocytes located beneath the tight junctions between epithelial cells, called intraepithelial lymphocytes that contribute to the immune responses.
The host to maintain its homeostatic relationship with the microbiota by combined action of epithelial cells, mucus, IgA, antimicrobial peptides and immune cells. First, by reducing the contact between the microbiome and the immune system via epithelial cells (physical barrier), or by the secretion of soluble factors, like antimicrobial peptides. Goblet cells present around the epithelial cells can produce mucus which limits exposure to the commensal microbiota.

5.2.1.2 INTESTINAL MUCOSA HOMEOSTASIS

Like the cellular composition, the architecture of the mucosa shapes the function of the gut. In the small intestine, the mucosal tissue is tightly folded to maximize the absorptive surface. Such folding produces a brush-shape surface called villi (Fig. 7). Along with the enterocytic microvilli, this architecture amplifies the absorptive surface (de Santa Barbara et al., 2003). These structural features are present in all the three compartments of the small intestine: duodenum, jejunum and ileum. Regarding the large intestine, it is divided into cecum, ascending colon, hepatic flexure, transverse colon, splenic flexure, descending colon, sigmoid colon, rectum, and anus. The function of these compartments resides in the absorption of water and lipids and the formation, transit and excretion of fecal material. Except from Paneth cells, the colon is populated by the same types of IEC than the small intestine. Nevertheless, the villi are absent. In turn, the epithelial barrier forms deep tubular pits that increase in depth toward the rectum (de Santa Barbara et al., 2003) (Peterson and Artis, 2014) (Fig 6). $CD4^+$ T lymphocytes, including ILC, γδT cells, MAITs, Invariant natural killer T (NKT) or NK cells can participate to the control of the intestinal homeostasis, tissue immunity and physiology via antimicrobial peptide and mucus stimulation, in regulating wound repair or in increasing epithelial regeneration (Belkaid and Harrison, 2017) (Aidy et al., 2013) (Okumura and Takeda, 2016) (Nielsen et al., 2017) (McCarthy and Eberl, 2018). γδT cells are also known to secrete IL-1 and IL-23 cytokines, important for activation and control of immune responses in the intestine (Belkaid and Harrison, 2017) (Aidy et al., 2013) (Okumura and Takeda, 2016) (Nielsen et al., 2017) (McCarthy and Eberl, 2018). Lymphocytes, such as T cells and ILC produce IL-17 and IL-22, that participate in the maintenance of intestinal barrier integrity.
Antigen-presenting cells loaded with microbial antigens can migrate from the lamina propria to the mesenteric lymph node, but do not circulate further (Spencer and Sollid, 2016) (Suzuki and Nakajima, 2014) (Mora and von Andrian, 2008) (Shacklett and Anton, 2010). The gut resident macrophages induction is associated with local expansion of regulatory CD4+ T cells (T_{reg}) (Belkaid and Harrison, 2017). Moreover, gut resident macrophages are also associated with IL-1β release that in turn promotes the accumulation of Th17 cells (Belkaid and Harrison, 2017) and GM-CSF production by ILC3 (Belkaid and Harrison, 2017) (Mortha et al., 2014). GM-CSF favorizes mucosal antigen-presenting cell to produce IL-10 and retinoic acid.

There are also IgA which can exclude microorganisms from the gut. Commensal-specific IgA responses are produced with the help of intestinal DCs and by their interaction with B and T cells in Peyer's Patches (PP) (described section 6.2.1.3.). Secretory IgA can be produced by T independent and T cell dependent ways.

Failure to regulate the microbiota, food derived antigens and/or pathogens can lead to severe pathological outcomes ranging from inflammatory bowel diseases to metabolic syndromes, and microbial translocation-induced systemic inflammation.

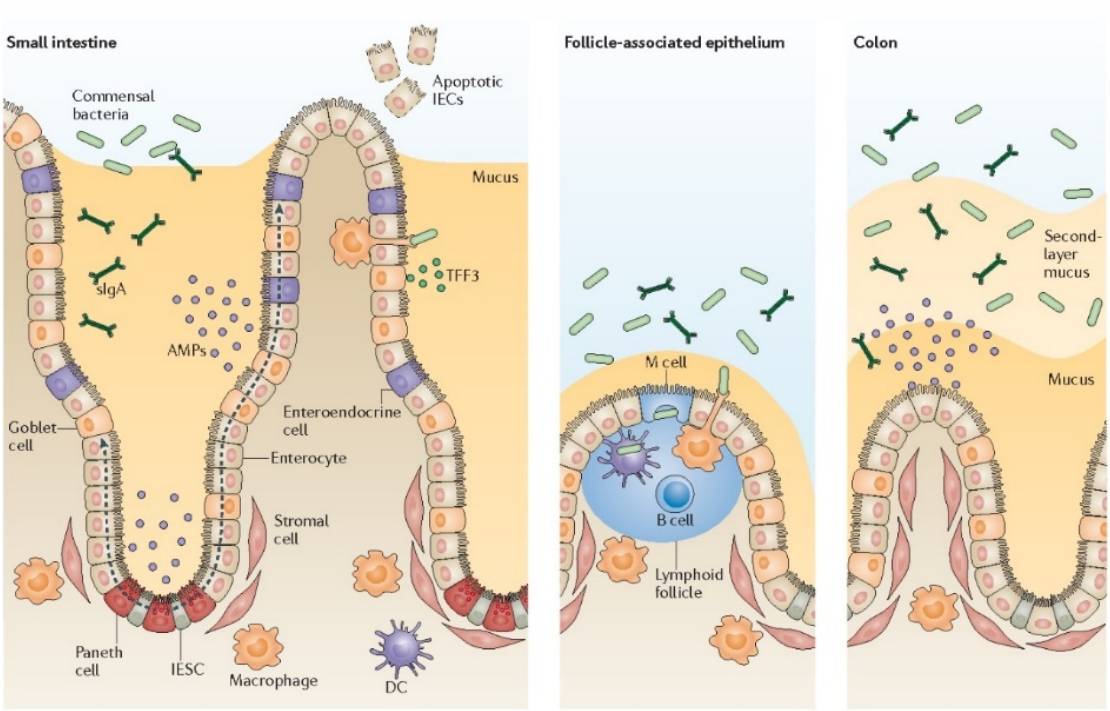


Figure 7. Structure of the intestinal mucosa in small and large intestine
Intestinal epithelial cells (IECs) form a biochemical and physical barrier that maintains segregation between luminal microbial communities and the mucosal immune system. Diverse types of differentiated IECs populate the villus while Paneth cells are found in the crypts. In the colon, the epithelium is conformed only by deep crypts. The mucosa also contains lymphoid aggregates as well as follicles (Peyer's patches) (Peterson and Artis, 2014).

5.2.1.3 GUT ASSOCIATED LYMPHOID TISSUE (GALT)

The GALT is contained in the lamina propria. It constitutes the largest pool of lymphocytes, Mφ and DCs in the body. The GALT also contains lymphoid aggregates, isolated lymphoid follicles and Peyer's patches (PP). All components of the GALT play a central role in primary mucosal tissue immune defenses.
Isolated lymphoid follicles are clusters of B cells, DCs and few CD4+ T cells, located in the terminal ileum and colon. ILFs formation can be promoted by recognition of antigens from commensal bacteria (Reboldi and Cyster, 2016) (Spencer and Sollid, 2016).

Peyer's patches are at the origin of majority IgA synthesis and surveillance of microbiome (Spencer and Sollid, 2016) (Suzuki and Nakajima, 2014) (Mora and von Andrian, 2008). The PPs are particularly abundant in the Ileum. They contain large amounts of B lymphocytes, T cells and DCs.

Lymphocytes enter PPs from the bloodstream via HEVs. Peyer's patches are organized in three major regions: BCF; follicle associated epithelium (FAE) and sub-epithelial dome (SED) that is localized between BCF and FAE (Figure 6). A small T zone is located next to the BCF. Antigen entry to PPs occurs majority via M cells. M cells do not express the poly-immunoglobulin receptor (polyIgR) but are able to capture and to realize transcytosis of IgA-coating antigens (Moor et al., 2017) (Kamada and Núñez, 2014) (Reboldi and Cyster, 2016). Dendritic cells from SED capture antigens transcytosed to stimulate CD4+ T cells. Germinal centers in PP contain FDC networks that are orientated toward the SED. FDCs can retain and display antigens by Fc and complement receptors, to stimulate B cells in the BCFs. PPs are continually exposed to mucosal-derived antigens and their follicles almost universally contain preformed GCs with Ig gene somatic hypermutation and B cell selection. Yet, Isolated lymphoid follicles (ILFs) can play a role as an IgA inductive site, although PPs are the main inductive sites for IgA in the intestine.

5.2.2. VIRAL REPLICATION PROFILES IN THE INTESTINE DURING HIV/SIV INFECTIONS

Intestine is one of major viral reservoir during HIV/SIV infection. Moreover, the gut is one of first important site of replication since acute phase of HIV/SIV infection (Crakes and Jiang, 2019) (Mora and von Andrian, 2008). With an important depletion of Th17 since day 14, the inflammatory environment favors the virus replication in this tissue (Hensley-McBain et al., 2018). Indeed, the pro-inflammatory environment favorizes the recruitment of virus target cells like $CD4^+$ T cells or macrophages (Koppensteiner et al., 2012).

Infected cells located is lamina propria, $CD4^+$ T cells in the GALT are 10-fold more frequently infected by the virus than $CD4^+$ T cells in the peripheral blood (Mehandru et al., 2007) (Mattapallil et al., 2005). *In vitro* experiments showed that Th17 cells can be infected by SIV/HIV (El Hed et al., 2010) (Cecchinato et al., 2008). Moreover, a study in the colon of chronically SIV-infected macaques indicates that mucosal T_{reg} were less susceptible to productive SIV infection than non-T_{reg} and thus were selectively spared from SIV-mediated cell death (Allers et al., 2010). Concerning intestinal macrophages, this resident population seems to be relatively resistant against HIV (Shen et al., 2009). However, the recruitment of circulating monocytes into the intestine leads to differentiate these monocytes into inflammatory macrophages, which become permissive for HIV infection (Porcheray et al., 2006). While rectal macrophages appear more susceptible, the role of intestinal macrophages in the establishment and spread in HIV/SIV infection stays uncertain (McElrath et al., 2013).

In natural host SIV infection, the virus replicates predominantly in lymphocytes but rarely in macrophages (Pandrea et al., 2008a) (Pandrea et al., 2007) (Milush et al., 2007) (Gordon et al., 2008). Moreover, natural host chronically infected with ART showed that the bulk of SIV replication occurs in short-lived cells (Pandrea et al., 2008a) (Gordon et al., 2008).

5.2.3 INTESTINAL TISSUE DAMAGE IN HIV/SIV INFECTIONS

The intestinal mucosa is impaired in untreated individuals at the level of:

- Disruption of the epithelial barrier
- Disruption of lymphoid follicles

These processes are briefly referred below and summarized in Figure 7. It has been shown that ART initiation in the chronic phase of infection does not restore the normal architecture and that the FDC networks and germinal centers remain damaged (Kök et al., 2015).

5.2.3.1 DISRUPTION OF THE EPITHELIAL BARRIER

During HIV infection, the damage of the intestinal barrier has been demonstrated by focal breaches, enterocyte apoptosis, increased gastrointestinal permeability, and changes in the expression of genes associated with growth of epithelial steam cells and tissue repair (Klatt et al., 2013) (Brenchley, 2013). A main consequence of the epithelial disruption is the translocation of luminal bacterial into the intestinal tissue. When such antigens are detected at the systemic level they drive or amplify immune activation at the systemic level (Fig. 8).

Whether the epithelial damage is the cause or consequence of the chronic inflammation or both, is still controversial. An increase of pro-inflammatory mediators in the intestine has been observed as early as 6-10 days p.i. in macaques, before evidence of microbial translocation. Despite some structural modifications, the damage in the epithelial barrier is generally not sufficient in primary infection to promote microbial translocation in the early phase of infection and seems to be clearly present only in the chronic phase of HIV/SIVmac infections (Hensley-McBain et al., 2018). Microbial translocation might occur if the damages of the epithelial barrier occurring in primary infection are not repaired and progressively become worse. However, it is important to remind that microbial translocation might be not the unique source of immune activation in chronically HIV-1/SIV-infected individuals (Hirao et al., 2014) (Hensley-McBain et al., 2018).

Several mechanisms have been proposed to explain the damage of the epithelial barrier. The latter correlates with the persistent production of pro-inflammatory factors. The overproduction of pro-inflammatory cytokines has been proven to damage the tight junctions. For instance, the excess of pro-inflammatory mediators such as TNF-α has been associated with the dysfunction of the epithelial barrier (Nazli et al., 2010). Moreover, and as we described above (section 3.2), the depletion of Th17 cells and $NKp44^+$ ILC3 that occurred already in acute HIV infection most likely participates to the loss of epithelial barrier regulation (Dandekar et al., 2010) (Li et al., 2014a) (Mudd et al., 2018) (Xu et al., 2012). Other studies showed that $CD8^+$ T cells producing IL-17, are maintained in the intestine from macaques during acute SIV infection but are also progressively depleted during chronic phase (Ponte et al., 2016). Also, $CD8^+$ T cells that produce GM-CSF and CCL5 increase in the intestine during SIV infection which could enhance recruitment into the gut of myeloid and lymphocyte populations that could further amplify the immune activation levels (Kenway-Lynch et al., 2013). Inhibitors of the inflammatory responses are induced early on (NLRX-1, Treg) and could inhibit viral control, further fueling inflammation. NLRX1 expression correlates with the magnitude of viral RNA in gastrointestinal tissues (Barouch et al., 2016). It was also shown that Treg increase in GALT and persist during chronic SIV infection (Ponte et al., 2016). This could explain the decrease in the Th17/Treg ratio described in the gut (Favre et al., 2009). Other cells, such as neutrophils were not increased in acute phase of SIV pathogenic infection, but in chronic phase neutrophils infiltrated colonic mucosa and their levels were correlated to epithelial barrier damage (Ponte et al., 2016). Collectively, all these changes and dysregulations might participate to variable extents to the epithelial

barrier disruption and/or decrease in repair mechanisms. Noteworthy, the epithelial barrier disruption has not been observed in natural hosts (Raehtz et al., 2020).

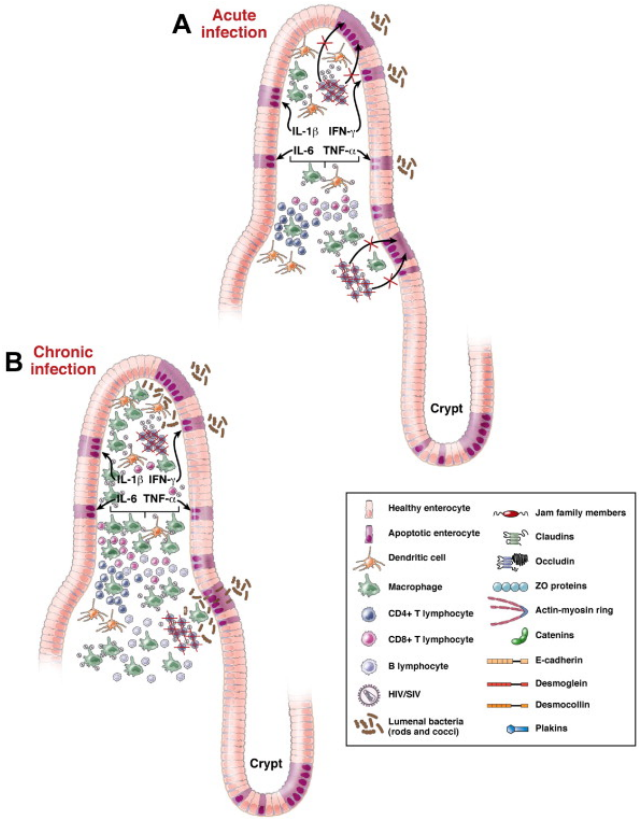


Figure 8. Schematic representation of pathological changes underlying intestinal epithelial barrier disruption during HIV/SIV infection

(*A*) Acute HIV/SIV infection depletes the mucosa of $CD4^+CCR5$ effector memory T cells and Th17 cells, leading to growth disruption, maintenance, and renewal of epithelial cells. (*B*) During chronic HIV/SIV infection there is increased infiltration of inflammatory cells into the lamina propria leading to more pro-inflammatory cytokine production and widespread distribution of the intestinal epithelial barrier facilitating bacterial translocation. Taken from (Lackner et al., 2009).

In PLWH with ART, the viremia is controlled and this leads to a decrease in systemic inflammation. However, in most of them, soluble markers of monocyte activation (sCD163), inflammation, and coagulation remain higher than in non-infected individuals (Paiardini and Müller-Trutwin, 2013). Moreover, neutrophil infiltration and apoptosis remain abnormally high in mucosal tissue despite ART. These inflammatory markers negatively correlated with epithelial barrier functional markers (such as I-FABP or zonulin-1) and predicted mortality in treated PLWH with a history of AIDS (Casado et al., 2020) (Raehtz et al., 2020) (Hunt et al., 2014).

Several studies with PLWH on long-term ART have evaluated the potential correlates of gut CD4+ T-cell restoration. Early ART initiation could reverse immune activation, preserve Th17 levels, help to maintain reactive memory B cells against HIV and maintain frequencies of functional T_{FH} cells in mucosal tissue (Schuetz et al., 2014) (Planchais et al., 2018). However, even very early ART (before Fiebig III) was not able to restore full function of Th17 cells (Schuetz et al., 2014). Also, signs of gut damages by measure of I-FABP and LPS plasmatic levels were still observed (Schuetz et al., 2014). And finally, as it was mentioned above (section 4.1) the viral reservoir is in majority present in the

intestine in PLWH under ART and that could be another factor (in case for example of viral protein production or low-level replication in follicles), which maintains at low levels a pro-inflammatory environment.

5.2.3.2 DISRUPTION OF THE LYMPHOID FOLLICLES

During early HIV infection, PP have a loss of germinal center architecture, with an important increase of apoptotic T and B cells (Shacklett and Anton, 2010) (Mora and von Andrian, 2008) (Veazey, 2019). But the disruption of PP is also due to the loss of the FDC network (Kök et al., 2015). A study showed that CD4+ T cell depletion in terminal ileum, including PP, is accompanied by extensive fibrotic damage and collagen deposition since acute phase (Mora and von Andrian, 2008) (Lane et al., 1983) (Veazey, 2019). However, CCR5+ CD4+ T cells are preferentially targeted by the virus. This phenomenon leads to show more extensive depletion in the lamina propria compare to PP (Mehandru et al., 2004) (Li et al., 2005). Moreover, the deletion of ILC in HIV/SIV infection lead to some difficulties to form the isolated lymphoid follicles in intestine (Buettner and Lochner, 2016) (Shah et al., 2017). Early treated, but not later treated PLWH, showed conserved intestinal lymphoid structure and were better able to repair lymphoid gut mucosal homeostasis (Kök et al., 2015) (Mudd and Brenchley, 2016).

CHAPTER 6: B CELLS AND NK CELLS IMMUNE RESPONSES IN TISSUES FROM HIV/SIV INFECTION

For the reasons mentioned above, we will focus the description of the B and NK cells immune responses in tissues, and in particular on those in LNs and intestine.

Indeed, previous studies have linked the potential role of IgA^+ B cells with the inflammatory control as it is the case in this study that showed a perturbation with the loss of IgA production from intestine that was linked with bacteria translocation in HIV infection (Hel et al., 2017) (Kulkarni and Ruprecht, 2017). In addition, in SIVagm infection, the depletion of B cells by anti-CD20 induced an upregulation of SIV production in intestine (Gaufin et al., 2009).

Regarding NK cell population in the LNs, most studies in the literature have focused their attention on CD8+ T cells (Kiniry et al., 2018). However, in SIVagm infection, CD8+ T cell was not observed to display a strong specific activity or localized in B follicles in LN (Zahn et al., 2008) (Diop et al., 2000). Jacquelin *et al.* noticed in natural hosts a stronger NK cell activity in LNs as compared to the blood (Jacquelin et al., 2014). Only little information is available on NK cells in tissues during HIV/SIV infections. We will summarize this information in the chapter below. In addition, unconventional CD8+ T cell, precisely MHC-E restricted $CD8^+$ T cells are interesting in HIV infection. Indeed, vaccination of MAC with a CMV-based vector, expressing HIV Gag, revealed a very strong MHC-E restricted $CD8^+$ T-cell response (Okoye et al., 2018) (Hansen et al., 2016). We were interested by a possible implication of MHC-E restricted $CD8^+$ T cells in intestine from SIVagm infection concerning a potential role in the inflammatory control. Another particular attention will be given to the immune responses in follicles, and therefore to B cell responses during HIV/SIV infections and their relationship with chronic immune activation damages.

6.1. B CELLS IN HUMAN AND NON-HUMAN PRIMATES

In humans, as in other primates, the bone marrow is the major site of B cell development and the repository of returning plasma cells following terminal differentiation of B cells in the periphery. During their developmental process, B cells way out bone marrow at the immature/transitional stage after having successfully completed the rearrangement of both heavy and light chain immunoglobulin genes to form a fully functional B-cell receptor (BCR). This process involves several checkpoints, designed to evaluate fitness and to eliminate B cells with self-reactive BCRs (Melchers, 2015). In the periphery, immature/transitional B cells develop into naive B cells following further selection, likely in the spleen, a process that is accompanied by a number of distinct phenotypic changes. In humans, a unique set of surface markers has proven useful for tracking maturing B cells in the periphery, in addition to the lineage defining markers of CD19, CD20, as well as IgM and IgD. Bone marrow B-cell emigrants maintain expression of the pre-B cell surface marker CD10, while expressing low levels of the complement receptor CD21. As immature/transitional B cells transition to naive B cells their expression of CD21 increases while levels of CD10 decrease to background and remain undetectable on mature B cells in the circulation. Then naive B cells circulate into peripheral tissues, like LNs.
Two types of memory B cells can be distinguished: conventional memory B cells and non-conventional memory B cells (Prieto and Felippe, 2017) (Sanz et al., 2019) (Kaminski et al., 2012). The conventional memory B cells represent the majority of circulating B-cell subsets in healthy donors and express both CD21 and CD27. They represent resting memory (RM) B cells, displaying low levels of activation markers. Non-conventional memory B cells are not seen in important numbers in healthy donors, including tissue-like memory (TLM) and activated memory (AM) B cells. Tissue-like memory B cells lack expression of CD27 and have low levels of CD21. The B_{AM} cells are CD21lo and express CD27, and are associated with apoptosis markers (Sims et al., 2005) (Prieto and Felippe, 2017) (Sanz et al., 2019) (Kaminski et al., 2012). The last differentiation stage are plasmablast/plasma cells (see also section 5.1.1.4).

There are differences in B cell memory subset distributions in blood between rhesus macaques and humans. Indeed, B_{RM} cells are predominant in healthy human blood while B_{AM} cells are a minor population. In blood of healthy macaques, it is the opposite, B_{RM} cells are the minor population and B_{AM} cells the major one (Brocca-Cofano et al., 2017). It has been suggested that this is dependent of environmental factors and host virome differences between both species (Brocca-Cofano et al., 2017). In a study describing the B cells from healthy AGM, the authors showed the same proportion of B cell subpopulations in blood than healthy macaques, except to B_{TLM} cells where this population is more important in AGM than in MAC (Brocca-Cofano et al., 2017). In tissues like the gut or LN, the proportion of B cell subpopulations were different between the species. In LNs, macaques have more B_{AM} cells than AGM, while in gut macaques have less B_{RM} and B_{TLM} cells than AGM (Brocca-Cofano et al., 2017). The reasons for it are unclear. There are in general many differences between species. For example, healthy AGMs display higher T cell counts than healthy macaques and humans. However, no relation between differences in immune cell subset frequencies of distinct species and SIV infection profiles could be established.

6.1.1. MUCOSAL B CELLS

The intestine is structured to prevent the entry of potentially pathogenic material into the body. In contrast, GALT is associated with an epithelial structure that facilitates antigen entry. The GALT contains diverse B-cell subsets. The central feature of most GALT in the small intestine and appendix are the prominent GC containing B cells that have been activated. B cells in GCs are surrounded by other cells, such as follicular dendritic cells, T follicular helper cells, and immune responses in the intestine are initiated and in gut regional lymph nodes, like mLN (Spencer and Sollid, 2016) (Suzuki and Nakajima, 2014) (Mora and von Andrian, 2008). Whereas food and ingested antigens are present in the small bowel, microbial antigens represent a major immune challenge in the colon.

Immune protection in the human intestinal mucosa heavily depends on the secretion of immunoglobulin A (IgA) by plasma cells. The latter occupy the diffuse subepithelial connective tissue of the intestinal lamina propria. Locally secreted IgA bound to polymeric Ig receptor (pIgR) is actively transported into the gut lumen where it regulates bacteria. The body commits considerable resources to the production of intestinal IgA (Spencer and Sollid, 2016) (Suzuki and Nakajima, 2014) (Mora and von Andrian, 2008). Human intestinal IgA is mostly dimeric and comprises both the IgA1and IgA2 subclass. Most plasma cells in the small intestine secrete IgA1. The proportion of IgA2 increases from the duodenum through to the terminal ileum and the subclasses are present in approximately equal numbers in the colon. IgA2 has a shorter hinge than IgA1 and as a consequence is less susceptible to bacterial proteases and would therefore have a functional advantage in the lumen of the colon that is rich in bacterial species. In contrast, while IgA is the second most common Ig isotype in blood after IgG, most IgA in serum is monomeric IgA1 (Steffen et al., 2020). Macaques and AGMs secreted only one subclass of IgA (Zhang et al., 2016).

Persistent humoral memory to gut pathogens and other gut antigens can be obtained by long-lived memory B cells replenishing dying plasma cells or by plasma cells that themselves are long-lived (Spencer and Sollid, 2016) (Suzuki and Nakajima, 2014) (Mora and von Andrian, 2008) (Shacklett and Anton, 2010). The longitudinal persistence of clonally related B cells in the IgA repertoire, despite major changes in the microbiota, was taken to support the notion of a continuous diversification of memory B cells and this was considered a central element in the shaping of the gut humoral response (Spencer and Sollid, 2016) (Suzuki and Nakajima, 2014) (Mora and von Andrian, 2008) (Shacklett and Anton, 2010). Secreted IgA primed in gut is also found in other body secretions, such as to high proportion in breast-milk or bone marrow due to IgA+ plasma cell migration in these compartment (Langel et al., 2020) (Fritz et al., 2012) (Lemke et al., 2016).

DCs in the subepithelial area are key regulators of the fate of responding B cells. They express the enzyme retinaldehyde dehydrogenase that catalyzes the production of retinoic acid that subsequently imprints homing via the induction of a4b7 and CCR9. They also secrete IgA-inducing protein (IGIP) and APRIL (a proliferation-inducing ligand) that together with derived transforming growth factor beta (TGFb) support IgA class switch recombination (Suzuki and Nakajima, 2014) (Mora and von Andrian, 2008).

6.1.2. B CELLS IN HIV/SIV INFECTION

In HIV/SIV infection, persistence of immune activation and pathogen leads to several alterations in the B cell population (Table 5). Hypergammaglobulinemia, polyclonal activation, increased B cell

turnover, lymph node germinal center hyperplasia, and altered antibody responses to HIV and other pathogens have been described (Brocca-Cofano et al., 2017). In addition, increased apoptosis by the Fas pathway or exhaustion by the PD-1 pathway has been reported in HIV-1/SIVmac infections (Brocca-Cofano et al., 2017). In early HIV/SIV pathogenic infection, B_{RM} cells are depleted in blood, while remaining at normal levels in SIVagm infection (Brocca-Cofano et al., 2017). However, in LNs, B_{RM} cells seem to be stable in SIVmac infection but increased in SIVagm infection. At the opposite, there are increases of B_{TLM} and B_{AM} cells in SIVmac infection, but not in SIVagm infection in LNs. While B_{TLM} increase in LNs in pathogenic HIV/SIV-infections, they display though a cell exhaustion profile similar to T-cell exhaustion (Brocca-Cofano et al., 2017) (Peruchon et al., 2009).
In HIV infection, a study showed a loss of IgA and IgG in gut because of dysfunction in switching of B cells in the gut, leading to enrichment of IgM+ B cells (Kulkarni and Ruprecht, 2017). This study showed a negative correlation between IgA titer in plasma and a bacterial translocation marker (sCD14) (Hel et al., 2017) (Kulkarni and Ruprecht, 2017).

In SIVagm there were not major variations in B cell population frequencies in the gut (Brocca-Cofano et al., 2017). The loss of total, naïve, resting memory B cells and progressive increase of B cell apoptosis does not occur in AGM SIV infection (Brocca-Cofano et al., 2017). In early SIVagm infection, there is however a strong proliferation of B cells inside GC to extent similar or higher than in SIVmac infection (Cumont et al., 2008). AGM rather developed higher-magnitude gp120-specific IgA/IgG responses and more robust gp140-specific IgG responses than SIV-infected macaques (Amos et al., 2013) (Zhang et al., 2016) (Amos et al., 2015) (Norley et al., 1990) (Brocca-Cofano et al., 2017). In particular, there is a robust anti-gp120 IgA response in mammary gland in SIVagm infection compare to SIVmac infection which appear later and in less amount (Amos et al., 2013) (Zhang et al., 2016) (Amos et al., 2015). Furthermore, AGM gp120-specific monoclonal antibodies displayed also important CD4-dependent virion capture and ADCC activity (Zhang et al., 2016). When B cells were depleted during SIVagm infection, there was no increase in viremia, but an increase of SIV in the intestine (Gaufin et al., 2009). This result could suggest a possible contribution of B cells in viral control in the gut (Gaufin et al., 2009). Yet, *in vitro* neutralization assays showed that in SIVagm infection, similar to HIV-1 and SIVmac infections, there are only few or no detectable neutralizing antibodies (Norley et al., 1990) (Gicheru et al., 1999). Allover, the B cell function seems to be less or not disturbed in SIVagm infection in contrast to HIV-1/SIVmac infection. The B cells responses are though not efficient in controlling viremia or viral replication in the gut. Of note, natural hosts of SIV display very rare mother to child transmission in contract to HIV infection (Chahroudi et al., 2011). It has been suggested that the high levels of anti-SIVagm IgA in the breast milk reduce mother to child transmission in natural hosts (Permar et al., 2010). Other mechanisms to explain this low mother to child transmission rate in natural hosts are though not excluded (Pandrea et al., 2008b).

Impediment	Consequence
High degree of HIV diversity	Challenge for vaccine-induced immunity
Poor immunological access to conserved HIV Env regions	Few broadly reactive neutralizing antibodies
Delay in neutralizing antibody response	Virus dissemination
Rapid viral mutation rate and selection pressure	Virus escape
Paucity of virus-specific IgAs at mucosal sites	Virus dissemination
Polyclonal activation	Few specific antibodies of low specificity; few memory B cells
Natural antibodies cross-react with self antigens	Tolerance
Functional exhaustion of B cells	Few specific antibodies of low specificity
Paucity of IgM^+ memory B cells	Decreased natural immunity
Interference by Nef	Suppressed class switching

Table 5: Abnormalities in HIV infection impacting B-cell function. The original table was taken from (Moir and Fauci, 2009)**.**

6.2. NK CELLS

NK cells are one of the components of so-called "innate" immunity and are considered as short-lived effectors with a turnover time of approximatively 2 weeks, as compared to months or years for some T cell subsets. Upon activation, the canonical function of NK cells is cytolysis but they also display immunomodulatory role via the secretions of cytokines (pro- / anti-inflammatory) such as IFN-γ, TNF-α and IL-10. Their cytotoxic capacity was discovered in the 1960-70s. ADCC is another known mechanism by which NK cells recognize and lyse antibody-coated target cells, through the engagement of antibody binding to the Fc gamma receptors expressed at the surface of NK cell according to maturation step or/and functional diversity (CD16, CD32, CD64).

NK cells have the capacity to spontaneously lyse tumor or infected cells in the absence of specific prior stimulation. This property distinguishes them from cytotoxic $CD8^+$ T lymphocytes, which need prior stimulation. T cells recognize specific antigens through their TCR. It was considered for long time that NK cells act non-specifically. Indeed, NK receptor genes do not perform gene rearrangements, unlike genes encoding TCR or BCR. However, more recently it has been demonstrated that NK cells can acquire memory-like properties (Stary and Stary, 2020) (Paust et al., 2017) (Alter et al., 2011).

NK cell activity is directed by a dynamic balance between different activating and inhibiting signals transmitted by membrane receptors. The receptors transmitting activating or inhibiting signals recognize the ligand C-type lectin-like receptors, classical and non-classical molecules of MHC-I. They belong to three large families, C-type lectin-like receptors, KIR and CD94 / NKG2A-C (Abel et al., 2018). The receptors of the KIR family recognize conventional MHC molecules of class I (-A, -B and –C). The CD94 / NKG2A/C receptor recognizes the non-classical MHC-I molecule, such as MHC-E. Unlike CD94 / NKG2A, which generally transmits an inhibitory signal, the CD94 / NKG2C receptor transmits an activating message to the NK cell. In contact with normal cells, NK cells are inhibited in their cytotoxic and cytokine functions and induce tolerance: this is the "missing-self" mechanism (Kumar, 2018) (Carrillo-Bustamante et al., 2016). On the other hand, during stress (transformation or infection), the cells often lose the expression of the MHC class I and/or increase

unconventional MHC-I presenting stress peptides and this stimulates NK cell activity (Kraemer et al., 2015) (Kaiser et al., 2005).

Combinations of KIR and HLA molecules also play an essential role during NK cell education. For human NK cells, education occurs through several inhibitory receptor/ligand combinations, such as KIR3DL1/HLA-Bw4, KIR2DL2/3/HLA-C1, KIR2DL1/HLA-C2 and NKG2A/HLA-E (He and Tian, 2017).

6.2.1. NK CELLS IN TISSUES

NK cells represent 10 to 20% of the lymphocytes in the circulating blood. NK cells populate multiple tissue sites including LNs, liver, lung, skin, kidneys, gut, uterus and bone marrow. However, the distribution of NK cells varies according to the tissue. Thus, they are frequent in organs such as liver and uterus, but rare in mucosa and SLT. Human NK cells have been for long time subdivided into two major subpopulations based on CD56 and CD16 expression and profiles displaying distinct differentiation and functional properties. The $CD56^{dim}CD16^{+}$ NK cells are predominant in the blood, spleen, bone marrow and lung. They are cytolytic effector cells with cytotoxic mediator secretion, such as Granzymes and Perforin, also rapidly secreting pro-inflammatory cytokines, such as IFN-γ or TNF-α. The $CD56^{bright}CD16^{+}$ NK cells are predominant in LNs, tonsils and intestine. They display reduced lytic capacity, but increased immuno-regulatory functions through pro-inflammatory cytokines production, in particular following stimulation by IL-12 and IL-18 (Poli et al., 2009) (Amand et al., 2017). In Old World monkeys (which include natural hosts of SIV and macaques), NK cells have been generally defined as CD3– CD20−/dim CD8αα+ NKG2A/C+, because the antibody against CD56 does not stain for all NK cell subpopulations in non-human primates, while nearly all NK cells in monkeys express NKG2A/C (Mavilio et al., 2005a). NK cell diversity and function are only poorly described in Old world monkeys.

It has been thought that most of the NK cell diversity is genetically determined, but environmental factors such as vaccinations, infections and age also strongly and durably modify the NK cell phenotypes (Hazeldine and Lord, 2013) (Harris et al., 2020) (Strauss-Albee et al., 2014). In addition, tissue localization is a critical determinant for the NK cell phenotype and functions (Dogra et al., 2020a) (Freud et al., 2017). Precursor and immature NK cells showed tissue-resident signatures and tissue-specific properties in LN and intestine (Hashemi and Malarkannan, 2020). NK cells have been described to be able to mature inside LNs (Dogra et al., 2020a) (Huntington et al., 2007).

In the intestine, NK cells are found in lamina propria in the middle of epithelial cells as intraepithelial lymphocytes. Similarly, to the BCF in LNs, NK cells are rare or not present in intestine lymphoid follicles (Poggi et al., 2019). Peripheral blood (PB)-derived NK cells can migrate into intestine in response to inflammation. Some of PB-derived NK cells express CD161, an important marker of intestinal infiltration (Poggi et al., 2019). Effector mucosal NK cells are defined in Humans as CD3−CD56+CD16− and have an important role in the regulation of gut homeostasis (Ivanova et al., 2014) (Poggi et al., 2019). The production of IL-22 by mucosal NK cells is essential for modulating epithelial cells from intestine and to favor epithelial cell remodeling and survival (Poggi et al., 2019) (Qiu et al., 2017).

6.2.2. NK CELLS IN HIV/SIV INFECTIONS

The strength of KIR-HLA interactions has a functional significance and can influence the susceptibility to or the outcome of infectious diseases (Figure 8). For instance, genomic studies in PLWH have clearly revealed that NK cells impact viremia levels (Ramsuran et al., 2018). In long-term non-progressors and HIV controllers, the co-expression of KIR3DS1 and HLABw480I that bind KIR3DL1, correlates with lower viral load. High expression of KIR3DS1, KIR3DL1 or KIR3DH were associated with lower viral set points in the presence of their ligands. NK cells can mediate control of HIV by KIR2DL2 and KIR2DL3 expression via HLA-C interaction. Enhanced of KIR3DL04 or KIR3DH04 expression is also associated with decreased loss of CD4+ T cells (Lucar et al., 2019). Unfortunately, there are a lot of disparities between human and NHP KIR repertoires. For example, 22 different KIR genes have been described for rhesus macaques, and 15 KIR genes with 2 pseudogenes in humans. Macaques harbor a unique KIR (KIR1D), while showing high diversity in lineage II and III KIR genes (Manickam et al., 2019). In addition, the KIR locus in African monkeys has not been characterized. Moreover, antibodies against the different KIR receptors are lacking for NHP cells. All this makes the study of KIR in monkeys difficult so far.
HIV NEF mediates decrease of HLA-A and -B expression, while Vpu-mediates downregulation of HLA-C (Manickam et al., 2019). Thus, the ligands of KIR are decreased on HIV-infected cells. The Nef protein of SIV from natural hosts also down-regulates MHC-I (Schindler et al., 2006). The decrease of MHC-I molecules allows the infected cells to escape CD8+ T cell surveillance but in the same time, makes the cells more vulnerable to NK-cell mediated suppression that is triggered in the absence of inhibitory signals. It has been shown that KIR-positive NK cells can place immunological pressure on HIV-1. Indeed, evidence has been provided that HIV mutates to evade such NK-cell-mediated immune pressure, similar to what was previously described for virus-specific T cells and neutralizing antibodies. This is another demonstration that NK cells play an important role in HIV control (Alter et al., 2011).

In contrast to conventional MHC-I, the expression of MHC-E is increased during HIV infection (Jabri Bana et al., 2005). MHC-E is increased on infected cells but mostly on un-infected CD4+ T cells during HIV infection. Indeed, there is a high proportion of CD4+ T cells with increased MHC-E expression in PLWH (Martini et al., 2016). However, a recent study demonstrated that some wild-type HIV isolates can reduce MHC-E levels on infected CD4+ T cells by Nef viral protein activity principally. This study revealed that the capacity of MHC-E downregulation varies between HIV strains, some downregulating MHC-E, other strains up-regulating MHC-E (Thans et al., 2019).

The KIRs and NKG2A/C receptors recognize their cognate MHC-E ligands in a peptide-dependent manner. Peptides derived from HIV and SIV Gag have been shown to bind to MHC-E (Hansen et al., 2016) (Jabri Bana et al., 2005). Some studies showed that these HIV/SIV Gag peptides when presented by MHC-E inhibit NK cells (Jabri Bana et al., 2005).

MHC-E expression levels are also genetically determined and therefore vary between individuals. In steady-state, MHC-E present cellular peptides that derive from the leader sequence of conventional MHC-I molecules. Binding of these peptides stabilizes MHC-E at the cell surface. Therefore, a genetic background that leads to high MHC-A expression is associated with high MHC-E expression. It has been shown that individuals with a genetic background favorable for high levels of MHC-E

display higher viremia levels (Ramsuran et al., 2018). It is considered that the higher viremia levels are the result of the MHC-E mediated inhibition of NK cells (Ramsuran et al., 2018).

It is unclear through which suppressive mechanism NK cells impact HIV replication in vivo. In addition to the cytotoxic and immunomodulatory activities of NK cells, ADCC might play a role. It has been shown that combinations of three broadly neutralizing antibodies mediated >30% killing by ADCC of HIV-infected primary CD4+ T cells in presence of autologous NK cells (Tuyishime et al., 2020).

HIV-1/SIVmac infection however impairs normal NK cell function (Jost and Altfeld, 2012). In early HIV-1/SIVmac infection, NK cells are already dysfunctional (Mavilio et al., 2005b) (Giavedoni et al., 2000). NK cells are impaired in their ability to secrete IL-2, IFN-γ, and TNF-α (LaBonte et al., 2006). They have been reported to significantly downregulate of NKG2C expression in blood of SIV-infected macaques (LaBonte et al., 2006). This impairment in NK cells could be due to the direct effect of HIV, CD4 or DC dysfunction and/or the effect of cytokine milieu on NKp30 and NKG2D expression (Altfeld et al., 2011) (Manickam et al., 2019). Some studies suggested an impact of HIV on NK cell education dysfunction (Ramsuran et al., 2018) (Kiani et al., 2019) (Kristensen et al., 2018). HIV-1/SIVmac infection also disrupt the overall homeostatic NK cell distribution in tissues. Thus, upon pathogenic infection, NK cells are directed to the mucosa (Mikulak et al., 2017), while there is a lack of functional NK cells in LN during HIV-1/SIVmac infections (Mikulak et al., 2017) (Schafer et al., 2015a). Conventional NK cells present in the gut produce IFN-γ in response to IL-12. Mucosal NK cells also produce IL-22 in response to IL-23. A study showed that IL-22 secretion by mucosal NKp44+ NK cells decreased in chronic SIVmac infection (Reeves et al., 2011). There was a positive correlation between mucosal intraepithelial lymphocytes NK cells and CD4+ T cells in the periphery in HIV chronic infection (Sips et al., 2012a). The authors also reported that persistent expansion of mucosal intraepithelial NK lymphocytes in the intestine was present in HIV controllers and linked with a protective KIR3DS1/L1-Bw4genotype (Jiang et al., 2013). Additionally, a significant increase of KIR3DL1+ NK cells in the intestine was detected during acute and chronic SIVmac infection, but an upregulation of KIR3DL1+ NK cell proliferation and activation was observed only in the acute phase (Ries et al., 2017).

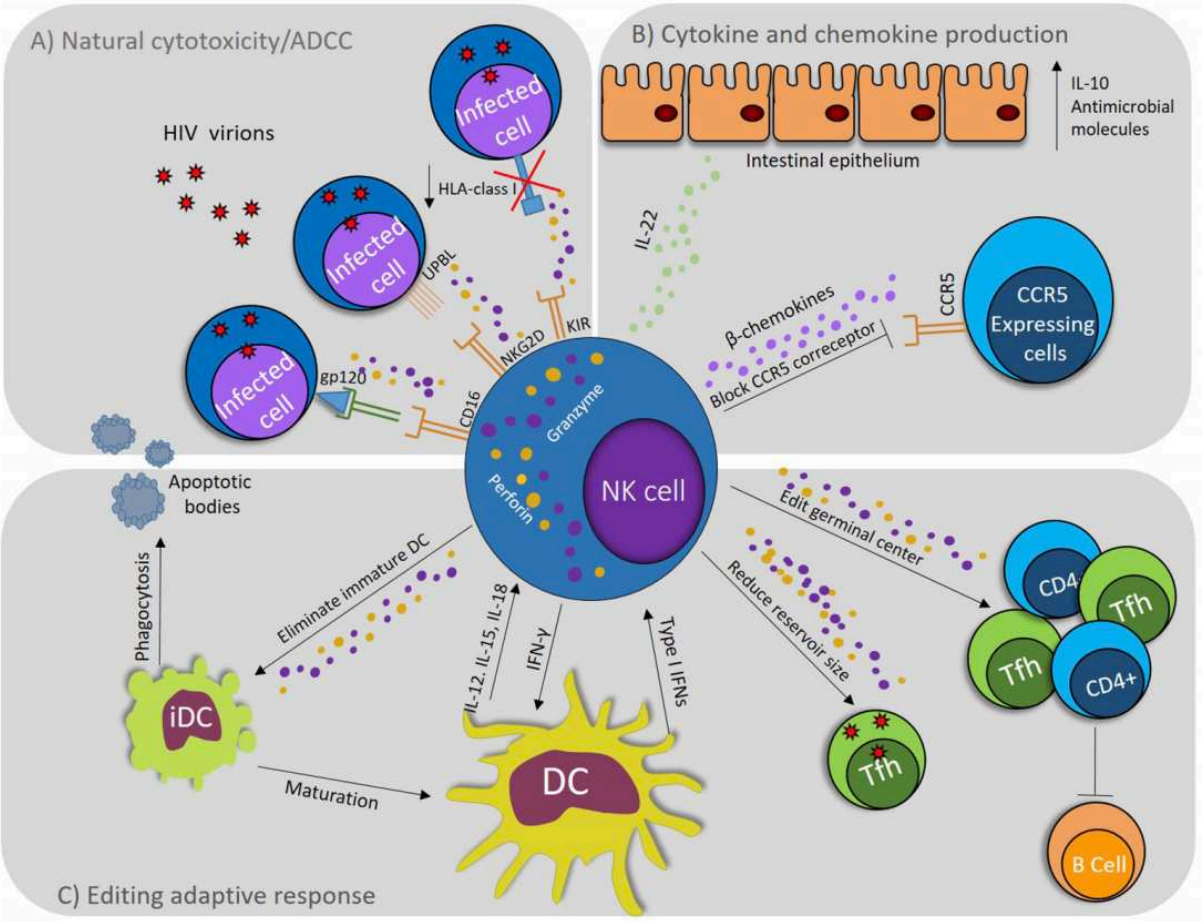


Figure 9: Multiple facets of NK cell in HIV-1 infection. **(A)** Cytotoxic NK cells response to via favoring of activator signals or downregulation of inhibitor signals. **(B)** Cytokine NK cells production, like IL-22 or β-chemokines. **(C)** Crosstalk mechanism between immature DC and NK cell. NK cells indirect impact on humoral response, via Tfh potential elimination. Taken from (Flórez-Álvarez et al., 2018).

In natural hosts of SIV, studies on NK cells are limited. The few reports that exist indicate a strong increase of NK cell activation and proliferation early on after SIVsm and SIVagm infection in respectively sooty mangabey and AGMs (Jacquelin et al., 2014) (Pereira et al., 2008). The NK cells detected in LN did not produce IFN-γ but had a high cytotoxic potential (Jacquelin et al., 2014) (Pereira et al., 2008). Their cytotoxic potential in LNs was stronger than in blood during SIVagm infection, which was counterintuitive since at steady-state, the LNs contains more cytokine-producing and less cytotoxic NK cells that the blood. The rapid and strong increase of NK cell proliferation and cytotoxicity in SIVagm infection was associated with plasma IFN-α and IL-15 levels (Jacquelin et al., 2014). It is known that that IL-15 and IFN-α stimulate the cytotoxicity activity and/or proliferation in NK cell population (Choi et al., 2004) (Madera et al., 2016). It is possible that natural hosts over evolution kept their capacity to produce high levels of IFN-α very early after SIV infection in order to stimulate NK cells. During chronic SIVagm infection, NK cells accumulate in BCF (Huot et al., 2017). It has been shown that the NK cells are responsible for the strong viral control in the BCF and in the T zone of LNs during chronic SIVagm infection (Huot et al., 2017).

6.3. NKG2A$^+$ CD8$^+$ T CELLS

CD8+ T cells can up-regulate NK cell receptors, such as NKG2A (Figure 9). The CD94/NKG2A heterodimer is expressed by NK cells and by a small fraction of activated CD8+ T lymphocytes. MHC-E bound peptides can be recognized by CD94/NKG2A/C on NK cells but also by NKG2A or TCR on CD8+T cells (Joosten et al., 2016). When the TCR engages an interaction with the MHC-E–peptide complex, that leads to activation and expansion of antigen-specific CD8+ T cells, while engagement of the CD94/NKG2A receptor expressed by CD8+ T cells generally attenuates the activities of these cells, similarly to NK cells (Kim and Cantor, 2011) (Stocks et al., 2017).

As mentioned above, MHC-E generally charges a nonamer peptide derived from the leader sequence of conventional MHC-I. However, MHC-E can also charge peptides derived from a stress protein, such as Hsp60. Hsp60 is capable of competing with the self-peptide. While the binding of peptides derived from MHC-I protects cells against their destruction, the presentation of the peptide derived from Hsp60 by MHC-E makes the cell sensitive to cell lysis by NK cells and by NKG2A+ expressing CD8$^+$ T cells because the HSP60 signal peptide is no longer recognized by the CD94/NKG2A inhibitory receptor (Michaëlsson et al., 2002) (Joosten et al., 2016).

MHC-E-restricted CD8$^+$ T cells have been described to play an important role in maintaining self-tolerance and preventing autoimmune diseases as shown in mouse models. Indeed, MHC-E-restricted CD8$^+$ T cells have been mainly studied in mice, where the Qa-1 molecule is the equivalent of MHC-E (Michaëlsson et al., 2002) (Shamaei-Tousi et al., 2006) (Jiang et al., 2010).

6.3.1. NKG2A+ CD8$^+$ T CELL FUNCTIONS

Interestingly, MHC-E bound peptides can be recognized either by the TCR on CD8+ T cells and/or by NKG2A/CD94 on NK and NKG2A$^+$CD8$^+$T cells (Joosten et al., 2016). When TCR engage an interaction with MHC-E–peptide that leads to activation and expansion of antigen-specific CD8$^+$ T cells, while engagement of the CD94/NKG2A receptor expressed by CD8$^+$ T attenuates the activities of these cells, as NK cells (Kim and Cantor, 2011) (Stocks et al., 2017). MHC-E is able to be charged by signal peptide derived from the leader sequence of a stress protein, such as Hsp60, is capable of competing with the self-peptide, which is the peptide derived from MHC-Ia. While the binding of peptides derived from MHC-I to MHC-E protects cells against their destruction, the presentation of the peptide derived from Hsp60 by MHC-E makes the cell sensitive to cell lysis by CD8$^+$ T cells restricted to MHC-E. (Michaëlsson et al., 2002). MHC-E-restricted CD8$^+$ T cells have already described such as important role in maintaining self-tolerance and preventing autoimmune diseases or cancer as shown in mouse models. Thus MHC-E-restricted CD8$^+$ T cells found in lung, blood or gut (Shamaei-Tousi et al., 2006) (Jiang et al., 2010) (Bhagat et al., 2008). NKG2A$^+$CD8$^+$ T population is defined by several receptor TCRgamma/delta, TCRalpha/beta, KIR, IL-15R, IL-12R, IL-18R, CD56, CD57, CD45RA expression in human or mice (Bhagat et al., 2008) (Uhrberg et al., 2001) (Barbarin et al., 2017). But their function associated stay few known, indeed it was observed an anticancer potential activity (Jiang et al., 2010) (Bhagat et al., 2008), an effector and proliferative responses in the case of virus persistence (Cush and Flaño, 2011), or could be representative marker of exhausted CD8$^+$ T cell population (Chen et al., 2020) (Rapaport et al., 2015).

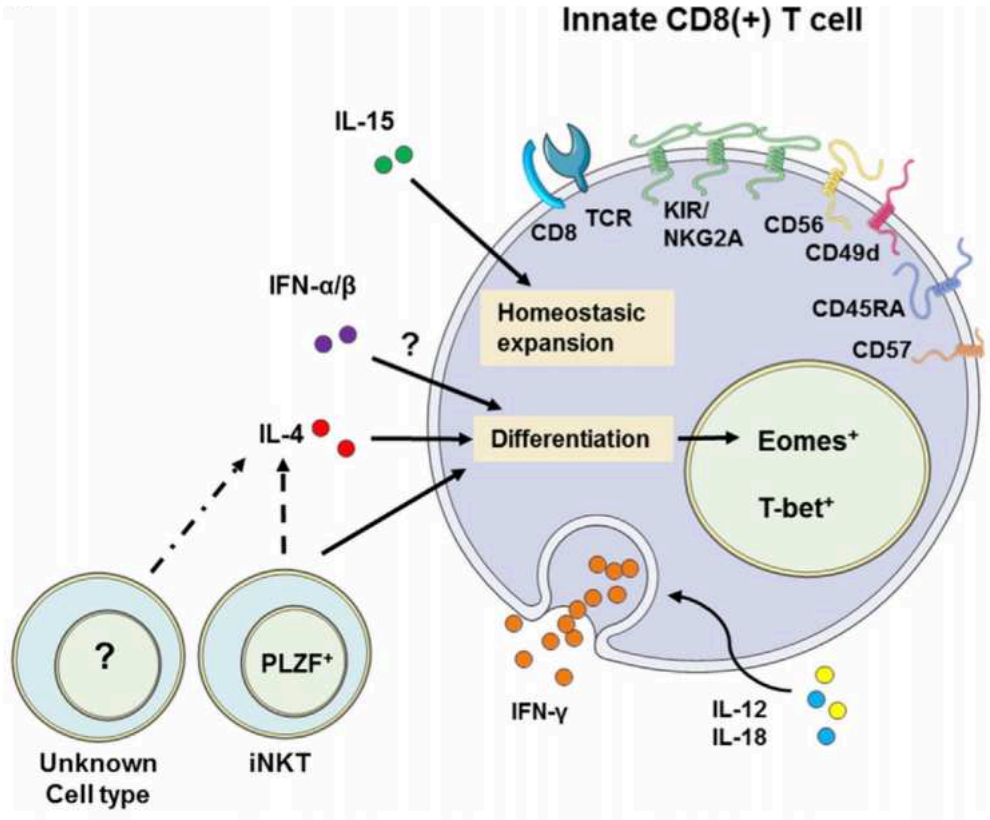


Figure 10: The NKG2A^{+} CD8^{+} T cells (also named innate CD8^{+} T cells) characterize in humans. The different receptors and transcription factors are represented, as defining this new unique population. This CD8^{+} T cell population in humans are susceptible to several cytokines such as IL-12, IL-18, IL-15 or IL-4. Adapted from (Barbarin et al., 2017).

6.3.2. NKG2A+ CD8 T CELLS IN HIV/SIV INFECTIONS

Hsp60 protein might be incorporated into HIV and SIV particles (Bartz et al., 1994). Hsp60 plasmatic levels correlated with viral load, circulating sCD14 and LPS plasmatic levels (Anraku et al., 2012) (d'Ettorre et al., 2017). Moreover, Hsp60 plasmatic levels in PLWH with ART remained higher than non-infected people. A study showed an improvement of mitochondrial morphology sustained in intraepithelial cells (IEC) and enterocyte by an observation of intracellular reduction of Hsp60 in PLWH with ART (d'Ettorre et al., 2017). The IEC has been proposed to act as a non-professional APC. In particular, the surface IEC expresses the MHC-E protein, while the cryptic cells express less or no unconventional MHC I molecules (Perera et al., 2007).

Tumors can display increased levels of MHC-E which is considered to inhibit immuno-surveillance by NK cells and may be also by CD94/NKG2A+ CD8+ T cells (Zeddou et al., 2007) (Gooden et al., 2011) (van Montfoort et al., 2018). In HIV-1 infection, MHC-E is also up-regulated on infected and uninfected cells, as mentioned above (section 6.2.2). The surface expression of CD94/NKG2A was increased on HIV-specific CD8+ T cells and has been suggested to inhibit efficient lysis of infected cells (Maria et al., 1997) (Thimme et al., 2005). Other studies though showed normal or low expression of inhibitory receptors such as CD94/NKG2A on HIV-specific CD8+ T cells (Costa et al., 2003). When analyzing the total CD8+T cells in blood of PLWH, a downregulation of the CD94/NKG2A inhibitory CD8+ T cells was observed (Zeddou et al., 2007). This decrease of

CD94/NKG2A expression was more pronounced in viremic patients than in patients with less than 50 copies/ml of viral RNA. No significant difference was detected in the proportion of CD8+ T lymphocytes expressing the activator CD94/NKG2C heterodimer (Zeddou et al., 2007).

Vaccination of macaques with a Gag-expressing CMV vector, revealed a strong, protective response of MHC-E restricted CD8 + T cells in half of the animals (Okoye et al., 2018) (Hansen et al., 2016). The Gag antigen-recognition by these cells was attributed mostly to the TCR and not to NKG2A/C (Früh and Picker, 2017) (Hansen et al., 2016) (Okoye et al., 2018). The plasmatic levels of Hsp60 are elevated in HIV-infected patients, with levels significantly reduced after cART, but still higher than those in HIV-negative individuals (Anraku et al., 2012). it is unclear if more cells are lysed in PLWH due to higher expression levels of Hsp60.

Natural hosts do not display strong SIV-specific CD8+ T cell responses (Zahn et al., 2008) (Reina et al., 2009). The CD8+ T cells expressing inhibitory NK cell receptors have not been studied to our knowledge. Even if CD8+ T cell responses most likely do not play a role in SIV control in natural hosts, a role of NKG2A+ CD8+ T cells in the regulation of immune activation in tissues during HIV/SIV infections is not excluded.

PART II. HYPOTHESES and OBJECTIVES

Antiretroviral therapy does not eradicate HIV from the infected person's body. The virus persists in anatomical sanctuaries and reservoir cells, such as in follicular helper T (T_{FH}) cells within the BCF of lymph nodes. This viral persistence is associated with several immune deregulations such as residual chronic inflammation, hypergammaglobulinemia and disorganization of the FDC network. SIVmac infection in the macaque summarizes the pathophysiology of HIV-1 infection in humans. In contrast, SIV infection in natural hosts, such as SIVagm infection in the AGM is non-pathogenic, despite a persistently high viremia. During infection with SIVagm, there is no systemic chronic inflammation, no disruption of the intestinal barrier and viral replication is strongly controlled in SLTs. The lab has recently shown that this strong, tissue-specific viral control in SIVagm-infected AGMs is mediated by NK cells.

Natural hosts for SIV are considered as an excellent model for studying the mechanism of protection against chronic inflammation and microbial translocation.
They are generally not supposed to be a model that could contribute in the search for a cure of HIV. This is due to the high viremia levels characterizing SIV infection in natural hosts. Such high viremia levels cannot be tolerated in humans because of the high risk of transmission. However, we propose that natural hosts can in addition also be an excellent model also for HIV cure research because of their peculiar strong viral control in SLTs, and in particular in BCF, which constitutes a sanctuary for HIV even in long-term treated people living with HIV.

The aims of my thesis work are elaborated as follows:

1) How do NK cells acquire the capacity to migrate into BCF? And why do their numbers increase in BCF during SIVagm infection allowing their long-term accumulation in BCFs?

2) How do NK cells control SIVagm infection in T_{FH} cells of SLT? What is the underlying mechanism and which NK cell subset(s) and target cell receptors are involved in the control?

3) What are the consequences of viral control and of NK cells present in BCF, respectively, on systemic inflammation profiles and B cell responses? Do NK cells also migrate into BCF of SLT associated to the intestinal mucosa, such as mesenteric LN, and what is the consequence of it?

4) Since there is no strong viral control in the intestine during SIVagm infection, similar to HIV-infected humans, could cells expressing NK cell receptors still be involved in the regulation of inflammation in the intestine in SIVagm infection?

PART III: RESULTS

1. NK cells migrate into and control SIV replication in lymph node follicles in African green monkeys

NK cells migrate into and control SIV replication in lymph node follicles in African green monkeys

Nicolas HUOt[1,2], Beatrice JACQUELIN[1], Thalia GARCIA-TELLEZ[1], Philippe RASCLE[1,2,3], Mickaël J PLOQUIN[1], Yoann MADEC[4], R Keith REEVES[5], Nathalie DERREUDRE-BOSQUET[6] & Michaela MÜLLER-TRUTWIN[1,2]

[1]Institut Pasteur, HIV, Inflammation and Persistence Unit, Paris, France; [2]Vaccine Research Institute, Créteil, France; [3]Université Paris Diderot, Sorbonne Paris Cité, Paris, France ; [4]Institut Pasteur, Epidemiology Unit, Paris, France; [5]Center for Virology and Vaccine Research, BIDMC, Harvard Medical School, Boston, MA, USA; [6]CEA-Université Paris Sud 11 INSERM U1184, Immunology of Viral Infections and Autoimmune Diseases (IMVA), IBJF, IDMIT Department, Fontenay-aux-Roses, France.

Keywords: NK cells, SIV, HIV, non-human primates, IL-15, CXCR5, lymph node, spleen, B cell follicles, natural hosts, viral reservoir

Corresponding author: Michaela Müller-Trutwin
Institut Pasteur
HIV, Inflammation and Persistence Unit
28 rue du Dr Roux
75015 Paris, France
mmuller@pasteur.fr

DOI: 10.1038/nm.4421

Abstract

Natural Killer (NK) cells play an essential role in anti-viral immunity, but knowledge of their function in secondary lymphoid organs is incomplete. Lymph node follicles constitute a major viral reservoir during HIV-1 and SIVmac infections. In contrast, during non-pathogenic SIVagm infection of African green monkeys (AGM), follicles remain generally virus-free. We show that NK cells in secondary lymphoid organs from chronically SIVagm-infected AGM were frequently $CXCR5^+$ and entered and persisted in lymph node follicles throughout the follow-up (240 days post-infection). These follicles were strongly positive for IL-15, which was primarily presented in its membrane-bound form by follicular dendritic cells. Anti-IL-15-induced NK cell-depletion during chronic SIVagm infection resulted in high viral replication (follicles and T zone) and viral DNA increase in lymph nodes. Our data reveal that in non-pathogenic SIV infection, NK cells migrate into follicles and play a major role for viral reservoir control in lymph nodes.

The persistence of Human immunodeficiency virus (HIV) in individuals treated efficiently with combined antiretroviral therapy (cART) remains a tremendous obstacle to achieving sustained virologic remission in HIV-infected individuals[1]. A major anatomical HIV reservoir are lymph nodes (LN)[2,3]. Studies in the non-human primate model for HIV, macaques (MAC) infected by SIVmac, showed that during the first weeks post-infection (p.i.), the virus replicates solely in the T cell zone of LNs[4]. Only later on the virus spreads to B cell follicles, where it replicates to a large extent in follicular helper T cells (T_{FH})[5–9]. Moreover, numerous viral particles are trapped by follicular dendritic cells (FDC) and remain infectious[10]. Finally, in chronic infection, more virus is present in follicles than in the T zone[11,12]. In HIV controllers, the virus also persists preferentially in these LN follicles and productive infection is markedly restricted to T_{FH} cells[13]. Follicles thus seem to constitute 'sanctuaries' for persistent viral replication even in HIV controllers who are capable of developing potent anti-viral $CD8^+$ T cell responses[13]. Indeed, B cell follicles are mostly devoid of $CD8^+$ T cells except for the rare follicular cytotoxic T cells[14]. In patients under long-term cART, T_{FH} cells equally represent the major viral reservoir, potentially complicating efforts to cure HIV infection with T cell immunotherapy[15,16].

NK cells play an essential role in viral infections[17,18]. Little attention has however been given to them in LN as their frequency is low in these tissues in contrast to other body compartments, such as liver or uterus[19]. In rodent LN, NK cells are more dense in the medulla than in T or B cell areas and they are mainly located within lymphatic sinuses[20,21]. Upon immunization or viral challenge in rodents, NK cells infiltrate draining LNs[22,23]. Little information is available regarding the trafficking of NK cells to LN during viral infections in humans and on NK cell migratory behavior within LN in general. During HIV-1 or SIVmac infections, LN display limited recruitment of NK cells that instead seems to be deviated toward the intestinal mucosa, and therefore provide a niche where the virus can replicate unabated by early NK-cell-mediated innate pressure[24,25].

Non-human primates from Africa, such as African Green monkeys (AGM), are natural hosts of SIV[25]. They usually do not experience disease progression, despite displaying high viremia and high viral replication in the intestine concomitant with massive acute depletion of mucosal $CD4^+$ T cells[26]. A major distinction of SIV infection in natural hosts is the rapid resolution of viral inflammation and the lack of microbial translocation[3,25]. In addition, AGM display a rapid control of viral replication in the secondary lymphoid organs and lack of viral trapping by FDC in follicles[27–33]. Another natural host of SIV, the sooty mangabey, also showed strong viral control in LN[6,34].

In AGM, most pro-inflammatory cytokines such as TNF-α, IL-6, IFN-γ and IL-8 are not or only weakly induced upon SIV infection[25]. However, AGM display high plasma levels of IFN-α and IL-15

during acute infection[35]. IL-15 is well known to promote mobilization and homeostatic proliferation of T cells and to be essential for the survival of NK cells[36,37]. Moroever, IL-15 contributes to the preservation of cytotoxic $CD8^+$T cells and also enhances NK cell suppressor function [38]. We have observed increases in NK cell proliferation as well as of $CD107a^+$ NK cells in peripheral LN during acute SIVagm infection[35]. We therefore raised the question whether NK cells play a role during non-pathogenic SIV infection in LN. Here we demonstrate that NK cells accumulate in a CXCR5- and IL-15-dependent manner in follicles of secondary lymphoid organs in SIV-infected AGM and exert efficient control of viral replication within LN contributing to a low viral reservoir in these organs.

RESULTS

Lack of virus in lymph node follicles during non-pathogenic SIV infection

We first determined the level and distribution of virus in LN of six AGM and six MAC infected with SIVagm.sab92018 and SIVmac251, respectively. Plasma viral RNA copies were always at least as high in AGM as in MAC (Supplementary Fig.1a-c). The viremia peak was reached around day 9 p.i. for all animals. The quantification of the cell-associated (ca) viral RNA and ca-viral DNA copy numbers in LN cells showed similar high levels for both SIVagm and SIVmac infections at peak viremia (Fig.1a and Supplementary Fig.1d). However, a strong decrease was observed after the viral peak in AGM LN ($p=0.001$). This viral control in AGM LN resulted in a strong difference compared to SIVmac infection, as the median quantity of ca-viral RNA and DNA in LN were, respectively, 2.5 log and 1.5 log lower in AGM than MAC during the chronic phase (Fig.1a and Supplementary Fig.1d). *In situ* evaluation of viral RNA showed indeed a dramatic decrease of productively infected cells in the T zone of AGM LN during the chronic phase of infection and a constant absence of productively infected cells within the follicles of AGM throughout the follow-up (240 days p.i.) (Fig.1b,c). These results contrast with SIVmac infection where, as expected, large amounts of viral RNA were detected both in the T zone and within follicles during chronic infection throughout the follow-up (Fig.1b,c).

Accumulation of NK cells in lymph node follicles during non-pathogenic SIV infection

NK cells were gated as previously reported (Supplementary Fig.2)[35,39]. A progressive and persistent reduction in the frequency of LN NK cells was observed during chronic infection as compared to pre-infection levels in the pathogenic model ($p<0.001$), but not in AGMs where, after a transient decline, NK cells recovered to pre-infection levels ($p=0.8$) (Fig.1d). The decrease in MAC was due to a decline of the major NK cell population in LN (i.e. $CD16^-$ NK cells), while, as in a previous report in

macaque LN[39], there was an increase in CD16$^+$ NK cells in SIVmac infection ($p<0.001$) (Fig.1g).
Evaluation of NK cell distribution *in situ* showed that in uninfected animals, NK cells were localized as expected in the marginal and parafollicular zone in both species (Supplementary Fig.3a). The localization of NK cells however changed dramatically in response to SIV infection. Indeed, many NK cells were found outside the marginal zones following SIV infection in both species (Supplementary Fig.3b+c). Of note, the distribution became highly distinct between pathogenic and non-pathogenic SIV infection. In SIV-infected AGM, NK cells were mostly found around or within follicles (Fig.1e,f and Supplementary Fig.3b), whereas MAC NK cells followed a random distribution within the LN after SIV infection and did not accumulate in follicles (Fig.1e,f and Supplementary Fig.3c). The total numbers of NK cells decreased in the T cell zone in both species after SIV infection. In contrast, NK cell numbers increased in follicles of AGM (Fig.1h).
These analyses reveal that NK cell distribution within LN changes significantly in response to SIV infection and differently between pathogenic and non-pathogenic infections. Moreover, the study in the non-pathogenic SIV infection uncovers that NK cells are able to migrate into follicles.

Decreases in LN homing receptors on NK cells in both pathogenic and non-pathogenic SIV infection

Since MAC showed persistently decreased NK cell levels in contrast to AGM, we wondered whether AGM NK cells have a better LN homing capacity than MAC during SIV infection. We examined the expression of major LN homing markers for NK cells (CCR7, CD62L, CX3CR1 and CXCR3). No significant changes as compared to pre-infection levels were detected on total peripheral blood NK cells for both species (Supplementary Fig.4a+b), while CD16$^-$ NK cells displayed decreases in CXCR3 and CX3CR1 (Supplementary Fig.5a+b).
In LN, the frequencies of NK cells expressing CCR7, CD62L or CX3CR1 were markedly down-regulated in both pathogenic and non-pathogenic SIV infections (Supplementary Fig.4). The decreases were again more pronounced in the CD16$^-$ than in the CD16$^+$ subsets (Supplementary Fig.5).
Altogether, strong decreases of homing receptors were observed for both species, in particular for CD16$^-$ NK cells. The homing receptor profiles were in most tissues similar between AGM and MAC and do not clearly explain the differences in NK cell levels in LN between AGM and MAC.

AGM NK cells express CXCR5 in secondary lymphoid organs during SIV infection

The preferential localization of NK cells in follicles during non-pathogenic SIV infection could be due to specific trafficking towards follicles and/or to an enhanced survival inside the follicles. In order to

address the hypothesis of specific trafficking, we measured the expression of CXCR5 on NK cells. CXCR5 is known to be both necessary and sufficient for B and T_{FH} cell migration into follicles[40,41]. We compared the level of CXCR5 expression on B cells, $CD8^+$ T cells and NK cells of LN from chronically infected animals (Fig.2a). As expected, the majority and minority of B and $CD8^+$T cells, respectively, expressed CXCR5 (Fig.2a,b). The frequencies of $CXCR5^+$NK cells were also low for MAC NK cells but, surprisingly, were elevated in AGM (Fig.2a,b). In contrast to spleen and LN, the levels of $CXCR5^+$NK cells were similarly low in AGM and MAC in blood and gut (jejunum, colon) (Fig.2b).

Thus we have identified high levels of $CXCR5^+$NK cells in LN of SIVagm-infected AGM. CXCR5 expression on AGM NK cells most likely allows their access to lymphoid tissue follicles.

Elevated frequencies of $CD107a^+$ and $CD32^+CXCR5^+$NK cells in secondary lymphoid organs during non-pathogenic SIVagm infection

We wondered whether these $CXCR5^+$NK cells could exert a suppressor function and characterized their functional phenotype. Major differences were observed between $CXCR5^+$ and $CXCR5^-$ NK cells in LN from SIV-infected AGM. Indeed $CXCR5^+$NK cells expressed more frequently CD69, CD16, CD107a and the Fcγ receptor CD32 and more rarely NKG2D and NKp46 (Fig.2 c,d). These cells might thus possess both an ADCC as well as cytoxic activity. The majority of $CXCR5^+$NK cells (median 60%) were $CD16^+$ (*not shown*). $CXCR5^+$ NK cells were also more often $PD\text{-}1^+$ than $CXCR5^-$ NK cells (Fig.2d), which might be associated with their location in follicles.

We wondered whether these results are representative of other secondary lymphoid organs and analyzed spleen NK cells from 10 AGM and 10 MAC in chronic infection (Fig.3). First we quantified the ca-viral RNA and DNA loads in spleen. As in LN, they were significantly lower in AGM than in MAC (Fig.3a). The viral DNA levels were negatively correlated with NK cell levels in AGM but not in MAC (Fig.3c). As in LN, NK cell frequencies in spleen were higher in SIVagm than in SIVmac infection (Fig.3d). The frequency of $CXCR5^+$NK cells in spleen was again significantly higher in AGM than in MAC, while the $CXCR5^+CD8^+$T cell frequencies were similar between the two species (Fig.3b,e). The major phenotypic difference between spleen $CXR5^+$NK and $CXCR5^-$NK cells consisted in the higher levels of cells positive for $CD107A^+$ and $CD32^+$ (Fig.3f). Also similar to LN, spleen $CXCR5^+$NK cells were more often $PD\text{-}1^+$ and less often $NKp46^+$.

We then compared the NK cell phenotypes between AGM and MAC in LN and spleen. Since $CXCR5^+$NK cells are rare in MAC, we compared total NK cells consisting in the majority of $CXCR5^-$ NK cells. No significant differences in the phenotype of these cells were observed between AGM and

MAC, except that total NK cells from AGM in spleen were more frequently $CD32^+$ than in MAC but the difference was weaker than for $CXCR5^+$NK cells and was not observed in LN (Fig.2e and Fig.3g). Altogether, we observed elevated levels of $CXCR5^+$NK cells expressing $CD32^+$ and $CD107a^+$ in secondary lymphoid organs from SIVagm-infected AGM.

Follicles of AGM lymph nodes constitute a niche for trans-presentation of IL-15

Since NK cell numbers increased in follicles during SIVagm infection without clearly showing a better homing receptor expression profile than in macaques, we wondered whether additional mechanisms, such as *in situ* proliferation or increased survival, participate in the accumulation of NK cells in follicles during SIVagm infection. The levels of NK cell proliferation in LN, as measured by Ki-67 staining, were not higher during SIVagm than SIVmac infection (*not shown*). Because IL-15 is essential for NK cell survival, we studied IL-15 production and distribution in LN in response to SIV infection. We detected IL-15 in LN during both infections, but IL-15 production was significantly higher in chronically infected AGM than MAC (Fig.4a,b and Supplementary Fig.6). In addition, it was primarily limited to follicles, whereas in MAC the production was diffuse (Fig.4b and Supplementary Fig.6). Remarkably, we observed NK cells in AGM follicles most often only if the follicles were IL-15 positive (Fig.4d).

To identify the cellular source of IL-15 in the follicles, we examined the *ex vivo* expression of IL-15 in distinct hematopoietic and stromal cell subpopulations from the LN of infected animals. The gating was performed in such a way as to allow the identification of as many as seven distinct cell populations (Supplementary Fig.7a). We did not detect significant Il-15 production by intracellular staining even if the cells were stimulated with PMA/Ionomycin (*data not shown*). Since intracellular detection of cytokines by flow cytometry was probably not sensitive enough, we evaluated *IL-15* mRNA *in situ* expression by FISH. Expression of *IL-15* mRNA was higher in AGM than in MAC LN (Fig.4e). Moreover, *IL-15* mRNA was expressed predominantly within follicles during SIVagm infection. Many mRNA-positive cells had dendritic-like shape and might thus correspond to FDC and/or dendritic cells located within the follicles.

IL-15 is particularly potent for stimulating immune responses if presented membrane-bound. We therefore co-stained the hematopoietic and stromal cell subpopulations for IL-15 and IL-15Rα surface expression (Supplementary Fig.7). Most of the cells that presented membrane-bound IL-15 (mbIL-15; i.e. $IL\text{-}15^+IL\text{-}15R\alpha^+$ cells) corresponded to APC-like cells ($CD3^-CD4^+$) and stromal cells, including follicular dendritic cells (FDC). The most pronounced difference in the levels of mbIL-15 between AGM and MAC was observed for FDC (Fig.4c).

We next addressed the question whether distinct levels of IL-15Rα between AGM and MAC could explain these profiles. IL-15Rα expression was measured on the same cell populations as above. The percentages of IL-15Rα$^+$ cells were highest for FDC, while the mean intensities of expression were highest on APC-like cells (CD3$^-$CD4$^+$) and FDC (Supplementary Fig.7b,c). This was the case for both AGM and macaques. Thus the IL-15Rα expression levels were not responsible for higher levels of mbIL-15 in AGM.

Altogether, NK cell accumulation in follicles during non-pathogenic SIVagm infection was associated with the presence of high levels of IL-15. IL-15 was produced within the follicles and presented membrane-bound, in particular on FDC.

Anti-IL15 treatment of SIVagm-infected AGM induces NK cell depletion

A major question is if NK cells in AGM LN have a crucial impact on viral load. We therefore aimed to deplete NK cells *in vivo* in AGM. While there is presently no antibody specific for NK cells in primates, it has been recently reported that anti-IL-15 treatment preferentially and dramatically depletes NK cells in MAC[36]. We treated five chronically infected AGM with this anti-IL-15 mAb using the same doses as previously described for MAC for a short period (2 weeks) (Fig.5a).

Blood NK cells were rapidly depleted (Fig.5b,c). The nadir was observed in 3 animals at day 7 post-treatment and for the two others at day 14. The latter two animals had higher NK cells at baseline. The levels remained low until autopsy at day 42 post-treatment. In contrast, the percentages of total blood CD4$^+$ T cells showed only a slight, transient increase ($p=0.043$) and the absolute CD4$^+$ T cell counts did not show any significant changes ($p=0.21$) (Fig.5d). The transient increases of CD4$^+$ T cells might be explained by strong proliferation at days 7 and 14 (Fig.5f). Blood CD8$^+$ T cell counts displayed a decrease that was mostly due to depletion of effector memory T cells (Fig.5e).

Anti-IL-15 depleted NK cells in all analyzed tissues, i.e. in LN, spleen and gut (Fig.5b and Supplementary Fig.8). In contrast to NK cells, the CD4$^+$ and CD8$^+$ T cell frequencies in LN were not different between day 0 and day 42 post-treatment (Fig.5g,h), with two exceptions. The frequencies of central memory CD4$^+$ and effector memory CD8$^+$ T cells were decreased in LN at days 21 and 42 post-treatment (Fig.5i,k).

Altogether, we show that anti-IL15 treatment induces a marked depletion of NK cells in SIVagm infected AGM in blood and tissues, including LN.

NK cell depletion during SIVagm infection leads to high viral replication in lymph nodes

We quantified the viral load in the anti-IL-15 treated animals. The viremia levels significantly increased and reached a median plateau around 10^5 viral RNA copies/ml at day 14 post-treatment (Fig.6a). Notably, in LN, both the ca-viral RNA and DNA were significantly increased (Fig.6b). *In situ* hybridization at days 21 and 42 post-treatment revealed many viral RNA-positive cells in LN of all treated animals (Fig.6c) and large foci of viral RNA-positive cells were detected in the T zone and within follicles. The increase in viremia in the blood of the anti-IL-15 treated animals is most likely the result of this increase in viral replication in the lymph nodes. There was no statistically significant correlation between the cell-associated vRNA or vDNA levels in LN and the proliferation (Ki-67) of total, naïve or or naïve, memory or effector $CD8^+$ T cells in LN. This is the first time that a high number of SIV-infected cells are observed within follicles of AGM.

DISCUSSION

We present here the first documented evidence for a distinct anatomical location of NK cells in response to a lentiviral infection within LN in any species. Previous studies in mice have shown, that infections by *L. major* induce NK cells to be recruited to the paracortex[20]. Similarly, we show that NK cells are recruited to the paracortex in response to SIV infection, but in addition we demonstrate here that NK cells can also accumulate around and within follicles of peripheral LNs in SIV-infected AGMs. This is an important observation, because it suggests the potential of NK cells to interact directly with other cells present in LN follicles, such as B cells and T_{FH} cells. It has been shown in murine models that NK cells can influence T_{FH} and germinal center B-cell responses[42–45]. Our results highlight the need for further studies on the effects of viral infections and vaccination on NK cell-B cell interactions and antibody responses, and on the potential role of NK cell localization within follicles in mediating these responses.

In contrast to B and T cells, the mechanisms governing NK cell trafficking remain poorly dissected. In this study, we correlated the capacity of NK cells to migrate into the follicles with CXCR5 expression. Moreover, we show that IL-15, a NK survival molecule, was found at high levels in follicles of SIVagm-infected AGM. IL-15 expression has been recently reported in LN of HIV-infected individuals, but only in the T zone[46]. We have shown that IL-15 is produced within follicles and presented as membrane-bound in particular by FDC, but also by APC-like cells during SIVagm infection. This finding agrees with previous reports showing that human APC and FDC can present mbIL-15[47,48]. The IL-15-mediated promotion of NK cell survival would then result in the

accumulation of these cells in a critical region of the LN. These results support previous reports suggesting the existence of *in situ* differentiated NK cells in LN[39,49].

The effect of IL-15 on NK cell survival, differentiation and function is much stronger when presented *in trans*, as it is the case here, than in its soluble form[50,51]. *In vitro* studies have indeed shown that the decreased control of HIV-1 infection in $CD4^+$ T cells by NK cells is due, at least *in vitro*, to the decreased presentation of mbIL-15[47]. IL-15 induces LFA-1 expression which is a late step required for cytotoxic differentiation[52]. Thus, in addition to promoting NK cell survival, the IL-15 in the AGM follicles might contribute to the differentiation toward a mature cytotoxic phenotype[53]. The study reveals that most of the $CXCR5^+$ NK cells were indeed within the $CD16^+$ subset and many expressed CD107a. In addition, the phenotypic analyses demonstrated that even more $CXCR5^+$ NK cells expressed the Fcγ receptors CD16 and CD32. These NK cells might thus display superior antibody-dependent cellular cytotoxicity (ADCC). This needs to be confirmed by functional studies. Altogether, $CXCR5^+$NK cells clearly showed a distinct phenotype that could explain their superior capacity for viral control.

We confirm here a strong viral control in LN during SIVagm infection. We cannot exclude that only follicles from peripheral secondary lymphoid organs are virus-free. It is still possible that lymphoid structures from the gut show viral replication and/or trapping since viral replication is not controlled in the gut in natural hosts. We also cannot exclude that in AGM the viral control in LN is stronger than in other natural hosts such as sooty mangabeys. However, our data are in line with previous reports on a strong SIVsm control in both the LN T zone and follicles of sooty mangabeys [6,34]. HIV infection in LN causes inflammation that when untreated leads to collagen deposition, fibrosis and disruption of the LN architecture[10]. In addition, persistent HIV infection in LN might severely impact the development of effective immune cells [54,55]. Our results highlight that AGM have the extraordinary capacity to mount a tissue-specific viral control. Together with other studies showing that memory $CD4^+$T cells are less infected in natural hosts[3], our data suggest that natural hosts, while unable to control viremia, developed mechanisms to specifically protect those key organs and cells which are critical for the education and memory of immune responses and protect secondary lymphoid structures from viral-induced damages. In addition, strong control of viral replication in the secondary lymphoid organs might contribute to the lack of inflammation during chronic infection in natural hosts.

NK cell depletion during SIVagm infection was associated with strong increases of viral replication in LN. This confirms the key role of NK cells for viral control in LN. The increase of viral replication was observed both in the T zone and within follicles. It is unclear which NK cell phenotype is

associated with viral control in the T zone. It is possible that in AGM, NK cells are not exhausted in contrast to MAC, since AGM are capable to resolve chronic inflammation[25,39]. We also cannot totally exclude that in the IL-15 treated animals, increases of $CD4^+$ target cells or decreases of $CD8^+$ T effector cells or their function contributed to the increases in viral load. However, in LN, the memory $CD4^+$T cells were either decreased or unchanged. Regarding $CD8^+$T cells, previous studies have shown that AGMs infected by SIVagm do not exhibit strong suppressive $CD8^+$T cell capacities nor significant infiltrations of $CD8^+$T cells into LN follicles[28,56,57]. In addition, *in vivo* depletion of $CD8^+$T cells in SIVagm-infected AGM have not lead to strong increases in viral load[58,59]. It is still possible that $CD8^+$T cells contribute to the control of viral load in the LN during SIVagm infection, but it is unlikely that they play a major role in this model.

Genetic and functional studies have long highlighted that NK cells impact significantly HIV infection[18]. However, the role of NK cells in the control of HIV/SIV reservoirs might have been underestimated in the past. NK cells play an important role for immune-surveillance in cancer. Clinical trials testing approaches for enhancing NK cell expansion and suppressor activity during cancer therapies are expanding. Based on our results, we anticipate that a better comprehension of NK cell biology in lymphoid tissues as provided here will endorse the search for novel NK-cell based immunotherapies in HIV infection.

Taken together, this study reveals that SIV infection induces a trafficking of NK cells within LNs. Most importantly, we discovered the potential of a unique, $CXCR5^+$ and IL-15 dependent localization of NK cells within LN follicles. This study therefore uncovers a new feature of NK cells during viral infections. Furthermore, we provide here the evidence that NK cells during non-pathogenic SIVagm infection play an unforeseen key role in the control of viral replication in lymph nodes. The discovery that NK cells have the potential to efficiently control the viral reservoir in follicles might have important implications for cure and vaccine research.

REFERENCES

1. Saez-Cirion, A., Jacquelin, B., Barré-Sinoussi, F. & Müller-Trutwin, M. Immune responses during spontaneous control of HIV and AIDS: what is the hope for a cure? *Philos. Trans. R. Soc. Lond. B. Biol. Sci.* **369,** 20130436 (2014).

2. Lederman, M. M. & Margolis, L. THE LYMPH NODE IN HIV PATHOGENESIS. *Semin. Immunol.* **20,** 187–195 (2008).

3. Paiardini, M. & Müller-Trutwin, M. HIV-associated chronic immune activation. *Immunol. Rev.* **254,** 78–101 (2013).

4. Chakrabarti, L. *et al.* Early stages of simian immunodeficiency virus infection in lymph nodes. *Amer J Pathol* **144,** 1226–1236 (1994).

5. Lindqvist, M. *et al.* Expansion of HIV-specific T follicular helper cells in chronic HIV infection. *J. Clin. Invest.* **122,** 3271–3280 (2012).

6. Brenchley, J. M. *et al.* Differential infection patterns of CD4+ T cells and lymphoid tissue viral burden distinguish progressive and nonprogressive lentiviral infections. *Blood* **120,** 4172–4181 (2012).

7. Petrovas, C. *et al.* CD4 T follicular helper cell dynamics during SIV infection. *J. Clin. Invest.* **122,** 3281–3294 (2012).

8. Xu, H. *et al.* Persistent Simian Immunodeficiency Virus Infection Drives Differentiation, Aberrant Accumulation, and Latent Infection of Germinal Center Follicular T Helper Cells. *J. Virol.* **90,** 1578–1587 (2016).

9. Chowdhury, A. *et al.* Decreased T Follicular Regulatory Cell/T Follicular Helper Cell (TFH) in Simian Immunodeficiency Virus-Infected Rhesus Macaques May Contribute to Accumulation of TFH in Chronic Infection. *J. Immunol. Baltim. Md 1950* **195,** 3237–3247 (2015).

10. Estes, J. D. Pathobiology of HIV/SIV-associated changes in secondary lymphoid tissues. *Immunol. Rev.* **254,** 65–77 (2013).

11. Tenner-Racz, K. & Racz, P. Follicular dendritic cells initiate and maintain infection of the germinal centers by human immunodeficiency virus. *Curr. Top. Microbiol. Immunol.* **201,** 141–159 (1995).

12. Fox, C. H. *et al.* Lymphoid Germinal Centers Are Reservoirs of Human Immunodeficiency Virus Type 1 RNA. *J. Infect. Dis.* **164,** 1051–1057 (1991).

13. Fukazawa, Y. *et al.* B cell follicle sanctuary permits persistent productive simian immunodeficiency virus infection in elite controllers. *Nat. Med.* **21,** 132–139 (2015).

14. Leong, Y. A. *et al.* CXCR5(+) follicular cytotoxic T cells control viral infection in B cell follicles. *Nat. Immunol.* (2016). doi:10.1038/ni.3543

15. Banga, R. *et al.* PD-1(+) and follicular helper T cells are responsible for persistent HIV-1 transcription in treated aviremic individuals. *Nat. Med.* (2016). doi:10.1038/nm.4113

16. Miles, B. & Connick, E. TFH in HIV Latency and as Sources of Replication-Competent Virus. *Trends Microbiol.* **24,** 338–344 (2016).

17. Vivier, E., Tomasello, E., Baratin, M., Walzer, T. & Ugolini, S. Functions of natural killer cells. *Nat. Immunol.* **9,** 503–510 (2008).

18. Carrington, M. & Alter, G. Innate immune control of HIV. *Cold Spring Harb. Perspect. Med.* **2,** a007070 (2012).

19. Carrega, P. & Ferlazzo, G. Natural killer cell distribution and trafficking in human tissues. *Front. Immunol.* **3,** (2012).

20. Bajénoff, M. *et al.* Natural killer cell behavior in lymph nodes revealed by static and real-time imaging. *J. Exp. Med.* **203,** 619–631 (2006).

21. Garrod, K. R., Wei, S. H., Parker, I. & Cahalan, M. D. Natural killer cells actively patrol peripheral lymph nodes forming stable conjugates to eliminate MHC-mismatched targets. *Proc. Natl. Acad. Sci. U. S. A.* **104,** 12081–12086 (2007).

22. Beuneu, H. *et al.* Dynamic behavior of NK cells during activation in lymph nodes. *Blood* **114,** 3227–3234 (2009).

23. Sagoo, P. *et al.* In vivo imaging of inflammasome activation reveals a subcapsular macrophage burst response that mobilizes innate and adaptive immunity. *Nat. Med.* **22,** 64–71 (2016).

24. Luteijn, R. *et al.* Early viral replication in lymph nodes provides HIV with a means by which to escape NK-cell-mediated control. *Eur. J. Immunol.* **41,** 2729–2740 (2011).

25. Huot, N., Rascle, P., Garcia-Tellez, T., Jacquelin, B. & Müller-Trutwin, M. Innate immune cell responses in non pathogenic versus pathogenic SIV infections. *Curr. Opin. Virol.* **19,** 37–44 (2016).

26. Pandrea, I. V. *et al.* Acute loss of intestinal CD4+ T cells is not predictive of simian immunodeficiency virus virulence. *J. Immunol. Baltim. Md 1950* **179,** 3035–3046 (2007).

27. Beer, B. *et al.* Lack of dichotomy between virus load of peripheral blood and lymph nodes during long-term simian immunodeficiency virus infection of African green monkeys. *Virology* **219,** 367–375 (1996).

28. Diop, O. M. *et al.* High levels of viral replication during primary simian immunodeficiency virus SIVagm infection are rapidly and strongly controlled in African green monkeys. *J. Virol.* **74,** 7538–7547 (2000).

29. Gueye, A. *et al.* Viral load in tissues during the early and chronic phase of non-pathogenic SIVagm infection. *J. Med. Primatol.* **33,** 83–97 (2004).

30. Goldstein, S. *et al.* Wide range of viral load in healthy african green monkeys naturally infected with simian immunodeficiency virus. *J Virol* **74,** 11744–53 (2000).

31. Broussard, S. R. *et al.* Simian immunodeficiency virus replicates to high levels in naturally infected African green monkeys without inducing immunologic or neurologic disease. *J Virol* **75,** 2262–75 (2001).

32. Cumont, M.-C. *et al.* Early divergence in lymphoid tissue apoptosis between pathogenic and nonpathogenic simian immunodeficiency virus infections of nonhuman primates. *J. Virol.* **82,** 1175–1184 (2008).

33. Müller, M. C. & Barré-Sinoussi, F. SIVagm: genetic and biological features associated with replication. *Front. Biosci. J. Virtual Libr.* **8,** d1170-1185 (2003).

34. Martinot, A. J. *et al.* Acute SIV infection in sooty mangabey monkeys is characterized by rapid virus clearance from lymph nodes and absence of productive infection in germinal centers. *PloS One* **8,** e57785 (2013).

35. Jacquelin, B. *et al.* Innate immune responses and rapid control of inflammation in African green monkeys treated or not with interferon-alpha during primary SIVagm infection. *PLoS Pathog.* **10,** e1004241 (2014).

36. DeGottardi, M. Q. *et al.* Effect of Anti-IL-15 Administration on T Cell and NK Cell Homeostasis in Rhesus Macaques. *J. Immunol. Baltim. Md 1950* **197,** 1183–1198 (2016).

37. Cooper, M. A. *et al.* In vivo evidence for a dependence on interleukin 15 for survival of natural killer cells. *Blood* **100,** 3633–3638 (2002).

38. Li, J. *et al.* Differential effects of IL-15 on the generation, maintenance and cytotoxic potential of adaptive cellular responses induced by DNA vaccination. *Vaccine* **33,** 1188–1196 (2015).

39. Schafer, J. L., Li, H., Evans, T. I., Estes, J. D. & Reeves, R. K. Accumulation of Cytotoxic CD16+ NK Cells in Simian Immunodeficiency Virus-Infected Lymph Nodes Associated with In Situ Differentiation and Functional Anergy. *J. Virol.* **89,** 6887–6894 (2015).

40. Gunn, M. D. *et al.* A B-cell-homing chemokine made in lymphoid follicles activates Burkitt's lymphoma receptor-1. *Nature* **391,** 799–803 (1998).

41. Moser, B., Schaerli, P. & Loetscher, P. CXCR5(+) T cells: follicular homing takes center stage in T-helper-cell responses. *Trends Immunol.* **23,** 250–254 (2002).

42. Rydyznski, C. *et al.* Generation of cellular immune memory and B-cell immunity is impaired by natural killer cells. *Nat. Commun.* **6,** 6375 (2015).

43. Abruzzo, L. V. & Rowley, D. A. Homeostasis of the antibody response: immunoregulation by NK cells. *Science* **222,** 581–585 (1983).

44. Blanca, I. R., Bere, E. W., Young, H. A. & Ortaldo, J. R. Human B cell activation by autologous NK cells is regulated by CD40-CD40 ligand interaction: role of memory B cells and CD5+ B cells. *J. Immunol. Baltim. Md 1950* **167,** 6132–6139 (2001).

45. Yuan, D., Koh, C. Y. & Wilder, J. A. Interactions between B lymphocytes and NK cells. *FASEB J. Off. Publ. Fed. Am. Soc. Exp. Biol.* **8,** 1012–1018 (1994).

46. Younes, S.-A. *et al.* IL-15 promotes activation and expansion of CD8+ T cells in HIV-1 infection. *J. Clin. Invest.* **126,** 2745–2756 (2016).

47. Moreno-Nieves, U. Y. *et al.* NK cells are primed by ANRS MVA(HIV)-infected DCs, via a mechanism involving NKG2D and membrane-bound IL-15, to control HIV-1 infection in CD4+ T cells. *Eur. J. Immunol.* **44,** 2370–2379 (2014).

48. Park, C.-S., Yoon, S.-O., Armitage, R. J. & Choi, Y. S. Follicular Dendritic Cells Produce IL-15 That Enhances Germinal Center B Cell Proliferation in Membrane-Bound Form. *J. Immunol.* **173,** 6676–6683 (2004).

49. Freud, A. G. *et al.* A human CD34(+) subset resides in lymph nodes and differentiates into CD56bright natural killer cells. *Immunity* **22,** 295–304 (2005).

50. Stonier, S. W. & Schluns, K. S. Trans-presentation: a novel mechanism regulating IL-15 delivery and responses. *Immunol. Lett.* **127,** 85–92 (2010).

51. Tamzalit, F. *et al.* IL-15.IL-15Rα complex shedding following trans-presentation is essential for the survival of IL-15 responding NK and T cells. *Proc. Natl. Acad. Sci. U. S. A.* **111,** 8565–8570 (2014).

52. Barao, I., Hudig, D. & Ascensao, J. L. IL-15-mediated induction of LFA-1 is a late step required for cytotoxic differentiation of human NK cells from CD34+Lin- bone marrow cells. *J. Immunol. Baltim. Md 1950* **171,** 683–690 (2003).

53. Castillo, E. F., Stonier, S. W., Frasca, L. & Schluns, K. S. Dendritic cells support the in vivo development and maintenance of NK cells via IL-15 trans-presentation. *J. Immunol. Baltim. Md 1950* **183,** 4948–4956 (2009).

54. Onabajo, O. O. & Mattapallil, J. J. Expansion or depletion of T follicular helper cells during HIV infection: consequences for B cell responses. *Curr. HIV Res.* **11,** 595–600 (2013).

55. Racz, P., Tenner-Racz, K. & Schmidt, H. Follicular dendritic cells in HIV-induced lymphadenopathy and AIDS. *APMIS. Suppl.* **8,** 16–23 (1989).

56. Zahn, R. C. *et al.* Simian immunodeficiency virus (SIV)-specific CD8+ T-cell responses in vervet African green monkeys chronically infected with SIVagm. *J. Virol.* **82,** 11577–11588 (2008).

57. Lozano Reina, J.-M. *et al.* Gag p27-specific B- and T-cell responses in Simian immunodeficiency virus SIVagm-infected African green monkeys. *J. Virol.* **83,** 2770–2777 (2009).

58. Schmitz, J. E. *et al.* Inhibition of adaptive immune responses leads to a fatal clinical outcome in SIV-infected pigtailed macaques but not vervet African green monkeys. *PLoS Pathog.* **5,** e1000691 (2009).

59. Gaufin, T. *et al.* Experimental depletion of CD8+ cells in acutely SIVagm-infected African Green Monkeys results in increased viral replication. *Retrovirology* **7,** 42 (2010).

60. Jacquelin, B. *et al.* Nonpathogenic SIV infection of African green monkeys induces a strong but rapidly controlled type I IFN response. *J. Clin. Invest.* **119,** 3544–3555 (2009).

ONLINE METHODS

Animals, SIV infections and anti-IL15 treatment

Fifteen African green monkeys (Caribbean *Chlorocebus aethiops*) and fifteen cynomolgus macaques (*Macaca fascicularis*) were used in this study. The animals were free of simian retrovirus type D and simian T-lymphotropic virus type 1 and were housed in single cages within level 3 biosafety facilities at the IDMIT Center (Fontenay-aux-Roses, France). Because H6 haplotypes are significantly associated with viral control in cynomolgus macaques, macaques with H6 haplotype were excluded from this study. The average weight of the monkeys was between 3 and 5 kg. All monkeys were young adults and with an average of 3 to 4 years at inclusion. Both males and females were used (60 % of females and 40 % of males for each species). The sample size varied between 5 and 10 animals per group (N=6 in most experiments), chosen according to the tripartite harmonized ICH Guideline on Methodology (previously coded Q2B). Sample collection was determined in a random order. The investigators were unblinded, while the animal handlers were blinded.

Animals were sedated with Ketamine Chlorhydrate (Rhone-Mérieux, Lyons, France) before handling. All experimental procedures were conducted in strict accordance with the international European guidelines 2010/63/UE on protection of animals use for experimentation and other scientific purposes (French decree 2013-118) and with the recommendations of the Weatherall report. IDMIT center complies with Standards for Human Care and Use of the Office for Laboratory Animal Welfare (OLAW, USA) under OLAW Assurance number #A5826-86. The monitoring of the animals was under the supervision of the veterinarians in charge of the animal facilities. Animal experimental protocols were approved by the Ethical Committee of Animal Experimentation (CETEA-DSV, IDF, France) (Notification #12-098). AGM and macaques were infected IV with, respectively, 250 $TCID_{50}$ of $SIVagm.sab_{92018}$ and 5000 AID_{50} of $SIVmac_{251}$, as previously reported[28,35].

From the six AGM and six MAC described in Figure 1, four of each species were randomly chosen for sacrifice at day 240 p.i., and the tissues (spleen and gut) collected at sacrifice used for the analyses

described in Figures 2 and 3. The spleens from the additional 6 animals described in Figure 3 correspond to randomly chosen, chronically SIVagm.sab92018-infected AGM from previous studies[35,60] . The two remaining AGM from Figure 1 were included in the group of animals treated with the simianized anti-IL15 mAb. The three other AGMs treated with the anti-IL-15 mAb derived from previous studies and were also randomly chosen[35]. The five AGMs were chronically infected with SIVagm.sab92018 for 1 to 3 years at the time of anti IL-15 administration.

Tissue collection and processing

Blood and LN biopsies were collected longitudinally. Whole venous blood was collected in EDTA tubes. Mononuclear cells were isolated by Ficoll density-gradient centrifugation. Biopsies of peripheral LNs were performed by excision. Other tissues (spleen, gut) were collected at autopsy. After careful removal of adhering connective and fat tissues, LN and spleen were digested using Collagenase IV, Collagenase D and DNase I and at 37°c for 5min. The tissue was then mechanically disrupted and filtered through a 40 µm cell strainer. Gut was washed with cold medium and cut in pieces. A 20 min digestion with Collagenase IV was performed at 37°C. The cell suspension was filtrated subsequently through 100 and 40 µm cell strainers and cells washed with cold PBS. Cells were either immediately stained for flow cytometry or cryopreserved in 90% FBS, 10% DMSO and stored in liquid nitrogen vapor.

Viral detection assays

Plasma viral load was determined by real-time PCR as described[28]. For cell-associated viral RNA, RNA was extracted as follows: samples were lysed in NaCl (3M), EDTA (0.5M, pH 8), SDS (10%, Bio-Rad) and Proteinase K (1mg/mL, Qiagen) in a 45min incubation at 55° C. Then, NaCl (5M) was added and incubated at 4° C between 15 and 60min, followed by centrifugation for 15min at 3000rpm at 4° C. DNA was precipitated in Phenol:Chloroform:isoamyl alcohol 25:24:1 (pH = 8, Sigma Aldrich). Viral RNA was measured by qPCR in duplicate. SIVagm and SIVmac products of T7 transcription from plasmids were used as standards to calculate SIV RNA copy numbers. 18SrRNA and CCR5 DNA quantification was used for normalization Sample preparation, enzyme mix preparation and PCR set-up were performed in three separate rooms to avoid PCR contamination. Negative controls were used to exclude sample contamination.

Flow cytometry

All analyses on blood cells and most analyses on LN cells, including those on the homing receptors, were performed on fresh cells. Hypotonic ammonium chloride solution was used to lyse contaminating red blood cells. Cytofix/Cytoperm (BD Biosciences, La Jolla, CA) was used for all intracellular stainings. Intra cellular staining for IL-15 was performed without and after stimulation with Phorbol Myristate Acetate (PMA) and Ionomycin at final concentrations of respectively 10ng/mL and 1µg/mL. After 1 hour of incubation, 10 µg/mL of Brefeldin A was added. FcR blocking reagent (Miltenyi) was used to block unspecific antibody binding. Antibodies used are shown in Supplementary Table 1. Flow cytometry acquisitions were done on an LSR Fortessa (BD Biosciences), and FlowJo software (version 9.6.4, Tree Star, Ashland, OR) was used for all analyses.

Immunohistology

Fresh LN tissues were embedded and snap frozen in optimum cold temperature compound (OCT) and 10µm frozen sections were stained using unconjugated primary antibodies followed by appropriate secondary antibodies conjugated to Alexa 488 (green), Alexa 568 (red) (Molecular Probes, Eugene, OR). Antibodies used are shown in Supplementary Table 2. Stained slides were incubated with 100–200µL of ice cold methanol and 5% acetic acid, placed at -20°C for 10 min and then washed. Image analysis was performed using a Leica TCS SP8 confocal microscope equipped with white lasers (Leica Microsystems, Exton, PA).

Fluorescent *in situ* hybridization

The probes were prepared as follows. SIV*env* and *IL-15* mRNA were RT-PCR amplified and cDNA was cloned, using the CloneJET PCR Cloning Kit (Thermo Fisher Scientific) as recommended by the manufacturer. The vectors were digested and *in vitro* transcribed using T7 RNA polymerase (Ambion) to make Alexa Fluor 488 [Life Technologies] single-strand RNA probes. The FISH assay combined with immunofluorescent staining was performed as follows: Cryosections were rehydrated in PBS for 15 minutes and then permeabilized by incubating in 0.5% (v/v) Triton X-100 in PBS for 20 minutes at RT. The slides were placed in container filled with 200 ml of 10 mM sodium citrate buffer (pH 6.0) and the RNA unmasked by putting the container in a microwave set at 700 W, before heating for 2.5 minutes or until first signs of boiling. This step was repeated seven times. The slides were transferred to 2X SSC and subsequently incubated in formamide-SSC solution for at least 4 hours. The probe was mounted using glass chambers. Prehybridization was performed by incubating the slides with the mounted probe for 1-2 hours at 37°C. Cellular RNA and RNA probes were simultaneously denatured by incubating the slides with a mounted probe on a heating block for 5

minutes at 80°C, followed by hybridization in humid dark chambers for 1 day at 37°C. Sections were washed three times at high stringency in 0.1X SSC at 60°C and three times in 2X SSC buffer. Finally they were incubated in 0.05 µg/ml DAPI in SSC/Tween for 10 minutes, rinsed briefly in 2X SSC and mounted. As negative controls, we used a RNAse degraded probe, as well as LNs from uninfected animals. Images were acquired on a Confocal Laser Scanning Microscope Leica TCS SP8, running LAS AF 3 (Leica Application Suite Advanced Fluorescence). Individual optical slices were collected at 1024 × 1024 pixel resolution. Image J software was used to assign colors to the channels collected.

Statistical analyses

Nonparametric Mann-Whitney *U*-tests was used to compare continuous factors between two groups, while non-parametric Wilcoxon signed rank test was used to compare paired variables. The Spearman rank correlation was used to assess the association between 2 continuous variables. These statistical analyses as well as graphic treatments were performed with GraphPad Prism 7.0 software (GraphPad Software, La Jolla, CA). To evaluate changes over time, mixed effect models were used to account for multiple repeated measurements, with testing of interactions between time and species, time being considered as a categorical or continuous variable depending on the number of values. We first assessed if the marker's distribution was Gaussian; if not, a logarithmic transformation was used and tested if efficient. Secondly, a LOWESS (locally weighted scatterplot smoothing) curve was used to assess whether the marker's trajectory was linear. Finally, a mixed effect linear or piecewise-linear model was applied. Stata 13 (Stata Corp., College Station, TX, USA) was used for the analyses. In all analyses, p-values <0.05 were considered significant.

ACKNOWLEDGMENTS

This work was supported by the « Investissements d'Avenir" program managed by the National Agency of Research (ANR) under reference ANR-10-LABX-77, the ANRS and the l'OREAL foundation. The Infectious Disease Models and Innovative Therapies (IDMIT) center in Fontenay-aux-Roses, France, was funded by the French government "Investissements d'Avenir" program for infrastructures (PIA) under grant ANR-11-INBS-0008, the PIA grant ANR-10-EQPX-02-01 funding the FlowCyTech facility at IDMIT. RKR was supported by NIH grant RO1 DE026014. The anti-IL-15 mAb was a gift from the NIH Non-Human Primate Reagent Resource supported by AI126683 and OD010976. NH and MJP were recipients of post-doctoral fellowships from, respectively, the French Vaccine Research Institute (Créteil, France) and SIDACTION. PR and TGT received a PhD fellowship from, respectively, the University Paris Diderot, Sorbonne Paris Cité, and the Pasteur-Paris University PhD program supported by the Institut Carnot Pasteur Microbes et Santé. We are grateful

to veterinarians and the staff of the IDMIT animal facility, in particular Vanessa Contreras, Benoit Delache, Jean-Marie Helies, Virgile Monnet, Julie Morin and Christophe Joubert for their excellent work. We thank Lamya Irbah, Thierry Kortulewski and Catherine Chapon for access to the stellar IDMIT imaging core facility as well as Christelle Cassan, Sabrina Guenounou and Antonio Cosma for access to the state-of-the art IDMIT Flowcytech core facility.

AUTHOR CONTRIBUTIONS

N.H. contributed to the project design, has set up methods and performed the experiments; N.D-B. provided samples; N.H., B.J., T.G-T, P.R. and M.J.P. proceeded the samples; P.R. prepared the anti-15 probe; N.H. and Y.M. performed the statistical analyses; N.H., B.J., R.K.R. and M.M-T. analyzed and interpreted the data; B.J. has prepared the ethical protocols; N.H. and M.M-T. wrote the manuscript. M.M-T. conceived the project and directed the research.

LEGENDS

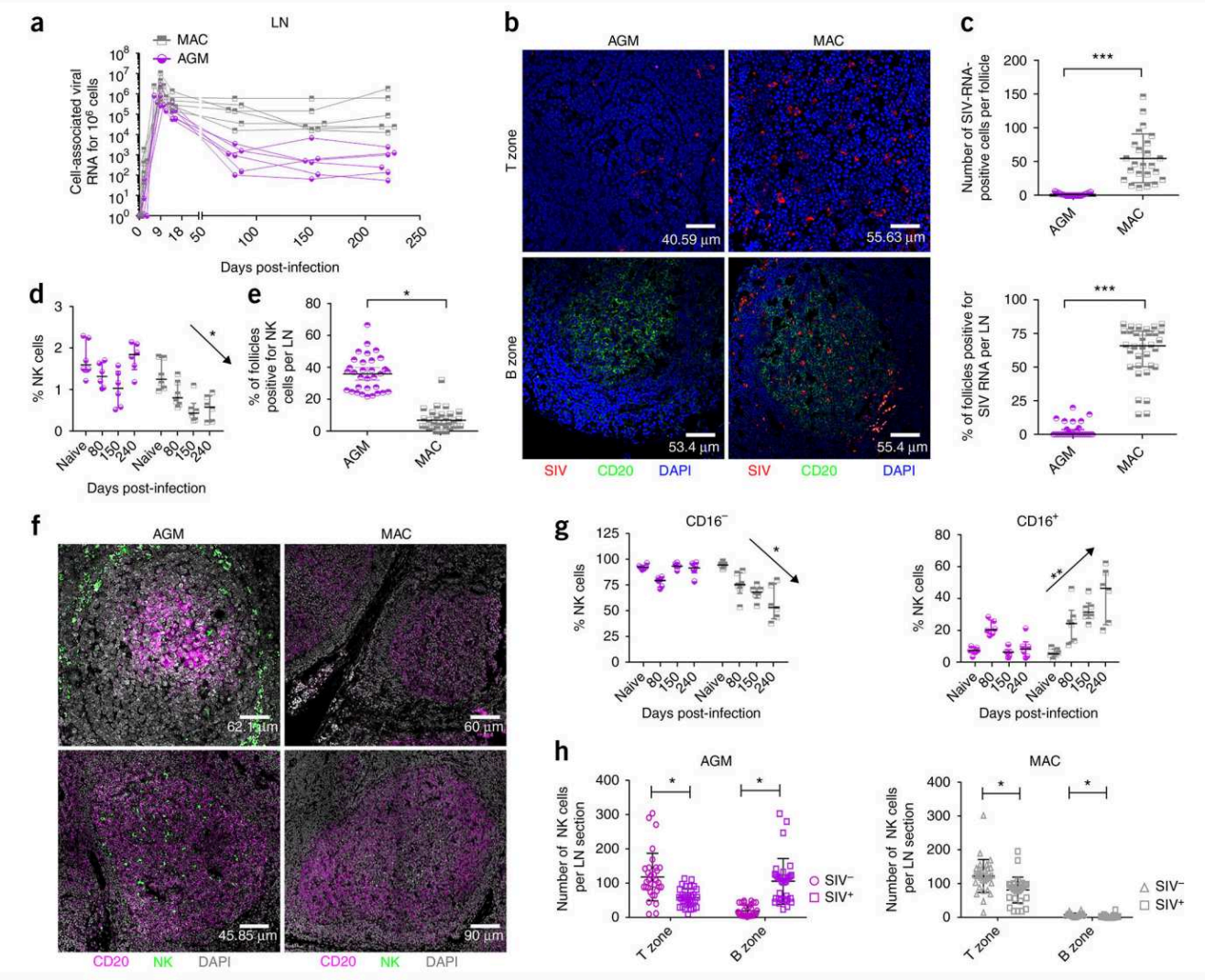


Figure 1. Numbers and distribution of SIV RNA and NK cells in lymph nodes. Peripheral LNs from six AGM and six macaques infected by SIVagm and SIVmac, respectively, were analyzed. **(a)** Cell-associated viral RNA in total LN cells. **(b)** Representative confocal images of LN sections from chronically infected animals stained for CD20 (green), SIV RNA (red) and total nucleus (blue). Cells containing viral RNA were detected by *in-situ* hybridization. The picture represents the distribution of the productively-infected cells in LNs. One representative picture in the B and T zones is shown for each species. The time points analyzed in chronic phase corresponded to days 80, 150 and 250 days p.i. **(c)** The graph on the left shows the numbers of SIV RNA positive-cells per follicle. A total of 24 follicles were counted. The graph on the right shows the numbers of follicles positive for SIV RNA. A total of 8 LN sections per animal were counted. **(d)** Frequencies of NK cells among total $CD45^+$ lymphocytes in LNs of AGM (purple) and MAC (grey). **(e)** Percentages of follicles positive for at

least one NK cell. A total of 32 LN sections were counted. **(f)** Examples of the distribution of NK cells in LNs during chronic SIVmac and SIVagm infections as evaluated by confocal imaging. NK cells were stained with anti-NKG2A (green) and B cells with anti-CD20 (purple). Staining of NK cells were verified with other markers, such as NKp30^{+} and NKp80^{+} (*not shown*). The analysis reveals the localization of NK cells in and around follicles during SIVagm infection in AGM. **(g)** Frequencies of CD16^{-} NK and CD16^{+} NK cells of LN in AGM (purple) and MAC (grey). **(h)** Numbers of NK cells in the T and B cell zones. A total of 32 LN sections from 6 animals per species were counted (4-6 sections per animal). A nonparametric Mann-Whitney *U*-tests, for panels c,e and h were applied. For panels d and g a mixed effect model was used. Asterisks indicate significant differences *p<0.05; **p<0.005; ***p<0.001. Median and inter-quartile range are shown. Dpi= days post-infection.

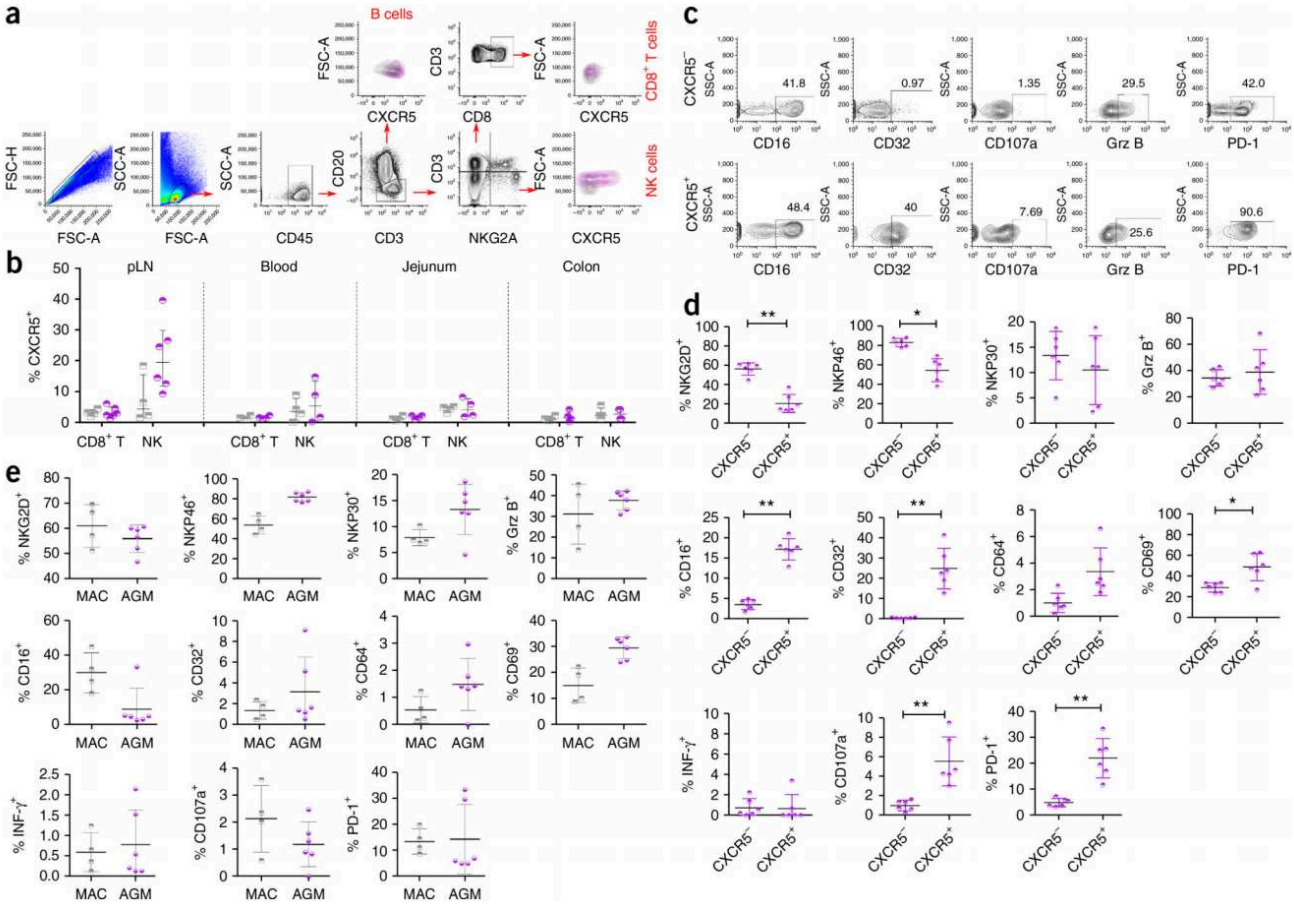


Figure 2. CXCR5 expression on NK cells and phenotyping of CXCR5^{+} NK cells in AGM. CXCR5 was measured on cells from six chronically infected AGM and six chronically infected macaques. **(a)** Gating

strategy used to analyze CXCR5 expression on B cells, $CD8^+$ T cells and NK cells. Cells from macaque are plotted in grey and from AGM in purple. Representative plots are shown. (**b**) Frequencies of $CXCR5^+$ cells for a given cell population in LNs from distinct tissues. (**c)** Phenotype of $CXCR5^-$ and $CXCR5^+$ lymph node NK cells in AGM. A representative dot plot for one animal is shown. (d) Frequencies of $CXCR5^+$ and $CXCR5^-$ NK cells expressing a given marker in AGM LN. (e) NK cell subset frequencies in LN from AGM and MAC. Individual values for AGM are shown as purple circles and for MAC as grey squares. A nonparametric Mann-Whitney *U*-test, was applied *$p<0.05$; **$p<0.005$; ***$p<0.001$.

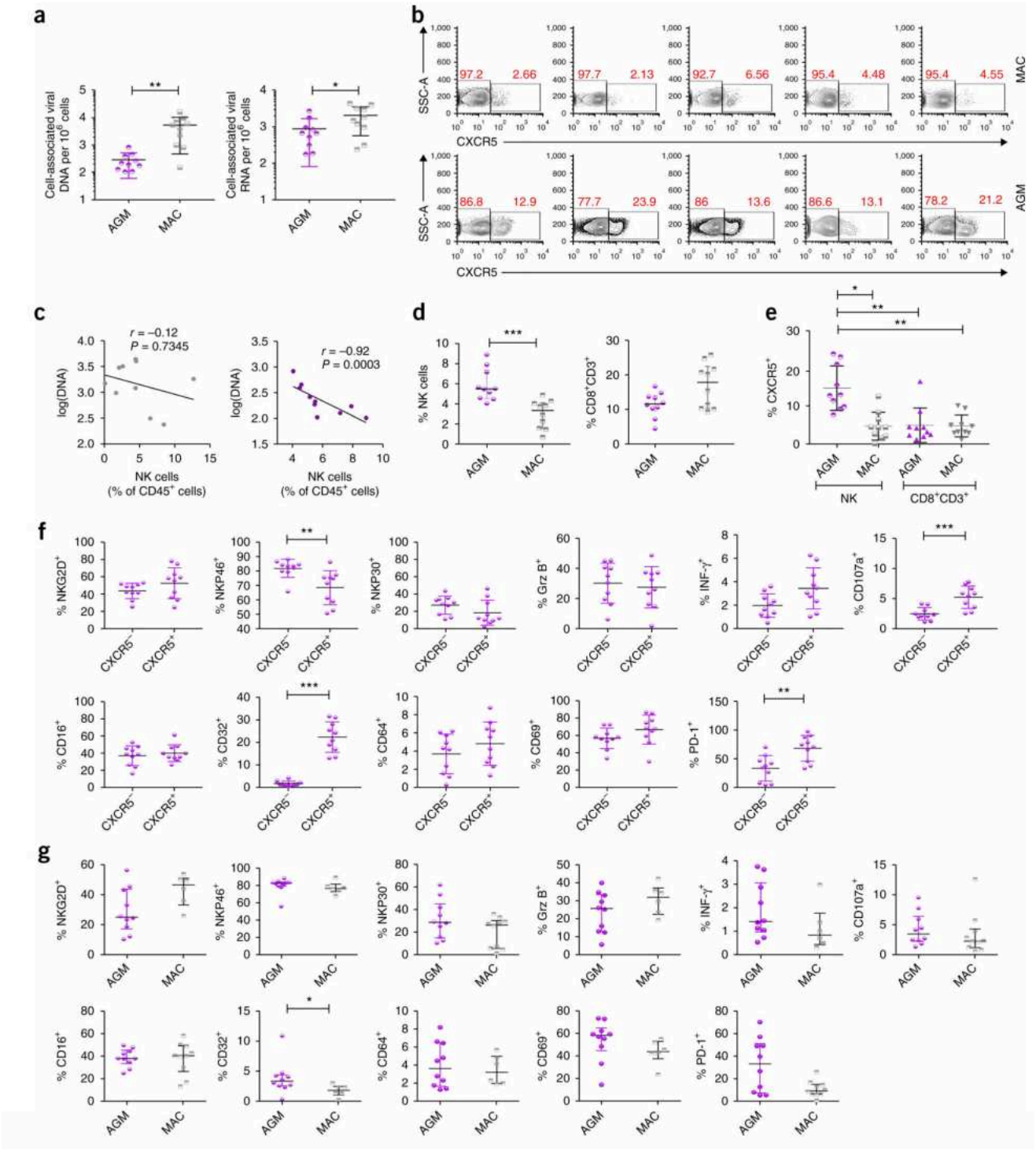


Figure 3. Viral load and NK cells in spleen from chronically infected AGM and MAC. Ten animals per species were analyzed. **(a)** Cell-associated SIV DNA and RNA in spleen (b) $CXCR5^+$ NK cells. Representative dot plots for 5 out of 10 randomly chosen animals (alphabetic order) are shown. **(c)** Cell-associated viral DNA in spleen was plotted against the frequency of spleen NK cells of MAC (left) and AGM (right). **(d)** Frequencies of NK cells among $CD45^+$ cells in spleen (e) Frequencies of $CXCR5^+$ among NK and $CD8^+$ T cells in spleen. **(f)** Frequencies of $CXCR5^+$ and $CXCR5^-$ NK cells expressing a given marker in spleen. (g) NK cell

subsets in spleen from AGM and MAC. Individual values for AGM are shown as purple circles and of MAC as grey squares. In panel c a nonparametric Spearman's rank-order correlation was run to determine the relationship between LOG(DNASIV) and NK cell frequencies for each species . For all panels exept panel c, a nonparametric Mann-Whitney *U*-test, was applied **p < 0.05; **p<0.005.*

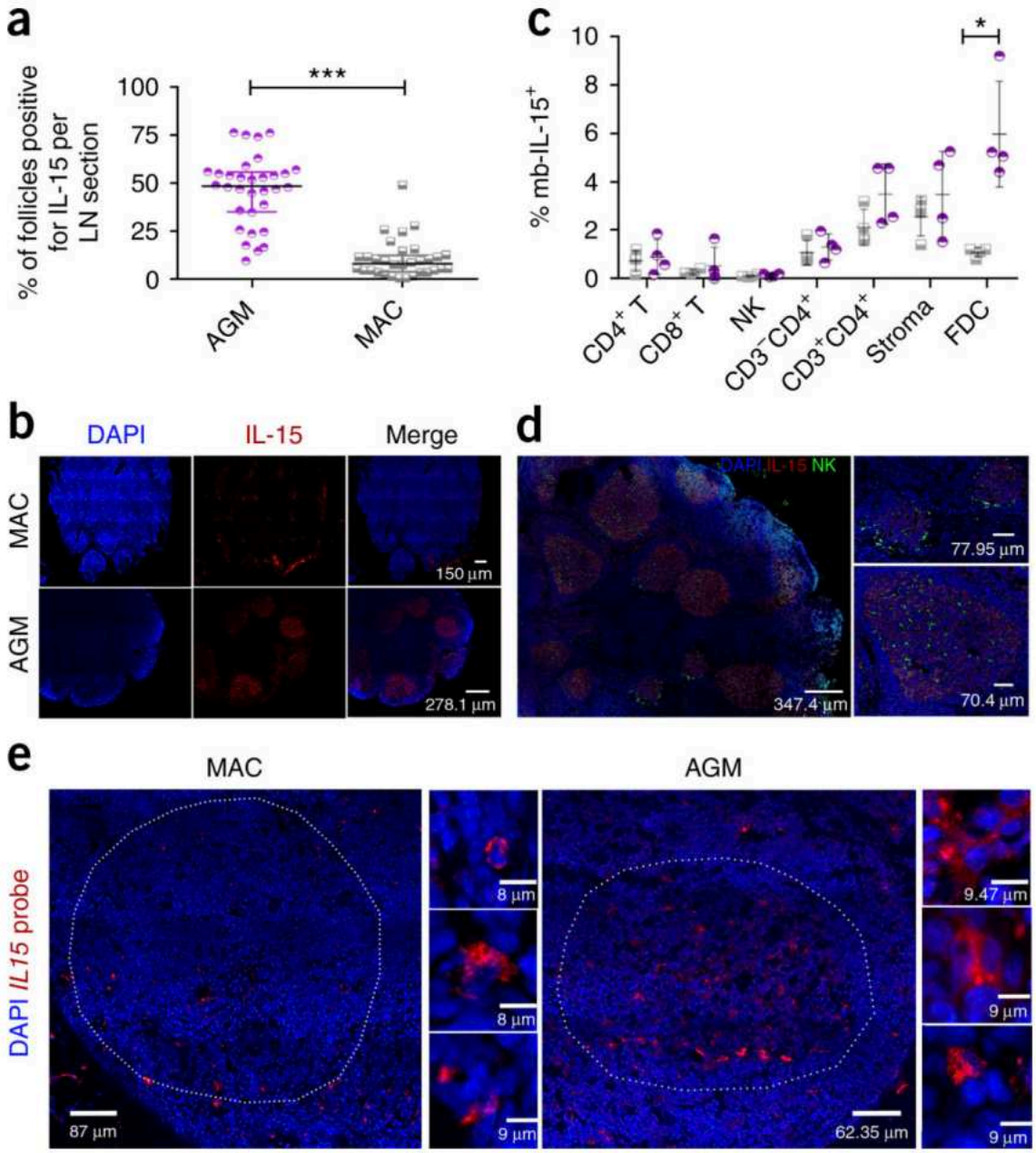


Figure 4. IL-15 expression in lymph nodes during SIV infection in AGM and macaques. LNs from six chronically infected AGM and six chronically infected macaques were analyzed. **(a)** Percentage of follicles positive for at least one IL-15^{+} cell per analyzed LN section. A total of 10 LN sections per animal were counted. **(b)** Confocal image of LN sections stained for IL-15 (red) and total

nucleus (blue). The picture represents the distribution of IL-15 positive cells for each species. IL-15 staining was strong in LN**s** from SIVagm-infected AGM and predominant in the follicles **(c)** Frequencies of cells positive for both IL-15 and IL-15Rα among distinct cell subpopulations of stromal (CD45-) and hematopoietic (CD45+) cells. **(d)** Confocal image of LN sections stained for NK cells (green), IL-15 (red) and nucleus (blue), showing the spatial association between IL-15 and NK cells. The zooms on the right side show enlarged images of AGM follicles showing typical NK cell distribution in AGM follicles, i.e. within and surrounding IL-15 positive follicles during SIVagm infection **(e)** Confocal image of LN sections hybridized with a IL-15 RNA probe (red) and stained with DAPI (blue). IL-15 mRNA positive cells were mainly detected in follicles in both species. The enlargements display representative examples of the shape of the IL-15 mRNA positive cells. Nonparametric Mann-Whitney *U*-tests were applied. Asterisks indicate significant differences ($p<0.05$). Median and interquartile range are shown. AGM : purple circle; MAC: grey squares. FDC= follicular dendritic cell.

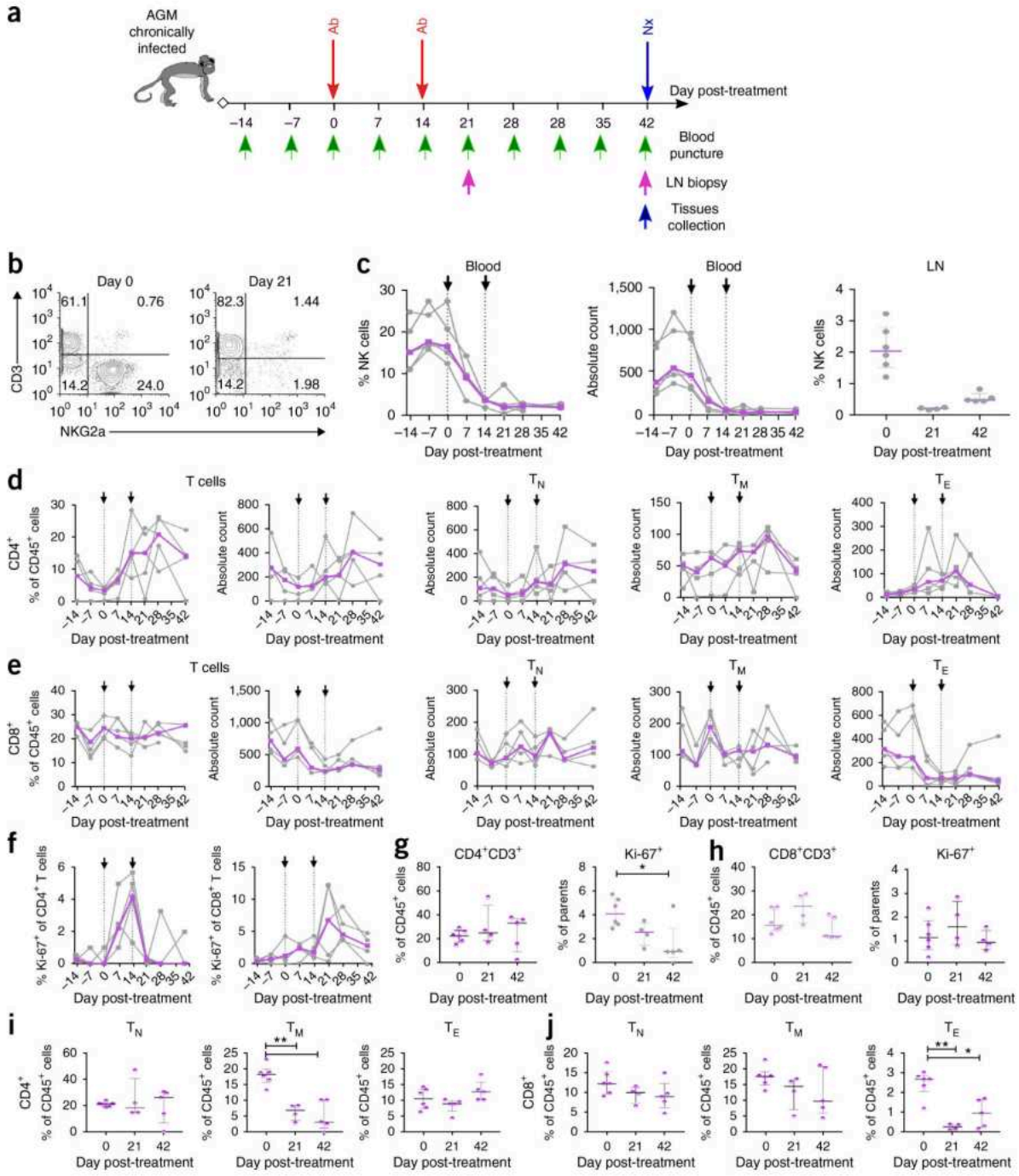


Figure 5. Anti–IL-15 administration results in near-complete NK cell depletion in AGM. (a) Schematic representation of the anti–IL-15 treatment schedule used in this study. Five chronically infected AGM received 20 mg/kg of anti–IL-15 mAb on day 0 and 10 mg/kg on day 14. The red arrows show the days of anti–IL-15 mAb administration. The blue arrow indicates the day of necropsy (Nx). (b) Dot plots showing NK cells ($CD3^-NKG2A^+$) in peripheral blood of one representative AGM before and after anti–IL-15 administration (c) Follow up of NK cells in blood and LN. In blood, five animals were followed. LN were available for 4 and 5 animals LN at day 21 and d42 post-treatment, respectively. In blood, grey and purple lines represent the trajectories for each animal and the median values from all animals, respectively. For the statistical analyses,

the mean values of the three pre-infection time points were used. (d) Follow up of $CD4^+$T cells and $CD4^+$T cell subpopulations in blood during anti-IL-15 treatment. (e) Follow up of $CD8^+$T cells and $CD8^+$T cell subpopulations in blood during anti-IL-15 treatment. (f) Levels of $CD4^+$T and $CD8^+$T positive for Ki-67 in blood. (g) $CD4^+$T cells in LN (h) CD8+ T cells in LN (i) $CD4^+$T cell subpopulations in LN (k) $CD8^+$T cell subpopulations in LN. Median values and interquartile range are indicated. Each dot represents the values of an individual animal. T_N: naïve T cells; T_M: central memory T cells; T_E: Effector memory T cells. Nonparametric Mann-Whitney *U*-tests were applied *$p < 0.05$; **$p<0.005$.

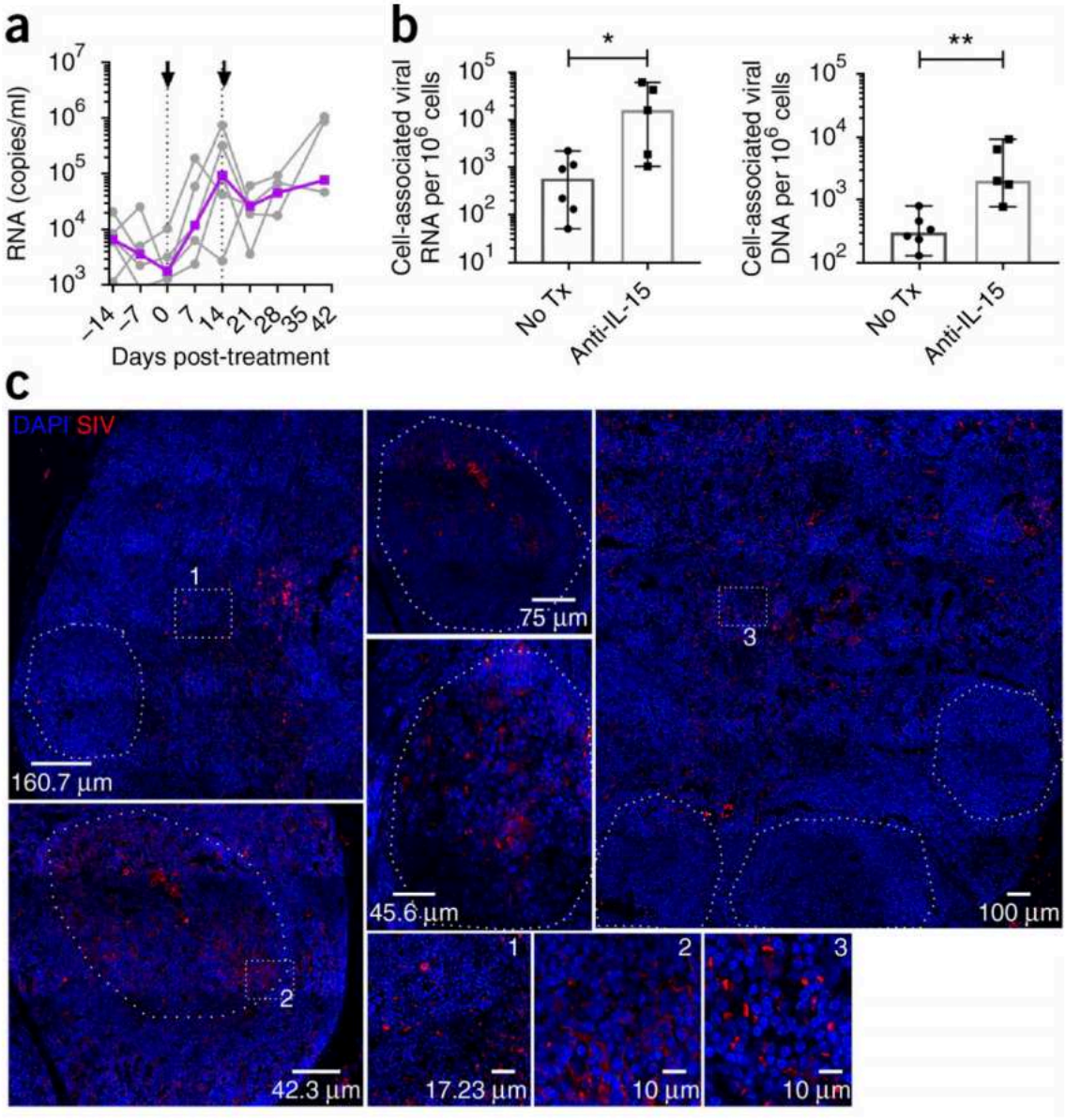
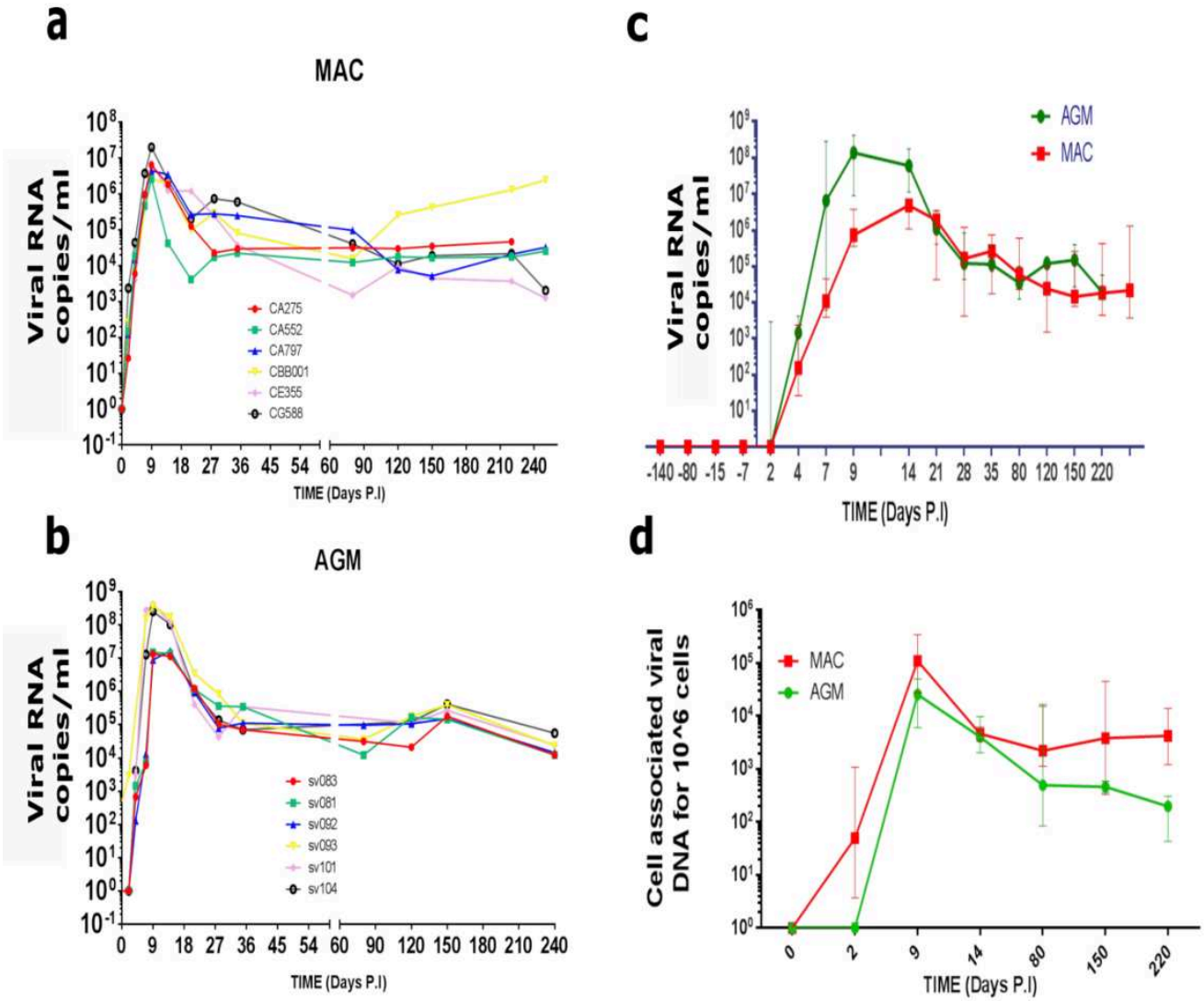


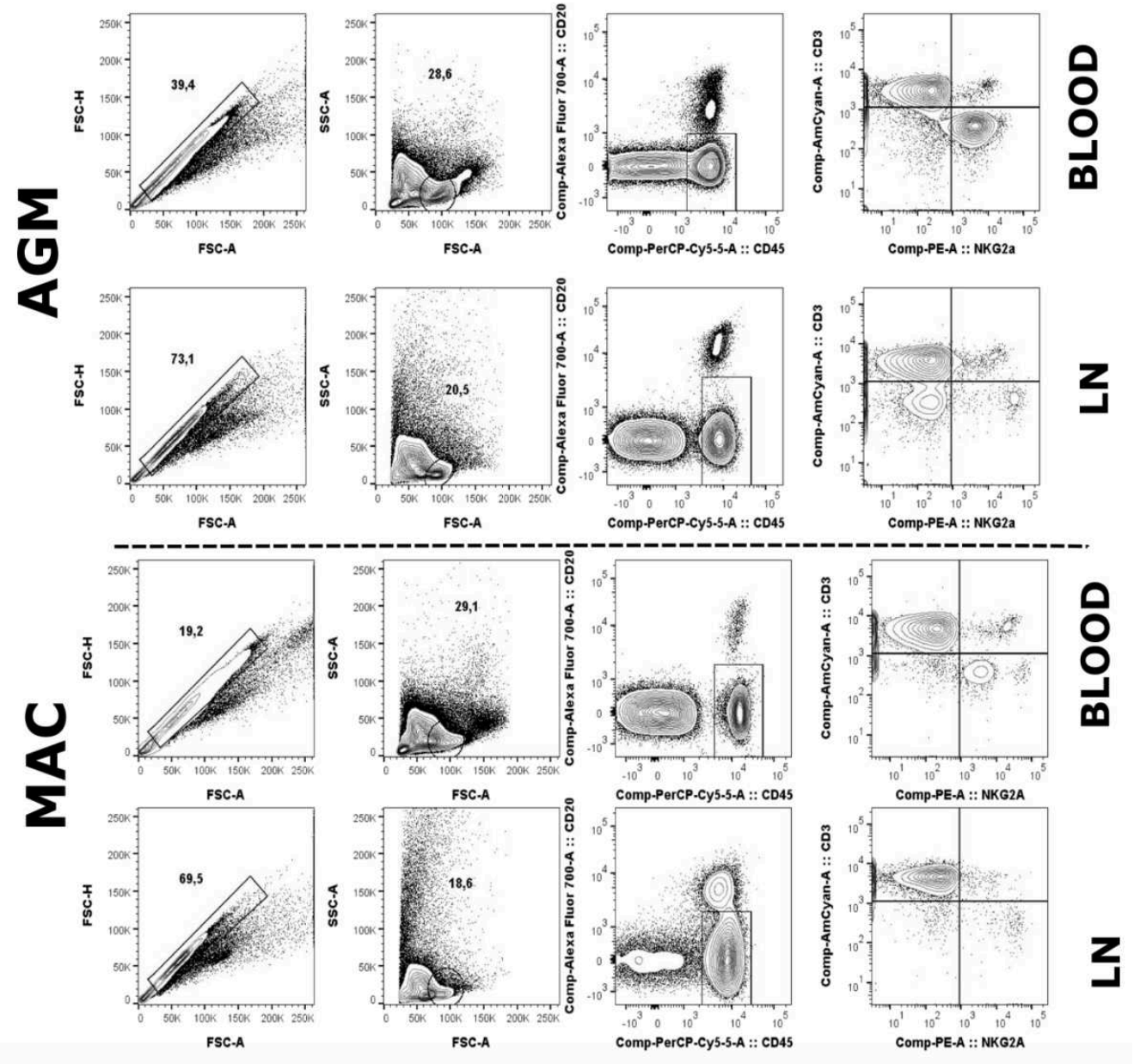
Figure 6. NK cell depletion results in increases of SIV RNA, SIV DNA and productively infected cells in lymph nodes. **(a)** Quantification of $SIVagm.sab_{92018}$ RNA in plasma by qRT-PCR in 5 chronically infected AGM (the same as in Fig.5), before and after anti–IL-15 administration. The grey line represents the viremia levels in individual monkeys over time and the purple line represents the median viremia. The black arrows

show the days of anti–IL-15 administration. **(b)** Quantification of the cell-associated SIV RNA and DNA in LN. The LN of 6 animals without treatment were compared to LN from 5 anti-IL-15 treated monkeys. Each dot represents an individual animal **(c)** Virus-producing cells (SIV RNA, red) in the LN of NK cell-depleted AGM. Representative images of an inguinal LN from five different animals. One image for each of the five anti-IL-15 treated animals is shown. Follicles are delineated by the dashed white lines. Images derived from mounted multiple confocal projected z-scans. Pictures were obtained using a Leica SP8 confocal microscope and processed with ImageJ software. Confocal images were collected with a 40X objective. Tx= anti-IL15 treatment. Nonparametric Mann-Whitney *U*-tests were applied *$p < 0.05$; **$p<0.005$.

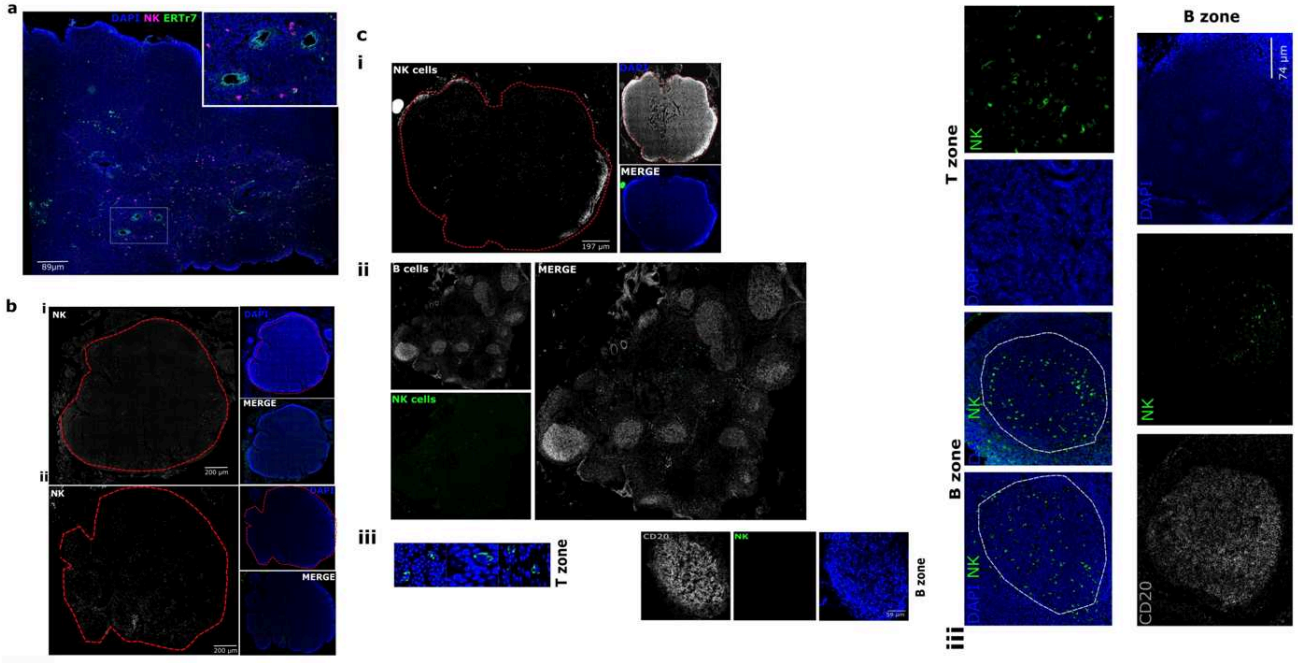


Supplementary Figure 1: Viral load in peripheral blood and lymph nodes from AGM and macaques (**a**) Quantification of SIVmac RNA in plasma in six macaques. (**b**) Quantification of SIVagm RNA in plasma in six AGM. **(c)** Median (interquartile range) values of plasma viral RNA in

the six AGM and six macaques **(d)** Median (interquartile range) values of ca-viral DNA load in peripheral LN of the six AGM and six macaques.

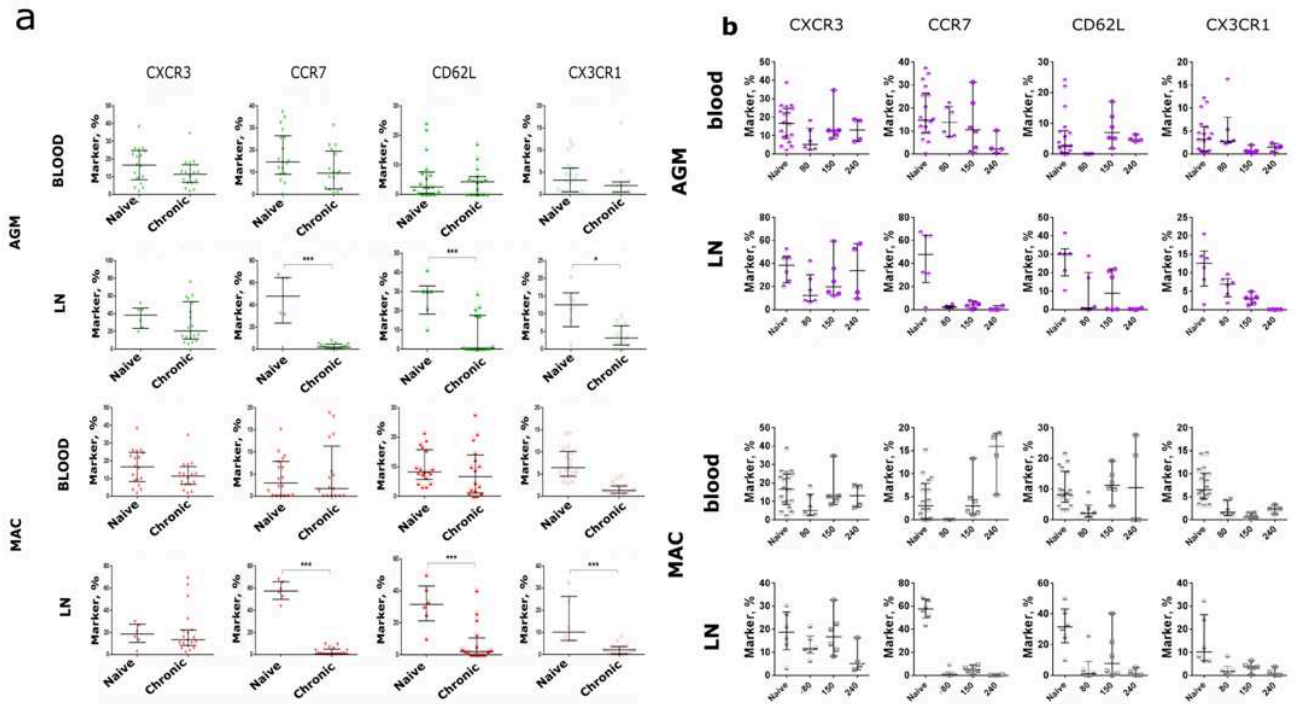


Supplementary Figure 2. Gating strategy for identifying NK cells within blood and lymph nodes from MAC and AGM. Dot plots represent the main steps of the gating strategy that was the same as reported for other NHP studies[35,39]. NK cells were defined by morphology and as $CD45^+$ $CD20^-$ $CD3^-$ $CD4^-$ $NKG2A^+$ $CD8^{+/-}$. NK cells from LN were $CD8^{low/neg}$ in contrast to blood NK cells that were $CD8^+$. NKG2A was identified as the most inclusive NK cell marker in both AGM and macaques, as previously reported[35,39].

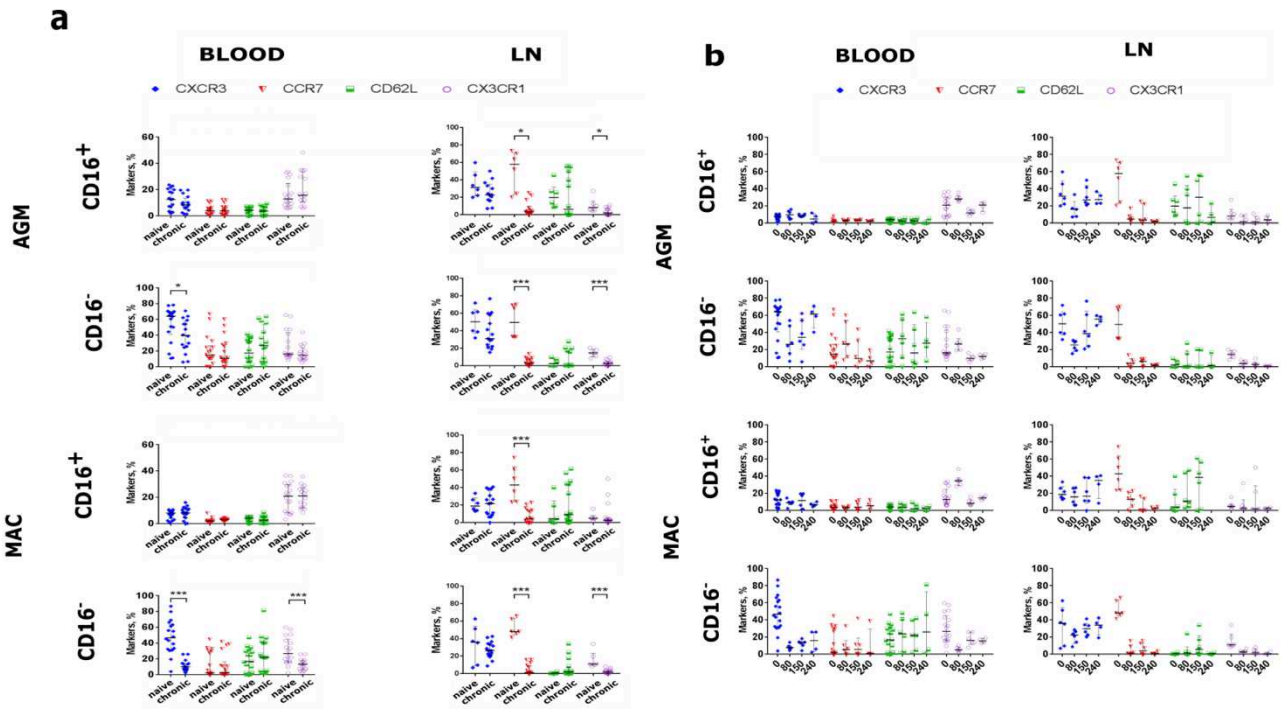


Supplementary Figure 3. Localization of NK cells in lymph nodes. (a) SIV-naive animals. Representative LN tissue section from a SIV-naive macaque, stained with anti-NKG2A (pink) to label NK cells, DAPI (blue) to label nucleus and anti-ER-TR7 (green) to label stromal cells (reticular fibroblasts). The enlarged figure shows NK cells (pink) and high endothelial venules (green). NK cells were mostly located in the medulla and sometimes in the paracortex. The same distribution was observed for NK cells in LN from non-infected AGMs. **(b)** Localization of NK cells in lymph nodes of chronically SIVagm-infected African green monkeys. ***(i+ii)*** Representative LN tissue sections stained with anti NKG2A (white) to label NK cells and with DAPI (blue) to label nucleus of all cells. ***(i)*** Inguinal LN from animal SV083 (AGM) at day 150 p.i. ***(ii)*** Axillary LN from animal SV091 (AGM) at150 day p.i. ***(iii)*** Magnification showing NK cells stained in green, B cells in white and nuclei in blue. Enlargements show examples of NK cells for both the B zone and T zone. NK cells were predominantly localized in the B zones (follicles), showing two types of predominant localization: most of the times they accumulated within follicles and sometimes they accumulated around the follicles (see also Fig.1f). **(c)** Localization of NK cells in lymph nodes of chronically SIVmac-infected macaques. ***(i+ii)*** Representative LN tissue sections stained with anti NKG2A (white) to label NK cells and DAPI (blue) to label nucleus of all cells. (**i**) Inguinal LN section from animal CA275 (macaque) at day 150 p.i. ***(ii)*** Axillary LN section from animal CBB001 (macaque) at 150 days p.i. ***(iii)*** Magnifications showing B cells in white, NK cells in green and cell nuclei in blue. Starting from the acute phase, the distribution of NK cells in LN from SIV-infected macaques was different from that of non-infected animals. While in infected AGM and MAC, NK cells were found

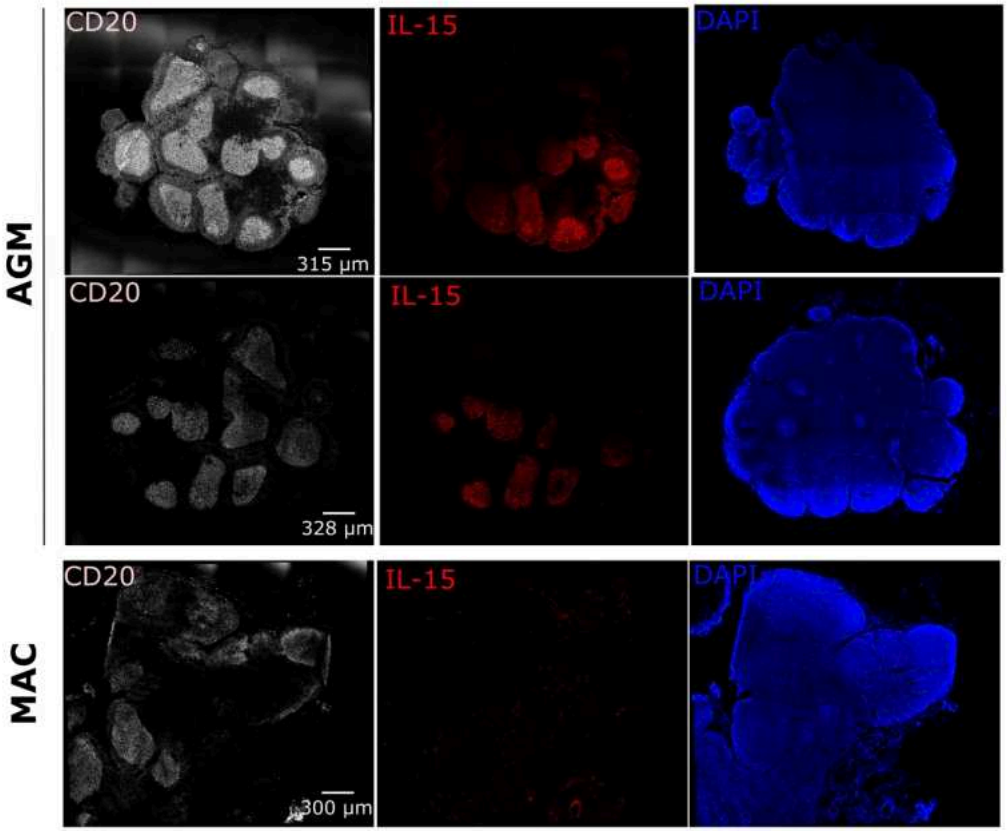
more often outside the medulla than in non-infected animals, NK cells in SIV-infected MAC were randomly distributed in the tissue and did not accumulate in follicles in contrast to SIVagm-infected AGM.



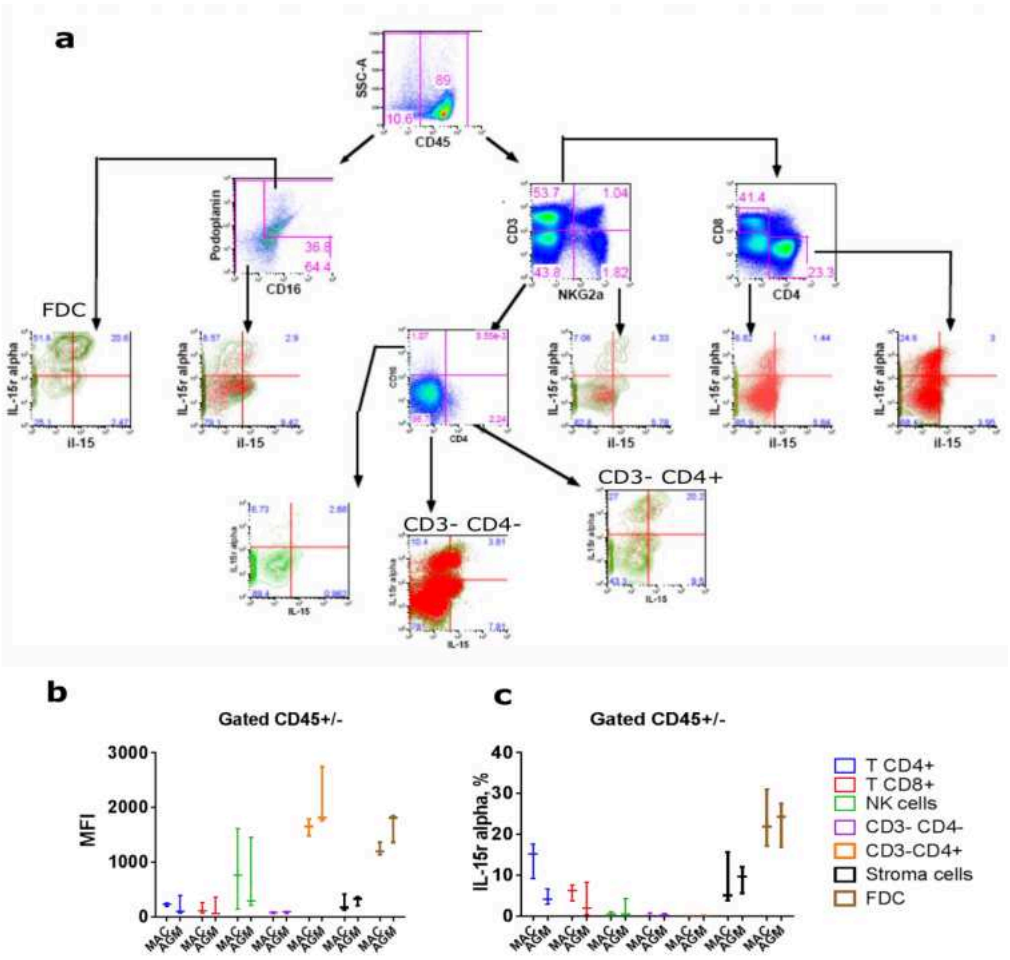
Supplementary Figure 4. Dynamics of lymph node homing markers on blood and lymph node NK cells in response to SIVmac and SIVagm infection. Blood and LN cells were analyzed, respectively, 3 times and one time before infection and 3 times during the chronic phase (days 80, 150, and 250 p.i.) **(a)** The levels of NK cells expressing homing markers were compared in the same animals before and in chronic infection. The values for the six AGM are depicted in green and for the six macaques in red. Statistically significant differences are indicated by asterisks (*p<0.05; ***p<0.001 ;). **(b)** The levels of NK cells expressing homing markers are shown before infection and longitudinally for each time point in chronic infection. The values for the six AGM are depicted in violet and for the six macaques in grey. Median and interquartile range are shown. Nonparametric Mann-Whitney *U*-tests were applied for each panel.



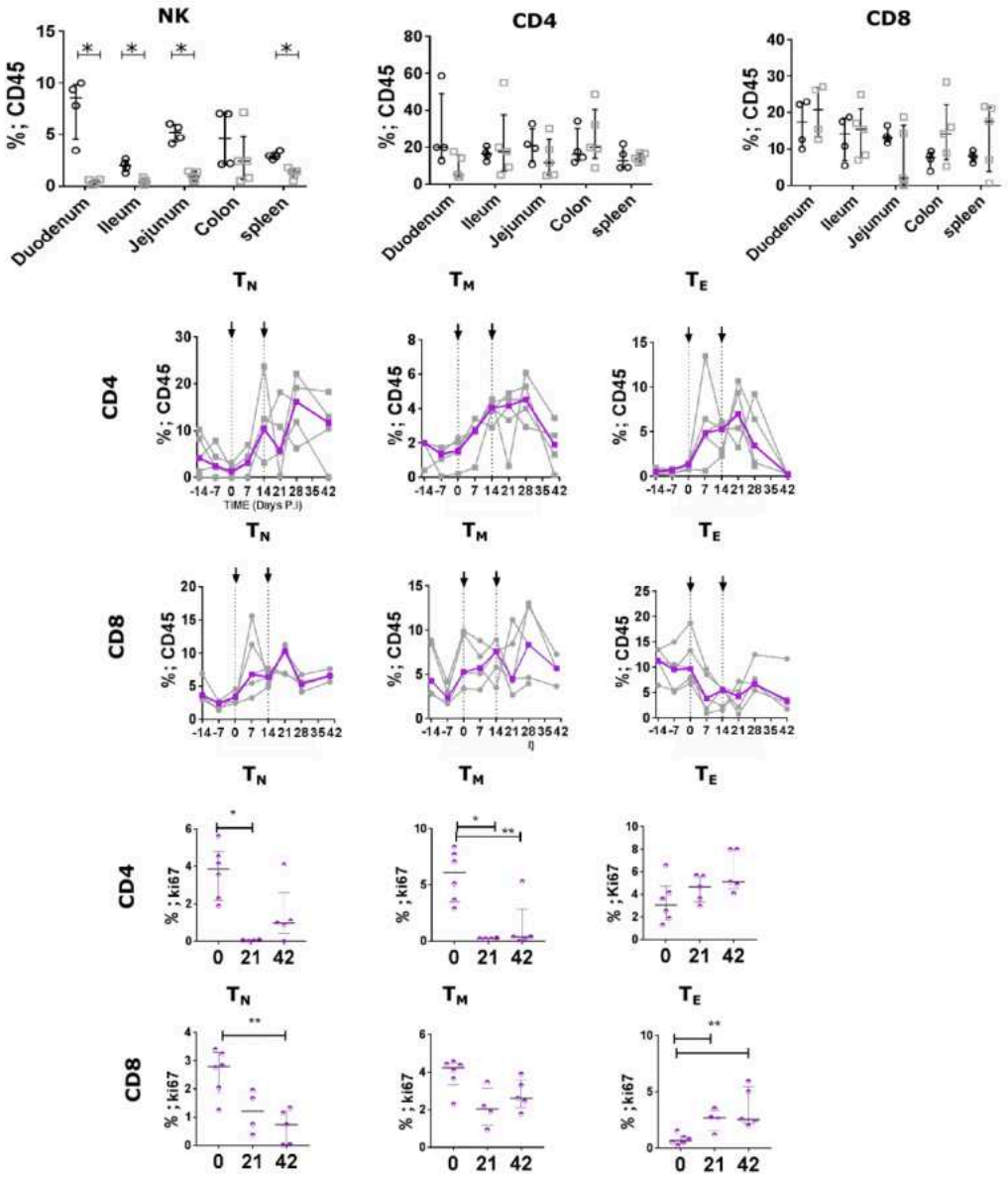
Supplementary Figure 5. Follow up of homing markers on CD16+ and CD16- NK cells in blood and lymph nodes from AGM and MAC before and in chronic SIV infection. Blood and LN cells were analyzed, respectively, 3 times and one time before infection and 3 times during the chronic phase (days 80, 150, and 250 p.i.) from six AGM and six macaques **(a).** The levels of $CD16^+$ and $CD16^-$ NK cells expressing specific homing markers were compared in the same animals before and in chronic infection. **(b)** The levels of CD16+ and CD16- NK cells expressing specific homing markers are shown before infection and for each time point in chronic infection. Nonparametric Mann-Whitney *U*-tests were applied. Statistically significant differences are indicated by asterisks (*** $p<0.001$; * $p<0.05$). Median and interquartile ranges are shown.



Supplementary Figure 6. IL-15 expression in lymph nodes from chronically SIV-infected AGM and macaques. Representative LN tissue sections stained with anti IL-15 (red), CD20 (white) and Dapi (blue). The first two rows at the top show inguinal and axillary LN sections from chronically infected AGM. The third row shows axillary LN section from a chronically infected macaque. More IL-15 staining was observed in AGM. In AGM, IL-15 positive cells were mainly present in follicles. In macaques, IL-15 was weak and IL-15-positive cells were distributed randomly in the LNs.



Supplementary Figure 7. **Representative gating strategy for identifying membrane-bound IL-15 in total lymph node cells from chronically SIV-infected AGM and macaques.** (**a**) Frozen LN cells from chronically SIV-infected animals were used for the analysis. Living cells were identified as Aqua dye-negative. LN cell sup-populations were defined as follows: stromal cells as $CD45^{-}$ $CD16^{-}$ $Podoplanin^{-}$; FDC as $CD45^{-}$ $CD16^{+}$ $Podoplanin^{+}$; CD4 T cells as $CD45^{+}$ $CD3^{+}$ $CD4^{+}$; CD8 T cells as $CD45^{+}$ $CD3^{+}$ $CD8^{+}$; NK cells as $CD45^{+}$ $CD3^{-}$ $NKG2A^{+}$; and two other population as $CD45^{+}$ $CD3^{-}$ $CD8^{-}$ $CD16^{-}$ $NKG2A^{-}$ $CD4^{+/-}$. Positive cells for mbIL-15 were defined when cells were double positive for IL-15 and IL-15Rα. (**b**) Mean of fluorescent intensity of IL-15Rα on the LN cell-subpopulations described above (**c**) Frequency of $IL\text{-}15R\alpha^{+}$ cells in LN cell-subpopulations. Nonparametric Mann-Whitney *U*-tests were applied. Statistically significant differences are indicated by asterisks (*** $p<0.001$; * $p<0.05$). Median and interquartile ranges are shown.



Supplementary Figure 8. Cell phenotypes and frequencies in chronically infected AGM treated with anti IL-15. (top) NK cell, T CD4 cell and T CD8 cell frequencies in tissues from chronically SIVagm-infected AGM without and after anti-IL-15 treatment**.** Tissues (spleen and four gut compartments) were obtained at necropsy. Samples from 4 non-treated (black circles) and five anti–IL-15 treated AGM (grey squares) were available for the analyses. NK cells were significantly depleted in duodenum, ileon, jejunum and spleen, while no significant changes were observed for CD4+ and CD8+ T cells in gut or spleen. **(middle)** Frequencies of each T cell subset within $CD45^+$ cells in blood. Five AGMs were studied. Individual animals are depicted by grey lines and the purple line represents the median values. (**bottom**) Frequencies of Ki-67+ cells for each T cell subset at days 0, 21 and 42 post-treatment. LN from 4 AGM at day 21 and 5 animals at day 42 post-treatment were available. Each circle represents the value of an individual AGM. The black arrows indicate the days

of anti-IL15 administration. T_N: naïve T cells; T_M: central memory T cells; T_E: effector memory T cells. Nonparametric Mann-Whitney *U*-tests were applied. Statistically significant differences are indicated by asterisks (*** $p<0.001$; * $p<0.05$). Median and interquartile ranges are shown.

2. Identification of a soluble factor inducing CXCR5 expression on NK cells

Identification of a soluble factor inducing CXCR5 expression on NK cells

Philippe RASCLE[1,2], Béatrice JACQUELIN[1], Caroline PETITDEMANGE[1], Vanessa CONTRERAS[3], Cyril PLANCHAIS[4,5,6], Marie LAZZERINI[1], Nathalie DEREUDDRE-BOSQUET[3], Hugo MOUQUET[4,5,6], Nicolas HUOT[1] and Michaela MÜLLER-TRUTWIN[1*].

[1]Institut Pasteur, Unité HIV Inflammation and Persistence, Paris, France ;

[2]Université Paris Diderot, Sorbonne Paris Cité, Paris, France ;

[3]CEA, Université Paris Sud 11, INSERM U1184, Immunology of Viral Infections and Autoimmune Diseases, IDMIT, IBFJ, CEA, Fontenay-aux-Roses, France ;

[4]Institut Pasteur, Humoral Response to Pathogens Laboratory, Paris, France;

[5]INSERM U1222, Paris, France;

[6]Vaccine Research Institute, Creteil, France.

Keywords:

*Correspondence :

Michaela Müller-Trutwin,

Institut Pasteur

28 rue du Dr Roux

75724 Paris Cedex 15, France

mmuller@pasteur.fr (Orcid ID: 0000-0002-3854-2396)

Abstract

B cell follicles are one of key site in the maturation of humoral immune responses. They also correspond to a major viral reservoir in HIV-1 infection. African green monkeys (AGM) infected by simian immunodeficiency virus (SIVagm) display a strong, NK-cell mediated viral control in B cell follicles. NK cells in secondary lymphoid organs from SIVagm-infected AGM frequently express CXCR5 in contrast to NK cells from blood and also in contrast to NK cells from humans and macaques infected respectively with HIV-1 and SIVmac. We aimed to identify the mechanism responsible for CXCR5 expression on NK cells. We observed a rapid increase of CXCR5+NK cells in lymph nodes after SIVagm infection concomitant with a progressive decrease of CCR7 on the CXCR5+NK cells. Imaging analyses showed that CXCR5+NK cells accumulated preferentially in follicles with high numbers of proliferating B cells. Cocultures of NK with B cells in transwell chambers induced CXCR5 on NK cells. Transcriptome analysis of CXCR5+NK cells revealed high expression of *Bcl6* and *IL6R*. *IL-6* mRNA was detected in the inter-follicular areas and B cell follicles of lymph nodes during SIVagm infection. IL-6 induced in a dose-dependent manner CXCR5 on NK cells from AGM *in vitro*. IL-6 also up-regulated CXCR5 on NK cells from humans *in vitro*. Our study reveals a novel B-NK cell cross-talk and that IL-6 participates in the induction of CXCR5+NK cells.

Introduction

Natural Killer (NK) cells contribute to the control of viral infections and defense against tumors[1,2,3]. These cells are characterized by a rapid effector response[2,3]. Depending on the strength and combination of multiple possible inhibitor and activator signals, NK cells can be either activated or inhibited[1,2]. Several clinical studies against tumors target the major inhibitor or activator receptors to favorize NK cell effector activities[4,5,6]. However, more information is needed regarding the phenotype and function of NK cells in tissues. For decades it has been appreciated that two major NK cell subsets (CD56bright and CD56dim) exist in humans and have distinct anatomical localization patterns, phenotypes and functions. It has become clear though that the spectrum of human NK cell diversity is broader than originally appreciated[7,8] and that NK cells have the capacity to adapt and also differentiate into long-lived memory cells[9,10,11]. NK cell diversity is influenced by age, history of infections and the tissue micro-environment as proven by the discovery of tissue-resident NK cell developmental intermediates[8,7,12].

Chronic viral infection can durably modulate NK cells toward improved or impaired function[13]. The presence of impaired NK cells in HIV infection were reported early on[14,15]. Similar observations have been made in the nonhuman primate model for HIV, i.e. the macaque infected with SIVmac[14,16,17,18,19,20,21,22]. NK cell modulation therapies are therefore being investigated in the context of HIV cure research[11,23,24]. Assays to improve NK cell-mediated viral control include NK cell-stimulation via IFN-a, TLR9 agonists or IL-15 superagonist associated with antiretroviral (ARV) treatment[25,26,27,28,29,30,31,32]. However, studies on NK cells in tissues during HIV and/or SIVmac infections are scarce, despite the fact that NK cells in blood and tissues show clear phenotypical and functional differences and that the major viral reservoirs reside in tissues. ARV treatment is not able to eradicate the virus during HIV infection. HIV/SIV viruses persist in cellular and anatomical reservoirs, such as in memory CD4+ T cells of the mucosa, in PD-1+ and CTLA4+ CD4+ T cells in the T zone of lymph nodes (LN) and in particular in T_{FH} cells in B cell follicles (BCF) from LNs[33,34]. To progress in therapies targeting NK cells in cancers and chronic viral infections, one must therefore also better understand NK cell trafficking and differentiation in tissues.

In LNs, NK cells are predominantly located in the medulla and paracortex at steady state[35,36]. Upon HIV-1 or SIVmac infection, NK cell numbers were unaltered or diminished in LNs and NK cells displayed a diminished migratory capacity toward LN[37,38]. African nonhuman primates, such as sooty mangabeys or African green monkeys (AGM) have most likely been natural hosts for SIV for over one million years[39]. Once these monkeys are infected by SIV they do not progress to AIDS, despite persistent high viremia[16,40,24]. Natural hosts show a difference in tissue viral distribution as compared to pathogenic HIV-1/SIVmac infections: a robust viral production in the intestine similar to HIV/SIVmac infections but a strong viral control in secondary lymphoid tissues (SLT) with a lack of virus in T_{FH} cells in contrast to HIV-1/SIVmac infections[16,41,42,43,44]. More recently we showed, that in AGMs chronically infected by SIVagm, NK cells accumulate in BCF from peripheral LN and spleen, which was associated with the presence of CXCR5+ NK cells[45]. NK cells present in SLT are at the origin of viral control in SIVagm infection[38]. The presence of CXCR5 on NK cells might allow them to enter into the BCF and exert the viral control in the T_{FH} cells.

It is important to understand how NK cells acquire the capacity to up-regulate CXCR5 and to migrate into BCF. It is important not only in the context of viral infections, but also because NK cells in BCF might contribute to the regulation of humoral responses in other settings. There is indeed evidence of an impact of NK cells on B cell responses[46,47]. CXCR5 expression was previously known for B cells and T_{FH} cells. Pre-T_{FH} cells derive from CXCR5-CD4+T cells after stimulation by dendritic cells (DC) and soluble factors (IL-6/IL-21/IL-27) which induce transcriptional factors including B-cell lymphoma 6 (Bcl-6). Bcl-6 represses other transcriptional factor lineages (T-bet, GATA3, RORγC) and favors expression of IL-21 and CXCR5[48]. These pre-T_{FH} cells co-express CXCR5 and CCR7. CCR7 maintains cells in the T cell zone. Co-expression of CCR7 with CXCR5 on CD4+ T cells leads to migration into the inter-follicular zone[49,50,51]. Here, pre-T_{FH} cells meet B cells and are exposed to activation (CD40L/CD40, MHC-II/TCR-CD4, CD80-CD86/CD28) and auto/paracrine (IL-6/IL-21/IL-27) contact between both cell types, allowing the pre-T_{FH} cells (CCR7+CXCR5+) to switch to T_{FH} cells with a CCR7-CXCR5+ phenotype and enter into BCF[49,50,51]. While the process of CXCR5 induction on T_{FH} and B cells has been well studied[52,49,53] little is currently known about the mechanism of CXCR5 induction on NK cells. Herein, we studied CXCR5 induction mechanism on NK cells by taking advantage of the AGM/SIVagm model.

Results

Early induction of CXCR5+ NK cells in lymph nodes after SIVagm infection and accumulation in activated B cell follicles

We first analyzed the kinetics of appearance of CXCR5+ NK cells shortly after SIVagm infection. To answer this question, we followed CXCR5+ NK cells in peripheral LN (pLN) at days 0, 2, 7, 9, 14 and 28 post-infection (p.i.). The cells were gated as previously reported[38] (Fig.1A, Fig.S1A). Before SIV infection, the median percentage of CXCR5+ NK cells in LN was 3.4% (Fig.1B). After SIVagm infection, the median percentage of CXCR5+ NK cells in the pLN was ranging from 7.7% to 33.1% between days 2 and 28 p.i. (Fig.1B) and thus in a similar range as previously reported for chronic SIVagm infection[38]. During follow up of primary SIVmac infection in macaques (Fig.S1B), there was no such an increase of CXCR5+ NK cells in pLN (Fig.S1C).

To better comprehend the spatial distribution of NK cells in LN during SIVagm infection, we investigated CCR7 expression on the NK cells. We followed CCR7 and CXCR5 expression on NK cells during early SIVagm infection in pLN (Fig.1C, Fig.S1D). Between days 0 and day 14 p.i., the dynamics between CCR7+ and CCR7- CXCR5+ NK cells were similar between the two subpopulations, while at day 28 p.i. the levels of CCR7- CXCR5+ NK cells seemed higher than the CCR7+ CXCR5+ NK cells (Fig.1C). These results suggest that CXCR5+ NK cells progressively increase their capacity to enter into BCF.

In chronic SIVagm infection, NK cells were found either around or inside BCF[38]. We wondered whether the distinct anatomical location of NK cells was related with the activation state of the BCF and whether NK cells would thus show a distinct accumulation profile with regard to primary follicles composed largely of naïve B cells and secondary (activated) BCFs generally characterized by a

germinal center with proliferating B cells[54]. To distinguish between primary from secondary BCF, we stained pLN collected during primary SIVagm infection with Ki-67 to identify proliferating B cells. NK cells localized predominantly inside those BCF which stained strongly positive for Ki-67 (Fig.1D and 1E). Not all Ki-67 positive follicles contained NK cells, but NK cells were preferentially localized inside Ki-67high follicles as compared to Ki-67low follicles. These results altogether suggest that NK cell migration into BCF is a multi-step event, CXCR5 being induced as soon as day 2 p.i. on NK cells, the migration of NK cells into BCF occurring progressively after the viremia peak[38] and when B cells in BCF are strongly proliferating.

Induction of CXCR5+ NK cells by soluble factor(s) produced during contact-independent autologous NK-B cell co-cultures

In order to understand whether there is a causative link between the presence of NK cells in BCF and B cells, we studied if there is a cross-talk between these two cell types. Previous studies already demonstrated direct or indirect effects of NK cells on B cell responses. For instance, human NK cells can induce autologous resting B cells to synthesize Ig[55]. Herein, we investigated if there is a direct impact of B cells on NK cells, in particular on CXCR5 expression. First, we analyzed the degree of proximity between NK and B cells inside the pLN of SIVagm-infected AGM. We observed multiple zones of possible direct contact between NK and B cells *in situ*, both in the inter-follicular areas around BCF and inside BCF (Fig.2A). Then, to further address the potential interactions, NK and B cells were isolated from blood of uninfected AGMs and co-cultured. Potential contacts between NK and B cells were analyzed at 2 days of co-culture. Close proximity between B and NK cell membranes was often observed (Fig.2B and S2A). Altogether, this confirms that NK and B cells can get in close contact.

NK and B cells from uninfected AGMs were then cultured during 6 days in different conditions: (i) NK cells alone, (ii) B cells alone, (iii) NK cells co-cultured with autologous B cells and (iv) NK cells co-cultured with autologous B cells separated in transwell chambers allowing no contact and letting pass through only soluble factors. We first analyzed the phenotype of the B cells in the cultures. We did not observe statistically significant changes (Fig.2C). We also cultured macaque NK cells with autologous B cells. IgG+ B memory cell increased in the transwell condition (Fig.S2B). We then analyzed the NK cells. The frequency of CD16+ NK cells increased in the co-cultures with B cells (Fig.2D). There was a trend for increase in NK cell activity, as measured by Granzyme B, IFN-g and/or IL-10 production in AGM and macaque NK cells co-cultured with B cells (Fig.2D, Fig.S2C).

We then measured CXCR5 expression on NK cells (Fig.S2D). The frequency of CXCR5+ NK cells was clearly increased in the co-cultures with B cells, as compared to NK cells cultured alone (Fig.S2D), both for AGM (Fig.3A, 3B and S3B) and macaque cells (Fig.S3A). The frequencies of CXCR5+NK cells in the cultures were in a similar range as CXCR5+NK cell levels in SIVagm infection *ex vivo* (Fig. S1A). However, CXCR5+NK cell levels were increased only in transwell condition, but not in cultures allowing contact (Fig.S2D, Fig.3A, Fig.S3A). These results indicate the presence of one or more soluble factor(s) produced during the co-culture of NK and B cells and which induces CXCR5 expression on NK cells. To address this, we cultured NK cells from SIV-negative AGM with supernatants from different culture conditions and analyzed after two days of culture the levels of CXCR5+ NK cells. The supernatant from NK and B cells cultured in transwell chambers induced CXCR5 expression on NK cells (Fig.3C, Fig.S3C). In contrast, the supernatants of NK and B

cells cultured together and the supernatant of B cells cultured alone did not change the levels of CXCR5+ NK cells (Fig.3C). Altogether, these data show that a contact-independent cross-talk between NK and B cells induces the secretion by B and/or NK cells of one or more soluble factor(s) which induces CXCR5 expression on NK cells.

CXCR5+ NK cells expressed high levels of IL-6 Receptor

We searched to determine the identity this soluble factor(s). For that, we analyzed the signaling pathways that are active in CXCR5+ NK cells present in pLN of SIVagm-infected AGM. We used RNAseq to map the transcriptional profile of the CXCR5+ NK cell subpopulation compared to the major NK cell population present in LN. The latter corresponds to CD45+CD3-NKG2A^{high}CD16- NK cells (Fig.S3E). We analyzed the expression profiles of genes coding for transcription factors, cytokines and cytokine-receptors (Fig.3D-F) (Supplementary Table 4). *Bcl-6* was highly expressed in CXCR5+ NK cells (Fig.3D). Among the cytokine-receptors showing high levels of expression in CXCR5+ NK cells were the colony stimulating factor 2 receptor alpha subunit (CSF2RA/B) coding for the GM-CSF receptor, IFNGR2, IL-6R, IL-15RA and IL21R (Fig.3E). CXCR5+ NK cells also expressed high levels of *IL-27, IL-6* and *LAMP1* (CD107a) and low levels of *IFN-g* and *IL-4* (Fig.3F). Previous studies have identified IL-6, IL-21 and IL-27 as major soluble factors at the origin of upregulation of CXCR5 on CD4+ T cells[49,50,51,56,57,58]. *IL6 receptor* was expressed more strongly on CXCR5+ NK cells than other receptors such as *IL-27R* (Fig.3E). Altogether, the CXCR5+NK cells expressed high levels of *bcl-6*, similar to what is known for the CXCR5-expressing T_{FH} lineage[59]. CXCR5+NK cells also expressed high levels of the *IL-6 Receptor*, suggesting that IL-6 might be one of the factors involved in CXCR5 up-regulation on NK cells.

IL-6 induced CXCR5 expression on NK cells *in vitro*

We evaluated if B cells in our cultures produce IL-6. Intra-cellular IL-6 was measured in B cells cultured alone in the same condition as described above (Fig.2C). A median of 24.5% B cells cultured alone were IL-6 positive (Fig. 4A). In order to define the level of IL-6 production *ex vivo*, we measured intracellular IL-6 in B cells from blood of uninfected and SIVagm-infected AGM. Median levels of 2.5% IL-6+ B cells were observed *ex vivo* (Fig.4A). This indicates a strong enrichment of IL-6 production by B cells in our culture condition.

In order to study the impact of IL-6 on CXCR5 expression on NK cells, we cultured NK cells from blood of uninfected AGM alone in the presence of IL-6. IL-6 induced dose-dependent increases of CXCR5+ NK cell levels (Fig.4B). In contrast, GM-CSF, which similar to IL-6 is known to be also produced by B cells[60,61] and whose receptor is highly expressed on CXCR5+ NK cells, did not induce any change in CXCR5+ NK cell levels in our culture condition (Fig.4B). We tested if the cytokines used in the culture medium (IL-2, IL-4, IL-15) alone or combined impact CXCR5 expression on NK cells and observed no impact (Fig.S3D). We investigated the IL-6 effect on NK cells from macaques and humans. We observed for human NK cells an upregulation of NK cells expressing CXCR5 when compared to NK cells cultured without IL-6 but not for MAC NK cells (Fig.4C). The fold increase of human CXCR5+NK cells was comparable to that observed with AGM cells (Fig. 4B and 4C). Therefore, we showed that IL-6 induced CXCR5 on AGM and human NK cells.

IL-6 expression *in vivo* in pLN during acute SIVagm infection

We addressed the question if IL-6 could be relevant *in vivo* during SIVagm infection regarding the induction of CXCR5+ NK cells. IL-6 is known to be increased in HIV-1 and SIVmac infections in plasma of untreated individuals and higher levels of IL-6 in plasma are associated with chronic inflammation and disease progression[62]. In contrast, in SIVagm infection, IL-6 is not increased in plasma[45,63,64]. Since CXCR5+ NK cells have been detected in LN but not in blood of SIVagm-infected AGM, we therefore evaluated whether IL-6 could be locally produced in pLN using *in situ* analysis by microscopy. We analyzed pLN during acute SIVagm infection and detected a local expression of *IL*-6 mRNA in pLN (Fig.4D-E). Cells expressing *IL-6* were detected both in BCF and in the T zone. In the inter-follicular area, foci *of IL*-6 mRNA expression were present. While B cells expressing *IL-6* were detected, for example in BCF, most of cells expressing *IL-6* in inter-follicular regions were not B cells (Fig.4E and 4D). NK cells could be detected in the same regions as *IL-6* mRNA positive cells (Fig.4D).

We analyzed IL-6 expression also in pLN of acutely SIVmac-infected macaques. Moderate levels of IL-6 mRNA were observed both in the T zone and in BCFs of pLN, similarly to acute SIVagm infection (Fig.S3F). However, we did not observe clusters of strong IL-6 mRNA expression in inter-follicular areas in contrast to SIVagm infection. Therefore, we detected local production of IL-6 mRNA in pLN during acute SIVagm and SIVmac infections and, in particular in the inter-follicular areas during SIVagm infection.

In order to quantify protein IL-6 production in pLN, we measured IL-6 in the supernatants of total cells from pLN collected before and during SIVagm infection. The protein levels of IL-6 did not change over time during SIVagm infection in AGM and also did not change for macaques during SIVmac infection (Fig.4F and Fig.S3G).

DISCUSSION

Here we investigated the mechanism at the origin of CXCR5 expression on NK cells. We determined the *in vivo* kinetics of CXCR5+ NK cell appearance *in vivo* in pLN in response to SIV infection. Our data indicate that CXCR5+CCR7- NK cells are induced progressively in pLN during acute SIVagm infection. These CXCR5+ NK cells isolated from pLN displayed similarities in their transcription factor profiles with T_{FH} cells as they expressed high levels of the *Bcl-6* transcription factor while low levels of *T-bet*, *Gata-3* and *RORC* when compared to other NK cells in pLN. We identified a soluble factor, IL-6, that by its own is capable of CXCR5 induction on NK cells from AGM and humans.

IL-6 production can increase by classical activation of B cell and/or by adding SIV on B cells[65,66,67]. We showed that NK cells preferentially accumulate in secondary follicles, i.e. follicles with high levels of proliferating B cells. These proliferative B cells might produce more IL-6 than the naïve B cells in primary follicles. We show that both in our *in vitro* culture conditions and *in vivo* in pLN, B cells expressed IL-6. We observed IL-6 expression in inter-follicular areas and also in BCF of pLN during acute SIVagm infection. We showed that NK and B cells can be in close proximity in these areas. It is possible that IL-6 produced by activated B cells in the inter-follicular area up-regulate

CXCR5 on NK cells which then enter into the BCFs. It is not mutually exclusive that IL-6 production in the pLN during SIV infection is also due to other cells, such as dendritic cells (DC). Indeed, many IL-6+ cells were neither B nor NK cells in the analyzed pLN. Dendritic cells are well-known to cross-talk with NK cells[68,69] and also to participate in the induction of CXCR5+ pre-T_{FH} cells[52,49,53]. DCs are also able to produce IL-6 and can be a major source of IL-6 in LN in some settings[70,71,72]. It is possible that DC in the T zone and B cells in the BCF are the major sources of IL-6 in the pLN during SIVagm infection.

We observed in CXCR5+ NK cells an upregulation of several cytokine receptors, in particular GM-CSF receptors (CSF2RA/B), IFNGR and IL-6R as compared to the main NK cell population in pLN of SIVagm-infected animals. The respective cytokines GM-CSF and IFN-g were not up-regulated and GMC-SF did not induce CXCR5 expression on NK cells. In contrast, IL-6 not only induced CXCR5 expression on NK cells but the CXCR5+ NK cells also expressed IL-6. Thus, there might be a mechanism of autocrine regulation for IL-6 in the CXCR5+ NK cell population. We observed NK cells predominantly in the BCF with proliferating B cells. We also have previously shown that NK cells accumulated preferentially inside those BCF where follicular dendritic cells (FDC) presented high levels of membrane-bound IL-15[38]. Such IL-15 is known to augment B cell proliferation in germinal centers[73] and could concomitantly augment the survival of the CXCR5+NK cells in BCF.

In SIVmac infection, we could not observe increases of CXCR5+ NK cells in pLN during acute SIV infection *in vivo*. This is in line with previous data in chronic SIVmac infection[38]. The reasons might be multiple. Since plasma IL-6 is increased in SIVmac and not in SIVagm infection, the lack of CXCR5+ NK cells in macaques during SIV infection is unlikely due to lower systemic levels of IL-6. However, only in SIVagm but not in SIVmac infection, we detected foci of strong IL-6 mRNA in T zone areas of the pLN. The lack of CXCR5+ NK cells in macaques might be explained by the need of high concentrations of IL-6 as observed in the inter-follicular areas during SIVagm infection and that were lacking in SIVmac infection. SIV infection considerably modifies dendritic cells, B cells and cytokine profiles in LN[56]. Multiple differences have been described between SIVmac and SIVagm infections regarding the micro-environment and/or maturation state of myeloid cells[45,74]. We cannot exclude that IL-6 production by DC in LN is different between AGM and MAC during SIV infection. However, the IL-6 protein levels measured in supernatants of total pLN cells did not differ between SIVagm and SIVmac infections. It could be that the method used here did not accurately reflect the *in vivo* production of total IL-6, because the protocol used to isolate LN cells is adapted for lymphocytes (B and NK cells) but not for obtaining DC[75]. The IL-6 production by DC in pLN could thus have been underestimated by the method used here. It could also be that the type of cells producing IL-6 and/or the location of the IL-6 producing cells are more important than the overall IL-6 concentrations in the pLN. Indeed, the anatomical distribution of IL-6 producing cells in pLN was distinct between SIVagm and SIVmac infections. Alternatively, NK cells from macaques might be less susceptible to IL-6 for other reasons such as a distinct differentiation stage in response to SIV infection, lower expression of IL6R and/or low levels of STAT3[76]. Indeed, *in vitro*, IL-6 induced CXCR5 on NK cells from AGM and humans but not on NK cells from macaques. However, the co-cultures of B cells with autologous NK cells from macaques induced CXCR5+ NK cells in transwell condition, which could indicate that IL-6 alone was not sufficient for macaque cells to induce CXCR5. Macaque NK cells might need additional stimuli. Such stimuli were probably present in the supernatants of the transwell co-

cocultures. Altogether the data show that CXCR5+ NK cells can be induced for MAC depending on the conditions.

The observation that CXCR5+ NK cells were induced in culture with supernatants from NK-B cell co-cultures (both for AGM and macaques) clearly provides evidence for a cross-talk between NK and B cells. The impact of the cross-talk on CXCR5+ NK cell levels might be explained by higher levels of IL-6 in the co-cultures, by the presence of eventual co-factors secreted by NK cells and/or B cells after co-culture, and/or a higher susceptibility of NK cells to IL-6 (such as for example IL6R expression) after co-culture with B cells in transwell conditions. Among the other cytokines known to participate in the induction of CXCR5 on CD4+T cells, are IL-21 and IL-27. It is possible that these cytokines or other soluble factors also play a role in CXCR5 up-regulation in NK cells.

There was a higher impact on CXCR5 up-regulation when adding supernatants from NK-B cell co-cultures than with supernatants from B cells cultured alone. While we did not see a statistically significant increase in CXC5+NK cell levels after culture with supernatants of B cells cultured alone, we cannot exclude a minor CXCR5 induction if we would have studied more animals. Of note, CXCR5+ NK cells were induced in the transwell chambers but not or less in the co-cultures allowing contact between NK and B cells. The fact that contact between NK cells and B cells was not necessary to induce CXCR5 demonstrated that CXCR5 on the NK cells was not acquired by trogocytosis. There could be several reasons why the contact inhibited CXCR5+ NK cell induction. The IL-6 production might have been lower for unknown reasons. Also, there was a trend for NK cells to up-regulate Granzyme B in the cultures with contact to B cells but not in the transwell chambers. It is thus conceivable that NK cells killed activated B cells producing IL-6 in the co-cultures.

The analysis of transcription factors revealed that Bcl-6 was upregulated in the CXCR5+ NK cells. BCL6 expression in T_{FH} cells is known to upregulate CXCR5, ICOS, PD1, IL-21R, IL-6R and to repress CCR7[77]. Surprisingly, the expression *PRDM1* was also upregulated in the CXCR5+ NK cells[78]. PRDM1 encodes B lymphocyte-induced maturation protein-1 (Blimp1)[79,80]. Blimp1 is an antagonist of Bcl-6 in B and T lymphocytes, however, in NK cells the interaction of Blimp1 with Bcl-6 is indeed distinct from B and T lymphocytes[78]. In human NK cells, Blimp1 is associated with Granzyme B expression and represses IFN-γ, TNF-α, and TNF-β production. In contrast to *blimp1* expression, the expressions of *RORC*, *t-bet*, *gata-3* and *EOMES* were downregulated in the CXCR5+ NK cells when compared to the predominant NK cell population in pLN of SIVagm-infected animals. This observation is in line with the literature regarding Bcl-6 and the capacity of this transcriptional factor to repress the other transcriptional factors in T_{FH} cells[81]. We also observed a lower expression of IL-2 receptors (IL2RA/B/G) which reminds GC-T_{FH} cells, for which it is known that the IL-6 pathway induction is leading to decreased IL-2 receptor expression[82]. We therefore observed major similarities between NK and T_{FH} cells in the transcriptional profiles that may lead to CXCR5 expression.

Knowledge on the mechanism regulating CXCR5 expression in NK cells was scarce. This study contributes to elucidate CXCR5 induction on NK cells. These novel insights can be of interest for efforts aiming at directing NK cells into BCF during HIV infections. They might also be of general relevance for other infections. IL-6 for instance is produced in elevated levels in SARS-Cov2 infections[83]. IL-6 is also produced in response to vaccinations[84,85]. Little attention has been given to CXCR5+ NK cells[86,76] and to NK cells in LN in general. More knowledge is needed on these cells in lymphoid tissues in distinct settings and on their potential influence on B cell responses. Indeed, B cell

responses might be under influence of NK cells during immunization strategies[87,88]. And vice-versa, activated B cells could influence NK cell responses. We show here for instance increases of CD16+NK cells after co-culture with B cells and the preferential presence of NK cells in BCF containing high levels of proliferating B cells during SIVagm infection.

In conclusion, we deliver here key elements for understanding how CXCR5+ NK cells are induced. Our studies underline the potential multiple interactions between NK and B cells in lymph nodes that deserve further attention. We provide novel evidence for a cross-talk between NK cells and B cells and, importantly, describe an interaction between IL-6 producing cells and NK cells that could be relevant also in other infections and for vaccine studies.

REFERENCES

1. Choucair, K. *et al.* Natural killer cells: a review of biology, therapeutic potential and challenges in treatment of solid tumors. *Future Oncol.* **15**, 3053–3069 (2019).
2. van Erp, E. A., van Kampen, M. R., van Kasteren, P. B. & de Wit, J. Viral Infection of Human Natural Killer Cells. *Viruses* **11**, 243 (2019).
3. Vivier, E. *et al.* Innate or adaptive immunity? The example of natural killer cells. *Science* **331**, 44–49 (2011).
4. Khan, M., Arooj, S. & Wang, H. NK Cell-Based Immune Checkpoint Inhibition. *Front. Immunol.* **11**, (2020).
5. Wagner, J. *et al.* A Two-Phase Expansion Protocol Combining Interleukin (IL)-15 and IL-21 Improves Natural Killer Cell Proliferation and Cytotoxicity against Rhabdomyosarcoma. *Front. Immunol.* **8**, (2017).
6. Di Vito, C. *et al.* NK cells to cure cancer. *Semin. Immunol.* **41**, 101272 (2019).
7. Strauss-Albee, D. M. & Blish, C. A. Human NK Cell Diversity in Viral Infection: Ramifications of Ramification. *Front. Immunol.* **7**, (2016).
8. Strauss-Albee, D. M. *et al.* Human NK cell repertoire diversity reflects immune experience and correlates with viral susceptibility. *Sci. Transl. Med.* **7**, 297ra115-297ra115 (2015).
9. Paust, S., Blish, C. A. & Reeves, R. K. Redefining Memory: Building the Case for Adaptive NK Cells. *J. Virol.* **91**, (2017).
10. Pahl, J. H. W., Cerwenka, A. & Ni, J. Memory-Like NK Cells: Remembering a Previous Activation by Cytokines and NK Cell Receptors. *Front. Immunol.* **9**, (2018).
11. Flórez-Álvarez, L., Hernandez, J. C. & Zapata, W. NK Cells in HIV-1 Infection: From Basic Science to Vaccine Strategies. *Front. Immunol.* **9**, (2018).
12. Freud, A. G., Mundy-Bosse, B. L., Yu, J. & Caligiuri, M. A. The Broad Spectrum of Human Natural Killer Cell Diversity. *Immunity* **47**, 820–833 (2017).
13. Hammer, Q. *et al.* Peptide-specific recognition of human cytomegalovirus strains controls adaptive natural killer cells. *Nat. Immunol.* **19**, 453–463 (2018).
14. Giavedoni, L. D., Velasquillo, M. C., Parodi, L. M., Hubbard, G. B. & Hodara, V. L. Cytokine Expression, Natural Killer Cell Activation, and Phenotypic Changes in Lymphoid Cells from Rhesus Macaques during Acute Infection with Pathogenic Simian Immunodeficiency Virus. *J. Virol.* **74**, 1648–1657 (2000).

15. Mavilio, D. *et al.* Natural killer cells in HIV-1 infection: Dichotomous effects of viremia on inhibitory and activating receptors and their functional correlates. *Proc. Natl. Acad. Sci.* **100**, 15011–15016 (2003).
16. Huot, N., Bosinger, S. E., Paiardini, M., Reeves, R. K. & Müller-Trutwin, M. Lymph Node Cellular and Viral Dynamics in Natural Hosts and Impact for HIV Cure Strategies. *Front. Immunol.* **9**, (2018).
17. LaBonte, M. L., McKay, P. F. & Letvin, N. L. Evidence of NK cell dysfunction in SIV-infected rhesus monkeys: Impairment of cytokine secretion and NKG2C/C2 expression. *Eur. J. Immunol.* **36**, 2424–2433 (2006).
18. Schafer, J. L., Li, H., Evans, T. I., Estes, J. D. & Reeves, R. K. Accumulation of Cytotoxic CD16+ NK Cells in Simian Immunodeficiency Virus-Infected Lymph Nodes Associated with In Situ Differentiation and Functional Anergy. *J. Virol.* **89**, 6887–6894 (2015).
19. Maria, A. D. *et al.* The impaired NK cell cytolytic function in viremic HIV-1 infection is associated with a reduced surface expression of natural cytotoxicity receptors (NKp46, NKp30 and NKp44). *Eur. J. Immunol.* **33**, 2410–2418 (2003).
20. Costanzo, M. C. *et al.* Transcriptomic signatures of NK cells suggest impaired responsiveness in HIV-1 infection and increased activity post-vaccination. *Nat. Commun.* **9**, 1212 (2018).
21. Alter, G. *et al.* Sequential deregulation of NK cell subset distribution and function starting in acute HIV-1 infection. *Blood* **106**, 3366–3369 (2005).
22. Mikulak, J., Oriolo, F., Zaghi, E., Vito, C. D. & Mavilio, D. Natural killer cells in HIV-1 infection and therapy. *Aids* **31**, 2317–2330 (2017).
23. Peppa, D. Entering a new era of harnessing natural killer cell responses in HIV infection. *EBioMedicine* **44**, 26–27 (2019).
24. Saez-Cirion, A., Jacquelin, B., Barré-Sinoussi, F. & Müller-Trutwin, M. Immune responses during spontaneous control of HIV and AIDS: what is the hope for a cure? *Philos. Trans. R. Soc. B Biol. Sci.* **369**, 20130436 (2014).
25. Davenport, M. P. *et al.* Functional cure of HIV: the scale of the challenge. *Nat. Rev. Immunol.* **19**, 45–54 (2019).
26. Vibholm, L. *et al.* Short-Course Toll-Like Receptor 9 Agonist Treatment Impacts Innate Immunity and Plasma Viremia in Individuals With Human Immunodeficiency Virus Infection. *Clin. Infect. Dis.* **64**, 1686–1695 (2017).
27. Jost, S. *et al.* CD4+ T-Cell Help Enhances NK Cell Function following Therapeutic HIV-1 Vaccination. *J. Virol.* **88**, 8349–8354 (2014).

28. Parsons, M. S., Chung, A. W. & Kent, S. J. Importance of Fc-mediated functions of anti-HIV-1 broadly neutralizing antibodies. *Retrovirology* **15**, 58 (2018).
29. Kumar, R., Qureshi, H., Deshpande, S. & Bhattacharya, J. Broadly neutralizing antibodies in HIV-1 treatment and prevention. *Ther. Adv. Vaccines Immunother.* **6**, 61–68 (2018).
30. van Hall, T. *et al.* Monalizumab: inhibiting the novel immune checkpoint NKG2A. *J. Immunother. Cancer* **7**, 263 (2019).
31. Papasavvas, E. *et al.* NK Response Correlates with HIV Decrease in Pegylated IFN-α2a–Treated ART-Suppressed Subjects. *J. Immunol.* (2019) doi:10.4049/jimmunol.1801511.
32. Garrido, C. *et al.* Interleukin-15-Stimulated Natural Killer Cells Clear HIV-1-Infected Cells following Latency Reversal Ex Vivo. *J. Virol.* **92**, (2018).
33. Vanhamel, J., Bruggemans, A. & Debyser, Z. Establishment of latent HIV-1 reservoirs: what do we really know? *J. Virus Erad.* **5**, 3–9.
34. Kuo, H.-H. & Lichterfeld, M. Recent progress in understanding HIV reservoirs. *Curr. Opin. HIV AIDS* **13**, 137–142 (2018).
35. Bajénoff, M. *et al.* Natural killer cell behavior in lymph nodes revealed by static and real-time imaging. *J. Exp. Med.* **203**, 619–631 (2006).
36. Ferlazzo, G. & Carrega, P. Natural killer cell distribution and trafficking in human tissues. *Front. Immunol.* **3**, (2012).
37. Luteijn, R. *et al.* Early viral replication in lymph nodes provides HIV with a means by which to escape NK-cell-mediated control. *Eur. J. Immunol.* **41**, 2729–2740 (2011).
38. Huot, N. *et al.* Natural killer cells migrate into and control simian immunodeficiency virus replication in lymph node follicles in African green monkeys. *Nat. Med.* **23**, 1277–1286 (2017).
39. Wertheim, J. O. & Worobey, M. A Challenge to the Ancient Origin of SIVagm Based on African Green Monkey Mitochondrial Genomes. *PLOS Pathog.* **3**, e95 (2007).
40. Garcia-Tellez, T. *et al.* Non-human primates in HIV research: Achievements, limits and alternatives. *Infect. Genet. Evol.* **46**, 324–332 (2016).
41. Estes, J. D. Pathobiology of HIV/SIV-associated changes in secondary lymphoid tissues. *Immunol. Rev.* **254**, 65–77 (2013).
42. Zeng, M. *et al.* Cumulative mechanisms of lymphoid tissue fibrosis and T cell depletion in HIV-1 and SIV infections. *J. Clin. Invest.* **121**, 998–1008 (2011).
43. Diop, O. *et al.* High Levels of Viral Replication during Primary Simian Immunodeficiency Virus SIVagm Infection Are Rapidly and Strongly Controlled in African Green Monkeys. *J. Virol.* **74**, 7538–47 (2000).

44. Gueye, A. *et al.* Viral load in tissues during the early and chronic phase of non-pathogenic SIVagm infection. *J. Med. Primatol.* **33**, 83–97 (2004).
45. Jacquelin, B. *et al.* Innate Immune Responses and Rapid Control of Inflammation in African Green Monkeys Treated or Not with Interferon-Alpha during Primary SIVagm Infection. *PLOS Pathog.* **10**, e1004241 (2014).
46. Gao, N. *et al.* Receptors and Counterreceptors Involved in NK-B Cell Interactions. *J. Immunol.* **174**, 4113–4119 (2005).
47. Bradley, T. *et al.* RAB11FIP5 Expression and Altered Natural Killer Cell Function Are Associated with Induction of HIV Broadly Neutralizing Antibody Responses. *Cell* **175**, 387-399.e17 (2018).
48. Kroenke, M. A. *et al.* Bcl6 and Maf Cooperate To Instruct Human Follicular Helper CD4 T Cell Differentiation. *J. Immunol.* **188**, 3734–3744 (2012).
49. Eivazi, S. *et al.* Development of T follicular helper cells and their role in disease and immune system. *Biomed. Pharmacother. Biomedecine Pharmacother.* **84**, 1668–1678 (2016).
50. Wu, H. *et al.* Molecular Control of Follicular Helper T cell Development and Differentiation. *Front. Immunol.* **9**, (2018).
51. Chavele, K.-M., Merry, E. & Ehrenstein, M. R. Cutting Edge: Circulating Plasmablasts Induce the Differentiation of Human T Follicular Helper Cells via IL-6 Production. *J. Immunol.* (2015) doi:10.4049/jimmunol.1401190.
52. Rao, D. A. T Cells That Help B Cells in Chronically Inflamed Tissues. *Front. Immunol.* **9**, (2018).
53. Suh, W.-K. Life of T Follicular Helper Cells. *Mol. Cells* **38**, 195–201 (2014).
54. Phan, T. G., Gray, E. E. & Cyster, J. G. The microanatomy of B cell activation. *Curr. Opin. Immunol.* **21**, 258–265 (2009).
55. Blanca, I. R., Bere, E. W., Young, H. A. & Ortaldo, J. R. Human B Cell Activation by Autologous NK Cells Is Regulated by CD40-CD40 Ligand Interaction: Role of Memory B Cells and CD5+ B Cells. *J. Immunol.* **167**, 6132–6139 (2001).
56. Moukambi, F. *et al.* Mucosal T follicular helper cells in SIV-infected rhesus macaques: contributing role of IL-27. *Mucosal Immunol.* **12**, 1038–1054 (2019).
57. Ma, C. S., Deenick, E. K., Batten, M. & Tangye, S. G. The origins, function, and regulation of T follicular helper cells. *J. Exp. Med.* **209**, 1241–1253 (2012).
58. de Wit, J. *et al.* Human B cells promote T-cell plasticity to optimize antibody response by inducing coexpression of T(H)1/T(FH) signatures. *J. Allergy Clin. Immunol.* **135**, 1053–1060 (2015).

59. Liu, X. *et al.* Bcl6 expression specifies the T follicular helper cell program in vivo. *J. Exp. Med.* **209**, 1841–1852 (2012).
60. Oleinika, K., Mauri, C. & Salama, A. D. Effector and regulatory B cells in immune-mediated kidney disease. *Nat. Rev. Nephrol.* **15**, 11–26 (2019).
61. Cyster, J. G. & Allen, C. D. C. B Cell Responses: Cell Interaction Dynamics and Decisions. *Cell* **177**, 524–540 (2019).
62. Petrovas, C. *et al.* CD4 T follicular helper cell dynamics during SIV infection. *J. Clin. Invest.* **122**, 3281–3294 (2012).
63. Favre, D. *et al.* Critical Loss of the Balance between Th17 and T Regulatory Cell Populations in Pathogenic SIV Infection. *PLOS Pathog.* **5**, e1000295 (2009).
64. Campillo-Gimenez, L. *et al.* AIDS Progression Is Associated with the Emergence of IL-17–Producing Cells Early After Simian Immunodeficiency Virus Infection. *J. Immunol.* **184**, 984–992 (2010).
65. Teleshova, N. *et al.* CpG-C ISS-ODN activation of blood-derived B cells from healthy and chronic immunodeficiency virus-infected macaques. *J. Leukoc. Biol.* **79**, 257–267 (2006).
66. Epeldegui, M. *et al.* CD40 Ligand (CD154) Incorporated into HIV Virions Induces Activation-Induced Cytidine Deaminase (AID) Expression in Human B Lymphocytes. *PLOS ONE* **5**, e11448 (2010).
67. Urashima, M. *et al.* CD40 ligand triggers interleukin-6 mediated B cell differentiation. *Leuk. Res.* **20**, 507–515 (1996).
68. Van Elssen, C. H. M. J., Oth, T., Germeraad, W. T. V., Bos, G. M. J. & Vanderlocht, J. Natural killer cells: the secret weapon in dendritic cell vaccination strategies. *Clin. Cancer Res. Off. J. Am. Assoc. Cancer Res.* **20**, 1095–1103 (2014).
69. Thomas, R. & Yang, X. NK-DC Crosstalk in Immunity to Microbial Infection. *Journal of Immunology Research* vol. 2016 e6374379 https://www.hindawi.com/journals/jir/2016/6374379/ (2016).
70. Garbers, C., Heink, S., Korn, T. & Rose-John, S. Interleukin-6: designing specific therapeutics for a complex cytokine. *Nat. Rev. Drug Discov.* **17**, 395–412 (2018).
71. Daudelin, J.-F., Mathieu, M., Boulet, S. & Labrecque, N. IL-6 Production by Dendritic Cells Is Dispensable for CD8+ Memory T-Cell Generation. *BioMed Research International* vol. 2013 e126189 https://www.hindawi.com/journals/bmri/2013/126189/ (2012).
72. Hope, J. C. *et al.* Identification of dendritic cells as a major source of interleukin-6 in draining lymph nodes following skin sensitization of mice. *Immunology* **86**, 441–447 (1995).

73. Park, C.-S., Yoon, S.-O., Armitage, R. J. & Choi, Y. S. Follicular Dendritic Cells Produce IL-15 That Enhances Germinal Center B Cell Proliferation in Membrane-Bound Form. *J. Immunol.* **173**, 6676–6683 (2004).
74. C, K. *et al.* Antiinflammatory profiles during primary SIV infection in African green monkeys are associated with protection against AIDS. *J. Clin. Invest.* **115**, 1082–1091 (2005).
75. Diop, O. M. *et al.* Plasmacytoid dendritic cell dynamics and alpha interferon production during Simian immunodeficiency virus infection with a nonpathogenic outcome. *J. Virol.* **82**, 5145–5152 (2008).
76. Theurich, S. *et al.* IL-6/Stat3-Dependent Induction of a Distinct, Obesity-Associated NK Cell Subpopulation Deteriorates Energy and Glucose Homeostasis. *Cell Metab.* **26**, 171-184.e6 (2017).
77. Yu, D. & Vinuesa, C. G. The elusive identity of T follicular helper cells. *Trends Immunol.* **31**, 377–383 (2010).
78. Kallies, A. *et al.* A role for Blimp1 in the transcriptional network controlling natural killer cell maturation. *Blood* **117**, 1869–1879 (2011).
79. Shaffer, A. L. *et al.* Blimp-1 Orchestrates Plasma Cell Differentiation by Extinguishing the Mature B Cell Gene Expression Program. *Immunity* **17**, 51–62 (2002).
80. Fu, S.-H., Yeh, L.-T., Chu, C.-C., Yen, B. L.-J. & Sytwu, H.-K. New insights into Blimp-1 in T lymphocytes: a divergent regulator of cell destiny and effector function. *J. Biomed. Sci.* **24**, 49 (2017).
81. Xu, W. *et al.* The Transcription Factor Tox2 Drives T Follicular Helper Cell Development via Regulating Chromatin Accessibility. *Immunity* **51**, 826-839.e5 (2019).
82. Papillion, A. *et al.* Inhibition of IL-2 responsiveness by IL-6 is required for the generation of GC-TFH cells. *Sci. Immunol.* **4**, (2019).
83. Costela-Ruiz, V. J., Illescas-Montes, R., Puerta-Puerta, J. M., Ruiz, C. & Melguizo-Rodríguez, L. SARS-CoV-2 infection: The role of cytokines in COVID-19 disease. *Cytokine Growth Factor Rev.* (2020) doi:10.1016/j.cytogfr.2020.06.001.
84. Vanden Bush, T. J., Buchta, C. M., Claudio, J. & Bishop, G. A. Cutting Edge: Importance of IL-6 and cooperation between innate and adaptive immune receptors in cellular vaccination with B lymphocytes. *J. Immunol. Baltim. Md 1950* **183**, 4833–4837 (2009).
85. Leal, I. S., Smedegård, B., Andersen, P. & Appelberg, R. Interleukin-6 and Interleukin-12 Participate in Induction of a Type 1 Protective T-Cell Response during Vaccination with a Tuberculosis Subunit Vaccine. *Infect. Immun.* **67**, 5747–5754 (1999).

86. Yang, C.-L. *et al.* CXCR5-negative natural killer cells ameliorate experimental autoimmune myasthenia gravis by suppressing follicular helper T cells. *J. Neuroinflammation* **16**, 282 (2019).
87. Cook, K. D., Kline, H. C. & Whitmire, J. K. NK cells inhibit humoral immunity by reducing the abundance of CD4+ T follicular helper cells during a chronic virus infection. *J. Leukoc. Biol.* **98**, 153–162 (2015).
88. Farsakoglu, Y. *et al.* Influenza Vaccination Induces NK-Cell-Mediated Type-II IFN Response that Regulates Humoral Immunity in an IL-6-Dependent Manner. *Cell Rep.* **26**, 2307-2315.e5 (2019).
89. Palgen, J.-L. *et al.* Innate and secondary humoral responses are improved by increasing the time between MVA vaccine immunizations. *NPJ Vaccines* **5**, 24 (2020).
90. Brocca-Cofano, E. *et al.* Pathogenic Correlates of Simian Immunodeficiency Virus-Associated B Cell Dysfunction. *J. Virol.* **91**, (2017).
91. Cokelaer, T., Desvillechabrol, D., Legendre, R. & Cardon, M. 'Sequana': a Set of Snakemake NGS pipelines. *J. Open Source Softw.* **2**, 352 (2017).
92. Martin, M. Cutadapt removes adapter sequences from high-throughput sequencing reads. *EMBnet.journal* (2011) doi:10.14806/ej.17.1.200.
93. Liao, Y., Smyth, G. K. & Shi, W. featureCounts: an efficient general purpose program for assigning sequence reads to genomic features. *Bioinforma. Oxf. Engl.* **30**, 923–930 (2014).
94. Love, M. I., Huber, W. & Anders, S. Moderated estimation of fold change and dispersion for RNA-seq data with DESeq2. *Genome Biol.* **15**, 550 (2014).
95. Benjamini, Y. & Hochberg, Y. Controlling the False Discovery Rate: A Practical and Powerful Approach to Multiple Testing. *J. R. Stat. Soc. Ser. B Methodol.* **57**, 289–300 (1995).
96. Mavilio, D. *et al.* Identification of NKG2A and NKp80 as specific natural killer cell markers in rhesus and pigtailed monkeys. *Blood* **106**, 1718–1725 (2005).

MATERIAL AND METHODS

Monkeys and ethics statement

Nineteen AGMs (Caribbean *Chlorocebus sabaeus*) were included in this study. Seven AGM were uninfected and twelve AGM were infected intravenously with the wild-type isolate SIVagm.sab92018 as previously reported[38,43]. Twenty-six cynomolgus macaques (*Macaca fascicularis* [MAC]) imported from Mauritius were included in the study. Seventeen of these MAC were uninfected and nine MAC were infected intravenously with the SIVmac251 isolate as previously reported[38] (Supplementary Table 1).

The AGM and MAC were housed at the IDMIT Center (Fontenay-aux-Roses, France). All non-human primate studies at IDMIT are conducted in accordance with French National Regulations and in strict accordance with the international European guidelines 2010/63/UE on the protection of animals used for experimentation and other scientific purposes, with the French law (French decree 2013-118) and the recommendations of the Weatherall report. The IDMIT center complies with the Standards for Human Care and Use of the Office for Laboratory Animal Welfare (OLAW, USA) under OLAW Assurance number A5826-86. Animals were generally housed in adjoining individual cages allowing social interactions, and maintained under controlled conditions with respect to humidity, temperature, and light (12 hours light/12 hours dark cycles). Water was available ad libitum. Animals were monitored and fed once or twice daily commercial monkey chow and fruit by trained personnel. Environmental enrichment was provided whenever possible including toys, novel foodstuffs, and music under the supervision of the CEA Animal Welfare Body. Animal experimental protocols were approved by the Ethical Committee of Animal Experimentation (CETEA-DSV, IDF, France) (Notification 12-098 and A17-044). The immunogenocity studies were approved by the "Ministère de l'Éducation Nationale, de l'Enseignement Supérieur et de la Recherche" (France) and the ethical committee "Comité d'éthique en expérimentation animale n°44" (France) under the reference 2015031314518254.02 (APAFIS#319). The animals used here had been purchased for other programs. Samples from these animals were shared with our study. Some results of these programs have already been published[38,89] (Huot et al, in press).

Monitoring of the monkeys was under the supervision of the veterinarians in charge of the animal facilities. They were handled in accordance with national regulations (CEA Permit Number A 92-03-02). Experimental procedures (animal handling, viral inoculations, and samplings) were conducted after sedation with ketamine hydrochloride (Rhone-Merieux, Lyon, France, 10 mg/kg). Tissues were collected at necropsy: animals were sedated with ketamine chlorhydrate (10 mg/kg) then humanely euthanized by intravenous injection of 180 mg/kg sodium pentobarbital. The sample size varied between three and eleven monkeys per group depending on the type of experiment. Sample collection was performed in random order, according to the tripartite harmonized International Council for Harmonization of Technical Requirements for Pharmaceuticals for Human Use (ICH) Guideline on Methodology (previously coded Q2B). The investigators were not blinded while the animal handlers were blinded to group allocation.

Human blood collection and isolation of PBMC

Human blood samples from healthy donors were obtained from the French Blood Bank (Etablissement Français du Sang, EFS) in agreement with national and European legislation (C CPSL UNT, number 15/EFS/023).
Peripheral blood mononuclear cells (PBMCs) were isolated by a density gradient (Eurobio, CMSMSL01-01). Red blood cells (RBC) were lysed by RBC lysis buffer (500mg $KHCO_3$ (Sigma P7682), 4.15g NH_4Cl (Sigma A0171), 500µL EDTA 100mM pH=7.5, qsp 500mL H_2O).

Processing of blood and tissues samples from nonhuman primates

Peripheral blood mononuclear cells were isolated on a density gradient (Eurobio, CMSMSL01-01). Red blood cells were lysed with RBC lysis buffer as described above and the PBMCs either used fresh or frozen in FBS (Eurobio, CVFSVF00-01) with 10% of DMSO (Sigma, D2650-100ML) for later use. After biopsy, the peripheral lymph nodes were transported to the laboratory and kept during the transport for 2-3 hours at 4°C in RPMI medium. The pLN were then cut into pieces, grinded with a gentleMACS Dissociator (Miltenyi Biotec, 130-093-235) in 500µl of RPMI per LN. The pLN cell suspension was centrifugated at 1500g for 5 min to pellet the cells. The cells were used fresh or were frozen in FBS with 10% of DMSO and stored in liquid nitrogen until further use. The supernatants were filtered at 70µm (Clearline, 141379C), centrifugated (1000g for 20 min) to clean from remaining cell debris and then stored at -80°C.

Isolation of NK cells and B cells from NHP for cell cultures

PBMCs were saturated for non-specific sites with FcR blocking reagent (Miltenyi, 130-059-901). Nonhuman primate NK and B cells respectively express NKG2A/C and CD20[38,90]. To isolate NK cells, cells were incubated with NKG2A/C antibodies (Z199-PE) for 20 minutes at 4°C. Using anti-PE microbeads (130-048-801), NKG2A/C+ cells were selected through magnetic columns (130-042-401). To isolate B cells from PBMCs, we used anti-CD20 microbeads (Miltenyi, 130-091-105). Cells were passed through magnetic columns (Miltenyi 130-042-401) to recover B cells.

Isolation and of human NK cells

NK cells were isolated from PBMC by RoboSep (Stemcell) using the human NK cell isolation kit (17955, Stemcell).

Culture of NK cells and B cells

Co-cultures were realized between autologous NK and B cells (ratio 1:5) in 96 well plates and 96 transwell plates (Life Sciences, 3381). Cells were cultured in IL-2 (100IU), IL-4 (25ng/mL) and IL-15 (100ng/mL). The supernatants were collected after 2 or 6 days of culture and used after centrifugation.

Tissue inclusion preparation

To conserve frozen tissues for ulterior image analyses, tissue pieces or small biopsies were incubated in PFA 4% (AlfaAesar, J61899) overnight. After that, the tissues were immersed into sucrose (Sigma, S0389-500G) 10% at 4°C during 72h. Then the incubation medium was changed to sucrose 20%, and after 72h to sucrose 30%. After these steps, tissues were placed in O.C.T. (Tissue-Tek, 4583) and snap-frozen in ethanol/dry ice solution. Tissues were conserved at -80°C or in liquid nitrogen. All tissues in O.C.T were cut at 10µm using a cryostat (LEICA CM 3050S) and put on slides (Thermo Scientific, J3800AMNZ). These slides were stored at -20°C.

Flow cytometry staining

Cells were thawed at room temperature. For the NK and B cell panels (Supplementary Table 2), we saturated non-specific sites by incubation with monkey sera during 20 min. We centrifuged at 1500 x g for 5 min. Then we added the antibodies to the samples (1 million of cells) and homogenized. We incubated the mix for 30 minutes at 4°C. We added 5 mL of PBS, centrifuged at 1500 x g for 5 min and discarded the supernatant. We permeabilized the cells by Cytofix solution (BD, 554655) for 20 min at 4°C. Five mL of PermWash(X1) solution (BD, 51-2091KZ) was added and we centrifuged at 1900 x g for 5 minutes. Antibodies were added on samples and homogenized followed by incubation for 20 min at 4°C. We added 5mL of PermWash(X1) solution and centrifuged at 1900 x g for 5 minutes. We homogenized the pellet in PFA 4%. The fluorescence staining was observed and captured by a flow cytometer (BD, LSR II) and software (BD, Diva). Images were analysed with FlowJo.

Immunofluorescent staining and fluorescent In Situ Hybridization

For immunofluorescent staining of the tissue sections, the epitope revelation protocol was realized with PBS incubation at room temperature (RT) for 15 min. Then, the slides were incubated in methanol (Fisher Chemical, M/3950/15) at -20°C during 2 hours (h) and subsequently in formaldehyde 2% at RT (Sigma, F8775-500mL) for 15 min. The non-specific sites were saturated with BSA 4% (Sigma, A6003-25G) during 2h at RT followed by a washing step for 1h with PBS. The primary antibodies (Supplementary Table 3; 1:200) were added overnight at 4°C. Then the slides were washed for 1h in PBS. Secondary antibodies (Supplementary Table 3; 1:200) and DAPI (Supplementary Table 3; 1:1000) were added for 1h at 4°C. After a washing step (1 h in PBS) the mounting medium was added (Invitrogen, 00-4958-02). We finally dropped off the cover (Fisher Scientific, 15165452 – Dutscher, 100038N) on the slide with mounting medium.
For the fluorescent in situ hybridization realized to measure IL-6 mRNA expression in LN, we followed the RNAscope protocol with IL-6 probe utilization (Advanced Cell Diagnostics Europe, 804341-C2) and ACD HybEZ Hybridization system (Advanced Cell Diagnostics Europe, 310013). The antibodies used for stainings were used as described above. The fluorescence staining was captured in all assays by a spinning-disk (Yokagawa, CellVoyager CV1000, x20). Images were analyzed by ImageJ (Fiji).

Immunostaining of *in vitro* cultured cells was realized using coated wells with poly-L-lysine (P8920-100ML) for 1h at 37°C incubation. NK and B cells were cultured one day before coating. Antibodies were added to the coated cells (Supplementary Table 3). The fluorescence staining was captured in all assays by a confocal microscope (Zeiss, LSM700, x40). Images were analyzed by ImageJ (Fiji).

ELISA

IL-6 was quantified using the IL-6 ELISA kit (U-CyTech; CT145A) according to the provider's instructions.

Cell sorting of NK cell subsets for transcriptional analysis

Eight-colour panels were used to phenotype, surface stain and sort NK cells. Total pLN cells were thawed in 20% FBS-containing media supplemented with benzonase nuclease, and counts and viabilities were performed (Life Technologies). Cells were washed and stained with Aqua Live/Dead stain (Molecular Probes). Cells were washed and the sites saturated using normal mouse IgG (Caltag). pLN cells were surface stained for CD45 (D058-1283, BD), CD3 (SP34.2, BD), CD8 (BW135/80, Miltenyi), CD16 (3G8, Beckman Coulter, Inc.), NKG2a/c (Z199, Beckman Coulter, Inc.), CD20 (2H7, Biolegend), CD14 (M5E2, BD) and CXCR5 (MU5UBEE, MABTech). The antibodies are listed in Supplementary Table 2. Post-staining, cells were washed, filtered and sorted on a FACS ARIA II (BD). Cells were directly collected in a lysis buffer that contained TCEP (tris(2-carboxyethyl) phosphine). The purity of the cells was >97%.

RNA extraction, library preparation and sequencing

RNA was isolated from the sorted NK cells using the RNeasy Mini Kit (205113, Qiagen). RNA integrity was verified with the Agilent Bioanalyser. DNase-treated RNA was submitted to library preparation using the Truseq Stranded mRNA Sample Preparation Kit (Illumina, San Diego, CA), according to manufacturer's instructions. An initial poly(A) RNA isolation step (included in the Illumina protocol) was performed on 10 ng of total RNA to keep only the polyadenylated RNA fraction and remove the ribosomal RNA. A step of fragmentation was then performed on the enriched fraction, by divalent ions at high temperature. The fragmented RNA samples were randomly primed for reverse transcription followed by second-strand synthesis to create double-stranded cDNA fragments. No end repair step was necessary. An adenine was added to the 3'-end and specific Illumina adapters were ligated. Ligation products were submitted to PCR amplification. The obtained oriented libraries were controlled by Bioanalyzer DNA1000 Chips (Agilent, # 5067-1504) and quantified by spectrofluorimetry (Quant-iT™ High-Sensitivity DNA Assay Kit, #Q33120, Invitrogen). Sequencing was performed on the Illumina Hiseq2500 platform to generate single-end 100 bp reads bearing strand specificity.

Bioinformatic analysis of the RNA sequence data

Bioinformatic analyses were performed using the RNA-seq pipeline from Sequana[91]. Reads were cleaned of adapter sequences, and low-quality sequences were removed using cutadapt version 1.11[92]. Only sequences ≥ 25 nucleotides (nt) in length were considered for further analysis. STAR version 2.5.0a, with default parameters, was used for alignment on the reference genome (*Chlorocebus sabaeus*, from Ensembl release 90). Genes were counted using featureCounts version 1.4.6-p3[93] from Subreads package (parameters: -t gene, -g ID and -s 1). Data were analyzed using R version 3.4.3 and the Bioconductor package DESeq2 version 1.18.1[94]. Normalization and dispersion estimation were performed with DESeq2, using the default parameters, and statistical tests for differential expression were performed by applying the independent filtering algorithm. A generalized linear model, including the monkey identifier as a blocking factor, was used to test for the differential expression between the biological conditions. For each pairwise comparison, raw p values were adjusted for multiple testing according to the Benjamini and Hochberg (BH) procedure[95]. Each list was used to query the Kyoto Encyclopedia of Genes and Genomes (KEGG), GO-biological function database and Wiki pathways. Genes with an adjusted p value <0.05 were considered differentially expressed (Supplemental table 4). Analyses and vizualisation of gene expressions by heat maps were performed using Prism (GraphPad, La Jolla, CA).

Data availability

Deep sequencing results have been deposited in the Gene Expression Omnibus database; the accession number is GSE140600. The authors declare that all other data supporting the findings of this study are available from the authors upon request.

Statistics

In order to illustrate specific gene sets, we draw heatmaps based on variance-stabilizing transformed counts. For the other data, a Wilcoxon matched-pairs signed rank test was used with subsequent Bonferroni correction to evaluate whether there was a statistically significant difference in the level of one given marker at a given time point post-infection when compared to the baseline medians (day 0). Baseline medians in blood consisted of 3–6 pre-infection values per animal. Statistical computations were performed using Prism (GraphPad, La Jolla, CA).

ACKNOWLEDGMENTS

We are grateful for the excellent contributions from the veterinarians and staff at the IDMIT Center (Benoit Delache, Jean-Marie Helies, Raphaël Ho Tsong Fang and Julie Morin). We also thank all the people from the Illumina Hiseq 2500 platform at the Institut Pasteur and especially Caroline Proux and Jean-Yves Coppee. NH was supported by the Fondation Beytout and Institut Pasteur. PR was recipient of a PhD fellowship from the University Paris Diderot, Sorbonne Paris Cité and also supported by the NIH (R01AI143457) and Institut Pasteur. CaP was recipient of a Roux-Cantarini Postdoctoral Fellowship. CyP was supported by the ERC-2013-StG 337146 program. We would like

to acknowledge grant support from ANRS, the Fondation J. Beytout and the Fondation Les Ailes to MMT, and from the NIH (R01AI143457) to MMT and RKR. We gratefully acknowledge the support to IDMIT from the French government: Investments for the Future program for infrastructures (PIA) through the ANR-11-INBS-0008 grant as well as from the PIA grant ANR-10-EQPX-02-01 to the FlowCyTech facility at IDMIT. We equally acknowledge the Investments for Future grant ANR-10–INSB–04 to support the UtechS Photonic BioImaging (Imagopole) and C2RT facilities at Institut Pasteur.

AUTHOR CONTRIBUTIONS

PR, NH, BJ, ML and CaP performed the experiments. PR, NH, BJ, CyP, HM and MMT designed the experiments. VC, NDB and BJ coordinated the animal studies. PR, NH, BJ, HM and MMT analyzed the data. MMT obtained the funding. PR and MMT wrote the manuscript and all co-authors reviewed it.

LEGENDS

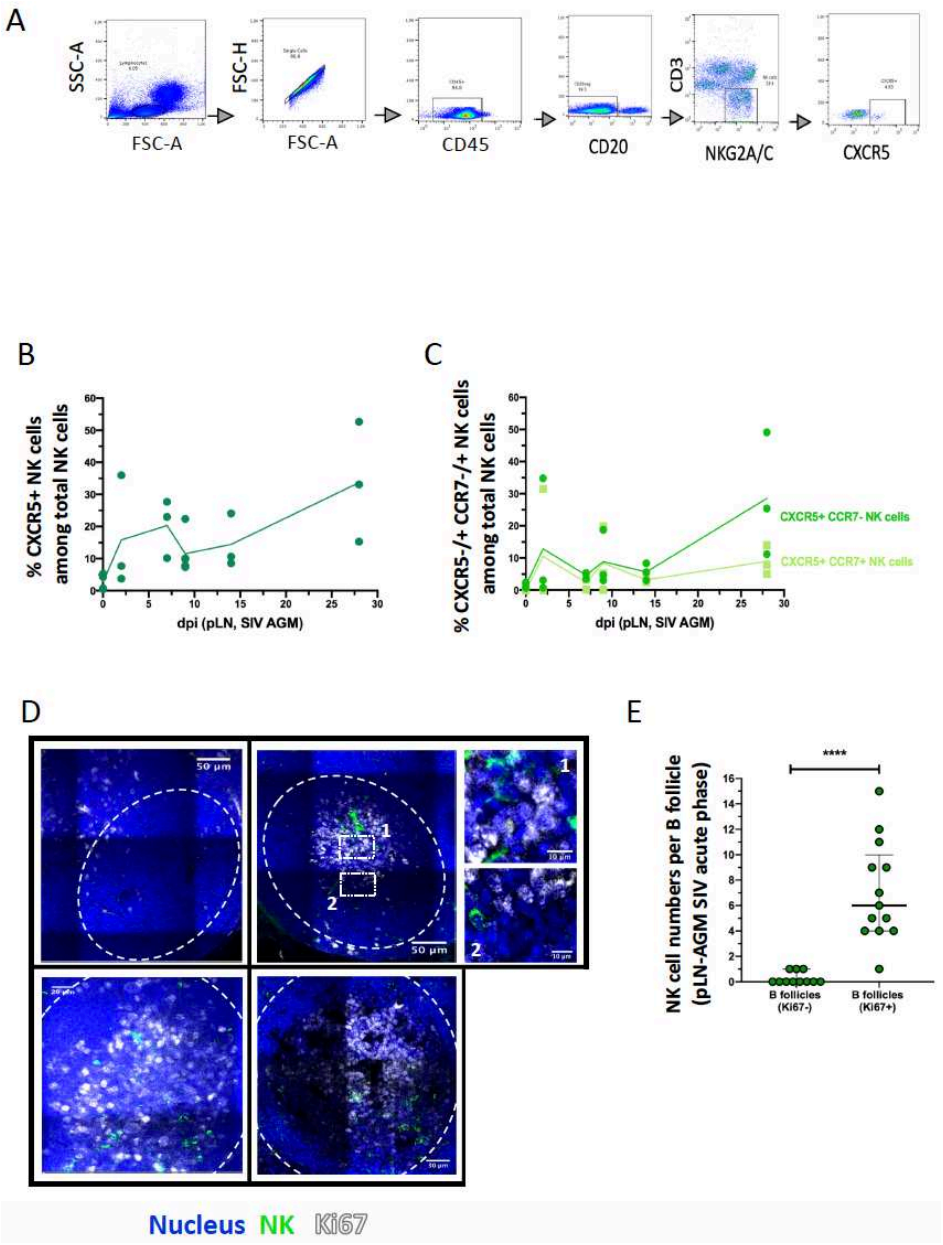


Figure 1: Temporal and spatial dynamics of CXCR5+ NK cells in peripheral lymph nodes during primary SIVagm infection. A) Gating strategy of CXCR5+ NK cells in pLN. NK cells were gated as $CD45^{+}CD3^{-}CD20^{-}NKG2A/C^{+}CXCR5^{+}$ cells as previously reported[38,96]. A representative image is shown. The example corresponds to pLN cells from an African Green Monkey infected by SIVagm at day 9 post-infection. **B)** Kinetic of $CXCR5^{+}$ NK cell percentages in pLN during primary SIVagm infection. Dpi= days post-infection. Each green circle indicates an individual animal, (n=3 AGM). **C)** Kinetic of CXCR5+CCR7- and CXCR5+CCR7+ NK cell frequencies in pLN during primary SIVagm infection. Light green rectangles indicate CXCR5+CCR7+ NK cells and dark green circles CXCR5+CCR7- NK cells. (n=3 AGM). **D)** Spatial distribution of NK cells and proliferating B cells in pLN during acute SIVagm infection (day 9 - 14 p.i.). The dashed with line delineates the B cell follicle (BCF). pLN from 5 individual AGMs were analyzed. The large images show

representative BCFs for 4 distinct animals. White numbered squares (1 & 2) show zoomed regions. **E)** NK cell counts in B cell follicles in presence or absence of proliferating B cells as indicated by Ki-67 staining. The pLN were analyzed at day 9-14 p.i. Each green circle indicates one BCF (BCF n= 24). (n=5 AGM). pvalue= *** <0.0001, Mann-Whitney test.

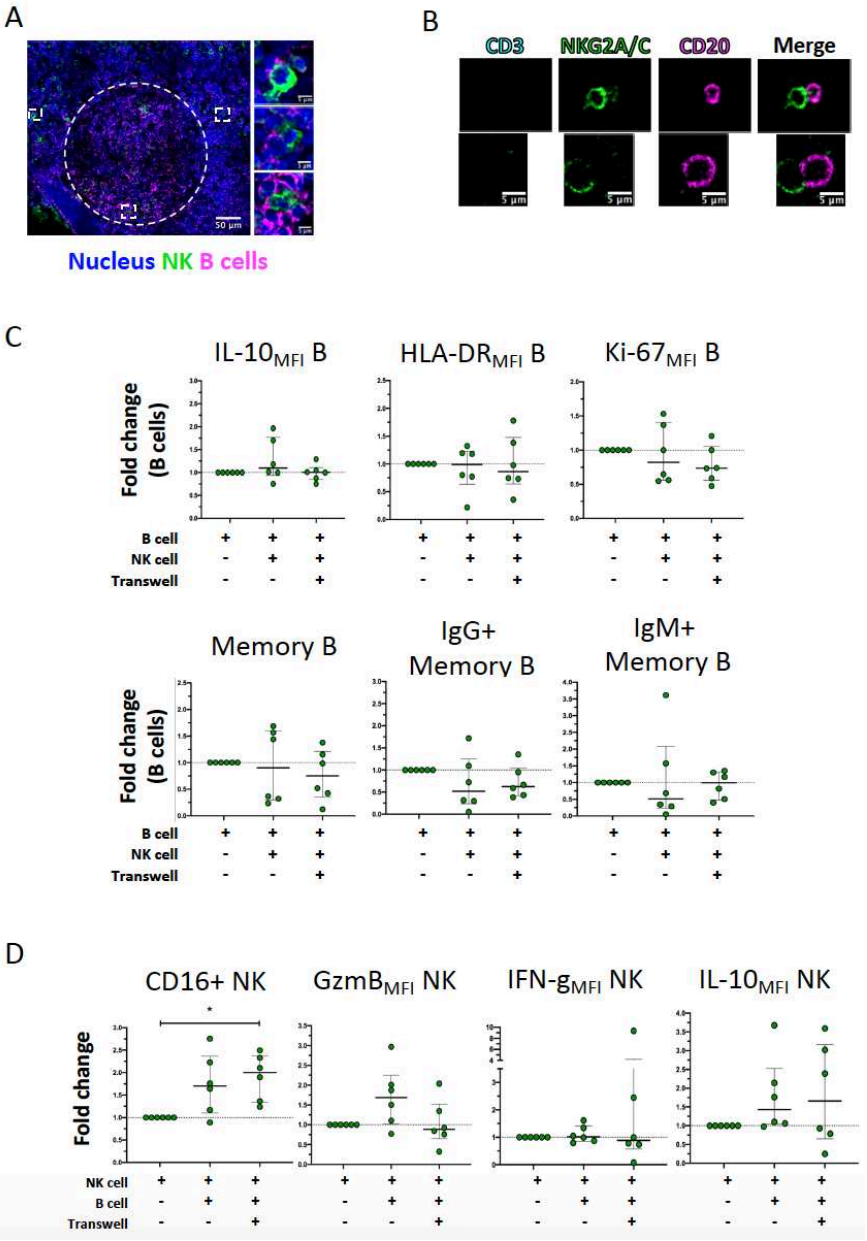


Figure 2: Contact and mutual impact between NK and B cells. A) Co-staining of B cells and NK cells in pLN during primary SIVagm infection. pLN were analyzed at day 9 p.i. A representative section showing a BCF and the surrounding interfollicular region is shown. The white dashed line delineates the BCF. White squares show zoomed regions. (n=3 AGM). **B)** Analysis of potential contacts between NK and B cells isolated from PBMC of non-infected AGM after 1 day of coculture. (n= 3 AGM). Two representative examples for each marker are shown (top and bottom, from the same culture). **C)** Analysis of the phenotype of B cells after co-culture with autologous NK cells or co-

culture with autologous NK cells separated by a transwell membrane. B and NK cells were isolated from blood of non-infected AGMs. The fold change in B cell frequency of a given phenotype among total B cells compared to B cells cultured alone is shown after 6 days of co-culture (n=6 AGM). **D)** Analysis of the phenotype of NK cells after co-culture with B cells or co-culture with B cells separated by a transwell membrane. NK and B cells were isolated from blood of non-infected AGMs. The fold change in NK cell frequency of a given phenotype among total NK cells compared to NK cells cultured alone is shown after 6 days of co-culture (n=6 AGM), (pvalue= * <0.05, Wilcoxon test).

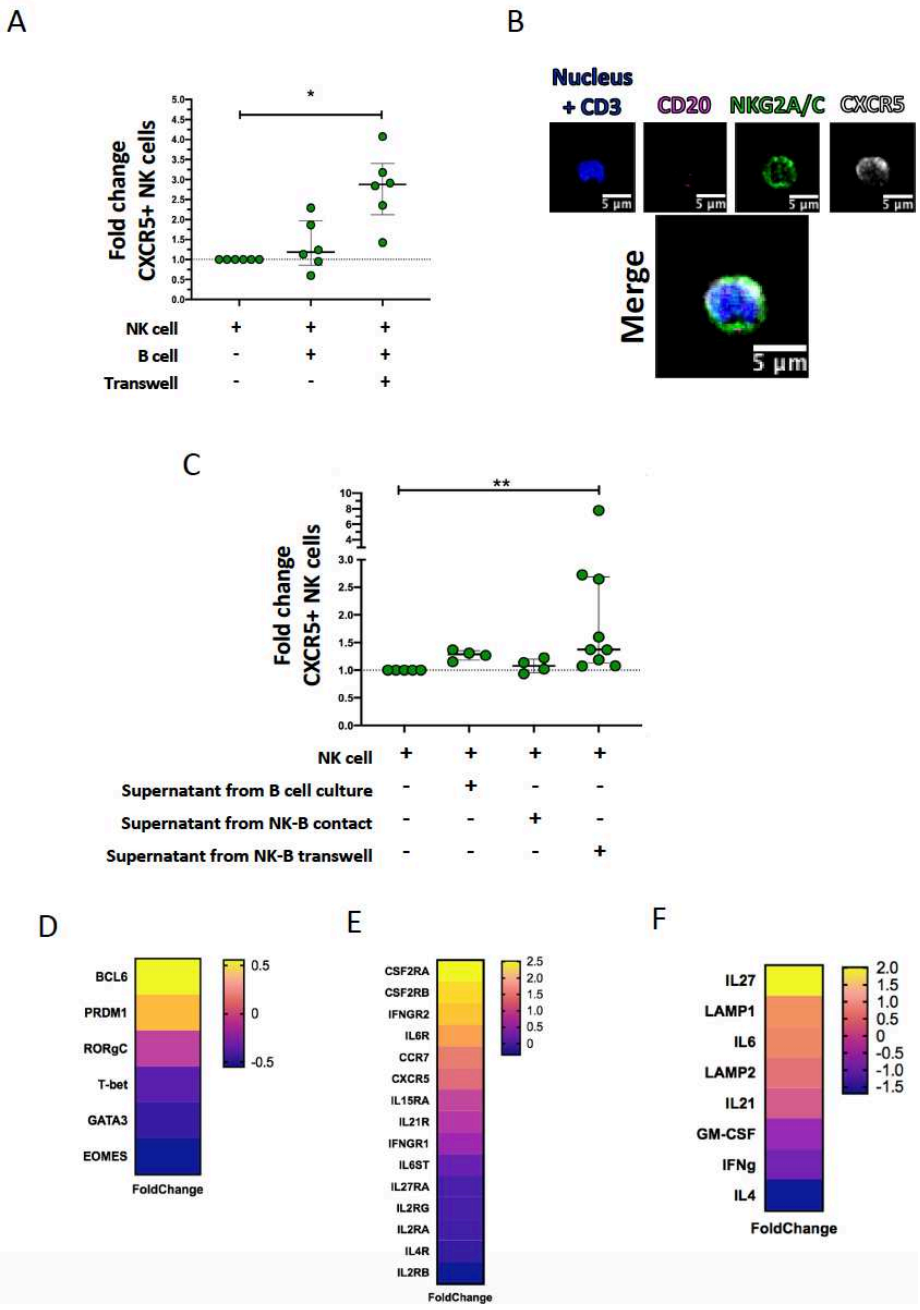


Figure 3: CXCR5+ NK cell induction and gene expression profile. A) Frequency of CXCR5+ NK cells after co-culture with autologous B cells or co-culture with autologous B cells separated by a transwell membrane. B and NK cells were isolated from blood of non-infected AGMs. The fold

change of CXCR5+ NK cells among total NK cells compared to the frequency of CXCR5+ NK cells in NK cells cultured alone is shown after 6 days of co-culture (n=6 AGM). (pvalue= * <0.05, Wilcoxon test). **B)** Staining of NK cells co-cultured with autologous B cells separated by a transwell membrane illustrating CXCR5 expression on NK cells. **C)** Measurement of CXCR5+ NK cell frequencies cultured 2 days with supernatants collected after 6 days of B cells cultured alone, of B and NK cell co-cultures and of B and NK cells cultured separated by a transwell membrane. Cells were from blood of uninfected AGM. The fold change for CXCR5+ NK cell frequencies as compared to NK cells cultured alone is shown (pvalue= ** <0.01, Wilcoxon test). Each green dot indicates an individual animal (Supplementary Table 5). **D-F)** Transcriptomic profile of CXCR5+ NK cells isolated from pLN of chronically SIVagm-infected AGM. The gene expression profiles of CXCR5+ NK cells were compared to that from the predominant NK cell subpopulation in pLN (n= 3 AGM). **D)** Expression profiles of genes coding for transcription factors known to be associated with the CXCR5 pathway on T_{FH} and B cells. **E)** Expression profiles of genes coding for cellular cytokine and chemokine receptors. **F)** Expression profiles of genes coding for soluble factors known to be associated with the CXCR5 pathway on T_{FH} and B cells.

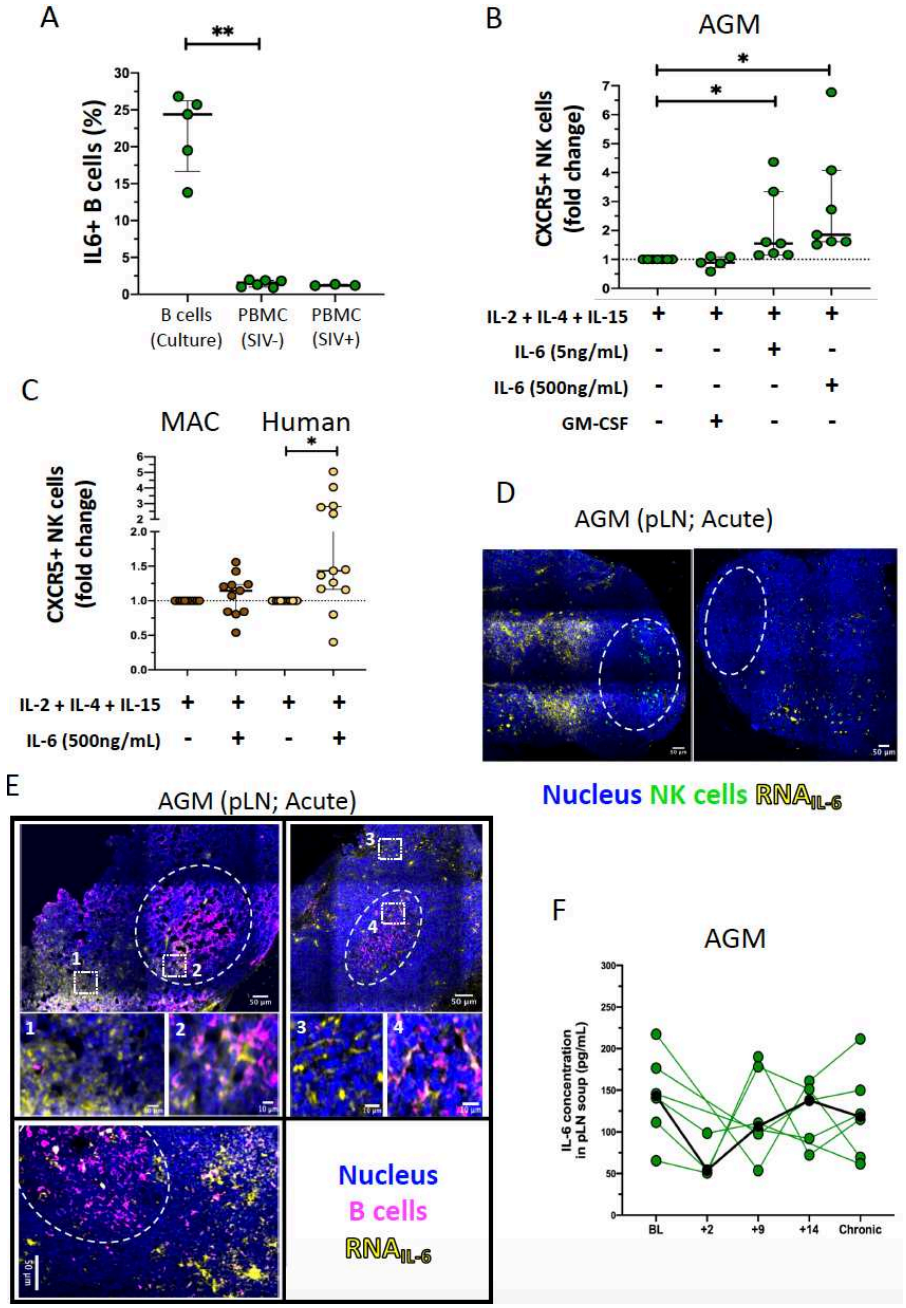
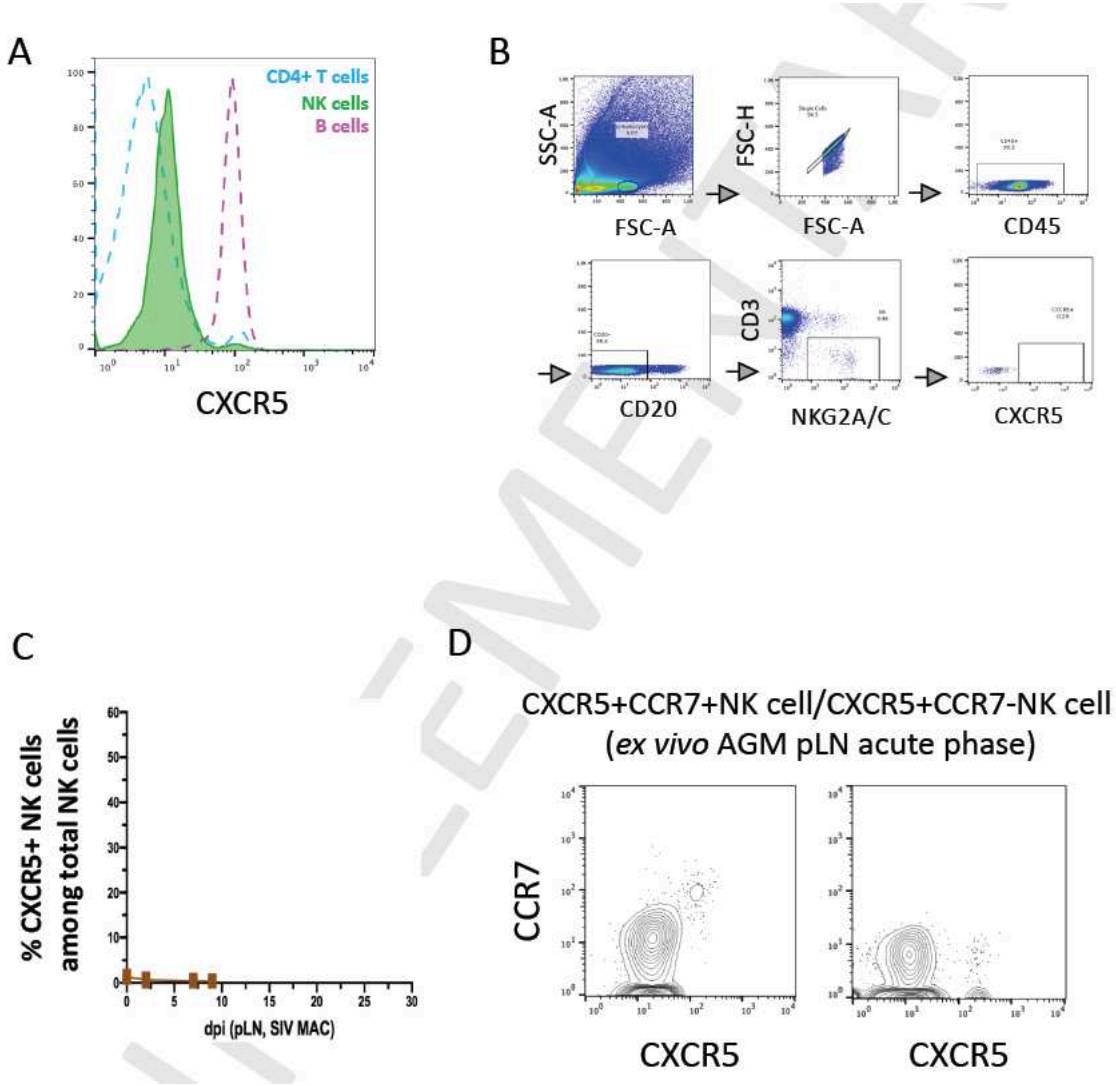
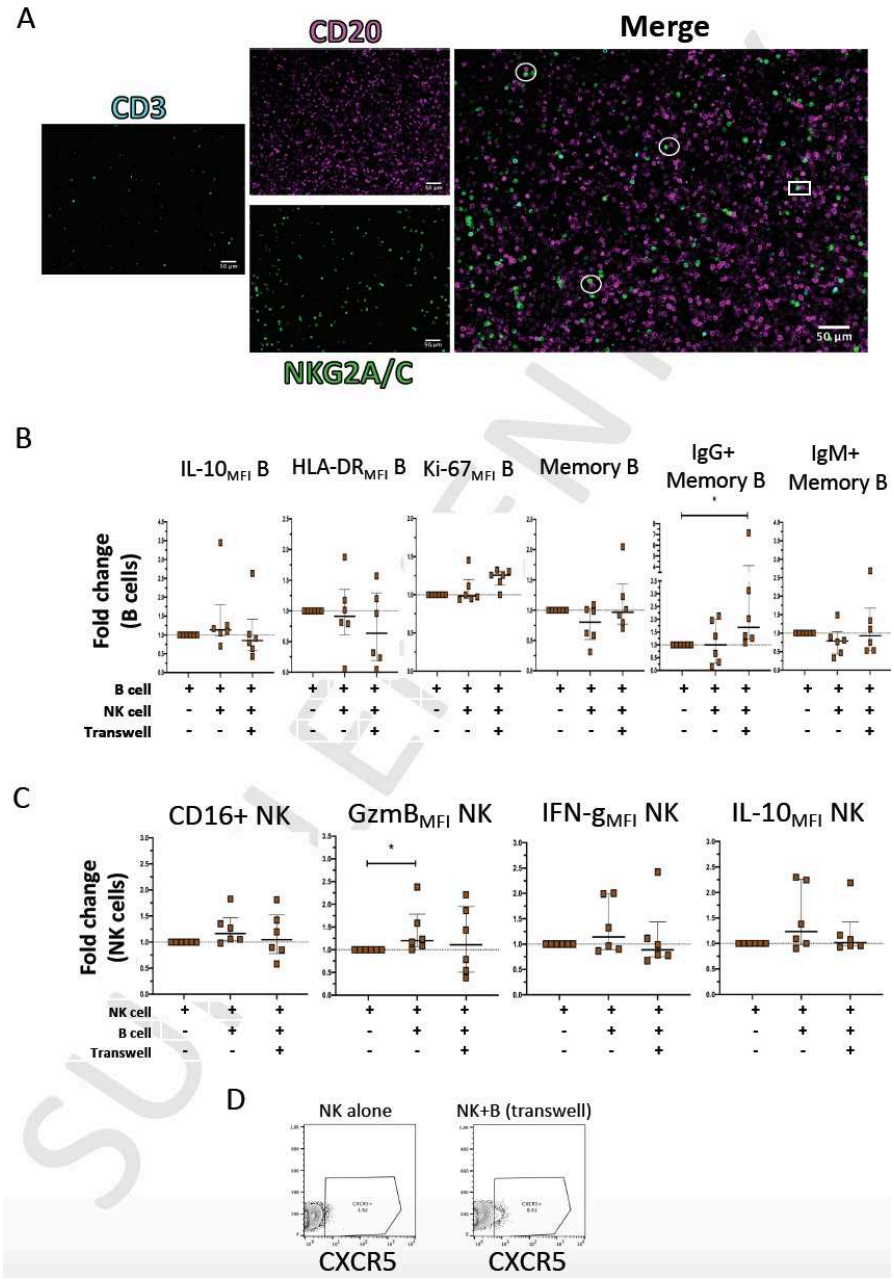


Figure 4: IL-6 a soluble factor inducer of CXCR5 expression on NK cells *in vitro*. A) Percentage of IL-6+ B cells isolated from blood of uninfected AGM after 6 days in culture or ex-vivo in PBMC of uninfected and chronically SIVagm-infected AGM. Each green circle indicates an individual animal (n=3-6 AGM), (pvalue= ** <0.01, Wilcoxon test). **B)** Impact of IL-6 on CXCR5+NK cell frequencies. NK cells were isolated from blood of uninfected AGMs and cultured for 2 days with distinct doses of IL-6 or with GM-CSF (250ng/ml). The fold change of CXCR5+ NK cell frequencies as compared to NK cells cultured without IL-6 or GM-CSF is shown. Each green circle indicates an individual animal (n=5-7 AGM), (pvalue= * <0.05, Wilcoxon test). **C)** Impact of IL-6 on NK cells from macaques and humans. NK cells were isolated from blood of uninfected animals and healthy donors and cultured for 2 days with IL-6. The fold change of CXCR5+ NK cell frequencies as compared to NK cells cultured without IL-6 is shown (n= 11 MAC, n= 13 healthy donors), (pvalue= * <0.05, Wilcoxon test). **D-E**) IL-6 mRNA production in pLN during acute SIVagm infection (day 9

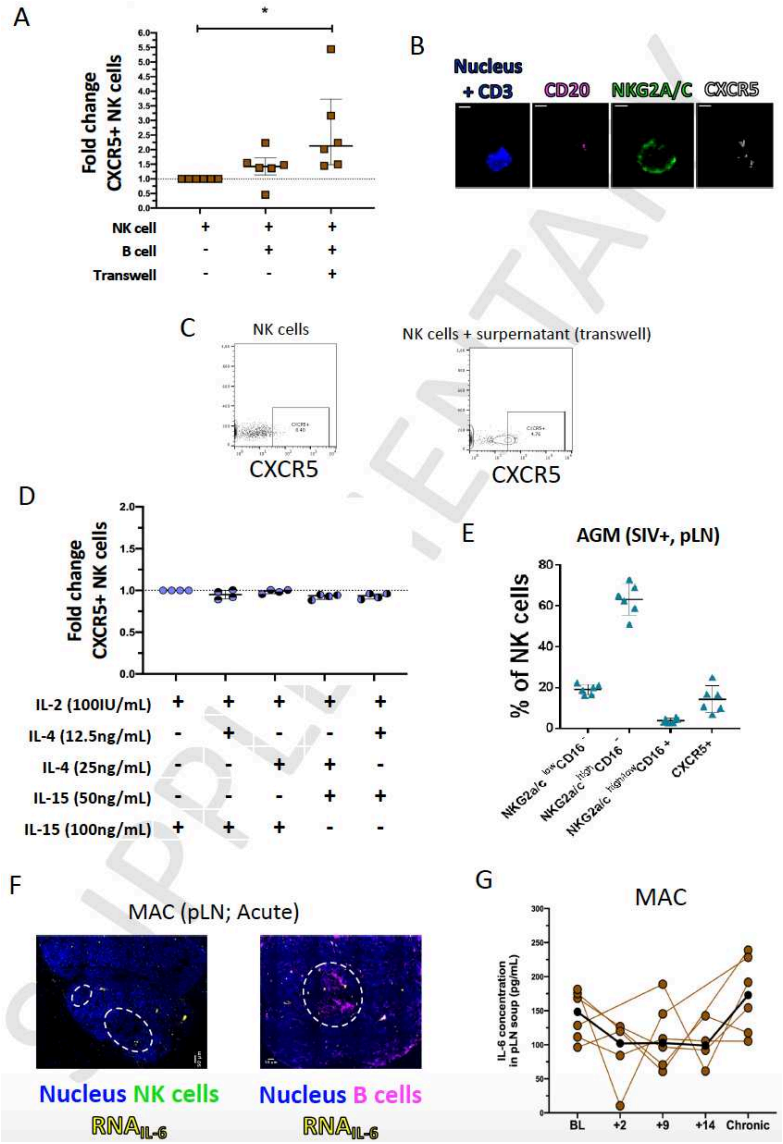
p.i.), (n=4 AGM). IL-6 mRNA was co-stained with antibodies labeling **D)** NK cells and **E)** B cells. White squares (numbered 1-4) show zoomed regions. BCF are indicated by a dash white line. Representative examples are shown. **F)** Concentrations of IL-6 in supernatants from total pLN cells. (n=3-6 AGM).



Supplementary Figure 1: A) Histogram of CXCR5 expression on CD4+ T cells, B cells and NK cells from pLN in acute SIVagm infection. A representative animal is shown (AGM at day 9 p.i.). **B)** Gating strategy of CXCR5+ NK cells in pLN from cynomolgus macaques. An example for cells from SIVmac-infected MAC at day 9 p.i. is shown. **C)** Kinetic of CXCR5+ NK cell percentages during acute SIVmac infection (n=3 MAC). **D)** Dot plot of CXCR5+CCR7+ and CXCR5+CCR7- NK cells in pLN from AGM during acute SIVagm infection (day 9 p.i.).



Supplementary Figure 2: A) Analysis of contacts between NK and B cells. Cells were isolated from PBMC of non-infected AGM (n=3). NK cell marker in green, B cell in magenta and CD3 in cyan. The white circles delineate NK and B cells and the white square T and B cells. **B)** Evaluation of the phenotype of B cells after 6 days of coculture with autologous NK cells, separated or not by a transwell membrane. Cells were isolated from PBMC of uninfected MAC (n= 6 MAC). Fold-change compared to B cells cultured alone (pvalue= * <0.05, Wilcoxon test). **C)** Evaluation of the phenotype of NK cells after 6 days of coculture with autologous B cells, separated or not by a transwell membrane. Cells were isolated from PBMC of uninfected MAC (n= 6 MAC). Fold-change compared to NK cells cultured alone (pvalue= * <0.05, Wilcoxon test). **D)** Dot plot representative of CXCR5+ NK cells from uninfected AGM after 6 days of culture: NK cells cultured alone and NK cells cocultured with autologous B cells separated by a transwell membrane.



Supplementary Figure 3: A) Evaluation of CXCR5+ NK cell frequencies in NK cells cultured for 6 days alone or in coculture with autologous B cells, separated or not by a transwell membrane. Cells were isolated from PBMCs of uninfected MAC. Fold-change as compared to NK cells cultured alone (p value= * <0.05, Wilcoxon test). **B)** Staining of NK cells after 1 day of culture. NK cell marker in green, B cell marker in magenta, Nucleus and CD3 in cyan, CXCR5 in grey. Scale bare upper left correspond to 2 micrometers. **C)** Dot plot representative of CXCR5+ NK cells from AGM after culture with the supernatant of NK-B cell cocultures in transwell chambers. **D)** Evaluation if the cytokines in the medium used for the cell cultures impacted on CXCR5+ NK cell frequencies. Cells were isolated from PBMC of uninfected AGM (n=4 AGM) and cultured for 6 days. Fold-change of CXCR5+ NK cell percentages compared to NK cells cultured alone (pvalue= * <0.05, Wilcoxon test). **E)** Frequencies of NK cell subpopulations in pLN of chronically SIVagm-infected AGM (n=6 AGM). **F)** IL-6 expression in pLN from MAC during acute SIVmac infection (at day 9 p.i.). Representative B follicles are shown. NK cell marker in green, B cell marker in magenta, $RNA_{IL\text{-}6}$ in yellow and nucleus in blue (n=3 MAC). **G)** Kinetic of IL-6 in supernatants of total pLN cells during SIVmac infection (n=3-6 MAC). BL = baseline (pre-infection).

https://www.dropbox.com/scl/fi/6448bid2qwliabi75yh0h/Manuscript-2_Supplemental-tables.xlsx?dl=0&rlkey=8983fy0acjiwar6ts3i1u573h

Supplemental table 1: Description of the animals used for the study. Left columns: AGM; right columns: macaques.

Supplemental table 2: Antibodies used to stain NK cells and B cells by flow cytometry using LSRII and antibodies used to stain NK cells during cell sorting by Aria II.

Supplemental table 3: Antibodies used to stain NK cells and B cells by microscopy in *in situ* and *in vitro* conditions.

Supplemental table 4: Gene expression data corresponding to the heat maps shown in Figure 3 D-E-F.

Supplemental table 5: Animals from which supernatants were collected and animals for which fresh NK cells were cultured with the respective supernatants (Figure 3C).

3. Expansion of terminally differentiated adaptive NK cells in lymph nodes of SIV-infected natural hosts associates with enhanced MHC-E restricted activity

Expansion of terminally differentiated adaptive NK cells in lymph nodes of SIV-infected natural hosts associates with enhanced MHC-E restricted activity

Nicolas Huot[1], Philippe Rascle[1,2], Caroline Petitdemange[1], Vanessa Contreras[3], Christina M Stürzel[4], Eduard Baquero[5], Justin L. Harper[6], Caroline Passaes[1], Rachel Legendre[7], Hugo Varet[7], Yoann Madec[8], Ulrike Sauermann[9], Christiane Stahl-Hennig[9], Jacob Nattermann[10], Asier Saez-Cirion[1], Roger Le Grand[3], R. Keith Reeves[11], Mirko Paiardini[6,12], Frank Kirchhoff[4], Beatrice Jacquelin[1] and Michaela Müller-Trutwin[1,*]

[1]*Institut Pasteur, Unité HIV, Inflammation et Persistance, Paris, France;*

[2]*Université Paris Diderot, Sorbonne Paris Cité, Paris, France;*

[3]*CEA-Université Paris Sud-Inserm, U1184, IDMIT Department, IBFJ, Fontenay-aux-Roses, France;*

[4]*Ulm University Medical Center, Germany;*

[5]*Institut Pasteur, Unité de Virologie Structurale, Paris, France;*

[6]*Division of Microbiology and Immunology, Yerkes National Primate Research Center (YNPRC), Atlanta, Georgia, USA.*

[7]*Institut Pasteur, HUB de Bioinformatique et Biostatistique – Départment de Biologie Computationnelle – USR 3756 CNRS, Paris, France;*

[8] *Institut Pasteur; Epidemiology Unit, Paris, France;*

[9]*Deutsches Primatenzentrum, Göttingen, Germany;*

[10]*Medizinische Klinik und Poliklinik I, Universitätsklinikum Bonn, Germany;* German Center for In- fection Research (DZIF).

[11]*BIDMC, Harvard Medical School, Boston, USA.*

[12]*Department of Pathology and Laboratory Medicine, Emory University School of Medicine, Atlanta, Georgia, USA.*

Keywords: SIV, HIV, NK cells, lymph node, natural hosts, adaptive, Env, CXCR5, viral control

***Correspondence:** mmuller@pasteur.fr

Abstract

Natural killer (NK) cells play a critical understudied role in HIV infection in tissues. In African green monkeys (AGM), NK cells mediate a strong control of SIVagm infection in secondary lymphoid tissues (SLT). We demonstrate that SIVagm infection induces the expansion of terminally differentiated NKG2a^{low} NK cells in SLT displaying an adaptive transcriptional profile and increased MHC-E-restricted cytotoxicity in response to SIV Env peptides while expressing little IFN-g. Such differentiation was lacking after day 2 post-infection in SIVmac-infected macaques. Adaptive NK cells were characterized by elevated levels of *Themi*s and no increased *NKG2C* expression. This study reveals an unprecedented NK cell adaptation to a viral infection and opens novel strategies toward NK-cell directed therapies and viral control in tissues.

Introduction

The impact of NK cells on viremia in HIV-1 infection has been clearly demonstrated through studies on HLA-I alleles[1–3]. Burgeoning data show that the NK cell repertoire is not stable and that its diversity increases with age[4–6]. The NK cell repertoire diversity reflects immune history and correlates with viral susceptibility[7]. This raises the possibility that there are unexpected functional specialization and distinct adaptive capabilities among NK cell subpopulations in response to viral infections and immunizations, a mechanism which could be exploited to promote antiviral immunity[8–12]. NK cells have been reported to differentiate not only in thymus and bone marrow but also within liver, uterus and secondary lymphoid tissues (SLT). However, data on NK cell differentiation in SLT during a viral infection are scarce[13–15]. African nonhuman primates, such asAfrican green monkeys (AGM), have been a natural host for simian immunodeficiency viruses (SIV) for > 1 million of years[16–18]. In contrast to people living with HIV (PLH), natural SIV hosts typically do not progress toward disease despite persistent high viremia[19]. We have previously shown that AGMs efficiently control viral replication in SLT (both in the T zone and in B follicles), and that this viral control is mediated predominantly by NK cells[20]. No such viral control is generally observed in lymph nodes (LN) of PLH and in the nonhuman primate model of HIV, i.e. SIVmac-infected macaques (MAC), where SLT constitute a major viral reservoir[21,22]. The capacity to control viral replication in B follicles of AGM was associated with the presence of $CXCR5^+$ NK cells[20]. We hypothesize that non-pathogenic (AGM) and pathogenic HIV-1/SIVmac infections differentially imprint NK cells and thereby contribute to the differences regarding the distinct capacity of the NK cells to control SIV/HIV replication in SLT.

Results

Blood NK cell diversity during SIV infection in the natural versus heterologous host

We first assessed if SIV viremia was linked with changes in NK cell diversity in blood of MAC and AGM (Fig.S1). The expression dynamics of nine NK cell markers studied longitudinally throughout infection were often inter-correlated in AGM, while less in MAC (Fig.1a, Table S1), suggesting a more coordinated maturation program in NK cells during SIVagm than SIVmac infection[23–26]. IFN- g and perforin showed the strongest correlations to each other both in AGM and MAC (Fig.1a, Table S1). Only CD16 showed a negative correlation with viremia and only in AGM (Fig.1a, Table S1).

We then analyzed the functional activity of blood NK cells using the classical assay with the MHC- I devoid K562 target cells. No difference was observed in NK cell activity when comparing total NK cells of SIV-infected MAC and AGM (Fig.S2a and b). We therefore analyzed distinct NK cell subpopulations stratified by CD16 and $NKG2_{a/c}$ (Fig.1b-e). The activity decreased in all subsets in response to SIV infection for both AGM and MAC (Fig.S2c and d). However, the activity of NKG2 $^{low}CD16^+$ NK cells

returned rapidly to normal levels in AGM but not in MAC. In order to evaluate the differentiation and functionality of the NK cells during SIV infection in a comprehensive way, we implemented a genome-wide transcriptional mapping. We sorted the four NK cell subpopulations stratified by CD16 and NKG2$_{a/c}$ expression from the blood of chronically infected monkeys. 2586 and 1895 genes were found to be differentially regulated between the distinct subpopulations in MAC and AGM, respectively (Fig.S3). We analyzed in more detail the expression profiles of NK cell receptors (Fig.1f), transcription factors (TF) (Fig.1g) and effector molecules (Fig.1h). Genes upregulated in NKG2$_{a/c}^{high}$CD16^{-} NK cells included those associated with tissue homing (*CCR7, SELL and CXCR3*), proliferation (*MKI67*), and transcription factors involved in cellular stemness and quiescence including *Tcf7* (TCF-1), indicating a low differentiation stage when compared to the other subsets. In contrast, NKG2$_{a/c}^{low}$CD16^{+} NK cells expressed elevated levels of genes associated with tissue egress and circulation (*CX3CR1*), transcription factors associated with terminal differentiation and effector function including *TBX21* (T-bet), and *ZEB2*[27,28]. The other two NK cell subpopulations displayed gene expression profiles of intermediate differentiation. Thus, the combination of NKG2$_{a/c}$ and CD16 allows the determination of distinct NK cell differentiation stages in NHP.

NK cell diversity and functional activity in LN is driven differentially between SIVagm and SIVmac infection

We analyzed the phenotype and function of NK cells in SLT, where we previously identified a strong capacity to control SIV replication in AGM in contrast to MAC[20]. SIVmac infection led to an expansion of the NKG2$_{a/c}^{high}$CD16^{+} NK cells, in contrast to SIVagm infection, where the two NKG2$_{a/c}^{low}$ subsets (NKG2$_{a/c}^{low}$CD16^{+}, NKG2$_{a/c}^{low}$CD16^{-}) were those that were increased in acute and chronic infection, respectively (Fig.2a and 2b). Thus, SIVmac infection led to an accumulation of only the intermediate stages of NK cell differentiation in LN with complete absence of fully differentiated NKG2$_{a/c}^{low}$CD16^{+} NK cells, except at day 2 p.i (Fig 2b). In MAC, only positive correlations were observed between NK cells (NKG2$_{a/c}^{high}$CD16^{+}) and viral load in LN (p=0.02 for cell-associated viral (ca-v)RNA and p=0.048 for ca-vDNA) (Fig.2c, Table S2). In AGM, a positive correlation was observed for NKG2$_{a/c}^{low}$CD16^{+} NK cells (p=0.009 for ca-vRNA and p=0.009 for ca-vDNA), while high viral load correlated with low levels of NKG2$_{a/c}^{high}$CD16^{-} NK cells (p<0.03) (Fig.2d and Table S2). The data suggest that viremia is driving the expansion of NKG2$_{a/c}^{high}$CD16^{+} NK cells in SIVmac infection but of NKG2$_{a/c}^{low}$CD16^{+} NK cells in SIVagm infection. The NKG2$_{a/c}^{low}$ NK cells from LN exhibited increased cytolytic activity during primary and chronic SIVagm infection (Fig.S4). In contrast, NK cells in LN from MAC displayed no increased functional activity after infection, except for a very transient response by the NKG2$_{a/c}^{low}$CD16^{+} NK cells at day 2 p.i. (Fig.S4). Therefore, the NK cells that showed the increased functionality were those that expanded in SIVagm infection and whose expansion stopped after day 2 p.i. in SIVmac infection. NK cell effector function is known to increase together with the repertoire on both CD8^{+} T and NK cells[23]. We

evaluated the levels of natural cytotoxicity receptors (NCR), including among others NKp30, NKp46, NKG2D, and effector molecules before and until day 150 p.i in LN (Fig.S5 and S6). We first focused on bulk NK cells. Strong differences in the dynamics were observed for the expression levels of $NKG2_{a/c}$, which increased on LN NK cells after SIVmac infection (Fig.S5) but not after SIVagm infection (Fig.S6). NK cells from MAC also showed *ex vivo* increases of IFN-γ expression in response to SIVmac infection, while in AGM, the expression level of IFN-γ decreased in LN NK cells. AGM rather displayed increased expression of perforin during primary SIVagm infection. In contrast, perforin expression was increased only at day 2 p.i. in SIVmac infection. A correlation matrix showed a strong positive correlation of $NKG2_{a/c}$ with CD16, IFN-γ and NKG2D for MAC (Fig S5). AGM also showed a positive albeit less strong correlation between $NKG2_{a/c}$ and IFN-γ, but in addition a strong negative correlation between $NKG2_{a/c}$ and perforin (*PRF*), that was absent in MAC (Fig.S6). Overall, more positive correlations were noticed for NK cells in SIVagm as compared to SIVmac infection. These data suggest, as in blood, a better coordination of NK cell differentiation in SIVagm than SIVmac infection, with a more pronounced cytokine (IFN-γ) profile in SIVmac infection, and cytotoxic profile (Perforin) in SIVagm infection.

We further analyzed the NK cell diversity in the LN through a boolean gating analysis performed on NK cell subsets. This uncovered 19 and 8 NK cell clusters during chronic SIVmac infection when compared to uninfected animals in the $NKG2_{a/c}^{high}$ and $NKG2_{a/c}^{low}$ subsets, respectively (Fig.S7), whereas in AGM this approach revealed 11 and 15 clusters during chronic infection when compared to uninfected animals in the $NKG2_{a/c}^{high}$ and $NKG2_{a/c}^{low}$ subsets, respectively (Fig.S8). In both infections, the expression of Ki-67 was increased in the $NKG2_{a/c}^{high}$ subsets (Fig.2g). The subsets showing the highest *ex vivo* expression of IFN-γ in SIVmac infection were the $NKG2_{a/c}^{high}$ NK cells and those expressing the highest levels of perforin in SIVagm infection were the $NKG2_{a/c}^{low}$ NK cells (Fig.2e and f). *Ex vivo* cell surface CD107a expression was increased throughout primary and chronic SIVagm infection in the $NKG2_{a/c}^{low}$ NK cells, while in SIVmac infection, the increases were more transient (day 2 or day 9 p.i.) (Fig.2h, Table S3). No negative correlations were apparent between NK cell subsets and viral load in LN in MAC or AGM (Fig.2i and Fig.2j, Table S3). Taken together, these data unraveled in SIVmac infection a higher diversity rate for $NKG2_{a/c}^{high}$

NK cells together with increased IFN-γ expression, while SIVagm infection was characterized by a more coordinated differentiation of NK cells, with higher diversity rate in the $NKG2_{a/c}^{low}$ NK cells concomitant with more pronounced expression of cytotoxicity markers.

$CXCR5^+$ NK cells are induced by SIVagm infection and resemble $NKG2_{a/c}^{low}CD16^-$ NK cells We next assessed how NK cell differentiation in the natural host could shape NK cells toward the control of viral replication in LN. We previously reported the presence of unprecedented $CXCR5^+$ NK cells during chronic SIVagm infection accumulating in B follicles of SLT allowing the control of viral replication in this otherwise immunoprivileged site[29]. Here, we analyzed the kinetic of appearance of the $CXCR5^+$ NK cells following SIVagm infection. There was no increase of $CXCR5^+$ NK cells in MAC LNs at day 9 p.i.

or during the chronic stage of SIVmac infection compared to baseline (Fig.3a). In contrast, the frequency of CXCR5$^+$ NK cells increased in AGM LN in primary infection compared to baseline to reach a median level of 12% of total NK cells at day 9 p.i. (p=0.001) and 8% in chronic infection (p=0.049; Fig.3b).
We next asked whether the expansion of CXCR5$^+$ NK cells in AGM LN is associated with changes in their phenotype. CXCR5$^+$ NK cells were frequently CD107a positive starting from day 2 p.i. (Fig.3c) and the majority was NKG2A^{low} during primary and chronic SIVagm infection (Fig.3d and 3e). These data suggest that most of the CXCR5$^+$ NK cells were differentiated, cytotoxic cells. However, CXCR5$^+$ NK cells did not all display the same differentiation stage but were heterogeneous. In order to compare comprehensively the differentiation stages of CXCR5$^+$ and CXCR5$^-$ NK cell subsets in SLT, we performed a genome-wide transcriptional mapping of the LN NK cells. Four NK cell subsets were sorted from the LN of the same animals and time points as described above for the blood. The four subsets were NKG2$_{a/c}^{low}$CD16$^-$, NKG2$_{a/c}^{high}$CD16$^-$, NKG2$_{a/c}^{low}$CD16$^+$ and CXCR5$^+$ NK cells. The NKG2$_{a/c}^{high}$CD16$^+$ subset was not sorted due to the extremely low number of these cells in LN. We analyzed surface markers specific for NK cells (Fig.3f), TF (Fig.3g), effector molecules (Fig.3h), and receptors associated with trafficking, differentiation and immune function (Fig.3i). The CXCR5$^+$ NK cells clustered separately from the other NK cell subpopulations in LN, but consistently closely to the NKG2$_{a/c}^{low}$CD16$^-$ NK cells (Fig.3f-i).

The genome-wide analysis of all subsets in LN showed, in agreement to the observations made in blood (Fig.1f-i, Fig.S9), that the LN NKG2$_{a/c}^{low}$CD16$^+$ NK cells expressed high levels of markers known to be associated with NK cell terminal differentiation, whereas the NKG2$_{a/c}^{high}$CD16$^-$ NK cells showed again the less differentiated profile and expressed high levels of transcripts coding for NKG2D (*KLRK1*), NKp46 (*NCR1*) and CD56 *(NCAM-1)* similar to the CD56^{high} NK cell population observed in human SLT[15]. Differential expression of NK cell markers at the transcription level were confirmed at the protein level by flow cytometry (Fig.S10). This analysis confirmed that combined with NKG2a/c allows to distinguish NK cells with distinct differentiation stages in LN. The findings moreover demonstrate that CXCR5$^+$ NK cells are not constitutive in AGMs but expanded in response to SIVagm infection, the majority of the CXCR5$^+$ NK being NKG2A^{low} CD16.

LN-specific NK cell gene signature during SIVagm infection in the natural host

We aimed to further investigate tissue-specific differences and define potential heterogeneity of putative tissue-resident NK cells in SLT. We compared the genome-wide transcriptome profiles between blood and LN (Fig.S11a and b). Surprisingly, the CD16$^-$ and CD16$^+$ NK cells from LN were more closely related to each other than to their respective subsets in the blood. The four NK cell subpopulations in the LN segregated clearly into distinct clusters, while they were less separated from each other in the blood. As many as 5489 genes displayed expression differences between LN and blood NK cells (Fig.S11a). Gene Ontology (GO) enrichment analysis indicated that in LN, NK cells displayed an enrichment for

pathways involved in viral responses, regulation of defense, IFN response, pattern recognition receptor signaling and inflammasome activation (NLRP3, NLRp1 and NLRC4) compared to blood NK cells (Fig.S11c-e) (Tables S4 and S5). In contrast, blood NK cells displayed an enrichment in biological process terms, such as regulation of stress-activated mitogen-activated protein kinase (MAPK) cascade and of histone modifications (Fig.S11f-h) (Tables S4 and S5). Thus, LN NK cells displayed a common gene signature distinct from blood during SIVagm infection in the natural host showing for instance stronger viral defense and inflammasome activation.

LN NKG2$_{a/c}^{low}$CD16^{+} NK cells display the strongest degranulation profile during SIVagm infection

We next addressed the question of the anti-viral activity profiles in the NK cells which expanded in LN upon acute (CXCR5^{+}, NKG2$_{a/c}^{low}$CD16^{+}) and/or chronic SIVagm infection (CXCR5^{+}, NKG2$_{a/c}^{low}$CD16^{-}) using the genome-wide expression data. We compared the expanding NK cells to to the remaining subset (NKG2$_{a/c}^{high}$CD16^{-}). The NKG2$_{a/c}^{low}$CD16^{+} NK cells were those with the highest number of up-regulated genes (1072 genes) compared to NKG2$_{a/c}^{high}$CD16^{-} NK cells followed by 432 upregulated genes in NKG2$_{a/c}^{low}$CD16^{-} and 294 genes in CXCR5^{+} NK cells (Fig.4a). 176 genes were commonly upregulated among the three expanded subsets, and one gene was downregulated, *CCDC102B* (Fig.4b,c and Table S6). The latter encodes a protein that regulates microtubules. Among the 176 upregulated genes, GO enrichment analysis uncovered pathways important for the lytic activity of NK cells, such as pathways associated with the biology of cytotoxic granules, including lytic vacuoles, secretion by cells, lysosomes and lytic vacuole membranes, cellular assembly and microtubule cytoskeleton (Fig.4b-c, Table S6). Among the genes related to cytokines were *CXCL11, CXCL12, IL-27, IFNGR*, *IL15RA* and *IL21R* as well as inflammasome-related proteins (i.e. *NLRP3, IL1B*) (Fig.3h,i and Fig.4c). Many other upregulated genes are known to be associated with metabolism, such as *GLUL* (glutamine synthetase); H6PD (Glucose-6-phosphate- dehydrogenase), *ENTPD1* (CD39), and *ATP13A2*. The NKG2 ^{low} NK cells also expressed high levels of *Lamp1* (CD107a) ($p<0.000000005$) and *CCL5* ($p=0.0003$) (Fig.3, Table S6). Perforin expression was not increased at the mRNA but at the protein level in the NKG2 ^{low} NK cells (Fig.2e). These data are consistent for CXCR5^{+} and NKG2^{low} NK cells, and in particular for NKG2 ^{low}CD16^{+} NK cells, displaying a strong degranulation activity in LN.

Adaptive NKG2$_{a/c}^{low}$CD16^{+} NK cells in LN during SIVagm infection

Strong cytotoxic potential and inflammasome activation is compatible with the generation of adaptive NK cells[30–32]. We addressed the question if NK cells present in LN in response to SIVagm infection could share adaptive NK cell features. We analyzed the expression of markers which are so far described as the most specific to adaptive NK cells, meaning the modulation of TFs as well as the variable loss of some intracellular adapter signaling molecules[10,33–35] (Fig.4d). NK cells with an adaptive transcriptional profile

were not detected in the blood (Fig.1). The $NKG2_{a/c}^{high}CD16^-$ NK cells also did not resemble adaptive NK cells, since they expressed high levels of *LCK*, *CD247* (CD3z), *ZAP70*, *SYK*, *Fyn*, *SH2D1B*, *TYROBP* (DAP12) and *HCST* (DAP10). In contrast, the $NKG2_{a/c}^{low}CD16^+$ NK cells in LN fully displayed gene expression profiles characteristic of adaptive NK cells, such as low expression of *LCK, ZAP70, FcεRγ and SYK* and high expression of *GRAP2* (Fig.4a). The $NKG2_{a/c}^{low}CD16^-$ and $CXCR5^+$ NK cells also shared several adaptive NK cell-like features, including low expression of *FcεRγ* and *VAV1* (Fig.4a). The levels of *KLRC2* (NKG2C) were negligible when compared to *KLRC1* (NKG2A) transcripts in all NK cell subsets. Altogether, these findings indicate that during SIVagm infection, LN $NKG2_{a/c}^{low}CD16^+$ NK cells, and to a certain extent also $NKG2_{a/c}^{low}CD16^-$ and CXCR5+ NK cells, displayed a transcriptional profile of adaptive NK cells.

We then searched for genes that could be a link to the generation of adaptive NK cells and analyzed the genes that were strongly expressed in $NKG2_{a/c}^{low}CD16^+$ NK cells. Among 15 highly expressed genes were those coding for ZNF831, JAKMIP2, PLBD1, UBASH3, S100A9 and THEMIS (Thymocyte-Expressed Molecule Involved in Selection) (Fig.4e). THEMIS showed a positive correlation with *GRAP2* ($p<0.004$, $r=0.74$) and a negative correlation with *NKG2A* ($p<0.002$, $r=-0.83$) expression (Fig.4f). Altogether, the data reveal the presence of adaptive NK cells during SIVagm infection expressing low levels of NKG2C and high levels of Themis.

High MHC-E expression on LN memory $CD4^+$ T cells

NKG2A is an inhibitory receptor recognizing peptides presented by the non-classical type I MHC-E. Before infection, we found that among all $CD4^+$ T cells in LN, MHC-E^+ cells were found most often among memory $CD4^+$ T cells and T_{FH} cells, both in MAC and AGM (Fig.S12f-i). After SIVmac infection in MAC, both the percentage of MHC-E^+ memory $CD4^+$ T cells as well as the expression intensity of MHC-E on $CD4^+$ T cells increased and were particularly high for T_{FH} cells (Fig.5a-e, Fig.S12). In SIVagm infection, MHC-E expression was only transiently increased in acute phase and the percentage of MHC-E^+ T_{FH} cells decreased. AGM B cell follicles showed accumulation of NK cells and absence of viral RNA, as previously reported (Fig.5a-c, Fig.5f, Fig.S13)[20]. Co-staining of MHC-E expression with SIV RNA could be observed (Fig 5a). Therefore, MHC-E expression was most frequent among preferential target cells for SIV infection and persistence.

MHC-E restricted SIV-specific NK cell activity increases after SIV infection in the natural host

We set up a functional assay to analyze MHC-E restricted viral suppressive activity of NK cells from AGM and MAC. To this end, we first designed SIVagm and SIVmac peptides that can bind to MHC-E. These peptides were nonamers containing the canonical sequence motif of MHC-E binding peptides. They were encoded by ENV close to the signal-peptidase cleavage site, as described in the methods section. These peptides stabilized HLA-E expression on MHC-I devoid K562 cells stably transduced with HLA-

E*0101 (K562-E*0101) (Fig.6a) indicating the ability of the SIV ENV peptides for HLA-E binding. To further analyze the efficacy of binding, competition- binding assays were performed (Fig.6b). They demonstrate the capacity of the SIV ENV peptides to displace peptides known to strongly bind to HLA-E (VL9 or HSP60) already at low concentrations (1μM). The concentrations needed by SIV ENV peptides for displacement of VL9 and HSP60 were in a similar range as those needed by other viral peptides known to efficiently bind to HLA-E (HIVgag, HCV) peptides[36] and even lower than for the previously reported SIVmac GAG peptide[37] (Fig.S14). These analyses confirm that peptides derived from SIV ENV efficiently bind to HLA-E. We analyzed the MHC-E-dependent activity of NK cells toward target cells presenting the SIV ENV peptides via HLA-E. We first studied NK cells from uninfected AGM and MAC. NK cells were co-cultured with K562-E*0101 cells pre-loaded or not with the peptides and activity was measured by CD107a expression (Fig.6c-d). As expected, the HLA-I-derived VL9 peptide inhibited NK cell activity, while the HSP60 peptide did not, validating our assay (Fig.6c). When pulsing the cells with the SIVmac ENV peptide, NK cell activity from both MAC and AGM were inhibited. The SIVagm peptide displayed an intermediate inhibitory activity on NK cells (Fig.6c). These peptides are not representative of all SIVagm and SIVmac variants. However, the data show that NK cells reacted differentially depending on the peptide sequence.

As a proof of concept of the capacity of the ENV peptides to be processed in primary cells and to be recognized differentially by NK cells depending on their sequence when presented by simian MHC- E, we applied a functional assay using AGM primary $CD4^+$ T cells as targets and full-length infectious SIV as source for the peptides. Two infectious molecular mutant viruses deriving from the wildtype $SIVagm._{sab92018}$ backbone were generated. In this backbone, the ENV sequence coding for the nonamer peptide of the wild type virus (IGIVVIVKL) was replaced by either the sequence coding for the $SIVmac_{239/251}$ peptide (NQLLIAILL) or by the VL9 sequence. The mutant viruses replicated efficiently in primary $CD4^+$ T cells from non-infected AGM (Fig.6e). The *in vitro* infected primary $CD4^+$ T cells were co-cultured with autologous NK cells. NK cells strongly suppressed replication of the wild-type SIVagm (Fig.6e). NK cells controlled the replication of the VL9 mutant less than the wild-type SIVagm, in line with a stronger inhibitory effect of the VL9 peptide. $CD4^+$ T cells infected with the virus coding for the SIVmac ENV peptide escaped NK cell suppressive capacity. These results confirm a distinct NK cell suppressive activity depending on the ENV sequence.

NKG2A synergizes regulation of NK cell education[38]. We reasoned that NK cells are educated through the NKG2a/MHC-E axis, leading to an increase in the MHC-E restricted viral suppressive capacity of the NK cells after SIVagm infection. We therefore compared the MHC-E dependent suppressive activity of NK cells before and after SIV infection. We exposed NK cells from blood and SLT to K562-E*0101 cells loaded or not with peptides. NK cells from LN of SIVmac-infected MAC showed a drop in their capacity to lyse target cells presenting the SIVmac ENV peptide via HLA-E when compared to NK cells from healthy animals (Fig.6f and Fig.S15a). SIVmac controllers did not show stronger ENV-specific NK cell

activities than viremic MAC, except for one animal (Fig.S15a). In contrast to MAC, NK cells from AGM showed an increased activity after SIVagm infection compared to non-infected AGM (Fig.6g and Fig.S15a).

We tested if the differential changes in NK cell activity after infection were unique for the two SIV peptides or applied to other ENV peptides as well. When using peptides from another SIVagm (SIVagm.sab1) and one more distant SIV (SIVgsn), we observed again strong MHC-E restricted activity with NK cells from LN of SIVagm-infected AGM, while NK cells from SIVmac-infected MAC displayed a weak MHC-E dependent NK cell activity in presence of all SIV ENV peptides tested (Fig 6h and i). We also analyzed NK cells from spleen. MHC-E restricted activity of NK cells from spleen showed trends for decreases in MAC after SIVmac infection with the SIV Env peptides, while this activity increased after SIVagm infection in the presence of $SIVagm.sab_{92018}$, $SIVagm._{sab1}$ and $SIVmac_{239/251}$ peptides (Fig.S15b).

Discussion

During HIV/SIV infection, previous studies mostly focused on circulating NK cells, and only a few studies with tissue NK cells have been reported[13,14,20,39]. We designed a study where we compared NK cells in LN associated with strong viral control (SIVagm infection) to that of NK cells lacking the capacity to efficient viral control (SIVmac infection). Our results show that SIV infection in the natural host induced terminally differentiated $NKG2A^{low}CD16^{+}$NK cells in LN displaying a strong degranulation activity and a transcriptional profile of adaptive NK cells. In line with this, the MHC- E restricted NK cell activity against target cells presenting SIV peptides was increased after SIVagm infection. In contrast, the process of terminal NK cell differentiation was blocked in LN during SIVmac infection of MAC after day 2 p.i., despite the generation of a highly diverse NK cell pool. Our results uncover that NK cells are educated to efficiently kill SIV-infected cells in nonpathogenic SIVagm infection while this education is not occurring in pathogenic SIV infection. The notion that NK cell differentiation is the result of a continuous process that can adapt in response to a viral infection is relatively new[4,7,28,40–42]. By analyzing distinct NK cell subsets from AGM and MAC at the transcriptomic and protein level we demonstrate here that NKG2A combined with CD16 defines distinct stages of NK cell differentiation in monkeys. This provides a novel tool for preclinical studies in NHP for the investigation of other infections and for vaccine studies.

The $NKG2_{a/c}{}^{low}CD16^{+}$ NK cells clearly displayed the most differentiated profile and strong cytotoxic activity. We also observed cytotoxic activity for the $NKG2_{a/c}{}^{low}CD16^{-}$ and $CXCR5^{+}$ NK cells. CD16 can be quickly shed from the NK cell surface upon activation[43]. Under these conditions, $NKG2_{a/c}{}^{low}CD16^{-}$ and $CXCR5^{+}$ NK cells might be a mixture of less differentiated NK cells together with terminal differentiated $NKG2_{a/c}{}^{low}CD16^{+}$ cells that exert the viral control. The $NKG2_{a/c}{}^{low}CD16^{+}CXCR5^{+}$ NK cells might be responsible for the viral control in B cell follicles and the $NKG2_{a/c}{}^{low}CD16^{+}CXCR5^{-}$ NK cells in the T cell zone. While our study demonstrates a superior MHC-E restricted NK cell activity in the natural host, this

might not be the unique mechanism of viral suppression, since terminally differentiated cells also up-regulate for example ADCC- mediated killing capacity[44]. The reasons why $NKG2_{a/c}^{low}$ NK cells expanded in SIVagm infection in AGM but not in SIVmac infection in MAC are unclear. These cells did not show increased proliferation and it is unlikely that they result from trafficking, since we reported that LN homing receptors decrease on NK cells from AGM in SIVagm infection similarly to SIVmac and HIV infection[20]. It is therefore more likely that this expansion of $NKG2_{a/c}^{low}$ NK cells is due to NK cell differentiation *in situ*. A major difference between the two infections consists in the persistence of an inflammatory environment in SLT during SIVmac infection while inflammation is resolved in SIVagm infection[19,39]. Systemic inflammation has been shown to drive the expansion of IFN-g producing NK cells in mice[45,46]. Similarly, it has been recently shown that inflammatory cytokines drive the expansion of $CD94^{-}CD56^{bright}$ NK cells with an increased capacity to produce IFN-g in HIV infection which could themselves contribute to the inflammation[47]. These cells might correspond to the $NKG2_{a/c}^{high}$ $CD16^{-}$ NK cells that were the predominant NK cell subset in LN of SIVmac-infected MAC. The terminally differentiated NK cells in AGM LN expressed high levels of IL15R and IL21R. Higher levels of IL-15 and IL-21 in the local environment during SIVagm infection as compared to SIVmac infection might allow the terminal differentiation. Considering that AGMs are ancient hosts of SIV, it is possible that the long-term co-existence in AGM selected for a specific tissue environment in response to SIV infection that allows proper education of NK cells. By driving NK cells toward a terminal differentiated, cytotoxic phenotype in SIVagm infection, this would allow the presence of NK cells with capacity to kill infected cells in LN, while avoiding the inflammation associated with NK-cell mediated IFN-g production.

The distinct MHC-E expression profiles on CD4+ T cells in LN between SIVmac and SIVagm infection might be determined by host and/or viral factors[45–50]. The frequency of productively infected cells in chronic SIVagm infection in SLT is too low to explain the decreased levels of MHC-E solely by virus-mediated down-regulation of MHC-E or NK-cell mediated killing of MHC- E+ cells. A distinct inflammatory environment between SIVmac and SIVagm infections, in particular higher levels of IFN-g in SIVmac than SIVagm infection[48–52], could be one reason for the higher MHC-E expressions in SIVmac infection.

It has been shown that genetic factors determining MHC-E expression levels strongly impact viral load in HIV-infected individuals[53], in line with reports on the importance of MHC-E in SIV control[37,54–56]. It has previously been reported that MHC-E dependent NK cell suppressive capacity is dependent of the nature of the peptide loaded by MHC-E[36,57–59] and that peptides derived from SIVmac can inhibit NK cells[36,56,60]. Only few MHC-E binding viral peptides have been described so far[55,58]. We define here a novel lentiviral region that can code for peptides with the capacity to bind to MHC-E. ENV might thus serve as a critical new target for NK cell directed HIV vaccines, cure strategies, or other therapeutic modalities. Further analyses are needed to identify the sequences of peptides bound to MHC-E *in vivo*. Of note, the target cells and peptides used in our assays were the same before and after SIV infection, clearly demonstrating

that the increased MHC-E restricted activity of NK cells in SIVagm infection must be due to changes at the level of the NK cells themselves.

A few examples are known where NKG2A-dependent NK cell education is a determining factor for NK cell responses in infectious conditions[6,44,61,62]. The increased functional activity here was not related to stronger expression of NKG2C and the NK cells that expanded here thus are not identical to the NK cells that expand upon CMV infection[63–65]. The signaling pathways of adaptive NK cells are poorly understood. The NK cells here expressed high level of transcripts coding for THEMIS. THEMIS has been reported to regulate signaling downstream of the T cell receptor (TCR) by interacting with SHP-1 and GRB2, both of which are supposed to participate in the transduction of the NKG2A signal after its ligation with MHC-E[66–68]. The data suggest a role of Themis for adaptive NK cell generation.

In conclusion, this study delivers unparalleled insights into functional differentiation of NK cells during a controlled viral infection in a tissue of crucial importance, the LNs, and key insights for an optimized guidance on NK-cell-based immunotherapies toward HIV cure.

ACKNOWLEDGEMENTS

We are grateful for the excellent help from the veterinarians and staff at the IDMIT Center (Benoit Delache, Jean-Marie Helies, Raphaël Ho Tsong Fang and Julie Morin). We thank M. Mietsch and M. Daskalaki for comprehensive veterinary support, and S. Heine, J. Hampe and N. Leuchte for excellent technical assistance. We also thank all the people from the Illumina Hiseq 2500 platform at the Institut Pasteur and especially Caroline Proux and Jean-Yves Coppee. NH was supported by the VRI Labex, the Fondation Beytout and Institut Pasteur, and PR was recipient of a PhD fellowship from the University Paris Diderot, Sorbonne Paris Cité. CP was supported by an MSDAvenir Post- doctoral Fellowship Grant. We would like to acknowledge grant support from ANRS, the Fondation J. Beytout and the Fondation Les Ailes to MMT, from the NIH (R01AI143457) to MMT and RKR and from MSDAvenir to ASC and MMT. JH and M. were supported by NIH grant R01AI116379. JN was supported by the DFG (SPP 1937, SFB TR57), the Hector Foundation, and the DZIF (TTU- HIV). We gratefully acknowledge the support to IDMIT from the French government: Investments for the Future program for infrastructures (PIA) through the ANR-11-INBS-0008 grant as well as from the PIA grant ANR-10-EQPX-02-01 to the FlowCyTech facility at IDMIT. We equally ac- knowledge the Investments for Future grant ANR-10–INSB–04 to support the UtechS Photonic BioImaging (Imagopole) and C2RT facilities at Institut Pasteur.

AUTHOR CONTRIBUTIONS

NH and MMT designed the study; NH designed the experiments; NH, PR, RG and BJ performed experiments; NH, PR and JN designed the peptides; NH, BJ and US quantified the viral loads; CS and FK

constructed the infectious SIVagm clones; NH and EB performed the prediction analyses; CSH provided samples; NH, RL and HV performed the bioinformatic analyses; NH, PR and YM performed the statistical analyses; NH, PR, JH, RLG, RKR, MP, ASC, BJ and MMT analyzed the data; VC, RLG and BJ coordinated the animal studies; MMT obtained the funding; NH and MMT wrote the manuscript and all co-authors reviewed it.

REFERENCES

1. Martin, M. P. & Carrington, M. Immunogenetics of HIV disease. *Immunol. Rev.* **254**, 245–264 (2013).
2. Alter, G. & Altfeld, M. NK cells in HIV-1 infection: Evidence for their role in the control of HIV-1 infection. *J. Intern. Med.* **265**, 29–42 (2009).
3. Goulder, P. J. R. & Watkins, D. I. Impact of MHC class I diversity on immune control of immunodeficiency virus replication. *Nat. Rev. Immunol.* **8**, 619–630 (2008).
4. Blish, C. A. Natural Killer Cell Diversity in Viral Infection: Why and How Much? *Pathog. Immun.* **1**, 165–192 (2016).
5. Freud, A. G., Mundy-Bosse, B. L., Yu, J. & Caligiuri, M. A. The Broad Spectrum of Human Natural Killer Cell Diversity. *Immunity* **47**, 820–833 (2017).
6. Goodridge, J. P., Önfelt, B. & Malmberg, K.-J. Newtonian cell interactions shape natural killer cell education. *Immunol. Rev.* **267**, 197–213 (2015).
7. Strauss-Albee, D. M. *et al.* Human NK cell repertoire diversity reflects immune experience and correlates with viral susceptibility. *Sci. Transl. Med.* **7**, 297ra115 (2015).
8. Palgen, J.-L. *et al.* NK cell immune responses differ after prime and boost vaccination. *J. Leukoc. Biol.* **105**, 1055–1073 (2019).
9. Reeves, R. K. *et al.* Antigen-specific NK cell memory in rhesus macaques. *Nat. Immunol.* **16**, 927–932 (2015).
10. Paust, S., Senman, B. & von Andrian, U. H. Adaptive Immune Responses Mediated by Natural Killer Cells. *Immunol. Rev.* **235**, 286–296 (2010).
11. Peng, H. & Tian, Z. Natural Killer Cell Memory: Progress and Implications. *Front. Immunol.* **8**, 1143 (2017).
12. Lucar, O., Reeves, R. K. & Jost, S. A Natural Impact: NK Cells at the Intersection of Cancer and HIV Disease. *Front. Immunol.* **10**, (2019).
13. Luteijn, R. *et al.* Early viral replication in lymph nodes provides HIV with a means by which to escape NK-cell-mediated control. *Eur. J. Immunol.* **41**, 2729–2740 (2011).
14. Schafer, J. L., Li, H., Evans, T. I., Estes, J. D. & Reeves, R. K. Accumulation of Cytotoxic CD16+ NK Cells in Simian Immunodeficiency Virus-Infected Lymph Nodes Associated with In Situ Differentiation and Functional Anergy. *J. Virol.* **89**, 6887–6894 (2015).
15. Freud, A. G. *et al.* A Human CD34(+) Subset Resides in Lymph Nodes and Differentiates into CD56brightNatural Killer Cells. *Immunity* **22**, 295–304 (2005).
16. Svardal, H. *et al.* Ancient hybridization and strong adaptation to viruses across African vervet monkey populations. *Nat. Genet.* **49**, 1705–1713 (2017).
17. Müller, M. C. *et al.* Simian immunodeficiency viruses from central and western Africa: evidence for a new species-specific lentivirus in tantalus monkeys. *J. Virol.* **67**, 1227–1235 (1993).
18. Raehtz, K., Pandrea, I. & Apetrei, C. The well-tempered SIV infection: Pathogenesis of SIV infection in natural hosts in the wild, with emphasis on virus transmission and early events post- infection that may contribute to protection from disease progression. *Infect. Genet. Evol.* **46**, 308–323 (2016).
19. Sodora, D. L. *et al.* Toward an AIDS vaccine: lessons from natural simian immunodeficiency virus

infections of African nonhuman primate hosts. *Nat. Med.* **15**, 861–865 (2009).
20. Huot, N. *et al.* Natural killer cells migrate into and control simian immunodeficiency virus replication in lymph node follicles in African green monkeys. *Nat. Med.* **23**, 1277–1286 (2017).
21. Hong, J. J., Chang, K.-T. & Villinger, F. The Dynamics of T and B Cells in Lymph Node during Chronic HIV Infection: TFH and HIV, Unhappy Dance Partners? *Front. Immunol.* **7**, 522 (2016).
22. Wong, J. K. & Yukl, S. A. Tissue reservoirs of HIV. *Curr. Opin. HIV AIDS* **11**, 362–370 (2016).
23. Strauss-Albee, D. M., Horowitz, A., Parham, P. & Blish, C. A. Coordinated regulation of natural killer receptor expression in the maturing human immune system. *J. Immunol. Baltim. Md 1950* **193**, 4871–4879 (2014).
24. Horowitz, A. *et al.* Genetic and environmental determinants of human NK cell diversity revealed by mass cytometry. *Sci. Transl. Med.* **5**, 208ra145 (2013).
25. Sivori, S. *et al.* TLR/NCR/KIR: Which One to Use and When? *Front. Immunol.* **5**, (2014).
26. Victor, A. R. *et al.* Epigenetic and Posttranscriptional Regulation of CD16 Expression during Human NK Cell Development. *J. Immunol. Baltim. Md 1950* **200**, 565–572 (2018).
27. Béziat, V., Descours, B., Parizot, C., Debré, P. & Vieillard, V. NK Cell Terminal Differentiation: Correlated Stepwise Decrease of NKG2A and Acquisition of KIRs. *PLoS ONE* **5**, (2010).
28. Luetke-Eversloh, M., Killig, M. & Romagnani, C. Signatures of Human NK Cell Development and Terminal Differentiation. *Front. Immunol.* **4**, (2013).
29. Huot, N., Bosinger, S. E., Paiardini, M., Reeves, R. K. & Müller-Trutwin, M. Lymph Node Cellular and Viral Dynamics in Natural Hosts and Impact for HIV Cure Strategies. *Front. Immunol.* **9**, (2018).
30. van den Boorn, J. G. *et al.* Inflammasome-Dependent Induction of Adaptive NK Cell Memory. *Immunity* **44**, 1406–1421 (2016).
31. Evavold, C. & Kagan, J. C. How inflammasomes inform adaptive immunity. *J. Mol. Biol.* **430**, 217–237 (2018).
32. O'Sullivan, T. E., Johnson, L. R., Kang, H. H. & Sun, J. C. BNIP3- and BNIP3L-Mediated Mitophagy Promotes the Generation of Natural Killer Cell Memory. *Immunity* **43**, 331–342 (2015).
33. Wagner, J. A. & Fehniger, T. A. Human Adaptive Natural Killer Cells: Beyond NKG2C. *Trends Immunol.* **37**, 351–353 (2016).
34. Tesi, B., Schlums, H., Cichocki, F. & Bryceson, Y. T. Epigenetic Regulation of Adaptive NK Cell Diversification. *Trends Immunol.* **37**, 451–461 (2016).
35. Paust, S., Blish, C. A. & Reeves, R. K. Redefining Memory: Building the Case for Adaptive NK Cells. *J. Virol.* **91**, (2017).
36. Walters, L. C. *et al.* Pathogen-derived HLA-E bound epitopes reveal broad primary anchor pocket tolerability and conformationally malleable peptide binding. *Nat. Commun.* **9**, 1–13 (2018).
37. Hansen, S. G. *et al.* Broadly targeted CD8+ T cell responses restricted by major histocompatibility complex-E. *Science* **351**, 714–720 (2016).
38. Anfossi, N. *et al.* Human NK cell education by inhibitory receptors for MHC class I. *Immunity* **25**, 331–342 (2006).
39. Jacquelin, B. *et al.* Innate Immune Responses and Rapid Control of Inflammation in African Green Monkeys Treated or Not with Interferon-Alpha during Primary SIVagm Infection. *PLoS Pathog.* **10**, (2014).
40. Cichicki, F. *et al.* Diversification and Functional Specialization of Human NK Cell Subsets. *Curr. Top. Microbiol. Immunol.* **395**, 63–94 (2016).
41. Wilk, A. J. & Blish, C. A. Diversification of human NK cells: Lessons from deep profiling. *J Leukoc.*

Biol. **103**, 629–641 (2018).
42. Schlums, H. *et al.* Cytomegalovirus Infection Drives Adaptive Epigenetic Diversification of NK Cells with Altered Signaling and Effector Function. *Immunity* **42**, 443–56 (2015).
43. Romee, R. *et al.* NK cell CD16 surface expression and function is regulated by a disintegrin and metalloprotease-17 (ADAM17). *Blood* **121**, 3599–3608 (2013).
44. Kristensen, A. B., Kent, S. J. & Parsons, M. S. Contribution of NK Cell Education to both Direct and Anti-HIV-1 Antibody-Dependent NK Cell Functions. *J. Virol.* **92**, (2018).
45. Rasid, O. *et al.* H3K4me1 Supports Memory-like NK Cells Induced by Systemic Inflammation. *Cell Rep.* **29**, 3933-3945.e3 (2019).
46. Wu, Y., Tian, Z. & Wei, H. Developmental and Functional Control of Natural Killer Cells by Cytokines. *Front. Immunol.* **8**, (2017).
47. Wang, Y. *et al.* HIV-1-induced cytokines deplete homeostatic innate lymphoid cells and expand TCF7 -dependent memory NK cells. *Nat. Immunol.* **21**, 274–286 (2020).
48. Zhou, F. Molecular mechanisms of IFN-gamma to up-regulate MHC class I antigen processing and presentation. *Int. Rev. Immunol.* **28**, 239–260 (2009).
49. Yang, I. *et al.* Modulation of major histocompatibility complex Class I molecules and major histocompatibility complex-bound immunogenic peptides induced by interferon-alpha and interferon-gamma treatment of human glioblastoma multiforme. *J. Neurosurg.* **100**, 310–319 (2004).
50. Nguyen, S. *et al.* HLA-E upregulation on IFN-γ-activated AML blasts impairs CD94/NKG2A-dependent NK cytolysis after haplo-mismatched hematopoietic SCT. *Bone Marrow Transplant.* **43**, 693–699 (2009).
51. Kornfeld, C. *et al.* Antiinflammatory profiles during primary SIV infection in African green monkeys are associated with protection against AIDS. *J. Clin. Invest.* **115**, 1082–1091 (2005).
52. Ploquin, M. J.-Y. *et al.* Distinct expression profiles of TGF-β1 signaling mediators in pathogenic SIVmac and non-pathogenic SIVagm infections. *Retrovirology* **3**, 37 (2006).
53. Ramsuran, V. *et al.* Elevated HLA-A expression impairs HIV control through inhibition of NKG2A-expressing cells. *Science* **359**, 86–90 (2018).
54. Thans, T. van S. *et al.* Primary HIV-1 Strains Use Nef To Downmodulate HLA-E Surface Expression. *J. Virol.* **93**, (2019).
55. Joosten, S. A., Sullivan, L. C. & Ottenhoff, T. H. M. Characteristics of HLA-E Restricted T- Cell Responses and Their Role in Infectious Diseases. *Journal of Immunology Research* vol. 2016 e2695396 https://www.hindawi.com/journals/jir/2016/2695396/ (2016).
56. Davis, Z. B. *et al.* A Conserved HIV-1-Derived Peptide Presented by HLA-E Renders Infected
57. T-cells Highly Susceptible to Attack by NKG2A/CD94-Bearing Natural Killer Cells. *PLOS Pathog.* **12**, e1005421 (2016).
58. Miller, J. D. *et al.* Analysis of HLA-E Peptide-Binding Specificity and Contact Residues in Bound Peptide Required for Recognition by CD94/NKG2. *J. Immunol.* **171**, 1369–1375 (2003).
59. Celik, A. A., Kraemer, T., Huyton, T., Blasczyk, R. & Bade-Döding, C. The diversity of the HLA-E-restricted peptide repertoire explains the immunological impact of the Arg107Gly mismatch. *Immunogenetics* **68**, 29–41 (2016).
60. Rölle, A., Jäger, D. & Momburg, F. HLA-E Peptide Repertoire and Dimorphism—Centerpieces in the Adaptive NK Cell Puzzle? *Front. Immunol.* **9**, (2018).
61. Hannoun, Z. *et al.* Identification of novel HIV-1-derived HLA-E-binding peptides. *Immunol. Lett.* **202**, 65–72 (2018).
62. Zhang, X., Feng, J., Chen, S., Yang, H. & Dong, Z. Synergized regulation of NK cell education by NKG2A and specific Ly49 family members. *Nat. Commun.* **10**, 1–12 (2019).

63. Hammer, Q. *et al.* Peptide-specific recognition of human cytomegalovirus strains controls adaptive natural killer cells. *Nat. Immunol.* **19**, 453–463 (2018).
64. Malmberg, K.-J., Beziat, V. & Ljunggren, H.-G. Spotlight on NKG2C and the human NK-cell response to CMV infection. *Eur. J. Immunol.* **42**, 3141–3145 (2012).
65. Pupuleku, A. *et al.* Elusive Role of the CD94/NKG2C NK Cell Receptor in the Response to Cytomegalovirus: Novel Experimental Observations in a Reporter Cell System. *Front. Immunol.* **8**, (2017).
66. Béziat, V. *et al.* CMV drives clonal expansion of NKG2C + NK cells expressing self-specific KIRs in chronic hepatitis patients. *Eur. J. Immunol.* **42**, 447–57 (2012).
67. Brockmeyer, C. *et al.* T Cell Receptor (TCR)-induced Tyrosine Phosphorylation Dynamics Identifies THEMIS as a New TCR Signalosome Component. *J. Biol. Chem.* **286**, 7535–7547 (2011).
68. Paster, W. *et al.* GRB2-mediated recruitment of THEMIS to LAT is essential for thymocyte development. *J. Immunol. Baltim. Md 1950* **190**, 3749–3756 (2013).
69. Choi, S. *et al.* THEMIS enhances TCR signaling and enables positive selection by selective inhibition of the phosphatase SHP-1. *Nat. Immunol.* **18**, 433–441 (2017).
70. Daskalaki, M. *et al.* Long-term efficient control of SIV infection in macaques is associated with an intact intestinal barrier. *J. Med. Primatol.* **46**, 144–148 (2017).
71. Mussil, B., Sauermann, U., Motzkus, D., Stahl-Hennig, C. & Sopper, S. Increased APOBEC3G and APOBEC3F expression is associated with low viral load and prolonged survival in simian immunodeficiency virus infected rhesus monkeys. *Retrovirology* **8**, 77 (2011).
72. Shen, A. *et al.* Resting CD4+ T lymphocytes but not thymocytes provide a latent viral reservoir in a simian immunodeficiency virus-Macaca nemestrina model of human immunodeficiency virus type 1-infected patients on highly active antiretroviral therapy. *J. Virol.* **77**, 4938–4949 (2003).
73. Gnanadurai, C. W. *et al.* Genetic identity and biological phenotype of a transmitted/founder virus representative of nonpathogenic simian immunodeficiency virus infection in African green monkeys. *J. Virol.* **84**, 12245–12254 (2010).
74. Diop, O. M. *et al.* High levels of viral replication during primary simian immunodeficiency virus SIVagm infection are rapidly and strongly controlled in African green monkeys. *J. Virol.* **74**, 7538–7547 (2000).
75. Ram, D. R. *et al.* Tracking KLRC2 (NKG2C)+ memory-like NK cells in SIV+ and rhCMV+ rhesus macaques. *PLoS Pathog.* **14**, e1007104 (2018).
76. Jacquelin, B. *et al.* Nonpathogenic SIV infection of African green monkeys induces a strong but rapidly controlled type I IFN response. *J. Clin. Invest.* **119**, 3544–3555 (2009).
77. Braud, V. M., Allan, D. S., Wilson, D. & McMichael, A. J. TAP- and tapasin-dependent HLA- E surface expression correlates with the binding of an MHC class I leader peptide. *Curr. Biol. CB* **8**, 1–10 (1998).
78. Michaëlsson, J. *et al.* A signal peptide derived from hsp60 binds HLA-E and interferes with CD94/NKG2A recognition. *J. Exp. Med.* **196**, 1403–1414 (2002).
79. Wu, H. L. *et al.* The Role of MHC-E in T Cell Immunity Is Conserved among Humans, Rhesus Macaques, and Cynomolgus Macaques. *J. Immunol. Baltim. Md 1950* **200**, 49–60 (2018).
80. Alter, G., Malenfant, J. M. & Altfeld, M. CD107a as a functional marker for the identification of natural killer cell activity. *J. Immunol. Methods* **294**, 15–22 (2004).
81. Webb, B. & Sali, A. Protein Structure Modeling with MODELLER. *Methods Mol. Biol. Clifton NJ* **1654**, 39–54 (2017).
82. Ashkenazy, H. *et al.* ConSurf 2016: an improved methodology to estimate and visualize evolutionary conservation in macromolecules. *Nucleic Acids Res.* **44**, W344-350 (2016).
83. Cokelaer, T., Desvillechabrol, D., Legendre, R. & Cardon, M. 'Sequana': a Set of Snakemake NGS

pipelines. *J. Open Source Softw.* **2**, 352 (2017).
84. Martin, M. Cutadapt removes adapter sequences from high-throughput sequencing reads. *EMBnet.journal* (2011) doi:10.14806/ej.17.1.200.
85. Liao, Y., Smyth, G. K. & Shi, W. featureCounts: an efficient general purpose program for assigning sequence reads to genomic features. *Bioinforma. Oxf. Engl.* **30**, 923–930 (2014).
86. Love, M. I., Huber, W. & Anders, S. Moderated estimation of fold change and dispersion for RNA-seq data with DESeq2. *Genome Biol.* **15**, 550 (2014).
87. Benjamini, Y. & Hochberg, Y. Controlling The False Discovery Rate - A Practical And Powerful Approach To Multiple Testing. *J R. Stat. Soc Ser. B* **57**, 289–300 (1995).
88. Bindea, G. *et al.* ClueGO: a Cytoscape plug-in to decipher functionally grouped gene ontology and pathway annotation networks. *Bioinformatics* **25**, 1091–1093 (2009).
89. Lundegaard, C., Lund, O. & Nielsen, M. Accurate approximation method for prediction of class I MHC affinities for peptides of length 8, 10 and 11 using prediction tools trained on 9mers. *Bioinforma. Oxf. Engl.* **24**, 1397–1398 (2008).
90. Nielsen, M. *et al.* Reliable prediction of T-cell epitopes using neural networks with novel sequence representations. *Protein Sci. Publ. Protein Soc.* **12**, 1007–1017 (2003).

MATERIAL AND METHODS

Monkeys and SIV infections

Twelve African green monkeys (Caribbean *Chlorocebus aethiops,* AGM), 9 cynomolgus macaques (*Macaca fascicularis,* cynMAC) and 18 rhesus macaques (*Macaca mulatta,* rhMAC) were studied (Supplementary method Fig 1). The AGM were infected with SIVagm.sab92018, the cynMAC with SIVmac251 and the rhMAC with SIVmac239 as previously described[20,69,70]. The viremia levels are shown in Supplementary method Fig 1. All cynMAC where viremic. Five rhMAC were used as uninfected controls. Six out of the 13 SIVmac-infected rhMAC were viremic and 7 were SIV Controllers (SIC). If not specified otherwise in the text, the species of macaques used was cynomolgus.

The AGM and cynMAC were housed at the IDMIT Center (Fontenay-aux-Roses, France) and the rhMAC at the German Primate Center (DPZ). All experimental procedures were conducted in strict accordance with the international European guidelines 2010/63/UE on the protection of animals used for experimentation and other scientific purposes and with the German and French law (French decree 2013-118), and the German Animal Welfare Act and also with the recommendations of the Weatherall report. The IDMIT center complies with the Standards for Human Care and Use of the Office for Laboratory Animal Welfare (OLAW, USA) under OLAW Assurance number A5826-86. Monitoring of the monkeys was under the supervision of the veterinarians in charge of the animal facilities. Animal experimental protocols were approved by the Ethical Committee of Animal Experimentation (CETEA-DSV, IDF, France) (Notification 12-098 and A17-044). The pVISCONTI study was approved and accredited under

statement number A15-035 by the ethics committee "*Comité d'Ethique en Expérimentation Animale du CEA"*, registered and authorized under Number 2453-2015102713323361v2 by the French Ministry of Education and Research. The study at DPZ was approved by the Lower Saxony State Office for Consumer Protection and Food Safety and performed with the project licences 33.19-42502-04-12/0820 and 33.19-42502-04- 17/2500. The DPZ has the permission to breed and house nonhuman primates under license number 392001/7 granted by the local veterinary office and conforming with § 11 of the German Animal Welfare act. Monkeys were sedated with Ketamine Chlorhydrate (Rhone-Mérieux, Lyons, France) before handling. The sample size varied between 3 and 9 monkeys per group (n = 6 in most experiments). Sample collection was performed in random order, according to the tripartite harmonized International Council for Harmonization of Technical Requirements for Pharmaceuticals for Human Use (ICH) Guideline on Methodology (previously coded Q2B). The investigators were not blinded while the animal handlers were blinded to group allocation.

Tissue collections and processing

Whole venous blood was collected in ethylenediaminetetraacetic acid (EDTA) tubes. Peripheral blood mononuclear cells (PBMCs) were isolated by Ficoll density-gradient centrifugation. Biopsies of peripheral LNs (pLN) were performed by excision. Other tissues were collected at autopsy. After careful removal of adhering connective and fat tissues, pLN and spleen cells were dissociated using the gentlemacS™ Dissociator technology (Miltenyi Biotec, Germany). The cell suspension was subsequently filtered through 100- and 40-µm cell strainers, and cells were washed with cold phosphate-buffered saline (PBS). Cells were either immediately stained for flow cytometry or cryopreserved in 90% foetal bovine serum (FBS) and 10% dimethyl sulfphoxide (DMSO) and stored in liquid nitrogen vapour.

Plasma viral load

The viral RNA copy numbers in plasma and the cell-asssociated viral DNA and RNA of the animals were quantified as previously described[20,39,71]. The cut-off value was 60 viral copies or below per ml plasma. Ultrasensitive determinations of plasma viral loads were achieved by concentrating virus from the larger volumes of material available by ultracentrifugation.

Viral RNA from rhesus macaques was extracted from 140 µl plasma using QiaAmp viral RNA isolation mini kit (Qiagen). For qRT-PCR, 8.5 µl RNA-solution were reverse transcribed and amplified using TaKaRa Prime-Script-One-Step-RT-PCR kit (TaKaRa Bio Europe) using primers gag forward (5′-ACCCAGTACAACAAATAGGTGGTAACT-3′), gag reverse (5′-TCAATTTTACCCAGGCATTTAATGT-3′) and a fluorescent probe (5′-6FAM (6- carboxyfluorescein)-TGTCCACCTGCCATTAAGCCCGAG-TAMRA (6-carboxytetramethylrhodamine-3′). Reverse transcription was performed at 45 °C for 5 min, amplification was started by an initial denaturation step at 95 °C for 10 s, followed by 45 cycles of denaturation for 5 s at 95 °C and annealing and elongation at 60 °C for 30 s using the Rotor-Gene Q apparatus and software

(Qiagen). The cut-off value was 40 viral copies per ml plasma.

Construction of the infectious molecular clones of SIVagm

Two infectious recombinant molecular clones were derived from the SIVagm.sab92018 clone (SIVagmSab92018ivTF) which itself derived from a SIVagm virus that was isolated from a naturally infected AGM and has never been *in vitro* cultured before cloning[72,73]. The recombinant clones harbor the ENV LS sequence coding either for the nonamer peptide of SIVmac$_{239/251}$ (NQLLIAILL; aatcagctgcttatcgccatcttgctt) or VL9 (VMAPRTLL; gtgatggcgccgcgcaccctgctgctg). The mutants were generated by replacement of the wildtype ENV LS sequence of SIVagm.sab using site-directed mutagenesis (cat:E0554; NEB New England Biolabs). The primers used were VL9_sense: caccctgctgctgGAACAATATGTTACAGTATTTTATG, VL9_reve: (cgcggcgccatcacCAAAAAGACTAAAAGAAAAAGC, mac$_{239/251_sense:}$ cgccatcttgcttGAACAATATGTTACAGTATTTTATG and mac$_{239/251_rev:}$ ataagcagctgattCAAAAAGACTAAAAGAAAAAGC.

Polychromatic flow cytometry

PBMCs and pLN cells were stained as previously described[20]. The antibodies are listed in Supplementary method Table 1. The anti-NKG2A antibody used recognizes both NKG2A and NKG2C on simian cells[74]. Flow cytometry acquisitions were done on a LSRFortessa (BD Biosciences). Intracellular staining was performed using BD Cytofix/Cytoperm™. The data were further analyzed using FlowJo 10.4.2 software (FlowJo, LLC, Ashland, OR, USA). Multiparametric analyses were performed using SPICE (version 5.1). *t*-SNE was performed with the *cytobank* (Cytobank, Inc.), using 2,000 iterations and a perplexity of 60.

Immunofluorescence staining

K562-E*0101 cells were incubated 16 hours (h) with biotinylated peptides. Cells were then fixed with PFA 4% and staining was performed using DAPI and Streptavidin coupled with Alexa 568 for 1 h at 37 °C followed by three washing steps. Cells were analyzed using a Nikon microscope. Appropriate filters for immunofluorescence analysis of labeled cells were used and images were imported into ImageJ software.

Fresh pLN tissues were embedded and snap frozen in optimum cold temperature compound (OCT) and 10µm frozen sections were stained using unconjugated primary antibodies followed by appropriate secondary antibodies conjugated to Alexa 488 (green), Alexa 568 (red) (Molecular Probes, Eugene, OR). Antibodies used are shown in Supplementary method table 1. FISH assay combined with immunofluorescent staining was performed as previously described[20]. Stained slides were incubated with 100–200 µL of ice cold methanol and 5% acetic acid, placed at -20°C for 10 min and then washed. Image analysis was performed using a Leica TCS SP8 confocal microscope equipped with white lasers (Leica Microsystems, Exton, PA).

Generation of a MHC-E$^+$K562 cell line

K562 were used as packaging cells to generate a lentivirus coding for HLA-E*0101 under the control of a CMV promotor (pLenti-GIII-CMV-RFP-2A-Puro lentiviral vectors (ABMGood)) according to manufacturer's instructions. Lentiviral particles were concentrated using Polybrene and Chondroitin Sulphate and viral pellets resuspended in one hundredth of the original volume in DMEM medium.

Before transduction, the coated plates were washed with dH_2O twice and then exposed to UV light for 45 min. K562 cells obtained from the American Type Culture Collection (ATCC) were seeded at a density of 2×10^4 cells per well (in coated and uncoated plates) and incubated at 37°*C* in a humidified 5% CO_2 incubator overnight. Cell culture medium in plates was removed leaving 100 μl medium in each well. Thirty minutes before transduction, the lentiviral vector was thawed on ice and 8 μg Polybrene was added to 100 μl of the virus in the tube. Viral vector-Polybrene complexes were added to each well, in coated and uncoated plates, at distinct multiplicities of infection (5, 10, 15 and 20 MOI). Plates were shaken gently and placed back in the incubator and incubated at 37°C and 5% CO2. Six hours after transduction, K562 cells were centrifuged at 800 × g for 10 seconds and cultured for 70 min at 32°C. After that, the cells were returned to the plates and incubated overnight. Cells were then seeded into 96 wells plated at the concentration of one cell per well in order to generate unique clones. After 5 weeks, transduction efficiency was evaluated by measuring the percentage of RFP-expressing cells by flow cytometry. One clone was selected, amplified and used for all the experiments.

Isolation of CD4+ T cells and NK cells

PBMC, pLN and spleen cells frozen at the day of their collection were thawed. CD4$^+$ T cells and NK cells were isolated using, respectively, anti-human CD4 or anti-NKG2a/c monoclonal antibody- conjugated microbeads with the Cell Separation Bead Miltenyi Biotec tools (USA), as previously described[75].

Cell culture

K562 (human HLA class I–negative erythroleukemia) (ATCC® CCL-243) as well as HLA-E transduced K562 cells were maintained in RPMI 1640 (Life Technologies) supplemented with 10% heat-inactivated foetal calf serum (FCS), 2 mM, l-glutamine, 100 U/ml penicillin, and 100µg/ml streptomycin. CD4$^+$ T cells were maintained in RPMI 1640 with Glutamax (Life Technologies) supplemented with 10% heat-inactivated FCS, 2 mM, l-glutamine, 100 U/ml penicillin, 100µg/ml streptomycin and 100 IU/ml of IL-2. NK cells were cultured in the same medium supplemented with 10 ng/mL of IL-15.

Infection of primary CD4$^+$ T cells with SIVagm viruses

CD4$^+$ T cells from SIV-negative AGMs rested overnight in the medium described above supplemented with IL-4 (20µg/ml). They were stimulated with anti-CD4 and -CD3. After 2 days, 5×10^6 cells CD4$^+$ T cells were exposed to virus (4ng of p27 capsid antigen) for 1h. Subsequently, cells were washed extensively to remove cell-free virus and maintained in IL-2 medium. Virus production in culture

supernatants was monitored at regular intervals by SIV p27 antigen capture assay (Zeptometrix) according to the manufacturer's instructions.

Design of SIVagm and SIVmac ENV peptides with potential for efficient binding to HLA-E We searched for SIV-derived peptides that would have a high probability for binding to MHC-E and examined whether the SIV genome sequence encodes amino acid sequences similar to the canonical MHC-E binding motif found in the leader sequence (LS) of classical MHC class I[76] and some cellular proteins such as the stress protein HSP60[77]. Since retroviral ENV proteins contain a LS, we focused on that region and screened the ENV LS sequences from 8 distinct SIV. We identified 28 peptides showing similarities with the MHC-E permissive motif (Supplementary method Figure 2a). We used a prediction algorithm to examine these 28 Env LS peptides as well as two control peptides (VL9 (VMAPRTVLL) derived from HLA-B*0701 and HSP60 (QMRPVSRVL)) for their binding affinity to HLA-E*0101 and HLA-E*0103, the only two functional HLA-E alleles in humans (Supplementary method Figure 2b and Supplementary method Table 2). We selected for each SIV the ENV peptide with a high probability to bind to MHC-E (Supplementary method Figure 2c and Supplementary method Table 2). The peptides selected for SIVmac239 and SVmac251 were identical to each other. The MHC-E peptide-binding groove is conserved among primates and it has been shown that human and MAC MHC-E are promiscuous and able to bind identical peptides[36,78]. Three-dimensional analyses indicated that AGM MHC-E was also conserved with respect to human and other nonhuman primate MHC-E (Supplementary method Figure 2d).

Peptides and HLA-E Stabilization assay

Synthetic peptides biotinylated or not were purchased from *Proimmune* (United Kingdom) and *Proteogenix* (France) and dissolved in DMSO at the concentration of 2mg/ml. The peptides used were VL9 (VMAPRTVLL), HSP60 (QMRPVSRVL), $SIV_{MAC239/251}$ (NQLLIAILL), $SIVagm_{SAB92018}$ (IGIVVIVKL), $SIVagm_{SAB-1}$ (SGCWSLVWL), $SIVagm_{TAN1}$ (GLGVGIVQL) and SIV_{GSN} (KMLVVSLTL). K562 and K562-E*0101 cells were incubated with synthetic peptides (3–300µM) at 37°C for 15–20 hours in serum-free AIM-V medium (GIBCO BRL) at a concentration of 1–3 10^6 cells/ml. Control cultures were kept at 37 °C for over 16 hours without peptides. Cells were then harvested, washed in PBS and cell-surface expression of HLA-E was determined by incubation with PE-conjugated anti-HLA-E antibody, washed twice with PBS and fixed in 100 µl of Cytofix (BD Biosciences). Cells were acquired using a LSR II (BD Biosciences), and FlowJo software (version 9.6.4, Tree Star, Ashland, OR) was used for all analyses. Results were expressed either directly as mean fluorescent intensity (MFI).

Peptide Competition Assay

Peptide-binding assays were performed according to methods described in the literature (36). In brief, K562-E*0101 cells were incubated overnight (18h) at 37°c with biotinylated peptides (20 µM) and dilutions of non-biotinylated competitor peptide were added to the culture binding buffer (0.01% Nonidet

P-40, 10 nM Citrate-phosphate buffer and Protease inhibitor cocktail (Roche, Nutley, NJ). Cell surface biotinylated peptides were determined by adding alexa-488 labeled Streptavidin to each sample well. The expression of biotinylated peptides was assessed by flow cytometry. Cells were acquired using a LSR II (BD Biosciences), and FlowJo software (version 9.6.4, Tree Star, Ashland, OR) was used for all analyses. Results were expressed either directly as mean fluorescent intensity (MFI).

NK cell cytotoxic *in vitro* assay

NK cell activity was determined through expression of cell surface CD107a, as previously described[79]. NK cells were cultured overnight in the presence or absence of the MHC-class-I-devoid target cell line K-562 at an effector:target ratio of 1:5 for a total of 6-8 h in the presence of anti- human CD107a. Monensin (BD GolgiStop, BD Biosciences, Franklin Lakes, NJ, USA) was added 1 h after setup of the co-culture, followed by an additional 5 h of incubation at 37°C in a humidified atmosphere with 5% (v/v) CO_2. Cells were then washed with PBS and stained for viability and expression of CD3, CD14, CD16, CD8, CD20, NKG2a/c, CD16 and CD107a.

MHC-E dependent NK cell viral suppressor assays

K562-E*0101 cells were incubated with 50 µM of a given peptide at 26°C for 15–20 h. NK cells were co-cultured with 2×10^4 K562-E*0101 target cells pulsed or not with peptides at a NK cell/target cell ratio of 5:1. Target cells were in parallel cultured in the absence of NK cells. Anti- CD107a antibody was added at the start of the assay, and GolgiStop and GolgiPlug (both BD Biosciences) were added 1 hour after start of the stimulation. After 6 hours of culture, cell suspensions were stained for viability and cytotoxic activity was analyzed through measurement of CD107a expression by flow cytometry. Percent activity was calculated as described above. $CD4^+$ T cells (5×10^6 cells) activated for 2 days as described above were co-cultured with autologous NK cells (ratio 1:1) and from the time of virus exposure on.

Cell sorting of NK cell sub-populations

Eight-colour panels were used to phenotype, surface stain and sort NK cells from blood and pLNs from chronically infected AGMs. Cells were thawed in 20% FBS-containing media supplemented with benzonase nuclease, and counts and viabilities were performed (Life Technologies). Cells were washed and stained with Aqua Live/Dead stain (Molecular Probes). Cells were washed and blocked using normal mouse IgG (Caltag). For the NKG2 $^{HIGH/low}CD16^{+/-}$ phenotyping panel, PBMCs and pLNs were surface stained for CD3 (SP34.2, 1:10 dilution; BD), CD8 ($_{a/c}$BW135/80, 1:20 dilution; Miltenyi), CD16 (3G8, 1:20 dilution; Beckman Coulter, Inc.), NKG2a/c (Z199, 1:20 dilution; Beckman Coulter, Inc.), CD20 (2H7, 1:20 dilution 1/20; Biolegend) and CD14 (M5E2, 1:25 dilution; BD). Post-staining, cells were washed, filtered and sorted on a FACS ARIA II (BD). Cells were directly collected in a lysis buffer that contained TCEP. The purity of the cells was >97%.

RNA extraction, library preparation and sequencing

RNA was isolated from the sorted NK cells using the RNeasy® Mini Kit (205113, Qiagen). RNA integrity was verified with the Agilent Bioanalyser. DNase-treated RNA was treated for library preparation using the Truseq Stranded mRNA Sample Preparation Kit (Illumina, San Diego, CA), according to manufacturer's instructions. An initial poly(A) RNA isolation step (included in the Illumina protocol) is performed on 10 ng of total RNA to keep only the polyadenylated RNA fraction and remove the ribosomal RNA. A step of fragmentation is then performed on the enriched fraction, by divalent ions at high temperature. The fragmented RNA samples were randomly primed for reverse transcription followed by second-strand synthesis to create double-stranded cDNA fragments. No end repair step was necessary. An adenine was added to the 3'-end and specific Illumina adapters were ligated. Ligation products were submitted to PCR amplification. The obtained oriented libraries were controlled by Bioanalyzer DNA1000 Chips (Agilent, # 5067-1504) and quantified by spectrofluorimetry (Quant-iT™ High-Sensitivity DNA Assay Kit, #Q33120, Invitrogen). Sequencing was performed on the Illumina Hiseq2500 platform to generate single-end 100 bp reads bearing strand specificity.

Homology modelling of MHC-E and model analysis

Since there is no X-ray structure available for MHC-E from nonhuman primates, structures for rhesus, cynomolgus, African green monkey, baboon and chimpanzee proteins were modeled with the software MODELLER using the crystal structure of HLA-E*01:03 (PDB code 3BZF) as template[80]. MHC-E amino acid sequence conservations were analyzed with the ConSurf server[81]. Illustrations were rendered with PyMol.

Bioinformatic analysis of the genome-wide sequence data

Bioinformatic analyses were performed using the RNA-seq pipeline from Sequana[82]. Reads were cleaned of adapter sequences, and low-quality sequences were removed using cutadapt version 1.11[83]. Only sequences ≥ 25 nucleotides (nt) in length were considered for further analysis. STAR version 2.5.0a, with default parameters, was used for alignment on the reference genome (*Chlorocebus sabaeus*, from Ensembl release 90). Genes were counted using featureCounts version 1.4.6-p3[84] from Subreads package (parameters: -t gene, -g ID and -s 1).

Data were analyzed using R version 3.4.3 and the Bioconductor package DESeq2 version 1.18.1[85]. Normalization and dispersion estimation were performed with DESeq2, using the default parameters, and statistical tests for differential expression were performed by applying the independent filtering algorithm. A generalized linear model, including the monkey identifier as a blocking factor, was used to test for the differential expression between the biological conditions. For each pairwise comparison, raw p values were adjusted for multiple testing according to the Benjamini and Hochberg (BH) procedure[86]. Genes with an adjusted p value <0.05 were considered differentially expressed.

Analyses and vizualization of GO terms associated with differentially expressed genes were performed

using ClueGO. Both groups of genes (up- and downregulated, p value < 0.05) were used as dual input for GO and pathway annotation networks of the expressed genes and proteins pathway enrichment analysis[87]. Each list was used to query the Kyoto Encyclopedia of Genes and Genomes (KEGG), GO-biological function database and Wiki pathways. ClueGo parameters were set as follows: Go Term Fusion selected; only display pathways with p values ≤ 0.05; GO tree interval, all levels; GO term minimum genes, 3; threshold of 4% of genes per pathway; and a kappa score of
0.42. GO terms are presented as nodes and clustered together based on the similarity of genes present in each term or pathway. The most significant term was chosen as a representative of the group (Benjamini-Hochberg correction).

Statistics

In order to illustrate specific gene sets, we draw heatmaps based on variance-stabilizing transformed counts. Comparisons among independent groups were conducted using nonparametric Mann- Whitney *U*-test (Fig1a and b, Fig2c). For the other data, a Wilcoxon matched-pairs signed rank test was used with subsequent Bonferroni correction to evaluate whether there was a statistically significant difference in the level of one given marker at a given time point post-infection when compared to the baseline medians (day 0). Baseline medians in blood consisted of 3–6 pre-infection values per animal. In pLNs, there were 1–2 pre-infection values per animal. Correlation analysis was performed according to Pearson test. A negative correlation coefficient (r) indicates inverse correlations. Statistical computations were performed using Prism (GraphPad, La Jolla, CA) and SigmaStat software (Systat). For the analyses with the mutated SIV clones, we also considered a model where target cells were assumed to be at a constant level in the absence of NK^+ cells and to decline exponentially in the presence of NK cells due to the changes in the NK/CD4 T cell ratio. The test was described by Betts M et al (J Virol 75:11983–11991).

Data availability

Deep sequencing results have been deposited in the Gene Expression Omnibus database; the accession number is GSE140600. The authors declare that all other data supporting the findings of this study are available within the article and its Supplementary Information files, or are available from the authors upon request.

LEGENDS

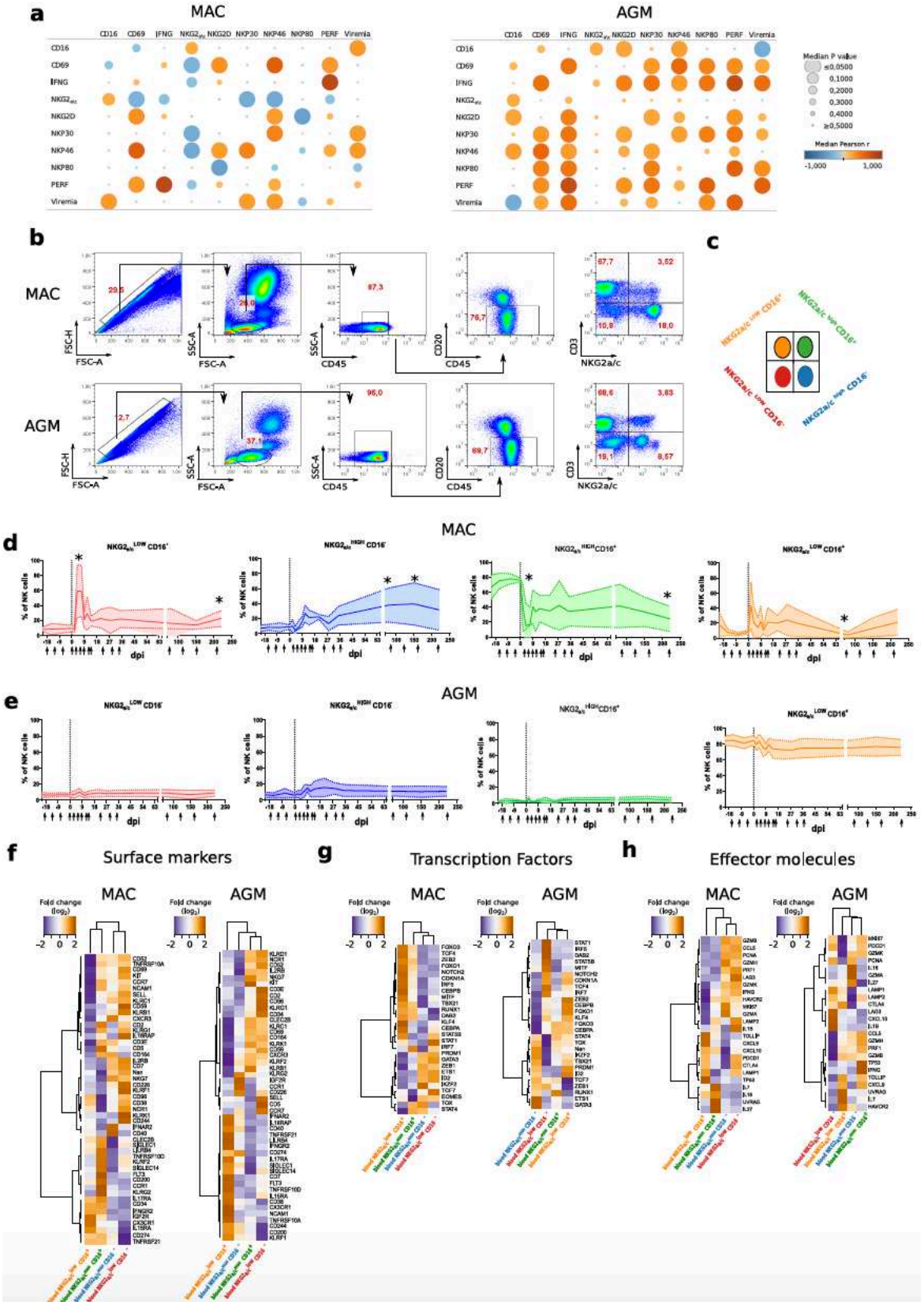


Figure 1. Phenotypic, genome-wide transcriptional and functional analysis of blood NK cells during SIV infection in the natural and heterologous hosts. (a) Correlation matrix of NK cell expression (MFI) and measures of viremia. The Pearson correlation is shown. The matrix was built using the values obtained between day 0 and day 150 p.i from 6 MAC (left panel) and 6 AGM (right panel). All p-values

are listed in Supplemental Table 1. (**b)** Gating strategy used to define NK cell subpopulations in MAC (upper panel) and AGM (lower panel). (**c)** Scheme showing NK cell subpopulations according to $NKG2_{a/c}$ and CD16 expression. The color code used to define each of the four subpopulations is the same throughout the manuscript. (**d-e)** Frequency of the NK cell subpopulations in blood longitudinally sampled from (d) six MAC and (e) six AGM at the indicated time points before and after SIV infection. In each graph, the arrows indicate the analyzed time points, the full line represents the median, and the interquartile range is indicated by the area between the dotted lines. (**f-h)** Heatmaps of the RNA-seq transcript signatures for (f) NK cell surface markers, (g) transcription factors and (h) activation markers. Each row represents a variable gene among clusters, and each column represents the median of 3 chronically infected monkeys for blood. In each panel, NK cell subsets are organized based on the overall similarity in gene expression patterns by an unsupervised hierarchical clustering algorithm of variable genes. A dendrogram, in which the length of the branches reflects the comparative difference in gene expression profiles between each of the NK samples is shown. A p-value adjustment was performed to account for multiple comparisons and control the false positive rate to a chosen level. The transcriptome similarity among clusters of the blood sample was evaluated by the Euclidean distance.

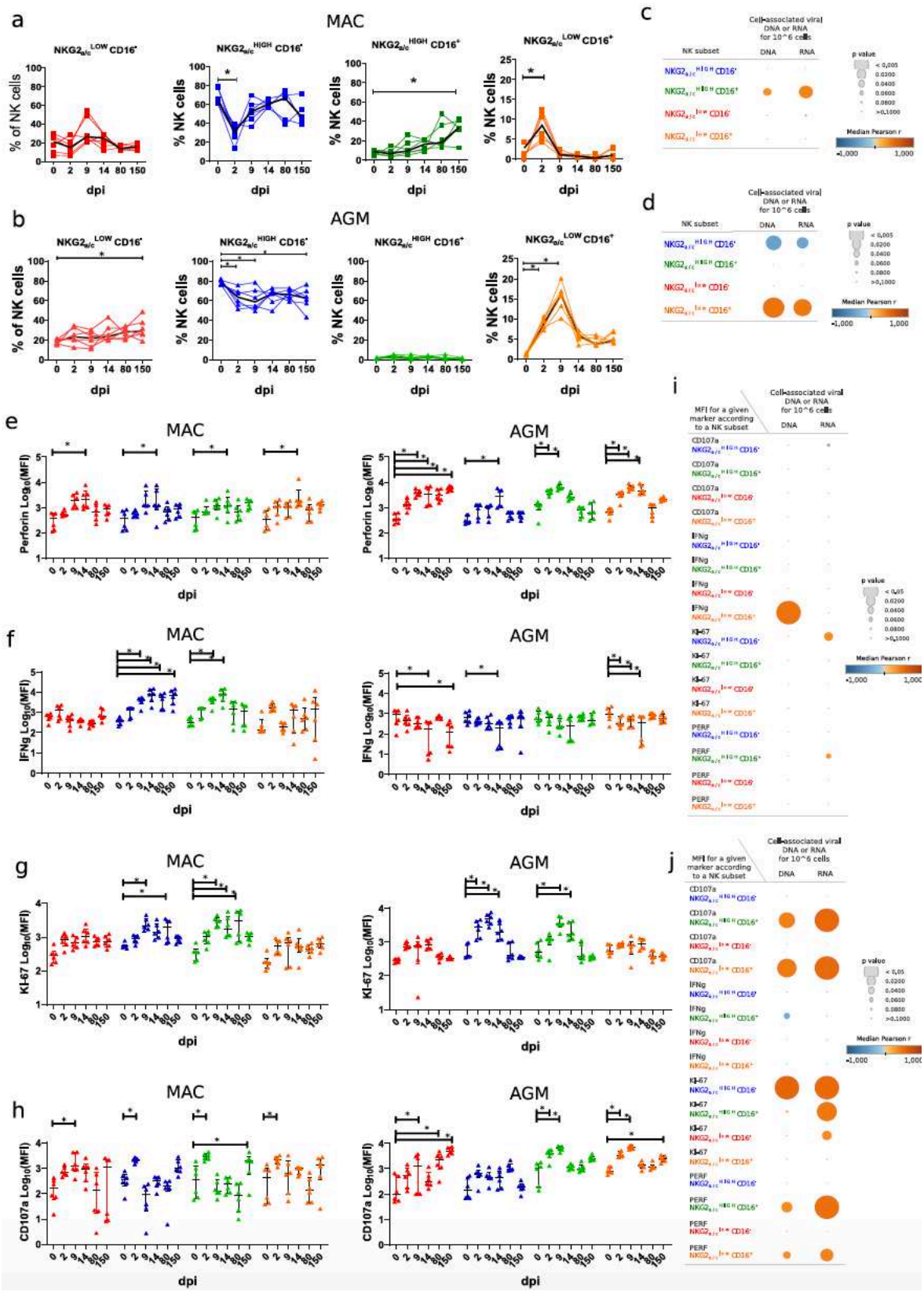


Figure 2. Dynamics of NK cell repertoire and activity in response to SIV infection in LN. (a-b) Frequency of NK cell subpopulations out of total NK cells in LN. Colors are the same as in Fig.1c. Cells were longitudinally sampled before and during (a) SIVmac and (b) SIVagm infection. The black line indicates the median and asterisks indicate significant differences ($p < 0.05$). **(c-d)** Correlation matrix between the frequency of NK cell subsets and cell-associated viral RNA (ca- vRNA) and DNA (ca-vDNA) in LN of (c) MAC and (d) AGM over time. The exact values are given in Table S2. **(e-h)** Graphs showing intracellular level of perforin (e), interferon gamma (f), Ki-67(g) and surface level of CD107a (h)

on NK cell subsets during SIVmac (left panel) and SIVagm (right panel) infections. Colors are the same as in Fig.1c. The black line indicates the median and asterisks indicate significant differences ($p < 0.05$). **(i-j)** Correlation matrix of level

markers measure in Fig.2i-j and the measures of LN ca-vRNA and ca-vDNA in (i) MAC and (j) AGM. The exact values are given in Table S3. Triangles indicate individual animals.

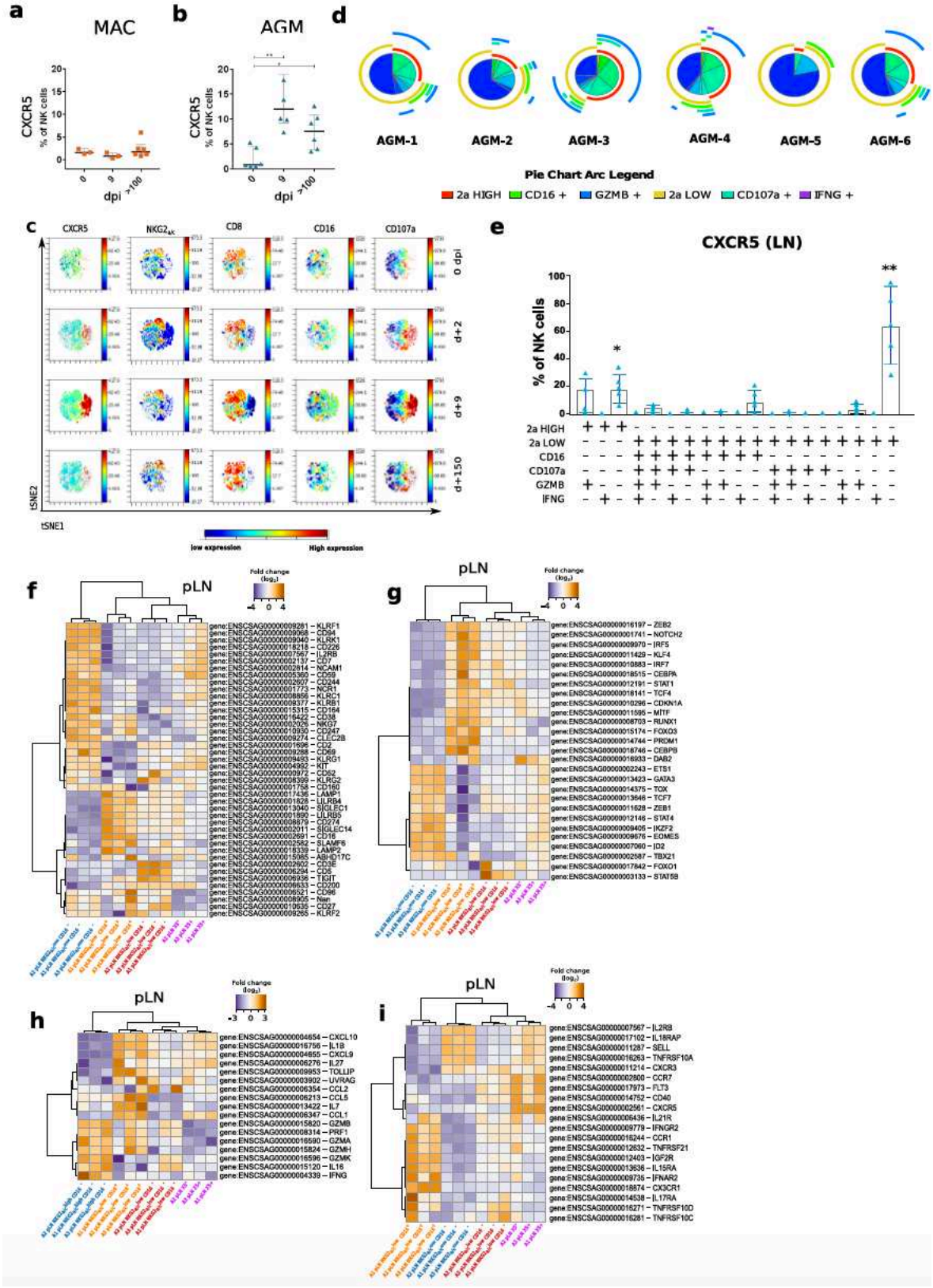


Figure 3. Dynamics, functional diversity and differentiation state of CXCR5$^+$ NK cells in LN during SIV infection in the natural host. (a-b) Frequency of CXCR5+ NK cells in LN during SIV infection in (a) MAC and (b) AGM). The y-axis indicates the percentage of CXCR5+ NK cells among total NK cells before and at day 9 and 150 p.i. Each symbol indicates an individual animal.

(c) viSNE analysis (Cytobank) on the concatenated flow cytometry data of LN NK cells from 6 AGM. Total LN cells were stained with 12 markers and measured by flow cytometry. viSNE analysis was run on

80000 live $CD45^+$ $CD3^-CD20^-CD14^-$ $NKG2^+$ single cells per sample using all surface markers. Data show surface expression of CXCR5, $NKG2_{a/c}$, CD8, CD16 and CD107a on all viable single cells from LN, subjected to the tSNE algorithm, at the given time point. (**d)** SPICE 5.3 analyses showing Pie charts and arcs representing the proportion of CXCR5+ NK cells expressing different combinations of CD107a, IFN-γ, GZMB, CD16 and $NKG2_{a/c}$ after surface staining for CD107a, CD16 and $NKG2_{a/c}$ and intracellular staining for GZMB and IFN-γ done on total cells from LN biopsies during the chronic phase of infection (150 days p.i.) (n=6). Each pie chart represents a monkey. The color of each arc represents a maker as indicated in the figure. **(e)** Graph showing the distribution of CXCR5+ NK cells from 6 chronically infected AGM in LN expressing different combinations CD107a, IFN-γ, GZMB + CD16+ and NKG2a. Data are given as mean ± SEM. *, $P < 0.05$ Wilcoxon Rank Test was used to compare each **s**ubset. (**f-i)** Heatmaps of the genome-wide transcript signatures for **(f)** NK cell surface markers, **(g)** transcription factors**, (h)** secreted molecules and**(i)** surface receptors. In each panel, NK cell subsets are organized as in Fig.1. Each row represents a variable gene among clusters, and each column represents one individual monkey.

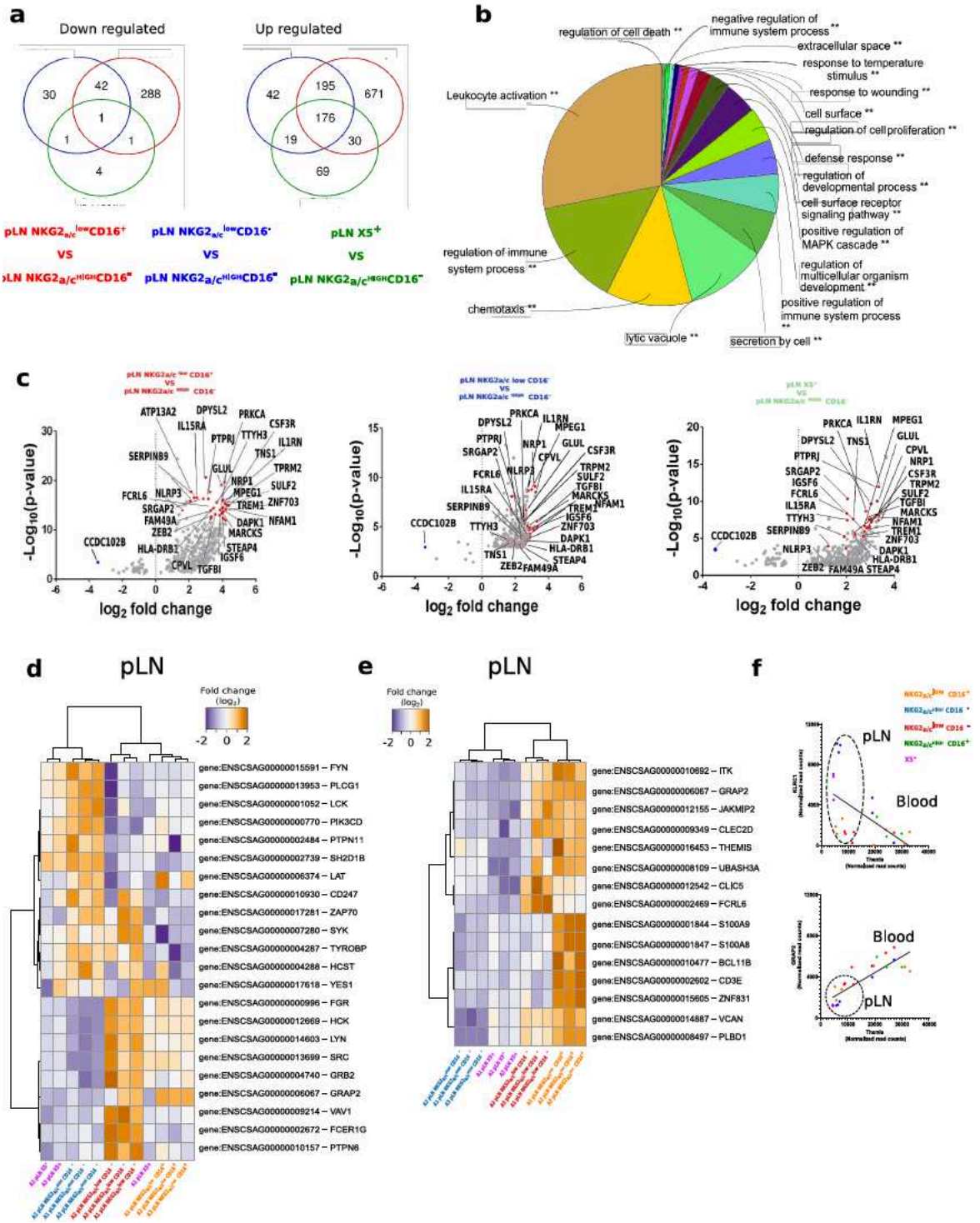


Figure 4: Transcriptomic signatures of adaption and degranulation activity in NK cells from LN during SIVagm infection. (a) Venn diagrams generated by the intersection of the list of up- and down-regulated genes with an adjusted p-value < 0.05 based on the genome-wide transcriptome. **(b)** The pie chart shows the enriched Gene Ontology (GO) terms for the 176 genes that were upregulated in $NKG2_{a/c}^{low}$ and $CXCR5^{+}$ NK cell subsets as compared to $NKG2_{a/c}^{high}CD16^{-}$ NK cells. The mRNAs were input for ClueGO plugged into Cytoscape for GO enrichment analysis. The 'cellular component', 'biological process', 'molecular function' and 'immune system process' GO terms were selected for this analysis. The two-sided hypergeometric test was used in the statistical inference. The term value corrected with the Bonferroni step down method was applied for p-value correlation. The adjusted p-value threshold was set to 0.001. The list of the associated

genes found for each GO term is given in Table S4. **(c)** Volcano plots that represent up- and down-regulated transcripts of each of the three NK cell subsets when compared to NKG2 $^{high}_{a/c}$CD16^{-} NK cells. The size of each data point is calculated as -log10 (p-value) x log2 (FC), with a p-value cutoff < 0.05. The red dots represent the 30 highest upregulated transcripts in NKG2 $^{low}_{a/c}$CD16^{+} versus NKG2 $^{high}_{a/c}$CD16^{-} NK cells. These transcripts were then highlighted on the volcano plots obtained for the two other comparisons. The blue dots represent the gene (*CCDC102B*), which was downregulated in all three comparisons. The list of all transcripts upregulated for each comparison is given in Table S6. **(d)** and **(e)** Genome-wide transcriptomes were used to define heatmaps of **(d)** markers linked to ITAM/ITIM signaling pathways and **(e)** genes strongly upregulated in NKG2$_{a/}$ ^{low}CD16^{+} NK cells with an adjusted p-value < 0.05. **(f)** Correlation between *KLRC1* (NKG2A) or *GRAP2* and *THEMIS* gene expressions. Each dot represents an individual animal.

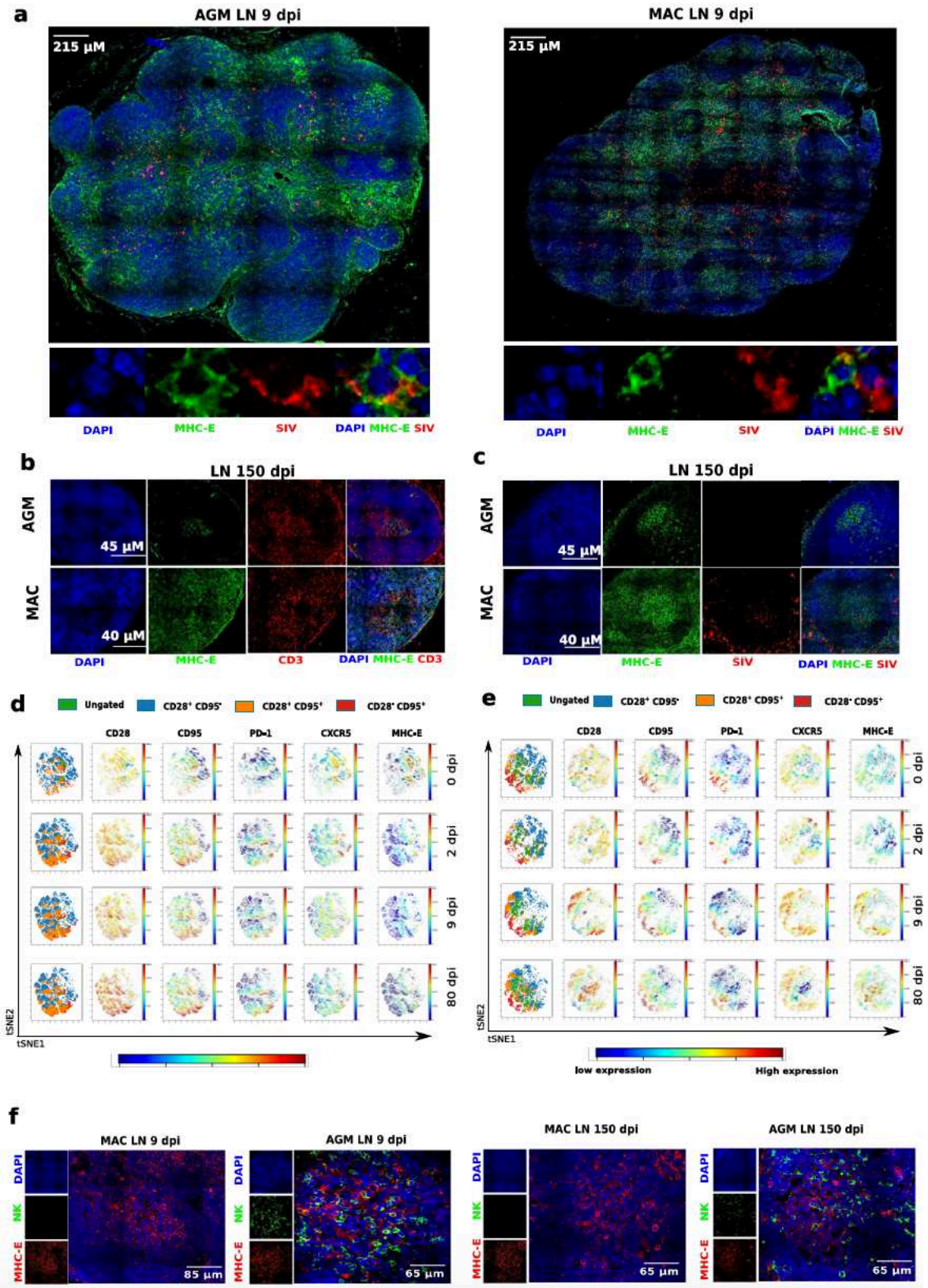


Figure 5. Staining of NK, MHC-E+ and SIV-RNA positive cells in LN during acute and chronic SIVmac and SIVagm infections. (a) Confocal image of MHC-E and SIV expression on frozen sections from LN samples. Pseudocolors were attributed to each marker (blue for DAPI, green for MHC-E and red for SIV RNA). Scale bars are indicated on the figure. Magnification represents a stained cell in chronic SIV infection showing staining for MHC-E and SIV RNA. Example is given for one animal among four studied. (**b-c)** B cell follicles stained for (b) MHC-E (green) and CD3 or (c) MHC-E (green) and SIV (red). Example is given for one animal among four studied. (**d-e)** Illustration of (d) the decrease during

SIVagm infection and (e) increase during SIVmac infection of MHC-E expression on memory $CD4^+$ T cells. Results are shown for a representative MAC and a representative AGM among six animals analyzed for each species. The time points analyzed are indicated on the right side of the panels. The viSNE plot was generated according to CD28, CD95, PD-1, CXCR5 and MHC-E expression gated on $CD45^+CD3^+CD14^-$ $CD4^+$ cells in LN using proportional sampling with 54422 events. The first column represents the distribution of $CD4^+$ T cell subpopulations based on CD28 and CD95 expression: naïve ($CD28^+CD95^-$, blue), memory ($CD28^+CD95^+$, orange), effector ($CD28^-CD95^+$, red) and remaining $CD28^-$ $CD95^-$ $CD4^+$ T cells (green). A color scale represents the level of expression of the indicated markers in the following columns. (**f)** Peripheral LNs from six AGM and six MAC infected by SIVagm and SIVmac, respectively, were analyzed at days 9 and 150 p.i. Representative confocal images of LN sections are shown with MHC-E (red), NKG2a (green) and total nucleus (blue).

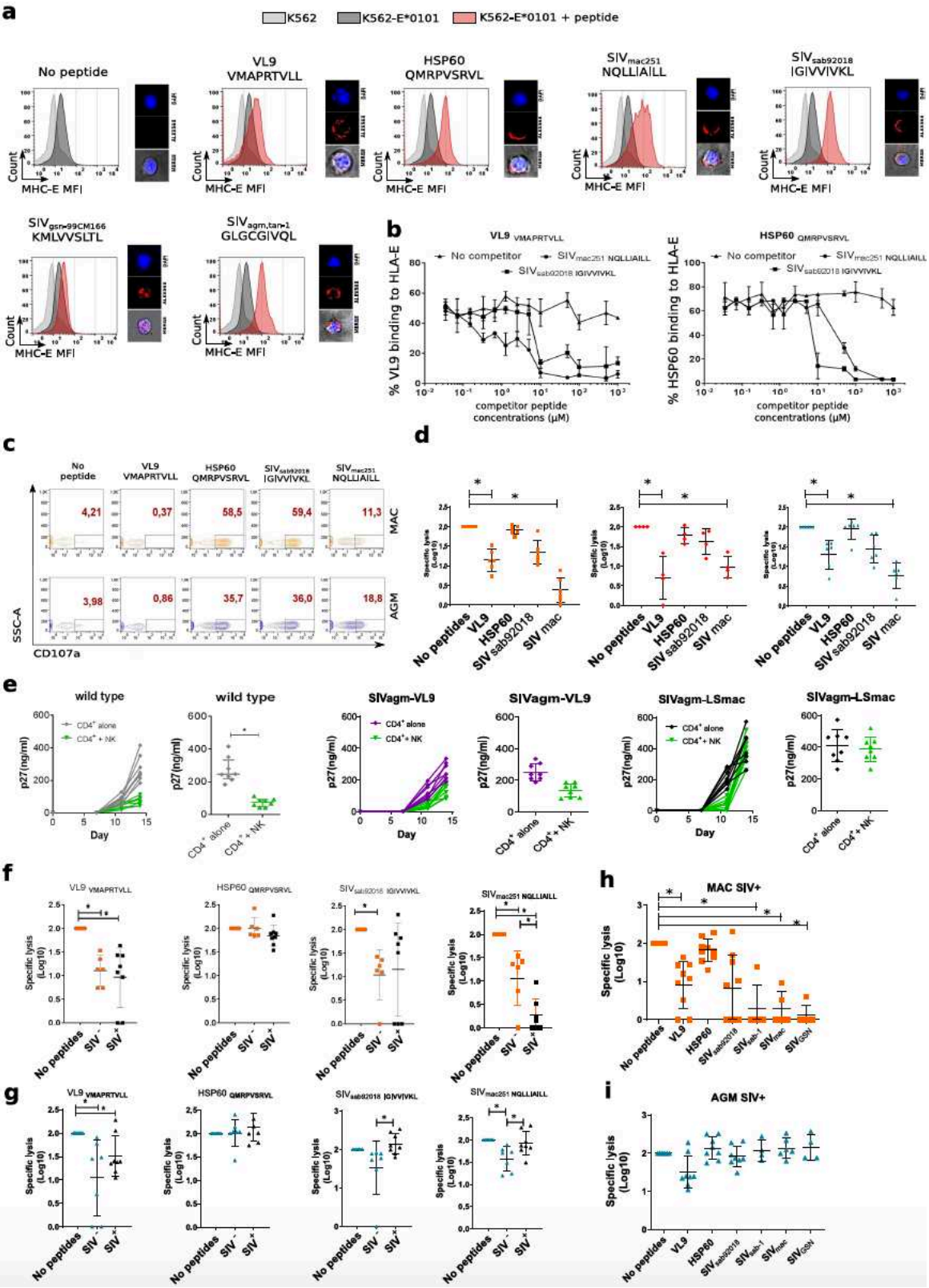
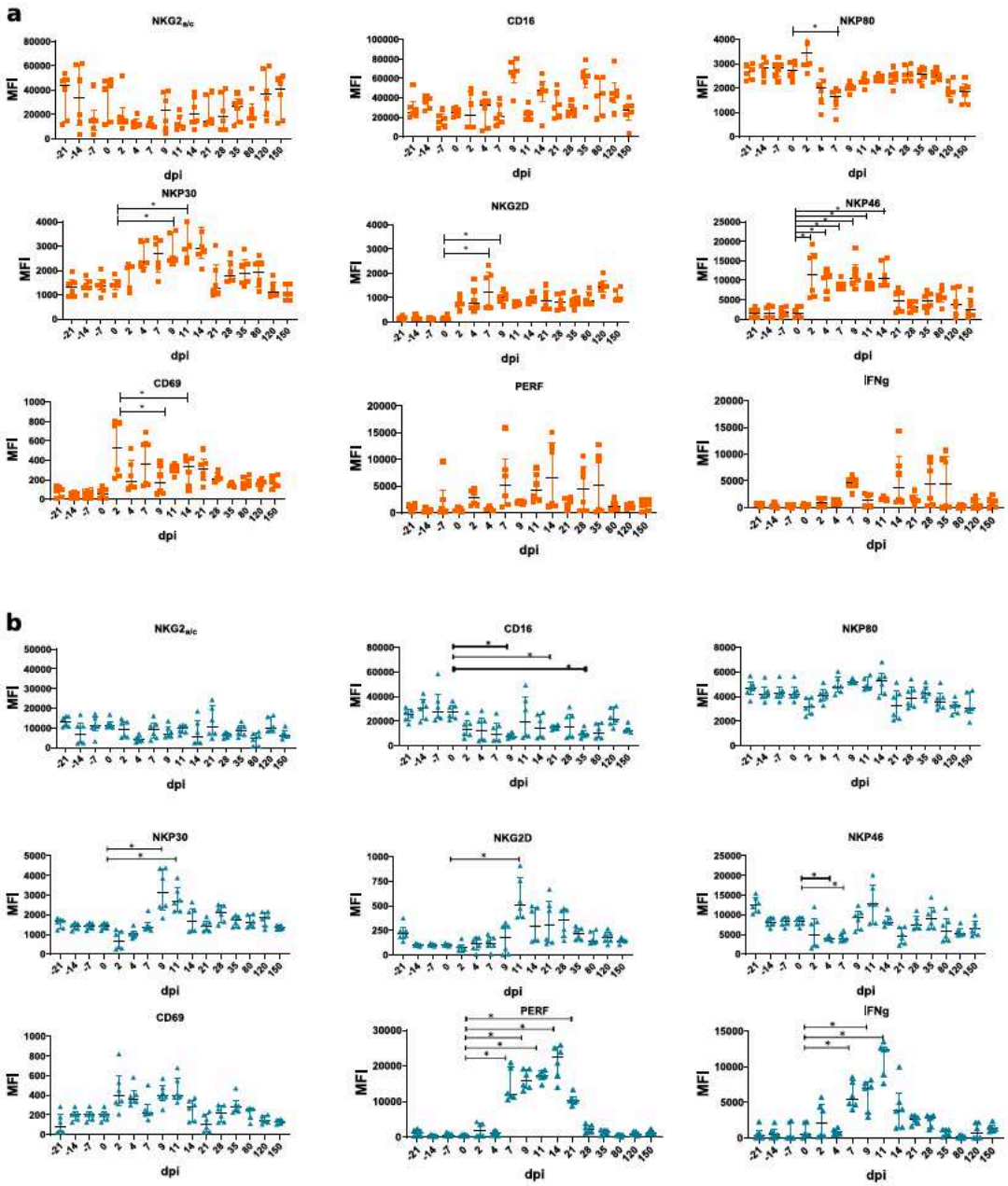


Figure 6. Analysis of MHC-E restricted NK cell activity a) Each histogram shows HLA-E expression after loading K562-E*0101 cells with the different peptides. Light grey curves indicate the mean fluorescent intensity (MFI) of HLA-E on K562 cells (control), the dark grey curves the

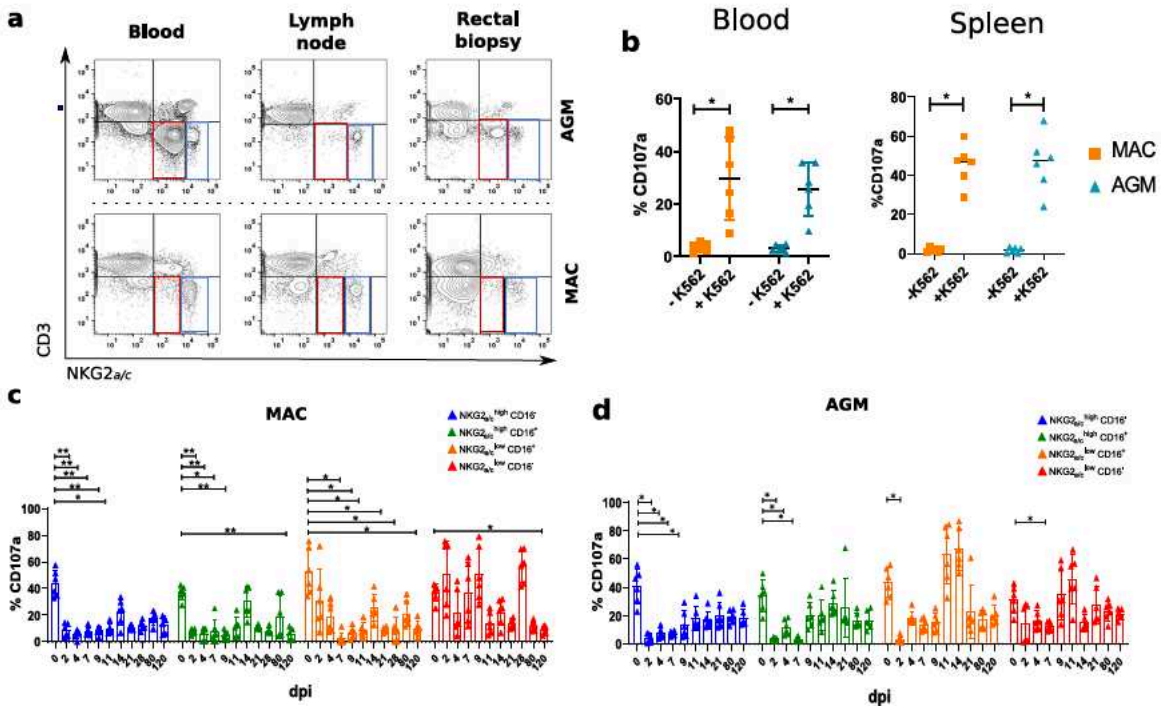
MFI of HLA-E on K562-E*0101 cells without peptides, and the red curves the MFI of HLA-E on K562-E*0101 cells loaded with the given peptide. VL9 and HSP60 are control peptides well known to bind to MHC-E and deriving respectively from HLA-I and heat-shock protein. The SIVmac251 and SIVmac239 peptide sequences were identical. One representative experiment out of more than three is shown. On the right side are shown the localization of the peptide stained with Alexa 568 (red). Nuclei were stained with

DAPI (blue). **(b)** Competition assay for binding to HLA-E. K562- E*0101 cells were loaded with biotin-A2 VL9 (left) or HSP60 peptides (right). An increasing concentration of the indicated unlabeled competitor peptides were introduced into the culture. HLA- E-bound biotinylated peptide was measured at the cell surface. Data represent the median of three independent experiments. **(c)** Analysis of HLA-E dependent activity of NK in presence of K562- E*0101 cells loaded or not with peptides. Activity was evaluated by CD107a cell surface expression. Dot plots show representative examples for one animal per species. **(d)** HLA-E dependent activity of NK cells from blood of six uninfected cynomolgus MAC (orange squares), four uninfected rhesus MAC (red circles) and six uninfected AGM (blue triangles) in the absence or presence of peptides, as indicated. **(e)** SIV suppressive capacity of autologous NK cells depending on the ENV nonamer sequence in the infectious virus. The panels show *in vitro* replication levels of SIVagm.sab92018 (grey), SIVagm.sab92018 mutant with the sequence coding for the VL9 peptide (purple) and the SIVagm.sab92018 mutant with the sequence coding for the SIVmac nonamer peptide (black) in primary $CD4^+$ T cells from 8 uninfected AGM cultured alone or in presence of autologous NK cells (green). For each of the three viruses, left panels show viral replication pattern longitudinally (days 0, 7, 11 and 15 p.i.) and right panels viral replication at the end time-point of the culture (day 15 p.i.). The y-axis reports viral replication level as quantified by SIV p27. **(f-g)** HLA-E dependent cytotoxic activity of NK cells isolated before infection and in chronic infection from LN of MAC (orange), and AGM (blue). K562-E*0101 were loaded or not with peptides. Uninfected MAC are indicated in orange squares and uninfected AGM in blue triangles. SIV infected animals are indicated in black. **(h-i)** HLA-E dependent cytotoxic activity of NK cells isolated from spleen of chronically infected MAC (h) and AGM **(i)** against distinct SIV ENV peptides. Each symbol in the figures represents a monkey. The asterisks indicate $p<0.05$. Horizontal bars indicate median values, and error bars indicate standard deviation.

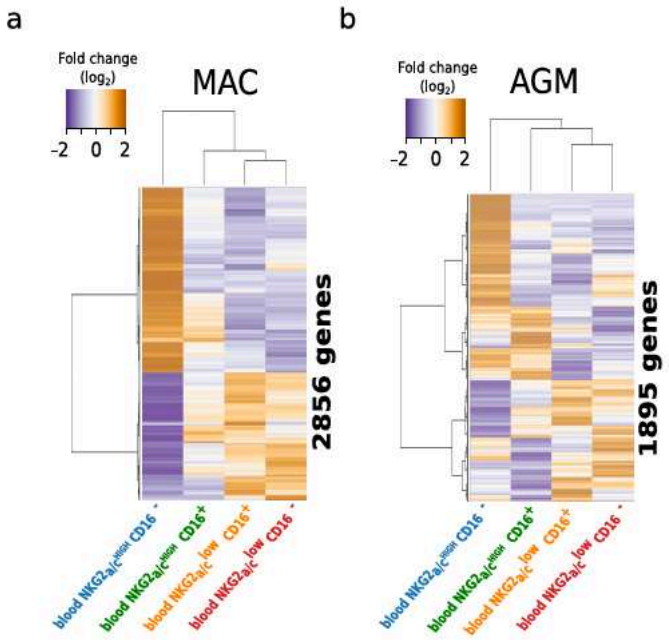
SUPPLEMENTARY FIGURE LEGENDS



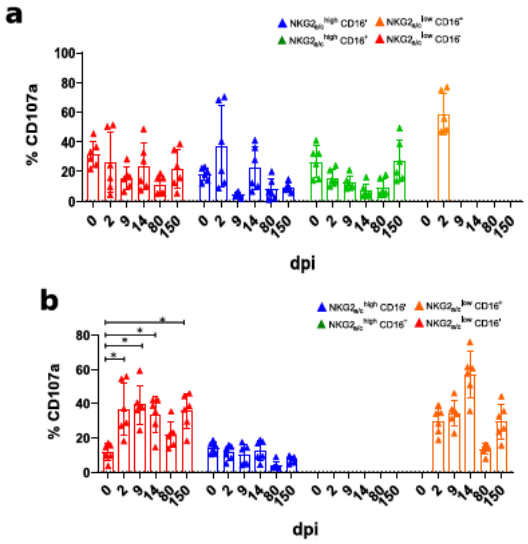
Supplementary Figure 1: (a, b) Graphs showing the evolution of the level of blood NK cell markers during (a) SIVmac (orange) and (b SIVagm (blue)) infection. Cells were analyzed by flow cytometry from blood collected longitudinally from six animals per species. Statistical analysis: Wilcoxon matched-pairs signed-rank test with subsequent Bonferroni correction. Bars represent the median, error bars indicate the quantifiable range, and asterisks indicate significant differences ($p < 0.05$). Each symbol represents an individual animal.



Supplementary Figure 2: (a) Dot plots showing an example of NK cell gating in blood, LN and intestine. NK cells were defined as CD45+CD20-CD3-NKG2A+. The dot plots represent one animal for AGM (upper part) and MAC (lower part). Red squares represent NK cells expressing a weak level of $NKG2_{a/c}$ and the blue squares represent NK cells with high level of $NKG2_{a/c}$. **(b)** Cytolytic activity of NK cells. NK cells were isolated from blood and spleen of chronically SIV- infected MAC and AGM. Each dot represents NK cells from a different animal. Activity was measured by CD107a expression on NK cells exposed to the MHC-I-devoid K562 cells. $*p<0.05$ **(c-d)** Functional activity of blood NK cells followed longitudinally**.** CD107a expression was measured on NKG2 ^{high} and NKG2 ^{low} NK cells after exposure to the MHC-I-devoid K562 target cells. Columns represent the median, the interquartile range is also indicated. Day 0 represents the median of all the time points before infection. The Wilcoxon matched-pairs signed-rank test with subsequent Bonferroni correction was used to compare each time point to day 0. Each triangle represents and individual animal.

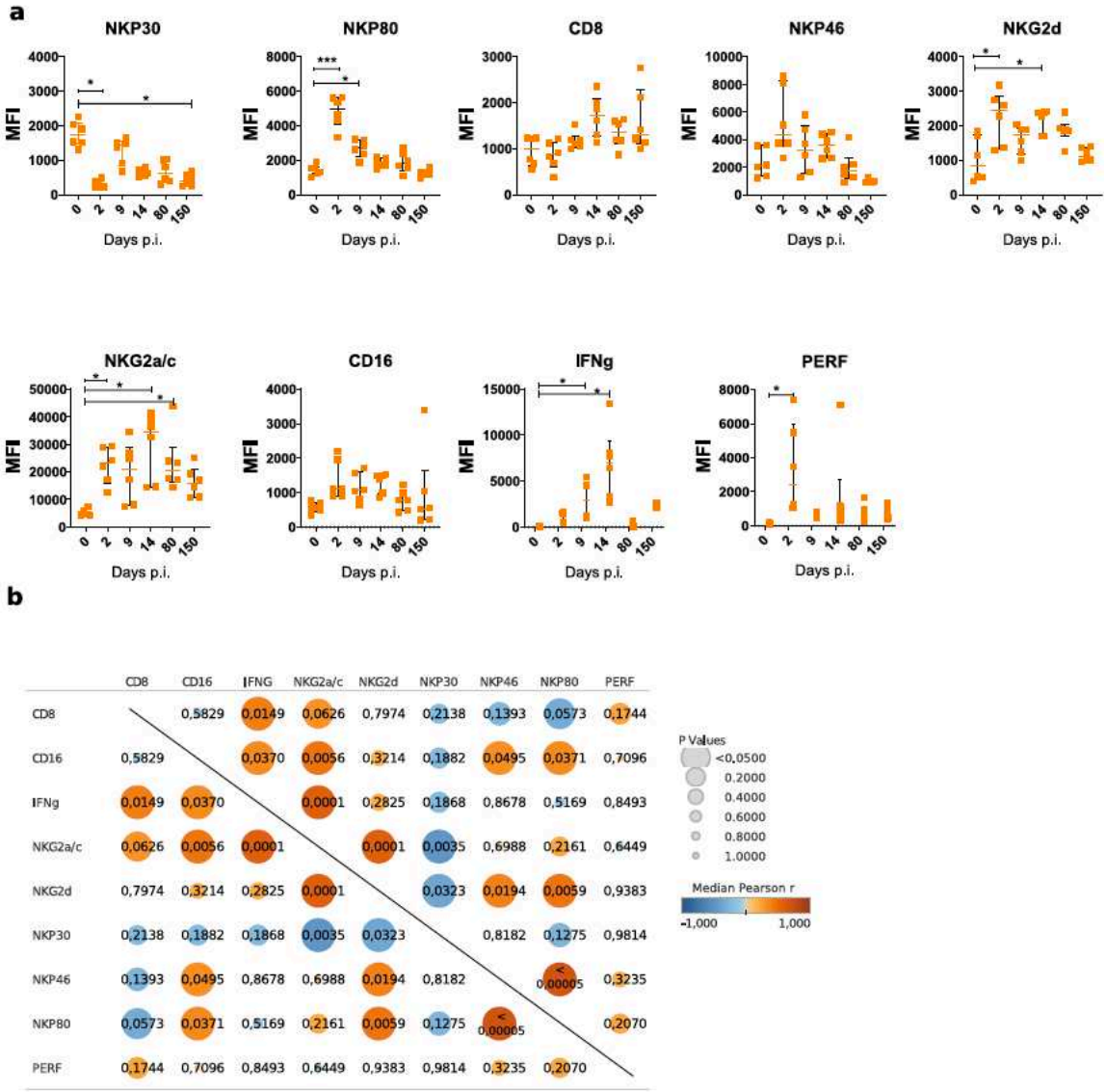


Supplementary Figure 3: Heatmaps of the total transcripts differently expressed between the different NK cell subsets in blood from chronically infected **(a)** MAC and **(b**) AGM**.** In each panel, NK cell subsets were organized based on the overall similarity in gene expression patterns by an unsupervised hierarchical clustering algorithm of variable genes. A dendrogram, in which the length of the branches reflects the comparative difference in gene expression profiles between each of the NK samples is shown. A p-value adjustment was performed to account for multiple comparisons and control the false positive rate to a chosen level. The transcriptome similarity among clusters of the blood sample was evaluated by the Euclidean distance. Each row represents a variable gene among clusters, and each column represents the median of 3 monkeys for blood.



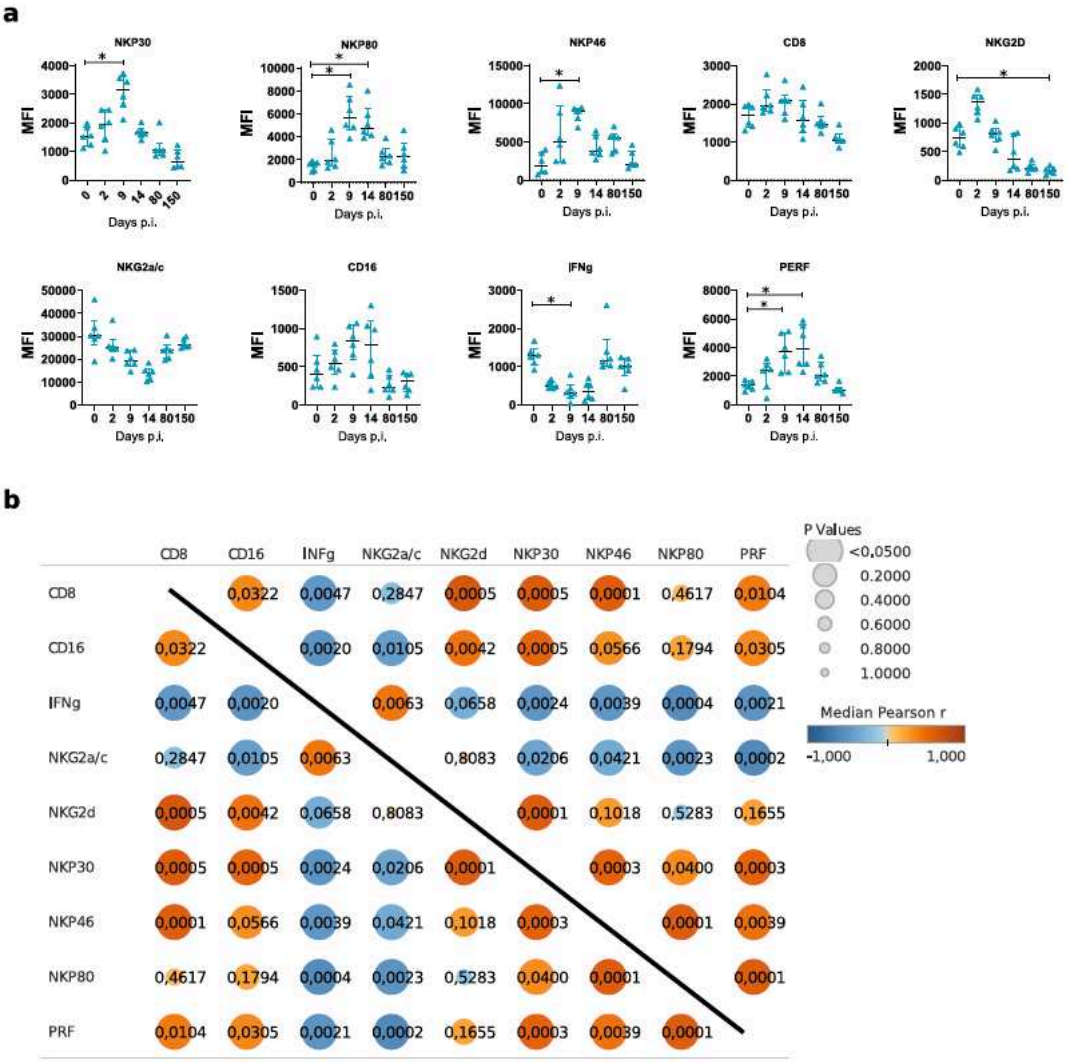
Supplementary Figure 4. Cytolytic activity of **(a)** MAC and **(b)** AGM NK cell subsets. Peripheral LN cells obtained before and during the infection were co-cultured with K562 cells. CD107a surface expression on NKG2$_{a/c}^{low}$CD16^{-} (red), NKG2$_{a/c}^{HIGH}$CD16^{-} (blue), NKG2$_{a/c}^{HIGH}$CD16^{+} (green) and NKG2$_{a/c}^{low}$CD16^{+} (orange) NK cells is shown. Columns represent the median, the interquartile range is

also indicated. Day 0 represents the median of all the time points before infection. The Wilcoxon matched-pairs signed-rank test with subsequent Bonferroni correction was used to compare each time point to day 0.



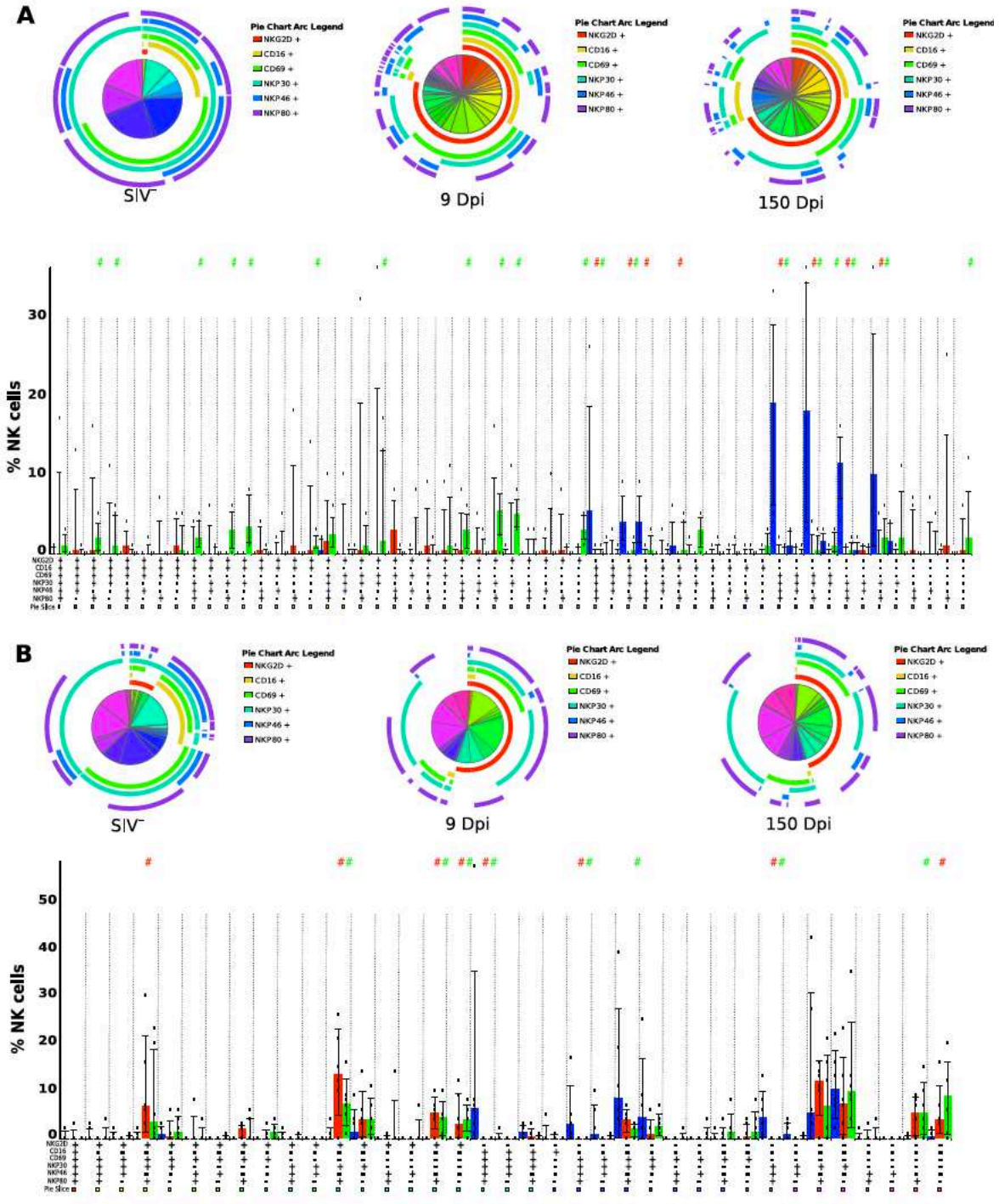
Supplementary Figure 5. Evolution of the level of LN NK cell markers during SIVmac infection.

(**a**) Cells were analyzed ex vivo by flow cytometry from LN collected longitudinally from six MAC. Statistical analysis: Wilcoxon matched-pairs signed-rank test with subsequent Bonferroni correction. Bars represent the median, error bars indicate the quantifiable range, and asterisks indicate significant differences ($p < 0.05$). (**b**) Correlation matrix of different LN MAC NK cell marker levels. The Pearson correlation is shown on a scale of −1 (blue) to 1 (red). Matrix were built using the value obtained since day 0 from day 150 p.i of 6 MAC. The size of the circle defines the median of the p-value.



Supplementary Figure 6. Evolution of the level of LN NK cell markers during SIVagm infection.

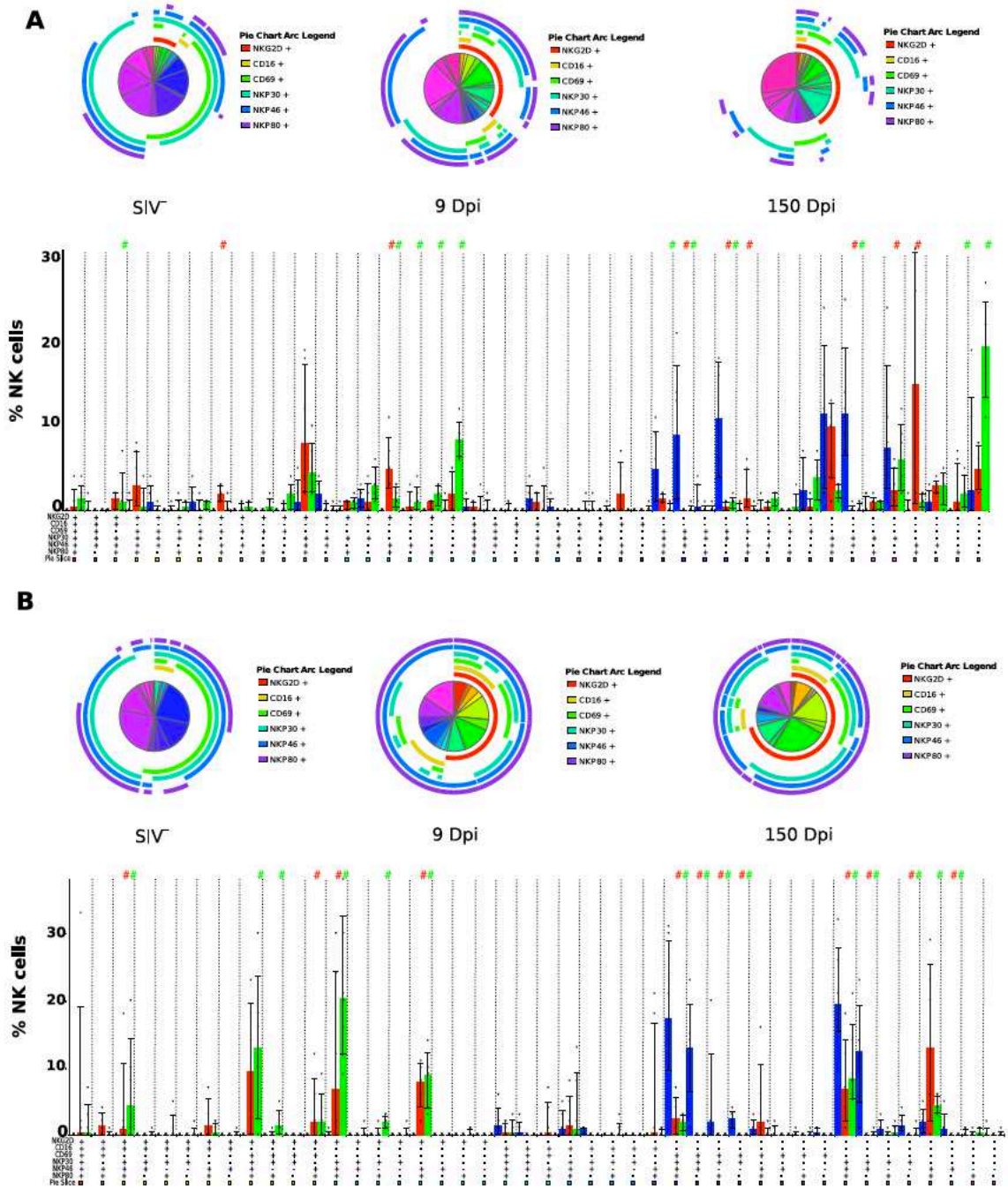
(**a)** Cells were analyzed by flow cytometry from LN collected longitudinally from six AGM. Statistical analysis: Wilcoxon matched-pairs signed-rank test with subsequent Bonferroni correction. Bars represent the median, error bars indicate the quantifiable range, and asterisks indicate significant differences ($p < 0.05$). (**b)** Correlation matrix of different LN AGM NK cell markers level. The Pearson correlation is shown on a scale of −1 (blue) to 1 (red). Matrix were built using the value obtained since day 0 from day 150 p.i of 6 AGM. The size of the circle defines the median of the p-value.



Supplementary Figure 7. NK cell diversity in LN during SIVmac infection. (**a**) Upper panel: SPICE 5.3 analyses showing the proportion of different combinations of markers on $NKG2_{a/c}^{HIGH}$ NK cells isolated from MAC LNs at the indicated time points. Each pie chart represents the median of 6 monkeys. The colour of each arc represents a maker (as indicated in the figure). Lower panel: Boolean analysis showing the range and mean frequencies of NK cell subpopulations according to the expression of NKG2D, NKP30, NKP46, CD16, CD69 and NKP80 on $NKG2_{a/c}^{HIGH}$ NK cells inMAC before infection (blue bar), at day 9 p.i. (red bar) and at day 150 p.i. (green bar). The red cross shows a significant change for a given population at day 9 p.i. compared to baseline. The green cross shows a significant change for a given population at day 150 p.i. compared to baseline. (**b**) Upper panel: SPICE 5.3 analyses showing the proportion of different combinations of markers on $NKG2_{a/c}^{low}$ NK cells isolated from MAC LN at the

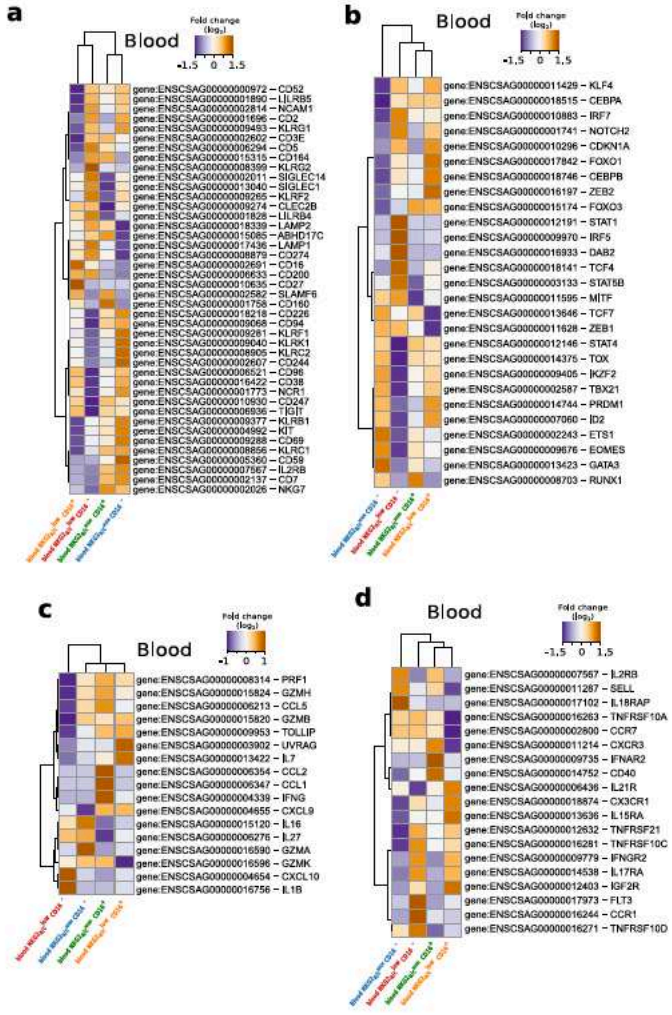
indicated time points. Each pie chart represents the median of 6 monkeys. The colour of each arc represents a maker (as indicated in the figure). Lower panel: Boolean analysis showing the range and mean frequencies of NK cell subpopulations according to the expression of NKG2D, NKP30, NKP46, CD16, CD69 and NKP80 on $NKG2_{a/c}^{low}$ NK cells in 6 MAC before infection (blue bar), at day 9 p.i. (red bar) and at day 150 p.i. (green bar). The red cross shows a significant change for a given population at day 9 p.i. compared to baseline.

The green cross shows a significant change for a given population at day 150 p.i. compared to baseline. For a) and b), the Wilcoxon rank test was used to compare each subset. The cut-off set to 0.03% of total LN cells was applied to exclude cell populations with limited biological significance.

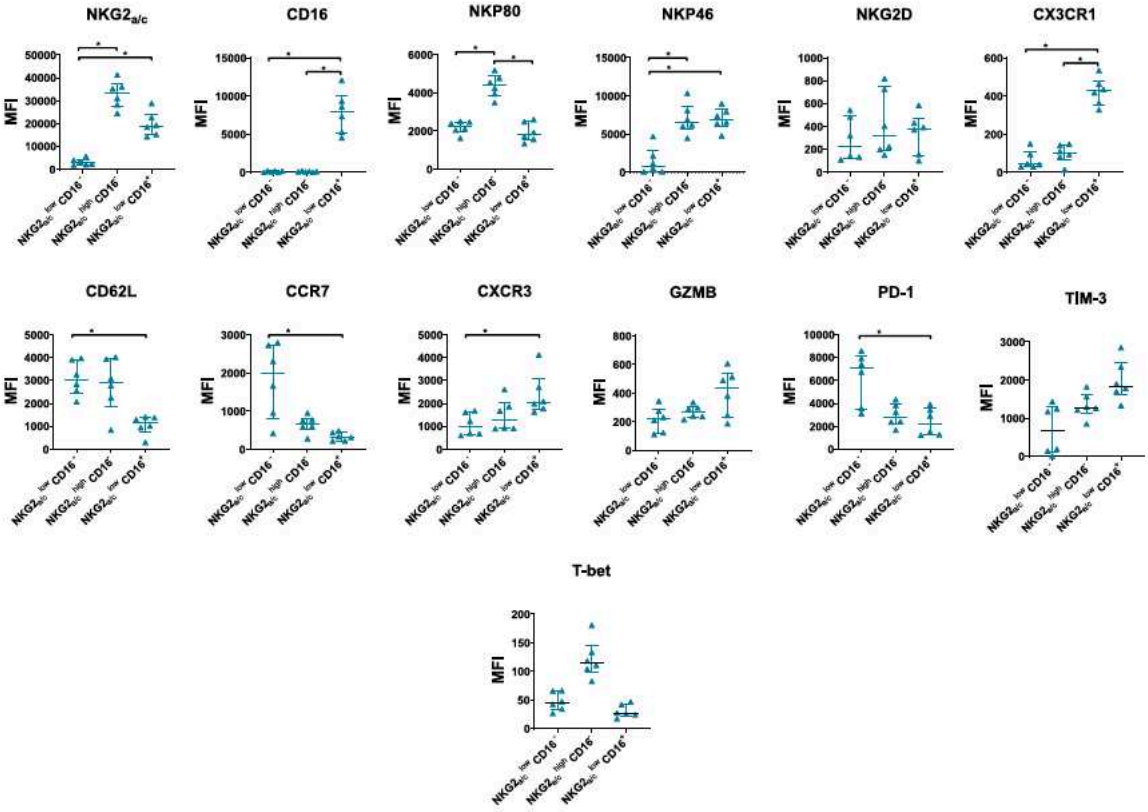


Supplementary Figure 8. NK cell diversity in LN during SIVmac infection. **(a)** Upper panel: SPICE 5.3 analyses showing the proportion of different combinations of markers on $NKG2_{a/c}^{HIGH}$ NK cells isolated

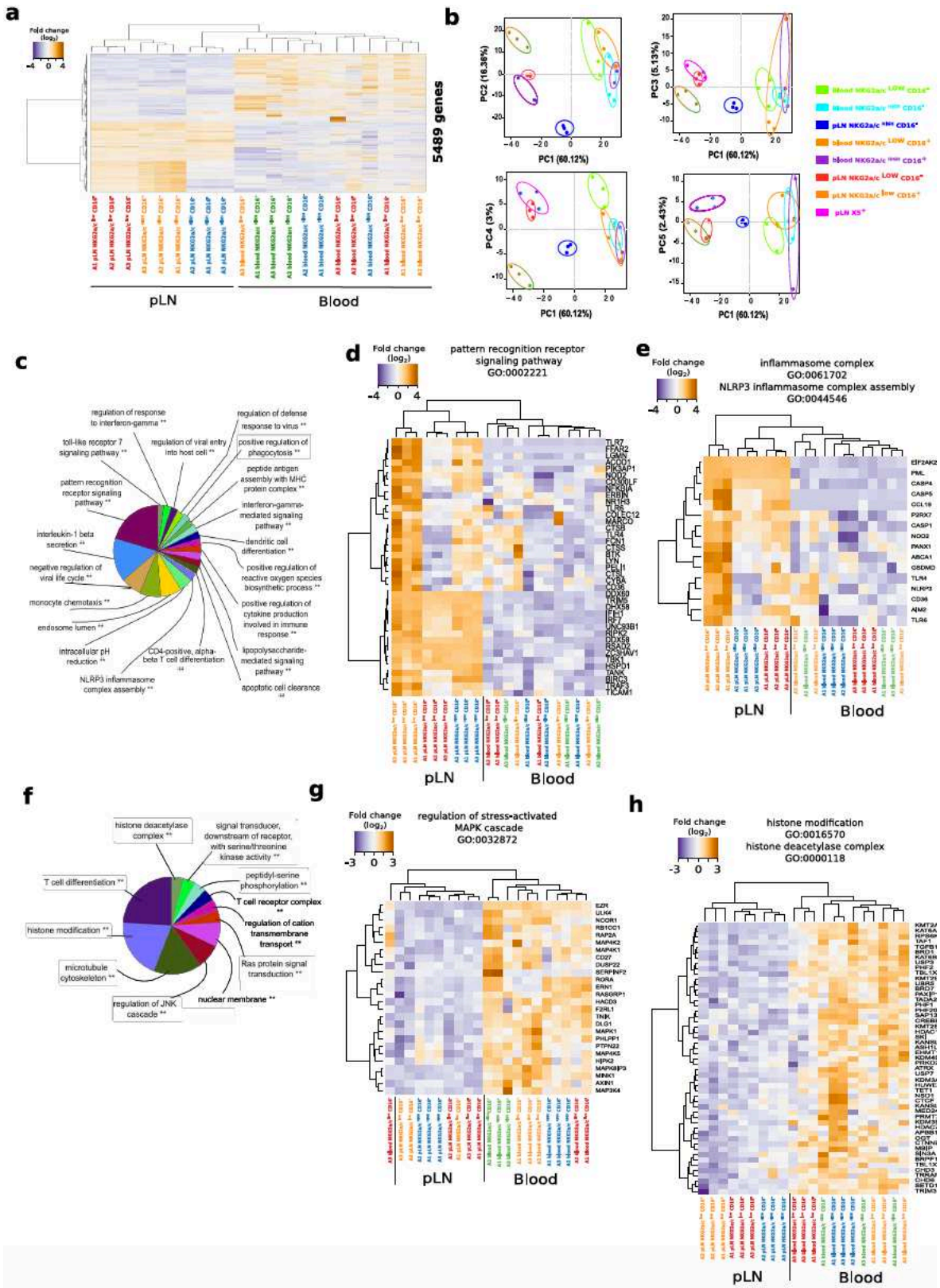
from AGM LN at the indicated time points. Each pie chart represents the median of 6 monkeys. The color of each arc represents a maker (indicated in the figure). Lower panel: Boolean analysis showing the range and mean frequencies of the 19 NK cell subpopulations according to the expression of NKG2D, NKP30, NKP46, CD16, CD69 and NKP80 on NKG2 ^{HIGH}NK cells in 6 AGMs before infection (blue bar), at day 9 p.i. (red bar) and at day 150 p.i. (green bar). The red cross shows a significant change for a given population at day 9 p.i. when compare to baseline. The green cross shows a significant change for a given population at day 150 p.i. when compared to baseline. **(b)** Upper panel: SPICE 5.3 analyses showing the proportion of different combinations of markers on NKG2 ^{low} NK cells isolated from AGM LNs at the indicated time points. Each pie chart represents the median of 6 monkeys. The colour of each arc represents a maker (as indicated in the figure). Lower panel: Boolean analysis showing the range and mean frequencies of the 19 NK cell subpopulations according to the expression of NKG2D, NKP30, NKP46, CD16, CD69 and NKP80 on NKG2 ^{low} NK cells in 6 AGMs before infection (blue bar), at day 9 p.i. (red bar) and at day 150 p.i. (green bar). The red cross shows significant change for a given population at day 9 p.i. compared to baseline. The green cross shows a significant change for a given population at day 150 p.i. compared to baseline. For **(a)** and **(b)**, the Wilcoxon rank test was used to compare each subset. The cut-off set to 0.03% of total pLN cells was applied to exclude cell populations with limited biological significance.



Supplementary Figure 9. Gene expression profiles in blood NK cells from chronically infected AGMs. Heatmaps of the transcript signatures for **(a)** NK cell surface markers, **(b)** transcription factors**, (c)** secreted molecules and **(d)** surface receptors. In each panel, NK cell subsets are organized as in Fig.1. Each row represents a variable gene among clusters, and each column represents the median of 3 monkeys.

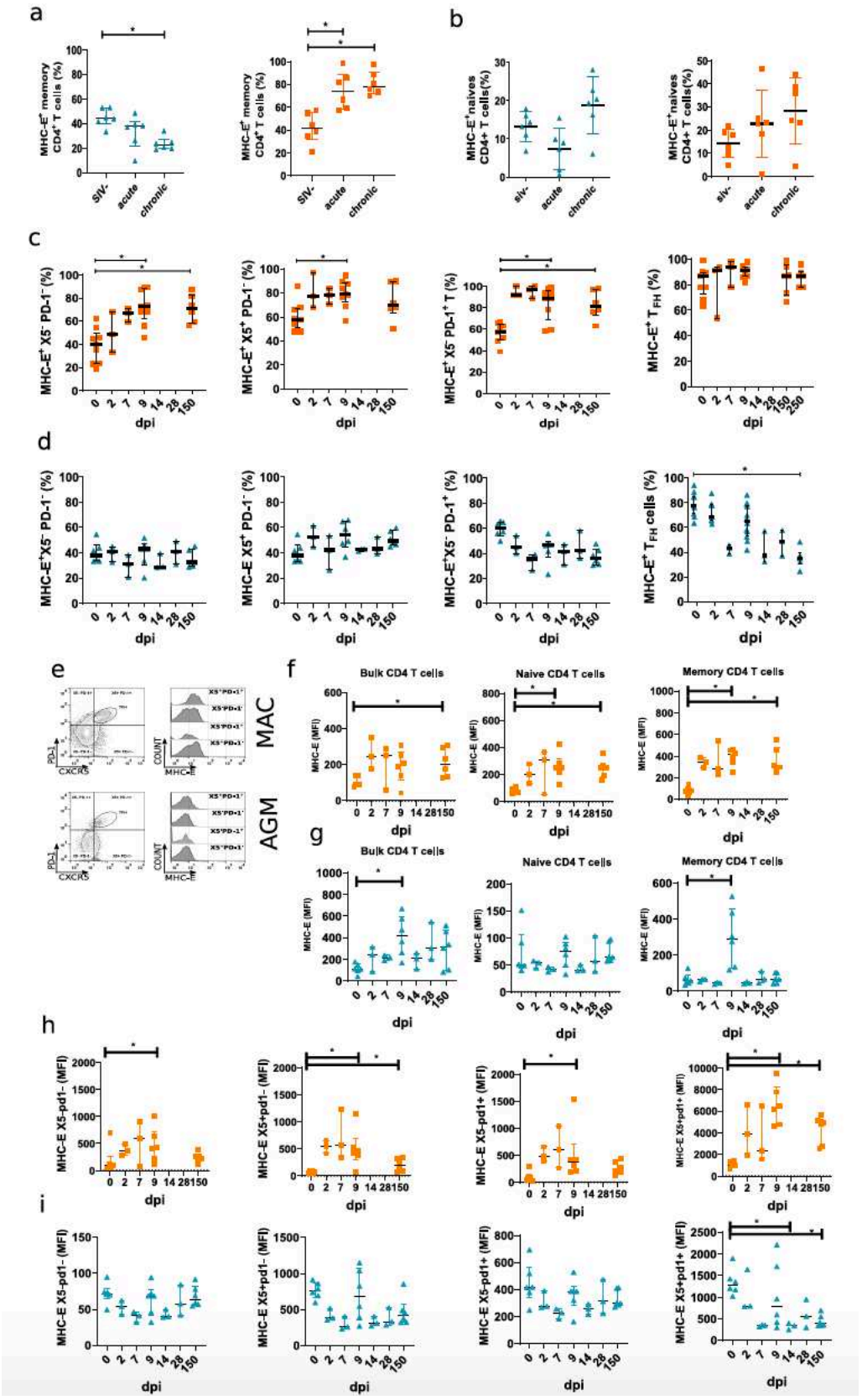


Supplementary Figure 10. Mean fluorescent intensity (MFI) for a given marker on NK cells during the chronic phase (day 150 p.i.) of SIVagm infection in AGM LN. Each monkey is represented by a triangle. The black bar represents the median, and the interquartile range is indicated. The asterisks indicate significant changes ($p<0.05$).



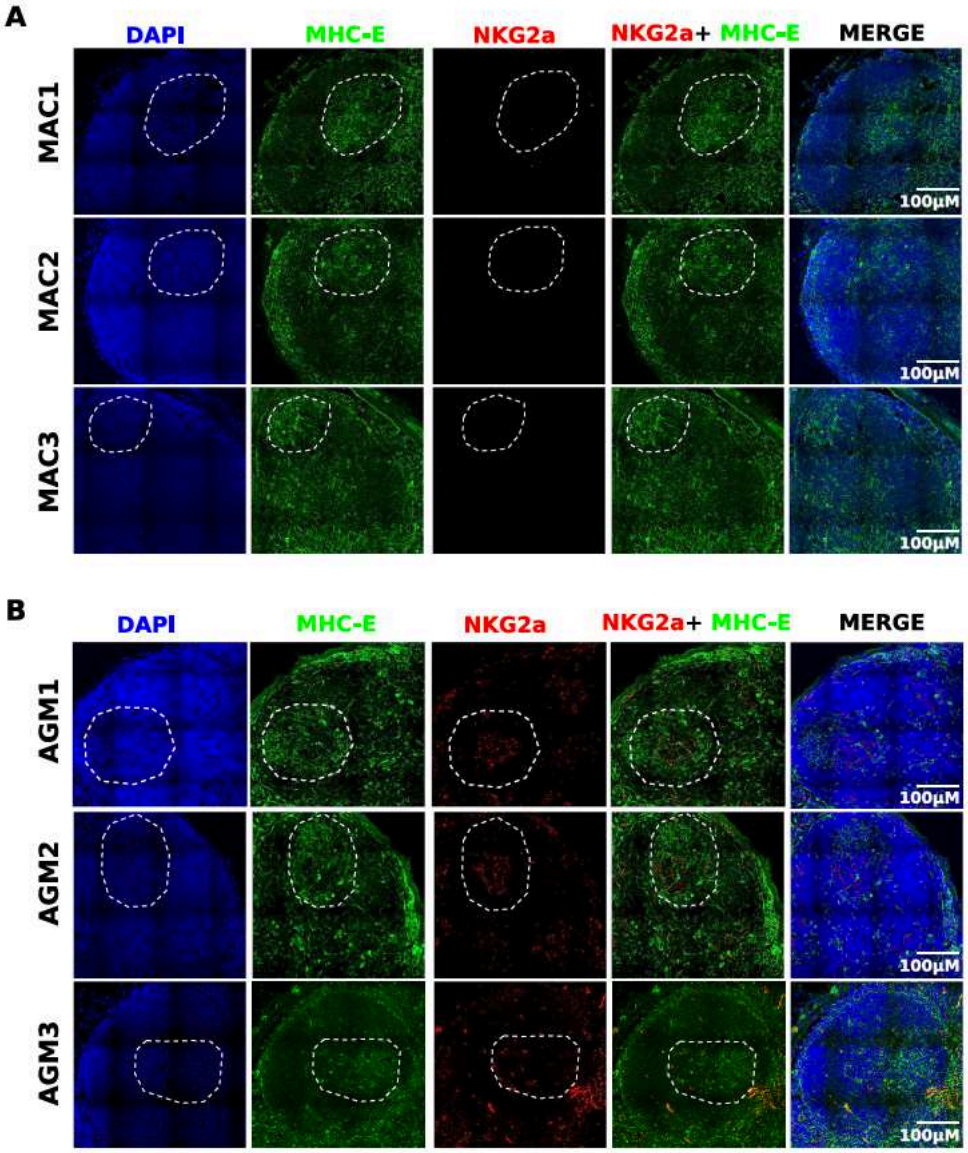
Supplementary Figure 11. Transcriptome analysis of NK cells in blood and LN from chronically SIVagm-infected AGMs. **(a)** Heatmap showing the 5,489 genes differentially regulated between blood and peripheral LN (pLN) NK cells in chronically SIVagm-infected AGM. Each row represents a variable gene among clusters, and each column represents the NK cell subset for an individual monkey. The NK cell subsets are indicated in distinct colors. **(b)** Principal component analysis for NK cells in blood and pLNs using the first five principal components (PC) of the indicated subsets, with percentages of variance associated with each axis based on the mean expression of the genes with variable expression. **(c)** The pie

chart shows the enriched Gene Ontology (GO) terms for the up-regulated genes shared by all pLN NK cell subsets when compared to blood subsets. The messenger RNAs (mRNAs) were input into ClueGO plugged in Cytoscape for GO enrichment analysis. The 'cellular component', 'biological process', 'molecular function' and 'immune system process' GO terms were selected for this analysis. The two-sided hypergeometric test was used in the statistical inference. The term value corrected with the Bonferroni step down method was applied for p-value correlation. The adjusted p-value threshold was set to 0.001. The list of the associated genes found for each GO term is given in Table S4. Each pie slice represents the percentage of genes found in a given pathway among the total genes up regulated in the pLN cells. **(d)** and **(e)** Heatmap showing all the genes found to be significantly up-regulated in pLN NK cells in at least one comparison between blood and pLN cell subsets in **(d)** the pattern recognition receptor signaling or **(e**) inflammasome pathway. **(f)** The pie chart shows the enriched GO terms for the downregulated genes shared by all pLN NK cells when compared to blood ones. The analysis was the same as described in **(c)**. The list of genes found in each pathway is given in Table S5. Each pie slice represents the percentage of genes found in a given pathway among the total genes downregulated in pLN NK cells. **(g)** and **(h)** Heatmap showing all the genes found to be significantly downregulated in pLN NK cells in at least one comparison between blood and pLN cell subsets for **(g)** the mitogen-activated protein kinase (MAPK) cascade and **(h)** epigenetic regulation. The NK cells from pLN and blood of three animals were analyzed.

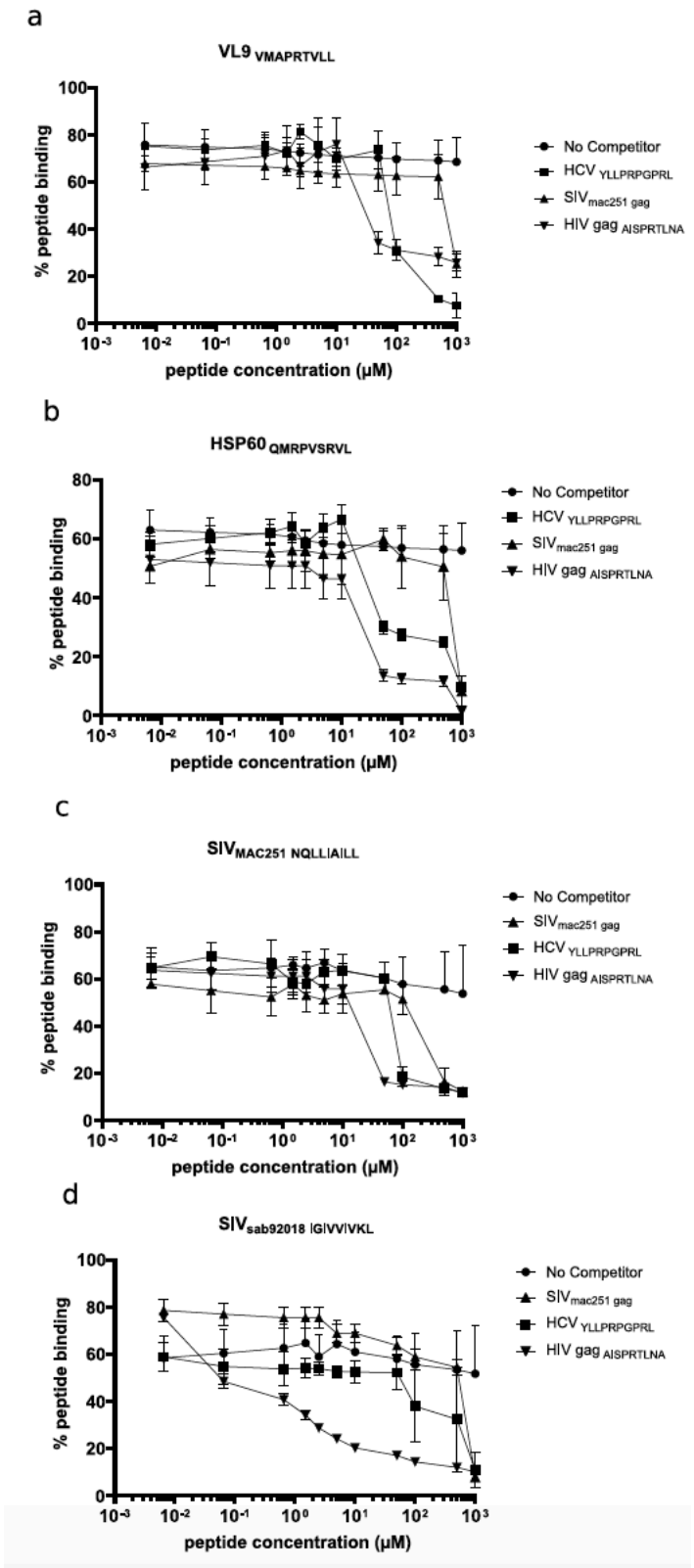


Supplementary Figure 12. MHC-E expression on CD4$^+$ T cells in LN during pathogenic and nonpathogenic SIV infection. **(a)** Frequencies of MHC-E$^+$ cells among memory CD4$^+$ T cells in LN from MAC (orange) and AGM (blue) before and during SIV infection. **(b)** Frequencies of MHC-E$^+$ cells among naive CD4$^+$ T cell in LN from MAC (orange) and AGM (blue) before and during SIV infection. **(c-d)** Longitudinal analyses of MHC-E$^+$ frequency on distinct CD4$^+$ T cell subpopulations in LN from infected MAC (orange) and AGM (blue). **(e)** A representative dot plot and histogram showing MHC-E levels on

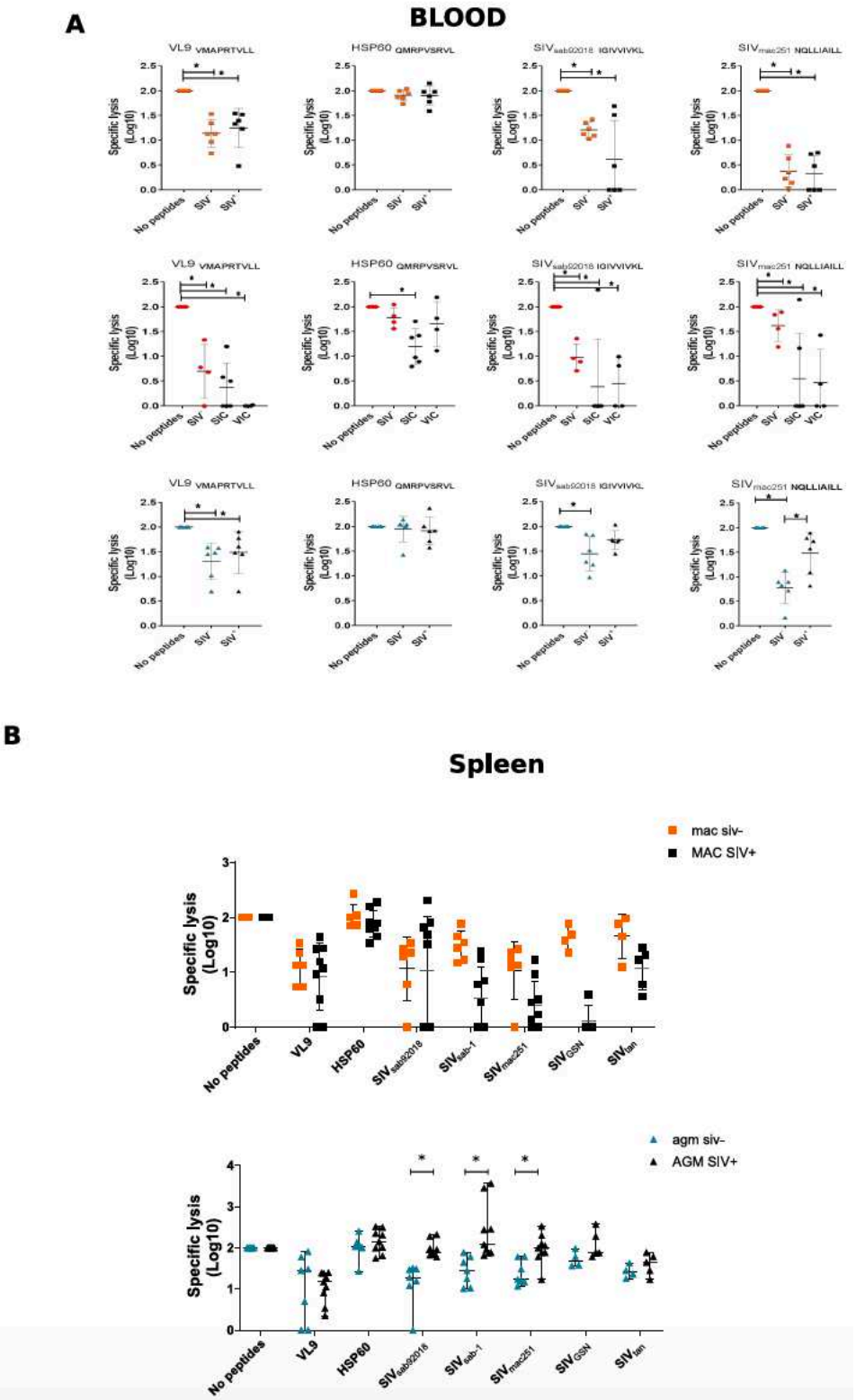
distinct CD4$^+$ T cell subpopulations in LN. **(f-g)** Longitudinal analyses of MHC-E$^+$ level on total, naive and memory CD4$^+$ T cells, in LN from infected MAC (orange) and AGM (blue). **(h-i)** Longitudinal analyses of MHC-E$^+$ level on distinct CD4$^+$ T cell subpopulations in LN from infected (h) MAC (orange) and (i) AGM (blue). In each graph, each symbol (squares for MAC and triangles for AGM) represents an individual animal. Asterisks indicate statistically significant differences: *: $p < 0.05$; **$p < 0.01$. Horizontal bars indicate median values, and error bars indicate standard deviation.



Supplementary Figure 13. Distribution of MHC-E and NKG2a/c positive cells in B cell follicles. Peripheral LNs from six AGM and six MAC were analyzed at day 150 p.i. The figure shows representative confocal images of LN sections from 3 MAC **(a)** and 3 AGM **(b)** stained for MHC-E (green), NKG2A (red) and total nucleus (blue).

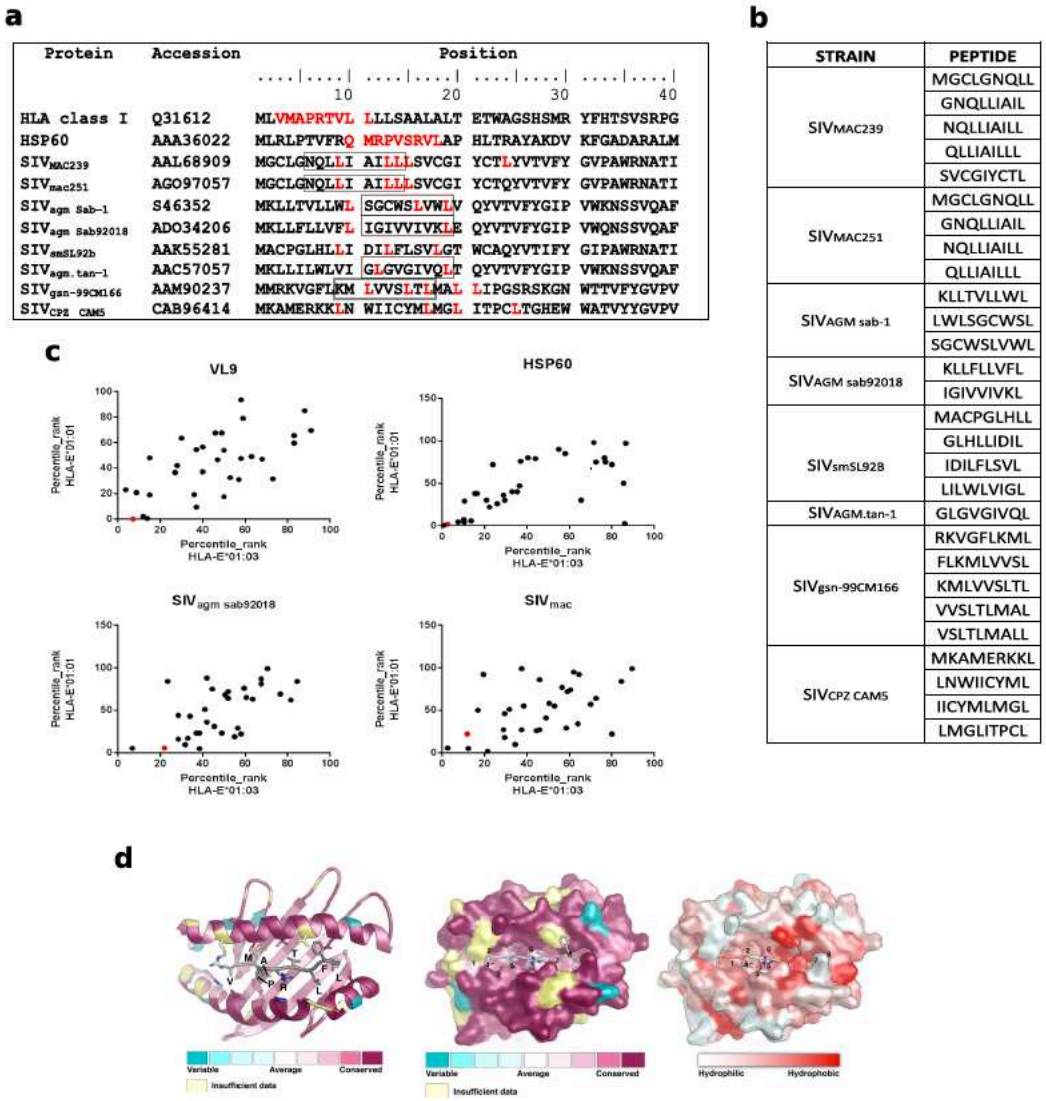


Supplementary Figure 14 Competition assay for binding to MHC-E. K562-HLA-E*0101 cells were loaded with biotin-A2 VL9 peptides **(a),** biotin-HSP60 peptides **(b),** biotin-SIVmac ENV LS peptides **(c)** and biotin-SIVagm ENV LS peptides **(d).** An increasing concentration of the indicated unlabeled competitor peptides was introduced into the culture. MHC-E-bound biotinylated peptide was measured at the surface of K562 cells. Data represent the median of three independent experiments. The sequence of the region coding for the SIVmac251 peptide is identical to that of SIVmac239.



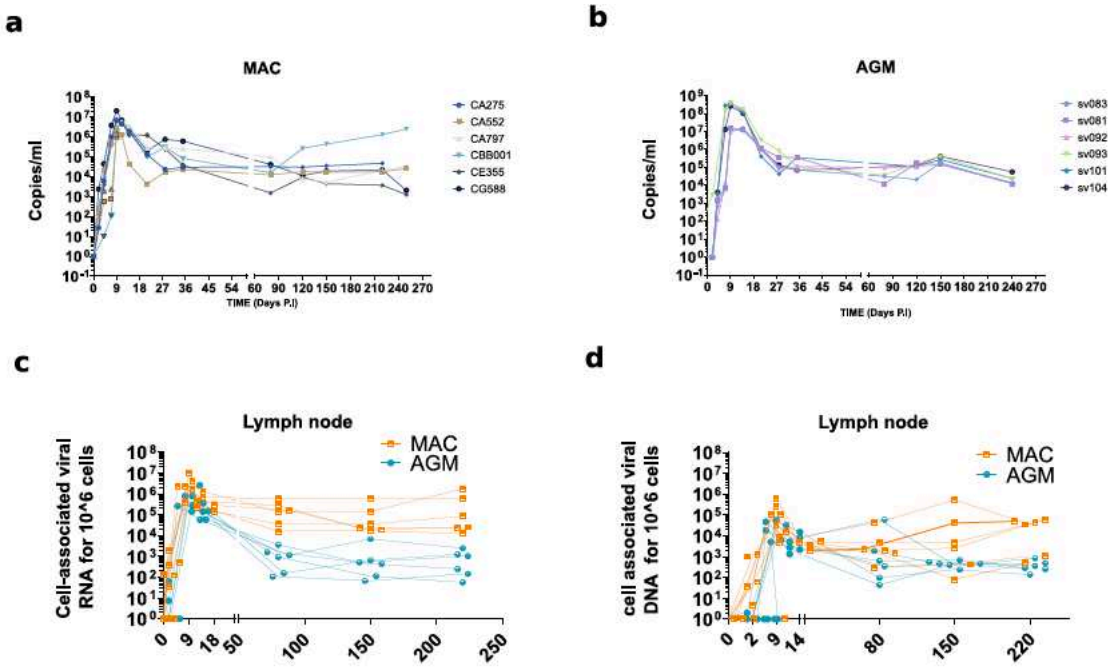
Supplementary Figure 15. MHC-E dependent cytotoxic activity of NK cells before and after SIV infection. **(a)** MHC-E dependent cytotoxic activity of NK cells from blood of cynomolgus MAC (orange/black), rhesus MAC (red/black) and AGM (blue/black) before and after infection. Rhesus MAC corresponded to 4 uninfected, 6 controller (SIC) and 4 viremic (VIC) animals. Uninfected cynomolgus MAC are indicated in orange squares, uninfected rhesus MAC in red circles and uninfected AGM in blue triangles. SIV infected animals are indicated in black. **(b)** MHC-E dependent cytotoxic activity of NK cells from spleen of AGM (grey/blue) and cynomolgus MAC (grey/orange) before and after SIV infection. Peptides derived from ENV LS of SIVagm.sab$_{92018}$, SIVagm.$_{sab1}$, SIVmac$_{239/251}$, SIVgsn and

SIVagm.tan were analyzed. NK cell activities for uninfected cynomolgus MAC are indicated in orange squares and uninfected AGM in blue triangles. NK cell activities for SIV infected animals are depicted in black. The SIVmac251 peptide is identical to the corresponding SIVmac239 region. The asterisks indicate $p < 0.05$.



Supplementary Figure 16. Design of peptides derived from the ENV leader sequence with a potential for HLA-E binding. (a) Sequence alignments of the region corresponding to the signal peptides of the human HLA-class I B-73 alpha chain, the human HSP60 protein and the envelope proteins of 8 SIV viruses. The sequences of the human nonamer peptides (VL9, HSP60) known to efficiently bind to MHC-E are shown in red, as well as the positions of the Leucine amino acids. The sequences corresponding to the selected ENV peptides are framed. **(b)** Table showing nonamer sequences from signal peptides in ENV of the 8 analyzed SIV viruses showing similarities with the canonical MHC-E binding motif, such as strong hydrophobicity and a leucine in the last position. (**c)** HLA-E binding predictions using the IEDB analysis resource. This is a T cell epitope prediction tool, which takes into account an amino acid sequence and determines each subsequence's ability to bind to a specific MHC class I molecule[88,89]. Here the sequence corresponds to the leader sequence. The multiple possible subsequences of it are represented by the black dots in the graph. Each of the subsequence and its predicted capacity for binding to HLA-E is indicated in Supplementary Method Table 2. The location of each dot represents the predicted capacity of binding to HLA-E. For each peptide, percentile ranks for binding to HLA-E*0101 are indicated on the y-axis, and percentile ranks for binding to HLA-E*0103 are

shown on the x-axis. A low percentile rank value indicates high affinity. The position of the known VL9 and HSP60 control peptides and of the selected SIV peptides are shown in red. The sequences for the selected SIVmac239 and SIVmac251 peptide are identical to each other. **(d)** Three-dimensional analysis of the binding pocket in the primate MHC-E molecule. Left and middle panel show the ribbon and surface representation of MHC-E with a peptide ligand (PDB code 3BZF) colored by degree of conservation based on the alignment of MHC-E amino acid sequences from *Homo sapiens*, *Pan troglodytes*, *Papio anubis, Chlorocebus sabaeus* (AGM), *Macaca mulatta* (rhMAC) and *Macaca fascicularis* (cynMAC). The MHC-E binding pocket was conserved between the species and the C-terminal binding part of the peptide highly hydrophobic for all species. The localization of a nonamer peptide with the canonical MHC- E binding motif is shown.



e

Animal #	Species	Duration of infection at necropsy (days)	SIV	Viral status	vRNA (copies/ml plasma)	SIV strain
RM 14222	Rh.Mac	n.a.	neg	n.a.	n.a.	n.a.
RM 2363	Rh.Mac	n.a.	neg	n.a.	n.a.	n.a.
RM 2564	Rh.Mac	n.a.	neg	n.a.	n.a.	n.a.
RM 14225	Rh.Mac	n.a.	neg	n.a.	n.a.	n.a.
AV556	Rh.Mac	n.a.	neg	n.a.	n.a.	n.a.
RM 13926	Rh.Mac	2512	+	Controller	$4.2x10^1$	SIVmac239
RM 12671	Rh.Mac	4367	+	Controller	<40	
RM 2139	Rh.Mac	4268	+	Controller	<40	
RM 2284	Rh.Mac	2483	+	Controller	<40	
RM 13919	Rh.Mac	2465	+	Controller	<40	
RM 13923	Rh.Mac	2150	+	Controller	<40	
RM2155	Rh.Mac	4373	+	Controller	4.2×10^1	
RM 2153	Rh.Mac	4107	+	Viremic	8.4×10^4	
RM 13909	Rh.Mac	2368	+	Viremic	$8.86x\ 10^4$	
RM 8644	Rh.Mac	6349	+	Viremic	2.3×10^4	
RM 15925	Rh.Mac	394	+	Viremic	$4.12x10^4$	
RM 13914	Rh.Mac	448	+	Viremic	$3.56x10^5$	
RM 2347	Rh.Mac	203	+	Viremic	$3.60x10^6$	

Supplementary method Figure 1. Plasma viral RNA copy numbers in the longitudinally followed animals. The longitudinal studies included (a) 6 cynomolgus macaques (cynMAC) infected with SIVmac251 and (b) 6 AGM infected with SIVagm.sab92018. (c) Cell associated viral RNA copy numbers in lymph nodes. (d) Cell-associated viral DNA copy numbers in lymph nodes. (e) Table showing immunological parameters at necropsy of rhesus macaques used in the study

https://www.dropbox.com/scl/fi/lmrd5valeynffpnoi0x5d/Manuscript-3_table-sup-1.ods?dl=0&rlkey=zxb5y776e6i3hoieuqr4pk9tu

Supplementary method table 1. Antibodies used for flow cytometry and histochemistry.

https://www.dropbox.com/scl/fi/zbsw5fo6rhp29tda5s9b0/Manuscript-3_table-sup-2.ods?dl=0&rlkey=1pfslb951tr2ozfw9lyxb7jpi

Supplementary method table 2. IEDB prediction values. Each row corresponds to one peptide binding prediction represented by a dot in Fig.S16c. The first six columns refer to the HLA-E allele, the peptide the prediction was made for, the start and end position of the peptide, its length, and the peptide sequence. The predicted output is given in units of IC50nM88,89. Peptides with IC50 values <50 nM are generally considered high affinity, <500 nM intermediate affinity and <5000 nM low affinity. In addition to the IC50 values for each peptide, a percentile rank is generated by comparing the peptide's IC50 against those of a set of random peptides from SWISSPROT database. A small numbered percentile rank indicates high affinity. The median percentile rank is reported.

4. Non-Human Primate Determinants of NK Cells in Tissues at steady-state and during SIV infection

Non-Human Primate Determinants of NK Cells in Tissues at steady-state and during SIV infection

Nicolas Huot[1], Philippe Rascle[1,2], Caroline Petitdemange[1], Vanessa Contreras[3], Jean-Louis Palgen[3], Christiane Stahl-Hennig[4], Roger Le Grand[3,] Anne-Sophie Beignon[3], Beatrice Jacquelin[1] and Michaela Müller-Trutwin[1'*]

[1]*Institut Pasteur, Unité HIV, Inflammation et Persistance, Paris, France;*

[2]*Université Paris Diderot, Sorbonne Paris Cité, Paris, France;*

[3]*CEA-Université Paris Saclay-Inserm, U1184, IMVA-HB/IDMIT Department, IBFJ, DRF, Fontenay-aux-Roses, France;*

[4]*Deutsches Primatenzentrum, Göttingen, Germany;*

Keywords: SIV, HIV, NK cells, lymph node, gut, tissue resident, CXCR5, CXCR3, CD8, CD69, NKp44.

***Correspondence:** mmuller@pasteur.fr

Frontier in press

Abstract

Natural killer (NK) cells play essential roles in immunity to viruses and tumors. Their function is genetically determined but also modulated by environmental factors. The distribution and functional regulation of these cells vary depending on the tissue. NK cell behavior in lymphoid tissues is so far understudied. Non-human primate (NHP) models are essential for the development of therapies and vaccines against human diseases and access to NHP tissues allows insights into spatial regulations of NK cells. Here, we investigated tissue-specific parameters of NK cells from NHP species, *i.e.* cynomolgus macaque (*Macaca cynomolgus*), African green monkey (*Chlorocebus aethiops*), rhesus macaque (*Macaca mulatta*) and baboon (*Papio, anubis*). By comprehensive multi-dimensional analysis of NK cells from secondary lymphoid organs, intestinal mucosa, liver and blood, we identified tissue- and species-specific patterns of NK cell frequencies, phenotypes and potential activity. In addition, we defined tissue-specific characteristics of NK cells during an infection by the simian immunodeficiency virus. Altogether, our results provide a comprehensive anatomic analysis of NK cells in different tissues of primates at steady state and during a viral infection.

Introduction

In recent years, it has become increasingly clear that human natural killer cells (NK cells) are far more diverse than previously assumed [1]. Some of the diversity is genetically determined, whereas substantial diversification seems to be also determined by environmental factors, including vaccinations and age [1–4]. NK cells are frequent in organs such as liver and uterus but are probably present in all tissues to various degrees, including bone marrow (BM), lymph nodes, spleen, kidneys, skin, lung and gut[2,5–9]. NK cells in secondary and tertiary lymphoid organs are still understudied given their low frequencies in these lymphoid tissues[10–12]. A proportion of them express molecules known as tissue-resident markers for T cells, such as CD69 and CD103[5]. The local tissue environment impacts NK cell diversity and function[5,13]. The role of tissue localization in human NK cell development and function, and how circulating NK cells relate to those in different sites, are however not yet sufficiently well understood. Also, markers for the identification of distinct tissue-resident NK cell subpopulations are still scarce. Characterization of NK cells is particularly challenging in tissues, mainly due to lack of hallmark lineage markers for tissue-derived innate lymphoid cells (ILCs) and NK cells in humans. In the context of viral infections, access limitations to organs in humans is an additional hurdle to fully understand the role of NK cells in tissues.

Non-human primates (NHP) are essential models for the development of therapies and vaccines against human diseases and allow insights into spatial cellular regulations of NK cells. African green monkeys (AGM), macaques and baboons are the most largely used NHP models in preclinical research. They have contributed essentially in the research or development of vaccines against viral diseases, including Sars-CoV-2, HIV, Influenza, Yellow fever and Ebola virus [14–18]. Efforts to identify sub-populations of NK cells in NHP were complicated by incomplete definitions of them, mainly due to the fact that the antibody against CD56 does not stain all NK cell subpopulations in NHP species[19]. Alternatively, NHP NK cells in blood have been defined as $CD3^{-}CD8\alpha\alpha^{+}CD20^{-/dim}NKG2a/c^{+}$, which is considered the most effective inclusive definition for NK cells from Old World monkeys, such as rhesus and pig-tailed macaques, sooty mangabeys and African green monkeys[20–23]; whereas this definition does not fully characterize neotropical primate blood NK cells[24].

Some of the NK cell diversity driven by environmental factors is linked to their maturation and differentiation. In Humans, the modulation of NKG2a/c expression among CD56dim cells defines a crucial step of their differentiation[25,26]. Immature and mature NK cells can be respectively defined as $CD56^{bright}NKG2a/c^{hi}CD62L^{hi}CD57^{-}$ and $CD56^{dim}NKG2a/c^{-}CD62L^{-}CD57^{+}$. Their distribution varies according to the tissue. NK cells in tissues also share several markers with innate lymphoid cells (ILCs). The natural cytotoxicity receptors (NCRs) NKp46 and NKp44 have been described on both NK cells and ILCs[27]. NKp46 is a major determinant of NK cell function and is implicated in tumor immune surveillance in acute myeloid leukemia [28,29]. NKp44 is expressed on activated human NK cells and is important for tumor target cell recognition by NK cells during natural cytotoxicity responses, whereas in the adult intestine, $NKp44^{+}$ ILC are the main ILC subset producing IL-22[30,31]. NKp44+CD103+CD69+ NK cells have been shown to persist in adult intestine, corresponding to previously described intraepithelial ILC1s [32]. The recent identification of the NKp44 receptor moreover indicates an important role of Nkp44 in viral infections [33]. NKp30 is another interesting NCR in viral infections due to is capacity to interact with dendritic cells (DC) and impact on the NK-DC cross-talk[34–36].

There is an urgent need for a better characterization of these NK cell subpopulations in lymphoid tissues. Until now, it has been very difficult to relate our knowledge of human NK cell biology to that of NHP and translate this information into pre-clinical practice. Among the different NHP models, African non-human primates, such as AGM, have been a natural host for simian immunodeficiency viruses (SIV) for probably more than 1 million of years[37–39]. In contrast to people living with HIV (PLH), natural hosts for SIV typically do not progress toward disease despite persistent high viremia[40]. At the opposite, Asian macaques are not natural hosts of SIV and experimental infection with SIVmac induces AIDS preceded by rapid loss of $CD4^{+}$ T cells in intestinal mucosa and systemic chronic inflammation as in PLH. We have previously shown that in contrast to HIV-1 infected humans and SIVmac-infected macaques, AGMs infected with SIVagm are free of chronic inflammation and efficiently control viral replication in SLT[41]. The viral control in SLT of SIVagm-infected AGMs is mediated predominantly by NK cells in a CXCR5 dependent manner[41]. Paradoxically, no viral control is observed in the intestine of SIVagm-infected monkeys[42]. AGM therefore represent a model of tissue-specific NK cell-mediated viral control.

In this study, we comprehensively determined tissue-specific frequencies, phenotypes and potential activity profiles of NK cells in major NHP primate models. We investigated NK cells in blood, liver, lymph nodes, spleen, ileum, jejunum, colon and rectum from uninfected animals and after infection with SIV. This work provides clues to better understand the behavior of tissue NK cells and delivers novel tools for the study of therapeutic and vaccinal approaches in NHP models for human diseases.

Results

Tissue-Intrinsic distribution of non-human primate NK cell subsets

To analyze NK cell distribution and phenotype profiles across different anatomic sites in Asian and African NHP, we collected blood, secondary lymphoid organs (spleen, and peripheral lymph nodes [pLN]), liver, and gut (small and large intestine) from Cynomolgus macaques (CM) and AGM (Fig.1A). NK cells were defined as previously reported by us and others[20–22,41] as $CD45^{+}CD3^{-}CD14^{-}CD20^{-}NKG2_{a/c}{}^{+}$ cells. The tissue distribution was analysed first in healthy CM and AGM. The distribution was consistent between animals for a given species with blood and liver having significantly higher frequencies of NK cells (5%–40%) compared to low frequencies (<0.1%–5%) of NK cells in the pLNs and gut (FIG.1B).

NK cells were further delineated into two NK cell subsets, $NKG2a/c^{HIGH}$ and $NKG2a/c^{LOW}$ (FIG 1C and D and Fig.S1). The distribution of $NKG2a/c^{HIGH}$ and $NKG2a/c^{LOW}$ NK cell subsets was also dependent on the tissue site (FIG.1C and D). $NKG2a/c^{HIGH}$ NK cells predominated in pLNs, spleen and ileum, whereas $NKG2a/c^{LOW}$ NK cells comprised the majority of NK cells in liver independently of the species (FIG.1E and F). Thus, $NKG2a/c^{HIGH}$ NK cells were more prevalent in sites known for containing an abundance of immature NK cells such as pLN, spleen and gut, and in liver potentially mature NK cells were predominant.

We also observed a difference between the species, as $NKG2a/c^{HIGH}$ NK cells were the main population in blood, jejunum and rectum of CM in contrast to AGM where $NKG2a/c^{LOW}$ NK cells dominated in these three compartments (FIG.1E and F). To clarify the difference observed between these two species, we analysed a higher number of animals and more species (FIG.1G). Thus, blood NK cells were analyzed in 12 CM, 11 AGM, 8 Rhesus macaques (RM) and 4 baboons. The $NKG2a/c^{HIGH}$ NK cells were again the major population in blood of the two Asian NHP (CM and RM), and not in the two African NHP (AGM and baboons) (Fig. 1H).

To summarize, the NK cell distributions across tissues varied similar to the ones described in humans[5]. The frequencies of total NK cells in different anatomical sites did not differ between NHP species. The frequency of $NKG2a/c^{LOW}$ NK cells in blood was higher in the NHP species from Africa compared to macaque species.

Evaluation of NK cell diversity in tissues from NHP

In order to further analyse the difference between the tissues, we implemented a high-dimensional flow cytometry analysis of simian NK cells, allowing notably the measurement of NK cell cytotoxicity receptors (NCRs), homing receptors and cellular exhaustion marker (PD-1). We included, as homing receptors, CXCR3 and CXCR5 which are respectively a major tissue homing receptor for NK cells[43] and a B cell follicle homing receptor for lymphocytes[44–46]. The NK cells from six anatomical sites (blood, pLN, spleen, liver, ileum and jejunum) collected from five healthy CM and four healthy AGM were analysed. A heatmap based on the MFI for each marker at cluster level was generated. Force-directed clustering analysis resulted in 11 distinct NK cell clusters for both AGM and CM (Fig. 2A - D). In both species, blood NK cells segregated into three distinct subclusters that did not reveal overlaps with NK cells from tissues. Liver NK cells either formed only one cluster or the clusters grouped together generally separate from other tissues. Spleen and pLN NK shared some clusters. Jejunum and ileum NK cells appeared to be closely linked but also sometimes were found in clusters with other tissue NK cells (Fig. 2A - D).

When comparing the two species, NK cells from pLN and spleen in AGM showed elevated levels of CXCR5 expression compared to other tissues. In contrast, for CM, highest CXCR5 expression was observed in the gut (Fig.2B

and D). CM also showed high frequencies of CXCR5+ NK cells in the liver (Fig.2E and F). Another distinct feature of the CM was a high frequency of NK cells with lower CD8 expression in tissues (Fig.2E).

In summary, NK cells showed tissue-specific clusters with LN and spleen NK cells closely related. Tissue NK cells in CM rarely expressed CD8. In the intestine and liver, NK cells in CM frequently expressed CXCR5.

Tissue NK cells are differentially impacted in pathogenic compared to non-pathogenic SIV infection

We evaluated if and how SIV infection modulates NK cell distribution and phenotype among tissues. We included in the analysis tissue homing markers and compared the distribution of NK cell subpopulations between the tissues. Seven CM and seven AGM were followed during SIVmac and SIVagm infection, respectively (Fig.S2). NK cells from blood, pLN and rectal biopsy were longitudinally monitored during the time course of infection (Fig.3A). To have access also to liver, ileum and jejunum during acute infection, we analysed tissues collected at necropsy from three monkeys of each species at day 9 p.i. and at the time of peak viremia, and from four animals of each species during the chronic phase of infection (day 240 p.i.). Assessment of absolute NK cell counts in blood did not reveal statistically significant differences during SIV infection, even if a trend for decrease was observed in each species during acute infection -up to day 3-4 p.i. (Fig.3B). In pLN, the frequency of NK cells rapidly decreased in CM during acute infection to never reach the level observed before infection throughout chronic infection, whereas no statistically significant change was observed in AGM (Fig.3C, left graph). In contrast, AGM NK cells in rectal biopsies showed a constant decrease during infection, while CM NK cells tended to drop at day 7 p.i., but only transiently and remained normal thereafter (Fig.3C, right graph).

Force-directed clustering analysis of NK cells from six tissues obtained at day 9 p.i. generated 7 distinct NK cell clusters per species (Fig. 3D-G). NK cells clustered again according to tissues as before infection, except some overlap between liver and blood or pLN. The highest density of expression was observed for CXCR5 on NK cells from SLT in AGM, while it was also elevated in some liver NK cells in CM. CXCR3 expression was high on NK cells from blood and SLT in AGM, while high on intestinal and blood NK cells for CM, suggesting that CXCR3 might be involved in the distinct tissue distribution of NK cells after SIVmac and SIVagm infection.

We then performed the same analysis on chronically infected animals. Due to the decrease and few amount of NK cells in gut tissues from AGM during SIVagm infection (Fig. 3C, right graph), we included an additional intestinal compartment (the colon) at the expense of liver in the analyses (Fig.4A-E). While in healthy animals, CXCR3 and CXCR5 were found in the same clusters (Fig.2B and D), they clustered separately in infected animals (Fig.4A-D), indicating that the CXCR3+ and CXCR5+ NK cells evolved differentially after SIV infection. In SIVmac infection, the frequencies of CXCR5+ NK cells in the gut decreased (Fig.4E) as compared to before infection (Fig.2E). CXCR5 expression on NK cells was also low in SLT of CM compared to AGM in chronic SIV infection (Fig.4A-D), correlating with previous data on the higher levels CXCR5+ NK cells in SLT during chronic SIVagm infection as compared to chronic SIVmac infection[41].

PD-1 is known to be expressed on exhausted CD8+ T cell lymphocytes. However, PD-1 expression is also high on CXCR5+ lymphocytes residing in the B cell follicles of SLT (T_{FH} and B cells). On NK cells, as shown here, PD-1 was often expressed on the same cell subset of CXCR5+ NK cells before infection but mostly on distinct NK cell subsets after SIV infection (Fig.4B and D). PD-1+ NK cells were increased in SLT during SIVagm infection (Fig.4F) as compared to healthy animals (Fig.2F), which might be related to their accumulation in B cell follicles during chronic SIVagm infection[41].

Allover, we demonstrate a distinct tissue distribution of NK cells after SIV infection as compared to healthy animals. In addition, the dynamic of NK cell frequencies was opposite between AGM and CM: decrease in SLT for CM and decrease in gut for AGM after SIV infection.

Resident tissue NK cells express a cytotoxic phenotype in the natural host of SIV infection

Next we analyzed the phenotype of the NK cells in the distinct tissues. We performed a first analysis on total NK cells and then on NK cells that express markers that have been associated with tissue residency of T cells, such as CD69,

and those present on mucosal innate lymphocytes, such as NKp44. We assessed the distribution of CD69+ and NKP44+ NK cells in distinct tissues from SIV-infected animals. (Fig.5A and B). CD69+ NK cells were generally more frequent in tissues than in blood, in particularly in the colon of CM (34% to 85%) (Fig.5A) and in all analysed tissues in AGM (pLN, spleen, ileum, jejunum, colon) (Fig.5B). As for CM, the highest frequencies of CD69+ NK cells in AGM where observed in the intestine compared to secondary lymphoid organs and blood (FIG5.B). NKP44+ NK cells were rare in blood and LN, while frequent in the intestine (FIG5.A and B). CM also harbored NKp44+ NK cells in the spleen. Altogether, CD69+ and NKp44+ NK cells were generally observed more often in tissues, and Nkp44+ NK cells were more frequent in the gut than in SLT, in particular in AGM, suggesting that these markers can be used in a similar way as in humans.

We evaluated the cytotoxic phenotype of the NK cells between the distinct tissues and combined the analysis with effector molecules: Granzyme B (GzmB), interferon gamma (IFNg), and tumor necrosis factor alpha (TNF-a). We performed *ex vivo* intra-cellular staining for GzmB, IFN-g, and TNF-a in the healthy AGM and CM (Fig.5A and B). We thus avoided any potential bias of *in vitro* cultures and provide profiles the most close to the physiological patterns *in vivo*. We observed high levels of IFN-g+ NK cells in all compartments (Fig.5A and B). In contrast, the frequencies of TNF-a+ NK cells and GzmB+ NK cells varied according to the tissues. The frequencies of GzmB+ NK cells were high in blood from both CM (65% to 80%) and AGM (72% to 96%) and low in SLT (FIG5.A and B). In the intestine, GzmB+ NK cells were sometimes as frequent as in blood, in particular in CM, and sometimes at intermediate levels between SLT and blood. Similar to GzmB+ NK cells, TNF-a+ NK cells were rare in SLT and sometimes frequent in the gut. There was however a high inter-individual variability, for example for TNF-a+ NK cells in blood. Altogether, NK cells with a cytotoxic phenotype were seen more often in effector sites (blood, gut) than in inductive sites (pLN, spleen). IFN-G+ NK cells were observed in all compartments including in inductive sites (SLT).

Finally, we studied if there was a link between tissue-specific residency of NK cells and their effector profiles. We analysed therefore the *ex vivo* expression of IFN-g and GzmB according to the expression of the potential tissue residency marker CD69 in the distinct lymphoid compartments of both species (Fig.5C and D). In SIV-infected CM, most of the GzmB+ cells did not express CD69, irrespective of the tissue studied (Fig.5E). These $CD69^{-}$GzmB+ NK cells in CM were more frequent in the intestine (colon, ileum) than in SLT. In AGM, the GzmB+ NK cells in blood were CD69- but in tissues CD69+ (Fig.5F). Similar to GzmB, the IFN-g+ NK cells in SIV-infected CM were mostly CD69- while in the SIV-infected AGM, many IFN-g+ NK cells were CD69+. In the SIV-infected CM, most NK cells were IFN-g+ in all lymphoid tissues analysed, in contrast to the SIV-infected AGM, where most NK cells were IFN-g-, in particular in the intestine. Altogether, most GzmB+ and IFN-g+ NK cells in the SLT and intestine of SIV-infected CM were CD69-, while CD69+ in AGM. Given that NK cells were increased in the intestine of CM in chronic SIV infection as compared to AGM (Fig.3C, right panel), this could suggest that most of the NK cells in the intestine during chronic SIVmac infection were infiltrating and not resident NK cells.

Discussion

In this study, we set out to investigate the tissue distribution, phenotype and function of NK cells in tissues of healthy and SIV-infected non-human primates. Moreover, we analyzed tissue-residence markers combined with effector molecules inside tissues. This study allowed to identify tissue- and species-specific patterns of NK cell frequencies and phenotype in lymphoid and non-lymphoid tissues of primates.

Studies on NK cells in lymphoid tissues are scarce because NK cell frequencies are low in these tissues. However, it is important to gather more information about NK cells in such tissues since their numbers and functions can be modulated by viral infections, and also given the importance of the NK-DC cross-talk in LN for shaping the adaptive immune responses[47,48]. While we did not analyse all possible tissues, we focused the study on lymphoid tissues where there is little information and which are key for the study of vaccine responses, i.e. mucosa as a site of viral entry and replication and SLT for education of B and T cell responses. We compared here the NK cells present in such anatomic sites to body compartments where NK cells are more frequent and more often described (blood and liver).

We performed these analyses in representative species from Asia and Africa. We thus studied four NHP species and only two of them extensively: one Asian (CM) and one African (AGM) species. Of note, these two species are among the most used NHP models in biomedical research. In addition, the data observed here for CM might be similar in related species, such as rhesus macaques.

Here we performed multiparameter flow cytometry. Even if we did not use NGS technology, such analysis allowed to focus on specific markers and to analyze a wide range of tissues (blood, liver, spleen, lymph nodes, ileum, jejunum, colon, rectum) concomitantly. We also performed a longitudinal analysis in two distinct tissues (SLT and intestine) in response to a viral infection. Most importantly, we provide *ex vivo* data for NK cell functionality in these tissues.

Our data demonstrate that NK cells of CM were rarely CD8+ in tissues. Previous reports have shown that CD8 engagement on NK cells delivers an activating signal which increases the synthesis and secretion of IFN-g[49]. CD8 may deliver an activating signal only when it is expressed at high density[50]. KIR and/or C-type lectin inhibitory receptors (CLIR) such as NKG2a/c can down-regulate CD8-mediated triggering[49]. The down-regulation of CD8-dependent IFN-g production exerted by inhibitory receptor superfamily (IRS) members may represent a mechanism to limit NK cell responses, as it has been proposed for the inhibiting signal delivered through inhibitory receptors to avoid lysis of autologous cells expressing the appropriate HLA-I ligand of a given IRS member[51]. Other NK cell surface receptors, including NKp30 and NKp44 [52–54] could thus rather be involved in the recognition of target cells and activation of NK cell-mediated lysis in CM tissues. Our data also imply that studies using anti-CD8a antibodies to deplete NK cells need to consider the low frequency of CD8+ NK cells in tissues of some species. Indeed, our study indicates that in CM, NK cells will not get efficiently depleted in tissues when using anti-CD8 antibodies.

CXCR5 is a chemokine receptor mainly expressed on B cells, as well as DCs and T cell subsets such as T_{FH} cells[55,56] present in B cell follicles. We have recently provided evidence that the capacity to control SIV viral replication in B cell follicles of AGM was associated with the presence of $CXCR5^+$ NK cells[41], showing that CXCR5 could be also be frequently expressed on NK cells under some circumstances. The role of CXCR5 in the gut is less studied[57]. Nevertheless in the gut, CXCR5 is known to support Solitary Intestinal Lymphoid Tissue (SILT) formation and B cell homing[58]. Here we show that CXCR5 is expressed to high frequency by ileum NK cells in healthy CM and AGM. This high frequency of CXCR5+ NK cells was also noticed in CM jejunum and colon. Strikingly, following SIV infection, the frequency of CXCR5+ NK cells strongly decreased in gut of CM for unknown reasons. It could be related to the increase of infiltrating, CXCR5- NK cells. Microbiota and other external stimuli can foster the formation of aberrant SILT distinguished by impaired development of B cell follicles in CXCR5-deficient mice[58–60]. In this context it could be interesting to investigate if the decrease of CXCR5+ NK cells in intestine during SIVmac infection, concomitant with the well-known induction of microbial translocation, may be associated with the formation of SILT in NHP and humans during HIV and SIVmac infections.

Although CD69 has long been viewed as an activation marker of both T cells and NK cells, it is now clear that it has an important role in retaining immune cells in tissues by inhibiting sphingosine-1-phosphate receptor 1 (S1P1)[61,62]. CD69 is now considered a tissue-resident marker for T cells[63,64]. For NK cells it is less clear if tissue-resident NK cells can be characterized on the basis of the expression of CD69. It has recently been shown that the CD69 expression displays subset- and site-specific variations by tissue NK cells in humans[5]. Here we show that during SIV infection in NHP, NK cells in peripheral blood largely lack expression of CD69. Our data in the tissues argue in in favor of CD69 as a tissue residence marker for NK cells in NHP. The main difference between the pathogenic and non-pathogenic SIV infection in the two species (CM, AGM) came from the observation that the frequency of CD69 cells in tissues during pathogenic infection was relatively low, whereas in natural host a high frequency of CD69+ NK cells was observed in tissues. The high frequency of CD69- NK cells in SIVmac infection might be the result of infiltrating NK cells. The combined analysis of CD69 with GzmB+ and IFN-g indicates that most of resident NK cells harbored a cytotoxic profile, while potentially infiltrating (CD69-) NK cells also expressed the pro-inflammatory IFN-g cytokine. It is not clear though if these changes are the result of blood NK cell infiltration or whether there are phenotypic changes in resident NK cell populations during SIV infection.

The role of tissue localization in NK cell development and function, and how circulating NK cells relate to those in different sites, are not well understood during HIV/SIV infection[22,65,66]. Only few data on NK cells in tissues are available during HIV/SIV infections[41,65,67] . Immediately after HIV/SIV infection, changes occur in NK cell populations in the GALT. Thus, the frequency of both intraepithelial and lamina propria NK cells was increased in

PLH with an incomplete blood CD4+ T cell recovery (CD4<350 cells / µl) despite several years of effective antiretroviral treatment [68]. Similarly, an increase in total and NKG2a/c$^+$ NK cells in rectum RM has been shown during SIVmac infection[66,69]. In contrast, the NKp44$^+$ lymphocytes were significantly depleted in acute HIV and SIV infections in mucosa and continued to decline in frequency during chronic phase[70]. Antiretroviral therapy significantly increased the frequency of mucosal NKG2a/c$^+$ NK cells[71]. SIV infection in pathogenic models drives a trafficking away from secondary lymphoid organs toward the intestine[22,72,73]. This is related to up-regulation of the gut-homing marker $\alpha_4\beta_7$ on NK cells as shown in chronic SIVmac infection coupled with down regulation of the LN-trafficking marker CCR7 [66,74]. Our data in the CM are in line with these reports. Strikingly, we observed opposite tissue dynamics in heterologous and natural hosts of SIV. In the natural host, NK cells were not directed toward the intestine and the frequencies of total NK cells in the gut were decreased in SIVagm infection in contrast to SIVmac infection. This could explain the lack of NK-cell mediated viral control in the intestine of SIVagm-infected AGMs. In CM, NK cells decreased in the LN but increased in the gut in contrast to SIVagm infection in AGM. These distinct NK cell tissue distributions were associated with CXCR3 expression, supporting its role as an inflammatory tissue homing marker for NK cells. The higher levels of the CXCR3 ligand (IP-10) in the intestine of SIVmac-infected macaques as compared to the SIVagm-infected AGMs[75,76] might explain in part, together with previously reported up-regulations of other receptors such as $\alpha_4\beta_7$, the higher levels of NK cells in the intestine of the SIVmac-infected macaques as compared to the natural host. The fact that NK cells seem to be redirected to intestine in SIVmac infection raises the question of their inefficient activity against the cells replicating the virus in the gut. In fact, an increase of these cells in this compartment should favor a better control of the viral replication. However, beyond the mechanisms established by the virus to escape NK cell lysis, the inflammatory environment as well as the loss of regulatory cells (i.e ILCs, TH17, CD4 T cells) might profoundly and durably alter NK cell functions. It has also previously been reported that NKG2a/c+ NK cells accumulate in vaginal mucosa during acute SIVmac infection, and that this occurred concomitant with an increase in HLA-E that could induce an inhibitory signal to the NKG2a/c+ NK cells[77]. Alternatively, it is not excluded that NK cells directed to the gut contribute to tissue damage in the intestine[78]. It has indeed been demonstrated in the macaque that microbial translocation increased the recruitment of cytotoxic NK cells in the liver[78]. This increase in cytotoxic NK cells resulted in an accelerated destruction of this organ. Recently NKp44+ NK cells have been implicated in autoimmune diseases, such as inflammatory bowel disease or Crohn Disease[79], however whether they participate in pathologic or protective processes of chronic inflammation in vivo remains controversial. HLA-DP molecules have recently been shown to directly bind NKp44[33]. HLA-DP is constitutively expressed on antigen-presenting cells, including B cells. HLA-DP molecules have been shown to be upregulated on non-hematopoietic tissues in response to inflammation[80]. Thus, it might be relevant to investigate the impact of NKP44+ NK cells on gut homeostasis in a context of gut inflammation such as HIV infection. The potential contribution on tissue damage and homeostasis by NK cells during chronic HIV/SIVmac infections will need to be addressed in future studies.

Given the remaining necessity in the use of NHP in biomedical research, as shown by the recent SARS-Cov2 outbreak, these data are highly relevant for establishing the validity and utility of such models for studying the role of NK cells in human diseases. More and more studies raise the question on the utility of NK cells in anti-tumor and anti-viral immunotherapies. Our data on the NK cell tissue distribution and functional profiles in the NHP contribute to the understanding of their role in lymphoid tissues during HIV infection as well as to efforts in the development of vaccines and therapies against human diseases.

Acknowledgements

We are grateful for the excellent help from the veterinarians and staff at the IDMIT Center (Benoit Delache, Jean-Marie Helies, Raphaël Ho Tsong Fang and Julie Morin). We thank M. Mietsch and M. Daskalaki for comprehensive veterinary support, and S. Heine, J. Hampe and N. Leuchte for excellent technical assistance. NH was supported by the VRI Labex, the Fondation Beytout and Institut Pasteur. PR was recipient of a PhD fellowship from the University Paris Diderot, Sorbonne Paris Cité and also supported by the NIH (R01AI143457). We would like to acknowledge

grant support from ANRS, the NIH (R01AI143457), the VRI, the Fondation J. Beytout and the Fondation Les Ailes to MMT. We gratefully acknowledge the support to IDMIT from the French government: Investments for the Future program for infrastructures (PIA) through the ANR-11-INBS-0008 grant as well as from the PIA grant ANR-10-EQPX-02-01 to the FlowCyTech facility at IDMIT.

Author contributions

NH and MMT designed the study; NH designed the experiments; NH, PR, CP and BJ performed experiments; CSH and ASB provided samples; NH performed the statistical analyses; NH, PR, CP, JLP, ASB, BJ and MMT analyzed the data; VC, RLG and BJ coordinated the animal studies; MMT obtained the funding; NH and MMT wrote the manuscript and all co-authors reviewed it.

References

1. Strauss-Albee, D. M. *et al.* Human NK cell repertoire diversity reflects immune experience and correlates with viral susceptibility. *Sci. Transl. Med.* **7**, 297ra115 (2015).
2. Freud, A. G., Mundy-Bosse, B. L., Yu, J. & Caligiuri, M. A. The broad spectrum of human natural killer cell diversity. *Immunity* **47**, 820–833 (2017).
3. Horowitz, A. *et al.* Genetic and environmental determinants of human NK cell diversity revealed by mass cytometry. *Sci. Transl. Med.* **5**, 208ra145 (2013).
4. Palgen, J.-L. *et al.* NK cell immune responses differ after prime and boost vaccination. *J. Leukoc. Biol.* **105**, 1055–1073 (2019).
5. Dogra, P. *et al.* Tissue Determinants of Human NK Cell Development, Function, and Residence. *Cell* **180**, 749-763.e13 (2020).
6. Carrega, P. & Ferlazzo, G. Natural killer cell distribution and trafficking in human tissues. *Front. Immunol.* **3**, (2012).
7. Gaynor, L. M. & Colucci, F. Uterine Natural Killer Cells: Functional Distinctions and Influence on Pregnancy in Humans and Mice. *Front. Immunol.* **8**, (2017).
8. Melsen, J. E. *et al.* Human Bone Marrow-Resident Natural Killer Cells Have a Unique Transcriptional Profile and Resemble Resident Memory CD8+ T Cells. *Front. Immunol.* **9**, (2018).
9. Hudspeth, K. *et al.* Human liver-resident CD56(bright)/CD16(neg) NK cells are retained within hepatic sinusoids via the engagement of CCR5 and CXCR6 pathways. *J. Autoimmun.* **66**, 40–50 (2016).
10. Karlsson-Parra, A. Chapter Twenty-Seven - Natural killer cells in the spleen and lymph node. in *Natural Killer Cells* (eds. Lotze, M. T. & Thomson, A. W.) 359–372 (Academic Press, 2010). doi:10.1016/B978-0-12-370454-2.00027-2.
11. Freud, A. G. *et al.* A human CD34(+) subset resides in lymph nodes and differentiates into CD56bright natural killer cells. *Immunity* **22**, 295–304 (2005).
12. Beuneu, H. *et al.* Dynamic behavior of NK cells during activation in lymph nodes. *Blood* **114**, 3227–3234 (2009).

13. Cichocki, F., Grzywacz, B. & Miller, J. S. Human NK Cell Development: One Road or Many? *Front. Immunol.* **10**, (2019).
14. Wit, E. de *et al.* Prophylactic and therapeutic remdesivir (GS-5734) treatment in the rhesus macaque model of MERS-CoV infection. *Proc. Natl. Acad. Sci.* **117**, 6771–6776 (2020).
15. Rockx, B. *et al.* Comparative pathogenesis of COVID-19, MERS, and SARS in a nonhuman primate model. *Science* **368**, 1012–1015 (2020).
16. Nalca, A., Totura, A., Livingston, V., Frick, O. & Dyer, D. African green monkey model of Middle East respiratory syndrome coronavirus (MERS-CoV) infection. *Int. J. Infect. Dis.* **79**, 99–100 (2019).
17. Smits, S. L. *et al.* Distinct severe acute respiratory syndrome coronavirus-induced acute lung injury pathways in two different nonhuman primate species. *J. Virol.* **85**, 4234–4245 (2011).
18. Bossart, K. N. *et al.* A Hendra virus G glycoprotein subunit vaccine protects African green monkeys from Nipah virus challenge. *Sci. Transl. Med.* **4**, 146ra107 (2012).
19. Webster, R. L. & Johnson, R. P. Delineation of multiple subpopulations of natural killer cells in rhesus macaques. *Immunology* **115**, 206–214 (2005).
20. Mavilio, D. *et al.* Identification of NKG2A and NKp80 as specific natural killer cell markers in rhesus and pigtailed monkeys. *Blood* **106**, 1718–1725 (2005).
21. Pereira, L. E., Johnson, R. P. & Ansari, A. A. Sooty mangabeys and rhesus macaques exhibit significant divergent natural killer cell responses during both acute and chronic phases of SIV infection. *Cell. Immunol.* **254**, 10–19 (2008).
22. Reeves, R. K. *et al.* CD16- natural killer cells: enrichment in mucosal and secondary lymphoid tissues and altered function during chronic SIV infection. *Blood* **115**, 4439–4446 (2010).
23. Jacquelin, B. *et al.* Innate immune responses and rapid control of inflammation in African green monkeys treated or not with interferon-alpha during primary SIVagm infection. *PLoS Pathog.* **10**, e1004241 (2014).
24. Carville, A., Evans, T. I. & Reeves, R. K. Characterization of Circulating Natural Killer Cells in Neotropical Primates. *PLoS ONE* **8**, (2013).
25. Béziat, V., Descours, B., Parizot, C., Debré, P. & Vieillard, V. NK Cell Terminal Differentiation: Correlated Stepwise Decrease of NKG2A and Acquisition of KIRs. *PLoS ONE* **5**, (2010).
26. Björkström, N. K. *et al.* Expression patterns of NKG2A, KIR, and CD57 define a process of CD56dim NK-cell differentiation uncoupled from NK-cell education. *Blood* **116**, 3853–3864 (2010).
27. Barrow, A. D., Martin, C. J. & Colonna, M. The Natural Cytotoxicity Receptors in Health and Disease. *Front. Immunol.* **10**, (2019).
28. Marcus, A. *et al.* Recognition of tumors by the innate immune system and natural killer cells. *Adv. Immunol.* **122**, 91–128 (2014).
29. Chretien, A.-S. *et al.* NKp46 expression on NK cells as a prognostic and predictive biomarker for response to allo-SCT in patients with AML. *Oncoimmunology* **6**, e1307491 (2017).

30. Hoorweg, K. *et al.* Functional Differences between Human NKp44− and NKp44+ RORC+ Innate Lymphoid Cells. *Front. Immunol.* **3**, (2012).
31. Parodi, M. *et al.* NKp44-NKp44 Ligand Interactions in the Regulation of Natural Killer Cells and Other Innate Lymphoid Cells in Humans. *Front. Immunol.* **10**, (2019).
32. Sagebiel, A. F. *et al.* Tissue-resident Eomes + NK cells are the major innate lymphoid cell population in human infant intestine. *Nat. Commun.* **10**, 975 (2019).
33. Niehrs, A. *et al.* A subset of HLA-DP molecules serve as ligands for the natural cytotoxicity receptor NKp44. *Nat. Immunol.* **20**, 1129–1137 (2019).
34. Ferlazzo, G. *et al.* Human Dendritic Cells Activate Resting Natural Killer (NK) Cells and Are Recognized via the NKp30 Receptor by Activated NK Cells. *J. Exp. Med.* **195**, 343–351 (2002).
35. Elssen, C. H. M. J. V., Oth, T., Germeraad, W. T. V., Bos, G. M. J. & Vanderlocht, J. Natural Killer Cells: The Secret Weapon in Dendritic Cell Vaccination Strategies. *Clin. Cancer Res.* **20**, 1095–1103 (2014).
36. Walzer, T., Dalod, M., Robbins, S. H., Zitvogel, L. & Vivier, E. Natural-killer cells and dendritic cells: "l'union fait la force". *Blood* **106**, 2252–2258 (2005).
37. Svardal, H. *et al.* Ancient hybridization and strong adaptation to viruses across African vervet monkey populations. *Nat. Genet.* **49**, 1705–1713 (2017).
38. Müller, M. C. *et al.* Simian immunodeficiency viruses from central and western Africa: evidence for a new species-specific lentivirus in tantalus monkeys. *J. Virol.* **67**, 1227–1235 (1993).
39. Raehtz, K., Pandrea, I. & Apetrei, C. The Well-Tempered SIV Infection: Pathogenesis of SIV Infection in Natural Hosts in the Wild, with Emphasis on Virus Transmission and Early Events Post-Infection that May Contribute to Protection from Disease Progression. *Infect. Genet. Evol. J. Mol. Epidemiol. Evol. Genet. Infect. Dis.* **46**, 308–323 (2016).
40. Sodora, D. L. *et al.* Toward an AIDS vaccine: lessons from natural simian immunodeficiency virus infections of African nonhuman primate hosts. *Nat. Med.* **15**, 861–865 (2009).
41. Huot, N. *et al.* Natural killer cells migrate into and control simian immunodeficiency virus replication in lymph node follicles in African green monkeys. *Nat. Med.* **23**, 1277–1286 (2017).
42. Pandrea, I. V. *et al.* Acute Loss of Intestinal CD4+ T Cells Is Not Predictive of Simian Immunodeficiency Virus Virulence. *J. Immunol.* **179**, 3035–3046 (2007).
43. Bernardini, G., Antonangeli, F., Bonanni, V. & Santoni, A. Dysregulation of Chemokine/Chemokine Receptor Axes and NK Cell Tissue Localization during Diseases. *Front. Immunol.* **7**, (2016).
44. Hardtke, S., Ohl, L. & Förster, R. Balanced expression of CXCR5 and CCR7 on follicular T helper cells determines their transient positioning to lymph node follicles and is essential for efficient B-cell help. *Blood* **106**, 1924–1931 (2005).
45. Junt, T. *et al.* CXCR5-dependent seeding of follicular niches by B and Th cells augments antiviral B cell responses. *J. Immunol. Baltim. Md 1950* **175**, 7109–7116 (2005).

46. Chevalier, N. *et al.* CXCR5 Expressing Human Central Memory CD4 T Cells and Their Relevance for Humoral Immune Responses. *J. Immunol.* (2011) doi:10.4049/jimmunol.1002828.
47. Lam, V. C. & Lanier, L. L. NK cells in host responses to viral infections. *Curr. Opin. Immunol.* **44**, 43–51 (2017).
48. Cook, K. D., Waggoner, S. N. & Whitmire, J. K. NK Cells and Their Ability to Modulate T Cells during Virus Infections. *Crit. Rev. Immunol.* **34**, 359–388 (2014).
49. Spaggiari, G. M. *et al.* IFN-gamma production in human NK cells through the engagement of CD8 by soluble or surface HLA class I molecules. *Eur. J. Immunol.* **33**, 3049–3059 (2003).
50. Massi, D. *et al.* The density and spatial tissue distribution of CD8+ and CD163+ immune cells predict response and outcome in melanoma patients receiving MAPK inhibitors. *J. Immunother. Cancer* **7**, 308 (2019).
51. Spaggiari, G. M. *et al.* Soluble HLA class I induces NK cell apoptosis upon the engagement of killer-activating HLA class I receptors through FasL-Fas interaction. *Blood* **100**, 4098–4107 (2002).
52. Bauer, S. *et al.* Activation of NK cells and T cells by NKG2D, a receptor for stress-inducible MICA. *Science* **285**, 727–729 (1999).
53. Chuang, S. S., Kumaresan, P. R. & Mathew, P. A. 2B4 (CD244)-mediated activation of cytotoxicity and IFN-gamma release in human NK cells involves distinct pathways. *J. Immunol. Baltim. Md 1950* **167**, 6210–6216 (2001).
54. Moretta, A. *et al.* Activating receptors and coreceptors involved in human natural killer cell-mediated cytolysis. *Annu. Rev. Immunol.* **19**, 197–223 (2001).
55. Moser, B. CXCR5, the Defining Marker for Follicular B Helper T (TFH) Cells. *Front. Immunol.* **6**, (2015).
56. León, B. *et al.* Regulation of TH2 development by CXCR5+ dendritic cells and lymphotoxin-expressing B cells. *Nat. Immunol.* **13**, 681–690 (2012).
57. Carlsen, H. S. B cell attracting chemokine 1 (CXCL13) and its receptor CXCR5 are expressed in normal and aberrant gut associated lymphoid tissue. *Gut* **51**, 364–371 (2002).
58. Velaga, S. *et al.* Chemokine receptor CXCR5 supports solitary intestinal lymphoid tissue formation, B cell homing, and induction of intestinal IgA responses. *J. Immunol. Baltim. Md 1950* **182**, 2610–2619 (2009).
59. Buettner, M. & Lochner, M. Development and Function of Secondary and Tertiary Lymphoid Organs in the Small Intestine and the Colon. *Front. Immunol.* **7**, (2016).
60. Eberl, G. & Lochner, M. The development of intestinal lymphoid tissues at the interface of self and microbiota. *Mucosal Immunol.* **2**, 478–485 (2009).
61. Mackay, L. K. *et al.* Cutting Edge: CD69 Interference with Sphingosine-1-Phosphate Receptor Function Regulates Peripheral T Cell Retention. *J. Immunol.* **194**, 2059–2063 (2015).

62. Bankovich, A. J., Shiow, L. R. & Cyster, J. G. CD69 Suppresses Sphingosine 1-Phosophate Receptor-1 (S1P1) Function through Interaction with Membrane Helix 4. *J. Biol. Chem.* **285**, 22328–22337 (2010).
63. Stelma, F. *et al.* Human intrahepatic CD69 + CD8+ T cells have a tissue resident memory T cell phenotype with reduced cytolytic capacity. *Sci. Rep.* **7**, (2017).
64. Walsh, D. A. *et al.* The Functional Requirement for CD69 in Establishment of Resident Memory CD8 $^{+}$ T Cells Varies with Tissue Location. *J. Immunol.* **203**, 946–955 (2019).
65. Luteijn, R. *et al.* Early viral replication in lymph nodes provides HIV with a means by which to escape NK-cell-mediated control. *Eur. J. Immunol.* **41**, 2729–2740 (2011).
66. Li, H. & Reeves, R. K. Functional perturbation of classical natural killer and innate lymphoid cells in the oral mucosa during SIV infection. *Front. Immunol.* **3**, 417 (2012).
67. Schafer, J. L., Li, H., Evans, T. I., Estes, J. D. & Reeves, R. K. Accumulation of Cytotoxic CD16+ NK Cells in Simian Immunodeficiency Virus-Infected Lymph Nodes Associated with In Situ Differentiation and Functional Anergy. *J. Virol.* **89**, 6887–6894 (2015).
68. Sips, M. *et al.* Altered distribution of mucosal NK cells during HIV infection. *Mucosal Immunol.* **5**, 30–40 (2012).
69. Takahashi, Y. *et al.* In Vivo Administration of a JAK3 Inhibitor during Acute SIV Infection Leads to Significant Increases in Viral Load during Chronic Infection. *PLoS Pathog.* **10**, (2014).
70. Li, H. *et al.* Hypercytotoxicity and Rapid Loss of NKp44+ Innate Lymphoid Cells during Acute SIV Infection. *PLOS Pathog.* **10**, e1004551 (2014).
71. Frias, M. *et al.* Persistence of Pathological Distribution of NK Cells in HIV-Infected Patients with Prolonged Use of HAART and a Sustained Immune Response. *PLoS ONE* **10**, (2015).
72. Estes, J. D. Pathobiology of HIV/SIV-Associated Changes in Secondary Lymphoid Tissues. *Immunol. Rev.* **254**, 65–77 (2013).
73. Wang, W. *et al.* The Secretion of IL-22 from Mucosal NKp44+ NK Cells Is Associated with Microbial Translocation and Virus Infection in SIV/SHIV-Infected Chinese Macaques. *Journal of Immunology Research* vol. 2014 e387950 https://www.hindawi.com/journals/jir/2014/387950/ (2014).
74. Reeves, R. K., Evans, T. I., Gillis, J. & Johnson, R. P. Simian immunodeficiency virus infection induces expansion of alpha4beta7+ and cytotoxic CD56+ NK cells. *J. Virol.* **84**, 8959–8963 (2010).
75. Ploquin, M. J. *et al.* Systemic DPP4 activity is reduced during primary HIV-1 infection and is associated with intestinal RORC + CD4+ cell levels: a surrogate marker candidate of HIV-induced intestinal damage. *J. Int. AIDS Soc.* **21**, (2018).
76. Ploquin, M. J. *et al.* Elevated Basal Pre-infection CXCL10 in Plasma and in the Small Intestine after Infection Are Associated with More Rapid HIV/SIV Disease Onset. *PLoS Pathog.* **12**, (2016).
77. Shang, L. *et al.* NK Cell Responses to SIV Vaginal Exposure in Naïve and Vaccinated Rhesus Macaques. *J. Immunol. Baltim. Md 1950* **193**, 277–284 (2014).

78. Evans, T. I. *et al.* SIV-induced Translocation of Bacterial Products in the Liver Mobilizes Myeloid Dendritic and Natural Killer Cells Associated With Liver Damage. *J. Infect. Dis.* **213**, 361–369 (2016).
79. Poggi, A. *et al.* Human Gut-Associated Natural Killer Cells in Health and Disease. *Front. Immunol.* **10**, (2019).
80. Stevanović, S. *et al.* HLA class II upregulation during viral infection leads to HLA-DP–directed graft-versus-host disease after CD4+ donor lymphocyte infusion. *Blood* **122**, 1963–1973 (2013).
81. Jacquelin, B. *et al.* Innate Immune Responses and Rapid Control of Inflammation in African Green Monkeys Treated or Not with Interferon-Alpha during Primary SIVagm Infection. *PLOS Pathog.* **10**, e1004241 (2014).
82. Daskalaki, M. *et al*, Long-term efficient control of SIV infection in macaques is associated with an intact intestinal barrier. *J. Med. Primatol*. **46**, 144-148. (2017)

MATERIAL AND METHODS

Monkeys and SIV infections

Samples from a total of thirty-six non-human primates were used in this study distributed across four different species. The numbers of animals per species was as follows: thirteen African green monkeys (Caribbean *Chlorocebus aethiops*, AGM), twelve cynomolgus macaques (*Macaca fascicularis*, CM), seven rhesus macaques (*Macaca mulatta*, RM) and four baboons (*Papio anubis*). Seven CM and seven AGM were infected with SIVmac251 and SIVagm.sab92018, respectively, as previously described[41,81]. The viremia levels are shown in Figure S2. All infected monkeys were highly viremic. All the animals were free of simian retrovirus type D and simian T-lymphotropic virus type 1.

The AGM, CM and baboons were housed at the IDMIT Center (Fontenay-aux-Roses, France) and the RM at at the German Primate Center (DPZ). All experimental procedures were conducted in strict accordance with the international European guidelines 2010/63/UE on the protection of animals used for experimentation and other scientific purposes and with the national laws (French decree 2013-118). The IDMIT center complies with the Standards for Human Care and Use of the Office for Laboratory Animal Welfare (OLAW, USA) under OLAW Assurance number A5826-86. Monitoring of the monkeys at IDMIT was under the supervision of the veterinarians in charge of the animal facilities. Animal experimental protocols were approved by the Ethical Committee of Animal Experimentation (CETEA-DSV, IDF, France) (Notification 12-098 and A17-044). The DPZ is allowed to breed and house nonhuman primates under license number 392001/7 approved by the local veterinary office and conforming with § 11 of the German Animal Welfare act. The collection of blood samples at the DPZ was granted by the Lower Saxony State Office for Consumer Protection and Food Safety with the project licence 33.9-42502-05-10A041. In compliance with the principles of the 3Rs (replacing, reducing and refining), all samples used here were from animals that were shared with other studies. Indeed, the animals have been purchased or infected for other programs. For instance, we used tissues that were collected from animals that have been sacrificed for other studies and some of these have already been published[4,41,82]. Monkeys were sedated with Ketamine Chlorhydrate (Rhone-Mérieux, Lyons, France) before handling. Sample collection was performed in random order, according to the tripartite harmonized International Council for

Harmonization of Technical Requirements for Pharmaceuticals for Human Use (ICH) Guideline on Methodology (previously coded Q2B). The investigators were not blinded while the animal handlers were blinded to group allocation.

Tissue collections and processing

Whole venous blood was collected in ethylenediaminetetraacetic acid (EDTA) tubes. Peripheral blood mononuclear cells (PBMCs) were isolated by Ficoll density-gradient centrifugation. Biopsies of peripheral LNs (pLN) were performed by excision. Other tissues were collected at autopsy. After careful removal of adhering connective and fat tissues, pLN and spleen cells were dissociated using the gentlemacS™ Dissociator technology (Miltenyi Biotec, Germany). The cell suspension was subsequently filtered through 100- and 40-µm cell strainers, and cells were washed with cold phosphate-buffered saline (PBS). Cells were either immediately stained for flow cytometry or cryopreserved in 90% foetal bovine serum (FBS) and 10% dimethyl sulphoxide (DMSO) and stored in liquid nitrogen vapour.

Viral RNA quantification

The viral RNA copy numbers in plasma of the animals were quantified as previously described [23,41].

Polychromatic flow cytometry

For flow cytometric analysis, cells were stained in U-bottom tubes in the dark. Cells were analyzed using 11-parameter flow cytometry. For surface staining, cells were incubated in PBS with the appropriate monoclonal antibodies and Zombie Aqua™ for 30 min at 4 °C, washed and fixed with 4% PFA. The following monoclonal antibodies were used for surface and intra cellular staining (clone, suppliers): CD3 (SP34-2, *BD Biosciences*), CD8 (BW135/80; Miltenyi Biotec), CD20 (2h7; ebioscience), CD16 (3G8,Coulter); NKG2A(Z199, Coulter), NKP30 (AF29-4D12, Miltenyi Biotec), CD45 (D058-1283, *BD Biosciences*), CD69 (FN50, *BD Biosciences*), NKP46 (BAB281,Coulter), CXCR5 (MU5UBEE,Thermo), CD279(PD-1) (EH12.2H7, Biolegend), CXCR3 (1C6/CXCR3, *BD Biosciences*), IFN-γ (4S.B3,*BD Biosciences*), Granzyme B (GB11, *BD Biosciences*), TNF-A(MAB11, *BD Biosciences*), NKP44 (REA1163, Miltenyi Biotec), CD14 (TÜK4, Miltenyi Biotec). References listing the cross reactivity of each antibody is listed in Supplemental Table 1. The anti-NKG2A antibody used recognizes both NKG2A and NKG2C on simian cells. Due to the lack of information on the KIR polymorphism in African NHP and the rare anti-KIR antibodies specific for NHP, the KIR expression has not been analysed. Flow cytometry acquisitions were performed on a LSRII (BD Biosciences). The data were further analyzed using FlowJo 10.4.2 software (FlowJo, LLC, Ashland, OR, USA). Intracellular staining was performed using BD Cytofix/Cytoperm™. *UMAP* was performed with Flojow, using 1000 iterations and a perplexity of 0,25.

Statistics

The GraphPad Prism 7 (GraphPad Software, San Diego, CA) was used to analyze data and to perform statistical analyses. Statistical significance of differences was assessed using non-parametric Mann-Whitney *U* tests (figure 1A, Figure 3B and C), or Wilcoxon matched-pairs signed rank test, for paired samples (Figure 1E, F and H). All group comparisons were carried out by means of a one-way analysis of variance (ANOVA) and followed by a Tukey's multiple-comparison test. The latter is a post-hoc test based on the studentized range distribution (Figure 2E and F; Figure 4E and F; and Figure 5A, B, E and F). Values of $p < 0.05$ were considered significant. NK cell populations were analyzed by uniform manifold approximation and projection (UMAP) method provided by the Flowjo plugin Version 3.1. Heatmap of the Log2(FC) of the marker expression compared to the median across all samples. Color-coded with blue for lower expression and red for higher expression. Dendrograms present clustering of samples (columns) and markers (row) which is based on hierarchical clustering with Euclidean distance metric and average linkage.

Data availability

The authors declare that all other data supporting the findings of this study are available within the article and its Supplementary Information files, or are available from the authors upon request.

LEGENDS

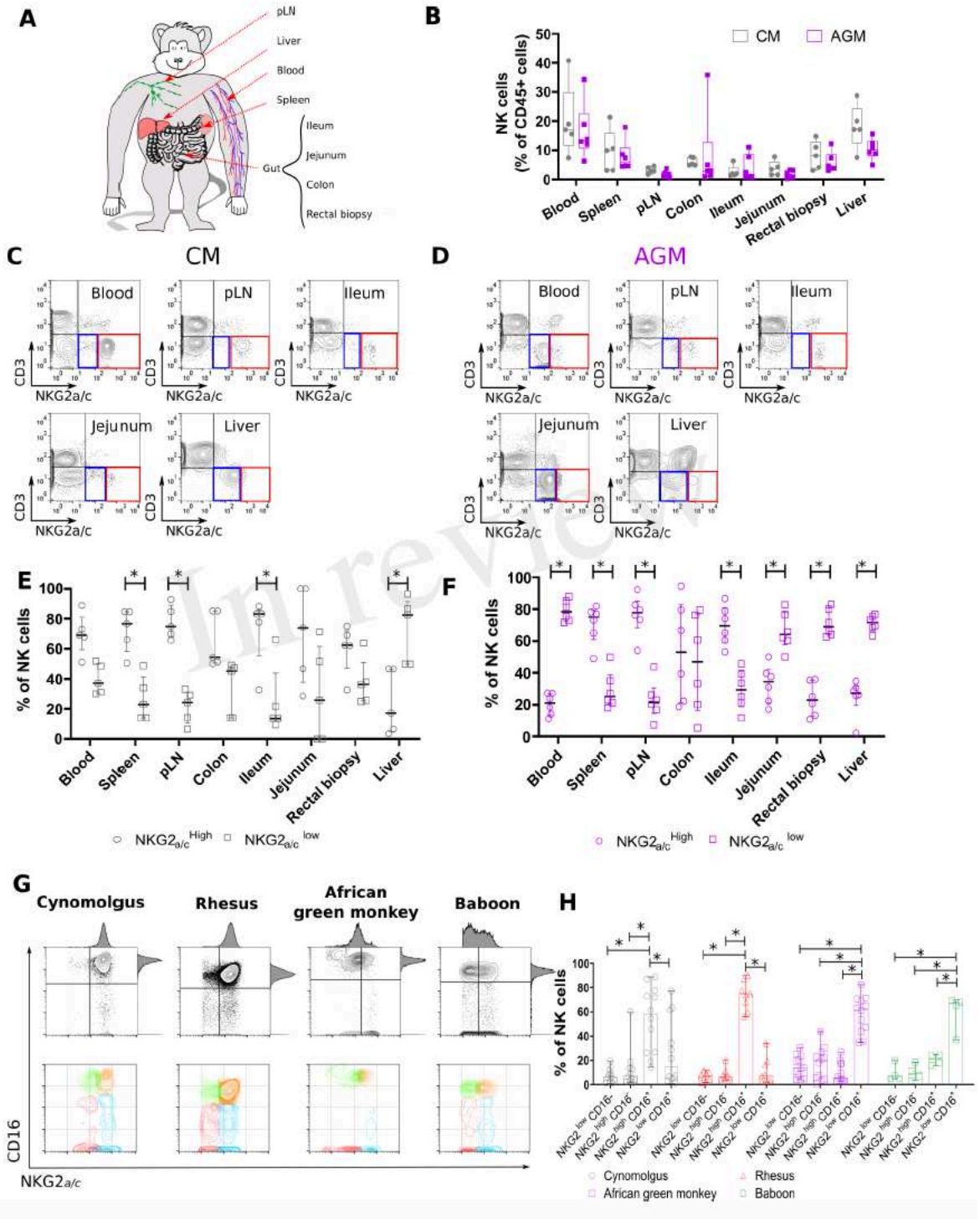


Figure 1. Non-human primate NK cell subset distributions in tissues. (A) Scheme of the NHP tissues obtained and experimental workflow presented in this study. (B) NK cell distribution in distinct tissue compartments. The frequencies are shown in boxplots and correspond to compiled data from 5 SIV negative CM (grey) and 6 SIV negative AGM (purple). (C and D) Representative flow cytometry plots for NKG2a/c^{LOW} (blue square) and NKG2a/c^{HIGH} (red square) NK cell subsets in multiple tissue sites obtained from (C) CM and

(D) AGM. (E and F) Distribution of NKG2a/c^{LOW} (empty circle) and NKG2a/c^{HIGH} (empty square) NK cell subsets in multiple tissue sites obtained from (E) 5 CM and (F) 6 AGM. (G) Representative dot plots showing blood NK cell subset distributions according to NKG2a/c and CD16 in four NHP species as indicated. (H) Frequency of blood NK cell subsets in four SIV negative NHP species. Each symbol depicts an individual animal among the 13 AGM, 12 CM, 7 RM and 4 baboons. Median and standard error bars are shown. Statistical significance of differences was assessed using non-parametric Mann-Whitney *U* tests (Figure 1B), or Wilcoxon matched-pairs signed rank test, for paired samples (Figure 1E, F and H). Asterix indicate p value < 0.05

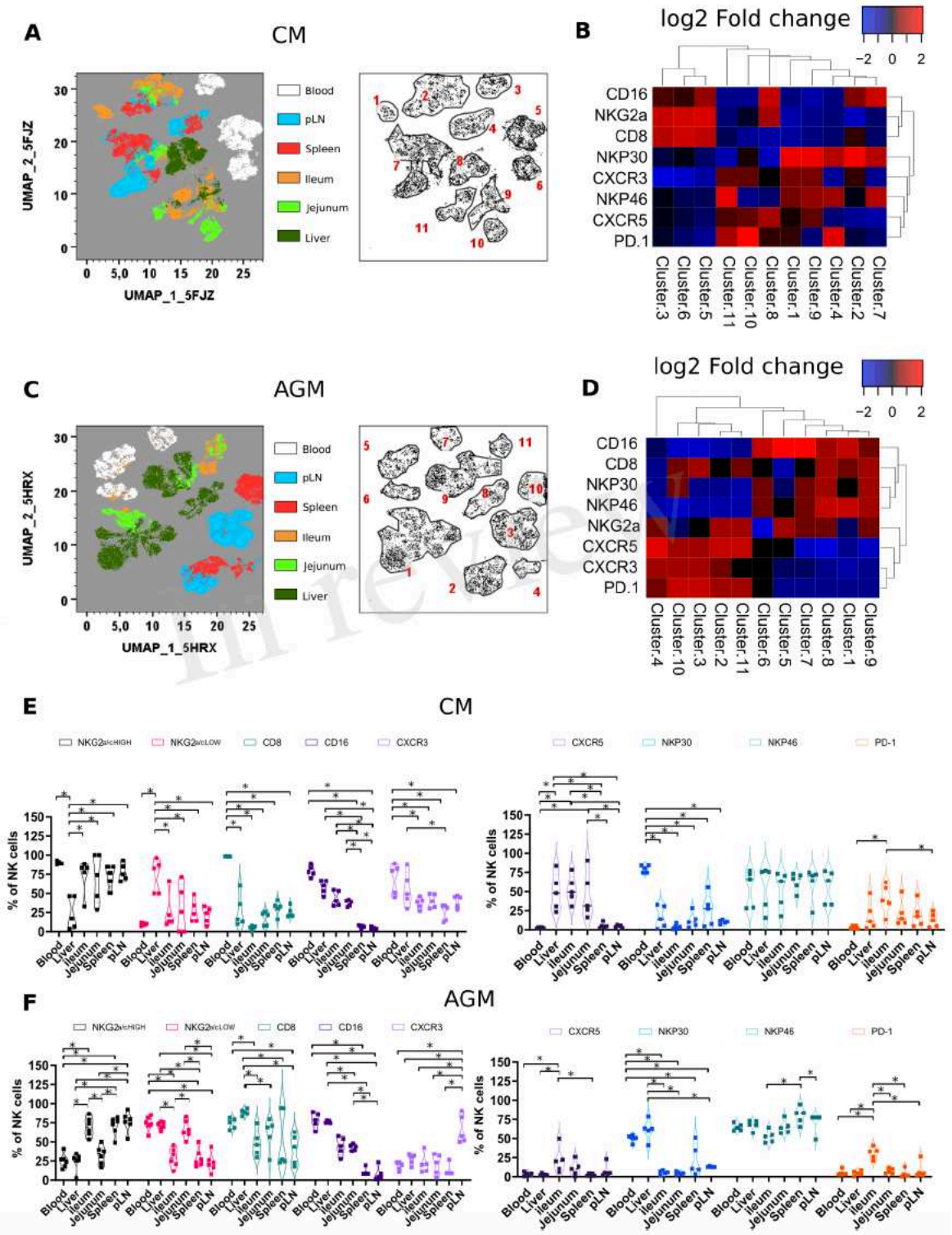


Figure 2. Tissue localization shapes the phenotype of NK cells (A) Force-directed plot showing the relationship between NK cells from distinct tissues identified by multi-dimensional analysis (data compiled from 5 healthy CM. Each node is an aggregation of phenotypically similar cells Resulting from several steps, including downsampling, merging and overall dimension reduction followed by gating (left panel), and collection of similar nodes forms 11 distinct NK cell clusters (right panel). (B) Heatmap showing the differential expression of cell surface markers used for clustering and community identification in the multi-

dimensional analysis in (A). (C) Same analyses as in (A) performed on 6 healthy AGM. (D) Heatmap showing the differential expression of cell surface markers used for clustering and community identification in the multi-dimensional analysis in (C). (E and F) Violplots showing the distribution of markers on bulk tissue NK cells from (E) healthy CM and (F) healthy AGM. Each marker is labeled with a unique color. All comparisons were carried out by means of a one-way analysis of variance (ANOVA) and followed by a Tukey's multiple-comparison test. The latter is a post-hoc test based on the studentized range distribution. Median and standard error bars are shown. Asterix indicate p value < 0.05

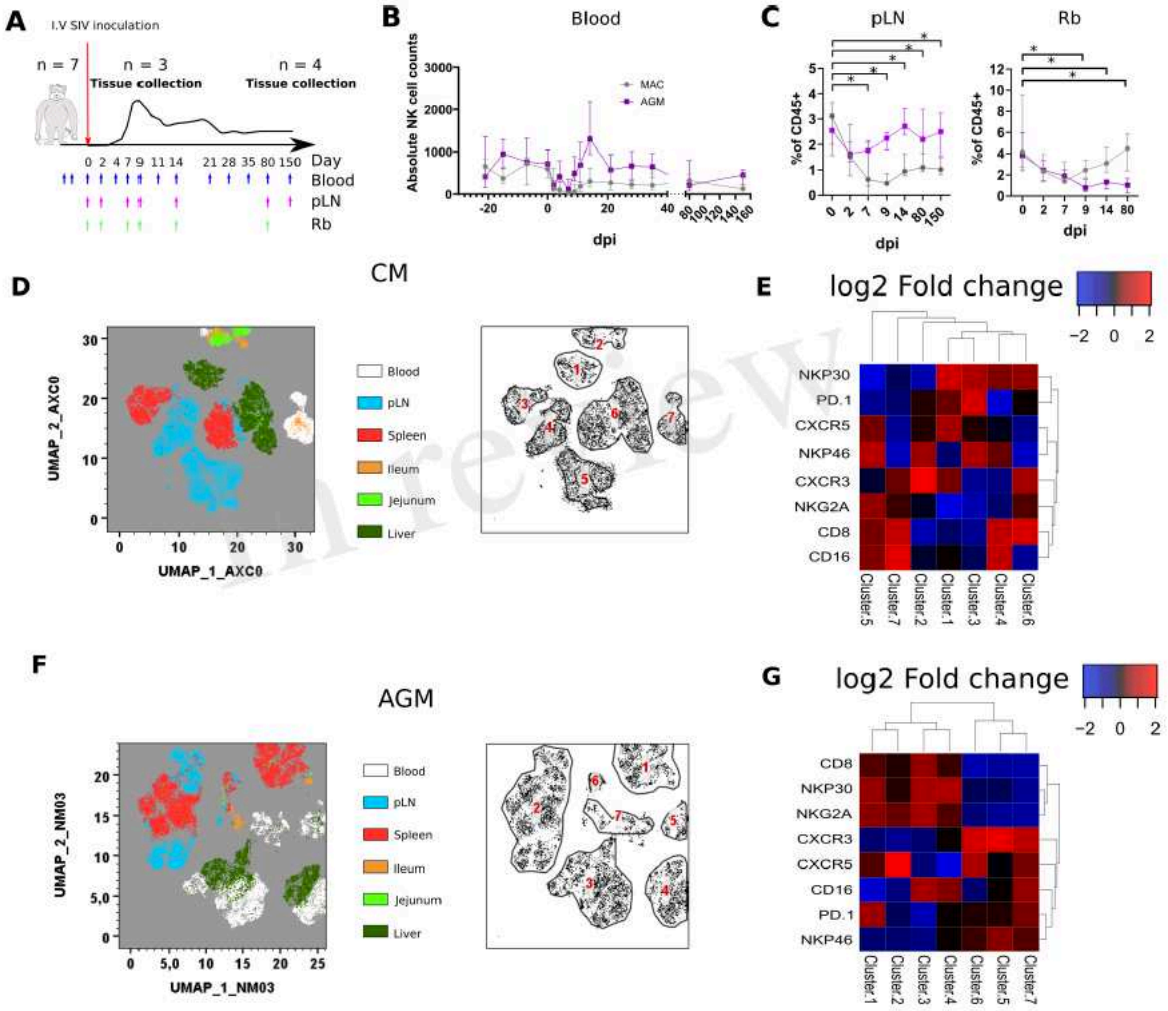


Figure 3. Rapid change in tissues NK cell phenotypes following SIV infection. (A) Schematic representation of the SIV infection schedule used in this study. Seven CM and seven AGM were intravenously injected with SIV (see method section). The blue arrows indicate blood sampling. The purple and the green arrows indicate peripheral lymph node (pLN) and rectal biopsies (Rb) samplings, respectively. Three monkeys per species were euthanized at day 9 p.i and the remaining animals were euthanized during the chronic phase (day 240 p.i). (B) Follow up of blood NK cell absolute counts before and during SIV infection in CM (grey line) and AGM (purple line). (C) Frequency of NK cells among CD45+ cells in pLN (left panel) and Rb (right panel) during

SIV infection in CM (grey line) and AGM (purple line). (D) Force-directed plot showing the relationship between NK cells from distinct tissues at day 9 p.i identified by multi-dimensional analysis (data compiled from 3 CM). Each node is an aggregation of similar cells resulting from downsampling of data (left panel), and collection of similar nodes forms 6 distinct NK cell clusters (right panel). (E) Heatmap showing the differential expression of cell surface markers used for clustering and community identification in the multi-dimensional analysis in (D). (F) Same analyses as in (A) performed on 3 AGM at day 9 p.i. (G) Heatmap showing the differential expression of cell surface markers used for clustering and community identification in the multi-dimensional analysis in (F). Median and standard error bars are shown. Asterix indicate p value < 0.05

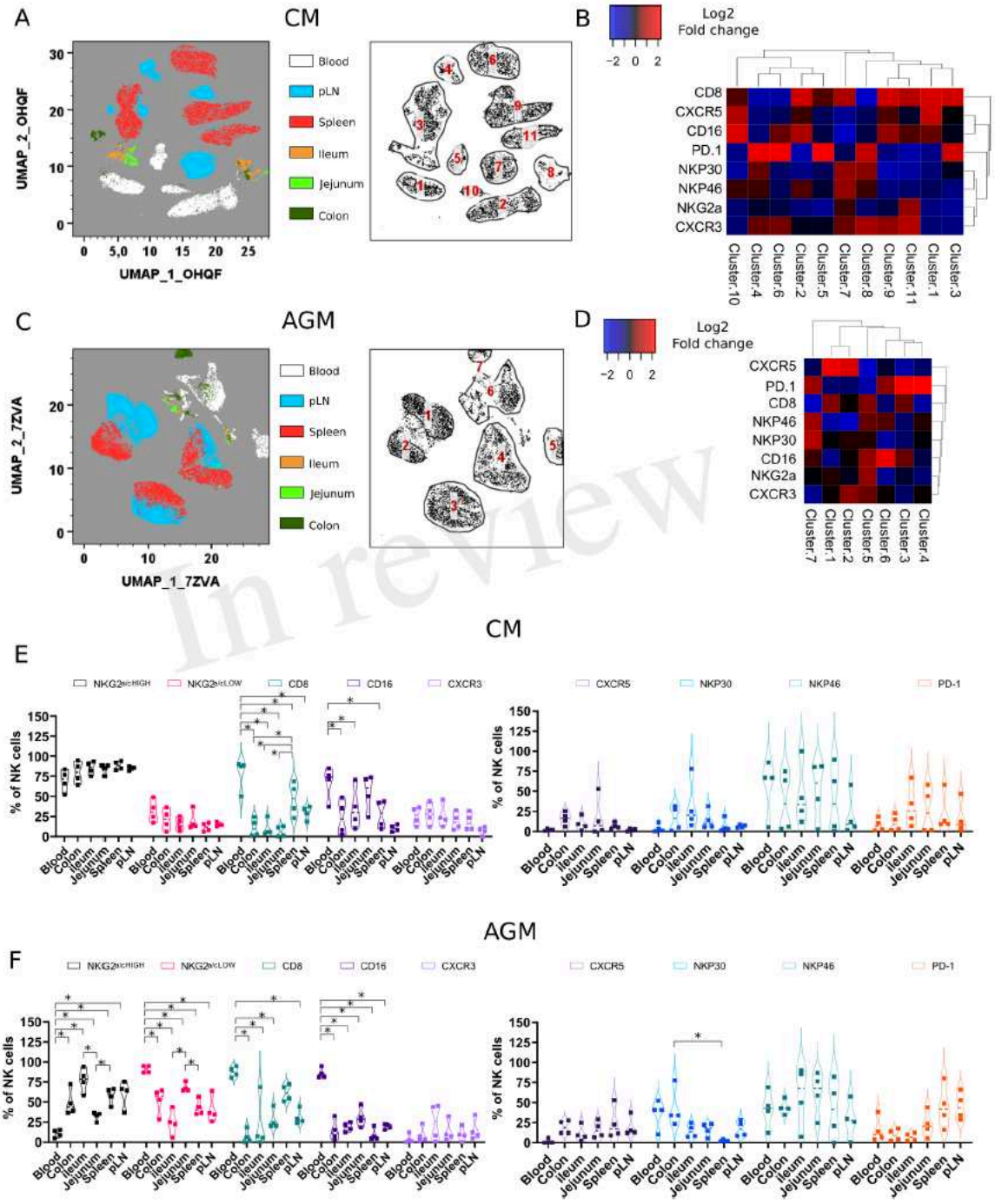


Figure 4. Phenotypic analysis of NK cells during chronic SIV infection across different tissue sites. (A) Force-directed plot showing the relationship between NK cells from distinct tissues identified by multi-dimensional analysis (data compiled from 5 chronically infected CM). Each node is an aggregation of similar cells resulting from downsampling of data (left panel), and collection of similar nodes forms 11 distinct NK cell clusters (right panel). (B) Heatmap showing the differential expression of cell surface markers used for clustering and community identification in the multi-dimensional analysis in (A). (C) Same analyses as in (A) performed on 4 chronically infected AGM. (D) Heatmap showing the differential expression of cell surface markers used for clustering and community identification in the multi-dimensional analysis in (C). (E and F)

In review

Vioplots showing the distribution of markers on bulk tissue NK cells from four chronically SIV-infected CM (E) and 4 chronically SIV-infected AGM (F). Each marker is presented with an unique color. All comparisons between NK cells were carried out by means of a one-way analysis of variance (ANOVA) and followed by a Tukey's multiple-comparison test. The latter is a post-hoc test based on the studentized range distribution. Median and standard error bars are shown. Asterix indicate p value < 0.05

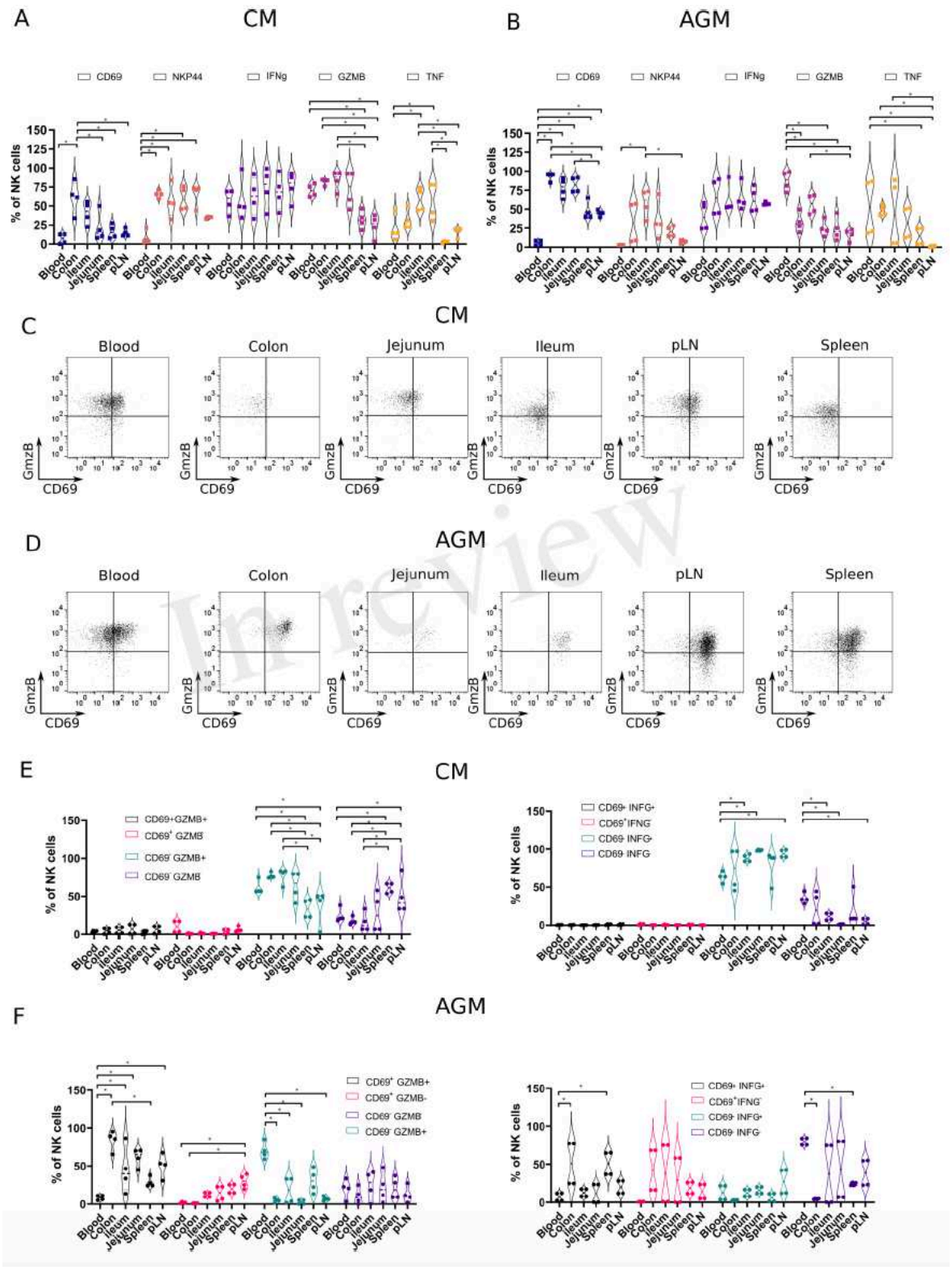
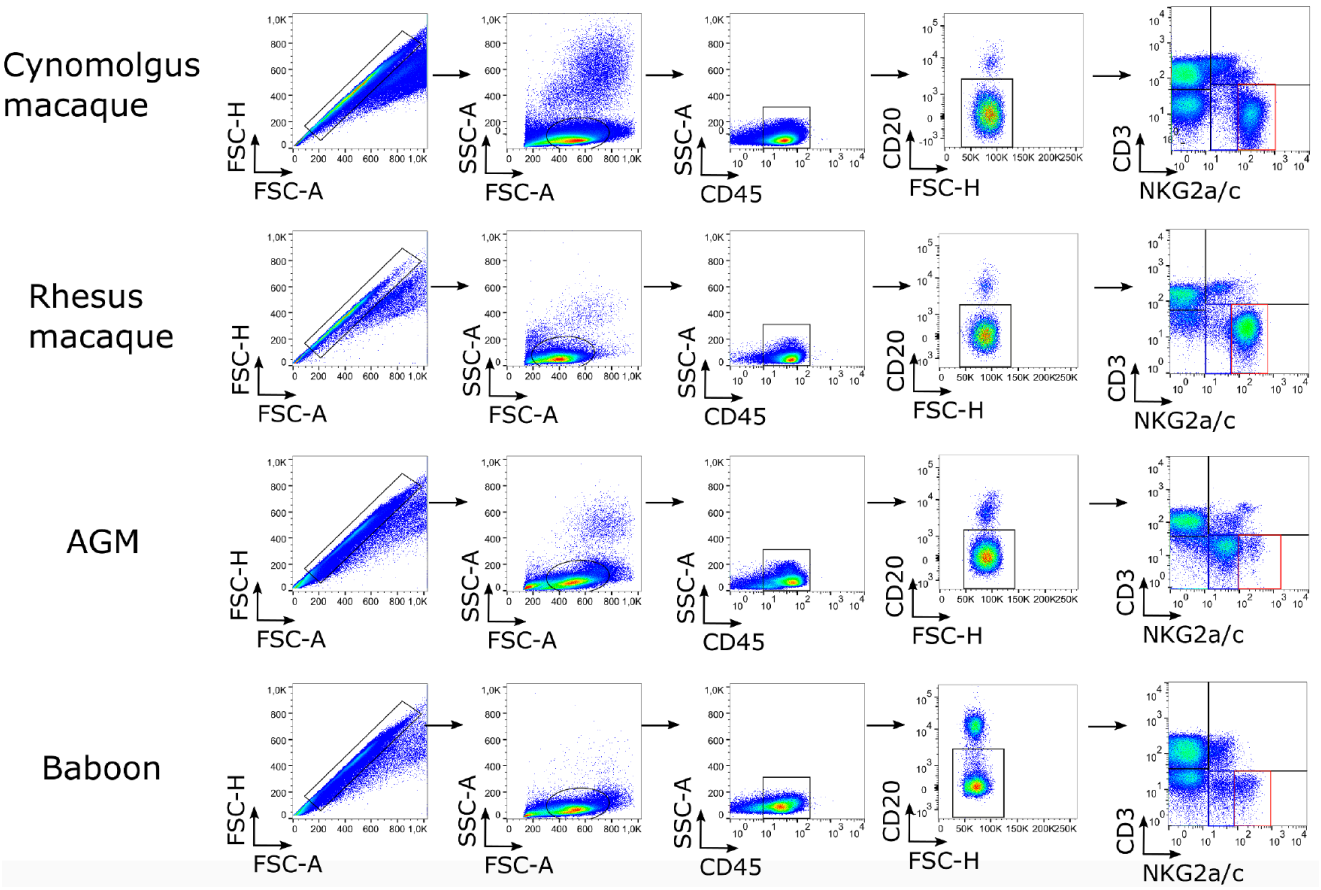
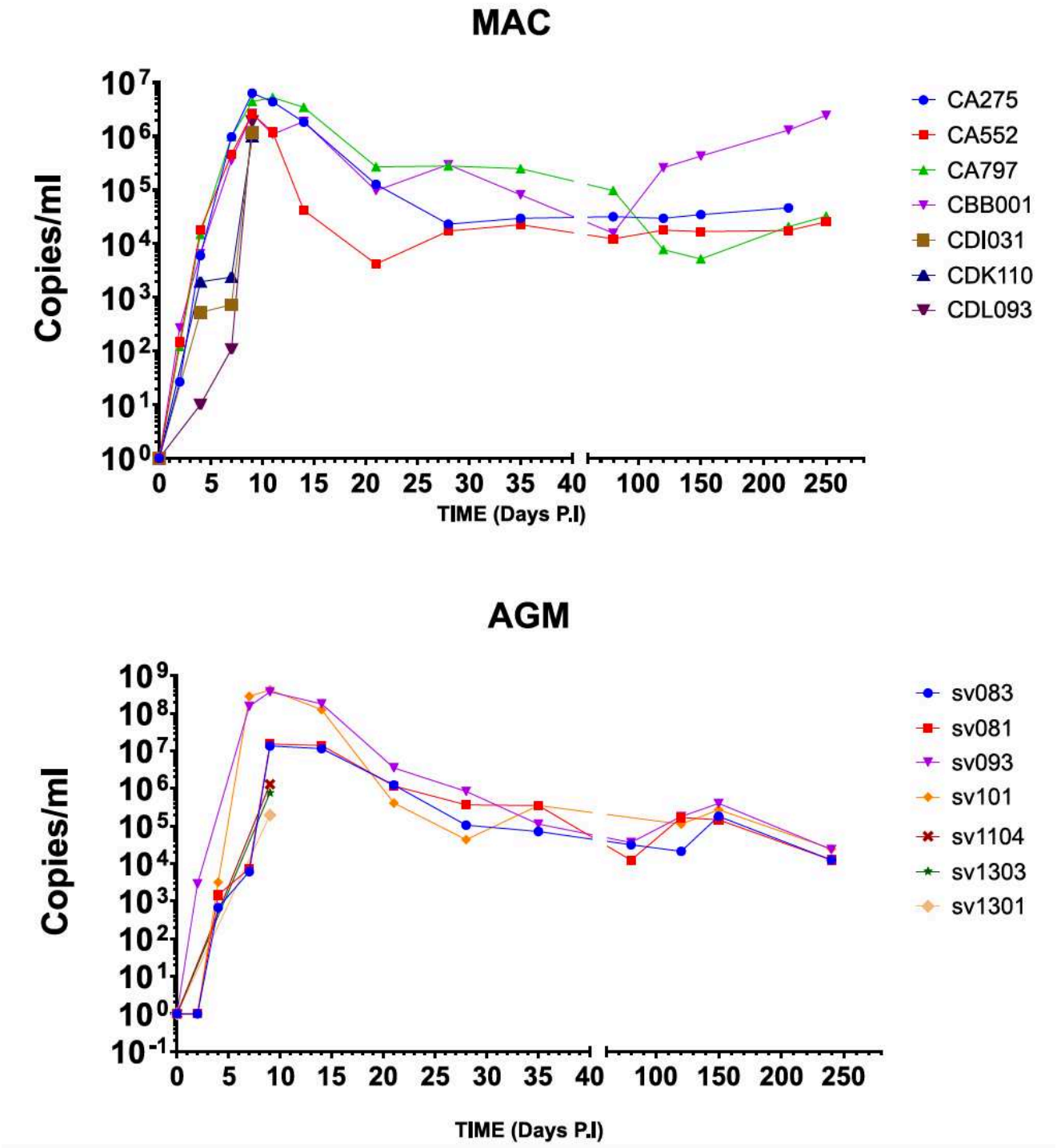


Figure 5. Functional profiles of NK cells in tissues from chronically SIV-infected non-human primates. NK cells from four SIVmac-infected CM and four SIVagm-infected AGM were analyzed**.** (A and B) Vioplots showing the distribution of markers on bulk tissue NK cells. Each marker is labeled with a unique color. All comparisons between NK cells were carried out by means of a one-way analysis of variance (ANOVA) and followed by a Tukey's multiple-comparison test. The latter is a post-hoc test based on the studentized range

distribution. (C and D) Representative dot plots showing NK cells according to CD69 surface expression and intracellular expression of GzmB in different tissues. Dot plots for a randomly chosen animal per species are shown. (E-F) Graphics showing frequencies of NK cells subsets in different tissues according to CD69 and Grzm B expression (left) or CD69 and IFN-g expression (right). All comparisons were carried out by means of a one-way analysis of variance (ANOVA) and followed by a Tukey's multiple-comparison test. The latter is a post-hoc test based on the studentized range distribution. Median and standard error bars are shown. Asterix indicate p value < 0.05.



Supplemental Figure 1: Gating strategy used to define NK cell subsets in the NHP.



Supplemental Figure 2: Viremia profiles during SIV infections. Seven CM and seven AGM were respectively infected with SIVmac251 and SIVagm.sab92018. The SIV copy numbers in the plasma over time are indicated.

5. NK cell profiles and IgA responses in mesenteric lymph nodes during SIV infections

NK cell profiles and IgA responses in mesenteric lymph nodes during SIV infections

Philippe RASCLE[1,2], Cyril PLANCHAIS[3,4], Béatrice JACQUELIN[1], Marie LAZZERINI[1], Vanessa CONTRERAS[5], Caroline PASSAES[1], Asier SAEZ-CIRION[1], Hugo MOUQUET[3,4], Nicolas HUOT[1] and Michaela MÜLLER-TRUTWIN[1,*].

[1]Institut Pasteur, Unité HIV Inflammation and Persistence, Paris, France;

[2]Université Paris Diderot, Sorbonne Paris Cité, Paris, France,

[3]Institut Pasteur, Laboratory of Humoral Immunology, Paris, France;

[4]INSERM U1222, Paris, France ;

[5]CEA, Université Paris Sud 11, INSERM U1184, Immunology of Viral Infections and Autoimmune Diseases, IDMIT, IBFJ, Fontenay-aux-Roses, France.

Keywords :

*Corresponding author :

Michaela Müller-Trutwin

Institut Pasteur

28, rue du Dr Roux

75724 Paris Cedex 15, France

mmuller@pasteur.fr (Orcid ID: 0000-0002-3854-2396)

Abstract

Lymph nodes (LN) and intestine are the major reservoirs of HIV in anti-retroviral treated people. African Green Monkeys (AGM) efficiently control SIVagm replication in lymph nodes and spleen, while in the intestine, SIVagm replicates at high levels without causing bacterial translocation nor chronic inflammation. IgA are important for the control of bacterial translocation and inflammation in the gut. In this study, we investigated the impact of NK cell-mediated viral control in BCF of mesenteric lymph nodes on IgA production and inflammation. Blood, mesenteric LN (mLN), jejunum, ileum and colon were collected from AGM and in the animal model of HIV infection (macaques) before and during acute and chronic SIV infection. Immunoglobulins were isolated by affinity chromatography. Trimeric SIVagm and SIVmac gp140-foldon Env proteins were produced. NK cells migrated into BCF of mLN during SIVagm infection. IgA+ memory B cells were increased in mLN during SIVagm infection in contrast to SIVmac infection and correlated positively with CXCR5+NK cell levels. Secretory IgA levels in the intestine (jejunum, ileum and colon) remained normal during acute and chronic SIVagm infection, while strongly decreased in chronically infected macaques. Systemic IgA correlated negatively with sCD14 levels in SIVmac infection. Our data support a major role of viral control in BCF on IgA production thereby contributing to inflammation regulation in non-pathogenic SIV infection.

Introduction

The immune system probably evolved to limit the negative effects exerted by pathogens on host homeostasis. Infections generally result in tissue damage, especially if replication of the pathogen is not controlled[1]. The tissue damage can be triggered directly by pathogens or indirectly by host responses to the infection. Disease tolerance is a defense strategy against tissue damage induced by chronic infection that sustains host homeostasis, without exerting a direct negative impact on pathogens[2]. In people living with HIV (PLWH), anti-retroviral treatment (ART) has transformed a deadly disease into a manageable chronic infection. However, a residual chronic inflammation persists in most PLWH, in particular in individuals who started ART in chronic infection, which is the most frequent case. Chronic inflammation in PLWH under efficient ART is associated with the risk of non-AIDS morbidities and mortality[3,4,5]. Moreover, ART treatment is not able to eliminate the virus from the body. The largest HIV reservoir resides in the intestine[6,7]. Moreover, residual viral replication can be observed in T_{FH} cells of B cell follicles (BCF) of lymph nodes (LN) during chronic infection in long-term treated PLWH[8]. One parameter that might largely contribute to the persistent inflammation is the disruption of the intestinal barrier and subsequent bacterial translocation in PLWH[9,10].

Natural hosts of SIV, such as African Green Monkeys (AGMs), do not display chronic inflammation despite stable high viremia during SIV infection[11,9]. Interestingly, SIV-infected AGMs do not show any tissue damage. Thus, LN do not display fibrosis and the Follicular dendritic cell (FDC) network is maintained in contrast to PLWH[12]. Also, the intestinal epithelial barrier remains intact[13,14] and no microbial translocation develops[14,15,16]. The maintenance of normal LN architecture is explained by a rapid and strong viral control in LN[17]. Indeed, AGM mount a tissue-specific viral control, i.e. SIVagm replication is strongly controlled in LN with no viral replication in BCF, while the virus continues to replicate efficiently in the intestine.

The reasons why SIVagm replication in the intestine does not lead to disruption of the intestinal barrier in AGM are unclear. The underlying mechanisms could be multiple. The maintenance of the gut barrier could be related with the preservation of Th17 cells in SIVagm-infected AGM[18]. Immunoglobulin A (IgA) is also known to have an important role in control of intestinal inflammation[19]. Immunoglobulin A is the dominant antibody isotype found in mucosal secretions[20]. The secretory IgA (SIgA) limit the penetration of commensal bacteria through the epithelium[21] achieving efficient protection of the epithelial barrier by immune exclusion[22]. Secretory IgA therefore have an anti-inflammatory function and play a key role in the prevention of tissue damage and recovery from infection[23,24]. IgA-deficient humans indeed exhibit gut microbiota dysbiosis[25].

B-cell dysregulation, including in mucosa, was noted at the very beginning of the HIV/AIDS epidemic. Damage to the B-cell compartment in HIV infection includes loss of normal BCF architecture in LN, polyclonal hypergammaglobulinemia, increased turnover of B cells, and eventually irreversible loss of memory B-cell responses with advancing HIV disease[26,27,28]. IgA-producing B cells and plasma cells are not spared from the HIV or SIV-induced damage[26]. There are unusually low anti-HIV IgA responses when compared to IgG responses in mucosal fluids[29]. The level of inflammation markers correlates with the loss of IgA in plasma and intestine during HIV infection[27]. PLWH showed dysfunction of isotype switch B cells, leading to less IgA in gut[27]. In contrast, AGMs developed higher-magnitude plasma gp120-specific IgA and IgG responses than RMs, whereas RMs developed more robust gp140-directed IgG responses[30,31].

IgA are produced from plasmablasts generated in BCF of Peyer's patches and mesenteric lymph nodes (mLN) that constitute major inductive sites of T-dependent IgA antibodies. Mesenteric lymph nodes draining the intestine are largely infected at early stage of infection and viral reservoirs during chronic infection[32]. We raise the hypothesis that the control of SIVagm replication in BCF in AGM could also have a beneficial impact on the maintenance of normal IgA levels and thereby on regulation of inflammation in the intestine. In order to address this question, we evaluated viral replication profiles, analyzed NK cells, quantified sIgA, and studied B cells producing IgA, IgM and IgG in mLN and intestine of AGM during non-pathogenic SIVagm infection

compared to the animal model of pathogenic HIV infection, i.e. SIVmac-infected macaques. We analyzed if there was a correlation between the IgA responses and intestine inflammation control. Our study reveals a correlation between NK cell mediated control and IgA levels in the mLN and deliver novel insights into the mechanisms that protect the mucosal tissue integrity during lentiviral infections.

RESULTS

Induction of CXCR5+ NK cells in B cell follicles from mesenteric lymph nodes during SIVagm infection

Previous studies have shown that the control of SIVagm replication in peripheral and mesenteric LN was associated with the presence of CXCR5+ NK cells[17,12,33]. However, so far, NK cells have only been studied in BCF of peripheral LN and spleen during SIVagm infection and only during the chronic stage of infection. No data are available on NK cells in mLN during SIVagm infection. We quantified viral replication in mLN. We investigated if NK cells from mLN up-regulate CXCR5 in response to SIVagm infection and whether they migrate into BCF of mLN. The viral replication profiles in mLN were analyzed *in situ* by FISH (Fig.1A). The mLN from four uninfected AGM and four uninfected cynomolgus macaques (MAC) were compared to mLN from four chronically SIVagm-infected AGM and four chronically SIVmac-infected MAC. We detected viral production in BCF from mLN of infected MAC (Fig.1A). We did not observe SIV RNA in BCF of mLN from non-infected animals. We also generally did not detect viral RNA in mLN of infected AGM. These data are in line with previous results showing a viral control in mLN of SIVagm-infected AGM[33]. We next stained the mLN for NK cells. We did not observe NK cells in mLN BCF from non-infected animals nor from infected MAC. However, we detected NK cells inside BCF of mLN BCF from infected AGM, both in acute (Fig.S1A) and chronic infection (Fig.1B). Indeed, CXCR5+ NK cells were induced after SIVagm infection in mLN of AGM starting from acute phase (Fig.1C, Fig.S1C). Moreover, we observed strong viral replication in BCF of mLN from chronically SIVagm-infected AGM once the animals were NK cell-depleted (Fig.S1B). These results showed that CXCR5+ NK cells are induced in mLN upon SIVagm infection and that, as previously shown for peripheral LN[17], BCF in mLN are protected from SIV replication in AGMs by NK cells.

Memory B cell IgA+ production is increased in mLN during SIVagm infection

We investigated the B cells and IgA responses in mLN during SIVagm and SIVmac infection. Six uninfected and six chronically SIV-infected animals were analyzed for each species. B cells were defined as CD45+ CD3- CD20+ and memory B cells as CD45+ CD3- CD20+ IgD- (Fig.S1D). As expected, the percentage of total B cells was higher in mLN and gut than in blood (Fig.S1E-F). The percentage of total B cells did not change after SIVmac and SIVagm infection in any compartment compared to uninfected animals (Fig.S1E-F). However, the memory B cells in mLN from SIV-infected MAC drastically decreased compared to non-infected MAC, while memory B cells in mLN from SIV-infected AGM were increased compared to non-infected AGM (Fig.S1G-H). We analyzed which types of Ig are produced by the memory B cells from mLN. We identified increases of IgA+ and IgM+ memory B cells in SIVagm-infected AGM compared to non-infected animals (Fig.1D, Fig.S1I-J). In contrast, there were no differences between non-infected and SIV-infected MAC regarding memory B cells positive for IgA+, IgM+, or IgG+ (Fig.1E, Fig.S1I-J). The increase of IgA+ memory B cells from mLN in SIVagm infection correlated positively with CXCR5+ NK cells present in mLN (Fig.1F). These results showed that IgA+ memory B cells were increased in mLN during SIVagm infection in contrast to SIVmac infection. They suggest that this increase is related with the NK cell-mediated control of viral replication in mLN.

Loss of total IgA in the intestinal lumen during chronic SIVmac in contrast to SIVagm infection

We explored the IgA response in the intestine (ileum, jejunum, colon). We stained intestinal mucosa for IgA. In non-infected AGM and MAC, the IgA signal was observed in lamina propria and in lumen (Fig.2A$_{\text{I-III \& X-XII}}$). During acute infection, the level and location of IgA staining showed no difference compared to uninfected AGM and MAC (Fig.2A$_{\text{I-VI \& X-XV}}$, Fig.S2A-C). However, the IgA signal was dramatically decreased in chronic SIVmac infection compared to non-infected MAC in all intestinal compartments (Fig.2A$_{\text{VII-IX}}$, Fig.S2A-C). IgA+ cells were still identified in lamina propria but we could not detect IgA signals in lumen of intestine any more during chronic SIVmac infection (Fig.2B-C). At the opposite to SIVmac infection, normal IgA signals were maintained in chronic SIVagm infection in all intestinal compartments (Fig.2A$_{\text{XVI-XVIII}}$, Fig.S2A-C).

To further analyze the IgA dynamics, we examined memory B cells from the intestine (jejunum, ileum and colon) by flow cytometry. There was a decrease of total memory B cells in jejunum and colon from SIV-infected MAC compared to non-infected MAC (Fig.S1G). In AGM, SIVagm infection did not induce changes in the frequencies of intestinal memory B cells (Fig.S1H). The IgA+ memory B cells in jejunum from SIV-infected MAC also decreased compared to non-infected animals (Fig.2D), while there was no change in SIVagm-infected AGM (Fig.2E). In contrast to IgA, the IgG+ memory B cells increased in jejunum and colon from SIV-infected MAC compared to uninfected animals (Fig.S2D), while intestinal IgG+ memory B cells remained normal in AGM after SIVagm infection (Fig.S2E). IgM+ memory B cells remained normal both in SIVmac and SIVagm infection (Fig.S2F-G). It is possible that the decrease of IgA+ memory B cells in the intestine during SIVmac infection was a consequence of IgG+ memory B cells increase. However, the total memory B cell levels as well as the IgA signal in the lumen was dramatically lost during SIVmac infection. Therefore, these results showed normal levels of intestinal memory B cells and IgA production in the intestine during SIVagm infection in contrast to chronic SIVmac infection, that was characterized by dramatically decreased IgA production. The major IgA signal loss in intestine of SIVmac-infected MAC came from a loss of IgA secreted in lumen.

Titers of total IgA but not IgA+ memory B cells in blood reflected the dynamics in intestine-associated tissues during SIVagm and SIVmac infections

We examined whether the changes in the gut-associated tissues were reflected in blood. There was no change in total memory B cells in SIVmac-infected compared to non-infected MAC (Fig.S1G), while memory B cell increased in blood after SIVagm infection (Fig.S1H). IgA+ and IgG+ memory B cells remained normal in blood during SIVmac and SIVagm infections (Fig.3A-B, Fig.S3A-D). We measured the immunoglobulin subtypes in plasma. There was no difference between non-infected and SIVagm-infected AGM for IgA and IgG titers present in plasma (Fig.3C, Fig.S3E). Yet, we found a decrease of the IgA and trend to increase (pvalue 0.0065) the IgG titers in plasma from SIVmac-infected MAC compared to non-infected MAC (Fig.3D, Fig.S3E). These data indicate that the soluble IgA levels in the plasma reflected the dynamics in the gut-associated tissues better than the levels of IgA+ memory B cell levels.

Inflammation in SIVmac infection correlated with less total IgA in blood

We measured systemic markers of inflammation and microbial translocation (sCD14, LBP and iFABP) (Fig.S3F-H). These markers are used in the literature to indicate inflammation through monocyte/macrophage activation (sCD14), intestinal epithelial barrier disruption (I-FABP) and microbial translocation (sCD14, I-FABP, LBP). We analyzed the potential correlation between these markers and the levels of total IgA and total

IgG in blood (Fig.3E-F, Fig.S4). As expected we detected an increase of sCD14 in chronic SIVmac infection as compared to baseline levels (Fig.S3F). Plasma IgA and sCD14 correlated negatively (r=-0.57; p= 0.04) (Fig.3E). The two other markers, I-FABP and LBP, were not increased in chronic SIVmac infection (Fig.S3G/H). However, plasma IgG, which can be a marker for hypergammaglobulinemia in HIV/SIVmac infections[34] and thus for abnormal B cell activation, correlated positively with LBP (r=0.89; p<0.0001) in SIVmac infection (Fig.S4C). At the opposite, SIVagm infection showed no increase of inflammation or microbial translocation markers nor correlations with Ig levels (Fig.3F and Fig.S4). Thus, higher levels of microbial translocation or inflammatory markers correlated with more IgG and less IgA in blood.

Stronger SIV-ENV specific memory B cell responses in mLN and intestine during SIVagm than SIVmac infection

We investigated the SIV-specific IgA responses in SIVagm versus SIVmac infection. SIVmac and SIVagm gp140 recombinant proteins were produced in order to analyze SIV ENV-specific memory B cells. In blood, we observed an increase of gp140-specific memory B cells after both SIVmac and SIVmac infections (Fig.4A-B). However, in the mLN and in all intestinal compartments gp140-specific memory B cells were increased only in SIVagm but not in SIVmac infection (Fig.4C-E). In the mLN, there were higher levels of gp140-specific IgM+ memory B compared to blood in both SIVagm and SIVmac infections (Fig.S5). Only 0.5% of the gp140-specific memory B cells in mLN from chronically-SIV infected MAC were IgA positive (Fig.S5C), while 4% were positive in chronically-SIV infected AGM (Fig.S5D). The frequencies of IgA+ gp140-specific memory B cells in chronic SIVagm infection were 8% in jejunum, 5% in ileum and 4% in colon (Fig.S5E). The levels of anti-gp140 IgA and IgG antibodies in blood of SIV-infected AGM and MAC were measured and the correlations with markers of inflammation evaluated (Figure 4F-G, Fig. S6). We observed no correlation. There was only a trend for a negative correlation in SIVmac-infected macaques between anti-gp140 IgA and I-FABP (Fig.4F). These results showed that gp140-specific memory B cells increased in blood during both SIVmac and SIVagm infection. However, in mLN and intestine, such increases were detected only in SIVagm and not in SIVmac infection.

DISCUSSION

Our study unravels major differences regarding the IgA response in the mLN and intestine between non-pathogenic SIVagm and pathogenic SIVmac infection. Previous studies have already analyzed IgA and B cell responses during SIVagm and SIVmac infections in distinct body compartments, including blood, milk, saliva, vaginal and rectal secretions[27],[34],[35]. SIV-infected AGMs were shown to display robust Env-binding antibody responses in milk, higher than those in rhesus MAC and humans, which may contribute to the rarity of postnatal transmission reported for natural SIV hosts[36]. Here we provide novel insights. We investigated if NK cells have the capacity to migrate into BCF of mLN during SIVagm infection. We furthermore analyzed the IgA and B cell responses in the mLN and distinct intestinal compartments. We evaluated the link with systemic inflammation.

We demonstrate that NK cells rapidly migrate into BCF of mLN during SIVagm infection where they control viral replication. We show that IgA+ memory B cells were increased in mLN during SIVagm infection in contrast to SIVmac infection. Moreover, normal intestinal IgA levels (jejunum, ileum and colon) were maintained during acute and chronic SIVagm infection, while they strongly decreased in chronically SIVmac-infected macaques. Our data in the pathogenic SIV model are in line with reports on HIV-1 infection in humans describing that HIV-1 does not induce vigorous specific IgA responses in any body fluid examined[26],[29]. Our

study underlines that in contrast to pathogenic HIV-1/SIVmac infections in respectively humans and macaques, IgA responses in the mLN are protected during SIVagm infection in AGM. The levels of CXCR5+ NK cells and IgA+ memory B cells in mLN were strongly correlated, suggesting that indeed the NK-cell mediated viral control is an important factor in the protection against dysfunction of the mucosal B cell responses in non-pathogenic SIV infection.

The protection of B cell dysfunction by NK cells in LN could be indirect through the viral control. The lack of chronic viral replication in BCF during SIVagm infection in opposite to untreated HIV-1/SIVmac infections would avoid chronic inflammation and destruction of the anatomical architecture, in particular fibrosis and disruption of the FDC network as described during early HIV infection[37], protecting thereby B cell responses in BCF[34]. Our data provide a further explanation of why early anti-retroviral treatment has a benefit with regard to treatment initiated in chronic HIV infection. Since early ARV is known to protect BCF structures in the intestine[37], thereby most likely improving IgA responses, early ARV might increase through IgA the control of chronic inflammation and thus also the chances for a durable remission. It is not excluded that NK cells also directly modulate B cell responses, including in HIV infection[38]. It has been shown that NK cells can influence humoral responses by diminishing T_{FH} cells and that they also can limit germinal center reaction[39,40]. The generation of CXCR5+ NK cells capable to migrate into BCF of mLN might facilitate the influence of NK cells on B cell responses.

In chronically SIVmac-infected macaques, the decrease of IgA signal was observed in all three intestinal compartments studied (ileum, jejunum, intestine). Since the decrease of the IgA production was due to a strong loss of signal in the lumen, and not in the lamina propria, this means that SIgA was lost while IgA+ cells were still present in the lamina propria. The results we observed in the macaque thus resemble those previously described in HIV infection[27]. A major difference between non-pathogenic and pathogenic SIVagm infection was thus the selective maintenance of SIgA that play a crucial role for the mucosal barrier integrity.

Although studies showed similar levels of SIV replication in the intestine of AGM and MAC[14,41], it was also reported that depletion of B cells in SIVagm infection leads to moderately increased viral production in the intestine[42]. Thus, a partial, weak contribution of B cells to viral replication in the gut during SIVagm infection is not excluded and could indirectly participate to inflammatory control. However, even if AGM develop better gp120 responses, they do not seem to develop more or better neutralizing antibodies than PLWH[43]. Total IgA was negatively correlated with sCD14 in SIVmac infection, while ENV-specific IgA did not show correlations. This suggests, that the inflammatory control in SIV infection in the intestine is more associated with the maintenance of non-specific IgA responses than with SIV-specific IgA responses. The total non-specific IgA responses in the intestine during SIVagm infection might strongly contribute to protect against translocation of bacteria together with the other proposed mechanisms protecting the epithelial barrier.

Blood did not reflect the IgA+ B cell dynamics occurring in the intestine. More than 90% of gut Igs are produced in situ by plasma cells in contrast to genital mucosa, where half of the Igs are coming from the blood[44]. In addition, the intestine is the largest lymphoid tissue in the body. This could explain why B cells in blood did not accurately reflected the dynamics in the intestine and further support that it is important to analyze intestinal tissue for understanding the in situ physiopathological virus-host interactions.

A limitation of our study is that we did not analyze viral replication pattern and NK cell distribution in Peyer's patches. The latter are known for being major sites for induction of IgA+ B cells[45,46,47]. The tissue sections we analyzed from the AGMs did not contain Peyer's patches. However, B cells are known to rapidly migrate from Peyer's patches to the regional mesenteric lymph nodes[47], which we studied here.

Overall, we show that IgA responses are normal or increased in the mLN and intestine during SIVagm infection. AGMs might have developed resilience mechanisms where tissues are synergistically protected.

Thus, NK cells control viral replication in LN, including mLN as shown here. This could protect the immune response, including the SIgA production in the intestine, contributing to the maintenance of bacterial control and epithelial barrier integrity, despite viral replication in the intestinal mucosa. In contrast, mesenteric lymph nodes are major viral reservoirs in pathogenic HIV/SIV infections[48] and IgA responses in intestine are damaged[26].

In conclusion, we show that NK cells of mLN upregulate CXCR5 in SIVagm infection and migrate into mLN BCF. This could have potentially important consequences on intestinal IgA responses and inflammation control. Enhancing HIV-specific IgA response in mucosa have been largely discussed in the context of vaccine studies[26]. Here our data suggest that total non-specific IgA contributes to the inflammatory control. Strategies allowing early and persisting viral control in BCF and/or restoring normal total IgA levels in the intestine could reveal beneficial for reducing inflammation in virologically controlled PLWH with persistent residual inflammation and in the research for therapies toward HIV cure.

REFERENCES

1. Soares, M. P., Teixeira, L. & Moita, L. F. Disease tolerance and immunity in host protection against infection. *Nat. Rev. Immunol.* **17**, 83–96 (2017).
2. Carlos, A. R., Weis, S. & Soares, M. P. Cross-Talk Between Iron and Glucose Metabolism in the Establishment of Disease Tolerance. *Front. Immunol.* **9**, (2018).
3. Sereti, I. *et al.* Persistent, Albeit Reduced, Chronic Inflammation in Persons Starting Antiretroviral Therapy in Acute HIV Infection. *Clin. Infect. Dis.* **64**, 124–131 (2017).
4. Hunt, P. W., Lee, S. A. & Siedner, M. J. Immunologic Biomarkers, Morbidity, and Mortality in Treated HIV Infection. *J. Infect. Dis.* **214 Suppl 2**, S44-50 (2016).
5. Hunt, P. W. Very Early ART and Persistent Inflammation in Treated HIV. *Clin. Infect. Dis.* **64**, 132–133 (2017).
6. Finzi, D. *et al.* Latent infection of CD4 + T cells provides a mechanism for lifelong persistence of HIV-1, even in patients on effective combination therapy. *Nat. Med.* **5**, 512–517 (1999).
7. Wong, J. K. & Yukl, S. A. Tissue reservoirs of HIV. *Curr. Opin. HIV AIDS* **11**, 362–370 (2016).
8. Banga, R. *et al.* PD-1 + and follicular helper T cells are responsible for persistent HIV-1 transcription in treated aviremic individuals. *Nat. Med.* **22**, 754–761 (2016).
9. Garcia-Tellez, T. *et al.* Non-human primates in HIV research: Achievements, limits and alternatives. *Infect. Genet. Evol.* **46**, 324–332 (2016).
10. Massanella, M., Fromentin, R. & Chomont, N. Residual inflammation and viral reservoirs: alliance against an HIV cure. *Curr. Opin. HIV AIDS* **11**, 234–241 (2016).
11. Huot, N., Rascle, P., Garcia-Tellez, T., Jacquelin, B. & Müller-Trutwin, M. Innate immune cell responses in non pathogenic versus pathogenic SIV infections. *Curr. Opin. Virol.* **19**, 37–44 (2016).
12. Diop, O. *et al.* High Levels of Viral Replication during Primary Simian Immunodeficiency Virus SIVagm Infection Are Rapidly and Strongly Controlled in African Green Monkeys. *J. Virol.* **74**, 7538–47 (2000).

13. Estes, J. D. *et al.* Damaged Intestinal Epithelial Integrity Linked to Microbial Translocation in Pathogenic Simian Immunodeficiency Virus Infections. *PLOS Pathog.* **6**, e1001052 (2010).
14. Raehtz, K. D. *et al.* African green monkeys avoid SIV disease progression by preventing intestinal dysfunction and maintaining mucosal barrier integrity. *PLOS Pathog.* **16**, e1008333 (2020).
15. Bochart, R. M. *et al.* Microbiome Stability with Chronic SIV Infection in AIDS-resistant Sooty Mangabeys. *bioRxiv* 780825 (2019) doi:10.1101/780825.
16. Pandrea, I. V. *et al.* Acute Loss of Intestinal CD4+ T Cells Is Not Predictive of Simian Immunodeficiency Virus Virulence. *J. Immunol.* **179**, 3035–3046 (2007).
17. Huot, N. *et al.* Natural killer cells migrate into and control simian immunodeficiency virus replication in lymph node follicles in African green monkeys. *Nat. Med.* **23**, 1277–1286 (2017).
18. Favre, D. *et al.* Critical Loss of the Balance between Th17 and T Regulatory Cell Populations in Pathogenic SIV Infection. *PLOS Pathog.* **5**, e1000295 (2009).
19. Leong, K. W. & Ding, J. L. The Unexplored Roles of Human Serum IgA. *DNA Cell Biol.* **33**, 823–829 (2014).
20. Cerutti, A., Chen, K. & Chorny, A. Immunoglobulin Responses at the Mucosal Interface. *Annu. Rev. Immunol.* **29**, 273–293 (2011).
21. Boullier, S. *et al.* Secretory IgA-Mediated Neutralization of Shigella flexneri Prevents Intestinal Tissue Destruction by Down-Regulating Inflammatory Circuits. *J. Immunol.* **183**, 5879–5885 (2009).
22. Phalipon, A. *et al.* Secretory Component: A New Role in Secretory IgA-Mediated Immune Exclusion In Vivo. *Immunity* **17**, 107–115 (2002).
23. Corthësy, B. Secretory immunoglobulin A: well beyond immune exclusion at mucosal surfaces. *Immunopharmacol. Immunotoxicol.* **31**, 174–179 (2009).
24. Fernandez, M. I. *et al.* Anti-Inflammatory Role for Intracellular Dimeric Immunoglobulin A by Neutralization of Lipopolysaccharide in Epithelial Cells. *Immunity* **18**, 739–749 (2003).
25. Catanzaro, J. R. *et al.* IgA-deficient humans exhibit gut microbiota dysbiosis despite secretion of compensatory IgM. *Sci. Rep.* **9**, 13574 (2019).
26. Kulkarni, V. & Ruprecht, R. M. Mucosal IgA Responses: Damaged in Established HIV Infection—Yet, Effective Weapon against HIV Transmission. *Front. Immunol.* **8**, (2017).
27. Hel, Z. *et al.* Dysregulation of Systemic and Mucosal Humoral Responses to Microbial and Food Antigens as a Factor Contributing to Microbial Translocation and Chronic Inflammation in HIV-1 Infection. *PLOS Pathog.* **13**, e1006087 (2017).
28. Planchais, C. *et al.* Early Antiretroviral Therapy Preserves Functional Follicular Helper T and HIV-Specific B Cells in the Gut Mucosa of HIV-1–Infected Individuals. *J. Immunol.* (2018) doi:10.4049/jimmunol.1701615.
29. Mestecky, J. *et al.* Paucity of Antigen-Specific IgA Responses in Sera and External Secretions of HIV-Type 1-Infected Individuals. *AIDS Res. Hum. Retroviruses* **20**, 972–988 (2004).

30. Amos, J. D. *et al.* Rapid Development of gp120-Focused Neutralizing B Cell Responses during Acute Simian Immunodeficiency Virus Infection of African Green Monkeys. *J. Virol.* **89**, 9485–9498 (2015).
31. Zhang, R. *et al.* Envelope-specific B-cell populations in African green monkeys chronically infected with simian immunodeficiency virus. *Nat. Commun.* **7**, 12131 (2016).
32. Rabezanahary, H. *et al.* Despite early antiretroviral therapy effector memory and follicular helper CD4 T cells are major reservoirs in visceral lymphoid tissues of SIV-infected macaques. *Mucosal Immunol.* **13**, 149–160 (2020).
33. Gueye, A. *et al.* Viral load in tissues during the early and chronic phase of non-pathogenic SIVagm infection. *J. Med. Primatol.* **33**, 83–97 (2004).
34. Brocca-Cofano, E. *et al.* Pathogenic Correlates of Simian Immunodeficiency Virus-Associated B Cell Dysfunction. *J. Virol.* **91**, (2017).
35. Amos, J. D. *et al.* Lack of B Cell Dysfunction Is Associated with Functional, gp120-Dominant Antibody Responses in Breast Milk of Simian Immunodeficiency Virus-Infected African Green Monkeys. *J. Virol.* **87**, 11121–11134 (2013).
36. Chahroudi, A. *et al.* Mother-to-infant transmission of SIV is rare in sooty mangabeys and is associated with low viremia. *J. Virol.* (2011) doi:10.1128/JVI.02690-10.
37. Kök, A. *et al.* Early initiation of combined antiretroviral therapy preserves immune function in the gut of HIV-infected patients. *Mucosal Immunol.* **8**, 127–140 (2015).
38. Bradley, T. *et al.* RAB11FIP5 Expression and Altered Natural Killer Cell Function Are Associated with Induction of HIV Broadly Neutralizing Antibody Responses. *Cell* **175**, 387-399.e17 (2018).
39. Cook, K. D., Kline, H. C. & Whitmire, J. K. NK cells inhibit humoral immunity by reducing the abundance of CD4+ T follicular helper cells during a chronic virus infection. *J. Leukoc. Biol.* **98**, 153–162 (2015).
40. Rydyznski, C. E. *et al.* Affinity Maturation Is Impaired by Natural Killer Cell Suppression of Germinal Centers. *Cell Rep.* **24**, 3367-3373.e4 (2018).
41. Estes, J. D. *et al.* Defining total-body AIDS-virus burden with implications for curative strategies. *Nat. Med.* **23**, 1271–1276 (2017).
42. Gaufin, T. *et al.* Effect of B-Cell Depletion on Viral Replication and Clinical Outcome of Simian Immunodeficiency Virus Infection in a Natural Host. *J. Virol.* **83**, 10347–10357 (2009).
43. Norley, S. G. *et al.* Immunological studies of the basis for the apathogenicity of simian immunodeficiency virus from African green monkeys. *Proc. Natl. Acad. Sci.* **87**, 9067–9071 (1990).
44. J, M., Z, M., Pd, S., Z, H. & Rc, A. Mucosal immunology of the genital and gastrointestinal tracts and HIV-1 infection. *J. Reprod. Immunol.* **83**, 196–200 (2009).
45. Lycke, N. Y. & Bemark, M. The regulation of gut mucosal IgA B-cell responses: recent developments. *Mucosal Immunol.* **10**, 1361–1374 (2017).
46. Cerutti, A. & Rescigno, M. The biology of intestinal immunoglobulin A responses. *Immunity* **28**, 740–750 (2008).

47. Macpherson, A. J., McCoy, K. D., Johansen, F.-E. & Brandtzaeg, P. The immune geography of IgA induction and function. *Mucosal Immunol.* **1**, 11–22 (2008).
48. Cumont, M. C. *et al.* TGF- β in intestinal lymphoid organs contributes to the death of armed effector CD8 T cells and is associated with the absence of virus containment in rhesus macaques infected with the simian immunodeficiency virus. *Cell Death Differ.* **14**, 1747–1758 (2007).
49. Jacquelin, B. *et al.* Nonpathogenic SIV infection of African green monkeys induces a strong but rapidly controlled type I IFN response. *J. Clin. Invest.* **119**, 3544–3555 (2009).
50. Jacquelin, B. *et al.* Innate Immune Responses and Rapid Control of Inflammation in African Green Monkeys Treated or Not with Interferon-Alpha during Primary SIVagm Infection. *PLOS Pathog.* **10**, e1004241 (2014).
51. C, P. *et al.* Optimal maturation of the SIV-specific CD8+ T-cell response after primary infection is associated with natural control of SIV. ANRS SIC study. (2019) doi:10.1101/2019.12.20.885459.
52. Ma, D. *et al.* Factors Associated with Siman Immunodeficiency Virus Transmission in a Natural African Nonhuman Primate Host in the Wild. *J. Virol.* **88**, 5687–5705 (2014).
53. He, T. *et al.* Critical Role for the Adenosine Pathway in Controlling Simian Immunodeficiency Virus-Related Immune Activation and Inflammation in Gut Mucosal Tissues. *J. Virol.* **89**, 9616–9630 (2015).
54. Planchais, C. *et al.* HIV-1 Envelope Recognition by Polyreactive and Cross-Reactive Intestinal B Cells. *Cell Rep.* **27**, 572-585.e7 (2019).
55. Gnanadurai, C. W. *et al.* Genetic Identity and Biological Phenotype of a Transmitted/Founder Virus Representative of Nonpathogenic Simian Immunodeficiency Virus Infection in African Green Monkeys. *J. Virol.* **84**, 12245–12254 (2010).

MATERIAL AND METHODS

Monkeys, SIV infection and ethics statement

Twenty-seven AGMs (Caribbean *Chlorocebus sabaeus*) were included in this study. Seven AGM were used as uninfected controls and twenty AGM were infected with SIVagm. Twenty-seven cynomolgus MACs (*Macaca fascicularis* [MAC]) imported from Mauritius island were included in the study, out of which twelve MAC were used as uninfected controls and fifteen MACs were infected with SIVmac. Macaques with a controller genotype (H6) were not included in the study. The AGMs were infected with the SIVagm.sab92018 wildtype isolate and the MAC with the SIVmac251 isolate as previously described[17]. The description of the animals is shown in Supplementary Table 1 A-B.

The AGM and MAC were housed at the IDMIT Center (Fontenay-aux-Roses, France). All experimental procedures were conducted in strict accordance with the international European guidelines 2010/63/UE on the protection of animals used for experimentation and other scientific purposes and the recommendations of the Weatherall report. The IDMIT center complies with the Standards for Human Care and Use of the Office for Laboratory Animal Welfare (OLAW, USA) under OLAW Assurance number A5826-86. Monitoring of the monkeys was under the supervision of the veterinarians in charge of the animal facilities. Animal experimental protocols were approved by the Ethical Committee of Animal Experimentation (CETEA-DSV, IDF, France;

Notification 12-098). The samples from the animals included here were from animals purchased and used for other studies. These studies were approved and accredited under statement numbers A17-044, A13-005 and A15-035 by the ethics committee, registered and authorized under Number 44 at the French Ministry of Education and Research. with the reference numbers 2453-2015102713323361v2 and 2015031314518254.02 (APAFIS#319). Some results of these other studies are already published[49,50,51] (Huot Frontier in press). Animals were handled by veterinarians in accordance with national regulations (CEA Permit Number A 92-32-02) and the European Directive (2010/63, recommendation no. 9) and in compliance with the Standards for Human Care and Use of Laboratory of the Office for Laboratory Animal Welfare (OLAW, USA) under OLAW Assurance number #A5826-01. Animals were housed in ASL3 confinement in adjoining individual cages allowing social interactions, and maintained under controlled conditions with respect to humidity, temperature, and light (12 hours light/12 hours dark cycles). Water was available ad libitum. Animals were monitored and fed once or twice daily commercial monkey chow and fruit by trained personnel. Environmental enrichment was provided including toys, novel foodstuffs, and music under the supervision of the CEA Animal Welfare Body. Experimental procedures (animal handling, viral inoculations, and samplings) were conducted after sedation with ketamine chlorhydrate (Rhone-Merieux, Lyon, France, 10 mg/kg). Tissues were collected at necropsy: animals were sedated with ketamine chlorhydrate 10 mg/kg) then humanely euthanized by intravenous injection of 180 mg/kg sodium pentobarbital. The sample size varied between three and nine monkeys per group (n = 6 in most experiments). Sample collection was performed in random order, according to the tripartite harmonized International Council for Harmonization of Technical Requirements for Pharmaceuticals for Human Use (ICH) Guideline on Methodology (previously coded Q2B). The investigators were not blinded while the animal handlers were blinded to group allocation.

Tissue collections and processing

Plasma was obtained by blood centrifugation 1800 x g for 10 minutes and stored at -80°C. PBMCs were isolated on density gradient (Eurobio, CMSMSL01-01). The cells were conserved in fetal bovine serum (FBS) (Eurobio, CVFSVF00-01) with 10% of DMSO (Sigma, D2650-100ML) in liquid nitrogren. The tissue samples (mesenteric lymph nodes, Jejunum, Ileum and Colon) were cut and grinded with the help of a gentleMACS Dissociator (Miltenyi Biotec, 130-093-235). The cells were then filtered (70µm, Clearline, 141379C) and stored in FBS with 10% of DMSO in liquid nitrogen.

To conserve tissues frozen in O.C.T. (Tissue-Tek, 4583), pieces were incubated in Paraformaldehyde (PFA) 4% (AlfaAesar, J61899) overnight. The next day, they were washed 3 times in PBS with 20 minutes of incubation at room temperature. After that, they were immersed into increasing concentrations of sucrose (Sigma, S0389-500G), i.e. 10%, 20% and 30% at 4°C. After these steps, the tissues were put into O.C.T. and freezed in ethanol/dry ice solution and conserved at -80°C.

Flow cytometry staining

For the NK and CD4 T cell panels, we saturated non-specific sites by monkey sera. For the B cell panel (Supplementary Table 2.B), we saturated non-specific sites by FBS. Then we added the antibody mixes to the samples (1 million of cells). The antibodies used are listed in Supplementary Table 2A. The B cell panels also included biotinylated gp140 proteins from SIVmac and SIVagm and streptavidin-PE (Fisher Scientific, 10503785). Cells were permeabilized using Cytofix solution (BD, 554655). The fluorescence staining was observed and captured by a flow cytometer (BD, LSR II) and DIVA software (BD). Images were analyzed using FlowJo.

Immunofluorescent staining

All tissues in O.C.T were cut at 10µm on a cryostat (LEICA CM 3050S) and put on slides (Thermo Scientific, J3800AMNZ). These slides were conserved at -20°C. The epitope revelation protocol was realized with PBS incubation at room temperature for 15 minutes. Then, we let the slide in methanol (Fisher Chemical, M/3950/15) at -20°C during 2 hours and incubated in formaldehyde 2% at room temperature (Sigma, F8775-500mL) for 15 minutes. We saturated non-specific sites by BSA 4% (Sigma, A6003-25G) during 2 hours at room temperature and washed for 1 hour with PBS. The primary antibodies (Supplementary Table 3; 1:200) were added overnight at 4°C. Then we washed the slide during 1 hour in PBS and we added secondary antibodies (Supplementary Table 3; 1:200) and DAPI (Supplementary Table 3; 1:1000) for 1 hour at 4°C. We washed the slide during 1 hour in PBS and we added mounting medium (Invitrogen, 00-4958-02). We finally dropped off the cover (Fisher Scientific, 15165452 – Dutscher, 100038N) from the slide with mounting medium. The fluorescence staining was observed and captured by a spinning-disk (Yokagawa, CellVoyager CV1000). We analyzed these images by ImageJ (Fiji).

Relative quantification by microscopy staining

On our acquired samples by ImageJ software (Fiji) the noise was deleted via threshold establishment. The threshold was determined by background staining analysis. Then the median of intensity fluorescence adjusted without background (MFIadj) was measured on our samples in channels corresponding to DAPI and the given marker to be measured, respectively. Finally, we calculated MFIadjIgA/MFIadjDAPI ratio on each sample.

Fluorescent In Situ Hybridization

All tissues in O.C.T were cut at 10µm on cryostat (LEICA CM 3050S) and put on slides (Thermo Scientific, J3800AMNZ). These slides were conserved at -20°C. The epitope revelation protocol was realized by two methods. For detection of SIVmac RNA, we followed the RNAscope protocol with SIVmac251-gag probe utilization (Advanced Cell Diagnostics Europe, 488091) and ACD HybEZ Hybridization system (Advanced Cell Diagnostics Europe, 310013). For detection of SIVagm RNA, the SIVagm probe was made based on the SIVagm.sab92018 backbone, as described in a previous study[17]. The primary antibodies (Supplementary Table 3; 1:200) were added overnight at 4°C. Then we washed the slide during 1 hour in PBS and added secondary antibodies (Supplementary Table 3; 1:200) and DAPI (Supplementary Table 3; 1:1000) for 1 hour at 4°C. We washed the slide during 1 hour in PBS and we added mounting medium (Invitrogen, 00-4958-02). We finally dropped off the cover (Fisher Scientific, 15165452 – Dutscher, 100038N) from the slide with mounting medium. The fluorescence staining was observed and captured by a spinning-disk (Yokagawa, CellVoyager CV1000). We analyzed these images by ImageJ (Fiji).

ELISA

The soluble markers for inflammation and microbial translocation in the plasma were measured by ELISA using the following commercial kits: iFABP (MyBiosource, MBS037632), sCD14 (R&D System, DC140) and LBP (Hycult Biotech, HK315-02). They have already been shown to cross-react with AGM samples[52,53].

The titers of total IgA and IgG in blood were quantified. Recombinant human antibodies and serum IgG from HIV-1 donors were purified by batch/gravity-flow affinity chromatography using peptide M-coupled agarose (Invivogen, San Diego, CA) and protein G Sepharose 4 fast flow beads (GE Healthcare, Chicago, IL) for IgAs and IgGs, respectively. By Anti-IgG and IgA was added and incubated on night at room temperature in plates covered by parafilm (Costar, 9018). Then, we washed 3x with PBS-0.001% tween (PBSt) and added ELISA buffer (0.5M EDTA, pH 8; 10X PBS; Tween 20 (Sigma); BSA (Sigma); H20), to incubate it for 2 h at room temperature. We washed 3x with PBSt. The plates were organized in accordance with samples to test Ig samples (1:4 dilution in PBS). The plates were incubated for 2 h at room temperature. We washed 3x with PBSt. We added HRP-conjugated goat anti-human IgG or IgA (Immunology Jackson ImmunoReseach)

(1:1000-diluted in ELISA buffer) and incubated for 1 h at room temperature. Then we washed 3x with PBSt and added ABTS solution (Invitrogen, Cat #: 00-2024). We finished by measured the optical density at 405nm.
For the quantification of the titers of SIVagm and SIVmac GP140-IgA and GP140-IgG, we constructed SIVagm and SIVmac gp140-foldon Env GP140 proteins using methods as described[54]. For SIVagm, we used as backbone the SIVagm.sab92018 molecular clone[12,55]. GP140 proteins was added and incubated on night at room temperature in plates covered by parafilm (Costar, 9018). Then, the same protocol was used like just above for IgA and IgG titer.

Statistics

Comparisons among independent groups were conducted using nonparametric Mann-Whitney U-test (pvalue<0.05=*; pvalue<0.01=**). Correlation analysis was performed according to Spearman r test. Statistical computations were performed using Prism (GraphPad, La Jolla, CA).

ACKNOWLEDGMENTS

We are grateful for the excellent contributions from the veterinarians and staff at the IDMIT Center (Benoit Delache, Jean-Marie Helies, Raphaël Ho Tsong Fang and Julie Morin). NH was supported by the Fondation Beytout and Institut Pasteur. PR was recipient of a PhD fellowship from the University Paris Diderot, Sorbonne Paris Cité and also supported by the NIH (R01AI143457) and Institut Pasteur. CaP was recipient of a Roux-Cantarini Postdoctoral Fellowship. CyP was supported by the ERC-2013-StG 337146 program. We would like to acknowledge grant support from Sidaction and the Fondation J. Beytout to MMT. We gratefully acknowledge the support to IDMIT from the French government: Investments for the Future program for infrastructures (PIA) through the ANR-11-INBS-0008 grant as well as from the PIA grant ANR-10-EQPX-02-01 to the FlowCyTech facility at IDMIT. We equally acknowledge the Investments for Future grant ANR-10–INSB–04 to support the UtechS Photonic BioImaging (Imagopole) and C2RT facilities at Institut Pasteur.

AUTHOR CONTRIBUTIONS

PR, NH, CyP, HM and MMT designed the experiments. PR, NH CyP, BJ, ML and CaP performed the experiments. VC and BJ coordinated the animal studies. PR, NH, BJ, ASC, HM and MMT analyzed the data. BJ, ASC and MMT obtained the funding. PR and MMT wrote the manuscript and all co-authors reviewed it.

LEGENDS

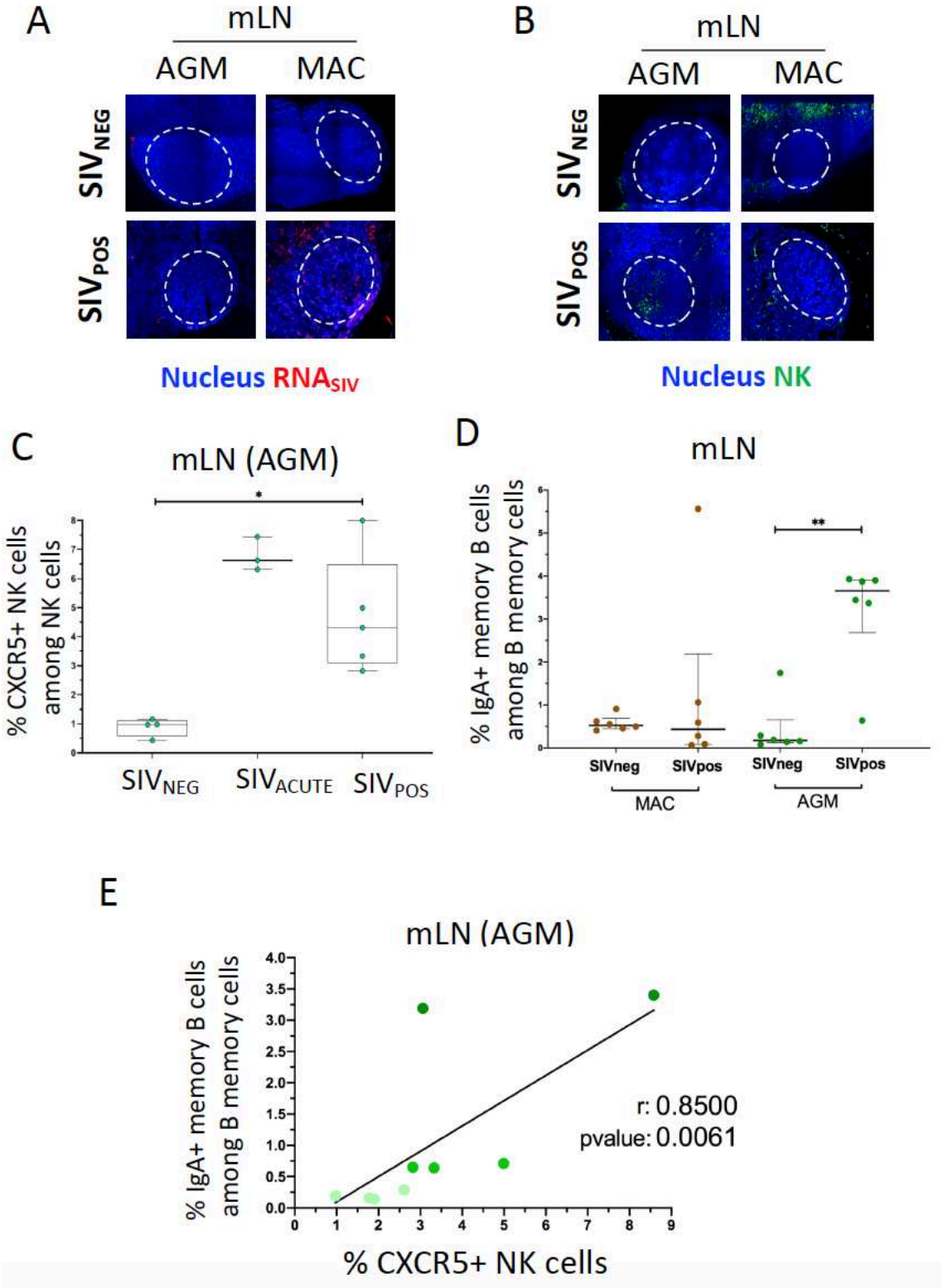


Figure 1: SIV replication, NK cells and IgA+ B cells in mesenteric lymph nodes during SIVagm and SIVmac infection. A) Immunofluorescence staining of viral RNA in B cell follicles (BCF) from mLN of AGM and MAC. Four uninfected and four chronically infected animals per species were studied. Nucleus is in blue, RNA_{SIV} is in red and dash white circle delineates the BCF areas. **B)** Immunofluorescence staining of NK cells in mLN. Four uninfected and four chronically infected animals per species were studied. Nucleus is in blue, NK cell is in green and dash white circle delineates the BCF areas. **C)** Evaluation of CXCR5+ NK cell frequencies in mLN in non-infected AGM, at day 9 p.i. (SIV acute) and in chronic SIVagm infection (SIVpos). Percentages of CXCR5+ NK cells among total NK cells are shown. Each green circle represents one individual AGM. **D)**

Measurement of IgA+ memory B cells in mLN from non-infected animals and from chronically infected (SIVpos) MAC (brown) and AGM (green). Percentages of among memory B cells in mLN are shown. Each dot indicates an individual animal. **E)** Correlation between CXCR5+ NK cells and IgA+ memory B cell in mLN from non-infected (light green) and chronically SIVagm-infected AGM (dark green). Each green circle indicates an individual animal. Mann-Whitney U-test was used.

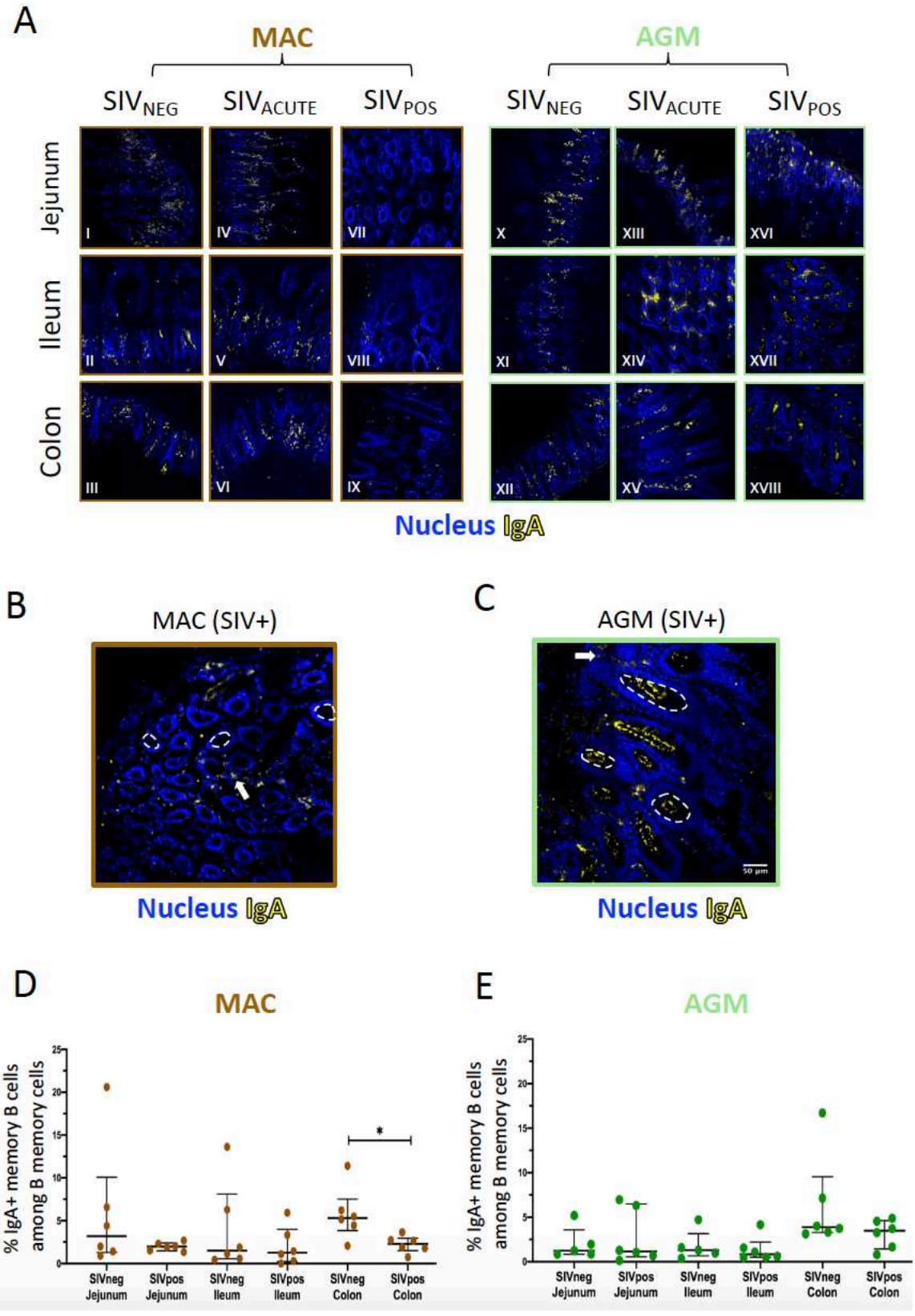


Figure 2: IgA dynamics and anatomical distributions during SIVagm and SIVmac infections in the intestine. A) Immunofluorescence staining of IgA in three compartments of the intestine (jejunum, ileum and

colon) from MAC (non-infected and chronically SIVmac-infected) and AGM (non-infected and chronically SIVagm-infected) (n= 3-5 animals per species). Representative sections for one animal per species are shown. **B-C)** Enlargements of the immunofluorescence staining of IgA (yellow) and nucleus (blue) in the intestine from **B)** chronically SIVmac-infected MAC and **C)** chronically SIVagm-infected AGM. Arrows represent IgA+ cells and circles delineate the lumen zone (n=3-5 animals per species). The images show a representative section in the ileum for one MAC and one AGM. **D-E)** Percentage of IgA+ memory B cells in three compartments of the intestine (jejunum, ileum and colon) from **D**) MAC (non-infected and chronically SIVmac-infected) (n = 5-6 animals) and **E)** AGM (non-infected and chronically infected) (n= 5-6 animals). Mann-Whitney U-test was used.

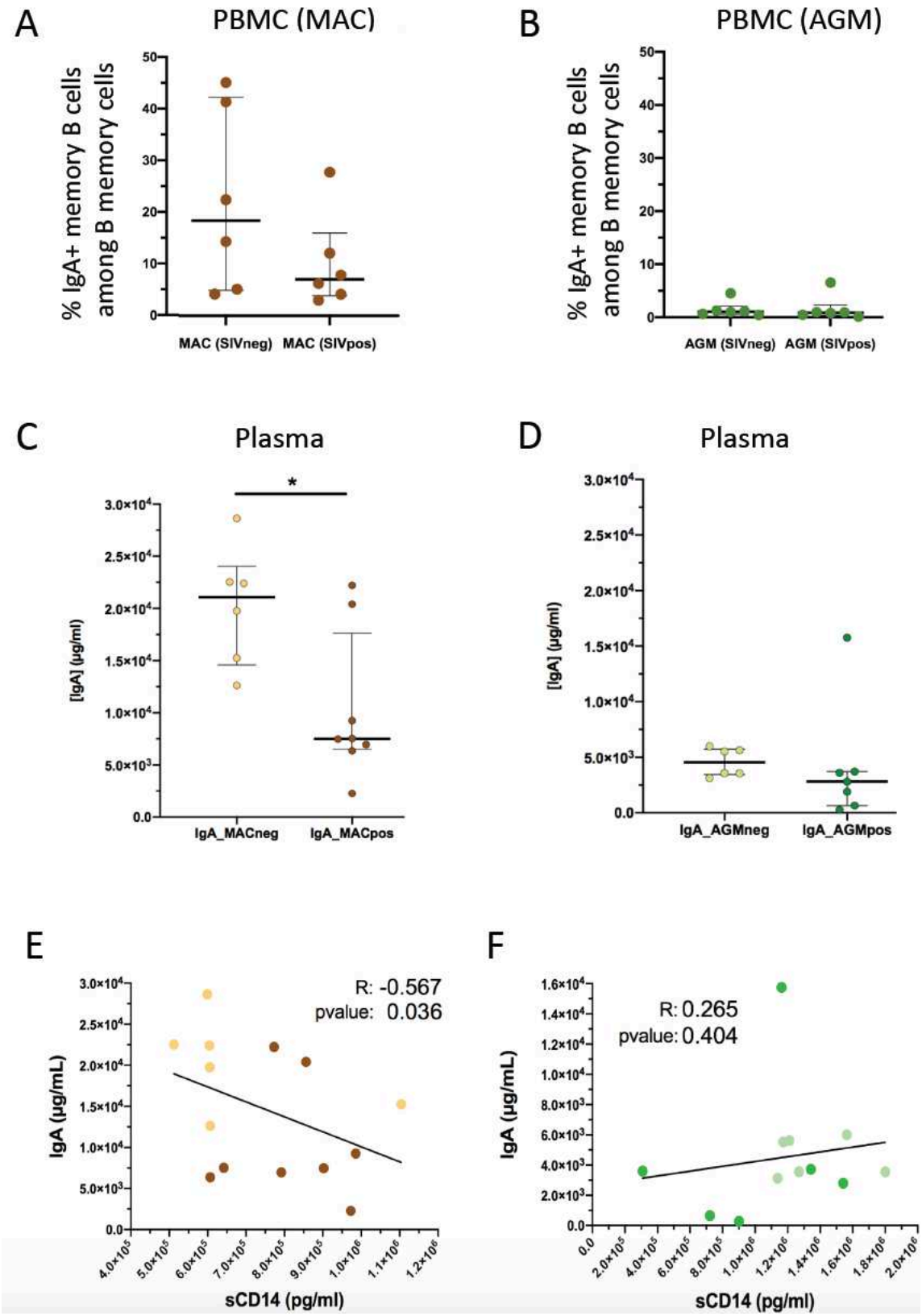


Figure 3: IgA titers in blood during SIVagm and SIVmac infections. A) Percentage of IgA+ memory B cells in blood from AGM (non-infected and chronically infected) (n= 6 animals). **B)** Percentage of IgA+ memory B cells in blood from MAC (non-infected and chronically SIVmac-infected) (n= 6-8 animals). **C)** IgA titers in plasma from AGM (non-infected and chronically SIVagm-infected) (n= 6 animals). **D)** IgA titers in plasma from MAC (non-infected and chronically SIVmac-infected) (n= 6-8 animals). Mann-Whitney U-test was used. **E)** Correlation between inflammatory and microbial translocation marker sCD14 in plasma and plasmatic-IgA in AGM (non-infected animals in light green and chronically infected animals in dark green) (n=6 animals). **F)** Correlation between inflammatory and microbial translocation marker sCD14 in plasma and

plasmatic-IgA in MAC (non-infected animals in light brown and chronically infected animals in dark brown) (n=6-8 animals). Spearman r test was used.

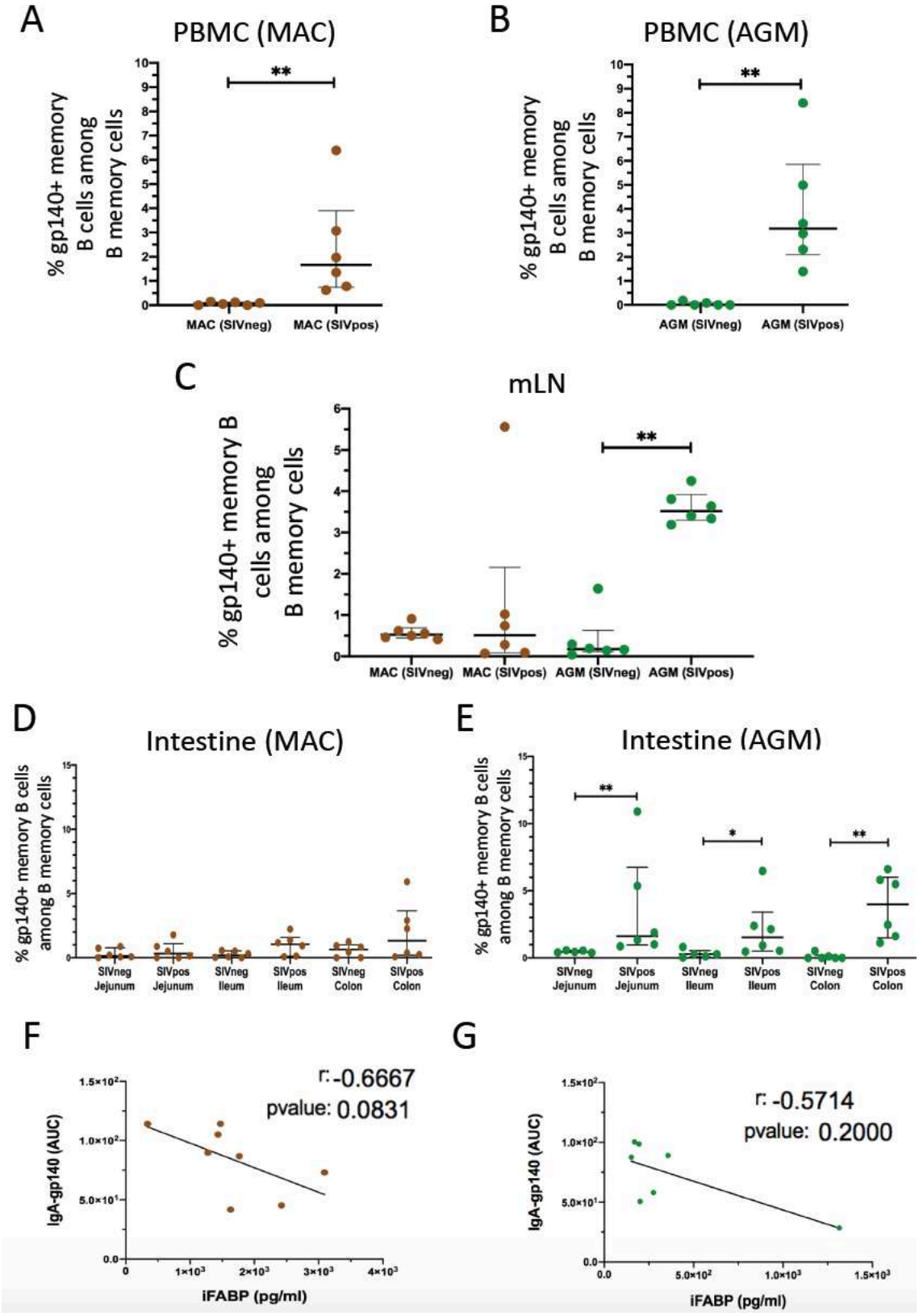
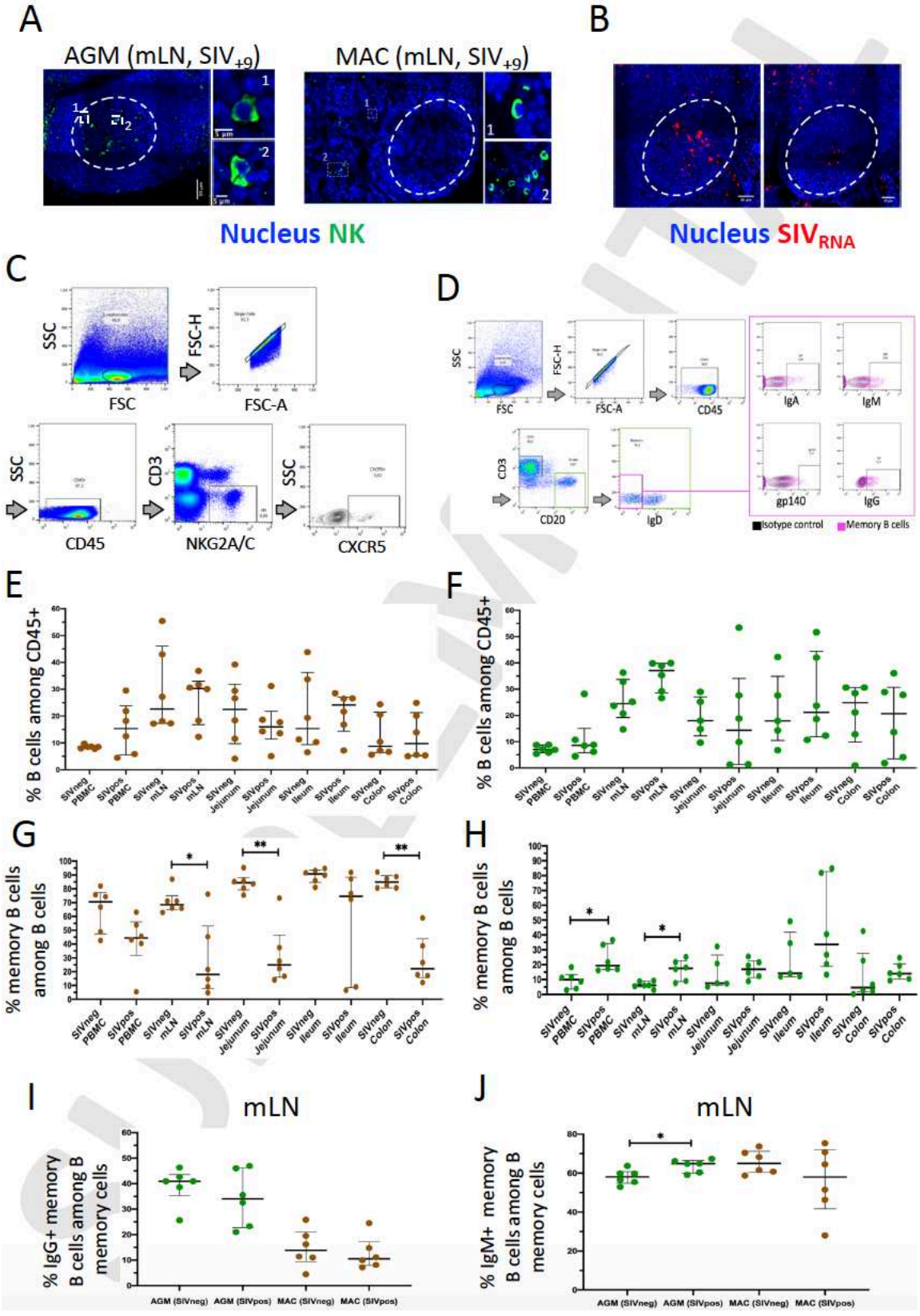


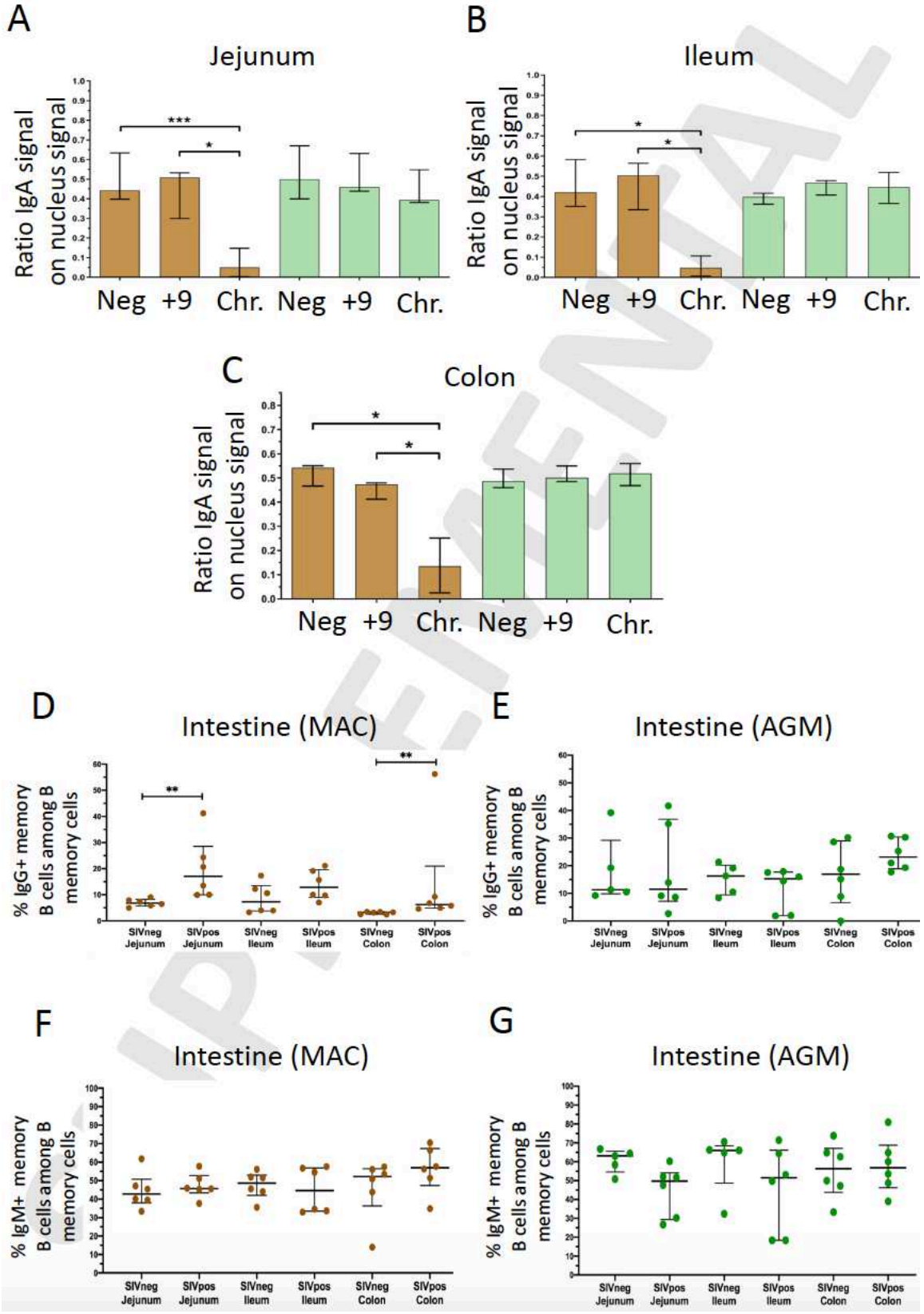
Figure 4: SIV ENV-specific memory B cells in blood, mesenteric lymph nodes and intestinal tissues during SIVmac and SIVagm infections. A) Percentage of gp140-specific memory B cells in blood from MAC (non-infected and chronically infected) (n=6). **B)** Percentage of gp140-specific memory B cells in blood from AGM (non-infected and chronically infected) (n=6). **C)** Percentage of gp140-specific memory B cells in mLN from AGM (non-infected and chronically infected) and MAC (non-infected and chronically infected) (n=6

animals per species). **D)** Percentage of gp140-specific B cells in the intestine from MAC (non-infected and chronically infected) (n=6 animals). **E)** Percentage of gp140-specific B cells in the intestine from AGM (non-infected and chronically infected) (n=6 animals). Mann-Whitney U-test was used. **F-G)** Correlation between anti-gp140 IgA levels in plasma and I-FABP in **F)** MAC (n=6 animals) and **G)** AGM (n=6 animals). Spearman r test was used.



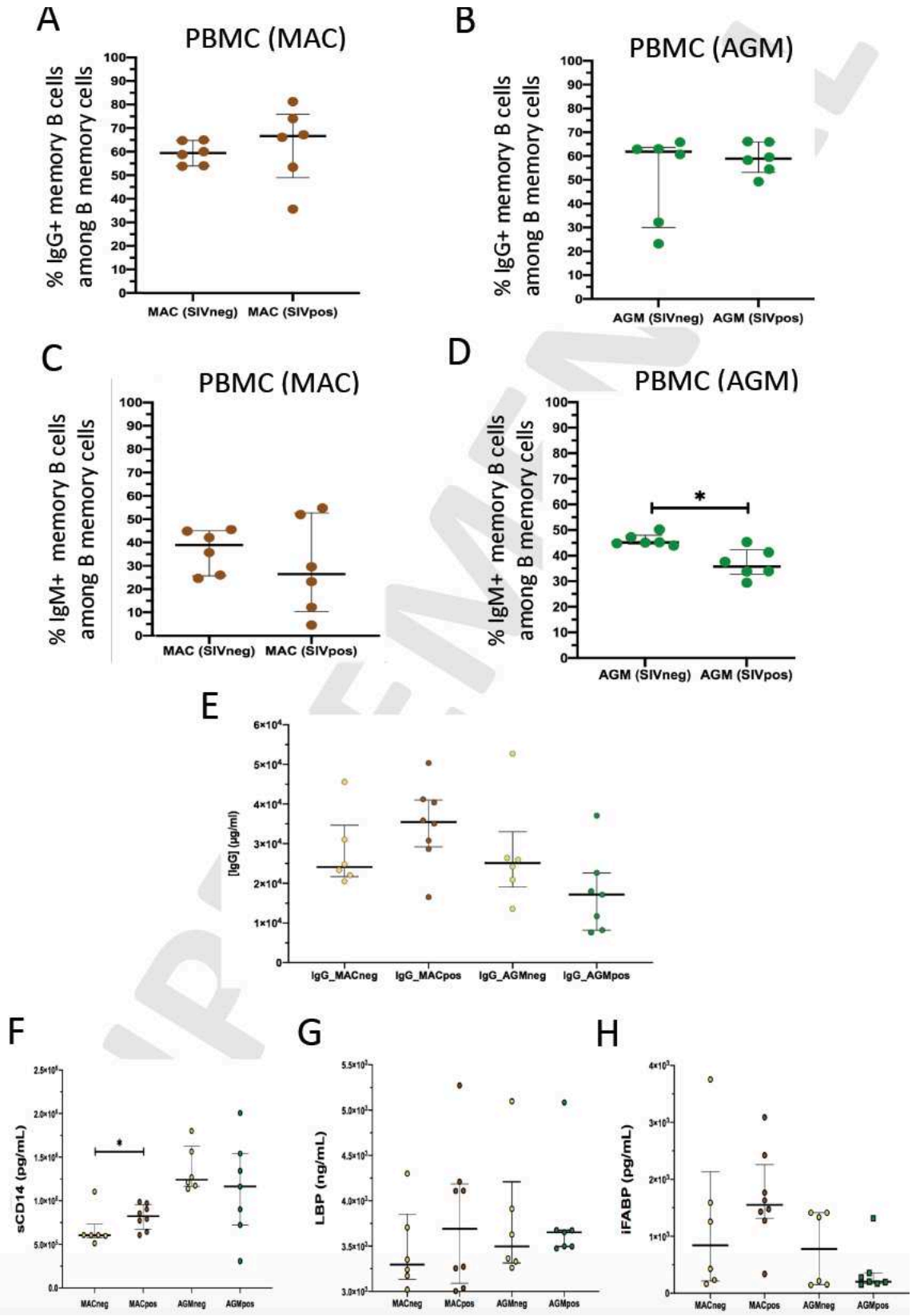
Supplementary Figure 1: A) Immunofluorescence staining of NK cells in mLN during acute SIVagm infection. Three animals per species were analyzed at day 9 p.i. Nucleus is stained in blue, NK cells in green.

The dash white circle delineates the B cell follicle area. **B)** Immunofluorescence staining of viral RNA in mLN from chronically SIVagm-infected AGM depleted for NK cells. The mLN were collected from four previously described animals[17]. Nucleus is stained in blue, RNA_{SIV} in red. The dash white circle delineates the B cell follicle area. Two representative BCF are shown from 2 distinct animals. **C) A** dot plot showing CXCR5+ NK cells. NK cells in MAC and AGM were gated as usual for NHP as CD45+CD3-NKG2A/C+ [17]. **D)** Gating strategy used for identifying IgG+/IgA+/IgM+/gp140+ memory B cells in MAC and AGM. **E-I)** Analyses of B cells in blood, mLN and intestine from six uninfected and six chronically SIV-infected animals for each species. **E)** Percentage of total B cells in distinct compartments (blood, mLN, jejunum, ileum and colon) in uninfected and chronically SIVmac-infected MAC. **F)** Percentage of total B cells in distinct compartments (blood, mLN, jejunum, ileum and colon) in uninfected and chronically SIVagm-infected AGM. **G)** Percentage of memory B cells in distinct compartments (blood, mLN, jejunum, ileum and colon) in uninfected and chronically SIV-infected MAC. **H)** Percentage of memory B cells in distinct compartments (blood, mLN, jejunum, ileum and colon) in uninfected and chronically SIVagm-infected AGM. **I)** Percentage of IgG+ memory B cells in mLN from uninfected and chronically SIV-infected AGM (green) and MAC (brown). **J)** Percentage of IgM+ memory B cells in mLN from uninfected and chronically SIV-infected AGM (green) and MAC (brown). Mann-Whitney U-test was used.



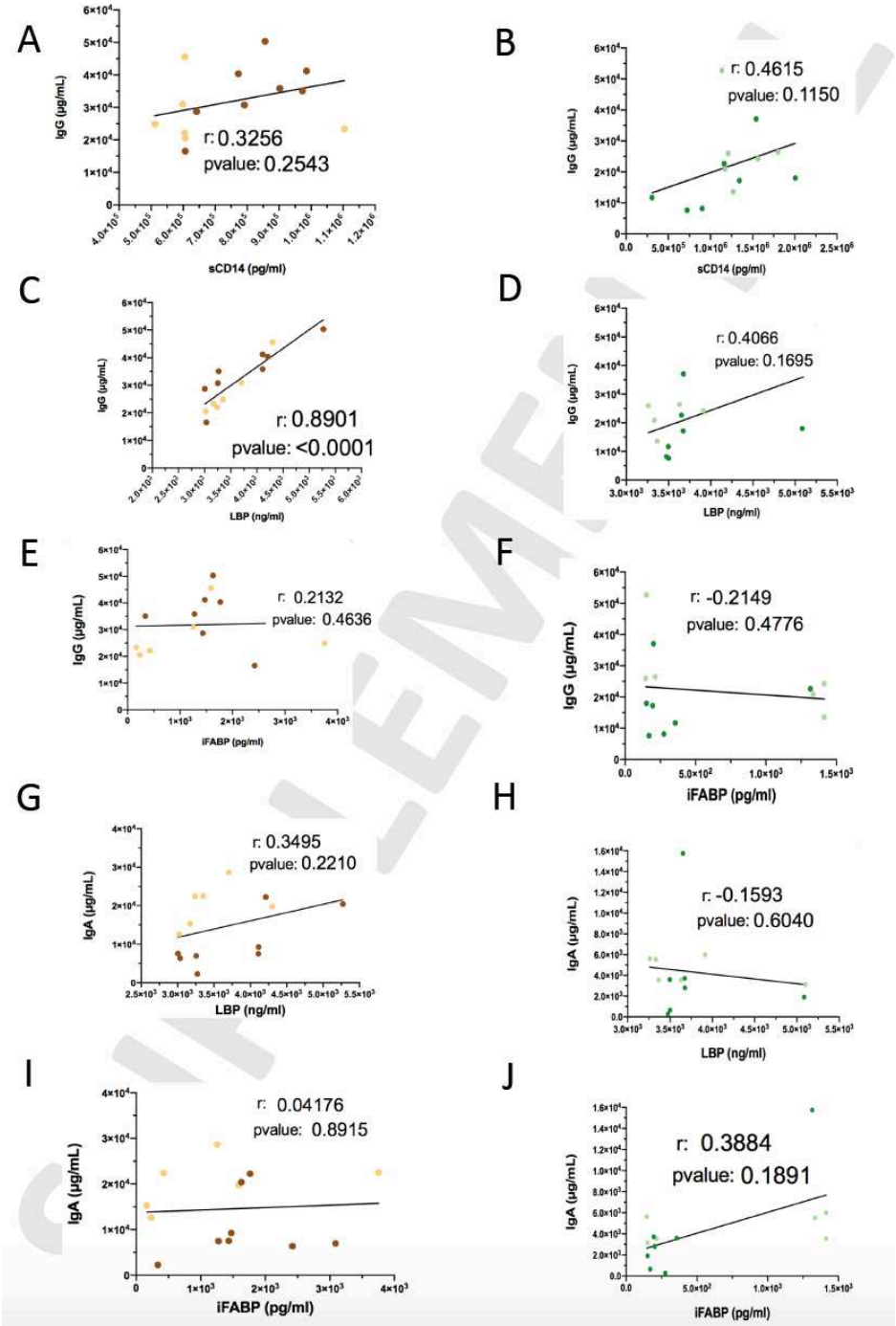
Supplementary Figure 2: IgA, IgM and IgG production in the intestine during SIVagm and SIVmac infections. A-C) Longitudinal evaluation of IgA levels in the intestine. The ratio of the IgA signal per nucleus signal was measured by microscopy in **A)** jejunum, **B)** ileum and **C)** colon in uninfected and SIV-infected MAC (brown) and AGM (green) during acute (day 9 p.i.) and chronic SIV infection (n=3 animals). **D)** Percentage of IgG+ memory B cells in the intestine (jejunum, ileum and colon) from uninfected and chronically SIVmac-infected MAC (n=6 animals). **E)** Percentage of IgG+ memory B cells in the intestine (jejunum, ileum and colon) from uninfected and chronically SIVagm-infected AGM (n=5-6 animals). **F)** Percentage of IgM+ memory B cells in the intestine (jejunum, ileum and colon) from uninfected and chronically SIVmac-infected

MAC (n=6 animals). **G)** Percentage of IgM+ memory B cells population in intestine (jejunum, ileum and colon) from uninfected and chronically SIVagm-infected AGM (n=5-6 animals). Mann-Whitney U-test was used.



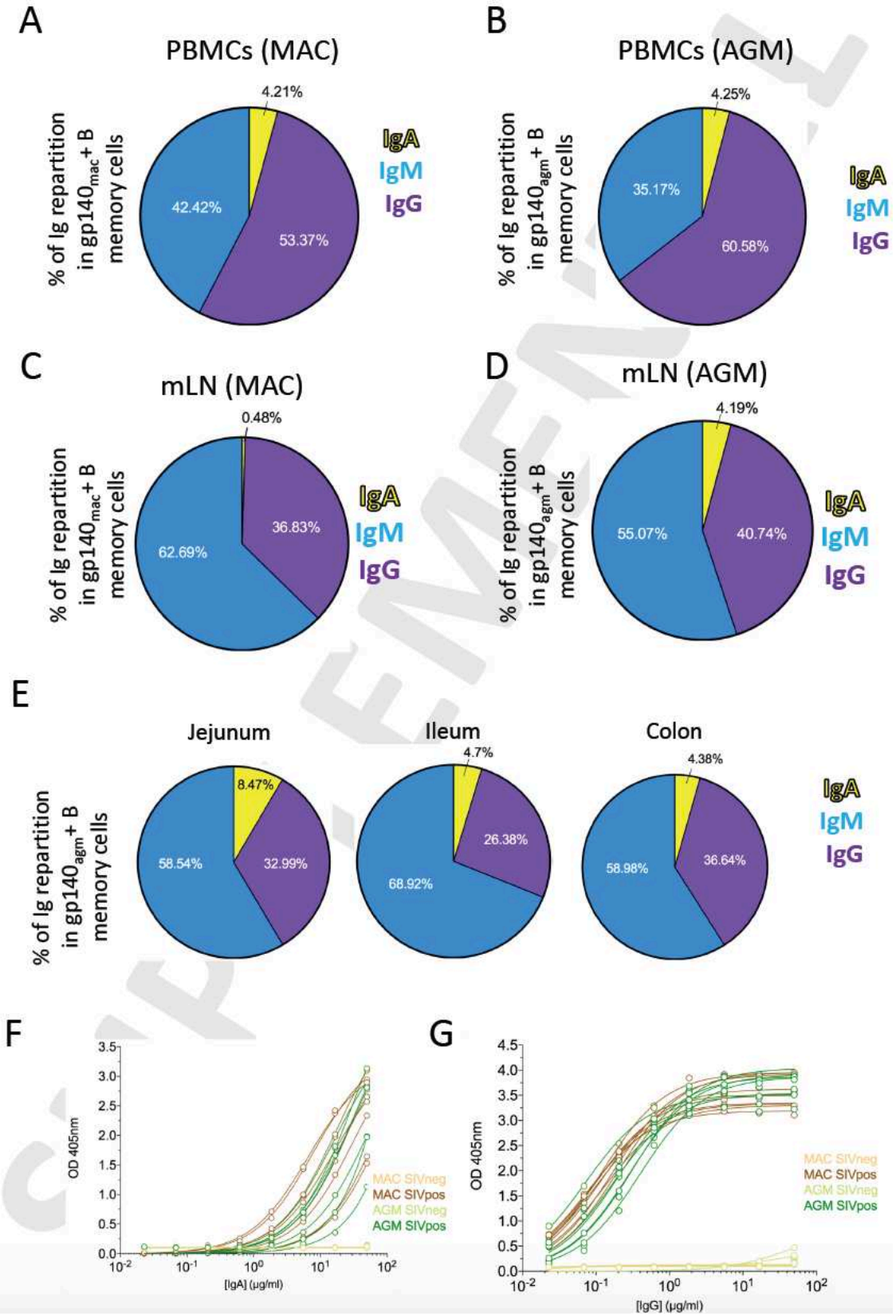
Supplementary Figure 3: A) Percentage of IgG+ memory B cells in blood from uninfected and chronically SIVmac-infected MAC (n=6 animals). **B)** Percentage of IgG+ memory B cells in blood from uninfected and chronically SIVagm-infected AGM (n=6 animals). **C)** Percentage of IgM+ memory B cells in blood from uninfected and chronically SIVmac-infected MAC (n=6 animals). **D)** Percentage of IgM+ memory B cells in

blood from uninfected and chronically SIVagm-infected AGM (n=5-6 animals). **E)** Plasma titer of IgG antibodies from uninfected and chronically SIV-infected MAC and AGM (n=6-8 animals per species). **F-H)** Plasmatic titer of **F)** sCD14, **G)** LBP and **H)** I-FABP from uninfected and chronically SIV-infected MAC and AGM (n=6-8 animals per species). Mann-Whitney U-test was used.



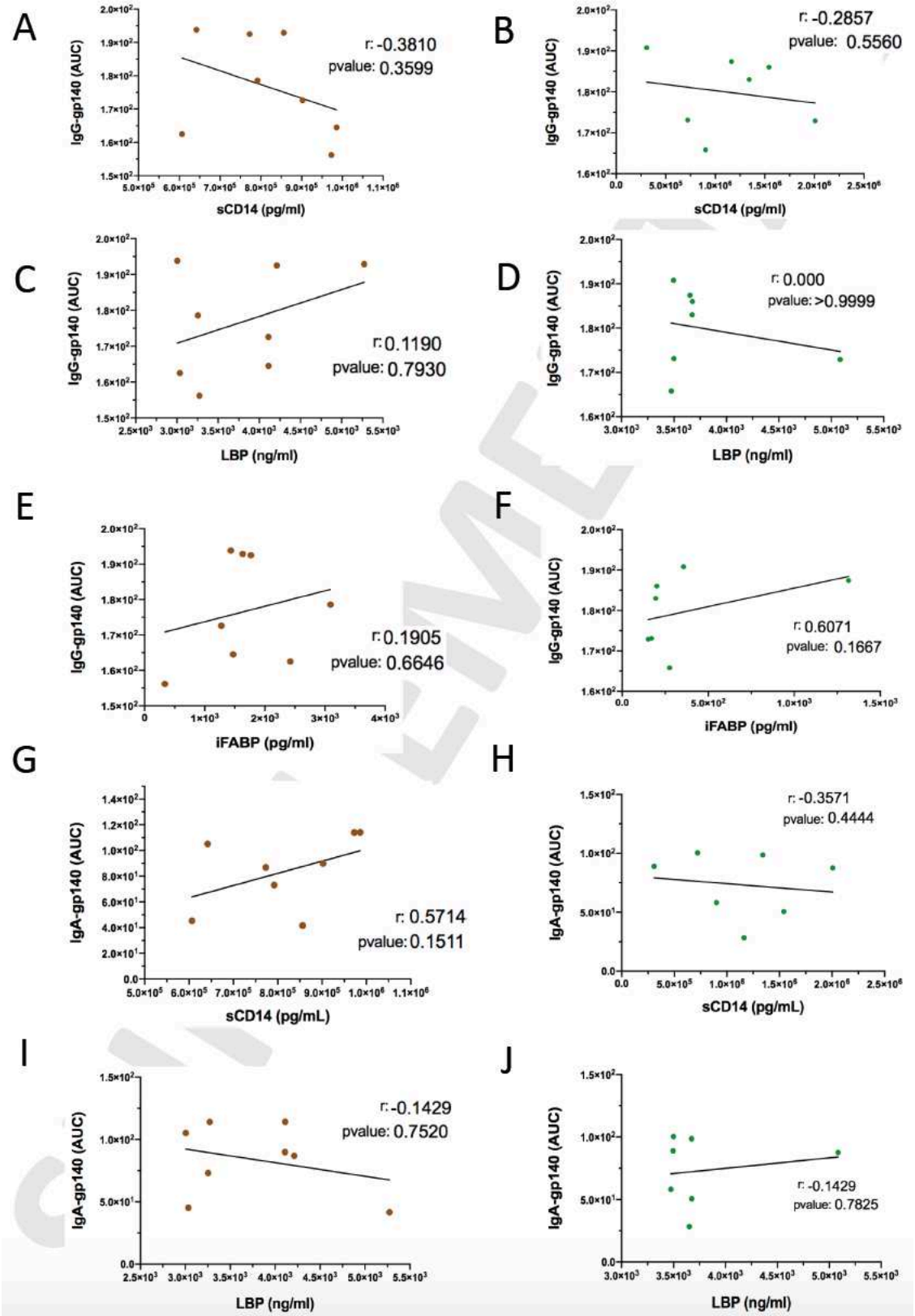
Supplementary Figure 4: Analyses of the correlations between plasmatic titers of IgG or IgA and soluble inflammation or microbial translocation markers in blood. A) Plasmatic IgG antibody levels were plotted against sCD14 in MAC. Non-infected MAC are in light brown and chronically infected in dark brown. **B)** The levels of IgG antibodies were plotted against those of sCD14 in AGM. Non-infected AGM are in light green and chronically infected in dark green. **C)** Plasmatic IgG antibody levels s were plotted against LBP in MAC. Non-infected MAC are in light brown and chronically infected in dark brown. **D)** Plasmatic IgG antibody levels were plotted against LBP in AGM. Non-infected AGM are in light green and chronically infected in dark green. **E)** Plasmatic IgG antibody levels were plotted against I-FABP in MAC. Non-infected MAC are in light brown

and chronically infected in dark brown. **F)** Plasmatic IgG antibody levels were plotted against I-FABP in AGM. Non-infected AGM are in light green and chronically infected in dark green. **G)** Plasmatic IgA antibody levels were plotted against and LBP in MAC. Non-infected MAC are in light brown and chronically infected in dark brown. **H)** Plasmatic IgA antibody levels were plotted against LBP in AGM. Non-infected AGM are in light green and chronically infected in dark green. **I)** Plasmatic IgA antibody levels were plotted against and I-FABP in MAC. Non-infected MAC are in light brown and chronically infected in dark brown. **J)** Plasmatic IgA antibody levels were plotted against and I-FABP in AGM. Non-infected AGM are in light green and chronically infected in dark green. Each dot indicates an individual animal. Spearman r test was used.



Supplementary Figure 5: A) Pie representation of median percentages of gp140+ IgA+, IgG+ and IgM+ memory B cells from blood in SIVmac-infected MAC (n=6). **B)** Pie representation of median percentages of gp140+ IgA+, IgG+ and IgM+ memory B cells from blood in SIVagm-infected AGM (n=6). **C)** Pie representation of median percentages of gp140+ IgA+, IgG+ and IgM+ memory B cells from mLN in SIVmac-infected MAC (n=6). **D)** Pie representation of median percentages of gp140+ IgA+, IgG+ and IgM+ memory B cells from mLN in SIVagm-infected AGM (n=6). **E)** Pie representation of median percentages of gp140+ IgA+, IgG+ and IgM+ memory B cells from intestine (jejunum, ileum and colon) of SIVagm-infected AGM (n=6). **F)** ELISA graphs show the binding of plasmatic SIV-specific IgA antibodies to trimeric gp140 proteins.

The green dotted line corresponds to the AGM (light green represents non-infected monkeys and dark green represents chronically infected monkeys, n= 6-7 animals). The brown dotted line corresponds to the MAC (light brown represents non-infected monkeys and dark brown represents chronically infected monkeys, n= 6-8 animals). **G)** ELISA graphs show the binding of plasmatic SIV-specific IgG antibodies to trimeric gp140 proteins. The green dotted line corresponds to the AGM (light green represents non-infected monkeys and dark green represents chronically infected monkeys, n= 6-7 animals). The brown dotted line corresponds to the MAC (light brown represents non-infected monkeys and dark brown represents chronically infected monkeys, n= 6-8 animals).



Supplementary Figure 6: Search for potential correlations between SIVagm and SIVmac Env-specific IgA and IgG in blood and markers of microbial translocation and systemic inflammation. (A-F) Plasma titers of gp140-specific IgG were plotted against sCD14, LBP or I-FABP concentrations in plasma of SIVmac infected MAC (brown) and SIVagm infected AGM (Green). Each dot indicates an individual animal. **(G-J)** Plasma titers of gp140-specific IgA were plotted against sCD14 or LBP concentrations in plasma of SIVmac infected MAC (brown) and SIVagm infected AGM (green). Each dot indicates an individual animal. Spearman r test was used.

Supplementary Tables

https://www.dropbox.com/scl/fi/bx3zafwmm7llxh2nvhsg4/Manuscript-5_Supplemental-tables.xlsx?dl=0&rlkey=p2y28wh0rfhh7860mby3obxnd

6. Tissue profiles of NKG2a/c^{+}CD8^{+} T cells in SIV infections

Tissue profiles of NKG2a/c^{+}CD8^{+} T cells in SIV infections

Nicolas Huot[1], Philippe Rascle[1,2], Nicolas Tchitchek[3], Benedikt Wimmer[1], Caroline Passaes[1], Vanessa Contreras[4], Desjardins Delphine[4], Christiane Stahl-Hennig[5], Roger Le Grand[4], Asier Saez-Cirion[1], Beatrice Jacquelin[1] and Michaela Müller-Trutwin[1]

[1]Institut Pasteur, Unité HIV, Inflammation et Persistance, Paris, France; [2]Université Paris Diderot, Sorbonne Paris Cité, Paris, France; [3]Sorbonne Université, INSERM, Immunology-Immunopathology-Immunotherapy (i3), Paris, France ; [4]CEA-Université Paris Sud-Inserm, U1184, IDMIT Department, IBFJ, Fontenay-aux-Roses, France; [4]Deutsches Primatenzentrum, Göttingen, Germany.

Keywords: SIV, HIV, NKG2A, CD8 T cells, CXCR5, HLA-E, stress, Hsp60, IL-23, non-human primates, lymph node, intestine.

Corresponding author: Michaela Müller-Trutwin

Institut Pasteur

HIV, Inflammation and Persistence Unit

28 rue du Dr Roux

75015 Paris, France

mmuller@pasteur.fr

Abstract

Some viruses present since a long time in primates have established an equilibrium with their host. African green monkeys (AGM) display persistent high viremia and viral replication in the intestine during infection by SIVagm. However, they efficiently resolve systemic inflammation after acute infection and do not display any intestinal immune or tissue damage during long-lasting chronic infection. We analyzed the tissue distribution and activity of $NKG2_{a/c}^{+}CD8^{+}$ T cells in blood, lymph nodes and intestine during non-pathogenic SIVagm infection in AGM compared to pathogenic SIVmac infection in macaques, the latter modeling HIV infection. $NKG2_{a/c}^{+}CD8^{+}$ T cells were expanded in blood and intestine but not in lymph nodes of AGM in response to SIVagm infection. Genome-wide transcriptome analysis of the $NKG2_{a/c}^{+}CD8^{+}$ T cells revealed the expression of NK cell receptors as well as cytotoxic effector function, gut homing and immunoregulatory molecules. NKG2a/c+CD8+T cells correlated negatively with IL-23 in the intestine during SIVmac infection. The data suggest a contribution of $NKG2_{a/c}^{+}CD8^{+}$ T cells in the control of inflammation and tissue protection in the intestine during non-pathogenic SIVagm infection.

Introduction

The implementation of combined antiretroviral therapy (ART) to treat HIV infection has been an incredible success and saved millions of lives. Anti-retroviral treatment reduces viremia to undetectable levels in blood of people living with HIV (PLWH). However, a residual inflammation persists in most PLWH, despite virological suppression, in particular in those individuals who started ART in chronic phase of infection, which still today is the most often case[1]. HIV-1 infection induces damages to the tissues, already at very early stages of infection. For instance, collagen deposition is observed in B cell follicles of the intestine and lymph nodes (LNs) causing fibrosis and a disruption of the follicular dendritic cell network already in HIV-1 primary infection[2]. The integrity of the intestinal barrier is also damaged during HIV infection leading to microbial translocation in chronic infection which most likely fuels systemic inflammation[3]. Anti-retroviral treatment initiated in chronic infection does not fully restore these tissue damages[4]. Anti-retroviral treatement initiated in acute HIV infection can avoid follicle damage in the intestine and restore intestinal Th17 cell levels, but does not fully restore the functional activity of these cells[5].

$CD8^+$ T-cells are critical in the control of viral replication and tumor cells[6,7] ; however, $CD8^+$ T-cells are highly affected by a persistent antigenic stimulation and chronic inflammation. During a variety of persistent infections, CD8 T cells upregulate immune check-point inhibitors, such as PD-1, CTLA-4, Lag-3 or Tim-3[8]. Such inhibitory receptors are generally induced to dampen inflammation, for example for the resolution of an infection-induced inflammation that otherwise would be harmful for the tissues[9]. However, it facilitates T cell exhaustion and is hampering the antiviral efficacy of the cells[10].

Inhibitory NK cell receptors (iNK), such as NKG2a, can also be induced on CD8+ T cells[11,12]. NKG2A forms a heterodimer with CD94. The expression of CD94/NKG2A complexes is induced on human CD8+ T cells after TCR triggering and stimulation by cytokines such as IL-10[13,14]. Commitment to expression of the inhibitory NKG2A generally is a clonal attribute restricted to a subset of memory/effector CD8+T cells[15]. NKG2A marks a unique immune effector T CD8+ subset preferentially co-expressing tissue-resident markers, but not immune checkpoint inhibitors[16,17]. CD94/NKG2A has been implicated in down-regulation of T-cell function in various cancers[18] and diminished responses against some viral infections, such as polyoma virus[19]. By contrast, NKG2A+ CD8+ T cells were also found in other settings to be more efficient at protecting against viral challenge than their counterparts[20]. For example, NKG2A does not inhibit responses against LCMV and even optimizes $CD8^+$ T cell responses during an acute poxvirus infection[21]. A regulatory function of the $NKG2_{a/c}{}^+CD8^+$ T cells is also not excluded[22].

CD8+ T cells expressing NKG2A have been observed during HIV-1 infection, ranging between 2 and 18% in peripheral blood of asymptomatic untreated PLWH[23]. There is evidence that HIV-specific NKG2A+ CD8+ T cells display impaired cytolytic function[23,24]. However, the percentage of NKG2A+ CD8+ T cells in blood is lower in PLWH than in healthy donors[25]. Within PLWH, the percentages were higher in PLWH controlling viremia than in viremic individuals[25]. Based on these reports, one might consider that the anti-HIV response of NKG2A+CD8+T cells is diminished, while the non-HIV-specific NKG2A+CD8+ T cells deliver some benefit to the host. It cannot be excluded though, in viremic PLWH, these cells home more intensively to the tissues and that this explains their lower levels in blood. Immunization of MAC with a CMV-based vector expressing HIV Gag induces a very efficient SIV control that was associated with MHC-E-restricted CD8+ T cells[26]. The vast majority of these cells were CD8a/b+ T cells lacking NKG2A/C expression[26].

The role of NKG2A+CD8+ T cells in HIV infection is not clearly understood. Their role might be particular important in tissues. Animal models allow to analyze immune responses in tissues. HIV originates from the Simian Immunodeficiency Virus (SIV) whose reservoir resides in African nonhuman primates (NHP). Natural

hosts of SIV, such as AGM, display high levels of replication in the blood and intestine, without inducing chronic inflammation[27]. They maintain a normal intestinal architecture, including intact FDC networks in the intestine and no loss of intestinal Th17 cells[27]. This contrasts with Asian monkeys (macaques, MAC) that do not carry SIV in their natural habitat and display the same physiopathology as HIV-1 infected humans[28]. African green monkeys infected by SIV therefore represent a good model to search for mechanisms that protect against chronic inflammation and tissue damage during a chronic viral infection. We raised the hypothesis that NKG2A+CD8+ T cells might be increased in tissues of AGM where the virus replicates (ie intestine) and contribute in tissue protection. We determined the genome-wide transcriptional profiles of these cells during SIVagm infection in AGM. We phenotyped and longitudinally followed NKG2a/c+ $CD8^+$ T cells in blood, LNs and intestine during pathogenic SIVmac infection in macaques and nonpathogenic SIVagm infection in AGM. Our study supports a protective role of NKG2a/c $CD8^+$ T cell during SIVagm infection in the gut.

Results

$NKG2_{a/c}$ expression on T cells in healthy nonhuman primates defines mainly a subset of CD8+T cells displaying an effector phenotype with effector tissue homing profile

We first performed a comparative analysis of the phenotype of $NKG2_{a/c}^+$ T cells in blood from six healthy AGM and six healthy cynomolgus MAC (CM). The data of peripheral blood-derived viable CD45+lin− lymphocytes was analyzed by dimensional reduction using viSNE algorithm. On nonhuman primate cells, the available antibodies against NKG2A also recognize NKG2C. viSNE plots revealed 8 spatially distinct populations in blood of healthy monkeys (Fig. 1a and 1b). $NKG2_{a/c}$ showed elevated expression of on a small cluster of CD8+ T cells. In AGM, this cluster of $NKG2_{a/c}^+CD8^+$ T cells was distinct from NK cells and conventional $NKG2_{a/c}^-$ $CD8^+$ T cells, whereas in MAC, this population clustered with conventional CD8+ T cells. These results indicate that $NKG2_{a/c}$ can be used to define a subset of CD8+ T cells in NHP. In both species, more than 75 % of the $NKG2_{a/c}^+$ $CD3^+$ T cells also expressed CD8a showing that CD3+NKG2a/c+ cells are mainly composed of CD8+ T cells in the blood of healthy AGM and CM ((Fig. 1c-d). NKG2a/c CD8+ T cell numbers in blood were low compared to conventional $CD8^+$ T or NK cells in both species (Fig 1d, e). Most of the $NKG2_{a/c}^+$ T cells were of the effector phenotype (Fig. 1f) and expressed both IFN-gamma and Perforin (Fig. 1g).

We measured chemokine receptor expression to evaluate their tissue homing potential. The large majority of the $NKG2_{a/c}^{++}$ T cells expressed CXCR3 and CD62L in AGM and MAC (Fig. 1h). Some of them also expressed CX3CR1, CCR7 and CXCR5 (Fig. 1h). For instance, the percentage of $CXCR5^+$ $NKG2_{a/c}^+$T cells were 11% and 6% in, respectively, AGM and MAC (Fig. 1h). We then assessed the expression of NK cell markers on $NKG2_{a/c}^+$T cells. The NK cell receptors NKG2D and NKP30 were expressed as frequently as on NK cells (Fig. 1i). $NKG2_{a/c}^+$T cells were also always positive for the other NK cell markers tested, i.e. CD16, NKp80, NKp46 and NKp44 (Fig. 1i). NKp44 marks NK cells that persist in intestine[29].

Taken together, our data show the existence of $NKG2_{a/c}^+$T cell populations in NHP peripheral blood mainly composed of CD8+ T cells with strong effector potential, expressing NK cell receptors and an inflammatory/effector tissue homing profile.

$NKG2_{a/c}$ $CD8^+$ T cells expand during primary SIVagm infection

We next deciphered the dynamics of $NKG2_{a/c}$ expressing T cells in response to SIV infection. The cells were followed in blood of twelve SIVagm.sab92018-infected AGMs and nine SIVmac251-infected CM between days 2 and 220 post-infection (pi). The viremia and $CD4^+$ T cell count of all animals are described in Supplementary

Figures 1 and 2 and in Supplementary Table 1. The viremia levels were as high in AGM than in the CM (Supplementary Fig.1). As expected, the CD4+ T cells counts decreased progressively in the CM while they rapidly recovered by the end of the primary infection in the AGM (Supplementary Fig.2).

In AGM, the $NKG2_{a/c}$ + T cells were readily detectable throughout the infection, whereas in CM, NKG2a/c staining on $CD3^+$ T cells sometimes failed to clearly define a population mainly due to a low number of cells (Fig. 2a). Analysis of CD8a expression on these NKG2a/c^+T cells showed that NKG2a/c^+T cells remained the vast majority throughout SIV infection (Fig. 2b).

We then assessed the dynamics of the NKG2a/c^+CD8^+ T cell counts during SIV infection. In CM, a transient decline of their absolute numbers in blood was observed at days 9 and 11 p.i. (Fig. 2c). This decline thus occurred concomitantly to the viremia peak (Suppl Fig. 1). In AGM, the cells expanded in primary infection and reached a peak at days 28 and 35 p.i. (Fig. 2c).

The differences observed in the dynamics of NKG2a/c^+CD8^+ T cells between pathogenic and non-pathogenic SIV infection could be a consequence of distinct tissue trafficking in response to infection. We assessed the frequencies of NKG2a/c^+CD8^+ T cells expressing tissue homing markers in blood. In both species, the $CCR7^+$NKG2a/c^+CD8^+ T cell frequencies did not show any significant changes in primary infection and remained low during chronic infection (Fig. 2d). The frequencies of $CD62L^+$, $CX3CR1^+$ and $CXCR3^+$ NKG2a/c^+CD8^+ T cells were strongly decreased after SIV infections in both CM and AGM (Fig. 2e-g). The levels of $CXCR3^+$ cells were partially recovered after day 80 p.i.

Here we show that AGM displayed an expansion of NKG2a/c^+CD8^+ T cells in blood during primary infection. Both in pathogenic and non-pathogenic SIV infection, NKG2a/c^+CD8^+ T cells expressing CCR7, CD62L, CXC3CR1 and CXCR3 were low or decreased in blood in response to SIV infection. These decreases could either mean that these cells are constantly recruited into tissues and/or that NKG2a/c^+CD8^+ T cells further differentiate into an effector profile upon SIV infection.

SIV infection sustains effector functions of $NKG2_{a/c}^+CD8^+$ T cells

We evaluated the effector activity profiles of $NKG2_{a/c}^+CD3^+CD8^+$ T cells following SIV infection. First, we examined the proliferative activity of these cells *ex vivo* by measuring intracellular expression of Ki-67, a cell-cycle marker expressed by cycling or recently divided cells (Fig. 3a). The $NKG2_{a/c}^+CD8^+$ T cells displayed more transient proliferative responses when compared to conventional $CD8^+$ T cells during SIVmac infection in contrast to AGMs. In AGM, the conventional CD8+ T cells did not show significant increases in proliferation, while $NKG2_{a/c}^+CD3^+CD8^+$T cells showed a strong increase in proliferative capacity in acute infection (day 7 p.i) (Fig.3a).

To evaluate the functional activity of the $NKG2_{a/c}^+CD8^+$ T cells, the surface expression of CD107a (a surrogate marker for cytolytic function) was measured *ex vivo* on unstimulated cells (Fig. 3b). In CM, increases in the cytotoxic activity of both conventional and $NKG2_{as/c}^+CD8^+$ T cells were detected in primary infection and for the $NKG2_{a/c}^+CD8^+$ T cells also in chronic infection. In AGMs, cytotoxic activity was observed for $NKG2_{a/c}^+CD3^+CD8^+$ T cells in primary and chronic infection (days 4, 9, 21 and 150 p.i) but was not increased on conventional $CD8^+$ T cells (Fig.3b).

We also measured Perforin and TNF-a expression levels by intracellular cytokine staining *ex vivo* in unstimulated cells. The data show the existence of $NKG2_{a/c}^+CD8^+$ T cells with increased levels of Perforin and TNF-a expressions during primary SIV infection in both species and in both $NKG2_{a/c}^+$ and conventional CD8+ T cells (Fig. 3c and d). In both species, the increases of Perforin and TNF-a in $NKG2_{a/c}^+CD8^+$ T cells were

observed as soon as day 7 and 2 p.i, respectively. In AGM, the increases of Perforin and TNF-a expressions were resolved earlier (day 14 and 28 p.i., respectively) than in MAC (day 35 and 80 p.i., respectively).

To analyze if these dynamics were associated with viral replication levels, a correlation matrix was generated between viremia levels and the different parameters measured on $NKG2_{a/c}^{+}CD8^{+}$ T cells (Fig. 3e and f). In both species, strong positive correlations were observed between viremia and KI-67 or Perforin levels of $NKG2_{a/c}^{+}CD8^{+}$ T cells, suggesting that viremia was driving the proliferation of these cells. Moreover, positive correlations were detected between Perforin and TNF-a levels for the $NKG2_{a/c}^{+}CD8^{+}$ T cells.

In summary, both AGM and CM showed increases in proliferation and cytotoxic activity of $NKG2_{a/c}^{+}CD8^{+}$ T cells in response to SIV infection in blood and these were associated with viremia levels.

No increases of total or CXCR5+$NKG2_{a/c}^{+}CD8^{+}$ T cells in secondary lymphoid tissues during SIVagm and SIVmac infections

To address the question of whether $NKG2_{a/c}^{+}CD8^{+}$ T cells home to the tissues during SIV infections, we examined their frequencies in secondary lymphoid tissues and in the intestine in AGM and CM. We analyzed non-infected, acutely infected and chronically infected AGM and CM. We did not find an enrichment of $NKG2_{a/c}^{+}CD8^{+}$ T cells in spleen from chronically infected animals when compared with healthy animals independently of the type of SIV infection studied (Fig. 4a). The longitudinal analysis of $NKG2_{a/c}^{+}CD8^{+}$ T cells in peripheral LN during the time course of SIV infection in both species also did not show significant changes (Fig. 4b). Similarly, no significant differences regarding the frequency of $NKG2_{a/c}^{+}CD8^{+}$ T cells were observed in the spleen of cART-treated CM where viremia was suppressed (Suppl. Table 1), when compared to viremic animals (Fig.4c). We also evaluated $NKG2_{a/c}^{+}CD8^{+}$ T cell frequencies in rhesus MAC (RM) that spontaneously controlled SIV (SIV controllers, SIC) (Suppl. Table 1a). The frequency of $NKG2_{a/c}^{+}CD8^{+}$ T cells in LN of chronically infected SIC was similar to that of viremic RM, but significantly increased compared to healthy animals (Fig. 4d). Thus, except for SIV controllers, $NKG2_{a/c}^{+}CD8^{+}$ T cells were not increased in peripheral secondary lymphoid organs.

We next assessed if $NKG2_{a/c}^{+}CD8^{+}$ T cells could access to the B cell follicles described as a sanctuary for HIV/SIV replication in secondary lymphoid tissues[30,31] and evaluated CXCR5 expression on tissue cells. The median frequencies of $CXCR5^{+}NKG2_{a/c}^{+}CD8^{+}$ T cells were more than 10 times lower in secondary lymphoid organs (LN, spleen) than in blood, including in SIV controllers (Fig.4e-h and Fig.1h). Furthermore, they decreased in the LN after SIV infection in both acutely and chronically infected viremic MAC (Fig.4e and h). In AGM, the levels of $CXCR5^{+}NKG2_{a/c}^{+}CD8^{+}$T in LN were also decreased in acute infection (Fig.4e). In the spleen, the median levels of $CXCR5^{+}$ $NKG2_{a/c}^{+}CD8^{+}$T were similar to that in LN and also did not increase after SIV infection in CM nor AGM (Fig. 4f). ART-treatment did not change the frequency of $CXCR5^{+}$ $NKG2_{a/c}^{+}CD8^{+}$ T cells in spleen of CM (Fig.4g). Thus, $NKG2_{a/c}^{+}CD8^{+}$ T cells showed no signs of increased capacity to migrate into B follicles within secondary lymphoid organs during SIV infection, neither in AGM nor in SIV controllers. The $CXCR5^{+}NKG2_{a/c}^{+}CD8^{+}$ T cells were lower in LN than in blood before infection and further decreased upon SIV infection in both species.

Rapid expansion of cytotoxic $NKG2_{a/c}^{+}CD8^{+}$ T cells during SIV infection in the the gut

Longitudinal follow up of $NKG2_{a/c}^{+}CD8^{+}$ T cells in the intestine (rectal biopsies) revealed differences with respect to secondary lymphoid organs and also between pathogenic and non-pathogenic SIV infection (Fig. 4i). In AGM, the $NKG2_{a/c}^{+}CD8^{+}$ T cells increased during primary infection in the intestine after SIV infection, and represented between 5 and 10% of the lymphoid cells between days 2 and 28 p.i. (Fig. 4i). In CM, the levels

never reached more than 5% (Fig. 4i). The increases of $NKG2_{a/c}^{+}CD8^{+}$ T cells also lasted longer in SIVagm than SIVmac infection (day 14 and day 2 p.i., respectively). In order to further comprehend the distribution of $NKG2_{a/c}^{+}CD8^{+}$T cells in the gut, we analyzed if their levels vary or not between distinct compartments of the intestine and analyzed ileum, jejunum and colon from healthy, acutely (day 9 p.i.) and chronically infected animals (Fig.4 j). In CM, the $NKG2_{a/c}^{+}CD8^{+}$T cell levels did not change in the three intestinal compartments compared to uninfected animals, besides a trend for decrease in acute (day 9 p.i.) infection. In AGM, the $NKG2_{a/c}^{+}CD8^{+}$ T cells showed a trend for increases in acute and chronic infection when compared to before infection. Thus, we did not observe differences between ileum, jejunum and colon and observed in all intestinal compartment signs for stronger and more long-lasting increases of the $NKG2_{a/c}^{+}CD8^{+}$ T cells in the gut during SIVagm than during SIVmac infection. Altogether, increases of $NKG2_{a/c}^{+}CD8^{+}$ T cells were seen in the intestine during SIVagm infection but not in secondary lymphoid organs.

We analyzed the functional phenotype of these intestinal $NKG2_{a/c}^{+}CD8^{+}$T cells before and during SIV infection by measuring *ex vivo* cell-surface CD107a as well as intra-cellular IFN-g and Perforin in unstimulated cells (Fig.4k-m). Perforin and CD107a expression were rapidly and strongly increased in $NKG2_{a/c}^{+}CD8^{+}$ T cells from rectal biopsies of SIV-infected CM and AGM starting from day 2 p.i. and throughout day 14 p.i. at least. The changes in IFN-g expression were not significant (Fig.4i). Altogether, the effector activity of $NKG2_{a/c}^{+}$ $CD8^{+}$ T cells was mobilized in the intestine upon SIV infection in both CM and AGM. This mobilization in the intestine occurred very early (day 2 p.i.) in both CM and AGM. In both species, the cytotoxic marker was more up-regulated than IFN-g. While the functional profile of the cells in the gut was similar between the two types of infection, the levels of $NKG2_{a/c}^{+}$ $CD8^{+}$ T cells expanded more in SIVagm than in SIVmac infection.

Transcriptional signatures in $NKG2_{a/c}^{+}CD8^{+}$T cells during SIVagm infection indicates cytotoxic effector concomitant with regulatory functions

The $NKG2_{a/c}^{+}CD8^{+}$ T cells were therefore expanded in blood and intestine during non-pathogenic SIV infection. In order to define them in-depth, we determined their genome-wide transcriptome. Three distinct $CD8^{+}$ T cell subpopulations were sorted from blood of five chronically SIVagm-infected AGM: the $NKG2_{a/c}^{+}CD8^{+}$ T cells as well as the conventional memory and effector $CD8^{+}$ T cells. As shown in the heatmaps, the $NKG2_{a/c}^{+}CD8^{+}$ T cells clustered clearly separately from both the memory and effector conventional $CD8^{+}$ T cells (Fig. 5a). The analysis revealed differential expression for 298 genes when $NKG2_{a/c}^{+}CD8^{+}$ T cells were compared to memory $CD8^{+}$ T cells (Fig. 5a) and 252 genes when compared to effector $CD8^{+}$ T cells (Fig. 5b). The number of total genes that were commonly differentially regulated in $NKG2_{a/c}^{+}$ versus conventional $CD8^{+}$ T cells are displayed in the Venn diagrams (Fig. 5c). All up- and down-regulated genes are listed in Supplementary Tables 2 and 3. The 37 genes that were up-regulated in $NKG2_{a/c}^{+}CD8^{+}$ T cells compared to the other $CD8^{+}$ T cells and the four 4 genes that were down-regulated are shown in Figure 5d.

Among the up-regulated genes in the $NKG2_{a/c}^{+}CD8^{+}$ T cells figured many NK cell receptors, such as NKp46, KIR2DL4, KIR3DL3, KIR2DL1, and both KLRC1 (NKG2A) and KLRC2 (NKG2C). The $NKG2_{a/c}^{+}CD8^{+}$ T cells also expressed higher levels of CXCR6 and of the cytokine receptor IL23R compared to the conventional effector $CD8^{+}$ T cells (Fig. 5a, b and d) suggesting a gut homing profile, in line with the data described above. Indeed, IL-23 is known to be expressed by intestinal myeloid cells, which is also the case of the CXCR6-ligand CXCL16 and CXCR6 can be expressed by intestinal activated lymphocytes[30,32]. The $NKG2_{a/c}^{+}CD8^{+}$ T cells expressed similar levels of IL-15R than the conventional memory and effector $CD8^{+}$ T cells. They expressed higher levels of cytolytic granules (ie Granzyme A and B, Perforin, NKG7, NCR1) as well as of CCL4 (MIP1-b) and TBX21 (t-bet) while lower levels of the immune checkpoint molecule Lag-3 when compared to the conventional memory $CD8^{+}$ T cells, in line with their effector phenotype (Fig. 5b and d). The molecular profiles

also revealed lower expression of LAMTOR1 and higher levels of CD73 (NT5E), IGFBP3, and CREM when compared to conventional effector $CD8^+$ T cells (Fig.5b and d). These molecules are associated with regulatory function of cellular metabolism and T cell activity. In addition, CD26 (DPP4), SerpinA3 and SerpinA5, the latest having anti-protease inhibitor and wound healing functions were also increased in the $NKG2_{a/c}^+CD8^+$ T cells compared to the conventional CD8+ T cells (Fig.5d)[33].

Together, these data demonstrate that the $NKG2_{a/c}^+CD8^+$ T cells present during SIVagm infection have a transcriptional expression profile clearly distinct from other $CD8^+$ T cell populations. They confirm the NK-cell like properties, the effector and cytotoxic profile as well as the preferential gut homing profile. Furthermore, they support a regulatory function of these cells.

NKG2a/c+CD8+T cells correlated negatively with IL-23 in the intestine during SIVmac infection

We next explored markers of intestinal inflammation and tissue stress. We therefore measured IL-23, CXCL10 and Hsp60. We chose IL-23 because the transcriptomic analysis revealed that NKG2a/c^+CD8^+ T cells express high levels of IL23R and because this cytokine is associated with inflammatory diseases in the gut. CXCL10 (IP-10) was selected because it was shown that it is increased in the gut during SIVmac infection (Ploquin et al, Plos Path 2016). It is the ligand of CXCR3 that is expressed on the majority of NKG2a/c^+CD8^+ T cells at steady state (Fig.1). CD26 that was up-regulated in the NKG2a/c^+CD8^+ T cells is known to cleave CXCL10. HSP60 is a stress protein which has shown to be an independent *marker for* inflammatory bold disease[34].

The levels of CXCL10 were increased already at day 2 p.i. in SIVagm infection, and not in SIVmac infection, as previously described (Fig. 6a-b)[35]. At the opposite, plasma levels of soluble Hsp60 showed significant increases at days 2 p.i in SIVmac infection, but not in SIVmac infection. HSP60 levels correlated with NKG2a/c^+CD8^+ T cell counts, in particular in SIVagm infection (Fig. 6c-d). We next investigated HSP60 levels in the intestine. Longitudinal analyses of Hsp60 protein in supernatants of rectal biopsies collected longitudinally showed high expression of HSP60 at day 2 p.i. and in chronic phase (day 80 p.i.) of SIVmac infection, whereas no increase was observed after SIVagm infection (Fig. 6e-f). IL-23 levels showed trends for increases in the gut. They correlated negatively with NKG2a/c^+CD8^+ T cell counts during SIVmac infection (Fig. 6g-h).

Altogether, the levels of Hsp60 in the intestine were increased in SIVmac but not in SIVagm infection. IL-23 in the gut correlated negatively with intestinal NKG2a/c^+CD8^+ T cell levels in SIVmac infection.

Discussion

Protection against viral-induced tissue damage can generally be achieved either through strong pathogen control or through resilience strategies[36]. The latter could include improved homeostatic mechanisms, improved wound healing, control of inflammation and/or resistance to stress[37]. In this report, we provide novel insights into the potential role of NKG2a/c expressing CD8+ T cells during SIV infection. We compared non-pathogenic SIVagm infection in the natural host (AGM) compared to pathogenic SIVmac infection in macaques, the latter modeling HIV infection. In both species, the SIV virus replicated to high titers in blood and intestine throughout chronic infection. Genome-wide transcriptome analysis of the NKG2a/c^+ $CD8^+$ T cells in SIVagm infection demonstrated the cytotoxic effector function and gut homing profile of these cells and also revealed the expression of immunoregulatory molecules. Based on the transcriptome profile, the cells detected here resemble most the regulatory $CD8^+$ T cells described in mice and humans during inflammatory conditions in the intestine[38]. In both SIVagm and SIVmac infection, the expression of the cytotoxic marker (Perforin) was more up-regulated than IFN-g, suggesting a more cytotoxic than pro-inflammatory activity of these cells in the intestine. We detected a negative correlation between IL-23 levels in intestine and intestinal NKG2a/c+CD8+ T

cells during pathogenic infection, whereas a low level of IL-23 was observed concomitantly to high frequency of NKG2a/c+CD8+ T cells in the gut during infection in the natural host. Together these results suggest that these cells might rather contribute to inflammatory control in the gut than to control of viral replication in the case of SIV, and thereby probably also HIV infection.

The cytotoxicity markers were upregulated very strongly in the gut of both CM and AGM. However, the overall frequencies of $NKG2_{a/c}^{+}CD8^{+}$ T cells in the intestine increased for a longer period in SIVagm than in SIVmac infection. The follow up of the tissue dynamics of NKG2a/c+CD8+ T cells indeed revealed differences between pathogenic and non-pathogenic SIV infection. By performing longitudinal studies simultaneously in distinct tissues, we show a more intense expansion of NKG2a/c+CD8+ T cells in the blood and intestine in response to SIVagm in AGM compared to SIVmac infection. The expansions were associated with viremia levels suggesting that antigenic stimulation is driving the expansions. NKG2A recognizes peptides presented via the non-classical MHC-E class I molecule. The peptides presented via MHC-E can be also be recognized by activatory NKG2C receptor as well as by the TCR. On NHP, the available antibodies cannot distinguish between the NKG2A and NKG2C and thus a phenotypic analysis was not possible. However, the transcriptome analyses showed that NKG2a/c+CD8+ T cells also expressed NKG2C mRNA. The expression levels of NKG2C were however not higher than those of NKG2A. Similarly, in humans, the proportion of CD8+ T expressing the activatory NKG2C receptor was similar between PLWH and healthy donors and also between viremic and non-viremic patients, suggesting that NKG2C regulation on these cells is not participating in a better control of HIV infection[25].

A clonal expansion of these cells, similar to what has been described for these cells in other settings is not excluded[39]. A scenario has been proposed whereby maintaining or upregulating NKG2A upon TCR engagement by subset of CTL clones could exerts a negative feed-back on TCR activation[16]. Such regulation is reminiscent of the CTLA-4/B7 regulatory loop[40] but has specific features adapted to the biology of memory/effector CTL in the intestinal epithelium. Indeed, CD94/NKG2A and MHC-E but not CTLA-4/B7 are significantly expressed in the intestinal environment[15]. Thereby, in natural host, the intestine environment with a high antigenic load might allow NKG2a/c+CD8+ T cells to respond initially and maximally to SIV antigens, submitting them later on to a fine-tuning of their TCR signaling threshold in order to down-modulate persisting immune reactions that might otherwise lead to chronic inflammation and tissue destruction. Concomitantly, the expansion of NKG2a/c+CD8+ T cells could facilitate viral persistence which agrees with the high level of viral replication observed in intestine of natural host.

MHC-E displays a selective preference for peptides derived from the leader sequence of various MHC class I alleles. Binding of a peptide is needed to stabilize and increase MHC-E expression at the cell surface. MHC-E is expressed on most cells, including on CD4+ T cells and also to high levels on intestinal epithelial cells. MHC-E has been described to be upregulated during HIV-1 and SIVmac infections in CD4+ T cells, both on infected and un-infected CD4+ T cells respectively in vitro and in vivo [41,42]. The up-regulation on un-infected cells might be a consequence of stronger expression of classical MHC-I molecules in activated CD4+ T cells and/or of HIV proteins that directly modify the expression levels of MHC-E in infected cells[41,43]. Among the small numbers of other cellular peptides that have been identified to bind to MHC-E and stimulate CD8+ T cells is a HSP60-derived peptide[44]. Under stress conditions, Hsp60 is sufficiently processed and competes with the MHC-I derived peptides for presentation by MHC-E. Therefore, changes in the level of the Hsp60 peptide presented by MHC-E during SIV infection, relative to the amount of MHC class Ia-derived leader, may result in the activation of NKG2a/c+CD8+ T cells in natural host and enhanced killing of un-infected, stressed cells in the intestine of SVagm-infected AGM. We report here increased levels of HSP60 protein in the intestine of SIVmac-infected MAC, while they were not increased in SIVagm infection. Therefore, either there are less stressed cells in SIVagm infection and thereby less uninfected cells would be killed by this mechanism, or alternatively, the stressed cells are more efficiently eliminated by NKG2A+CD8+ T cells in SIVagm infection

allowing improved tissue repair. In order to differentiate between these mechanisms, and between NKG2A and TcR mediated recognition, the tetramers would be useful in the future. An intervention study to prove the immunoregulatory role of these cells in the gut of SIV-infected animals could not be performed. Indeed, by targeting NKG2A, one would also inhibit NK cell responses in the animals, NKG2A being expressed on >80% of NK cells in NHP (Huot Frontiers in press).

The up-regulation of CD94/NKG2A and other NK cell receptors on CD8+ T cells is a general feature of the immune response and the extent of up-regulation is variable. It is notable that expression of CD94/NKG2A is known to be influenced by a number of cytokines. Indeed, IL-6, IL-10, and IL-21, increases CD94/NKG2A expression, whereas IL-4, IL-23, and TGF-β are strongly inhibitory[13]. Unlike IL-2, the capacity of IL-4, IL-23, and TGF-β to inhibit CD94/NKG2A expression is CD28 independent. Differences in the tissue cytokine environment between SIVagm and SIVmac infection, as described[45–48] could explain the differences we observed regarding the dynamics of the NKG2a/c+CD8+ T cells.

This is a large study, in multiple tissues, that were analyzed transversally and longitudinally including ex vivo analyses on functional profiles of unstimulated cells and a genome-wide transcriptomic study. Altogether we demonstrate that NKG2a/c+CD8 T cells do not expand in LN but in the blood and intestine during non-pathogenic SIV infections. They display a strong cytotoxic and immunoregulatory function. We show that they correlate negatively with intestinal inflammation. This study suggests that NKG2a/c+CD8 T cells do not contribute to viral control, as expected, but that they participate in the control of immunopathology in the intestine during SIV and may be also HIV infection.

REFERENCES

1. Hunt, P. W. *et al.* A Low T Regulatory Cell Response May Contribute to Both Viral Control and Generalized Immune Activation in HIV Controllers. *PLOS ONE* **6**, e15924 (2011).
2. Zeng, M. *et al.* Lymphoid Tissue Damage in HIV-1 Infection Depletes Naïve T Cells and Limits T Cell Reconstitution after Antiretroviral Therapy. *PLOS Pathog.* **8**, e1002437 (2012).
3. Brenchley, J. M., Silvestri, G. & Douek, D. C. Nonprogressive and Progressive Primate Immunodeficiency Lentivirus Infections. *Immunity* **32**, 737–742 (2010).
4. Hunt, P. W. *et al.* Gut Epithelial Barrier Dysfunction and Innate Immune Activation Predict Mortality in Treated HIV Infection. *J. Infect. Dis.* **210**, 1228–1238 (2014).
5. Schuetz, A. *et al.* Initiation of ART during Early Acute HIV Infection Preserves Mucosal Th17 Function and Reverses HIV-Related Immune Activation. *PLOS Pathog.* **10**, e1004543 (2014).
6. Collins, D. R., Gaiha, G. D. & Walker, B. D. CD8 + T cells in HIV control, cure and prevention. *Nat. Rev. Immunol.* **20**, 471–482 (2020).
7. Cao, Y. (ORCID:0000000258800006), Cartwright, E., Silvestri, G. & Perelson, A. S. (ORCID:0000000224550002). CD8+ lymphocyte control of SIV infection during antiretroviral therapy. *PLoS Pathog.* **14**, (2018).
8. Kaufmann, D. & Walker, B. PD-1 and CTLA-4 Inhibitory Cosignaling Pathways in HIV Infection and the Potential for Therapeutic Intervention. *J. Immunol. Baltim. Md 1950* **182**, 5891–7 (2009).

9. L, T., R, S., R, V. & O, M. Immune checkpoint inhibitors and radiotherapy-concept and review of current literature. *Ann. Transl. Med.* **6**, 155–155 (2018).
10. Odorizzi, P. M. & Wherry, E. J. Inhibitory receptors on lymphocytes: insights from infections. *J. Immunol. Baltim. Md 1950* **188**, 2957–2965 (2012).
11. Mingari, M. C., Pietra, G. & Moretta, L. Immune Checkpoint Inhibitors: Anti-NKG2A Antibodies on Board. *Trends Immunol.* **40**, 83–85 (2019).
12. Thimme, R. *et al.* Increased expression of the NK cell receptor KLRG1 by virus-specific CD8 T cells during persistent antigen stimulation. *J. Virol.* **79**, 12112–12116 (2005).
13. Cho, J.-H. *et al.* Calcineurin-dependent negative regulation of CD94/NKG2A expression on naive CD8+ T cells. *Blood* **118**, 116–128 (2011).
14. Hj, K. & H, C. Regulation of self-tolerance by Qa-1-restricted CD8(+) regulatory T cells. *Semin. Immunol.* **23**, 446–452 (2011).
15. Jabri, B. *et al.* TCR specificity dictates CD94/NKG2A expression by human CTL. *Immunity* **17**, 487–499 (2002).
16. Eugène, J. *et al.* The inhibitory receptor CD94/NKG2A on CD8 + tumor-infiltrating lymphocytes in colorectal cancer: a promising new druggable immune checkpoint in the context of HLAE/β2m overexpression. *Mod. Pathol.* **33**, 468–482 (2020).
17. Sun, H., Sun, C., Xiao, W. & Sun, R. Tissue-resident lymphocytes: from adaptive to innate immunity. *Cell. Mol. Immunol.* **16**, 205–215 (2019).
18. N, van M. *et al.* NKG2A Blockade Potentiates CD8 T Cell Immunity Induced by Cancer Vaccines. *Cell* **175**, 1744-1755.e15 (2018).
19. CD94-NKG2A receptors regulate antiviral CD8+ T cell responses. *Nat. Immunol.* **3**, (2002).
20. Früh, K. & Picker, L. CD8+ T cell programming by cytomegalovirus vectors: applications in prophylactic and therapeutic vaccination. *Curr. Opin. Immunol.* **47**, 52–56 (2017).
21. Miller, J. D. *et al.* CD94/NKG2 Expression Does Not Inhibit Cytotoxic Function of Lymphocytic Choriomeningitis Virus-Specific CD8+ T Cells. *J. Immunol.* **169**, 693–701 (2002).
22. Keynan, Y. *et al.* The Role of Regulatory T Cells in Chronic and Acute Viral Infections. *Clin. Infect. Dis. Off. Publ. Infect. Dis. Soc. Am.* **46**, 1046–52 (2008).
23. Maria, A. D. *et al.* Expression of HLA class I-specific inhibitory natural killer cell receptors in HIV-specific cytolytic T lymphocytes: Impairment of specific cytolytic functions. *Proc. Natl. Acad. Sci.* **94**, 10285–10288 (1997).
24. D, W. & D, K. Differential expression of natural killer receptors on Vdelta1 gammadelta T cells in HIV-1-infected individuals. *J. Acquir. Immune Defic. Syndr. 1999* **33**, 420–425 (2003).
25. Zeddou, M. *et al.* Downregulation of CD94/NKG2A inhibitory receptors on CD8+T cells in HIV infection is more pronounced in subjects with detected viral load than in their aviraemic counterparts. *Retrovirology* **4**, 72 (2007).

26. Hansen, S. G. *et al.* Broadly targeted CD8+ T cell responses restricted by major histocompatibility complex E. *Science* (2016) doi:10.1126/science.aac9475.
27. M, P. Th17 cells in natural SIV hosts. *Curr. Opin. HIV AIDS* **5**, 166–172 (2010).
28. Garcia-Tellez, T. *et al.* Non-human primates in HIV research: Achievements, limits and alternatives. *Infect. Genet. Evol.* **46**, 324–332 (2016).
29. Sagebiel, A. F. *et al.* Tissue-resident Eomes+ NK cells are the major innate lymphoid cell population in human infant intestine. *Nat. Commun.* **10**, (2019).
30. Sato, T. *et al.* Role for CXCR6 in Recruitment of Activated CD8+ Lymphocytes to Inflamed Liver. *J. Immunol.* **174**, 277–283 (2005).
31. Maloy, K. J. & Kullberg, M. C. IL-23 and Th17 cytokines in intestinal homeostasis. *Mucosal Immunol.* **1**, 339–349 (2008).
32. Diegelmann, J. *et al.* Expression and regulation of the chemokine CXCL16 in Crohn's disease and models of intestinal inflammation. *Inflamm. Bowel Dis.* **16**, 1871–1881 (2010).
33. Miyagawa, I. *et al.* Induction of Regulatory T Cells and Its Regulation with Insulin-like Growth Factor/Insulin-like Growth Factor Binding Protein-4 by Human Mesenchymal Stem Cells. *J. Immunol.* **199**, 1616–1625 (2017).
34. Cappello, F. *et al.* Hsp60 as a Novel Target in IBD Management: A Prospect. *Front. Pharmacol.* **10**, (2019).
35. Ploquin, M. J. *et al.* Elevated Basal Pre-infection CXCL10 in Plasma and in the Small Intestine after Infection Are Associated with More Rapid HIV/SIV Disease Onset. *PLOS Pathog.* **12**, e1005774 (2016).
36. Chovatiya, R. & Medzhitov, R. Stress, inflammation, and defense of homeostasis. *Mol. Cell* **54**, 281–288 (2014).
37. Cohen, S. *et al.* Chronic stress, glucocorticoid receptor resistance, inflammation, and disease risk. *Proc. Natl. Acad. Sci. U. S. A.* **109**, 5995–5999 (2012).
38. Allez, M. & Mayer, L. Regulatory T CellsPeace Keepers in the Gut. *Inflamm. Bowel Dis.* **10**, 666–676 (2004).
39. Warren, H. S. *et al.* CD8 T cells expressing killer Ig-like receptors and NKG2A are present in cord blood and express a more naïve phenotype than their counterparts in adult blood. *J. Leukoc. Biol.* **79**, 1252–1259 (2006).
40. Griffin, M. *et al.* Blockade of T Cell Activation Using a Surface-Linked Single-Chain Antibody to CTLA-4 (CD152)1. *J. Immunol.* **164**, 4433–4442 (2000).
41. J, N. *et al.* HIV-1 infection leads to increased HLA-E expression resulting in impaired function of natural killer cells. *Antivir. Ther.* **10**, 95–107 (2005).
42. Wu, H. L. *et al.* The role of MHC-E in T cell immunity is conserved among humans, rhesus macaques, and cynomolgus macaques. *J. Immunol. Baltim. Md 1950* **200**, 49–60 (2018).

43. Takao, S., Ishikawa, T., Yamashita, K. & Uchiyama, T. The rapid induction of HLA-E is essential for the survival of antigen-activated naive CD4 T cells from attack by NK cells. *J. Immunol. Baltim. Md 1950* **185**, 6031–6040 (2010).
44. Michaëlsson, J. *et al.* A Signal Peptide Derived from hsp60 Binds HLA-E and Interferes with CD94/NKG2A Recognition. *J. Exp. Med.* **196**, 1403–1414 (2002).
45. Micci, L. *et al.* Paucity of IL-21-producing CD4(+) T cells is associated with Th17 cell depletion in SIV infection of rhesus macaques. *Blood* **120**, 3925–3935 (2012).
46. Hong, J. J. *et al.* Early initiation of antiretroviral treatment post SIV infection does not resolve lymphoid tissue activation. *AIDS Lond. Engl.* **31**, 1819–1824 (2017).
47. Ploquin, M. J.-Y. *et al.* Distinct expression profiles of TGF-β1 signaling mediators in pathogenic SIVmac and non-pathogenic SIVagm infections. *Retrovirology* **3**, 37 (2006).
48. Manickam, C., Shah, S. V., Lucar, O., Ram, D. R. & Reeves, R. K. Cytokine-Mediated Tissue Injury in Non-human Primate Models of Viral Infections. *Front. Immunol.* **9**, (2018).
49. Diop, O. *et al.* High Levels of Viral Replication during Primary Simian Immunodeficiency Virus SIVagm Infection Are Rapidly and Strongly Controlled in African Green Monkeys. *J. Virol.* **74**, 7538–47 (2000).
50. Jacquelin, B. *et al.* Nonpathogenic SIV infection of African green monkeys induces a strong but rapidly controlled type I IFN response. *J. Clin. Invest.* **119**, 3544–3555 (2009).
51. Huot, N. *et al.* Natural killer cells migrate into and control simian immunodeficiency virus replication in lymph node follicles in African green monkeys. *Nat. Med.* **23**, 1277–1286 (2017).
52. Jacquelin, B. *et al.* Innate immune responses and rapid control of inflammation in African green monkeys treated or not with interferon-alpha during primary SIVagm infection. *PLoS Pathog.* **10**, e1004241 (2014).

MATERIAL AND METHODS

Monkeys and SIV infections

Nineteen African green monkeys (Caribbean *Chlorocebus sabaeus,* AGM), 22 cynomolgus macaques (*Macaca fascicularis,* CM) and 18 rhesus macaques (*M. mulatta*, RM) were included in the study. The AGM were infected with SIVagm.sab92018 and the macaques with either SIVmac251 or SIVmac239 as previously described[49–51]. The ART-treated CM are part of the SIVART cohort from the ANRS. They were infected with SIVmac251 and treated for >12 months with the combination of TDF, FTC and DTG and virologically suppressed at the time of the study. Viral load in AGM, CM and RM was quantified as previously described[51,52]. The description of the animals (viremia, $CD4^+$ T cell counts) is given in Supplementary Figures 1 and 2 and Supplemental Method Figure 1.

The AGM and CM were housed at the IDMIT Center (Fontenay-aux-Roses, France) and the RM at the German Primate Center (DPZ). All experimental procedures were conducted in strict accordance with the international European guidelines 2010/63/UE on the protection of animals used for experimentation and other scientific purposes, with the German and French law (French decree 2013-118) and the recommendations of the Weatherall report. The IDMIT center complies with the Standards for Human Care and Use of the Office for

Laboratory Animal Welfare (OLAW, USA) under OLAW Assurance number A5826-86. The DPZ has the permission to breed and house NHPs under license number 392001/7 granted by the local veterinary office and conforming with §11 of the German Animal Welfare act. Monitoring of the monkeys was under the supervision of the veterinarians in charge of the animal facilities. The animals used here were shared with other studies[51] (Huot Frontiers in press). Animal experimental protocols were approved by the Ethical Committee of Animal Experimentation (CETEA-DSV, IDF, France) (Notification 12-098 and A17-044) and the Lower Saxony State Office for Consumer Protection and Food Safety and performed with the project licenses 33.19-42502-04-12/0820 and 33.19-42502-04-17/2500.
Monkeys were sedated with Ketamine Chlorhydrate (Rhone-Mérieux, Lyons, France) before handling. The sample size varied between 3 and 9 monkeys per group (n = 6 in most experiments). Sample collection was performed in random order, according to the tripartite harmonized International Council for Harmonization of Technical Requirements for Pharmaceuticals for Human Use (ICH) Guideline on Methodology (previously coded Q2B). The investigators were not blinded while the animal handlers were blinded to group allocation.

Tissues collection and processing for flow analysis
Whole blood was collected in EDTA tubes. Mononuclear cells were isolated by Ficoll density-gradient centrifugation. Lymph node and rectal biopsies were collected longitudinally before and during infection and cleaned of adhering connective and fat tissues. The other tissues were collected at autopsy. Fractions of the ileum, jejunum and colon were removed immediately after sacrifice, trimmed free of adjacent tissue and cleaned of stool. Adhering connective and fat tissues were carefully removed **and** approximately 7cm intestinal pieces were placed in PBS supplemented with 20 % of SVF, 1.0% Glutamine,0.8% antibiotics/antimycotics (all Sigma-Aldrich, St Louis, MO), 1 mM dithiothreitol (Roth, Karlsruhe, Germany) and 1.5 mM EDTA (Roth) and then cut in little pieces with a scissors. Cells were dissociated using the gentleMACS™ Dissociator technology (Miltenyi Biotec (Germany). The suspensions were centrifuged (7 min, 300g, RT) and cell pellets were re-suspended in DMEM containing fetal calf serum, L-glutamine and antibiotics. For each tissue cell suspension was filtrated subsequently through 100- and 40-µm cell strainers, and cells were washed with cold PBS. Cells were either immediately stained for flow cytometry or cryopreserved in 90% FBS, 10% DMSO and stored in liquid nitrogen vapor.

Tissue processing for immunofluorescence staining
Pieces of the gastrointestinal tract were fixed in 4% PBS buffered formaldehyde during 12 hours then washed in PBS and incubated in PBS with different concentration (10%, 20%, 30%) of sucrose during 72 h, and embedded in cryopreserved media Immuno Mount™. Immunofluorescence (IF) staining was performed on 5 mm sections of tissue obtained using a Cryostat (Leica Biosystems). Antigen unmasking was performed by cooking the sections in 10mM Citrate buffer at pH 6.0 in a pressure cooker for 23 min. Specimens were blocked in blocking buffer containing 5% serum gained from serum the host species of the respective secondary antibody. Antibodies and dilutions are listed in Supplementary Method Table 1. Images were acquired on the CellVoyager CV1000 Confocal Scanner System, (Yokogawa). Individual optical slices were collected at 1024 × 1024 pixel resolution. ImageJ software was used to assign colors to the channels collected.

Polychromatic flow cytometry
Cells were stained as previously described . Briefly, FcR blocking reagent (Miltenyi) was used to block unspecific antibody binding. Antibodies used are shown in Supplementary method Table 2. Flow cytometry acquisitions were done on an LSR II (BD Biosciences). Intra-cellular staining was performed using BD Cytofix/Cytoperm™. Intracellular cytokines were measured *ex vivo* without prior *in vitro* stimulation. The data were further analyzed using FlowJo 10.4.2 software (FlowJo, LLC, Ashland, OR, USA). *t*-SNE (*t*-distributed

stochastic neighbor embedding) was carried out using the *t*-SNE feature in FlowJo using 2000 iterations and a perplexity of 50.

Hsp60, IL-23 and IP-10 quantification

Hsp60, IL-23 and IP-10 were quantified in plasma and in supernatants of tissue biopsies. These supernatants consisted of the medium in which the biopsy was collected and kept for 2–3 hours at 4°C (500µl for one biopsy of similar size). Cells were prepared by homogenization in the same medium and the supernatant was collected after centrifugation. The proteins were quantified using the Mouse HSP60 ELISA Kit (AbCAM) according to the provider's instructions.

Cell sorting

Cells were thawed in 20% fetal bovine serum-containing media supplemented with Benzonase nuclease, washed and stained with Aqua Live/Dead stain (Molecular Probes). Cell counts and viabilities were determined (Life Technologies). After a washing step, cells were blocked using normal mouse IgG (Caltag). Cells were surface-stained for CD3 (SP34-2, dilution 1/10, BD), CD8 (BW135/80, dilution 1/20, Miltenyi), CD95 (DX2, dilution 1/20, BD), NKG2a/c (Z199, dilution 1/20, Beckman Coulter, Inc.), CD20 (2H7, dilution 1/20, Biolegend), CD14 (M5E2, dilution 1/25, BD) and CD28 (CD28.2, dilution 1/20, BD). Post-surface staining, cells were washed, filtered and $CD45^+$ $CD14^-$ $CD20^-CD3^+$ effector ($NKG2_{a/c}^-CD28^-CD95^+$), memory ($NKG2_{a/c}^-$ $CD28^+CD95^+$) and $NKG2_{a/c}^+$ $CD8^+$ T cells sorted on a FACS ARIA II (BD Biosciences). Cells were directly collected in a lysis buffer containing TCEP. All samples were re-examined by flow cytometry following sorting, to ensure purity above 99%.

RNA-seq profiling

RNA was isolated from the sorted cells using the RNeasy® Plus Micro Kit (74034, Qiagen). RNA integrity was verified with the Agilent Bioanalyzer. RNA molecules were treated for library preparation using the Truseq Stranded mRNA sample preparation kit (Illumina, San Diego, California) according to manufacturer's instructions. An initial poly(A) RNA isolation step (included in the Illumina protocol) is performed on 10 ng of total RNA to keep only the polyadenylated RNA fraction and remove the ribosomal RNA. A step of fragmentation is then performed on the enriched fraction, by divalent ions at high temperature. The fragmented RNA samples were randomly primed for reverse transcription followed by second-strand synthesis to create double-stranded cDNA fragments. No end repair step was necessary. An adenine was added to the 3'-end and specific Illumina adapters were ligated. Ligation products were submitted to PCR amplification. The obtained oriented libraries were controlled by Bioanalyzer DNA1000 Chips (Agilent, # 5067-1504) and quantified by spectrofluorimetry (Quant-iT™ High-Sensitivity DNA Assay Kit, #Q33120, Invitrogen). Sequencing was performed on the Illumina Hiseq2500 platform to generate single-end 100 bp reads bearing strand specificity.

RNA-seq data analyses

Reads were cleaned of adapter sequences and low-quality sequences using cutadapt version 1. 1162.Bowtie version 1.2.2, with default parameters, was used for alignment of reads on the reference genomes (Chlorocebus sabaeus from Ensembl release 90). Genes were counted using HTseq-count version 0.11.1. Count data were analyzed using R version 3.4.361 and the Bioconductor package DESeq2 version 1.18.162. The normalization and dispersion estimation were performed with DESeq2 using the default parameters and statistical tests for differential expression were performed applying the independent filtering algorithm. For each comparison, p-values were adjusted for multiple testing according to the Benjamini and Hochberg procedure and genes with an adjusted p-value lower than 0.05 were considered as differentially expressed.

Statistical analyses

Statistically significant differences were determined by the non-parametric unpaired t-test or by one-way analysis of variance followed by appropriate post hoc tests. Wilcoxon signed-rank tests were used to evaluate whether there was a statistically significant difference in the level of one given marker at a given time post-infection when compared to the baseline medians (day 0). Baseline medians in blood consisted of 3 to 6 pre-infection values per animal. In LNs, it consisted of 1 to 2 pre-infection values per animal. Wilcoxon rank-sum tests were used to compare continuous factors between two groups. Correlation analyses were performed according to the Spearman coefficient of correlation. Statistical computations were performed using Prism software (Graph Pad, La Jolla, CA) and SigmaStat software (Systat).

Data availability

RNA-seq data have been deposited in the ArrayExpress database under the accession number is E-MTAB-8664. The authors declare that all other data supporting the findings of this study are available within the article and its Supplementary Information files, or are available from the authors upon request.

ACKNOWLEDGMENTS

We are grateful for the excellent help from the veterinarians and staff at the IDMIT Center (Benoit Delache, Jean-Marie Helies, Raphaël Ho Tsong Fang, Julie Morin). We thank M. Mietsch and M. Daskalaki for comprehensive veterinary support and S. Heine, J. Hampe and N. Leuchte for excellent technical assistance. We also thank all the people who work on the Illumina Hiseq 2500 platform at the Institut Pasteur and specially R. Legendre and JY Coppee. NH was a recipient of a post-doctoral fellowship from the Fondation Beytout and PR of a PhD fellowship from the University Paris Diderot, Sorbonne Paris Cité. We gratefully acknowledge grant support from the ANRS, the Fondation Beytout and Fondation les Ailes to MMT and from MSDAvenir to ASC and MMT. We gratefully acknowledge the support from the ANRS for the SIVART cohort, from the French infrastructure investment through the ANR-11-INBS-0008 grant to the IDMIT center and through the PIA grant ANR-10-EQPX-02-01 to the FlowCyTech facility at IDMIT. We gratefully aknowledge the UtechS Photonic BioImaging (Imagopole), C2RT, Institut Pasteur, supported by the French National Research Agency (France BioImaging; ANR 10-INSB-04-01, Investments for the Future), for advice and access to the CV1000 system.

AUTHOR CONTRIBUTIONS

NH designed the experiments and the overall study; NH, PR, BW, CP and BJ performed the experiments; NH and PR developed the cytotoxic assay; NH and NT performed the transcriptome big data analyses; NH, PR, BJ, ASC and MMT analyzed the data; NH performed the statistical analyses; VC, BJ, DD, RLG, CSH and MMT coordinated the animal studies; CSH, CP and ASC provided samples; NH and MMT wrote the manuscript and all co-authors reviewed it; MMT supervised the study.

LEGENDS

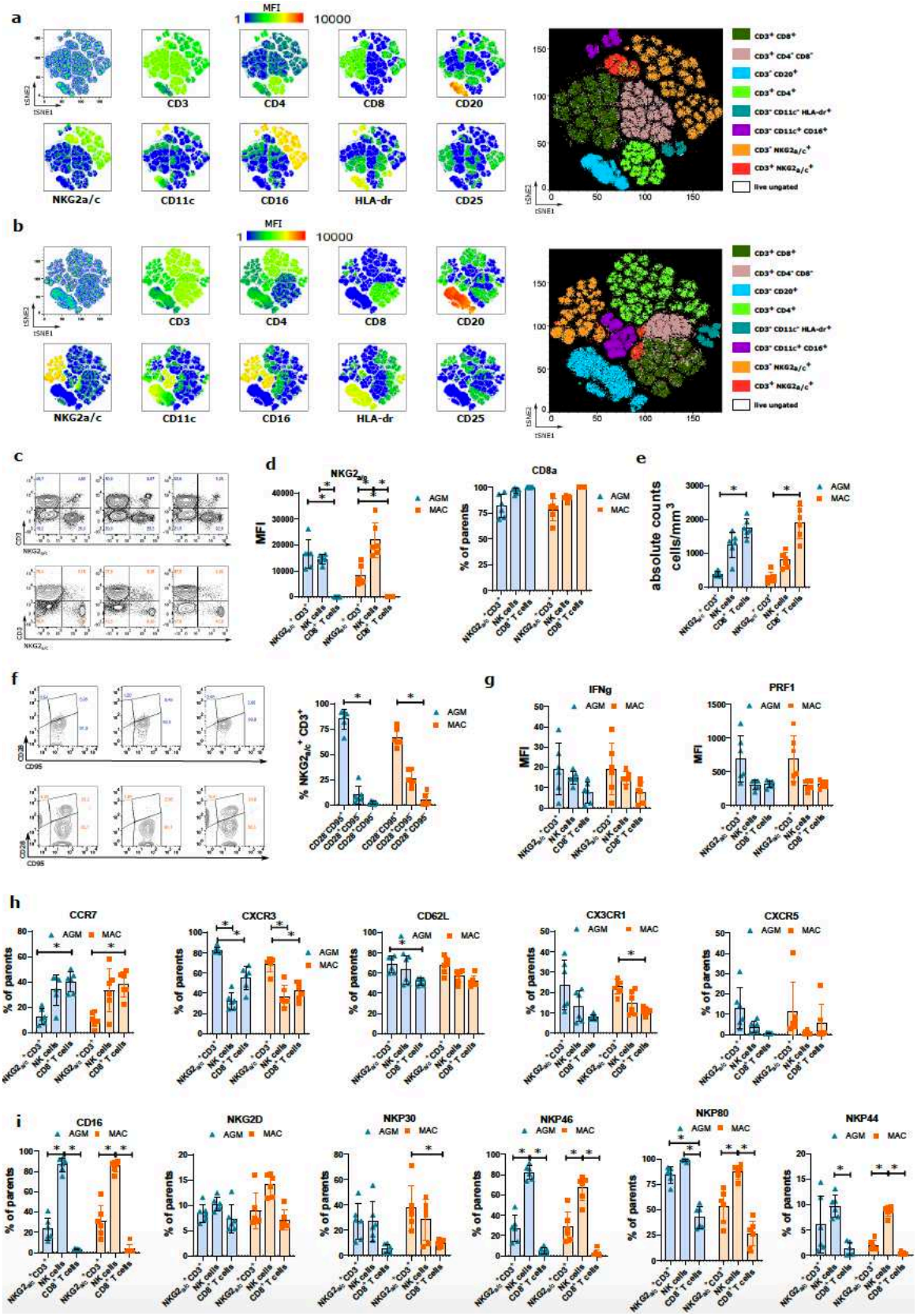


Figure 1. Identification and analysis of NKG2$_{a/c}$$^{+}$T cells in blood of healthy nonhuman primates. Analyses were performed on six monkeys per species. (**A and B)** Multidimensional viSNE analysis in blood cells of (**A**) AGM and (**B**) cynomolgus macaques (CM). Cells were stained with 16 markers and measured by flow cytometry. viSNE analysis was run on 60000 live CD45^{+} single cells per sample using all surface markers. (**C**) Gating of the NKG2$_{a/c}$$^{+}$T cells based on CD45^{+} lin^{-}CD3^{+}NKG2$_{a/c}$$^{+}$ cells. The numbers in each quadrant represent the percentage among CD45^{+} Lin^{-} cells in AGM (upper panel, blue) and CM (lower panel, orange).

Each panel represents a distinct animal. Data from three representative animals per species are shown. (**D**) Mean fluorescence intensity (MFI) of $NKG2_{A/C}$ at the surface $NKG2_{a/c}^{+}$ T cells, NK cells and conventional $CD8a^{+}$ T cells (left). Frequency of CD8a among $NKG2_{a/c}^{+}$T cells, NK cells and conventional $CD8a^{+}$ T cells (right). (**E**) Absolute numbers of $NKG2_{a/c}^{+}CD3^{+}$ T cell compared to NK and conventional $CD8a^{+}$ T cells. (**F**) Frequencies of naïve, memory and effector $NKG2_{a/c}^{+}$ T cells according to CD28 and CD95 expression. Dot plots with three representative animals per species are shown on the left. (**G**) Mean intensity fluorescence of intracellular cytokine expression *ex vivo*. (**H**) Frequency of cells expressing homing markers. (**K**) Frequencies of cells expressing NK cell markers. A nonparametric Mann–Whitney *U*-test was applied; $*p < 0.05$, $**p < 0.005$. Horizontal bars indicate median values, and error bars indicate standard deviation. Each symbol (triangles for AGM and rectangles for CM) represents a distinct animal.

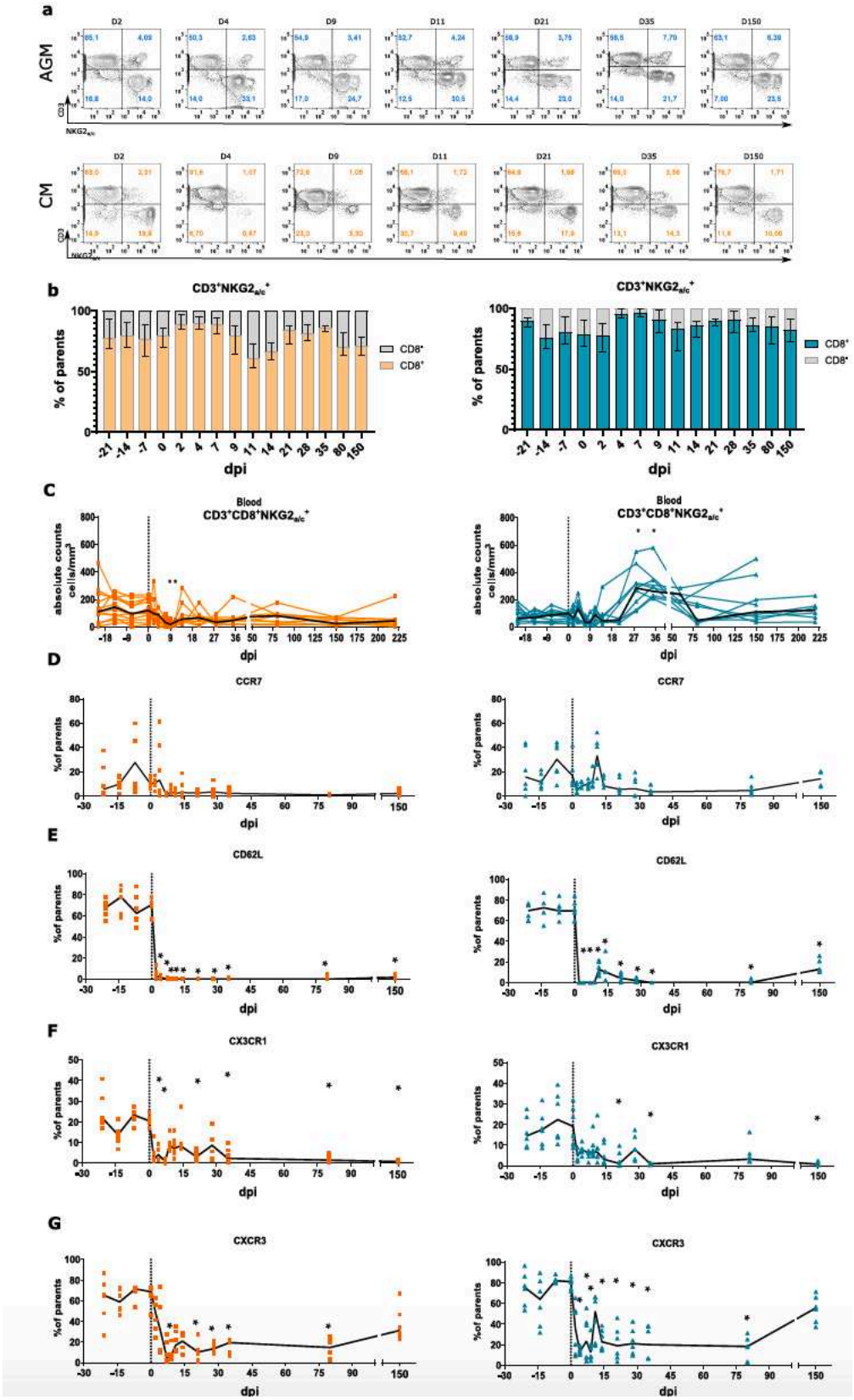


Figure 2. Dynamics of NKG2$_{a/c}^{+}$CD8^{+} T cells in blood during pathogenic SIVmac infection and non-pathogenic SIVagm infection. Nine animals per species were analysed. AGM are represented in blue and CM in orange. (**A**) Dot plots illustrating the dynamics of CD45^{+}CD20^{-}NKG2$_{A/C}^{+}$ T cells during SIV infection in AGM (upper panel) and CM (lower panel). The days after SIV infection are indicated at the top of each dot plot. The dot plots show a representative animal for each species. The numbers in each quadrant indicate the percentage of NKG2$_{A/C}^{+}$ T cells among CD45^{+} cells. (**B**) Frequency of CD8a+ cells among NKG2$_{a/c}^{+}$ T cells during SIV infection in CM (left) and AGM (right). (**C**) NKG2$_{a/c}^{+}$CD8^{+} T cell dynamics in response to SIV infection. The dark line represents the median. Day 0 represents the median value from all the time points

analyzed before infection. (**E-G**) Dynamics of $NKG2_{a/c}^{+}CD8^{+}$ T cells expressing homing markers. The cells were followed in blood before and during the time course of SIV infection in nine AGM (blue) and nine CM (orange). Each symbol represents an individual monkey, the black line the median values and day 0 the median values of all time points before infection. dpi: days post infection. *$p < 0.05$.

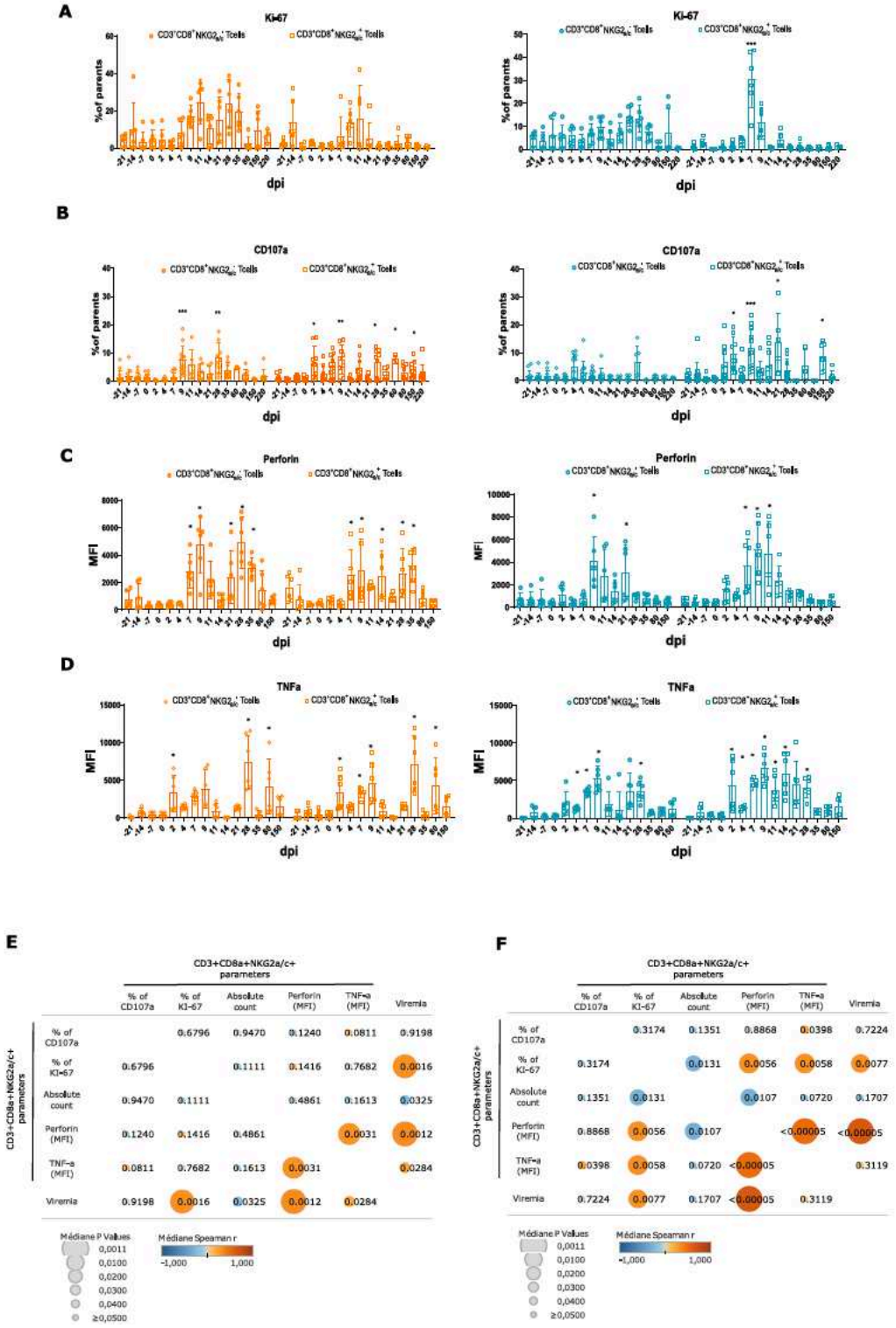


Figure 3. Longitudinal analysis of $NKG2_{a/c}^{+}CD8^{+}$ T cell proliferation and functional phenotypes in blood and evaluation of correlation with viremia. (**A-D)** Longitudinal analyses. Orange symbols indicate CM (left) and blue symbols AGM (right). Each symbol corresponds to a distinct animal. (**A)** Cell proliferation as evaluated by intracellular staining of Ki-67^{+}. (**B-D)** Ex vivo suppressor activity as evaluated by (**B**) surface staining of CD107a and intra cellular staining (**C**) of perforin and (**D**) TNF-a. Each symbol represents a distinct animal. dpi: days post infection. A nonparametric Mann–Whitney *U*-test was applied *$p < 0.05$, **$p < 0.005$,

***$p < 0.0005$. (**E-F**) Correlation matrix of measures of viremia and NKG2$_{a/c}^{+}$CD8^{+} T cells parameters. The Pearson correlation is shown. The matrix was built using the values obtained between day 0 and day 150 p.i from (**E**) 6 MAC and (**F**) 6 AGM.

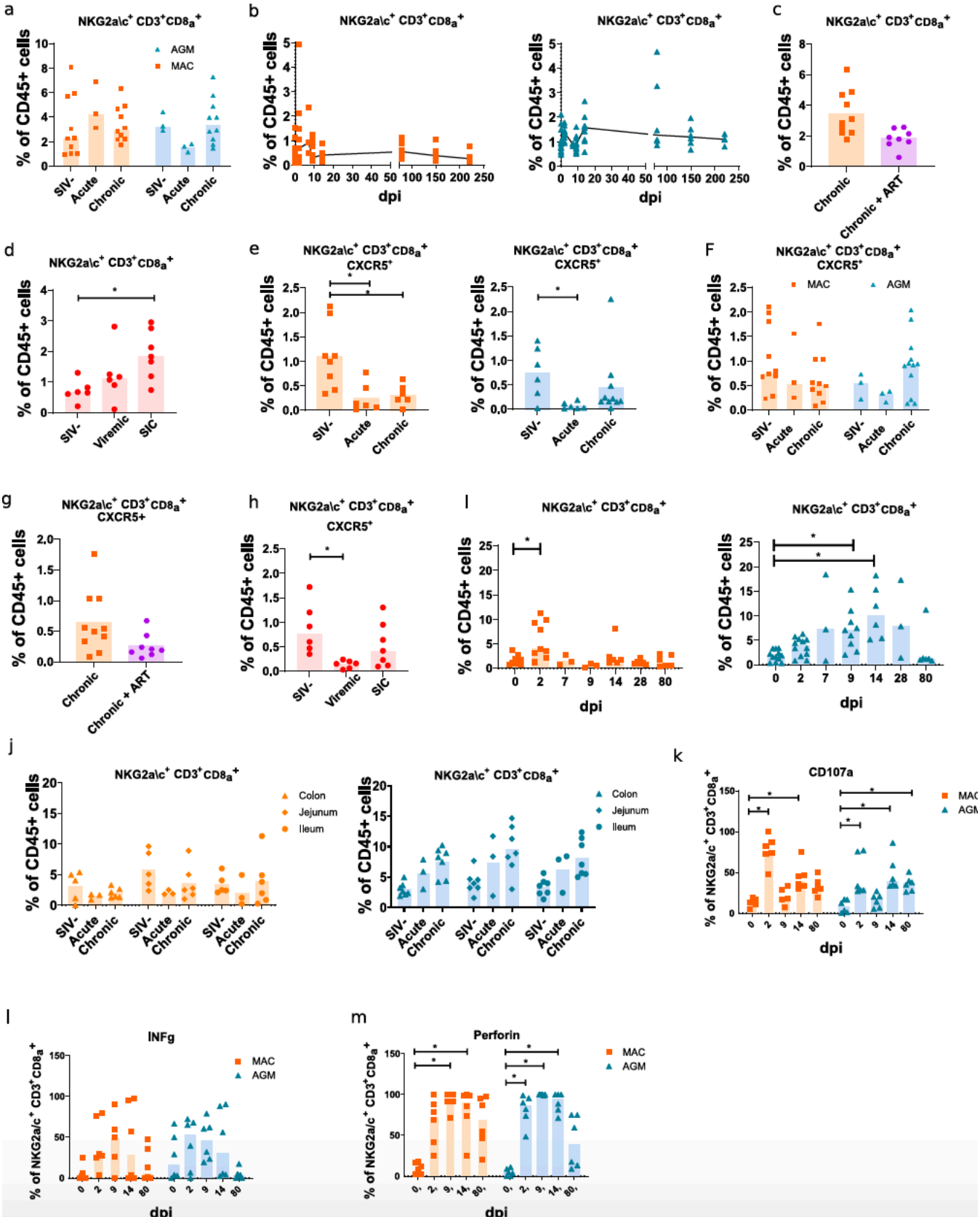


Figure 4. Dynamics and functional phenotype of NKG2$_{a/c}^{+}$CD8^{+} T cells in secondary lymphoid organs and intestine from naive and SIV-infected monkeys. Each symbol corresponds to a distinct animal. Orange symbols indicate CM, blue symbols AGM, violet symbols ART-treated CM and red symbols rhesus macaques

(RM). (**A**) Frequencies of $NKG2_{a/c}^{+}CD8^{+}$ T cells among $CD45^{+}$ cells in spleen from CM (orange) and AGM (blue). (**B**) Dynamics of $NKG2_{a/c}^{+}CD8^{+}$ T cells during SIV infection in peripheral lymph nodes (pLN) from CM (orange) and AGM (blue). The black line indicates the median values. (**C**) $NKG2_{a/c}^{+}CD8^{+}$ T cells in spleen of viremic and ART-treated virologically suppressed CM. **(D**) $NKG2_{a/c}^{+}CD8^{+}$ T cells in pLN of naive, viremic and virological controller (SIC) RM. (**E and F**) Frequencies of $NKG2_{a/c}^{+}CD8^{+}$ T cells expressing CXCR5 in (**E**) pLN and (**F**) spleen from CM (orange) and AGM (blue). (**G**) $NKG2_{a/c}^{+}CD8^{+}$ T cells expressing CXCR5 in spleen from viremic and ART-treated virologically suppressed CM. (**H**) $NKG2_{a/c}^{+}CD8^{+}$ T cells expressing CXCR5 in LN from naive, viremic and virological controller (SIC) RM. (**I**) Dynamics of $NKG2_{a/c}^{+}CD8^{+}$ T cells in rectal biopsies (RB) from CM (orange) and AGM (blue). (**J**) Dynamics of $NKG2_{a/c}^{+}CD8^{+}$ T cells in distinct intestinal compartments from CM (orange) and AGM (blue). (**K-M**) Lymphocytes were isolated from rectal biopsies and surface (CD107a) or intracellular staining (IFN-gamma and Perforin) were assessed *ex vivo* in $NKG2_{a/c}^{+}CD8^{+}$ T cells for CM (orange) and AGM (blue). dpi: days post infection. $*p < 0.05$.

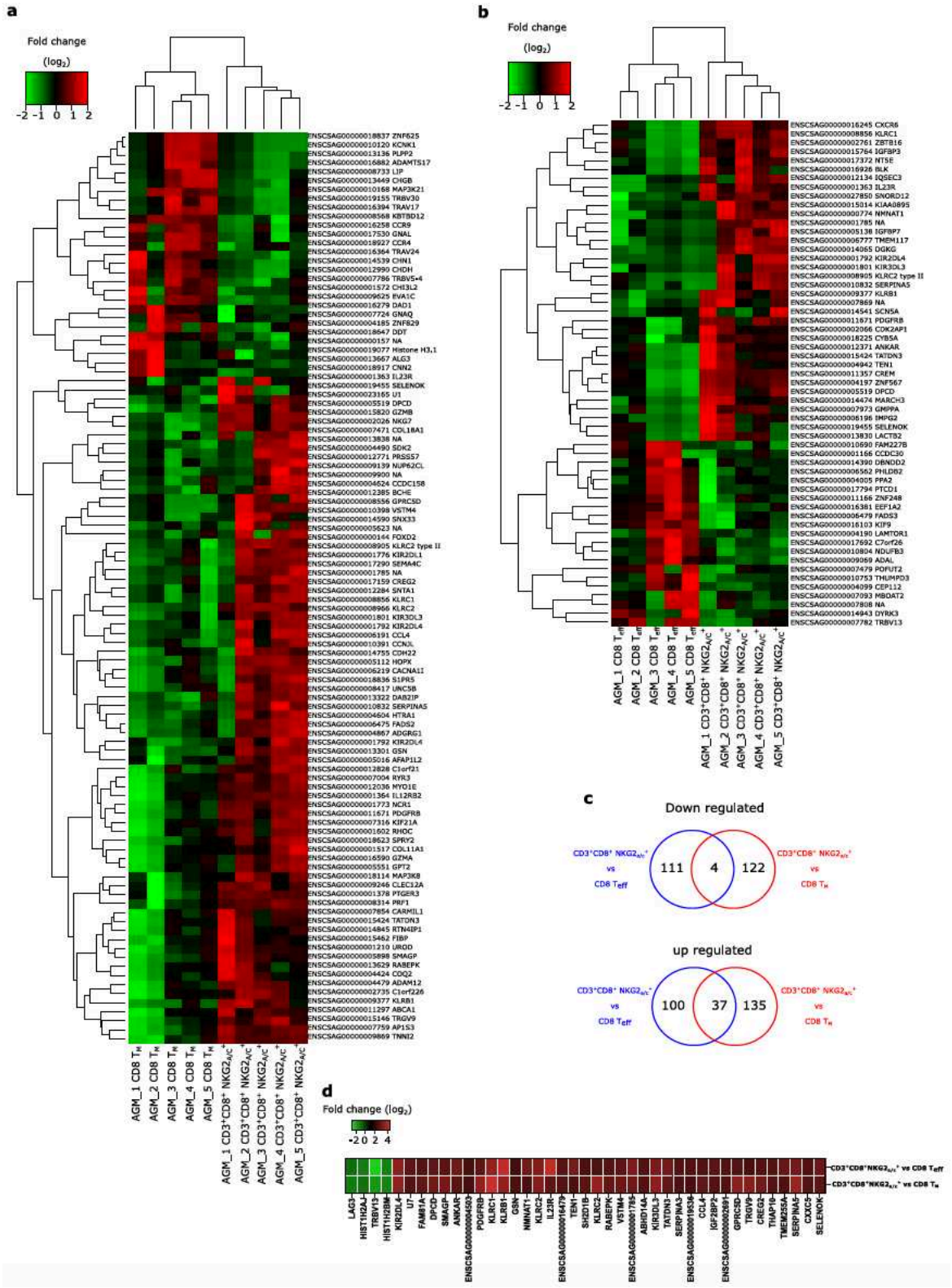


Figure 5. Genome-wide transcriptome analysis of NKG2$_{a/c}$$^{+}$CD8^{+} T cells. NKG2$_{a/c}$$^{+}$CD8^{+} T cells, conventional memory CD8^{+} T cells (CD95^{+}CD28^{+}) and conventional effector CD8^{+} T cells (CD95^{+}CD28^{-}) were sorted from blood of five chronically SIVagm-infected AGM. **(A-B)** Heat maps of unsupervised hierarchical clustering showing differentially expressed genes (**A**) between NKG2$_{a/c}$$^{+}$CD8^{+} T cells and conventional memory CD8^{+} T cells and (**B**) between NKG2$_{a/c}$$^{+}$CD8^{+} T cells and conventional effector CD8^{+} T cells. A p-value adjustment was performed to consider multiple testing and control the false positive rate to a chosen level. The level of controlled false positive rate was set to Padj <0.05. (**C**) Venn diagrams generated by the intersection of the down- or up-regulated genes with a padj <0.05. (**D**) Unsupervised heat map showing the

four down- and 37 up-regulated genes in the NKG2$_{a/c}^{+}$CD8^{+} T cells compared to both memory and effector conventional CD8^{+} T cells.

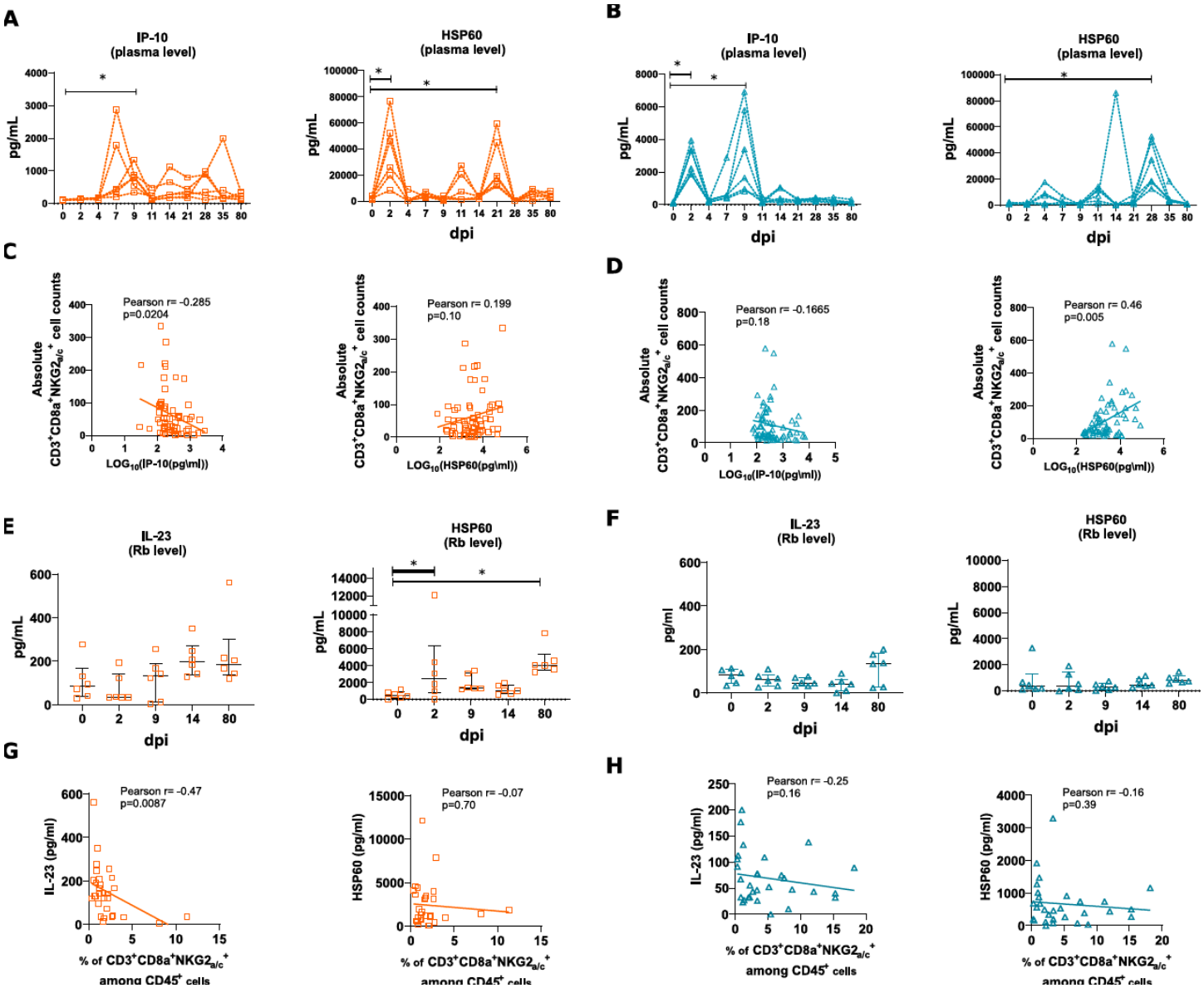
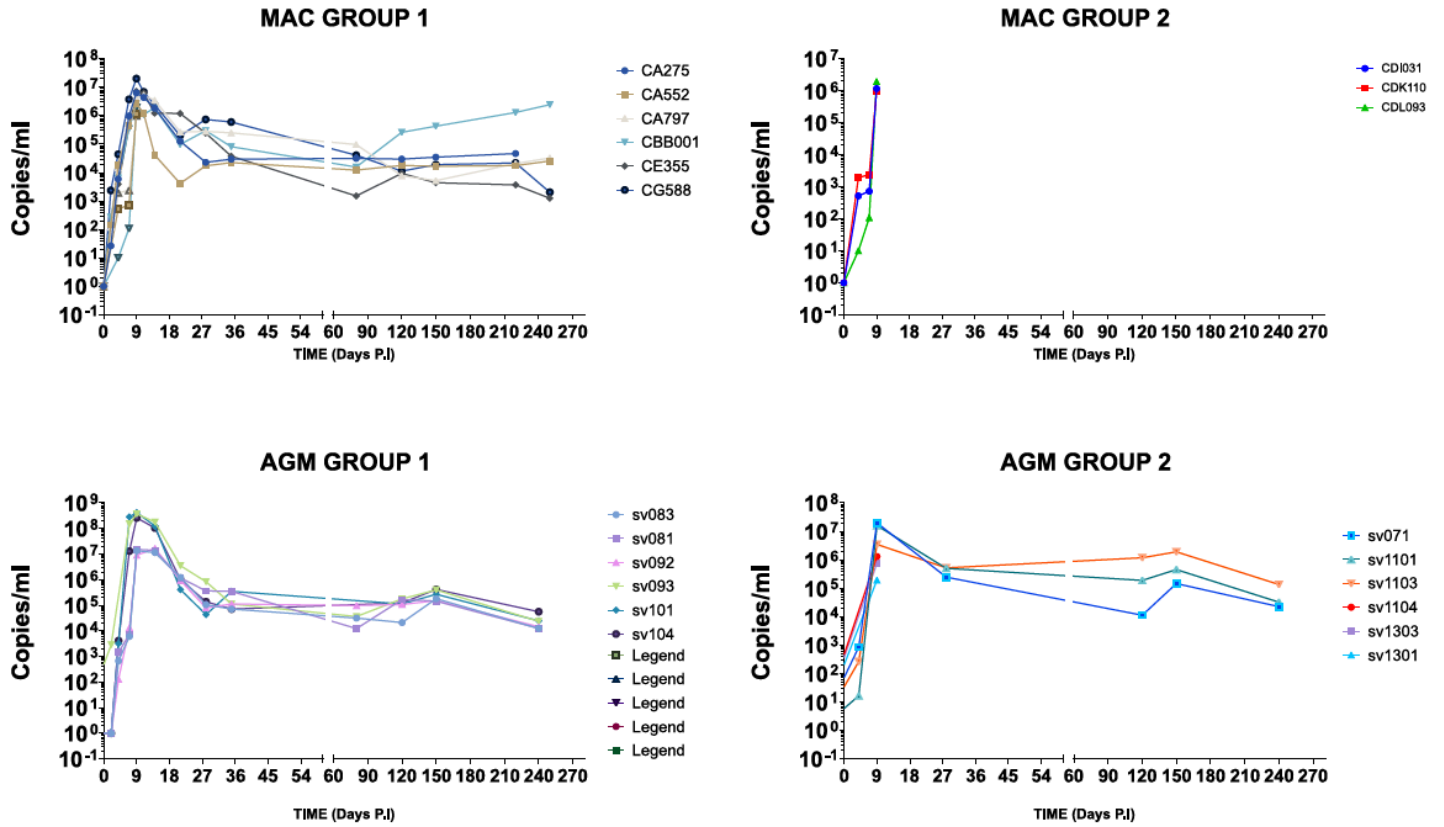
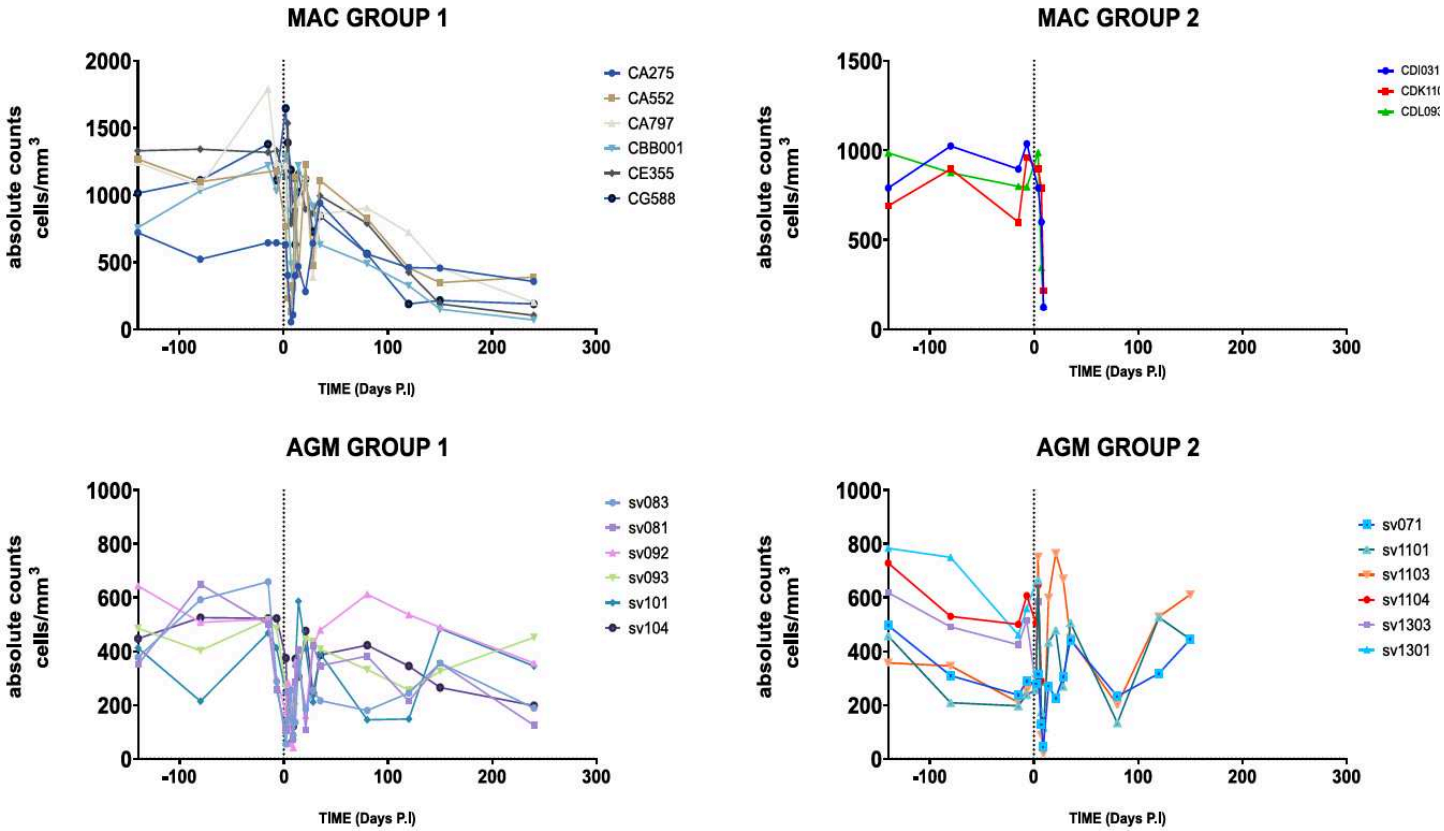


Figure 6. Levels of systemic and intestinal inflammatory and cellular stress markers. Each symbol corresponds to a distinct animal. Orange symbols indicate CM and blue symbols AGM. **(A-B)** Longitudinal IP-10 and Hsp60 concentrations in plasma during SIV infection in (**A**) CM and (**B**) AGM. (**C-D**) IP-10 and Hsp60 plasma concentrations were plotted against NKG2$_{a/c}^{+}$CD8^{+} T cell counts in blood of (**C**) CM and (**D**) AGM. (**E-F**) Longitudinal measurement of IL-23 and HSP60 concentrations produced by total rectal biopsy cells from (**E**) CM and (**F**) AGM. (**G-H**) IL-23 and HSP60 levels from rectal biopsies were plotted against NKG2$_{a/c}^{+}$CD8^{+} T cells of (**C**) CM and (**D**) AGM. NKG2$_{a/c}^{+}$CD8^{+} T cells corresponded to the percentage among CD45+ measured in the respective rectal biopsy. The Pearson correlation is shown and r and p Value are indicated in each graph. A nonparametric Mann–Whitney *U*-test was applied *$p < 0.05$, **$p < 0.005$, ***$p < 0.0005$

SUPPLEMENTARY FIGURES



Supplementary Figure 1. Plasma viral RNA copy numbers in the longitudinally followed animals. The longitudinal studies included 9 cynomolgus macaques (CM) infected with SIVmac251 and 12 AGM infected with SIVagm.sab92018. The animals were followed until 280 days p.i. except for three per species that were sacrificed at day 9 p.i. for tissue collections in the acute phase of infection. The same animals have already been served for other studies[51] (Huot Frontier in press).



Supplementary Figure 2. CD4+ T cell counts were determined by staining whole-blood leukocytes with a pre-titrated antibody cocktail. Following staining with the antibody mixture, red blood cells were lysed with BD FACS lysing solution and labeled lymphocytes were analyzed for their expression of cell surface markers by flow cytometry on an LSR II flow cytometer (BD Biosciences). Data were generated with BD FACS Diva 6.1.3 Software before analysis with FlowJo 8.8 Software.

a

Animal #	Species	Euthanasia	Duration of infection at necropsy (days)	SIV status	vRNA (copies/ml plasma)	% of CD4+ T cells in thawed PBMC
RM 2153	Rh. Mac	13.12.2016	4107	Viremic	7.00 x10^4	1,21%
RM 13909	Rh. Mac	23.12.2016	2368	Viremic	7.91 x10^4	1,16%
RM 8644	Rh. Mac	05.01.2017	6349	Viremic	approx. 5x10^4	6,67%
RM 15925	Rh. Mac	16.11.2017	394	Viremic	4.12 x10^4	26,00%
RM 13914	Rh. Mac	14.12.2011	448	Viremic	3,56E+05	19,70%
RM 2347	Rh. Mac	17.01.2012	203	Viremic	3,60E+06	28,20%
RM 14222	Rh. Mac	05.12.2017	n.a.	Healthy	n.a.	16,30%
RM 2363	Rh. Mac	15.05.2017	n.a.	Healthy	n.a.	8,39%
RM 2564	Rh. Mac	27.06.2017	n.a.	Healthy	n.a.	36,40%
RM 14225	Rh. Mac	11.12.2017	n.a.	Healthy	n.a.	52,50%
RM 13926	Rh. Mac	27.06.2017	2512	Controller	< 40	23,10%
RM 12671	Rh. Mac	08.08.2017	4367	Controller	< 40	33,20%
RM 2139	Rh. Mac	23.05.2017	4268	Controller	< 40	27,50%
RM 2284	Rh. Mac	15.05.2017	2483	Controller	< 40	27,40%
RM 13919	Rh. Mac	04.05.2017	2465	Controller	< 40	12,80%
RM 13923	Rh. Mac	02.05.2017	2150	Controller	< 40	44,80%
RM 2155	Rh. Mac	05.09.2017	4373	Controller	< 40	29,40%

b

Animal #	Species	Euthanasia	SIV status	Duration after ART initiation	vRNA (copies/ml plasma)	% of CD4+ T cells in thawed PBMC
AA840K	Cyn. Mac	23.01.2019	ART treated	117 weeks	< 40	19%
AM28F	Cyn. Mac	28.01.2019	ART treated	118 weeks	< 40	23.15%
GA342F	Cyn. Mac	30.01.2019	ART treated	118 weeks	< 40	18.15%
SL44B	Cyn. Mac	04.02.2019	ART treated	119 weeks	< 40	19.45%
PS6C	Cyn. Mac	06.02.2019	ART treated	119 weeks	< 40	23.45%

Supplementary Table 1. Description of the macaque animals. (A) CD4+ T cell counts and plasma viremia levels of rhesus macaques at the time point of the study, corresponding to the day of necropsy. (**B)** Description of the treated animals. Five CM initiated ART treatment at 28 days following SIVmac251 infection. They belonged to the ANRS SIVART cohort. CD4+ T cell counts and plasma viremia levels are shown for the time point of this study (day of necropsy).

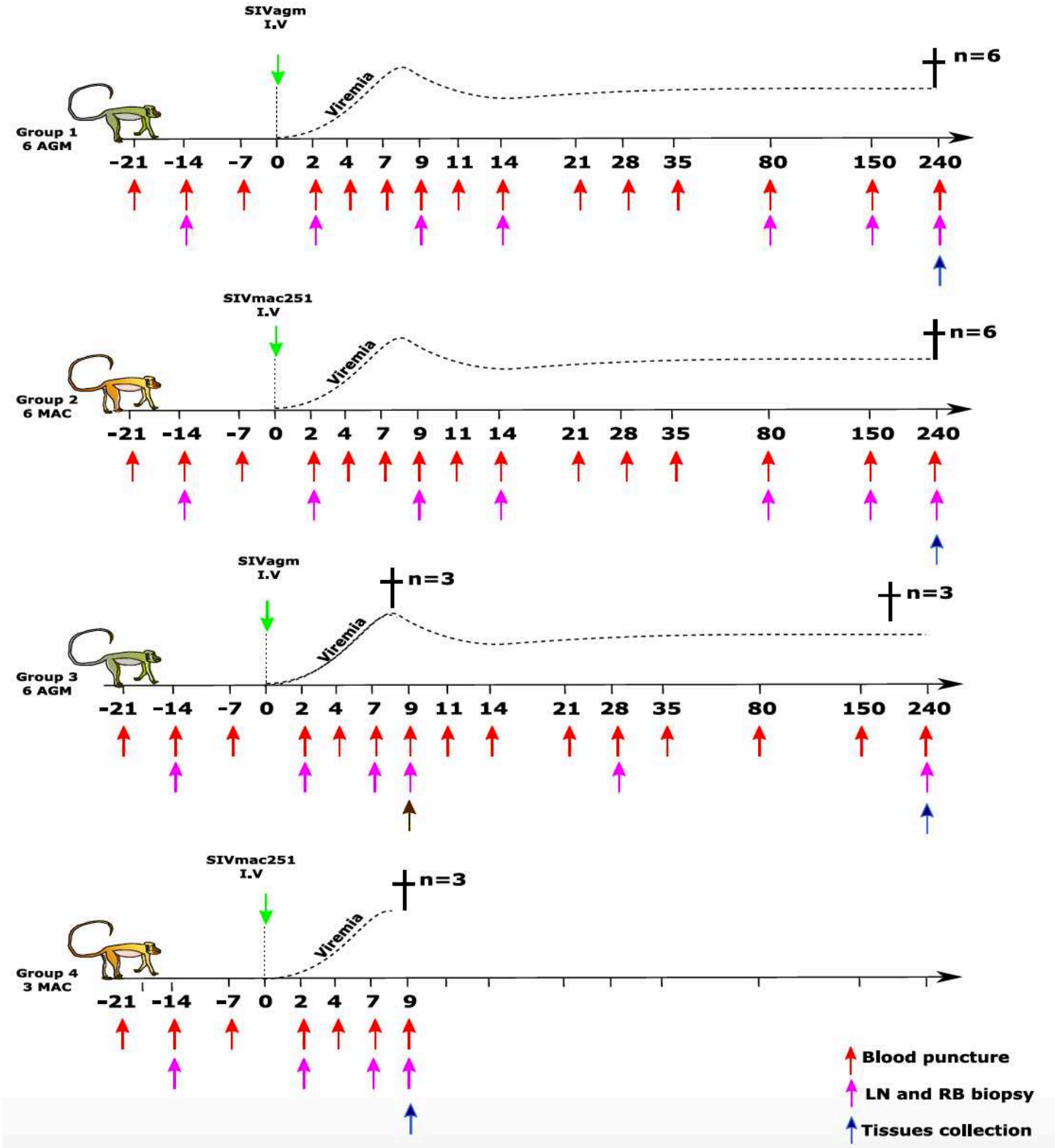
https://www.dropbox.com/scl/fi/cwp0zzy4po8pfh3ptc9k6/Manuscript-4_supplementary-Table-2.xlsx?dl=0&rlkey=xi02m0r4bt2suzijyffc7gr0h

Supplementary Table 2. Table showing all genes that displayed differential expression (p<00.5) between $NKG2_{a/c}^{+}CD8^{+}$ T cells and conventional effector $CD8^{+}$ T cells.

https://www.dropbox.com/scl/fi/lexg79hqefuy9qfq3p2vi/Manuscript-4_supplementary-Table-3.xlsx?dl=0&rlkey=7pylzk6x2ic8qg3wq2qz5htyt

Supplementary Table 3. Table showing all genes that displayed differential expression (p<00.5) between $NKG2_{a/c}^{+}CD8^{+}$ T cells conventional memory $CD8^{+}$ T cells.

SUPPLEMENTARY METHODS



Supplementary Method Figure 1. Scheme showing longitudinal sample collections for AGM and CM used in the study. Peripheral lymph nodes and rectal biopsies were collected longitudinally. Spleen, ileum, jejunum and colon was collected at sacrifice of the animals.

Supplementary method Table 1 Antibodies used for flow cytometry.

Antibody	Clone	Suppliers	Control
CD3	SP34-2	BD biosciences	Isotype + FMO
CD45	D058-1283	BD biosciences	Isotype + FMO
CD20	2H7	Biolegend	Isotype + FMO
NKG2A/C	Z199	Beckman Coulter, Inc.	Isotype + FMO
CD16	3G8	Beckman Coulter, Inc.	Isotype + FMO
CXCR5	710D82.1	NHP reagent	Isotype + FMO
CD8	BW135/80	Miltenyi	Isotype + FMO
CD4	L200	BD biosciences	Isotype + FMO
CXCR3	1C6/CXCR3	BD biosciences	Isotype + FMO
NKp80	4A4.D10	Miltenyi	Isotype + FMO
NKP30	AF29-4D12	Miltenyi	Isotype + FMO
CD279(PD-1)	EH12.2H7	BD biosciences	Isotype + FMO
CD107a	H4A3	BD biosciences	Isotype + FMO
CD28	CD28.2	BD biosciences	Isotype + FMO
CD95	DX2	BD biosciences	Isotype + FMO
CD69	FN50	BD biosciences	Isotype + FMO
HLA-DR	TU36	BD biosciences	Isotype + FMO

Antibody	Clone	Suppliers	Control
PRF1	PF-344	mabtech	Isotype + FMO
CXCR3	1C6/CXCR3	BD biosciences	Isotype + FMO
CCR7	3d12	eBioscience	Isotype + FMO
CD62L	150503	R&D	Isotype + FMO
CX3CR1	2a9-1	biolegends	Isotype + FMO
CXCR5	MU5UBEE	eBioscience	Isotype + FMO
NKG2d	ON72	Beckman Coulter, Inc	Isotype + FMO
NKP46	BAB281	Beckman Coulter, Inc	Isotype + FMO
NKP44	2.29	Miltenyi	Isotype + FMO
Ki-67	MIB-1	Dako	Isotype + FMO
CD107a	H4A3	BD biosciences	Isotype + FMO
TNF-a	MAb11	BD biosciences	Isotype + FMO
IFNg	45-15	Miltenyi	Isotype + FMO

Supplementary Method Table 1. Antibodies used for confocal microscopy.

PART IV. Discussion

Our studies aim to provide a better understanding of mechanisms that lead to a control of HIV/SIV replication in tissues and to protection against tissue damage during a persistent viral infection. We take advantage of the SIVagm/AGM model, a natural host of SIV. AGMs have been carrying SIV since probably > 1 million of years according to recent estimates. Today, the virus and the host live in an equilibrium, where the virus can replicate to sufficient titers to be efficiently transmitted but without damaging the tissues nor the immune responses. We aim to better understand these mechanisms. In the past, natural hosts have been studied mostly to understand how they avoid chronic immune activation despite high viremia. However, natural hosts also strongly control viral replication in lymph nodes, including in T_{FH} cells of BCF. Therefore, we believe that natural hosts are also an excellent model for discovering novel mechanism of viral reservoir control in tissues, i.e. in particular in LNs. Herein, we studied SIV natural host model to understand how this NHP model can control the virus in key anatomical sites and resolve general inflammation in SIV infection despite continuous replication.

I. LYMPH NODE VIRAL RESERVOIR: EFFICIENT VIRUS CONTROL by NK CELLS DURING SIVagm INFECTION

In the first aim, we were interested in the identification of SIVagm reservoir control by NK cells in LN.

I.1. MECHANISMS UNDERLYING THE ABILITY OF NK CELLS TO ACCUMULATE INSIDE B CELL FOLLICLES DURING CHRONIC SIVagm INFECTION

The host lab has shown that in acute SIVagm infection, NK cells display strong increases in proliferation and activity in lymph nodes but not or less in blood (Jacquelin et al., 2014). Subsequently, they demonstrated that the viral control in secondary lymphoid tissues is mediated by NK cells (Huot et al., 2017). The lab also showed that between 7% and 40% of NK cells from chronically-infected AGM express CXCR5 and that NK cells accumulate in BCF during chronic SIVagm infection allowing to control the viral productive reservoirs in T_{FH} cells from peripheral lymph nodes and spleen (Huot et al., 2017). The first aim of my thesis work consisted in understanding why NK cells not only migrate into BCF but in addition increase in numbers in BCF during chronic SIVagm infection.

Previous studies from the lab have shown that IL-15 is among the first cytokines that increased in plasma upon SIVagm infection (Jacquelin et al., 2014). IL-15 is known as the key survival factor of NK cells. We raised the hypothesis that AGMs produce high amounts of IL-15 in BCF of lymph nodes. In order to address this question, I constructed an anti-IL-15 probe that is specific for AGM and macaque IL-15. I stained by FISH lymph node tissue sections of peripheral LNs. These analyses revealed high amounts of IL-15 mRNA in BCF of peripheral LNs of the chronically infected AGM (Huot et al., 2017). The cells that were expressing IL-15 often displayed long dendrites suggesting that they corresponded to FDCs. FDCs are indeed known to produce IL-15 and express it in membrane-bound form on their surface and which is known to stimulate B cells. This contrasted with SIVmac-infected macaques that did not show high IL-15 expression in FDCs. The lack of IL-15 production in BCF of SIVmac-infected macaques might be related to the damaged FDC characteristic of

SIVmac infection. We also showed by flow cytometry that IL-15 was presented on FDC membranes in SIVagm infection. We demonstrated that NK cells preferentially accumulated in those BCF with high IL-15. IL-15 presented as membrane-bound can stimulate NK cell survival, differentiation and effector function (Stonier and Schluns, 2010; Tamzalit et al., 2014). Thus, we showed that BCF of SIVagm-infected AGM produce high amounts of IL-15 by FDCs and this membrane-bound IL-15 probably is an important factor for the survival of NK cells explaining their accumulation and persistence in numbers in BCF and most likely contributing to their efficient activity in BCF.

IL-15 superagonist (ALT-803) combined with an antibody (NEO-201) has been shown to increase NK cell ADCC activity, activation and cytotoxicity (Fantini et al., 2019). Another study showed that IL-15 superagonist (ALT-803) treatment in SIVmac infection induces proliferation of NK and $CD8^+$ T cells and redistributing them to BCFs in LNs (Webb et al., 2020). However, it is not excluded, that the NK and $CD8^+$ T cells could migrate into the BCF because the structure of the BCF was already damaged. Indeed, no increases of CXCR5+ NK cells were described during SIVmac or HIV-1 infection so far. Moreover, the IL-15 treatment did not consistently diminish the viral reservoir (Webb et al., 2020). It therefore seems that membrane-bound presentation of IL-15 might be necessary, in particular for the survival of NK cells, but not sufficient to induce efficient NK-cell mediated control of HIV/SIV. It thus raises the question how NK cells in the T-zone of SLT control SIVagm infection and why NK cells don't exert such a control in HIV/SIVmac infections.

We noticed that CXCR5+ NK cells expressed more frequently CD107a, and Fcγ receptors (CD16 and CD32) but little IFN-γ compared to other NK cells in LNs of SIVagm infected AGMs. These findings showed that NK cells might display superior cytotoxicity or/and ADCC function, while little pro-inflammatory activity.

Interestingly, sooty mangabeys also control viral replication in the T cell zone and BCF of SLT (Le et al., 2008). While the underlying mechanism in sooty mangabeys has not been studied yet, it is not excluded that this might be mediated as well by NK cells. Indeed, SIV-infected sooty mangabeys showed an earlier and stronger NK cell response in blood than SIVmac-infected macaques (Le et al., 2008). Future studies need to determine NK cell activity in LNs of sooty mangabeys.

Conclusion

Taken together, this study revealed strong IL-15 production by FDC during SIVagm infection and indicates that in SIVagm infection, CXCR5-expression on NK cells together with BCF-associated IL-15 contribute to the control of SIVagm in BCF of peripheral SLT. The results of this study lead to two major questions: the mechanism underlying CXCR5 receptor acquisition at the surface of NK cells during SIVagm infection and the mechanism of viral control in B follicles and the T cell zone by NK cells.

I.2. IDENTIFCIATION OF A SOLUBLE FACTOR INDUCING CXCR5 ON NK CELLS

Specific aims

Following these observations, it seemed important to study the mechanisms at the origin of NK cell migration into B follicles during SIVagm infection. Up to 40% of NK cells in lymph nodes during chronic SIVagm infection are CXCR5 positive, allowing the migration of NK cells into BCF (Huot et al., 2017). In the second part of my thesis, I searched for the mechanisms responsible of CXCR5 acquisition at the surface of NK cells during SIVagm infection and identified a factor that can up-regulate CXCR5 on NK cells (Rascle et al, manuscript #2).

Discussion

The literature about CXCR5 induction at the surface of NK is scarce. On the contrary, CXCR5 expression on T_{FH} and B cells is well described (Estes, 2013b). We started by determining the *in vivo* kinetics of CXCR5+ NK cell appearance in pLN in response to SIVagm infection. Indeed, in our previous study, we had analyzed the frequency of CXCR5+ NK cells only in chronic phase of SIVagm infection. Our data showed that the frequency of CXCR5+NK+ cells is up-regulated starting from day 2 p.i. and that CXCR5+CCR7- NK cells are induced progressively in peripheral lymph nodes during acute SIVagm infection. We identified a soluble factor, IL-6, that by its own is capable of CXCR5 induction on NK cells from AGMs and humans. These CXCR5+ NK cells isolated from pLNs displayed similarities in their transcription factor profiles with T_{FH} cells as they expressed high levels of the *Bcl-6* transcription factor while low levels of *T-bet*, *Gata-3* and *RORC*.

Here I thus demonstrated that a soluble factor (IL-6) induced CXCR5 on NK cells and that the contact between NK cells and B cells was not necessary to induce CXCR5. This provides a proof that CXCR5 on the NK cells was not acquired by trogocytosis. We measured IL-6 production and showed that it's production by B cells was increased during our *in vitro* culture condition and that it was produced locally *in vivo* in pLNs during SIVagm infection. We observed this production of IL-6 in inter-follicular areas of pLNs from SIVagm-infected AGMs and also in BCFs, and showed that NK and B cells can be in close proximity in these areas. IL-6 production can increase by classical activation of B cell and/or by adding SIV on B cells (Epeldegui et al., 2010; Teleshova et al., 2006; Urashima et al., 1996). It is possible that IL-6 produced by activated B cells in the inter-follicular area up-regulate CXCR5 on NK cells which then enter into the BCFs. It is therefore more likely and not mutually exclusive that IL-6 production is in majority due to other cells, such as dendritic cells (DCs). Indeed, many IL-6+ cells were neither B nor NK cells in the analyzed pLN. DCs are well-known to cross-talk with NK cells (Elssen et al., 2014; Zitvogel et al., 2006) and also to participate in the induction of CXCR5+ pre-T_{FH} (Eivazi et al., 2016; Rao, 2018; Suh, 2014). DCs are also able to produce IL-6 and can be a major source of IL-6 in LNs in some settings (Daudelin et al., 2012; Garbers et al., 2018; Hope et al., 1995).

We observed in CXCR5+ NK cells an upregulation of several cytokine receptors, in particular GM-CSF receptors (CSF2RA/B), IFNGR and IL-6R as compared to the main NK cell population in pLN of SIVagm infected animals. The respective cytokines GM-CSF and IFN-γ were not up-regulated and GMC-SF did not induce CXCR5 expression on NK cells. In contrast, IL-6 not only induced CXCR5 expression on NK cells but

its expression was also up-regulated in the CXCR5+ NK cells. Thus, there might be a mechanism of autocrine regulation for IL-6 in the CXCR5+ NK cell population. This mechanism could participate at the induction or maintenance of CXCR5 expression on CXCR5+ NK cells once they entered BCF. We observed NK cells preferentially in the BCF with proliferating B cells, that might express higher levels of IL-6 as compared to primary follicles. We have previously shown that NK cells accumulated preferentially inside those BCF where FDCs produced high levels of membrane-bound IL-15 (Huot et al., 2017). IL-15 presented by FDCs is known to augment B cell proliferation in germinal centers (Park et al., 2004) and could concomitantly enhance the survival of the CXCR5+NK cells in BCF.

CXCR5+ NK cells were induced in culture with supernatants from NK-B cell co-cultures but not with supernatants from NK or B cells cultured alone. This clearly provides evidence for a cross-talk between NK and B cells. Of note, CXCR5+ NK cells were induced only in the transwell chambers but not in the co-cultures allowing contact between NK and B cells. While we did not see a statistically significant difference of CXC5+ NK cells cultured alone and in contact with B cells, we cannot exclude a minor difference if we would have studied more animals. Still, the upregulation was higher in transwell than in contact condition. There could be several reasons why they were not induced during contact. The IL-6 production might be inhibited or lower when contacts are allowed between NK and B cells. Also, there was a trend for NK cells to up-regulate Granzyme B in the cultures with contact to B cells but not in the transwell chambers. It is thus possible that NK cells killed preferentially activated B cells producing IL-6 in the co-cultures.

In SIVmac infection, we could not observe increases of CXCR5+ NK cells after SIV infection *in vivo*. The reasons might be multiple. We show that NK and B cells can be in close proximity in LNs. However, only in AGM we detected foci of strong IL-6 mRNA in T zone areas of the pLNs and not in macaques during acute SIV infection. The lack of CXCR5+ NK cells in macaques might be in part explained by this. SIV infection considerably modifies cytokine profiles in LN. Mesenteric LN of SIV-infected macaques display lower mRNA transcripts encoding for IL-12, IL-23 and IL-35 (F et al., 2019). The micro-environment and/or maturation state of the DCs in LN has also been shown to be different between SIVmac and SIVagm infections (C et al., 2005; Jacquelin et al., 2014). It is possible that IL-6 expression by DCs in LN was different between AGM and MAC during SIV infection. Paradoxically, the IL-6 protein levels secreted by total pLN cells did not differ between SIVagm and SIVmac infections. There might be post-translational regulations of IL-6. It could also be that the method used here did not accurately reflect the *in vivo* production of total IL-6, because the protocol used to isolate LN cells is adapted for isolating lymphocytes (B and NK cells) but not for obtaining DCs (Diop et al., 2008). The IL-6 production by DCs in pLN could thus have been underestimated by the method used here. It could also be that the type of cells and/or the location of the IL-6 producing cells play a role. Indeed, the anatomical distribution of IL-6 producing cells in pLN was distinct between SIVagm and SIVmac infections. Alternatively, NK cells from macaques in pLN might need additional stimuli or are less susceptible to IL-6 for other reasons such as a distinct differentiation stage in response to SIV infection, lower expression of IL6R or low levels of STAT3 (Theurich et al., 2017). Indeed, *in vitro*, IL-6 induced CXCR5 on NK cells from non-infected AGMs and humans but not on NK cells from non-infected macaques. However, the co-cultures of B cells with autologous NK cells from macaques induced CXCR5+ NK cells in transwell condition, which could indicate that IL-6 alone was not sufficient for macaque cells to induce CXCR5. It shows though that CXCR5+ NK cells can be induced both for MAC and humans, depending on the conditions.

There was a higher impact on CXCR5 up-regulation when adding supernatants from NK-B cell co-cultures (transwell) than with supernatants from B cells cultured alone. This could be explained by higher levels of IL-6 in the co-cultures, by the presence of co-factors secreted by NK cells and or B cells after co-culture and/or a higher susceptibility of NK cells to IL-6 (such as for example IL6R expression) after co-culture with B cells in transwell conditions. Among the other cytokines known to participate in the induction of CXCR5 on CD4+T cells, are IL-21 and IL-27. It is possible that these cytokines or other soluble factors also play a role in CXCR5 up-regulation in NK cells.

The analysis of transcription factors revealed that Bcl-6 was upregulated in the CXCR5+ NK cells. BCL6 expression in T_{FH} cells is known to upregulate CXCR5, ICOS, PD1, IL-21R, IL-6R and to repress CCR7 (Yu and Vinuesa, 2010). Surprisingly, the expression *PRDM1* was also upregulated in the CXCR5+ NK cells (Kallies et al., 2011). PRDM1 encodes B lymphocyte-induced maturation protein-1 (Blimp1) (Fu et al., 2017; Shaffer et al., 2002). Blimp1 is an antagonist of Bcl-6 in B and T lymphocytes, however, in NK cells the interaction of Blimp1 with Bcl-6 is distinct from B and T lymphocytes (Kallies et al., 2011). In human NK cells, Blimp1 is associated with Granzyme B expression and represses IFN-γ, TNF-α, and TNF-β production. In contrast to *blimp1* expression, the expressions of *RORC*, *t-bet*, *gata-3* and *EOMES* were downregulated in the CXCR5+ NK cells when compared to the predominant NK cell population in pLN of SIVagm-infected animals. This observation is in line with the literature regarding Bcl-6 and the capacity of this transcriptional factor to repress the other transcriptional factors in T_{FH} cells (Xu et al., 2019). We also observed a lower expression of IL-2 receptors (IL2RA/B/G) which reminds GC-T_{FH} cells, for which it is known that the IL-6 pathway induction is leading to decreased IL-2 receptor expression (Papillion et al., 2019). The transcriptional factors leading to CXCR5 expression in NK cells might thus be similar between NK and T_{FH} cells.

Knowledge on the mechanisms regulating CXCR5 expression in NK cells was scarce. This study contributes to elucidate CXCR5 induction on NK cells present during SIVagm infection. These novel insights can be of interest for efforts aiming at directing NK cells into BCF during HIV infection. They might also be of general relevance for other infections. IL-6 for instance is produced in elevated levels in SARS-Cov2 infections (Costela-Ruiz et al., 2020). IL-6 is also produced in response to vaccinations (Bush et al., 2009; Leal et al., 1999). Little attention has been given to CXCR5+ NK cells (Theurich et al., 2017; Yang et al., 2019) and to NK cells in LNs in general. More knowledge is needed on the frequency of these cells in distinct settings and on their potential influence on B cell responses. Indeed, B cell responses might be under influence of NK cells during immunization strategies (Cook et al., 2015; Farsakoglu et al., 2019). And vice-versa, activated B cells could influence NK cell responses. We show here for instance increases of CD16+NK cells after co-culture with B cells and the preferential presence of NK cells in BCF containing high levels of proliferating B cells during SIVagm infection.

Conclusions

Our studies underline the potential multiple interactions between NK and B cells in lymph nodes that deserve further attention. Importantly, we provide here novel evidence for a cross-talk between NK cells and B cells. We reveal an interaction between IL-6 producing cells and NK cells and we provide key elements for understanding how CXCR5+ NK cells are induced.

I.3. MHC-E RESTRICTED NK CELL SUPPRESSION OF SIVagm REPLICATION

Specific aims

As mentioned above, the induction of CXCR5 on NK cells in SIVagm infection in contrast to SIVmac and HIV-1 infection is not sufficient to explain the difference in viral control pattern in LN (Webb et al., 2020). It is important to decipher how NK cells are able to kill infected target cells. So, we were interested by the identification of the receptors/ligands combinations between NK cells and the infected target cells implicated in the NK cell mediated control. It is known that HIV/SIV viruses reduce KIR ligands, such as MHC-A and -B expression on infected cells by Nef viral protein, while Vpu mediates reduction of MHC-C (Manickam et al., 2019). In contrast, MHC-E has been shown to be up-regulated (Jabri Bana et al., 2005; Martini et al., 2016). A recent study demonstrated that primary HIV strains can down-or up-regulate MHC-E levels on infected $CD4^+$ T cells by Nef viral protein (Thans et al., 2019). MHC-E generally impairs NK cell lysis and high MHC-E expression has been associated with higher viremia *in vivo* (Ramsuran et al., 2018). Indeed, a study showed that presentation of SIV-Gag via MHC-E inhibits NK cells (Hansen et al., 2016). However, other studies could not confirm an inhibitory effect by HIV or SIV Gag proteins on MHC-E dependent NK cell activity. Interestingly, MHC-E expression is known to be higher on T_{FH} than on other CD4+ T cells. We raised the hypothesis that SIVagm encodes for antigens that can be presented by MHC-E and that do not inhibit NK cells. Therefore, we studied if there is a mechanism link between MHC-E/Peptide recognition by NK cells and viral control in SIVagm infection. In this study, I was particularly involved in the design of the MHC-E binding SIV peptides. I also constructed the MHC-E expressing cell line and performed functional suppressor assays (manuscript #3).

Discussion

In order to set up a functional assay to analyze MHC-E restricted viral suppressive activity of NK cells from AGM and MAC, we first designed SIVagm and SIVmac peptides that can bind to MHC-E. HLA-E usually presents hydrophobic nonamer peptides derived from the leader sequence of other HLA class I or from the leader sequence of other cellular proteins such as HSP60 (Michaëlsson et al., 2002). We searched for peptides in SIV that share such properties. The retroviral Env proteins have a signal peptide leader sequence (LS). We screened the full length ENV LS from 8 distinct SIV viruses for peptides displaying the MHC-E permissive motif. We identified regions that encode for nonamers containing the canonical sequence motif of MHC-E binding peptides. They were encoded close to the signal-peptidase cleavage site and thus have a high probability to be processed by the canonical pathway in contrast to Gag peptides. We showed that these ENV peptides stabilized MHC-E expression on MHC-I devoid K562 cells stably transduced with HLA-E*0101 (K562-E*0101) indicating the ability of the SIV ENV peptides for MHC-E binding. To further analyze the efficacy of binding, competition-binding assays were performed. They demonstrate the capacity of the SIV ENV peptides to displace peptides known to strongly bind to HLA-E (MHC-I derived VL9 or HSP60) already at low concentrations (1μM). The concentrations needed by SIV ENV peptides for displacement of VL9 and HSP60 were in a similar range as those needed by other viral peptides known to efficiently bind to HLA-E (HIVgag, HCV) peptides (Walters et al., 2018) and even lower than for the previously reported SIVmac GAG peptide (Hansen et al., 2016). These analyses confirm that peptides derived from SIV ENV efficiently bind to HLA-E. Only few MHC-E binding viral peptides have been described so far (Joosten et al., 2016). We define

here a novel lentiviral region that can code for peptides with the capacity to bind to MHC-E. ENV might thus serve as a critical new target for NK cell directed HIV vaccines, cure strategies, or other therapeutic modalities.

We analyzed the MHC-E-dependent activity of NK cells toward target cells presenting the SIV ENV peptides via MHC-E. We first studied NK cells from uninfected AGM and MAC. NK cells were co-cultured with K562-E*0101 cells pre-loaded or not with the peptides and activity was measured by CD107a expression. As expected, the MHC-I-derived VL9 peptide inhibited NK cell activity, while the HSP60 peptide did not, validating our assay. When pulsing the cells with the SIVmac ENV peptide, NK cell activity from both MAC and AGM were inhibited. The SIVagm peptide displayed an intermediate inhibitory activity on NK cells. These peptides are not representative of all SIVagm and SIVmac variants. However, the data show that NK cells reacted differentially depending on the peptide sequence.

As a proof of concept of the capacity of the ENV peptides to be processed in primary cells and to be recognized differentially by NK cells depending on their sequence when presented by simian MHC-E, we applied a functional assay using AGM primary $CD4^+$ T cells as targets and full-length infectious SIV as source for the peptides. Two infectious molecular mutant viruses deriving from the wildtype $SIVagm._{sab92018}$ backbone were generated by our collaborator Frank Kirchhoff. In this backbone, the ENV sequence coding for the nonamer peptide of the wild type SIVagm virus (IGIVVIVKL) was replaced by either the sequence coding for the $SIVmac_{239/251}$ peptide (NQLLIAILL) or by the VL9 sequence. The mutant viruses replicated efficiently in primary $CD4^+$ T cells from non-infected AGM. The *in vitro* infected primary $CD4^+$ T cells were co-cultured with autologous NK cells. NK cells strongly suppressed replication of the wild-type SIVagm. NK cells controlled the replication of the VL9 mutant less than the wild-type SIVagm, in line with a strong inhibitory effect of the VL9 peptide. $CD4^+$ T cells infected with the virus coding for the SIVmac ENV peptide escaped NK cell suppressive capacity. These results confirm that the SIVmac ENV peptide inhibits viral suppression of NK cells isolated from noninfected animals while the SIVagm ENV peptide didn't, showing a distinct NK cell suppressive activity depending on the ENV sequence.

We then compared the MHC-E dependent suppressive activity of NK cells before and after SIV infection. We exposed NK cells from blood and SLT to K562-E*0101 cells loaded or not with peptides. NK cells from LN of SIVmac-infected MAC showed a drop in their capacity to lyse target cells presenting the SIVmac ENV peptide via MHC-E when compared to NK cells from healthy animals. SIVmac controllers did not show stronger ENV-specific NK cell activities than viremic MAC, except for one animal. In contrast to MAC, NK cells from AGM showed an increased activity after SIVagm infection compared to non-infected AGM.

We tested if the differential changes in NK cell activity after infection were unique for the two SIV peptides or applied to other SIV ENV peptides as well. When using peptides from another SIVagm (SIVagm.sab1) and one more distant SIV (SIVgsn), we observed again strong MHC-E restricted activity with NK cells from LN of SIVagm-infected AGM, while NK cells from SIVmac-infected MAC displayed a weak MHC-E dependent NK cell activity in presence of all SIV ENV peptides tested. We also analyzed NK cells from spleen. MHC-E restricted activity of NK cells from spleen showed trends for decreases in MAC after SIVmac infection with the SIV Env peptides, while this activity increased after SIVagm infection in the presence of $SIVagm.sab_{92018}$, $SIVagm._{sab1}$ and $SIVmac_{239/251}$ peptides.

Of note, the target cells and peptides used in our assays were the same before and after SIV infection, demonstrating that the increased MHC-E restricted activity of NK cells in SIVagm infection was not related to the SIV sequence but must be due to changes at the level of the NK cells themselves.

Conclusions

We defined ENV sequences coding for nonamer peptides with a strong capacity to bind to MHC-E. We show that the MHC-E restricted suppressive activity of NK cells varies depending on the SIV ENV peptide sequence. We demonstrate that SIVagm infection trains NK cells towards efficient MHC-E dependent SIV control, while SIVmac infection doesn't. These data suggest that NK cells during SIVagm infection are educated toward a better control of SIVagm via peptides presented by MHC-E to it is receptor (NKG2A/C) on NK cells. A similar education of NK cells was lacking in SIVmac infection. This discrepancy might contribute to explain the superior viral control of NK cells in the B cell and T cell zone of SLT in SIVagm versus SIVmac infection.

I.4. EXPANSION OF TERMINALLY DIFFERENTIATED ADAPTIVE NK CELLS IN LYMPH NODES OF SIV-INFECTED NATURAL HOSTS

Specific aims

The results described above indicated that NK cells are imprinted differentially in SIVagm and SIVmac infections. Given the strong cytotoxic and weak pro-inflammatory profile of the NK cells in LN, we raised the hypothesis that NK cells in AGM are highly differentiated. Interestingly, LN have been described as a major site for NK-cell differentiation (Freud et al., 2006). We therefore longitudinally analyzed the phenotype and genotype of NKG2A^{high} and NKG2A^{low} NK cells during SIVagm and SIVmac infection in blood and tissues (manuscript #3). We hope that by this study we contribute to better explain why NK cells already in the early phase of HIV infection are dysfunctional (Giavedoni et al., 2000; Mavilio et al., 2005b). I contributed in the study in particular at the tissue processing of the NK cells.

Discussion

Our study showed that SIV infection in the natural host induced terminally differentiated NKG2A^{low}CD16+ NK cells in LN displaying a strong degranulation activity and a transcriptional profile of adaptive NK cells. In contrast, the process of terminal NK cell differentiation was blocked in LN during SIVmac infection of MAC after day 2 p.i., despite the generation of a highly diverse NK cell pool. Our results uncover that NK cells are educated to efficiently kill SIV-infected cells in nonpathogenic SIVagm infection while this education is not occurring in pathogenic SIV infection. The notion that NK cell differentiation is the result of a continuous process that can adapt in response to a viral infection is raising increasing interest (Cichocki et al., 2015; H et al., 2015; Wilk et al., 2018).

By analyzing distinct NK cell subsets from AGM and MAC at the transcriptomic and protein level we demonstrated here that NKG2A combined with CD16 defines distinct stages of NK cell differentiation in monkeys. This provides a novel tool for preclinical studies in NHP for the investigation of other infections and for vaccine studies.

The NKG2a/c^{low}CD16+ NK cells clearly displayed the most differentiated profile and strong cytotoxic activity. We also observed cytotoxic activity for the NKG2a/c^{low}CD16- and CXCR5+ NK cells. CD16 can be quickly shed from the NK cell surface upon activation (Romee et al., 2013). Under these conditions, NKG2a/c^{low}CD16- and CXCR5+ NK cells might be a mixture of less differentiated NK cells together with terminal differentiated NKG2a/c^{low}CD16+ cells that exert the viral control. The NKG2a/c^{low}CD16+CXCR5+ NK cells might be responsible for the viral control in B cell follicles and the NKG2a/c^{low}CD16+CXCR5- NK cells for the viral control in the T cell zone.

The reasons why NKG2a/c^{low} NK cells expanded after SIVagm infection in AGM but not during SIVmac infection in MAC are unclear. These cells did not show increased proliferation and it is unlikely that they result from trafficking, since we reported that LN homing receptors decrease on NK cells from AGM in SIVagm infection similarly to SIVmac and HIV infection (Huot et al., 2017). It is therefore more likely that this expansion of NKG2a/c^{low} NK cells is due to NK cell differentiation *in situ*. A major difference between the two infections consists in the persistence of an inflammatory environment in SLT during SIVmac infection while inflammation is resolved in SIVagm infection (Jacquelin et al., 2009). Systemic inflammation has been shown to drive the expansion of IFN-γ producing NK cells in mice (Wu et al., 2017). Similarly, it has been recently shown that inflammatory cytokines drive the expansion of CD94-CD56^{bright} NK cells with an increased capacity to produce IFN-γ in HIV infection which could themselves contribute to the inflammation (Wang et al., 2020). These cells might correspond to the NKG2a/c^{high}CD16- NK cells that were the predominant NK cell subset in LN of SIVmac-infected MAC. The terminally differentiated NK cells in AGM LN expressed high levels of IL15R and IL21R. Higher levels of IL-15 and IL-21 in the local environment during SIVagm infection as compared to SIVmac infection might allow the terminal differentiation. Considering that AGMs are ancient hosts of SIV, it is possible that the long-term co-existence in AGM selected for a specific tissue environment in response to SIV infection that allows proper education of NK cells. By driving NK cells toward a terminal differentiated, cytotoxic phenotype in SIVagm infection, this would allow the presence of NK cells with capacity to kill infected cells in LN, while avoiding the inflammation associated with NK-cell mediated IFN-γ production.

While our study demonstrates a superior MHC-E restricted NK cell activity in the natural host, this might not be the unique mechanism of viral suppression, since terminally differentiated cells also up-regulate for example ADCC mediated killing capacity[44] and these were also up-regulated on the CXCR5+ NK cells.

Other examples are known where NKG2A-dependent NK cell education is a determining factor for NK cell responses in infectious conditions, in particular CMV infection (Hammer et al., 2018). In contrast to CMV infection (Malmberg et al., 2012), the increased functional activity of the NK cells here was not related to stronger expression of NKG2C. The signaling pathways of adaptive NK cells are poorly understood. The NK cells here expressed high level of transcripts coding for THEMIS. THEMIS has been reported to regulate signaling downstream of the T cell receptor (TCR) by interacting with SHP-1 and GRB2, both of which are supposed to participate in the transduction of the NKG2A signal after its ligation with MHC-E (Choi et al., 2017; Paster et al., 2013). Our data suggest a role of Themis for adaptive NK cell generation.

Conclusions

We demonstrate that SIVagm infection induces the expansion of terminally differentiated NKG2a^{low} NK cells in SLT in contrast to SIVmac infection. The NK cells that expanded in LN during SIVagm infection displayed an adaptive transcriptional profile. This adaptation could explain the increased MHC-E-restricted in response to SIV Env peptides during SIVagm infection. In conclusion, our study delivers insights into functional differentiation of NK cells during a controlled viral infection in LN. These results could be useful for future approaches to improve NK cell activity during HIV infection, in particular to control viral reservoirs in the context of HIV cure strategies.

II. INTESTINE-ASSOCIATED VIRAL RESERVOIR and INFLAMMATION CONTROL

SIVagm-infected AGMs show a tissue-specific viral control. While viral replication is controlled in LN it is not controlled in the gut. This raises the question how SIVagm avoids chronic inflammation and tissue damage in the intestine. The underlying mechanisms could be multiple. The maintenance of the gut barrier could be related with the preservation of Th17 cells in SIVagm-infected AGM (Favre et al., 2009). Immunoglobulin A (IgA) is also known to have an important role in control of intestinal inflammation (Leong and Ding, 2014). However, additional and still not yet uncovered mechanisms are not excluded.

II.1. NON-HUMAN PRIMATE DETERMINANTS OF NK CELLS IN TISSUES AT STEADY-STATE AND DURING SIV INFECTION

Specific aims

In order to better understand the lack of viral control in the gut of SIVagm-infected AGM, we investigate the tissue distribution, phenotype and function of NK cells in the intestine of healthy and SIV-infected AGM and macaques. Moreover, we analyzed tissue-residence markers combined with function inside tissues to provide a better general insight on NK cells in lymphoid tissues. This study allowed to identify tissue- and species-specific patterns of NK cell frequencies, phenotype and function in lymphoid tissues (manuscript #4). I participated in all steps of the tissue processing of the cells.

Discussion

Studies on NK cells in lymphoid tissues are scarce because NK cell frequencies are low in these tissues. However, it is important to gather more information about NK cells in such tissues since their numbers and functions can be modulated by viral infections, and also given the importance of the NK-DC cross-talk in LN for shaping the adaptive immune responses (Cook et al., 2014; Lam and Lanier, 2017). While we did not analyze all possible tissues, we focused the study on lymphoid tissues where there is little information and

which are key for the study of vaccine responses, i.e. mucosa as a site of viral entry and replication and SLT for education of B and T cell responses. We compared here the NK cells present in such anatomic sites to body compartments where NK cells are more frequent and more often described (blood and liver).

We performed these analyses in representative species from Asia and Africa. We thus studied four NHP species and only two of them extensively: one Asian (CM) and one African (AGM) species. Of note, these two species are among the most used NHP models in biomedical research. In addition, the data observed here for CM might be similar in related species, such as rhesus macaques.

Here we performed multiparameter flow cytometry. Even if we did not use NGS technology, such analysis allowed to focus on specific markers and to analyze a wide range of tissues (blood, liver, spleen, lymph nodes, ileum, jejunum, colon, rectum) concomitantly. We also performed a longitudinal analysis in two distinct tissues (SLT and intestine) in response to a viral infection. Most importantly, we provide *ex vivo* data for NK cell functionality in these tissues.

Our data demonstrate that NK cells of CM were rarely CD8+ in tissues. Our data also imply that studies using anti-CD8a antibodies to deplete NK cells need to consider the low frequency of CD8+ NK cells in tissues of some species. Indeed, our study indicates that in CM, NK cells will not get efficiently depleted in tissues when using anti-CD8 antibodies.

Here we show that CXCR5 is expressed to high frequency by ileum NK cells in healthy CM and AGM. This high frequency of CXCR5+ NK cells was also noticed in CM jejunum and colon. Strikingly, following SIV infection, the frequency of CXCR5+ NK cells strongly decreased in gut of CM for unknown reasons. It could be related to the increase of infiltrating, CXCR5- NK cells. CXCR5 is known to support Solitary Intestinal Lymphoid Tissue (SILT) formation and B cell homing (Velaga et al., 2009). Microbiota and other external stimuli can foster the formation of aberrant SILT distinguished by impaired development of B cell follicles in CXCR5-deficient mice (Buettner and Lochner, 2016; Eberl and Lochner, 2009; Velaga et al., 2009). In this context it could be interesting to investigate if the decrease of CXCR5+ NK cells in intestine during SIVmac infection, concomitant with the well-known induction of microbial translocation, may be associated with the formation of SILT in NHP and humans during HIV and SIVmac infections.

Although CD69 has long been viewed as an activation marker of both T cells and NK cells, it is now clear that it has an important role in retaining immune cells in tissues by inhibiting sphingosine-1-phosphate receptor 1 (S1P1) (Bankovich et al., 2010; Mackay et al., 2015). CD69 is now considered a tissue-resident marker for T cells (Stelma et al., 2017; Walsh et al., 2019). For NK cells it is less clear if tissue-resident NK cells can be characterized on the basis of the expression of CD69. It has recently been shown that the CD69 expression displays subset- and site-specific variations by tissue NK cells in humans(Dogra et al., 2020b). Here we show that during SIV infection in NHP, NK cells in peripheral blood largely lack expression of CD69. Our data of higher levels of CD69+ NK cells in the tissues argue in in favor of CD69 as a tissue residence marker for NK cells in NHP. The main difference between the pathogenic and non-pathogenic SIV infection in the two species (CM, AGM) came from the observation that the frequency of CD69 cells in tissues during pathogenic infection was relatively low, whereas in natural host a high frequency of CD69+ NK cells was observed in tissues. The high frequency of CD69- NK cells in SIVmac infection might be the result of infiltrating NK cells.

The combined analysis of CD69 with GzmB+ and IFN-γ indicates that most of resident NK cells harbored a cytotoxic profile, while potentially infiltrating (CD69-) NK cells also expressed the pro-inflammatory IFN-γ cytokine. It is not clear though if these changes are the result of blood NK cell infiltration or whether there are phenotypic changes in resident NK cell populations during SIV infection.

The role of tissue localization in NK cell development and function, and how circulating NK cells relate to those in different sites, are not well understood during HIV/SIV infection (Li and Reeves, 2012; Luteijn et al., 2011; Reeves et al., 2010a). Only few data on NK cells in tissues are available during HIV/SIV infections in particular in LN while more data have been described for the gut (Huot et al., 2017; Luteijn et al., 2011; Schafer et al., 2015b) . Immediately after HIV/SIV infection, changes occur in NK cell populations in the GALT. Thus, the frequency of both intraepithelial and lamina propria NK cells was increased in PLWH with an incomplete blood CD4+ T cell recovery (CD4<350 cells / µl) despite several years of effective antiretroviral treatment (Sips et al., 2012b). Similarly, an increase in total and NKG2a/c^{+} NK cells in rectum of RM has been shown during SIVmac infection (Li and Reeves, 2012; Takahashi et al., 2014). In contrast, the NKp44^{+} lymphocytes were significantly depleted in acute HIV and SIV infections in mucosa and continued to decline in frequency during chronic phase (Li et al., 2014b). Antiretroviral therapy significantly increased the frequency of mucosal NKG2a/c^{+} NK cells (Frias et al., 2015). SIV infection in pathogenic models drives a trafficking away from secondary lymphoid organs toward the intestine (Estes, 2013b; Reeves et al., 2010a; Wang et al., 2014). This is related to up-regulation of the gut-homing marker $\alpha_4\beta_7$ on NK cells as shown in chronic SIVmac infection coupled with down regulation of the LN-trafficking marker CCR7 (Li and Reeves, 2012; Reeves et al., 2010b). Our data in the CM on decreased NK cells in the LN and increased levels in the gut are in line with these reports. Strikingly, we observed opposite tissue dynamics in heterologous and natural hosts of SIV. In the natural host, NK cells were not directed toward the intestine and the frequencies of total NK cells in the gut were decreased in SIVagm infection in contrast to SIVmac infection. This could explain the lack of NK-cell mediated viral control in the intestine of SIVagm-infected AGMs.

These distinct NK cell tissue distributions were associated with CXCR3 expression, supporting its role as an inflammatory tissue homing marker for NK cells. The higher levels of the CXCR3 ligand (IP-10) in the intestine of SIVmac-infected macaques as compared to the SIVagm-infected AGMs (Ploquin et al., 2016, 2018) might explain in part, together with previously reported up-regulations of other receptors such as $\alpha_4\beta_7$, the higher levels of NK cells in the intestine of the SIVmac-infected macaques as compared to the natural host.

The fact that NK cells seem to be redirected to intestine in SIVmac infection raises the question of their inefficient activity against the cells replicating the virus in the gut. In fact, an increase of these cells in this compartment should favor a better control of the viral replication. However, beyond the mechanisms established by the virus to escape NK cell lysis, the inflammatory environment as well as the loss of regulatory cells (i.e ILCs, TH17, CD4 T cells) might profoundly and durably alter NK cell functions. It has also previously been reported that NKG2a/c+ NK cells accumulate in vaginal mucosa during acute SIVmac infection, and that this occurred concomitant with an increase in MHC-E that could induce an inhibitory signal to the not well educated NKG2a/c+ NK cells (Shang et al., 2014).

It is furthermore not excluded that NK cells directed to the gut contribute to tissue damage in the intestine (Evans et al., 2016). It has indeed been demonstrated in the macaque that microbial translocation increased the

recruitment of cytotoxic NK cells in the liver (Evans et al., 2016). This increase in cytotoxic NK cells resulted in an accelerated destruction of this organ. Recently NKp44+ NK cells have been implicated in autoimmune diseases, such as inflammatory bowel disease or Crohn Disease (Poggi et al., 2019), however whether they participate in pathologic or protective processes of chronic inflammation *in vivo* remains controversial. HLA-DP molecules have recently been shown to directly bind NKp44 (Niehrs et al., 2019). HLA-DP is constitutively expressed on antigen-presenting cells, including B cells. HLA-DP molecules have been shown to be upregulated on non-hematopoietic tissues in response to inflammation (Stevanović et al., 2013). Thus, it might be relevant to investigate the impact of NKP44+ NK cells on gut homeostasis in a context of gut inflammation such as HIV infection. The potential contribution on tissue damage and homeostasis by NK cells in the gut during chronic HIV/SIVmac infections will need to be addressed in future studies.

Conclusions

Given the remaining necessity in the use of NHP in biomedical research, as shown by the recent SARS-Cov2 outbreak, these data are highly relevant for establishing the validity and utility of such models for studying the role of NK cells in human diseases. More and more studies raise the question on the utility of NK cells in anti-tumor and anti-viral immunotherapies. Our data on the NK cell tissue distribution and functional profiles in the NHP contribute to the understanding of their role in lymphoid tissues during HIV infection as well as to efforts in the development of vaccines and therapies against human diseases.

II.2. NK CELL PROFILES AND IgA RESPONSES IN MESENTERIC LYMPH NODES DURING SIV INFECTIONS

Specific aims

As described above, we showed that in SIVagm infection, the number of NK cells increase in BCF (manuscript #1), while they decrease in the gut (manuscript #4). The very low numbers of NK cells in the gut during SIVagm infection most likely provides an explanation why NK cells are not capable to efficiently control SIVagm replication in the gut. This does not explain though how AGM avoid tissue damage in the gut.

Immunoglobulin A is the dominant antibody isotype found in mucosal secretions (Cerutti et al., 2011). SIgA limit the penetration of commensal bacteria through the epithelium (Boullier et al., 2009) achieving efficient protection of the epithelial barrier by immune exclusion (Phalipon et al., 2002). SIgA is known to have got an important role in control of intestine inflammation and homeostasis (Catanzaro et al., 2019; Leong and Ding, 2014; Phalipon et al., 2002). SIgA therefore have an anti-inflammatory function and play a key role in the prevention of tissue damage and recovery from infection (Corthësy, 2009; Fernandez et al., 2003). IgA-deficient humans indeed exhibit gut microbiota dysbiosis (Catanzaro et al., 2019). IgA responses, in particular SIgA, are decreased in HIV infection (Kulkarni and Ruprecht, 2017). IgA+ producing cells an induced in Peyer's patches and then migrate to mesenteric lymph nodes (Macpherson et al., 2008). As described above, NK cells accumulate around and inside B follicles of pLNs in SIVagm infection. We raise the hypothesis that NK cells also control viral replication in mesenteric lymph nodes (mesLN) draining the intestine and thereby

protect immune responses, in particular the IgA response. I was involved in all parts of the study and designed and performed all key experiments (manuscript #5).

Discussion

Our study unravels major differences regarding the IgA response in the mLN and intestine between non-pathogenic SIVagm and pathogenic SIVmac infection. Previous studies have already analyzed IgA and B cell responses during SIVagm and SIVmac infections in distinct body compartments, including blood, milk, saliva, vaginal and rectal secretions (Amos et al., 2013; Brocca-Cofano et al., 2017; Hel et al., 2017). SIV-infected AGMs were shown to display robust Env-binding antibody responses in milk, higher than those in rhesus MAC and humans, which may contribute to the rarity of postnatal transmission reported for natural SIV hosts (Chahroudi et al., 2011). Here we provide novel insights. We investigated if NK cells have the capacity to migrate into BCF of mesLN during SIVagm infection. We furthermore analyzed the IgA and B cell responses in the mesLN and distinct intestinal compartments. We evaluated the link with systemic inflammation.

We demonstrate that NK cells rapidly migrate into BCF of mesLN during SIVagm infection where they control viral replication. We show that IgA+ memory B cells were increased in mesLN during SIVagm infection in contrast to SIVmac infection. Moreover, normal intestinal IgA levels (jejunum, ileum and colon) were maintained during acute and chronic SIVagm infection, while they strongly decreased in chronically SIVmac-infected macaques. Our data in the pathogenic SIV model are in line with reports on HIV-1 infection in humans describing that HIV-1 does not induce vigorous specific IgA responses in any body fluid examined (Kulkarni and Ruprecht, 2017; Mestecky et al., 2004). Our study underlines that in contrast to pathogenic HIV-1/SIVmac infections in respectively humans and macaques, IgA responses in the mesLN are protected during SIVagm infection in AGM. The levels of CXCR5+ NK cells and IgA+ memory B cells in mesLN were strongly correlated, suggesting that indeed the NK-cell mediated viral control is an important factor in the protection against dysfunction of the mucosal B cell responses in non-pathogenic SIV infection.

The protection of B cell dysfunction by NK cells in LN could be indirect through the viral control. The lack of chronic viral replication in BCF during SIVagm infection in opposite to untreated HIV-1/SIVmac infections would avoid chronic inflammation and destruction of the anatomical architecture, in particular fibrosis and disruption of the FDC network as described during early HIV infection (Kök et al., 2015), protecting thereby B cell responses in BCF.

It is not excluded that NK cells also directly modulate B cell responses, including in HIV infection (Bradley et al., 2018). It has been shown that NK cells can influence humoral responses by diminishing T_{FH} cells and that they also can limit germinal center reaction (Cook et al., 2015; Rydyznski et al., 2018). The generation of CXCR5+ NK cells capable to migrate into BCF of mLN might facilitate the direct influence of NK cells on B cell responses. In chronically SIVmac-infected macaques, the decrease of IgA signal was observed in all three intestinal compartments studied (ileum, jejunum, intestine). Since the decrease of the IgA production was due to a strong loss of signal in the lumen, and not in the lamina propria, this means that SIgA was lost while IgA+ cells were still present in the lamina propria. The results we observed in the macaque thus resemble those previously described in HIV infection (Hel et al., 2017). A major difference between non-pathogenic and pathogenic SIVagm infection was therefore the selective maintenance of SIgA in SIVagm infection that is known to play a crucial role for the maintenance of the mucosal barrier integrity.

Although studies showed similar levels of SIV replication in the intestine of AGM and MAC (Estes et al., 2017; Raehtz et al., 2020), it was also reported that depletion of B cells in SIVagm infection leads to moderately increased viral production in the intestine (Gaufin et al., 2009). Thus, a partial, weak contribution of B cells to

viral replication in the gut during SIVagm infection is not excluded and could indirectly participate to inflammatory control. However, even if AGM develop better gp120 responses, they do not seem to develop more or better neutralizing antibodies than PLWH (Norley et al., 1990). Total IgA was negatively correlated with sCD14 in SIVmac infection, while ENV-specific IgA did not show correlations. This suggests, that the inflammatory control in SIV infection in the intestine is more associated with the maintenance of non-specific IgA responses than with SIV-specific IgA responses. The total non-specific IgA responses in the intestine during SIVagm infection might strongly contribute to protect against translocation of bacteria together with the other proposed mechanisms protecting the epithelial barrier. Blood did not reflect the IgA+ B cell dynamics occurring in the intestine. More than 90% of gut Igs are produced in situ by plasma cells in contrast to genital mucosa, where half of the Igs are coming from the blood (Jacob Nattermann et al., 2009). In addition, the intestine is the largest lymphoid tissue in the body. This could explain why B cells in blood did not accurately reflected the dynamics in the intestine and further support that it is important to analyze intestinal tissue for understanding the in situ pathophysiological virus-host interactions.

Our data provide a further explanation of why early anti-retroviral treatment has a benefit with regard to treatment initiated in chronic HIV infection. Since early ARV is known to protect BCF structures in the intestine (Kök et al., 2015), thereby most likely improving IgA responses, early ARV might increase through IgA the control of chronic inflammation and thus also protect against tissue damage.

Conclusions

In conclusion, we show that NK cells of mesLN upregulate CXCR5 in SIVagm infection and migrate into mesLN BCF. Hence, we propose that the viral control in BCF could help maintaining normal IgA responses and a better control of gut inflammation. Indeed, we found that CXCR5+ NK cell induction in mesLN correlated positively with IgA+ memory B cells in mesLN from SIVagm infection. Moreover, our data unraveled a negative correlation between gut IgA titers and inflammation in SIVmac infection, with a dramatic loss of intestinal IgA in SIV-infected MAC while IgA levels in chronic SIVagm infection remained stable. And interestingly, IgA+ memory B cells were increased in mesLN in response to SIVagm infection but not in SIVmac infection.
Enhancing HIV-specific IgA response in mucosa have been largely discussed in the context of vaccine studies (Kulkarni and Ruprecht, 2017). Here our data suggest that total non-specific IgA contributes to the inflammatory control. Strategies allowing early and persisting viral control in BCF and/or restoring normal total IgA levels in the intestine could reveal beneficial for reducing inflammation in virologically controlled PLWH with persistent residual inflammation.

II.3. TISSUE PROFILES OF NKG2A/C^{+}CD8^{+} T CELLS IN SIV INFECTIONS

Specific aims

CD8^{+} T-cells are critical in the control of viral replication. However, CD8^{+} T-cells are highly affected by a persistent antigenic stimulation and chronic inflammation. During HIV infection, CD8 T cells upregulate immune check-point inhibitors, such as PD-1, CTLA-4, Lag-3 or Tim-3 (Kaufmann and Walker, 2009). Such inhibitory receptors are generally induced to dampen inflammation, for example for the resolution of an

infection-induced inflammation that otherwise would be harmful for the tissues. However, it is hampering the antiviral efficacy of the cells (Odorizzi and Wherry, 2012). Inhibitory NK cell receptors (iNK), such as NKG2a, can also be induced on CD8+ T cells (Pereira et al., 2019; Thimme et al., 2005). NKG2A marks a unique immune effector T CD8+ subset preferentially co-expressing tissue-resident markers, but not immune checkpoint inhibitors (van Montfoort et al., 2018). CD94/NKG2A has been implicated in down-regulation of T-cell function in various cancers (Ruggeri et al., 2016) and diminished responses against some viral infections, such as polyoma virus (2002). By contrast, NKG2A+ CD8+ T cells were also found in other settings to be more efficient at protecting against viral challenge than their counterparts (Andrew J McMichael and Louis J Picker, 2017). CD8+ T cells expressing NKG2A have been observed during HIV-1 infection (Md et al., 1999). Contrasting results on their role in HIV infection have been reported (D Wesch and D Kabelitz, 2003; Maria et al., 1997; Zeddou et al., 2007). Based on these reports, we raised the hypothesis that the anti-HIV response of NKG2A+CD8+T cells is diminished, while the non-HIV-specific NKG2A+CD8+ T cells contribute to dampen inflammation in the tissues. We postulated that if this is true, NKG2A+CD8+ T cells should be increased in tissues, and in particular in the intestine, of AGM where the virus replicates (ie intestine) and contribute in tissue protection. I contributed in the tissue processing of the NKG2A+CD8+ T cells (manuscript #6).

Discussion

Here, we compared NKG2a/c expressing CD8+ T cells in non-pathogenic SIVagm infection in the natural host (AGM) compared to pathogenic SIVmac infection in macaques. Genome-wide transcriptome analysis of the NKG2a/c^{+} CD8^{+} T cells in SIVagm infection demonstrated a cytotoxic effector function and gut homing profile of these cells and also revealed the expression of immunoregulatory molecules.

In both SIVagm and SIVmac infections, the expression of the cytotoxic marker (Perforin) was more up-regulated than IFN-γ, suggesting a more cytotoxic than pro-inflammatory activity of these cells in the intestine. We detected a negative correlation between IL-23 levels in intestine and intestinal NKG2a/c+CD8+ T cells during pathogenic infection, whereas a low level of IL-23 was observed concomitantly to high frequency of NKG2a/c+CD8+ T cells in the gut during infection in the natural host. Together these results suggest that these cells might rather contribute to inflammatory control in the gut than to control of viral replication in the case of SIV, and thereby probably also HIV infection.

The cytotoxicity markers were upregulated very strongly in the gut of both CM and AGM. However, the overall frequencies of NKG2a/c+CD8+ T cells in the intestine increased for a longer period in SIVagm than in SIVmac infection. The follow up of the tissue dynamics of NKG2a/c+CD8+ T cells indeed revealed differences between pathogenic and non-pathogenic SIV infection. By performing longitudinal studies simultaneously in distinct tissues, we show a more intense expansion of NKG2a/c+CD8+ T cells in the blood and intestine in response to SIVagm in AGM compared to SIVmac infection. The expansions were associated with viremia levels suggesting that antigenic stimulation is driving the expansions. NKG2A recognizes peptides presented via the non-classical MHC-E class I molecule. The peptides presented via MHC-E can also be recognized by activatory NKG2C receptor as well as by the TCR. On NHP, the available antibodies cannot distinguish between the NKG2A and NKG2C and thus a phenotypic analysis was not possible. However, the transcriptome analyses showed that NKG2a/c+CD8+ T cells also expressed NKG2C mRNA. The expression levels of NKG2C were however not higher than those of NKG2A. Similarly, in humans, the proportion of CD8+ T expressing the activatory NKG2C receptor was similar between PLWH and healthy donors and also between viremic and non-viremic patients, suggesting that NKG2C regulation on these cells is not participating in a better control of HIV infection (Zeddou et al., 2007).

A clonal expansion of these cells, similar to what has been described for these cells in other settings is not excluded (Jabri et al., 2002). It has been proposed whereby maintaining or upregulating NKG2A upon TCR engagement by subset of CTL clones could exerts a negative feed-back on TCR activation (2002). Thereby, in natural hosts, the intestine environment with a high antigenic load might allow NKG2a/c+CD8+ T cells to respond initially and maximally to SIV antigens, submitting them later on to a fine-tuning of their TCR signaling threshold in order to down-modulate persisting immune reactions that might otherwise lead to chronic inflammation and tissue destruction. Concomitantly, the expansion of NKG2a/c+CD8+ T cells could facilitate viral persistence, which agrees with the high level of viral replication observed in intestine of natural host.

MHC-E is expressed on most cells, including on CD4+ T cells and also to high levels on intestinal epithelial cells. MHC-E has been described to be upregulated during HIV-1 and SIVmac infection in CD4+ T cells, both on infected and un-infected CD4+ T cells respectively in vitro and in vivo (Jabri Bana et al., 2005)(Wu et al., 2018). The up-regulation on un-infected cells might be a consequence of stronger expression of classical MHC-I molecules in activated CD4+ T cells and/or of HIV proteins that directly modify the expression levels of MHC-E in infected cells (Jabri Bana et al., 2005) (Takao et al., 2010). Among the small numbers of other cellular peptides that have been identified to bind to MHC-E and stimulate CD8+ T cells is a HSP60-derived peptide (Michaëlsson et al., 2002). Under stress conditions, Hsp60 is sufficiently processed and competes with the MHC-I derived peptides for presentation by MHC-E. Therefore, changes in the level of the Hsp60 peptide presented by MHC-E during SIV infection, relative to the amount of MHC class Ia-derived leader, may result in the activation of NKG2a/c+CD8+ T cells in natural host and enhanced killing of un-infected, stressed cells in the intestine of SVagm-infected AGM. We report here increased levels of HSP60 protein in the intestine of SIVmac-infected MAC, while they were not increased in SIVagm infection. Therefore, either there are less stressed cells in SIVagm infection and thereby less uninfected cells would be killed by this mechanism, or alternatively, the stressed cells are more efficiently eliminated by NKG2A+CD8+ T cells in SIVagm infection allowing improved tissue repair.

The up-regulation of CD94/NKG2A and other NK cell receptors on CD8+ T cells is a general feature of the immune response and the extent of up-regulation is variable. It is notable that expression of CD94/NKG2A is known to be influenced by a number of cytokines. Indeed, IL-6, IL-10, and IL-21, increases CD94/NKG2A expression, whereas IL-4, IL-23, and TGF-β are strongly inhibitory (Cho et al., 2011). Unlike IL-2, the capacity of IL-4, IL-23, and TGF-β to inhibit CD94/NKG2A expression is CD28 independent. Differences in the tissue cytokine environment between SIVagm and SIVmac infection, as described (Ploquin et al., 2006) might explain the differences we observed regarding the dynamics of the NKG2a/c+CD8+ T cells.

Conclusions

This is a large study, in multiple tissues, that were analyzed transversally and longitudinally including *ex vivo* analyses on functional profiles of unstimulated cells and a genome-wide transcriptomic study. Altogether we demonstrate that NKG2a/c+CD8 T cells do not expand in LN but do increase in the blood and intestine during non-pathogenic SIV infection. They display a strong cytotoxic and immunoregulatory function. We show that they correlate negatively with intestinal inflammation. This study suggests that NKG2a/c+CD8 T cells do not contribute to viral control, as expected, but that they participate in the control of immunopathology in the intestine during SIV and may be also HIV infection.

PART V. General conclusions and Perspectives

Protection against viral-induced tissue damage can generally be achieved either through strong pathogen control or through resilience strategies (Chovatiya and Medzhitov, 2014). The latter could include improved homeostatic mechanisms, improved wound healing, control of inflammation and/or resistance to stress (Galluzzi et al., 2018)(Cohen et al., 2012).

Our studies provide important novel information to better understand the mechanisms of how AGM avoid tissue damage during SIVagm infection. AGMs developed an original tissue-specific mechanism of resilience, with viral replication control essentially and only occurring in secondary lymphoid tissues. Indeed, we found that SIVagm infection induces an up-regulation of CXCR5 on NK cells, allowing NK cells to migrate into B cell follicles, where follicular dendritic cells present high levels of membrane-bound IL-15. We observed an early NK cell migration into follicles during the acute phase of SIVagm infection (day 9 post-infection) and throughout chronic phase of SIVagm infection. Our study reveals that IL-6 participates in the induction of CXCR5 on NK cells in acute SIVagm infection. Also, our results highlight an unprecedented crosstalk between NK and B cells.

Future studies might investigate the cross-talk between CXCR5+ NK cells and B cells. It would for example be interesting to analyze why only contact-independent co-cultures of NK and B cells enhance the susceptibility of NK cells to express CXCR5. It will also be important to better understand the impact of DC on the NK cell phenotypes in the LN.

The description of CXCR5+ NK cells supports the potential of these cells to interact directly with other cells present in B follicles, such as T_{FH} cells or/and B cells. It might be useful to further investigate how NK cells might impact B cell activity in BCF during vaccine studies.

We also demonstrated that T_{FH} cells in LN of MAC and AGM express high levels of MHC-E, which expand in pathogenic SIVmac infection in MAC but decrease upon SIVagm infection in AGM. We identified peptides derived from the ENV signal sequence that strongly bind to MHC-E. We deciphered a differential MHC-E restricted SIV suppressive capacity of NK cells from AGM and MAC. We demonstrate that SIVagm infection induces the expansion of terminally differentiated NKG2a^{low} NK cells in LN displaying an adaptive transcriptional profile. Such differentiation was lacking after day 2 post-infection in SIVmac-infected macaques. Adaptive NK cells were characterized by elevated levels of Themis and no increased NKG2C expression. This study reveals an unprecedented NK cell adaptation to a viral infection and opens novel strategies toward NK-cell directed therapies and viral control in tissues. Since we observed that NK cells in SIVagm infected AGM display a terminally differentiated phenotype, molecules that enhance such differentiation might be used in the future in pre-clinical assays in SIVmac-infected macaques.

AGMs might have developed resilience mechanisms where tissues are synergistically protected. Thus, NK cells control viral replication in LN, including mLN as shown here. This could protect the immune responses, including the SIgA production in the intestine, contributing to the maintenance of bacterial control and epithelial barrier integrity, despite viral replication in the intestinal mucosa. In contrast, mesenteric lymph nodes

are major viral reservoirs in pathogenic HIV/SIV infections (Cumont et al., 2007) and IgA responses in intestine are damaged.

It is unclear which mechanism in the gut is the principal factor for maintaining the gut barrier intact in SIVagm infection. Multiple factors, including Th17 cells, IL-21 production, IgA and NKG2A+ CD8 T cells could be involved. The exact role of each factor still needs to be established.

An intervention study to prove the immunoregulatory role of these NKG2A+ CD8 T cells in the gut of SIV-infected animals could not be performed. Indeed, by targeting NKG2A, one would also inhibit NK cell responses in the animals, NKG2A being expressed on >80% of NK cells in NHP (Huot et al, Frontiers in Immunol, in press). A functional assay is also lacking. For instance, in order to differentiate between NKG2A and TCR mediated recognition by NKG2A+ CD8 T cells, the development of tetramers would be useful in the future.

Altogether, our study provides novel insights into virus-host interactions in tissues in an original and complex model that might be helpful to provide novel ideas for better control of human viral infections.

PART VI. References (Introduction & Discussion)

Aarnink, A., Dereuddre-Bosquet, N., Vaslin, B., Le Grand, R., Winterton, P., Apoil, P.-A., and Blancher, A. (2011). Influence of the MHC genotype on the progression of experimental SIV infection in the Mauritian cynomolgus macaque. Immunogenetics *63*, 267–274.

Abdel-Mohsen, M., Kuri-Cervantes, L., Grau-Exposito, J., Spivak, A.M., Nell, R.A., Tomescu, C., Vadrevu, S.K., Giron, L.B., Serra-Peinado, C., Genescà, M., et al. (2018). CD32 is expressed on cells with transcriptionally active HIV but does not enrich for HIV DNA in resting T cells. Sci. Transl. Med. *10*.

Abel, A.M., Yang, C., Thakar, M.S., and Malarkannan, S. (2018). Natural Killer Cells: Development, Maturation, and Clinical Utilization. Front. Immunol. *9*.

Abrahams, M.-R., Joseph, S.B., Garrett, N., Tyers, L., Moeser, M., Archin, N., Council, O.D., Matten, D., Zhou, S., Doolabh, D., et al. (2019). The replication-competent HIV-1 latent reservoir is primarily established near the time of therapy initiation. Sci. Transl. Med. *11*.

Abreu, C.M., Veenhuis, R.T., Avalos, C.R., Graham, S., Parrilla, D.R., Ferreira, E.A., Queen, S.E., Shirk, E.N., Bullock, B.T., Li, M., et al. (2019a). Myeloid and CD4 T Cells Comprise the Latent Reservoir in Antiretroviral Therapy-Suppressed SIVmac251-Infected Macaques. MBio *10*.

Abreu, C.M., Veenhuis, R.T., Avalos, C.R., Graham, S., Queen, S.E., Shirk, E.N., Bullock, B.T., Li, M., Pate, K.A.M., Beck, S.E., et al. (2019b). Infectious Virus Persists in CD4+ T Cells and Macrophages in Antiretroviral Therapy-Suppressed Simian Immunodeficiency Virus-Infected Macaques. J. Virol. *93*.

Aid, M., Dupuy, F.P., Moysi, E., Moir, S., Haddad, E.K., Estes, J.D., Sekaly, R.P., Petrovas, C., and Ribeiro, S.P. (2018). Follicular CD4 T Helper Cells As a Major HIV Reservoir Compartment: A Molecular Perspective. Front. Immunol. *9*.

Aidy, S.E., Hooiveld, G., Tremaroli, V., Bäckhed, F., and Kleerebezem, M. (2013). The gut microbiota and mucosal homeostasis. Gut Microbes *4*, 118–124.

Andrew J, McMichael, and Louis J, Picker (2017). Unusual antigen presentation offers new insight into HIV vaccine design. Curr. Opin. Immunol. *46*, 75–81.

Allers, K., Loddenkemper, C., Hofmann, J., Unbehaun, A., Kunkel, D., Moos, V., Kaup, F.-J., Stahl-Hennig, C., Sauermann, U., Epple, H.-J., et al. (2010). Gut mucosal FOXP3+ regulatory CD4+ T cells and Nonregulatory CD4+ T cells are differentially affected by simian immunodeficiency virus infection in rhesus macaques. J. Virol. *84*, 3259–3269.

Allers, K., Fehr, M., Conrad, K., Epple, H.-J., Schürmann, D., Geelhaar-Karsch, A., Schinnerling, K., Moos, V., and Schneider, T. (2014). Macrophages Accumulate in the Gut Mucosa of Untreated HIV-infected Patients. J. Infect. Dis. *209*, 739–748.

Alter, G., Heckerman, D., Schneidewind, A., Fadda, L., Kadie, C.M., Carlson, J.M., Oniangue-Ndza, C., Martin, M., Li, B., Khakoo, S.I., et al. (2011). HIV-1 adaptation to NK-cell-mediated immune pressure. Nature *476*, 96–100.

Altfeld, M., Fadda, L., Frleta, D., and Bhardwaj, N. (2011). DCs and NK cells: critical effectors in the immune response to HIV-1. Nat. Rev. Immunol. *11*, 176–186.

Amand, M., Iserentant, G., Poli, A., Sleiman, M., Fievez, V., Sanchez, I.P., Sauvageot, N., Michel, T., Aouali, N., Janji, B., et al. (2017). Human CD56dimCD16dim Cells As an Individualized Natural Killer Cell Subset. Front. Immunol. *8*.

Amos, J.D., Wilks, A.B., Fouda, G.G., Smith, S.D., Colvin, L., Mahlokozera, T., Ho, C., Beck, K., Overman, R.G., DeMarco, C.T., et al. (2013). Lack of B Cell Dysfunction Is Associated with Functional, gp120-Dominant Antibody Responses in Breast Milk of Simian Immunodeficiency Virus-Infected African Green Monkeys. J. Virol. *87*, 11121–11134.

Amos, J.D., Himes, J.E., Armand, L., Gurley, T.C., Martinez, D.R., Colvin, L., Beck, K., Overman, R.G., Liao, H.-X., Moody, M.A., et al. (2015). Rapid Development of gp120-Focused Neutralizing B Cell Responses during Acute Simian Immunodeficiency Virus Infection of African Green Monkeys. J. Virol. *89*, 9485–9498.

Ananworanich, J., Eller, L.A., Pinyakorn, S., Kroon, E., Sriplenchan, S., Fletcher, J.L., Suttichom, D., Bryant, C., Trichavaroj, R., Dawson, P., et al. (2017). Viral kinetics in untreated versus treated acute HIV infection in prospective cohort studies in Thailand. J. Int. AIDS Soc. *20*, 21652.

von Andrian, U.H., and Mempel, T.R. (2003). Homing and cellular traffic in lymph nodes. Nat. Rev. Immunol. *3*, 867–878.

Anraku, I., Rajasuriar, R., Dobbin, C., Brown, R., Lewin, S.R., and Suhrbier, A. (2012). Circulating Heat Shock Protein 60 Levels Are Elevated in HIV Patients and Are Reduced by Anti-Retroviral Therapy. PLOS ONE *7*, e45291.

Bachmann, N., von Siebenthal, C., Vongrad, V., Turk, T., Neumann, K., Beerenwinkel, N., Bogojeska, J., Fellay, J., Roth, V., Kok, Y.L., et al. (2019). Determinants of HIV-1 reservoir size and long-term dynamics during suppressive ART. Nat. Commun. *10*, 3193.

Badia, R., Ballana, E., Castellví, M., García-Vidal, E., Pujantell, M., Clotet, B., Prado, J.G., Puig, J., Martínez, M.A., Riveira-Muñoz, E., et al. (2018). CD32 expression is associated to T-cell activation and is not a marker of the HIV-1 reservoir. Nat. Commun. *9*, 2739.

Bagnara, D., Squillario, M., Kipling, D., Mora, T., Walczak, A.M., Da Silva, L., Weller, S., Dunn-Walters, D.K., Weill, J.-C., and Reynaud, C.-A. (2015). A Reassessment of IgM Memory Subsets in Humans. J. Immunol. Baltim. Md 1950 *195*, 3716–3724.

Bajénoff, M., Breart, B., Huang, A.Y.C., Qi, H., Cazareth, J., Braud, V.M., Germain, R.N., and Glaichenhaus, N. (2006). Natural killer cell behavior in lymph nodes revealed by static and real-time imaging. J. Exp. Med. *203*, 619–631.

Banga, R., Procopio, F.A., Noto, A., Pollakis, G., Cavassini, M., Ohmiti, K., Corpataux, J.-M., de Leval, L., Pantaleo, G., and Perreau, M. (2016). PD-1 + and follicular helper T cells are responsible for persistent HIV-1 transcription in treated aviremic individuals. Nat. Med. *22*, 754–761.

Bankovich, A.J., Shiow, L.R., and Cyster, J.G. (2010). CD69 Suppresses Sphingosine 1-Phosophate Receptor-1 (S1P1) Function through Interaction with Membrane Helix 4. J. Biol. Chem. *285*, 22328–22337.

Barbarin, A., Cayssials, E., Jacomet, F., Nunez, N.G., Basbous, S., Lefèvre, L., Abdallah, M., Piccirilli, N., Morin, B., Lavoue, V., et al. (2017). Phenotype of NK-Like CD8(+) T Cells with Innate Features in Humans and Their Relevance in Cancer Diseases. Front. Immunol. *8*.

Barouch, D.H., Ghneim, K., Bosche, W.J., Li, Y., Berkemeier, B., Hull, M., Bhattacharyya, S., Cameron, M., Liu, J., Smith, K., et al. (2016). Rapid Inflammasome Activation following Mucosal SIV Infection of Rhesus Monkeys. Cell *165*, 656–667.

Barrenas, F., Raehtz, K., Xu, C., Law, L., Green, R.R., Silvestri, G., Bosinger, S.E., Nishida, A., Li, Q., Lu, W., et al. (2019). Macrophage-associated wound healing contributes to African green monkey SIV pathogenesis control. Nat. Commun. *10*, 5101.

Barton, K., Winckelmann, A., and Palmer, S. (2016). HIV-1 Reservoirs During Suppressive Therapy. Trends Microbiol. *24*, 345–355.

Bartz, S.R., Pauza, C.D., Ivanyi, J., Jindal, S., Welch, W.J., and Malkovsky, M. (1994). An Hsp60 related protein is associated with purified HIV and SIV. J. Med. Primatol. *23*, 151–154.

Belkaid, Y., and Harrison, O.J. (2017). Homeostatic Immunity and the Microbiota. Immunity *46*, 562–576.

Benson, D.M., Bakan, C.E., Mishra, A., Hofmeister, C.C., Efebera, Y., Becknell, B., Baiocchi, R.A., Zhang, J., Yu, J., Smith, M.K., et al. (2010). The PD-1/PD-L1 axis modulates the natural killer cell versus multiple myeloma effect: a therapeutic target for CT-011, a novel monoclonal anti-PD-1 antibody. Blood *116*, 2286–2294.

Bevins, C.L., and Salzman, N.H. (2011). Paneth cells, antimicrobial peptides and maintenance of intestinal homeostasis. Nat. Rev. Microbiol. *9*, 356–368.

Bhagat, G., Naiyer, A.J., Shah, J.G., Harper, J., Jabri, B., Wang, T.C., Green, P.H.R., and Manavalan, J.S. (2008). Small intestinal $CD8^+TCR\gamma\delta^+NKG2A^+$ intraepithelial lymphocytes have attributes of regulatory cells in patients with celiac disease. J. Clin. Invest. *118*, 281–293.

Blackard, J.T., Ma, G., Martin, C.M., Rouster, S.D., Shata, M.T., and Sherman, K.E. (2011). HIV Variability in the Liver and Evidence of Possible Compartmentalization. AIDS Res. Hum. Retroviruses *27*, 1117–1126.

Bordet, E., Frétaud, M., Crisci, E., Bouguyon, E., Rault, S., Pezant, J., Pleau, A., Renson, P., Giuffra, E., Larcher, T., et al. (2019). Macrophage-B Cell Interactions in the Inverted Porcine Lymph Node and Their Response to Porcine Reproductive and Respiratory Syndrome Virus. Front. Immunol. *10*.

Bordoni, V., Bibas, M., Abbate, I., Viola, D., Rozera, G., Agrati, C., Rinaldi, A., Amendola, A., Ammassari, A., Capobianchi, M.R., et al. (2015). Bone marrow CD34+ progenitor cells may harbour HIV-DNA even in successfully treated patients. Clin. Microbiol. Infect. Off. Publ. Eur. Soc. Clin. Microbiol. Infect. Dis. *21*, 290.e5-8.

Bosinger, S.E., Li, Q., Gordon, S.N., Klatt, N.R., Duan, L., Xu, L., Francella, N., Sidahmed, A., Smith, A.J., Cramer, E.M., et al. (2009). Global genomic analysis reveals rapid control of a robust innate response in SIV-infected sooty mangabeys. J. Clin. Invest. *119*, 3556–3572.

Boullier, S., Tanguy, M., Kadaoui, K.A., Caubet, C., Sansonetti, P., Corthésy, B., and Phalipon, A. (2009). Secretory IgA-Mediated Neutralization of Shigella flexneri Prevents Intestinal Tissue Destruction by Down-Regulating Inflammatory Circuits. J. Immunol. *183*, 5879–5885.

Bradley, T., Peppa, D., Pedroza-Pacheco, I., Li, D., Cain, D.W., Henao, R., Venkat, V., Hora, B., Chen, Y., Vandergrift, N.A., et al. (2018). RAB11FIP5 Expression and Altered Natural Killer Cell Function Are Associated with Induction of HIV Broadly Neutralizing Antibody Responses. Cell *175*, 387-399.e17.

Brenchley, J.M. (2013). Mucosal immunity in human and simian immunodeficiency lentivirus infections. Mucosal Immunol. *6*, 657–665.

Brenchley, J.M., and Paiardini, M. (2011). Immunodeficiency lentiviral infections in natural and non-natural hosts. Blood *118*, 847–854.

Brenchley, J.M., Paiardini, M., Knox, K.S., Asher, A.I., Cervasi, B., Asher, T.E., Scheinberg, P., Price, D.A., Hage, C.A., Kholi, L.M., et al. (2008). Differential Th17 CD4 T-cell depletion in pathogenic and nonpathogenic lentiviral infections. Blood *112*, 2826–2835.

Brocca-Cofano, E., Kuhrt, D., Siewe, B., Xu, C., Haret-Richter, G.S., Craigo, J., Labranche, C., Montefiori, D.C., Landay, A., Apetrei, C., et al. (2017). Pathogenic Correlates of Simian Immunodeficiency Virus-Associated B Cell Dysfunction. J. Virol. *91*.

Buettner, M., and Lochner, M. (2016). Development and Function of Secondary and Tertiary Lymphoid Organs in the Small Intestine and the Colon. Front. Immunol. *7*.

Bush, T.J.V., Buchta, C.M., Claudio, J., and Bishop, G.A. (2009). Cutting Edge: Importance of IL-6 and Cooperation between Innate and Adaptive Immune Receptors in Cellular Vaccination with B Lymphocytes1. J. Immunol.

C Kornfeld, Ploquin Mj, Pandrea I, Abdourahmane F, Richard O, et al. (2005). Antiinflammatory profiles during primary SIV infection in African green monkeys are associated with protection against AIDS. J. Clin. Invest. *115*, 1082–1091.

Calantone, N., Wu, F., Klase, Z., Deleage, C., Perkins, M., Matsuda, K., Thompson, E.A., Ortiz, A.M., Vinton, C.L., Ourmanov, I., et al. (2014). Tissue Myeloid Cells in SIV-Infected Primates Acquire Viral DNA through Phagocytosis of Infected T Cells. Immunity *41*, 493–502.

Carrillo-Bustamante, P., Keşmir, C., and de Boer, R.J. (2016). The evolution of natural killer cell receptors. Immunogenetics *68*, 3–18.

Casado, C., Colombo, S., Rauch, A., Martínez, R., Günthard, H.F., Garcia, S., Rodríguez, C., Romero, J. del, Telenti, A., and López-Galíndez, C. (2010). Host and Viral Genetic Correlates of Clinical Definitions of HIV-1 Disease Progression. PLOS ONE *5*, e11079.

Casado, C., Galvez, C., Pernas, M., Tarancon-Diez, L., Rodriguez, C., Sanchez-Merino, V., Vera, M., Olivares, I., De Pablo-Bernal, R., Merino-Mansilla, A., et al. (2020). Permanent control of HIV-1 pathogenesis in exceptional elite controllers: a model of spontaneous cure. Sci. Rep. *10*, 1902.

Cassol, E., Rossouw, T., Malfeld, S., Mahasha, P., Slavik, T., Seebregts, C., Bond, R., du Plessis, J., Janssen, C., Roskams, T., et al. (2015). CD14+ macrophages that accumulate in the colon of African AIDS patients express pro-inflammatory cytokines and are responsive to lipopolysaccharide. BMC Infect. Dis. *15*, 430.

Catanzaro, J.R., Strauss, J.D., Bielecka, A., Porto, A.F., Lobo, F.M., Urban, A., Schofield, W.B., and Palm, N.W. (2019). IgA-deficient humans exhibit gut microbiota dysbiosis despite secretion of compensatory IgM. Sci. Rep. *9*, 13574.

Cecchinato, V., Trindade, C.J., Laurence, A., Heraud, J.M., Brenchley, J.M., Ferrari, M.G., Zaffiri, L., Tryniszewska, E., Tsai, W.P., Vaccari, M., et al. (2008). Altered balance between Th17 and Th1 cells at mucosal sites predicts AIDS progression in simian immunodeficiency virus-infected macaques. Mucosal Immunol. *1*, 279–288.

Cerutti, A., Chen, K., and Chorny, A. (2011). Immunoglobulin Responses at the Mucosal Interface. Annu. Rev. Immunol. *29*, 273–293.

Chahroudi, A., Meeker, T., Lawson, B., Ratcliffe, S., Else, J., and Silvestri, G. (2011). Mother-to-infant transmission of SIV is rare in sooty mangabeys and is associated with low viremia. J. Virol.

Chahroudi, A., Bosinger, S.E., Vanderford, T.H., Paiardini, M., and Silvestri, G. (2012). Natural SIV Hosts: Showing AIDS the Door. Science *335*, 1188–1193.

Chakrabarti, L., Isola, P., Cumont, M.C., Claessens-Maire, M.A., Hurtrel, M., Montagnier, L., and Hurtrel, B. (1994). Early stages of simian immunodeficiency virus infection in lymph nodes. Evidence for high viral load and successive populations of target cells. Am. J. Pathol. *144*, 1226–1237.

Chen, Y., Xin, Z., Huang, L., Zhao, L., Wang, S., Cheng, J., Wu, P., and Chai, Y. (2020). CD8+ T Cells Form the Predominant Subset of NKG2A+ Cells in Human Lung Cancer. Front. Immunol. *10*.

Chéret, A., Durier, C., Mélard, A., Ploquin, M., Heitzmann, J., Lécuroux, C., Avettand-Fenoël, V., David, L., Pialoux, G., Chennebault, J.-M., et al. (2017). Impact of early cART on HIV blood and semen compartments at the time of primary infection. PLOS ONE *12*, e0180191.

Cho, J.-H., Kim, H.-O., Webster, K., Palendira, M., Hahm, B., Kim, K.-S., King, C., Tangye, S.G., and Sprent, J. (2011). Calcineurin-dependent negative regulation of CD94/NKG2A expression on naive CD8+ T cells. Blood *118*, 116–128.

Choi, S., Warzecha, C., Zvezdova, E., Lee, J., Argenty, J., Lesourne, R., Aravind, L., and Love, P.E. (2017). THEMIS enhances TCR signaling and enables positive selection by selective inhibition of the phosphatase SHP-1. Nat. Immunol. *18*, 433–441.

Choi, S.S., Chhabra, V.S., Nguyen, Q.H., Ank, B.J., Stiehm, E.R., and Roberts, R.L. (2004). Interleukin-15 Enhances Cytotoxicity, Receptor Expression, and Expansion of Neonatal Natural Killer Cells in Long-Term Culture. Clin. Diagn. Lab. Immunol. *11*, 879–888.

Chomont, N., El-Far, M., Ancuta, P., Trautmann, L., Procopio, F.A., Yassine-Diab, B., Boucher, G., Boulassel, M.-R., Ghattas, G., Brenchley, J.M., et al. (2009). HIV reservoir size and persistence are driven by T cell survival and homeostatic proliferation. Nat. Med. *15*, 893–900.

Chovatiya, R., and Medzhitov, R. (2014). Stress, inflammation, and defense of homeostasis. Mol. Cell *54*, 281–288.

Ciccone, E.J., Read, S.W., Mannon, P.J., Yao, M.D., Hodge, J.N., Dewar, R., Chairez, C.L., Proschan, M.A., Kovacs, J.A., and Sereti, I. (2010). Cycling of gut mucosal CD4+ T cells decreases after prolonged anti-retroviral therapy and is associated with plasma LPS levels. Mucosal Immunol. *3*, 172–181.

Cichocki, F., Schlums, H., Theorell, J., Tesi, B., Miller, J., Ljunggren, H.-G., and Bryceson, Y. (2015). Diversification and Functional Specialization of Human NK Cell Subsets. Curr. Top. Microbiol. Immunol. *395*.

Clayton, K.L., Garcia, J.V., Clements, J.E., and Walker, B.D. (2017). HIV Infection of Macrophages: Implications for Pathogenesis and Cure. Pathog. Immun. *2*, 179–192.

Cohen, S., Janicki-Deverts, D., Doyle, W.J., Miller, G.E., Frank, E., Rabin, B.S., and Turner, R.B. (2012). Chronic stress, glucocorticoid receptor resistance, inflammation, and disease risk. Proc. Natl. Acad. Sci. U. S. A. *109*, 5995–5999.

Cook, K.D., Waggoner, S.N., and Whitmire, J.K. (2014). NK Cells and Their Ability to Modulate T Cells during Virus Infections. Crit. Rev. Immunol. *34*, 359–388.

Cook, K.D., Kline, H.C., and Whitmire, J.K. (2015). NK cells inhibit humoral immunity by reducing the abundance of CD4+ T follicular helper cells during a chronic virus infection. J. Leukoc. Biol. *98*, 153–162.

Corthësy, B. (2009). Secretory immunoglobulin A: well beyond immune exclusion at mucosal surfaces. Immunopharmacol. Immunotoxicol. *31*, 174–179.

Costa, P., Rusconi, S., Fogli, M., Mavilio, D., Murdaca, G., Puppo, F., Mingari, M.C., Galli, M., Moretta, L., and De Maria, A. (2003). Low expression of inhibitory natural killer receptors in CD8 cytotoxic T lymphocytes in long-term non-progressor HIV-1-infected patients. AIDS Lond. Engl. *17*, 257–260.

Costela-Ruiz, V.J., Illescas-Montes, R., Puerta-Puerta, J.M., Ruiz, C., and Melguizo-Rodríguez, L. (2020). SARS-CoV-2 infection: The role of cytokines in COVID-19 disease. Cytokine Growth Factor Rev.

Couturier, J., Suliburk, J.W., Brown, J.M., Luke, D.J., Agarwal, N., Yu, X., Nguyen, C., Iyer, D., Kozinetz, C.A., Overbeek, P.A., et al. (2015). Human adipose tissue as a reservoir for memory CD4+ T cells and HIV. AIDS Lond. Engl. *29*, 667–674.

Crakes, K.R., and Jiang, G. (2019). Gut Microbiome Alterations During HIV/SIV Infection: Implications for HIV Cure. Front. Microbiol. *10*.

Cribbs, S.K., Lennox, J., Caliendo, A.M., Brown, L.A., and Guidot, D.M. (2014). Healthy HIV-1-Infected Individuals on Highly Active Antiretroviral Therapy Harbor HIV-1 in Their Alveolar Macrophages. AIDS Res. Hum. Retroviruses *31*, 64–70.

Crosse, K.M., Monson, E.A., Beard, M.R., and Helbig, K.J. (2018). Interferon-Stimulated Genes as Enhancers of Antiviral Innate Immune Signaling. J. Innate Immun. *10*, 85–93.

Cumont, M.C., Monceaux, V., Viollet, L., Lay, S., Parker, R., Hurtrel, B., and Estaquier, J. (2007). TGF- β in intestinal lymphoid organs contributes to the death of armed effector CD8 T cells and is associated with the absence of virus containment in rhesus macaques infected with the simian immunodeficiency virus. Cell Death Differ. *14*, 1747–1758.

Cumont, M.-C., Diop, O., Vaslin, B., Elbim, C., Viollet, L., Monceaux, V., Lay, S., Silvestri, G., Grand, R.L., Müller-Trutwin, M., et al. (2008). Early Divergence in Lymphoid Tissue Apoptosis between Pathogenic and Nonpathogenic Simian Immunodeficiency Virus Infections of Nonhuman Primates. J. Virol. *82*, 1175–1184.

Cush, S.S., and Flaño, E. (2011). KLRG1+NKG2A+ CD8 T Cells Mediate Protection and Participate in Memory Responses during γ-Herpesvirus Infection. J. Immunol.

Cyster, J.G., and Allen, C.D.C. (2019). B Cell Responses: Cell Interaction Dynamics and Decisions. Cell *177*, 524–540.

D, Wesch, and D, Kabelitz. (2003). Differential expression of natural killer receptors on Vdelta1 gammadelta T cells in HIV-1-infected individuals. J. Acquir. Immune Defic. Syndr. 1999 *33*, 420–425.

DaFonseca, S., Niessl, J., Pouvreau, S., Wacleche, V.S., Gosselin, A., Cleret-Buhot, A., Bernard, N., Tremblay, C., Jenabian, M.-A., Routy, J.-P., et al. (2015). Impaired Th17 polarization of phenotypically naive CD4+ T-cells during chronic HIV-1 infection and potential restoration with early ART. Retrovirology *12*, 38.

Dandekar, S., George, M.D., and Bäumler, A.J. (2010). Th17 cells, HIV and the gut mucosal barrier. Curr. Opin. HIV AIDS *5*, 173–178.

Darcis, G., Kootstra, N.A., Hooibrink, B., van Montfort, T., Maurer, I., Groen, K., Jurriaans, S., Bakker, M., van Lint, C., Berkhout, B., et al. (2020). CD32+CD4+ T Cells Are Highly Enriched for HIV DNA and Can Support Transcriptional Latency. Cell Rep. *30*, 2284-2296.e3.

Daudelin, J.-F., Mathieu, M., Boulet, S., and Labrecque, N. (2012). IL-6 Production by Dendritic Cells Is Dispensable for CD8+ Memory T-Cell Generation (Hindawi).

Deeks, S.G., and Phillips, A.N. (2009). HIV infection, antiretroviral treatment, ageing, and non-AIDS related morbidity. BMJ *338*.

Deeks, S.G., Kitchen, C.M.R., Liu, L., Guo, H., Gascon, R., Narváez, A.B., Hunt, P., Martin, J.N., Kahn, J.O., Levy, J., et al. (2004). Immune activation set point during early HIV infection predicts subsequent CD4+ T-cell changes independent of viral load. Blood *104*, 942–947.

Descours, B., Petitjean, G., López-Zaragoza, J.-L., Bruel, T., Raffel, R., Psomas, C., Reynes, J., Lacabaratz, C., Levy, Y., Schwartz, O., et al. (2017). CD32a is a marker of a CD4 T-cell HIV reservoir harbouring replication-competent proviruses. Nature *543*, 564–567.

DiNapoli, S.R., Ortiz, A.M., Wu, F., Matsuda, K., Twigg, H.L., Hirsch, V.M., Knox, K., and Brenchley, J.M. (2017). Tissue-resident macrophages can contain replication-competent virus in antiretroviral-naive, SIV-infected Asian macaques. JCI Insight *2*.

Diop, O., Gueye, A., Dias-Tavares, M., Kornfeld, C., Faye, A., Ave, P., Huerre, M., Corbet, S., Barre-Sinoussi, F., and Müller-Trutwin, M. (2000). High Levels of Viral Replication during Primary Simian Immunodeficiency

Virus SIVagm Infection Are Rapidly and Strongly Controlled in African Green Monkeys. J. Virol. *74*, 7538–7547.

Diop, O.M., Ploquin, M.J.-Y., Mortara, L., Faye, A., Jacquelin, B., Kunkel, D., Lebon, P., Butor, C., Hosmalin, A., Barré-Sinoussi, F., et al. (2008). Plasmacytoid dendritic cell dynamics and alpha interferon production during Simian immunodeficiency virus infection with a nonpathogenic outcome. J. Virol. *82*, 5145–5152.

Dogra, P., Rancan, C., Ma, W., Toth, M., Senda, T., Carpenter, D.J., Kubota, M., Matsumoto, R., Thapa, P., Szabo, P.A., et al. (2020a). Tissue Determinants of Human NK Cell Development, Function, and Residence. Cell *180*, 749-763.e13.

Dogra, P., Rancan, C., Ma, W., Toth, M., Senda, T., Carpenter, D.J., Kubota, M., Matsumoto, R., Thapa, P., Szabo, P.A., et al. (2020b). Tissue Determinants of Human NK Cell Development, Function, and Residence. Cell *180*, 749-763.e13.

Domingues, R.G., and Hepworth, M.R. (2020). Immunoregulatory Sensory Circuits in Group 3 Innate Lymphoid Cell (ILC3) Function and Tissue Homeostasis. Front. Immunol. *11*.

Eberl, G., and Lochner, M. (2009). The development of intestinal lymphoid tissues at the interface of self and microbiota. Mucosal Immunol. *2*, 478–485.

Echebli, N., Tchitchek, N., Dupuy, S., Bruel, T., Passaes, C.P.B., Bosquet, N., Grand, R.L., Bourgeois, C., Favier, B., Cheynier, R., et al. (2018). Stage-specific IFN-induced and IFN gene expression reveal convergence of type I and type II IFN and highlight their role in both acute and chronic stage of pathogenic SIV infection. PLOS ONE *13*, e0190334.

Eivazi, S., Bagheri, S., Hashemzadeh, M.S., Ghalavand, M., Qamsari, E.S., Dorostkar, R., and Yasemi, M. (2016). Development of T follicular helper cells and their role in disease and immune system. Biomed. Pharmacother. Biomedecine Pharmacother. *84*, 1668–1678.

El Hed, A., Khaitan, A., Kozhaya, L., Manel, N., Daskalakis, D., Borkowsky, W., Valentine, F., Littman, D.R., and Unutmaz, D. (2010). Susceptibility of Human Th17 Cells to Human Immunodeficiency Virus and Their Perturbation during Infection. J. Infect. Dis. *201*, 843–854.

Elssen, C.H.M.J.V., Oth, T., Germeraad, W.T.V., Bos, G.M.J., and Vanderlocht, J. (2014). Natural Killer Cells: The Secret Weapon in Dendritic Cell Vaccination Strategies. Clin. Cancer Res. *20*, 1095–1103.

Epeldegui, M., Thapa, D.R., Cruz, J.D.L., Kitchen, S., Zack, J.A., and Martínez-Maza, O. (2010). CD40 Ligand (CD154) Incorporated into HIV Virions Induces Activation-Induced Cytidine Deaminase (AID) Expression in Human B Lymphocytes. PLOS ONE *5*, e11448.

Estes, J.D. (2013a). Pathobiology of HIV/SIV-associated changes in secondary lymphoid tissues. Immunol. Rev. *254*, 65–77.

Estes, J.D. (2013b). Pathobiology of HIV/SIV-Associated Changes in Secondary Lymphoid Tissues. Immunol. Rev. *254*, 65–77.

Estes, J.D., Haase, A.T., and Schacker, T.W. (2008). The role of collagen deposition in depleting CD4+ T cells and limiting reconstitution in HIV-1 and SIV infections through damage to the secondary lymphoid organ niche. Semin. Immunol. *20*, 181–186.

Estes, J.D., Reilly, C., Trubey, C.M., Fletcher, C.V., Cory, T.J., Piatak, M., Russ, S., Anderson, J., Reimann, T.G., Star, R., et al. (2015). Antifibrotic Therapy in Simian Immunodeficiency Virus Infection Preserves CD4+ T-Cell Populations and Improves Immune Reconstitution With Antiretroviral Therapy. J. Infect. Dis. *211*, 744–754.

Estes, J.D., Kityo, C., Ssali, F., Swainson, L., Makamdop, K.N., Del Prete, G.Q., Deeks, S.G., Luciw, P.A., Chipman, J.G., Beilman, G.J., et al. (2017). Defining total-body AIDS-virus burden with implications for curative strategies. Nat. Med. *23*, 1271–1276.

Etemad, B., Esmaeilzadeh, E., and Li, J.Z. (2019). Learning From the Exceptions: HIV Remission in Post-treatment Controllers. Front. Immunol. *10*.

d'Ettorre, G., Rossi, G., Scagnolari, C., Andreotti, M., Giustini, N., Serafino, S., Schietroma, I., Scheri, G.C., Fard, S.N., Trinchieri, V., et al. (2017). Probiotic supplementation promotes a reduction in T-cell activation, an increase in Th17 frequencies, and a recovery of intestinal epithelium integrity and mitochondrial morphology in ART-treated HIV-1-positive patients. Immun. Inflamm. Dis. *5*, 244–260.

Evans, T.I., Li, H., Schafer, J.L., Klatt, N.R., Hao, X.-P., Traslavina, R.P., Estes, J.D., Brenchley, J.M., and Reeves, R.K. (2016). SIV-induced Translocation of Bacterial Products in the Liver Mobilizes Myeloid Dendritic and Natural Killer Cells Associated With Liver Damage. J. Infect. Dis. *213*, 361–369.

F Moukambi, Rabezanahary H, Fortier Y, et al. (2019). Mucosal T follicular helper cells in SIV-infected rhesus macaques: contributing role of IL-27. Mucosal Immunol. *12*, 1038–1054.

Fang, V., Chaluvadi, V.S., Ramos-Perez, W.D., Mendoza, A., Baeyens, A., Rivera, R., Chun, J., Cammer, M., and Schwab, S.R. (2017). Gradients of the signaling lipid S1P in lymph nodes position natural killer cells and regulate their interferon-γ response. Nat. Immunol. *18*, 15–25.

Fantini, M., David, J.M., Wong, H.C., Annunziata, C.M., Arlen, P.M., and Tsang, K.Y. (2019). An IL-15 Superagonist, ALT-803, Enhances Antibody-Dependent Cell-Mediated Cytotoxicity Elicited by the Monoclonal Antibody NEO-201 Against Human Carcinoma Cells. Cancer Biother. Radiopharm. *34*, 147–159.

Farsakoglu, Y., Palomino-Segura, M., Latino, I., Zanaga, S., Chatziandreou, N., Pizzagalli, D.U., Rinaldi, A., Bolis, M., Sallusto, F., Stein, J.V., et al. (2019). Influenza Vaccination Induces NK-Cell-Mediated Type-II IFN Response that Regulates Humoral Immunity in an IL-6-Dependent Manner. Cell Rep. *26*, 2307-2315.e5.

Farzan, M., Choe, H., Martin, K., Marcon, L., Hofmann, W., Karlsson, G., Sun, Y., Barrett, P., Marchand, N., Sullivan, N., et al. (1997). Two Orphan Seven-Transmembrane Segment Receptors Which Are Expressed in CD4-positive Cells Support Simian Immunodeficiency Virus Infection. J. Exp. Med. *186*, 405–411.

Favre, D., Lederer, S., Kanwar, B., Ma, Z.-M., Proll, S., Kasakow, Z., Mold, J., Swainson, L., Barbour, J.D., Baskin, C.R., et al. (2009). Critical Loss of the Balance between Th17 and T Regulatory Cell Populations in Pathogenic SIV Infection. PLOS Pathog. *5*, e1000295.

Fernandez, M.I., Pedron, T., Tournebize, R., Olivo-Marin, J.-C., Sansonetti, P.J., and Phalipon, A. (2003). Anti-Inflammatory Role for Intracellular Dimeric Immunoglobulin A by Neutralization of Lipopolysaccharide in Epithelial Cells. Immunity *18*, 739–749.

Février, M., Dorgham, K., and Rebollo, A. (2011). CD4+ T Cell Depletion in Human Immunodeficiency Virus (HIV) Infection: Role of Apoptosis. Viruses *3*, 586–612.

Fletcher, C.V., Staskus, K., Wietgrefe, S.W., Rothenberger, M., Reilly, C., Chipman, J.G., Beilman, G.J., Khoruts, A., Thorkelson, A., Schmidt, T.E., et al. (2014). Persistent HIV-1 replication is associated with lower antiretroviral drug concentrations in lymphatic tissues. Proc. Natl. Acad. Sci.

Flórez-Álvarez, L., Hernandez, J.C., and Zapata, W. (2018). NK Cells in HIV-1 Infection: From Basic Science to Vaccine Strategies. Front. Immunol. *9*.

Freud, A.G., Yokohama, A., Becknell, B., Lee, M.T., Mao, H.C., Ferketich, A.K., and Caligiuri, M.A. (2006). Evidence for discrete stages of human natural killer cell differentiation in vivo. J. Exp. Med. *203*, 1033–1043.

Freud, A.G., Mundy-Bosse, B.L., Yu, J., and Caligiuri, M.A. (2017). The Broad Spectrum of Human Natural Killer Cell Diversity. Immunity *47*, 820–833.

Frias, M., Rivero-Juarez, A., Gordon, A., Camacho, A., Cantisan, S., Cuenca-Lopez, F., Torre-Cisneros, J., Peña, J., and Rivero, A. (2015). Persistence of Pathological Distribution of NK Cells in HIV-Infected Patients with Prolonged Use of HAART and a Sustained Immune Response. PLoS ONE *10*.

Fritz, J.H., Rojas, O.L., Simard, N., McCarthy, D.D., Hapfelmeier, S., Rubino, S., Robertson, S.J., Larijani, M., Gosselin, J., Ivanov, I.I., et al. (2012). Acquisition of a multifunctional IgA + plasma cell phenotype in the gut. Nature *481*, 199–203.

Fromentin, R., Bakeman, W., Lawani, M.B., Khoury, G., Hartogensis, W., DaFonseca, S., Killian, M., Epling, L., Hoh, R., Sinclair, E., et al. (2016). CD4+ T Cells Expressing PD-1, TIGIT and LAG-3 Contribute to HIV Persistence during ART. PLOS Pathog. *12*, e1005761.

Früh, K., and Picker, L. (2017). CD8+ T cell programming by cytomegalovirus vectors: applications in prophylactic and therapeutic vaccination. Curr. Opin. Immunol. *47*, 52–56.

Fu, S.-H., Yeh, L.-T., Chu, C.-C., Yen, B.L.-J., and Sytwu, H.-K. (2017). New insights into Blimp-1 in T lymphocytes: a divergent regulator of cell destiny and effector function. J. Biomed. Sci. *24*, 49.

Fukazawa, Y., Lum, R., Okoye, A.A., Park, H., Matsuda, K., Bae, J.Y., Hagen, S.I., Shoemaker, R., Deleage, C., Lucero, C., et al. (2015). B cell follicle sanctuary permits persistent productive simian immunodeficiency virus infection in elite controllers. Nat. Med. *21*, 132–139.

Galluzzi, L., Yamazaki, T., and Kroemer, G. (2018). Linking cellular stress responses to systemic homeostasis. Nat. Rev. Mol. Cell Biol. *19*, 731–745.

Ganor, Y., Real, F., Sennepin, A., Dutertre, C.-A., Prevedel, L., Xu, L., Tudor, D., Charmeteau, B., Couedel-Courteille, A., Marion, S., et al. (2019). HIV-1 reservoirs in urethral macrophages of patients under suppressive antiretroviral therapy. Nat. Microbiol. *4*, 633–644.

Garbers, C., Heink, S., Korn, T., and Rose-John, S. (2018). Interleukin-6: designing specific therapeutics for a complex cytokine. Nat. Rev. Drug Discov. *17*, 395–412.

García-Lerma, J.G., Cong, M., Mitchell, J., Youngpairoj, A.S., Zheng, Q., Masciotra, S., Martin, A., Kuklenyik, Z., Holder, A., Lipscomb, J., et al. (2010). Intermittent Prophylaxis with Oral Truvada Protects Macaques from Rectal SHIV Infection. Sci. Transl. Med. *2*, 14ra4-14ra4.

Garcia-Tellez, T., Huot, N., Ploquin, M.J., Rascle, P., Jacquelin, B., and Müller-Trutwin, M. (2016). Non-human primates in HIV research: Achievements, limits and alternatives. Infect. Genet. Evol. *46*, 324–332.

Gaufin, T., Pattison, M., Gautam, R., Stoulig, C., Dufour, J., MacFarland, J., Mandell, D., Tatum, C., Marx, M.H., Ribeiro, R.M., et al. (2009). Effect of B-Cell Depletion on Viral Replication and Clinical Outcome of Simian Immunodeficiency Virus Infection in a Natural Host. J. Virol. *83*, 10347–10357.

Gaya, M., Barral, P., Burbage, M., Aggarwal, S., Montaner, B., Warren Navia, A., Aid, M., Tsui, C., Maldonado, P., Nair, U., et al. (2018). Initiation of Antiviral B Cell Immunity Relies on Innate Signals from Spatially Positioned NKT Cells. Cell *172*, 517-533.e20.

Geskus, R.B., Prins, M., Hubert, J.-B., Miedema, F., Berkhout, B., Rouzioux, C., Delfraissy, J.-F., and Meyer, L. (2007). The HIV RNA setpoint theory revisited. Retrovirology *4*, 65.

Giavedoni, L.D., Velasquillo, M.C., Parodi, L.M., Hubbard, G.B., and Hodara, V.L. (2000). Cytokine Expression, Natural Killer Cell Activation, and Phenotypic Changes in Lymphoid Cells from Rhesus Macaques during Acute Infection with Pathogenic Simian Immunodeficiency Virus. J. Virol. *74*, 1648–1657.

Gicheru, M.M., Otsyula, M., Spearman, P., Graham, B.S., Miller, C.J., Robinson, H.L., Haigwood, N.L., and Montefiori, D.C. (1999). Neutralizing antibody responses in Africa green monkeys naturally infected with simian immunodeficiency virus (SIVagm). J. Med. Primatol. *28*, 97–104.

Gooden, M., Lampen, M., Jordanova, E.S., Leffers, N., Trimbos, J.B., Burg, S.H. van der, Nijman, H., and Hall, T. van (2011). HLA-E expression by gynecological cancers restrains tumor-infiltrating CD8+ T lymphocytes. Proc. Natl. Acad. Sci.

Gordon, S.N., Dunham, R.M., Engram, J.C., Estes, J., Wang, Z., Klatt, N.R., Paiardini, M., Pandrea, I.V., Apetrei, C., Sodora, D.L., et al. (2008). Short-lived infected cells support virus replication in naturally SIV-infected sooty mangabeys: implications for AIDS pathogenesis. J. Virol.

Gordon, S.N., Cervasi, B., Odorizzi, P., Silverman, R., Aberra, F., Ginsberg, G., Estes, J.D., Paiardini, M., Frank, I., and Silvestri, G. (2010). Disruption of Intestinal CD4+ T Cell Homeostasis Is a Key Marker of Systemic CD4+ T Cell Activation in HIV-Infected Individuals. J. Immunol. *185*, 5169–5179.

Gray, F., Lescure, F., Adle-Biassette, H., Polivka, F., Gallien, S., Pialoux, G., and Moulignier, A. (2013). Encephalitis with Infiltration by CD8+Lymphocytes in HIV Patients Receiving Combination Antiretroviral Treatment. Brain Pathol. Zurich Switz. *23*.

Gueye, A., Diop, O.M., Ploquin, M.J.Y., Kornfeld, C., Faye, A., Cumont, M.-C., Hurtrel, B., Barré-Sinoussi, F., and Müller-Trutwin, M.C. (2004). Viral load in tissues during the early and chronic phase of non-pathogenic SIVagm infection. J. Med. Primatol. *33*, 83–97.

Heinrich S., Frank C., Bianca T., Jakob T., Vivien B., Tim H., Hongya H., Samuel C C., et al. (2015). Cytomegalovirus infection drives adaptive epigenetic diversification of NK cells with altered signaling and effector function. Immunity *42*, 443–456.

Haley, P.J. (2017). The lymphoid system: a review of species differences. J. Toxicol. Pathol. *30*, 111–123.

Hammer, Q., Rückert, T., Borst, E.M., Dunst, J., Haubner, A., Durek, P., Heinrich, F., Gasparoni, G., Babic, M., Tomic, A., et al. (2018). Peptide-specific recognition of human cytomegalovirus strains controls adaptive natural killer cells. Nat. Immunol. *19*, 453–463.

Hansen, S.G., Wu, H.L., Burwitz, B.J., Hughes, C.M., Hammond, K.B., Ventura, A.B., Reed, J.S., Gilbride, R.M., Ainslie, E., Morrow, D.W., et al. (2016). Broadly targeted CD8+ T cell responses restricted by major histocompatibility complex E. Science.

Harris, L.D., Tabb, B., Sodora, D.L., Paiardini, M., Klatt, N.R., Douek, D.C., Silvestri, G., Müller-Trutwin, M., Vasile-Pandrea, I., Apetrei, C., et al. (2010). Downregulation of robust acute type I interferon responses distinguishes nonpathogenic simian immunodeficiency virus (SIV) infection of natural hosts from pathogenic SIV infection of rhesus macaques. J. Virol. *84*, 7886–7891.

Harris, L.D., Khayumbi, J., Ongalo, J., Sasser, L.E., Tonui, J., Campbell, A., Odhiambo, F.H., Ouma, S.G., Alter, G., Gandhi, N.R., et al. (2020). Distinct Human NK Cell Phenotypes and Functional Responses to Mycobacterium tuberculosis in Adults From TB Endemic and Non-endemic Regions. Front. Cell. Infect. Microbiol. *10*.

Hasegawa, A., Liu, H., Ling, B., Borda, J.T., Alvarez, X., Sugimoto, C., Vinet-Oliphant, H., Kim, W.-K., Williams, K.C., Ribeiro, R.M., et al. (2009). The level of monocyte turnover predicts disease progression in the macaque model of AIDS. Blood *114*, 2917–2925.

Hashemi, E., and Malarkannan, S. (2020). Tissue-Resident NK Cells: Development, Maturation, and Clinical Relevance. Cancers *12*, 1553.

Hatziioannou, T., Prete, G.Q.D., Keele, B.F., Estes, J.D., McNatt, M.W., Bitzegeio, J., Raymond, A., Rodriguez, A., Schmidt, F., Trubey, C.M., et al. (2014). HIV-1–induced AIDS in monkeys. Science *344*, 1401–1405.

Hazeldine, J., and Lord, J.M. (2013). The impact of ageing on natural killer cell function and potential consequences for health in older adults. Ageing Res. Rev. *12*, 1069–1078.

He, Y., and Tian, Z. (2017). NK cell education via nonclassical MHC and non-MHC ligands. Cell. Mol. Immunol. *14*, 321–330.

Hel, Z., Xu, J., Denning, W.L., Helton, E.S., Huijbregts, R.P.H., Heath, S.L., Overton, E.T., Christmann, B.S., Elson, C.O., Goepfert, P.A., et al. (2017). Dysregulation of Systemic and Mucosal Humoral Responses to Microbial and Food Antigens as a Factor Contributing to Microbial Translocation and Chronic Inflammation in HIV-1 Infection. PLOS Pathog. *13*, e1006087.

Henrich, T.J., Hatano, H., Bacon, O., Hogan, L.E., Rutishauser, R., Hill, A., Kearney, M.F., Anderson, E.M., Buchbinder, S.P., Cohen, S.E., et al. (2017). HIV-1 persistence following extremely early initiation of

antiretroviral therapy (ART) during acute HIV-1 infection: An observational study. PLOS Med. *14*, e1002417.

Hensley-McBain, T., Berard, A.R., Manuzak, J.A., Miller, C.J., Zevin, A.S., Polacino, P., Gile, J., Agricola, B., Cameron, M., Hu, S.-L., et al. (2018). Intestinal damage precedes mucosal immune dysfunction in SIV infection. Mucosal Immunol. *11*, 1429–1440.

Hirao, L.A., Grishina, I., Bourry, O., Hu, W.K., Somrit, M., Sankaran-Walters, S., Gaulke, C.A., Fenton, A.N., Li, J.A., Crawford, R.W., et al. (2014). Early Mucosal Sensing of SIV Infection by Paneth Cells Induces IL-1β Production and Initiates Gut Epithelial Disruption. PLOS Pathog. *10*, e1004311.

Hodge, J.N., Srinivasula, S., Hu, Z., Read, S.W., Porter, B.O., Kim, I., Mican, J.M., Paik, C., DeGrange, P., Di Mascio, M., et al. (2011). Decreases in IL-7 levels during antiretroviral treatment of HIV infection suggest a primary mechanism of receptor-mediated clearance. Blood *118*, 3244–3253.

Hogan, L.E., Vasquez, J., Hobbs, K.S., Hanhauser, E., Aguilar-Rodriguez, B., Hussien, R., Thanh, C., Gibson, E.A., Carvidi, A.B., Smith, L.C.B., et al. (2018). Increased HIV-1 transcriptional activity and infectious burden in peripheral blood and gut-associated CD4+ T cells expressing CD30. PLOS Pathog. *14*, e1006856.

Honeycutt, J.B., Wahl, A., Baker, C., Spagnuolo, R.A., Foster, J., Zakharova, O., Wietgrefe, S., Caro-Vegas, C., Madden, V., Sharpe, G., et al. (2016). Macrophages sustain HIV replication in vivo independently of T cells. J. Clin. Invest. *126*, 1353–1366.

Hong, J.J., Silveira, E.L.V., Amancha, P.K., Byrareddy, S.N., Gumber, S., Chang, K.-T., Ansari, A.A., and Villinger, F. (2017). Early initiation of antiretroviral treatment post SIV infection does not resolve lymphoid tissue activation. AIDS Lond. Engl. *31*, 1819–1824.

Hope, J.C., Cumberbatch, M., Fielding, I., Dearman, R.J., Kimber, I., and Hopkins, S.J. (1995). Identification of dendritic cells as a major source of interleukin-6 in draining lymph nodes following skin sensitization of mice. Immunology *86*, 441–447.

Huang, L., Deng, J., Xu, W., Wang, H., Shi, L., Wu, F., Wu, D., Nei, W., Zhao, M., Mao, P., et al. (2018). CD8+ T cells with high TGF-β1 expression cause lymph node fibrosis following HIV infection. Mol. Med. Rep. *18*, 77–86.

Hunt, P.W., Martin, J.N., Sinclair, E., Bredt, B., Hagos, E., Lampiris, H., and Deeks, S.G. (2003). T Cell Activation Is Associated with Lower CD4+ T Cell Gains in Human Immunodeficiency Virus-Infected Patients with Sustained Viral Suppression during Antiretroviral Therapy. J. Infect. Dis. *187*, 1534–1543.

Hunt, P.W., Sinclair, E., Rodriguez, B., Shive, C., Clagett, B., Funderburg, N., Robinson, J., Huang, Y., Epling, L., Martin, J.N., et al. (2014). Gut Epithelial Barrier Dysfunction and Innate Immune Activation Predict Mortality in Treated HIV Infection. J. Infect. Dis. *210*, 1228–1238.

Huntington, N.D., Vosshenrich, C.A.J., and Di Santo, J.P. (2007). Developmental pathways that generate natural-killer-cell diversity in mice and humans. Nat. Rev. Immunol. *7*, 703–714.

Huot, N., Rascle, P., Garcia-Tellez, T., Jacquelin, B., and Müller-Trutwin, M. (2016). Innate immune cell responses in non pathogenic versus pathogenic SIV infections. Curr. Opin. Virol. *19*, 37–44.

Huot, N., Jacquelin, B., Garcia-Tellez, T., Rascle, P., Ploquin, M.J., Madec, Y., Reeves, R.K., Derreudre-Bosquet, N., and Müller-Trutwin, M. (2017). Natural killer cells migrate into and control simian immunodeficiency virus replication in lymph node follicles in African green monkeys. Nat. Med. *23*, 1277–1286.

Huot, N., Bosinger, S.E., Paiardini, M., Reeves, R.K., and Müller-Trutwin, M. (2018). Lymph Node Cellular and Viral Dynamics in Natural Hosts and Impact for HIV Cure Strategies. Front. Immunol. *9*.

Igarashi, T., Brown, C.R., Endo, Y., Buckler-White, A., Plishka, R., Bischofberger, N., Hirsch, V., and Martin, M.A. (2001). Macrophage are the principal reservoir and sustain high virus loads in rhesus macaques after the depletion of CD4+ T cells by a highly pathogenic simian immunodeficiency virus/HIV type 1 chimera (SHIV): Implications for HIV-1 infections of humans. Proc. Natl. Acad. Sci. *98*, 658–663.

Iglesias-Ussel, M., Vandergeeten, C., Marchionni, L., Chomont, N., and Romerio, F. (2013). High Levels of CD2 Expression Identify HIV-1 Latently Infected Resting Memory CD4+ T Cells in Virally Suppressed Subjects. J. Virol. *87*, 9148–9158.

Ivanova, D., Krempels, R., Ryfe, J., Weitzman, K., Stephenson, D., and Gigley, J.P. (2014). NK Cells in Mucosal Defense against Infection (Hindawi).

Jintanat A., Karine D., and Nicolas C. (2015). How does the timing of antiretroviral therapy initiation in acute infection affect HIV reservoirs? Curr. Opin. HIV AIDS *10*, 18–28.

Jiri Mestecky, Zina M., Phillip D S., Zdenek H., and Rashada C A. (2009). Mucosal immunology of the genital and gastrointestinal tracts and HIV-1 infection. J. Reprod. Immunol. *83*, 196–200.

Jacob Nattermann, Hans Dieter N., Hans Dieter H., et al. (2005). HIV-1 infection leads to increased HLA-E expression resulting in impaired function of natural killer cells. Antivir. Ther. *10*, 95–107.

Jabri, Bana, Selby, J.M., Negulescu, H., Lee, L., Roberts, A.I., Beavis, A., Lopez-Botet, M., Ebert, E.C., and Winchester, R.J. (2002). TCR specificity dictates CD94/NKG2A expression by human CTL. Immunity *17*, 487–499.

Jacquelin, B., Mayau, V., Targat, B., Liovat, A.-S., Kunkel, D., Petitjean, G., Dillies, M.-A., Roques, P., Butor, C., Silvestri, G., et al. (2009). Nonpathogenic SIV infection of African green monkeys induces a strong but rapidly controlled type I IFN response. J. Clin. Invest. *119*, 3544–3555.

Jacquelin, B., Petitjean, G., Kunkel, D., Liovat, A.-S., Jochems, S.P., Rogers, K.A., Ploquin, M.J., Madec, Y., Barré-Sinoussi, F., Dereuddre-Bosquet, N., et al. (2014). Innate Immune Responses and Rapid Control of Inflammation in African Green Monkeys Treated or Not with Interferon-Alpha during Primary SIVagm Infection. PLOS Pathog. *10*, e1004241.

Jiang, H., Canfield, S.M., Gallagher, M.P., Jiang, H.H., Jiang, Y., Zheng, Z., and Chess, L. (2010). HLA-E–restricted regulatory $CD8^+$ T cells are involved in development and control of human autoimmune type 1 diabetes. J. Clin. Invest. *120*, 3641–3650.

Jiang, Y., Chen, O., Cui, C., Zhao, B., Han, X., Zhang, Z., Liu, J., Xu, J., Hu, Q., Liao, C., et al. (2013). KIR3DS1/L1 and HLA-Bw4-80I are associated with HIV disease progression among HIV typical progressors and long-term nonprogressors. BMC Infect. Dis. *13*, 405.

Joas, S., Parrish, E.H., Gnanadurai, C.W., Lump, E., Stürzel, C.M., Parrish, N.F., Learn, G.H., Sauermann, U., Neumann, B., Rensing, K.M., et al. (2018). Species-specific host factors rather than virus-intrinsic virulence determine primate lentiviral pathogenicity. Nat. Commun. *9*, 1371.

Jochems, S.P., Jacquelin, B., Chauveau, L., Huot, N., Petitjean, G., Lepelley, A., Liovat, A.-S., Ploquin, M.J., Cartwright, E.K., Bosinger, S.E., et al. (2015a). Plasmacytoid dendritic cell infection and sensing capacity during pathogenic and non-pathogenic SIV infection. J. Virol.

Jochems, S.P., Petitjean, G., Kunkel, D., Liovat, A.-S., Ploquin, M.J., Barré-Sinoussi, F., Lebon, P., Jacquelin, B., and Müller-Trutwin, M.C. (2015b). Modulation of type I interferon-associated viral sensing during acute simian immunodeficiency virus infection in African green monkeys. J. Virol. *89*, 751–762.

Joosten, S.A., Sullivan, L.C., and Ottenhoff, T.H.M. (2016). Characteristics of HLA-E Restricted T-Cell Responses and Their Role in Infectious Diseases (Hindawi).

Jost, S., and Altfeld, M. (2012). Evasion from NK cell-mediated immune responses by HIV-1. Microbes Infect. *14*, 904–915.

Kaiser, B.K., Barahmand-pour, F., Paulsene, W., Medley, S., Geraghty, D.E., and Strong, R.K. (2005). Interactions between NKG2x Immunoreceptors and HLA-E Ligands Display Overlapping Affinities and Thermodynamics. J. Immunol. *174*, 2878–2884.

Kallies, A., Carotta, S., Huntington, N.D., Bernard, N.J., Tarlinton, D.M., Smyth, M.J., and Nutt, S.L. (2011). A role for Blimp1 in the transcriptional network controlling natural killer cell maturation. Blood *117*, 1869–1879.

Kamada, N., and Núñez, G. (2014). Regulation of the immune system by the resident intestinal bacteria. Gastroenterology *146*, 1477–1488.

Kaminski, D.A., Wei, C., Qian, Y., Rosenberg, A.F., and Sanz, I. (2012). Advances in Human B Cell Phenotypic Profiling. Front. Immunol. *3*.

Kandasamy, J., Huda, S., Ambalavanan, N., and Jilling, T. (2014). Inflammatory signals that regulate intestinal epithelial renewal, differentiation, migration and cell death: Implications for necrotizing enterocolitis. Pathophysiol. Off. J. Int. Soc. Pathophysiol. *21*, 67–80.

Karris, M.A., and Smith, D.M. (2011). Tissue-specific HIV-1 infection: why it matters. Future Virol. *6*, 869–882.

Kaufmann, D., and Walker, B. (2009). PD-1 and CTLA-4 Inhibitory Cosignaling Pathways in HIV Infection and the Potential for Therapeutic Intervention. J. Immunol. Baltim. Md 1950 *182*, 5891–5897.

Keating, S.M., Heitman, J.W., Wu, S., Deng, X., Stacey, A.R., Zahn, R.C., Rosa, M. de la, Finstad, S.L., Lifson, J.D., Piatak, M., et al. (2016). Magnitude and quality of cytokine and chemokine storm during acute infection

distinguish non-progressive and progressive simian immunodeficiency virus infections of nonhuman primates. J. Virol.

Kenway-Lynch, C.S., Das, A., Pan, D., Lackner, A.A., and Pahar, B. (2013). Dynamics of cytokine/chemokine responses in intestinal CD4+ and CD8+ T-cells during acute simian immunodeficiency virus infection. J. Virol.

Kiani, Z., Dupuy, F.P., Bruneau, J., Lebouché, B., Retière, C., Geraghty, D.E., and Bernard, N.F. (2019). The Education of NK Cells Determines Their Responsiveness to Autologous HIV-Infected CD4 T Cells. J. Virol.

Kim, H.-J., and Cantor, H. (2011). Regulation of self-tolerance by Qa-1-restricted CD8+ regulatory T cells. Semin. Immunol. *23*, 446–452.

Kiniry, B.E., Hunt, P.W., Hecht, F.M., Somsouk, M., Deeks, S.G., and Shacklett, B.L. (2018). Differential Expression of CD8+ T Cell Cytotoxic Effector Molecules in Blood and Gastrointestinal Mucosa in HIV-1 Infection. J. Immunol.

Klatt, N.R., Funderburg, N.T., and Brenchley, J.M. (2013). Microbial translocation, immune activation, and HIV disease. Trends Microbiol. *21*, 6–13.

Kök, A., Hocqueloux, L., Hocini, H., Carrière, M., Lefrou, L., Guguin, A., Tisserand, P., Bonnabau, H., Avettand-Fenoel, V., Prazuck, T., et al. (2015). Early initiation of combined antiretroviral therapy preserves immune function in the gut of HIV-infected patients. Mucosal Immunol. *8*, 127–140.

Koppensteiner, H., Brack-Werner, R., and Schindler, M. (2012). Macrophages and their relevance in Human Immunodeficiency Virus Type I infection. Retrovirology *9*, 82.

Kraemer, T., Celik, A.A., Huyton, T., Kunze-Schumacher, H., Blasczyk, R., and Bade-Döding, C. (2015). HLA-E: Presentation of a Broader Peptide Repertoire Impacts the Cellular Immune Response—Implications on HSCT Outcome (Hindawi).

Kristensen, A.B., Kent, S.J., and Parsons, M.S. (2018). Contribution of NK cell education to both direct and anti-HIV-1 antibody-dependent NK cell functions. J. Virol.

Kulkarni, V., and Ruprecht, R.M. (2017). Mucosal IgA Responses: Damaged in Established HIV Infection—Yet, Effective Weapon against HIV Transmission. Front. Immunol. *8*.

Kumar, S. (2018). Natural killer cell cytotoxicity and its regulation by inhibitory receptors. Immunology *154*, 383–393.

LaBonte, M.L., McKay, P.F., and Letvin, N.L. (2006). Evidence of NK cell dysfunction in SIV-infected rhesus monkeys: Impairment of cytokine secretion and NKG2C/C2 expression. Eur. J. Immunol. *36*, 2424–2433.

Lackner, A.A., Mohan, M., and Veazey, R.S. (2009). The gastrointestinal tract and AIDS pathogenesis. Gastroenterology *136*, 1965–1978.

Lam, V.C., and Lanier, L.L. (2017). NK cells in host responses to viral infections. Curr. Opin. Immunol. *44*, 43–51.

Lambotte, O., Boufassa, F., Madec, Y., Nguyen, A., Goujard, C., Meyer, L., Rouzioux, C., Venet, A., and Delfraissy, J.-F. (2005). HIV Controllers: A Homogeneous Group of HIV-1—Infected Patients with Spontaneous Control of Viral Replication. Clin. Infect. Dis. *41*, 1053–1056.

Lane, H.C., Masur, H., Edgar, L.C., Whalen, G., Rook, A.H., and Fauci, A.S. (1983). Abnormalities of B-Cell Activation and Immunoregulation in Patients with the Acquired Immunodeficiency Syndrome. N. Engl. J. Med. *309*, 453–458.

Langel, S.N., Wang, Q., Vlasova, A.N., and Saif, L.J. (2020). Host Factors Affecting Generation of Immunity Against Porcine Epidemic Diarrhea Virus in Pregnant and Lactating Swine and Passive Protection of Neonates. Pathogens *9*, 130.

Le, Pereira, et al. (2008). Sooty mangabeys and rhesus macaques exhibit significant divergent natural killer cell responses during both acute and chronic phases of SIV infection. Cell. Immunol. *254*, 10–19.

Leal, I.S., Smedegård, B., Andersen, P., and Appelberg, R. (1999). Interleukin-6 and Interleukin-12 Participate in Induction of a Type 1 Protective T-Cell Response during Vaccination with a Tuberculosis Subunit Vaccine. Infect. Immun. *67*, 5747–5754.

Lemke, A., Kraft, M., Roth, K., Riedel, R., Lammerding, D., and Hauser, A.E. (2016). Long-lived plasma cells are generated in mucosal immune responses and contribute to the bone marrow plasma cell pool in mice. Mucosal Immunol. *9*, 83–97.

Leong, K.W., and Ding, J.L. (2014). The Unexplored Roles of Human Serum IgA. DNA Cell Biol. *33*, 823–829.

Letvin, N.L., Eaton, K.A., Aldrich, W.R., Sehgal, P.K., Blake, B.J., Schlossman, S.F., King, N.W., and Hunt, R.D. (1983). Acquired immunodeficiency syndrome in a colony of macaque monkeys. Proc. Natl. Acad. Sci. *80*, 2718–2722.

Levy, J.A. (2011). Virus-Host Interactions in HIV Pathogenesis: Directions for Therapy. Adv. Dent. Res.

Li, H., and Reeves, R.K. (2012). Functional perturbation of classical natural killer and innate lymphoid cells in the oral mucosa during SIV infection. Front. Immunol. *3*, 417.

Li, H., Richert-Spuhler, L.E., Evans, T.I., Gillis, J., Connole, M., Estes, J.D., Keele, B.F., Klatt, N.R., and Reeves, R.K. (2014a). Hypercytotoxicity and Rapid Loss of NKp44+ Innate Lymphoid Cells during Acute SIV Infection. PLOS Pathog. *10*, e1004551.

Li, H., Richert-Spuhler, L.E., Evans, T.I., Gillis, J., Connole, M., Estes, J.D., Keele, B.F., Klatt, N.R., and Reeves, R.K. (2014b). Hypercytotoxicity and Rapid Loss of NKp44+ Innate Lymphoid Cells during Acute SIV Infection. PLOS Pathog. *10*, e1004551.

Li, Q., Duan, L., Estes, J.D., Ma, Z.-M., Rourke, T., Wang, Y., Reilly, C., Carlis, J., Miller, C.J., and Haase, A.T. (2005). Peak SIV replication in resting memory CD4+ T cells depletes gut lamina propria CD4+ T cells. Nature *434*, 1148–1152.

Louie, D.A.P., and Liao, S. (2019). Lymph Node Subcapsular Sinus Macrophages as the Frontline of Lymphatic Immune Defense. Front. Immunol. *10*.

Ltd, B.P.G. (2004). Scientists Find HIV-Blocking Protein in Monkeys. J. Investig. Med. *52*, 235–235.

Lucar, O., Reeves, R.K., and Jost, S. (2019). A Natural Impact: NK Cells at the Intersection of Cancer and HIV Disease. Front. Immunol. *10*.

Luteijn, R., Sciaranghella, G., van Lunzen, J., Nolting, A., Dugast, A.-S., Ghebremichael, M.S., Altfeld, M., and Alter, G. (2011). Early viral replication in lymph nodes provides HIV with a means by which to escape NK-cell-mediated control. Eur. J. Immunol. *41*, 2729–2740.

Mackay, L.K., Braun, A., Macleod, B.L., Collins, N., Tebartz, C., Bedoui, S., Carbone, F.R., and Gebhardt, T. (2015). Cutting Edge: CD69 Interference with Sphingosine-1-Phosphate Receptor Function Regulates Peripheral T Cell Retention. J. Immunol. *194*, 2059–2063.

Macpherson, A.J., McCoy, K.D., Johansen, F.-E., and Brandtzaeg, P. (2008). The immune geography of IgA induction and function. Mucosal Immunol. *1*, 11–22.

Madera, S., Rapp, M., Firth, M.A., Beilke, J.N., Lanier, L.L., and Sun, J.C. (2016). Type I IFN promotes NK cell expansion during viral infection by protecting NK cells against fratricide. J. Exp. Med. *213*, 225–233.

Malmberg, K.-J., Beziat, V., and Ljunggren, H.-G. (2012). Spotlight on NKG2C and the human NK-cell response to CMV infection. Eur. J. Immunol. *42*, 3141–3145.

Manickam, C., Shah, S.V., Nohara, J., Ferrari, G., and Reeves, R.K. (2019). Monkeying Around: Using Non-human Primate Models to Study NK Cell Biology in HIV Infections. Front. Immunol. *10*.

Maria, A.D., Ferraris, A., Guastella, M., Pilia, S., Cantoni, C., Polero, L., Mingari, M.C., Bassetti, D., Fauci, A.S., and Moretta, L. (1997). Expression of HLA class I-specific inhibitory natural killer cell receptors in HIV-specific cytolytic T lymphocytes: Impairment of specific cytolytic functions. Proc. Natl. Acad. Sci. *94*, 10285–10288.

Martinelli, E., Derby, N., and Robbiani, M. (2014). Nonhuman Primate Models of HIV Transmission. In Encyclopedia of AIDS, T.J. Hope, M. Stevenson, and D. Richman, eds. (New York, NY: Springer), pp. 1–9.

Martini, F., Agrati, C., D'Offizi, G., and Poccia, F. (2016). HLA-E Up-Regulation Induced by HIV Infection May Directly Contribute to CD94-Mediated Impairment of NK Cells: Int. J. Immunopathol. Pharmacol.

Martinot, A.J., Meythaler, M., Pozzi, L.-A., Boisvert, K.D., Knight, H., Walsh, D., Westmoreland, S., Anderson, D.C., Kaur, A., and O'Neil, S.P. (2013). Acute SIV Infection in Sooty Mangabey Monkeys Is Characterized by Rapid Virus Clearance from Lymph Nodes and Absence of Productive Infection in Germinal Centers. PLOS ONE *8*, e57785.

Mattapallil, J.J., Douek, D.C., Hill, B., Nishimura, Y., Martin, M., and Roederer, M. (2005). Massive infection and loss of memory CD4 + T cells in multiple tissues during acute SIV infection. Nature *434*, 1093–1097.

Mavilio, D., Benjamin, J., Kim, D., Lombardo, G., Daucher, M., Kinter, A., Nies-Kraske, E., Marcenaro, E., Moretta, A., and Fauci, A.S. (2005a). Identification of NKG2A and NKp80 as specific natural killer cell markers in rhesus and pigtailed monkeys. Blood *106*, 1718–1725.

Mavilio, D., Lombardo, G., Benjamin, J., Kim, D., Follman, D., Marcenaro, E., O'Shea, M.A., Kinter, A., Kovacs, C., Moretta, A., et al. (2005b). Characterization of CD56–/CD16+ natural killer (NK) cells: A highly dysfunctional NK subset expanded in HIV-infected viremic individuals. Proc. Natl. Acad. Sci. *102*, 2886–2891.

McCarthy, N.E., and Eberl, M. (2018). Human γδ T-Cell Control of Mucosal Immunity and Inflammation. Front. Immunol. *9*.

McElrath, M.J., Smythe, K., Randolph-Habecker, J., Melton, K.R., Goodpaster, T.A., Hughes, S.M., Mack, M., Sato, A., Diaz, G., Steinbach, G., et al. (2013). Comprehensive assessment of HIV target cells in the distal human gut suggests increasing HIV susceptibility toward the anus. J. Acquir. Immune Defic. Syndr. 1999 *63*, 263–271.

McGary, C.S., Deleage, C., Harper, J., Micci, L., Ribeiro, S.P., Paganini, S., Kuri-Cervantes, L., Benne, C., Ryan, E.S., Balderas, R., et al. (2017). CTLA-4+PD-1- Memory CD4+ T Cells Critically Contribute to Viral Persistence in Antiretroviral Therapy-Suppressed, SIV-Infected Rhesus Macaques. Immunity *47*, 776-788.e5.

McHeyzer-Williams, M., Okitsu, S., Wang, N., and McHeyzer-Williams, L. (2012). Molecular programming of B cell memory. Nat. Rev. Immunol. *12*, 24–34.

Md, Galiani, E, Aguado, R, Tarazona, P, Romero, I, Molina, et al. (1999). Expression of killer inhibitory receptors on cytotoxic cells from HIV-1-infected individuals. Clin. Exp. Immunol. *115*, 472–476.

Mehandru, S., Poles, M.A., Tenner-Racz, K., Horowitz, A., Hurley, A., Hogan, C., Boden, D., Racz, P., and Markowitz, M. (2004). Primary HIV-1 Infection Is Associated with Preferential Depletion of CD4+ T Lymphocytes from Effector Sites in the Gastrointestinal Tract. J. Exp. Med. *200*, 761–770.

Mehandru, S., Poles, M.A., Tenner-Racz, K., Manuelli, V., Jean-Pierre, P., Lopez, P., Shet, A., Low, A., Mohri, H., Boden, D., et al. (2007). Mechanisms of gastrointestinal CD4+ T-cell depletion during acute and early human immunodeficiency virus type 1 infection. J. Virol. *81*, 599–612.

Melchers, F. (2015). Checkpoints that control B cell development. J. Clin. Invest. *125*, 2203–2210.

Mestecky, J., Jackson, S., Moldoveanu, Z., Nesbit, L.R., Kulhavy, R., Prince, S.J., Sabbaj, S., Mulligan, M.J., and Goepfert, P.A. (2004). Paucity of Antigen-Specific IgA Responses in Sera and External Secretions of HIV-Type 1-Infected Individuals. AIDS Res. Hum. Retroviruses *20*, 972–988.

Michaëlsson, J., Teixeira de Matos, C., Achour, A., Lanier, L.L., Kärre, K., and Söderström, K. (2002). A Signal Peptide Derived from hsp60 Binds HLA-E and Interferes with CD94/NKG2A Recognition. J. Exp. Med. *196*, 1403–1414.

Mikulak, J., Oriolo, F., Zaghi, E., Vito, C.D., and Mavilio, D. (2017). Natural killer cells in HIV-1 infection and therapy. Aids *31*, 2317–2330.

Milush, J.M., Reeves, J.D., Gordon, S.N., Zhou, D., Muthukumar, A., Kosub, D.A., Chacko, E., Giavedoni, L.D., Ibegbu, C.C., Cole, K.S., et al. (2007). Virally Induced CD4+ T Cell Depletion Is Not Sufficient to Induce AIDS in a Natural Host. J. Immunol. *179*, 3047–3056.

Mogensen, T.H., Melchjorsen, J., Larsen, C.S., and Paludan, S.R. (2010). Innate immune recognition and activation during HIV infection. Retrovirology *7*, 54.

Moir, S., and Fauci, A.S. (2009). B cells in HIV infection and disease. Nat. Rev. Immunol. *9*, 235–245.

van Montfoort, N., Borst, L., Korrer, M.J., Sluijter, M., Marijt, K.A., Santegoets, S.J., van Ham, V.J., Ehsan, I., Charoentong, P., André, P., et al. (2018). NKG2A Blockade Potentiates CD8 T Cell Immunity Induced by Cancer Vaccines. Cell *175*, 1744-1755.e15.

Moor, K., Diard, M., Sellin, M.E., Felmy, B., Wotzka, S.Y., Toska, A., Bakkeren, E., Arnoldini, M., Bansept, F., Co, A.D., et al. (2017). High-avidity IgA protects the intestine by enchaining growing bacteria. Nature *544*, 498–502.

Mora, J.R., and von Andrian, U.H. (2008). Differentiation and homing of IgA-secreting cells. Mucosal Immunol. *1*, 96–109.

Mortha, A., Chudnovskiy, A., Hashimoto, D., Bogunovic, M., Spencer, S.P., Belkaid, Y., and Merad, M. (2014). Microbiota-Dependent Crosstalk Between Macrophages and ILC3 Promotes Intestinal Homeostasis. Science *343*.

Mudd, J.C., and Brenchley, J.M. (2016). Gut Mucosal Barrier Dysfunction, Microbial Dysbiosis, and Their Role in HIV-1 Disease Progression. J. Infect. Dis. *214*, S58–S66.

Mudd, J.C., Busman-Sahay, K., DiNapoli, S.R., Lai, S., Sheik, V., Lisco, A., Deleage, C., Richardson, B., Palesch, D.J., Paiardini, M., et al. (2018). Hallmarks of primate lentiviral immunodeficiency infection recapitulate loss of innate lymphoid cells. Nat. Commun. *9*, 3967.

Nascimbeni, M., Perié, L., Chorro, L., Diocou, S., Kreitmann, L., Louis, S., Garderet, L., Fabiani, B., Berger, A., Schmitz, J., et al. (2009). Plasmacytoid dendritic cells accumulate in spleens from chronically HIV-infected patients but barely participate in interferon-α expression. Blood *113*, 6112–6119.

Nazli, A., Chan, O., Dobson-Belaire, W.N., Ouellet, M., Tremblay, M.J., Gray-Owen, S.D., Arsenault, A.L., and Kaushic, C. (2010). Exposure to HIV-1 Directly Impairs Mucosal Epithelial Barrier Integrity Allowing Microbial Translocation. PLOS Pathog. *6*, e1000852.

Ndungʾu, T., Dong, K.L., Kwon, D.S., and Walker, B.D. (2018). A FRESH approach: Combining basic science and social good. Sci. Immunol. *3*.

Niehrs, A., Garcia-Beltran, W.F., Norman, P.J., Watson, G.M., Hölzemer, A., Chapel, A., Richert, L., Pommerening-Röser, A., Körner, C., Ozawa, M., et al. (2019). A subset of HLA-DP molecules serve as ligands for the natural cytotoxicity receptor NKp44. Nat. Immunol. *20*, 1129–1137.

Nielsen, M.M., Witherden, D.A., and Havran, W.L. (2017). γδ T cells in homeostasis and host defence of epithelial barrier tissues. Nat. Rev. Immunol. *17*, 733–745.

Norley, S.G., Kraus, G., Ennen, J., Bonilla, J., König, H., and Kurth, R. (1990). Immunological studies of the basis for the apathogenicity of simian immunodeficiency virus from African green monkeys. Proc. Natl. Acad. Sci. *87*, 9067–9071.

Odorizzi, P.M., and Wherry, E.J. (2012). Inhibitory receptors on lymphocytes: insights from infections. J. Immunol. Baltim. Md 1950 *188*, 2957–2965.

Ohno, H. (2016). Intestinal M cells. J. Biochem. (Tokyo) *159*, 151–160.

Okoye, A.A., and Picker, L.J. (2013). CD4+ T-cell depletion in HIV infection: mechanisms of immunological failure. Immunol. Rev. *254*, 54–64.

Okoye, A.A., Hansen, S.G., Vaidya, M., Fukazawa, Y., Park, H., Duell, D.M., Lum, R., Hughes, C.M., Ventura, A.B., Ainslie, E., et al. (2018). Early antiretroviral therapy limits SIV reservoir establishment to delay or prevent post-treatment viral rebound. Nat. Med. *24*, 1430–1440.

Okumura, R., and Takeda, K. (2016). Maintenance of gut homeostasis by the mucosal immune system. Proc. Jpn. Acad. Ser. B *92*, 423–435.

Onabajo, O.O., and Mattapallil, J.J. (2013). Expansion or depletion of T follicular helper cells during HIV infection: consequences for B cell responses. Curr. HIV Res. *11*, 595–600.

Paiardini, M., and Müller-Trutwin, M. (2013). HIV-associated chronic immune activation. Immunol. Rev. *254*, 78–101.

Paiardini, M., Cervasi, B., Reyes-Aviles, E., Micci, L., Ortiz, A.M., Chahroudi, A., Vinton, C., Gordon, S.N., Bosinger, S.E., Francella, N., et al. (2011). Low levels of SIV infection in sooty mangabey central memory CD4 + T cells are associated with limited CCR5 expression. Nat. Med. *17*, 830–836.

Pallikkuth, S., Micci, L., Ende, Z.S., Iriele, R.I., Cervasi, B., Lawson, B., McGary, C.S., Rogers, K.A., Else, J.G., Silvestri, G., et al. (2013). Maintenance of Intestinal Th17 Cells and Reduced Microbial Translocation in SIV-infected Rhesus Macaques Treated with Interleukin (IL)-21. PLOS Pathog. *9*, e1003471.

Pandrea, I., Silvestri, G., Onanga, R., Veazey, R.S., Marx, P.A., Hirsch, V., and Apetrei, C. (2006). Simian immunodeficiency viruses replication dynamics in African non-human primate hosts: common patterns and species-specific differences. J. Med. Primatol. *35*, 194–201.

Pandrea, I., Ribeiro, R.M., Gautam, R., Gaufin, T., Pattison, M., Barnes, M., Monjure, C., Stoulig, C., Dufour, J., Cyprian, W., et al. (2008a). SIVagm Dynamics in African Green Monkeys. J. Virol.

Pandrea, I., Onanga, R., Souquiere, S., Mouinga-Ondéme, A., Bourry, O., Makuwa, M., Rouquet, P., Silvestri, G., Simon, F., Roques, P., et al. (2008b). Paucity of CD4+ CCR5+ T Cells May Prevent Transmission of Simian Immunodeficiency Virus in Natural Nonhuman Primate Hosts by Breast-Feeding. J. Virol. *82*, 5501–5509.

Pandrea, I.V., Gautam, R., Ribeiro, R.M., Brenchley, J.M., Butler, I.F., Pattison, M., Rasmussen, T., Marx, P.A., Silvestri, G., Lackner, A.A., et al. (2007). Acute Loss of Intestinal CD4+ T Cells Is Not Predictive of Simian Immunodeficiency Virus Virulence. J. Immunol. *179*, 3035–3046.

Papillion, A., Powell, M.D., Chisolm, D.A., Bachus, H., Fuller, M.J., Weinmann, A.S., Villarino, A., O'Shea, J.J., León, B., Oestreich, K.J., et al. (2019). Inhibition of IL-2 responsiveness by IL-6 is required for the generation of GC-TFH cells. Sci. Immunol. *4*.

Park, C.-S., Yoon, S.-O., Armitage, R.J., and Choi, Y.S. (2004). Follicular Dendritic Cells Produce IL-15 That Enhances Germinal Center B Cell Proliferation in Membrane-Bound Form. J. Immunol. *173*, 6676–6683.

Parsons, M.S., Le Grand, R., and Kent, S.J. (2018). Neutralizing Antibody-Based Prevention of Cell-Associated HIV-1 Infection. Viruses *10*, 333.

Paster, W., Brockmeyer, C., Fu, G., Simister, P.C., Wet, B. de, Martinez-Riaño, A., Hoerter, J.A.H., Feller, S.M., Wülfing, C., Gascoigne, N.R.J., et al. (2013). GRB2-Mediated Recruitment of THEMIS to LAT Is Essential for Thymocyte Development. J. Immunol. *190*, 3749–3756.

Paust, S., Blish, C.A., and Reeves, R.K. (2017). Redefining Memory: Building the Case for Adaptive NK Cells. J. Virol. *91*.

Peperzak, V., Veraar, E.A.M., Xiao, Y., Bąbała, N., Thiadens, K., Brugmans, M., and Borst, J. (2013). CD8+ T Cells Produce the Chemokine CXCL10 in Response to CD27/CD70 Costimulation To Promote Generation of the CD8+ Effector T Cell Pool. J. Immunol.

Perdomo-Celis, F., Taborda, N.A., and Rugeles, M.T. (2017). Follicular CD8+ T Cells: Origin, Function and Importance during HIV Infection. Front. Immunol. *8*.

Pereira, B.I., Devine, O.P., Vukmanovic-Stejic, M., Chambers, E.S., Subramanian, P., Patel, N., Virasami, A., Sebire, N.J., Kinsler, V., Valdovinos, A., et al. (2019). Senescent cells evade immune clearance via HLA-E-mediated NK and CD8 + T cell inhibition. Nat. Commun. *10*, 2387.

Pereira, L.E., Johnson, R.P., and Ansari, A.A. (2008). Sooty mangabeys and rhesus macaques exhibit significant divergent natural killer cell responses during both acute and chronic phases of SIV infection. Cell. Immunol. *254*, 10–19.

Perera, L., Shao, L., Patel, A., Evans, K., Meresse, B., Blumberg, R., Geraghty, D., Groh, V., Spies, T., Jabri, B., et al. (2007). Expression of nonclassical class I molecules by intestinal epithelial cells. Inflamm. Bowel Dis. *13*, 298–307.

Perera, P.-Y., Lichy, J.H., Waldmann, T.A., and Perera, L.P. (2012). The role of interleukin-15 in inflammation and immune responses to infection: implications for its therapeutic use. Microbes Infect. *14*, 247–261.

Permar, S.R., Wilks, A.B., Ehlinger, E.P., Kang, H.H., Mahlokozera, T., Coffey, R.T., Carville, A., Letvin, N.L., and Seaman, M.S. (2010). Limited contribution of mucosal IgA to SIV-specific neutralizing antibody response and virus Envelope evolution in breast milk of SIV-infected, lactating rhesus monkeys. J. Virol.

Perreau, M., Savoye, A.-L., De Crignis, E., Corpataux, J.-M., Cubas, R., Haddad, E.K., De Leval, L., Graziosi, C., and Pantaleo, G. (2013). Follicular helper T cells serve as the major CD4 T cell compartment for HIV-1 infection, replication, and production. J. Exp. Med. *210*, 143–156.

Peruchon, S., Chaoul, N., Burelout, C., Delache, B., Brochard, P., Laurent, P., Cognasse, F., Prévot, S., Garraud, O., Grand, R.L., et al. (2009). Tissue-Specific B-Cell Dysfunction and Generalized Memory B-Cell Loss during Acute SIV Infection. PLOS ONE *4*, e5966.

Peterson, L.W., and Artis, D. (2014). Intestinal epithelial cells: regulators of barrier function and immune homeostasis. Nat. Rev. Immunol. *14*, 141–153.

Petrovas, C., Yamamoto, T., Gerner, M.Y., Boswell, K.L., Wloka, K., Smith, E.C., Ambrozak, D.R., Sandler, N.G., Timmer, K.J., Sun, X., et al. (2012). CD4 T follicular helper cell dynamics during SIV infection. J. Clin. Invest. *122*, 3281–3294.

Phalipon, A., Cardona, A., Kraehenbuhl, J.-P., Edelman, L., Sansonetti, P.J., and Corthésy, B. (2002). Secretory Component: A New Role in Secretory IgA-Mediated Immune Exclusion In Vivo. Immunity *17*, 107–115.

Planchais, C., Hocqueloux, L., Ibanez, C., Gallien, S., Copie, C., Surenaud, M., Kök, A., Lorin, V., Fusaro, M., Delfau-Larue, M.-H., et al. (2018). Early Antiretroviral Therapy Preserves Functional Follicular Helper T and HIV-Specific B Cells in the Gut Mucosa of HIV-1–Infected Individuals. J. Immunol.

Ploquin, M.J., Madec, Y., Casrouge, A., Huot, N., Passaes, C., Lécuroux, C., Essat, A., Boufassa, F., Jacquelin, B., Jochems, S.P., et al. (2016). Elevated Basal Pre-infection CXCL10 in Plasma and in the Small Intestine after Infection Are Associated with More Rapid HIV/SIV Disease Onset. PLOS Pathog. *12*, e1005774.

Ploquin, M.J., Casrouge, A., Madec, Y., Noël, N., Jacquelin, B., Huot, N., Duffy, D., Jochems, S.P., Micci, L., Lécuroux, C., et al. (2018). Systemic DPP4 activity is reduced during primary HIV-1 infection and is

associated with intestinal RORC + CD4+ cell levels: a surrogate marker candidate of HIV-induced intestinal damage. J. Int. AIDS Soc. *21*.

Ploquin, M.J.-Y., Desoutter, J.-F., Santos, P.R., Pandrea, I., Diop, O.M., Hosmalin, A., Butor, C., Barre-Sinoussi, F., and Müller-Trutwin, M.C. (2006). Distinct expression profiles of TGF-β1 signaling mediators in pathogenic SIVmac and non-pathogenic SIVagm infections. Retrovirology *3*, 37.

Poggi, A., Benelli, R., Venè, R., Costa, D., Ferrari, N., Tosetti, F., and Zocchi, M.R. (2019). Human Gut-Associated Natural Killer Cells in Health and Disease. Front. Immunol. *10*.

Poli, A., Michel, T., Thérésine, M., Andrès, E., Hentges, F., and Zimmer, J. (2009). CD56bright natural killer (NK) cells: an important NK cell subset. Immunology *126*, 458–465.

Ponte, R., Mehraj, V., Ghali, P., Couëdel-Courteille, A., Cheynier, R., and Routy, J.-P. (2016). Reversing Gut Damage in HIV Infection: Using Non-Human Primate Models to Instruct Clinical Research. EBioMedicine *4*, 40–49.

Porcheray, F., Samah, B., Léone, C., Dereuddre-Bosquet, N., and Gras, G. (2006). Macrophage activation and human immunodeficiency virus infection: HIV replication directs macrophages towards a pro-inflammatory phenotype while previous activation modulates macrophage susceptibility to infection and viral production. Virology *349*, 112–120.

Poultsidi, A., Dimopoulos, Y., He, T.-F., Chavakis, T., Saloustros, E., Lee, P.P., and Petrovas, C. (2018). Lymph Node Cellular Dynamics in Cancer and HIV: What Can We Learn for the Follicular CD4 (Tfh) Cells? Front. Immunol. *9*.

Price, D.A., West, S.M., Betts, M.R., Ruff, L.E., Brenchley, J.M., Ambrozak, D.R., Edghill-Smith, Y., Kuroda, M.J., Bogdan, D., Kunstman, K., et al. (2004). T Cell Receptor Recognition Motifs Govern Immune Escape Patterns in Acute SIV Infection. Immunity *21*, 793–803.

Prieto, J.M.B., and Felippe, M.J.B. (2017). Development, phenotype, and function of non-conventional B cells. Comp. Immunol. Microbiol. Infect. Dis. *54*, 38–44.

Qin, S., Fallert Junecko, B.A., Trichel, A.M., Tarwater, P.M., Murphey-Corb, M.A., Kirschner, D.E., and Reinhart, T.A. (2010). Simian Immunodeficiency Virus Infection Alters Chemokine Networks in Lung Tissues of Cynomolgus Macaques: Association with Pneumocystis carinii Infection. Am. J. Pathol. *177*, 1274–1285.

Qiu, Y., Jiang, Z., Hu, S., Wang, L., Ma, X., and Yang, X. (2017). Lactobacillus plantarum Enhanced IL-22 Production in Natural Killer (NK) Cells That Protect the Integrity of Intestinal Epithelial Cell Barrier Damaged by Enterotoxigenic Escherichia coli. Int. J. Mol. Sci. *18*, 2409.

Rabezanahary, H., Moukambi, F., Palesch, D., Clain, J., Racine, G., Andreani, G., Benmadid-Laktout, G., Zghidi-Abouzid, O., Soundaramourty, C., Tremblay, C., et al. (2020). Despite early antiretroviral therapy effector memory and follicular helper CD4 T cells are major reservoirs in visceral lymphoid tissues of SIV-infected macaques. Mucosal Immunol. *13*, 149–160.

Raehtz, K.D., Barrenäs, F., Xu, C., Busman-Sahay, K., Valentine, A., Law, L., Ma, D., Policicchio, B.B., Wijewardana, V., Brocca-Cofano, E., et al. (2020). African green monkeys avoid SIV disease progression by preventing intestinal dysfunction and maintaining mucosal barrier integrity. PLOS Pathog. *16*, e1008333.

Ramsuran, V., Naranbhai, V., Horowitz, A., Qi, Y., Martin, M.P., Yuki, Y., Gao, X., Walker-Sperling, V., Del Prete, G.Q., Schneider, D.K., et al. (2018). Elevated HLA-A expression impairs HIV control through inhibition of NKG2A-expressing cells. Science *359*, 86–90.

Rao, D.A. (2018). T Cells That Help B Cells in Chronically Inflamed Tissues. Front. Immunol. *9*.

Rapaport, A.S., Schriewer, J., Gilfillan, S., Hembrador, E., Crump, R., Plougastel, B.F., Wang, Y., Le Friec, G., Gao, J., Cella, M., et al. (2015). The Inhibitory Receptor NKG2A Sustains Virus-Specific CD8+ T Cells in Response to a Lethal Poxvirus Infection. Immunity *43*, 1112–1124.

Reboldi, A., and Cyster, J.G. (2016). Peyer's patches: organizing B-cell responses at the intestinal frontier. Immunol. Rev. *271*, 230–245.

Reeves, R.K., Gillis, J., Wong, F.E., Yu, Y., Connole, M., and Johnson, R.P. (2010a). CD16- natural killer cells: enrichment in mucosal and secondary lymphoid tissues and altered function during chronic SIV infection. Blood *115*, 4439–4446.

Reeves, R.K., Evans, T.I., Gillis, J., and Johnson, R.P. (2010b). Simian immunodeficiency virus infection induces expansion of alpha4beta7+ and cytotoxic CD56+ NK cells. J. Virol. *84*, 8959–8963.

Reeves, R.K., Rajakumar, P.A., Evans, T.I., Connole, M., Gillis, J., Wong, F.E., Kuzmichev, Y.V., Carville, A., and Johnson, R.P. (2011). Gut inflammation and indoleamine deoxygenase inhibit IL-17 production and promote cytotoxic potential in NKp44+ mucosal NK cells during SIV infection. Blood *118*, 3321–3330.

Reeves, R.K., Evans, T.I., Gillis, J., Wong, F.E., Kang, G., Li, Q., and Johnson, R.P. (2012). SIV Infection Induces Accumulation of Plasmacytoid Dendritic Cells in the Gut Mucosa. J. Infect. Dis. *206*, 1462–1468.

Reina, J.-M.L., Favre, D., Kasakow, Z., Mayau, V., Nugeyre, M.-T., Ka, T., Faye, A., Miller, C.J., Scott-Algara, D., McCune, J.M., et al. (2009). Gag p27-Specific B- and T-Cell Responses in Simian Immunodeficiency Virus SIVagm-Infected African Green Monkeys. J. Virol. *83*, 2770–2777.

Reynolds, M.R., Rakasz, E., Skinner, P.J., White, C., Abel, K., Ma, Z.-M., Compton, L., Napoé, G., Wilson, N., Miller, C.J., et al. (2005). CD8+ T-Lymphocyte Response to Major Immunodominant Epitopes after Vaginal Exposure to Simian Immunodeficiency Virus: Too Late and Too Little. J. Virol. *79*, 9228–9235.

Ries, M., Reynolds, M.R., Bashkueva, K., Crosno, K., Iii, S.C., Prall, T.M., Wiseman, R., O'Connor, D.H., Rakasz, E.G., Uno, H., et al. (2017). KIR3DL01 upregulation on gut natural killer cells in response to SIV infection of KIR- and MHC class I-defined rhesus macaques. PLOS Pathog. *13*, e1006506.

Rodda, L.B., Lu, E., Bennett, M.L., Sokol, C.L., Wang, X., Luther, S.A., Barres, B.A., Luster, A.D., Ye, C.J., and Cyster, J.G. (2018). Single-Cell RNA Sequencing of Lymph Node Stromal Cells Reveals Niche-Associated Heterogeneity. Immunity *48*, 1014-1028.e6.

Romee, R., Foley, B., Lenvik, T., Wang, Y., Zhang, B., Ankarlo, D., Luo, X., Cooley, S., Verneris, M., Walcheck, B., et al. (2013). NK cell CD16 surface expression and function is regulated by a disintegrin and metalloprotease-17 (ADAM17). Blood *121*, 3599–3608.

Rothenberger, M.K., Keele, B.F., Wietgrefe, S.W., Fletcher, C.V., Beilman, G.J., Chipman, J.G., Khoruts, A., Estes, J.D., Anderson, J., Callisto, S.P., et al. (2015). Large number of rebounding/founder HIV variants emerge from multifocal infection in lymphatic tissues after treatment interruption. Proc. Natl. Acad. Sci.

Ruggeri, L., Urbani, E., André, P., Mancusi, A., Tosti, A., Topini, F., Bléry, M., Animobono, L., Romagné, F., Wagtmann, N., et al. (2016). Effects of anti-NKG2A antibody administration on leukemia and normal hematopoietic cells. Haematologica *101*, 626–633.

Rydyznski, C.E., Cranert, S.A., Zhou, J.Q., Xu, H., Kleinstein, S.H., Singh, H., and Waggoner, S.N. (2018). Affinity Maturation Is Impaired by Natural Killer Cell Suppression of Germinal Centers. Cell Rep. *24*, 3367-3373.e4.

Saeidi, A., Zandi, K., Cheok, Y.Y., Saeidi, H., Wong, W.F., Lee, C.Y.Q., Cheong, H.C., Yong, Y.K., Larsson, M., and Shankar, E.M. (2018). T-Cell Exhaustion in Chronic Infections: Reversing the State of Exhaustion and Reinvigorating Optimal Protective Immune Responses. Front. Immunol. *9*.

Sáez-Cirión, A., Lacabaratz, C., Lambotte, O., Versmisse, P., Urrutia, A., Boufassa, F., Barré-Sinoussi, F., Delfraissy, J.-F., Sinet, M., Pancino, G., et al. (2007). HIV controllers exhibit potent CD8 T cell capacity to suppress HIV infection ex vivo and peculiar cytotoxic T lymphocyte activation phenotype. Proc. Natl. Acad. Sci. *104*, 6776–6781.

Sandler, N.G., Bosinger, S.E., Estes, J.D., Zhu, R.T.R., Tharp, G.K., Boritz, E., Levin, D., Wijeyesinghe, S., Makamdop, K.N., del Prete, G.Q., et al. (2014). Type I interferon responses in rhesus macaques prevent SIV infection and slow disease progression. Nature *511*, 601–605.

de Santa Barbara, P., van den Brink, G.R., and Roberts, D.J. (2003). Development and differentiation of the intestinal epithelium. Cell. Mol. Life Sci. CMLS *60*, 1322–1332.

Santangelo, P.J., Rogers, K.A., Zurla, C., Blanchard, E.L., Gumber, S., Strait, K., Connor-Stroud, F., Schuster, D.M., Amancha, P.K., Hong, J.J., et al. (2015). Whole-body immunoPET reveals active SIV dynamics in viremic and antiretroviral therapy–treated macaques. Nat. Methods *12*, 427–432.

Sanz, I., Wei, C., Jenks, S.A., Cashman, K.S., Tipton, C., Woodruff, M.C., Hom, J., and Lee, F.E.-H. (2019). Challenges and Opportunities for Consistent Classification of Human B Cell and Plasma Cell Populations. Front. Immunol. *10*.

Schacker, T.W., Nguyen, P.L., Beilman, G.J., Wolinsky, S., Larson, M., Reilly, C., and Haase, A.T. (2002). Collagen deposition in HIV-1 infected lymphatic tissues and T cell homeostasis. J. Clin. Invest. *110*, 1133–1139.

Schafer, J.L., Li, H., Evans, T.I., Estes, J.D., and Reeves, R.K. (2015a). Accumulation of Cytotoxic CD16+ NK Cells in Simian Immunodeficiency Virus-Infected Lymph Nodes Associated with In Situ Differentiation and Functional Anergy. J. Virol. *89*, 6887–6894.

Schafer, J.L., Li, H., Evans, T.I., Estes, J.D., and Reeves, R.K. (2015b). Accumulation of Cytotoxic CD16+ NK Cells in Simian Immunodeficiency Virus-Infected Lymph Nodes Associated with In Situ Differentiation and Functional Anergy. J. Virol. *89*, 6887–6894.

Scharko, A.M., Perlman, S.B., PW2nd, H., Hanson, J.M., Uno, H., and Pauza, C.D. (1996). Whole body positron emission tomography imaging of simian immunodeficiency virus-infected rhesus macaques. Proc. Natl. Acad. Sci. *93*, 6425–6430.

Schindler, M., Münch, J., Kutsch, O., Li, H., Santiago, M.L., Bibollet-Ruche, F., Müller-Trutwin, M.C., Novembre, F.J., Peeters, M., Courgnaud, V., et al. (2006). Nef-Mediated Suppression of T Cell Activation Was Lost in a Lentiviral Lineage that Gave Rise to HIV-1. Cell *125*, 1055–1067.

Schoggins, J.W. (2014). Interferon-stimulated genes: roles in viral pathogenesis. Curr. Opin. Virol. *6*, 40–46.

Schuetz, A., Deleage, C., Sereti, I., Rerknimitr, R., Phanuphak, N., Phuang-Ngern, Y., Estes, J.D., Sandler, N.G., Sukhumvittaya, S., Marovich, M., et al. (2014). Initiation of ART during Early Acute HIV Infection Preserves Mucosal Th17 Function and Reverses HIV-Related Immune Activation. PLOS Pathog. *10*, e1004543.

Serra-Peinado, C., Grau-Expósito, J., Luque-Ballesteros, L., Astorga-Gamaza, A., Navarro, J., Gallego-Rodriguez, J., Martin, M., Curran, A., Burgos, J., Ribera, E., et al. (2019). Expression of CD20 after viral reactivation renders HIV-reservoir cells susceptible to Rituximab. Nat. Commun. *10*, 3705.

Shacklett, B.L., and Anton, P.A. (2010). HIV Infection and Gut Mucosal Immune Function: Updates on Pathogenesis with Implications for Management and Intervention. Curr. Infect. Dis. Rep. *12*, 19–27.

Shaffer, A.L., Lin, K.-I., Kuo, T.C., Yu, X., Hurt, E.M., Rosenwald, A., Giltnane, J.M., Yang, L., Zhao, H., Calame, K., et al. (2002). Blimp-1 Orchestrates Plasma Cell Differentiation by Extinguishing the Mature B Cell Gene Expression Program. Immunity *17*, 51–62.

Shah, S.V., Manickam, C., Ram, D.R., and Reeves, R.K. (2017). Innate Lymphoid Cells in HIV/SIV Infections. Front. Immunol. *8*.

Shamaei-Tousi, A., Stephens, J.W., Bin, R., Cooper, J.A., Steptoe, A., Coates, A.R.M., Henderson, B., and Humphries, S.E. (2006). Association between plasma levels of heat shock protein 60 and cardiovascular disease in patients with diabetes mellitus. Eur. Heart J. *27*, 1565–1570.

Shang, L., Smith, A.J., Duan, L., Perkey, K.E., Qu, L., Wietgrefe, S., Zupancic, M., Southern, P.J., Masek-Hammerman, K., Reeves, R.K., et al. (2014). NK Cell Responses to SIV Vaginal Exposure in Naïve and Vaccinated Rhesus Macaques. J. Immunol. Baltim. Md 1950 *193*, 277–284.

Shen, R., Richter, H.E., Clements, R.H., Novak, L., Huff, K., Bimczok, D., Sankaran-Walters, S., Dandekar, S., Clapham, P.R., Smythies, L.E., et al. (2009). Macrophages in Vaginal but Not Intestinal Mucosa Are Monocyte-Like and Permissive to Human Immunodeficiency Virus Type 1 Infection. J. Virol. *83*, 3258–3267.

Shive, C.L., Biancotto, A., Funderburg, N.T., Pilch-Cooper, H.A., Valdez, H., Margolis, L., Sieg, S.F., McComsey, G.A., Rodriguez, B., and Lederman, M.M. (2012). HIV-1 is not a major driver of increased plasma IL-6 levels in chronic HIV-1 disease. J. Acquir. Immune Defic. Syndr. 1999 *61*, 145–152.

Simmons, R.P., Scully, E.P., Groden, E.E., Arnold, K.B., Chang, J.J., Lane, K., Lifson, J., Rosenberg, E., Lauffenburger, D.A., and Altfeld, M. (2013). HIV-1 infection induces strong production of IP-10 through TLR7/9-dependent pathways. AIDS *27*, 2505–2517.

Simon, V., Ho, D.D., and Karim, Q.A. (2006). HIV/AIDS epidemiology, pathogenesis, prevention, and treatment. The Lancet *368*, 489–504.

Sims, G.P., Ettinger, R., Shirota, Y., Yarboro, C.H., Illei, G.G., and Lipsky, P.E. (2005). Identification and characterization of circulating human transitional B cells. Blood *105*, 4390–4398.

Sips, M., Sciaranghella, G., Diefenbach, T., Dugast, A.-S., Berger, C.T., Liu, Q., Kwon, D., Ghebremichael, M., Estes, J.D., Carrington, M., et al. (2012a). Altered distribution of mucosal NK cells during HIV infection. Mucosal Immunol. *5*, 30–40.

Sips, M., Sciaranghella, G., Diefenbach, T., Dugast, A.-S., Berger, C.T., Liu, Q., Kwon, D., Ghebremichael, M., Estes, J.D., Carrington, M., et al. (2012b). Altered distribution of mucosal NK cells during HIV infection. Mucosal Immunol. *5*, 30–40.

Sozzani, S., Vermi, W., Del Prete, A., and Facchetti, F. (2010). Trafficking properties of plasmacytoid dendritic cells in health and disease. Trends Immunol. *31*, 270–277.

Spencer, J., and Sollid, L.M. (2016). The human intestinal B-cell response. Mucosal Immunol. *9*, 1113–1124.

Stacey, A.R., Norris, P.J., Qin, L., Haygreen, E.A., Taylor, E., Heitman, J., Lebedeva, M., DeCamp, A., Li, D., Grove, D., et al. (2009). Induction of a Striking Systemic Cytokine Cascade prior to Peak Viremia in Acute Human Immunodeficiency Virus Type 1 Infection, in Contrast to More Modest and Delayed Responses in Acute Hepatitis B and C Virus Infections. J. Virol. *83*, 3719–3733.

Stary, V., and Stary, G. (2020). NK Cell-Mediated Recall Responses: Memory-Like, Adaptive, or Antigen-Specific? Front. Cell. Infect. Microbiol. *10*.

Steffen, U., Koeleman, C.A., Sokolova, M.V., Bang, H., Kleyer, A., Rech, J., Unterweger, H., Schicht, M., Garreis, F., Hahn, J., et al. (2020). IgA subclasses have different effector functions associated with distinct glycosylation profiles. Nat. Commun. *11*, 120.

Stelma, F., de Niet, A., Sinnige, M.J., van Dort, K.A., van Gisbergen, K.P.J.M., Verheij, J., van Leeuwen, E.M.M., Kootstra, N.A., and Reesink, H.W. (2017). Human intrahepatic CD69 + CD8+ T cells have a tissue resident memory T cell phenotype with reduced cytolytic capacity. Sci. Rep. *7*.

Stevanović, S., van Bergen, C.A.M., van Luxemburg-Heijs, S.A.P., van der Zouwen, B., Jordanova, E.S., Kruisselbrink, A.B., van de Meent, M., Harskamp, J.C., Claas, F.H.J., Marijt, E.W.A., et al. (2013). HLA class II upregulation during viral infection leads to HLA-DP–directed graft-versus-host disease after CD4+ donor lymphocyte infusion. Blood *122*, 1963–1973.

Stieh, D.J., Matias, E., Xu, H., Fought, A.J., Blanchard, J.L., Marx, P.A., Veazey, R.S., and Hope, T.J. (2016). Th17 Cells Are Preferentially Infected Very Early after Vaginal Transmission of SIV in Macaques. Cell Host Microbe *19*, 529–540.

Stocks, B.T., Wilson, C.S., Marshall, A.F., Brewer, L.A., and Moore, D.J. (2017). Host Expression of the CD8 Treg/NK Cell Restriction Element Qa-1 is Dispensable for Transplant Tolerance. Sci. Rep. *7*, 11181.

Stonier, S.W., and Schluns, K.S. (2010). Trans-presentation: a novel mechanism regulating IL-15 delivery and responses. Immunol. Lett. *127*, 85–92.

Strauss-Albee, D.M., Horowitz, A., Parham, P., and Blish, C.A. (2014). Coordinated Regulation of NK Receptor Expression in the Maturing Human Immune System. J. Immunol.

Suh, W.-K. (2014). Life of T Follicular Helper Cells. Mol. Cells *38*, 195–201.

Suzuki, K., and Nakajima, A. (2014). New aspects of IgA synthesis in the gut. Int. Immunol. *26*, 489–494.

Swan, Z.D., Wonderlich, E.R., and Barratt-Boyes, S.M. (2016). Macrophage accumulation in gut mucosa differentiates AIDS from chronic SIV infection in rhesus macaques. Eur. J. Immunol. *46*, 446–454.

Takahashi, Y., Byrareddy, S.N., Albrecht, C., Brameier, M., Walter, L., Mayne, A.E., Dunbar, P., Russo, R., Little, D.M., Villinger, T., et al. (2014). In Vivo Administration of a JAK3 Inhibitor during Acute SIV Infection Leads to Significant Increases in Viral Load during Chronic Infection. PLoS Pathog. *10*.

Takao, S., Ishikawa, T., Yamashita, K., and Uchiyama, T. (2010). The rapid induction of HLA-E is essential for the survival of antigen-activated naive CD4 T cells from attack by NK cells. J. Immunol. Baltim. Md 1950 *185*, 6031–6040.

Tamzalit, F., Barbieux, I., Plet, A., Heim, J., Nedellec, S., Morisseau, S., Jacques, Y., and Mortier, E. (2014). IL-15.IL-15Rα complex shedding following trans-presentation is essential for the survival of IL-15 responding NK and T cells. Proc. Natl. Acad. Sci. U. S. A. *111*, 8565–8570.

Teleshova, N., Kenney, J., Williams, V., Nest, G.V., Marshall, J., Lifson, J.D., Sivin, I., Dufour, J., Bohm, R., Gettie, A., et al. (2006). CpG-C ISS-ODN activation of blood-derived B cells from healthy and chronic immunodeficiency virus-infected macaques. J. Leukoc. Biol. *79*, 257–267.

Thans, T. van S., Akko, J.I., Niehrs, A., Garcia-Beltran, W.F., Richert, L., Stürzel, C.M., Ford, C.T., Li, H., Ochsenbauer, C., Kappes, J.C., et al. (2019). Primary HIV-1 Strains Use Nef To Downmodulate HLA-E Surface Expression. J. Virol. *93*.

Theurich, S., Tsaousidou, E., Hanssen, R., Lempradl, A.M., Mauer, J., Timper, K., Schilbach, K., Folz-Donahue, K., Heilinger, C., Sexl, V., et al. (2017). IL-6/Stat3-Dependent Induction of a Distinct, Obesity-Associated NK Cell Subpopulation Deteriorates Energy and Glucose Homeostasis. Cell Metab. *26*, 171-184.e6.

Thimme, R., Appay, V., Koschella, M., Panther, E., Roth, E., Hislop, A.D., Rickinson, A.B., Rowland-Jones, S.L., Blum, H.E., and Pircher, H. (2005). Increased expression of the NK cell receptor KLRG1 by virus-specific CD8 T cells during persistent antigen stimulation. J. Virol. *79*, 12112–12116.

Ting, H.-A., and Moltke, J. von (2019). The Immune Function of Tuft Cells at Gut Mucosal Surfaces and Beyond. J. Immunol. *202*, 1321–1329.

Tortorec, A.L., Grand, R.L., Denis, H., Satie, A.-P., Mannioui, K., Roques, P., Maillard, A., Daniels, S., Jégou, B., and Dejucq-Rainsford, N. (2008). Infection of Semen-Producing Organs by SIV during the Acute and Chronic Stages of the Disease. PLOS ONE *3*, e1792.

Tsai, C.-C., Follis, K.E., Sabo, A., Beck, T.W., Grant, R.F., Bischofberger, N., Benveniste, R.E., and Black, R. (1995). Prevention of SIV Infection in Macaques by (R)-9-(2-Phosphonylmethoxypropyl)adenine. Science *270*, 1197–1199.

Tuyishime, M., Garrido, C., Jha, S., Moeser, M., Mielke, D., LaBranche, C., Montefiori, D., Haynes, B.F., Joseph, S.B., Margolis, D.M., et al. (2020). Improved Killing of HIV-infected Cells Using Three Neutralizing and Non-neutralizing Antibodies. J. Clin. Invest.

Uhrberg, M., Valiante, N.M., Young, N.T., Lanier, L.L., Phillips, J.H., and Parham, P. (2001). The Repertoire of Killer Cell Ig-Like Receptor and CD94:NKG2A Receptors in T Cells: Clones Sharing Identical αβ TCR Rearrangement Express Highly Diverse Killer Cell Ig-Like Receptor Patterns. J. Immunol. *166*, 3923–3932.

Urashima, M., Chauhan, D., Hatziyanni, M., Ogata, A., Hollenbaugh, D., Aruffo, A., and Anderson, K.C. (1996). CD40 ligand triggers interleukin-6 mediated B cell differentiation. Leuk. Res. *20*, 507–515.

Vaccari, M., and Franchini, G. (2018). T Cell Subsets in the Germinal Center: Lessons from the Macaque Model. Front. Immunol. *9*.

Valle-Casuso, J.C., Angin, M., Volant, S., Passaes, C., Monceaux, V., Mikhailova, A., Bourdic, K., Avettand-Fenoel, V., Boufassa, F., Sitbon, M., et al. (2019). Cellular Metabolism Is a Major Determinant of HIV-1 Reservoir Seeding in CD4+ T Cells and Offers an Opportunity to Tackle Infection. Cell Metab. *29*, 611-626.e5.

Valverde-Villegas, J.M., Matte, M.C.C., Medeiros, R.M. de, and Chies, J.A.B. (2015). New Insights about Treg and Th17 Cells in HIV Infection and Disease Progression (Hindawi).

Vásquez, J.J., Aguilar-Rodriguez, B.L., Rodriguez, L., Hogan, L.E., Somsouk, M., McCune, J.M., Deeks, S.G., Laszik, Z.G., Hunt, P.W., and Henrich, T.J. (2019). CD32-RNA Co-localizes with HIV-RNA in CD3+ Cells Found within Gut Tissues from Viremic and ART-Suppressed Individuals. Pathog. Immun. *4*, 147–160.

Veazey, R.S. (2019). Intestinal CD4 Depletion in HIV / SIV Infection. Curr. Immunol. Rev. *15*, 76–91.

Veazey, R.S., and Lackner, A.A. (2017). Nonhuman Primate Models and Understanding the Pathogenesis of HIV Infection and AIDS. ILAR J. *58*, 160–171.

Veazey, R.S., DeMaria, M., Chalifoux, L.V., Shvetz, D.E., Pauley, D.R., Knight, H.L., Rosenzweig, M., Johnson, R.P., Desrosiers, R.C., and Lackner, A.A. (1998). Gastrointestinal Tract as a Major Site of CD4+ T Cell Depletion and Viral Replication in SIV Infection. Science *280*, 427–431.

Veazey, R.S., Marx, P.A., and Lackner, A.A. (2003). Vaginal CD4+ T Cells Express High Levels of CCR5 and Are Rapidly Depleted in Simian Immunodeficiency Virus Infection. J. Infect. Dis. *187*, 769–776.

Velaga, S., Herbrand, H., Friedrichsen, M., Jiong, T., Dorsch, M., Hoffmann, M.W., Förster, R., and Pabst, O. (2009). Chemokine receptor CXCR5 supports solitary intestinal lymphoid tissue formation, B cell homing, and induction of intestinal IgA responses. J. Immunol. Baltim. Md 1950 *182*, 2610–2619.

Velu, V., Mylvaganam, G.H., Gangadhara, S., Hong, J.J., Iyer, S.S., Gumber, S., Ibegbu, C.C., Villinger, F., and Amara, R.R. (2016). Induction of Th1-Biased T Follicular Helper (Tfh) Cells in Lymphoid Tissues during Chronic Simian Immunodeficiency Virus Infection Defines Functionally Distinct Germinal Center Tfh Cells. J. Immunol. *197*, 1832–1842.

Velu, V., Mylvaganam, G., Ibegbu, C., and Amara, R.R. (2018). Tfh1 Cells in Germinal Centers During Chronic HIV/SIV Infection. Front. Immunol. *9*.

Wacleche, V.S., Landay, A., Routy, J.-P., and Ancuta, P. (2017). The Th17 Lineage: From Barrier Surfaces Homeostasis to Autoimmunity, Cancer, and HIV-1 Pathogenesis. Viruses *9*, 303.

Walker, B., and McMichael, A. (2012). The T-Cell Response to HIV. Cold Spring Harb. Perspect. Med. *2*, a007054.

Wallet, C., De Rovere, M., Van Assche, J., Daouad, F., De Wit, S., Gautier, V., Mallon, P.W.G., Marcello, A., Van Lint, C., Rohr, O., et al. (2019). Microglial Cells: The Main HIV-1 Reservoir in the Brain. Front. Cell. Infect. Microbiol. *9*.

Walsh, D.A., Borges da Silva, H., Beura, L.K., Peng, C., Hamilton, S.E., Masopust, D., and Jameson, S.C. (2019). The Functional Requirement for CD69 in Establishment of Resident Memory CD8 $^{+}$ T Cells Varies with Tissue Location. J. Immunol. *203*, 946–955.

Walters, L.C., Harlos, K., Brackenridge, S., Rozbesky, D., Barrett, J.R., Jain, V., Walter, T.S., O'Callaghan, C.A., Borrow, P., Toebes, M., et al. (2018). Pathogen-derived HLA-E bound epitopes reveal broad primary anchor pocket tolerability and conformationally malleable peptide binding. Nat. Commun. *9*, 3137.

Wang, L., and Müschen, M. (2018). Portending death in germinal centers — when B cells know their time is up. Cell Res. *28*, 5–6.

Wang, C.-C., Thanh, C., Gibson, E.A., Ball-Burack, M., Hogan, L.E., Descours, B., Jones, N., Carvidi, A.B., Munter, S., Bakkour, S., et al. (2018). Transient loss of detectable HIV-1 RNA following brentuximab vedotin anti-CD30 therapy for Hodgkin lymphoma. Blood Adv. *2*, 3479–3482.

Wang, W., Wu, F., Cong, Z., Liu, K., Qin, C., and Wei, Q. (2014). The Secretion of IL-22 from Mucosal NKp44+ NK Cells Is Associated with Microbial Translocation and Virus Infection in SIV/SHIV-Infected Chinese Macaques (Hindawi).

Wang, X., Cho, B., Suzuki, K., Xu, Y., Green, J.A., An, J., and Cyster, J.G. (2011). Follicular dendritic cells help establish follicle identity and promote B cell retention in germinal centers. J. Exp. Med. *208*, 2497–2510.

Wang, Y., Lifshitz, L., Gellatly, K., Vinton, C.L., Busman-Sahay, K., McCauley, S., Vangala, P., Kim, K., Derr, A., Jaiswal, S., et al. (2020). HIV-1-induced cytokines deplete homeostatic innate lymphoid cells and expand TCF7 -dependent memory NK cells. Nat. Immunol. *21*, 274–286.

Webb, G.M., Molden, J., Busman-Sahay, K., Abdulhaqq, S., Wu, H.L., Weber, W.C., Bateman, K.B., Reed, J.S., Northrup, M., Maier, N., et al. (2020). The human IL-15 superagonist N-803 promotes migration of virus-specific CD8+ T and NK cells to B cell follicles but does not reverse latency in ART-suppressed, SHIV-infected macaques. PLOS Pathog. *16*, e1008339.

Wetzel, K.S., Yi, Y., Elliott, S.T.C., Romero, D., Jacquelin, B., Hahn, B.H., Muller-Trutwin, M., Apetrei, C., Pandrea, I., and Collman, R.G. (2017). CXCR6-Mediated Simian Immunodeficiency Virus SIVagmSab Entry into Sabaeus African Green Monkey Lymphocytes Implicates Widespread Use of Non-CCR5 Pathways in Natural Host Infections. J. Virol. *91*.

Whitney, J.B., Hill, A.L., Sanisetty, S., Penaloza-MacMaster, P., Liu, J., Shetty, M., Parenteau, L., Cabral, C., Shields, J., Blackmore, S., et al. (2014). Rapid seeding of the viral reservoir prior to SIV viraemia in rhesus monkeys. Nature *512*, 74–77.

Wilk, A.J., Wilk, A.J., and Blish, C.A. (2018). Diversification of human NK cells: Lessons from deep profiling. J. Leukoc. Biol.

Withers, D.R. (2016). Innate lymphoid cell regulation of adaptive immunity. Immunology *149*, 123–130.

Wong, J.K., and Yukl, S.A. (2016). Tissue reservoirs of HIV. Curr. Opin. HIV AIDS *11*, 362–370.

Wong, E., Xu, R.-H., Rubio, D., Lev, A., Stotesbury, C., Fang, M., and Sigal, L.J. (2018). Migratory Dendritic Cells, Group 1 Innate Lymphoid Cells, and Inflammatory Monocytes Collaborate to Recruit NK Cells to the Virus-Infected Lymph Node. Cell Rep. *24*, 142–154.

Wong, M.E., Jaworowski, A., and Hearps, A.C. (2019). The HIV Reservoir in Monocytes and Macrophages. Front. Immunol. *10*.

Wu, H.L., Wiseman, R.W., Hughes, C.M., Webb, G.M., Abdulhaqq, S.A., Bimber, B.N., Hammond, K.B., Reed, J.S., Gao, L., Burwitz, B.J., et al. (2018). The role of MHC-E in T cell immunity is conserved among humans, rhesus macaques, and cynomolgus macaques. J. Immunol. Baltim. Md 1950 *200*, 49–60.

Wu, Y., Tian, Z., and Wei, H. (2017). Developmental and Functional Control of Natural Killer Cells by Cytokines. Front. Immunol. *8*.

Xu, H., Wang, X., Liu, D.X., Moroney-Rasmussen, T., Lackner, A.A., and Veazey, R.S. (2012). IL-17-producing innate lymphoid cells are restricted to mucosal tissues and are depleted in SIV-infected macaques. Mucosal Immunol. *5*, 658–669.

Xu, W., Zhao, X., Wang, X., Feng, H., Gou, M., Jin, W., Wang, X., Liu, X., and Dong, C. (2019). The Transcription Factor Tox2 Drives T Follicular Helper Cell Development via Regulating Chromatin Accessibility. Immunity *51*, 826-839.e5.

Yelina Alvarez, M, Tuen, G, Shen, F, Nawaz, J, Arthos, et al. (2013). Preferential HIV infection of CCR6+ Th17 cells is associated with higher levels of virus receptor expression and lack of CCR5 ligands (J Virol).

Yang, C.-L., Zhang, P., Liu, R.-T., Zhang, N., Zhang, M., Li, H., Du, T., Li, X.-L., Dou, Y.-C., and Duan, R.-S. (2019). CXCR5-negative natural killer cells ameliorate experimental autoimmune myasthenia gravis by suppressing follicular helper T cells. J. Neuroinflammation *16*, 282.

Yero, A., Farnos, O., Rabezanahary, H., Racine, G., Estaquier, J., and Jenabian, M.-A. (2019). Differential Dynamics of Regulatory T-Cell and Th17 Cell Balance in Mesenteric Lymph Nodes and Blood following Early Antiretroviral Initiation during Acute Simian Immunodeficiency Virus Infection. J. Virol. *93*.

Yu, D., and Vinuesa, C.G. (2010). The elusive identity of T follicular helper cells. Trends Immunol. *31*, 377–383.

Zahn, R.C., Rett, M.D., Korioth-Schmitz, B., Sun, Y., Buzby, A.P., Goldstein, S., Brown, C.R., Byrum, R.A., Freeman, G.J., Letvin, N.L., et al. (2008). Simian Immunodeficiency Virus (SIV)-Specific CD8+ T-Cell Responses in Vervet African Green Monkeys Chronically Infected with SIVagm. J. Virol. *82*, 11577–11588.

Zeddou, M., Rahmouni, S., Vandamme, A., Jacobs, N., Frippiat, F., Leonard, P., Schaaf-Lafontaine, N., Vaira, D., Boniver, J., and Moutschen, M. (2007). Downregulation of CD94/NKG2A inhibitory receptors on CD8+T cells in HIV infection is more pronounced in subjects with detected viral load than in their aviraemic counterparts. Retrovirology *4*, 72.

Zeng, M., Southern, P.J., Reilly, C.S., Beilman, G.J., Chipman, J.G., Schacker, T.W., and Haase, A.T. (2012). Lymphoid Tissue Damage in HIV-1 Infection Depletes Naïve T Cells and Limits T Cell Reconstitution after Antiretroviral Therapy. PLOS Pathog. *8*, e1002437.

Zhang, R., Martinez, D.R., Nguyen, Q.N., Pollara, J., Arifin, T., Stolarchuk, C., Foulger, A., Amos, J.D., Parks, R., Himes, J.E., et al. (2016). Envelope-specific B-cell populations in African green monkeys chronically infected with simian immunodeficiency virus. Nat. Commun. *7*, 12131.

Zhang, Z.-Q., Schuler, T., Zupancic, M., Wietgrefe, S., Staskus, K.A., Reimann, K.A., Reinhart, T.A., Rogan, M., Cavert, W., Miller, C.J., et al. (1999). Sexual Transmission and Propagation of SIV and HIV in Resting and Activated CD4+ T Cells. Science *286*, 1353–1357.

Zitvogel, L., Terme, M., Borg, C., and Trinchieri, G. (2006). Dendritic cell-NK cell cross-talk: regulation and physiopathology. Curr. Top. Microbiol. Immunol. *298*, 157–174.

Zolla-Pazner, S., Alvarez, R., Kong, X.-P., and Weiss, S. (2019). Vaccine-induced V1V2-specific antibodies control and or protect against infection with HIV, SIV and SHIV. Curr. Opin. HIV AIDS *14*, 309–317.

(2002). CD94-NKG2A receptors regulate antiviral CD8+ T cell responses. Nat. Immunol. *3*.

Acquired immunodeficiency syndrome in a colony of macaque monkeys.

Page 333-341

- Garcia-Tellez T, Huot N, Ploquin MJ, Rascle P, Jacquelin B, Müller-Trutwin M. Non-human primates in HIV research: Achievements, limits and alternatives. Infect Genet Evol. 2016 ; 46:324-332.

Page 342-349

- Huot N*, Rascle P*, Garcia-Tellez T, Jacquelin B, Müller-Trutwin M. Innate immune cell responses in non Pathogenic versus pathogenic SIV infections. Curr Opin Virol. 2016; 19:37-44.

Page 350-361

- Huot N, Rascle P, Müller-Trutwin M. Contribution of animal models to HIV research. Virologie 2019, 23 (4):229-40.

ARTICLE IN PRESS
MEEGID-02841; No of Pages 9
Infection, Genetics and Evolution xxx (2016) xxx–xxx
Contents lists available at ScienceDirect
Infection, Genetics and Evolution
journal homepage: www.elsevier.com/locate/meegid

Non-human primates in HIV research: Achievements, limits and alternatives

Thalía Garcia-Tellez [a], Nicolas Huot [a,b], Mickaël J. Ploquin [a], Philippe Rascle [a], Beatrice Jacquelin [a], Michaela Müller-Trutwin [a,b,*]

[a] Institut Pasteur, Unité HIV, Inflammation and Persistence. 25–28 Rue du Doctor Roux,75015 Paris, France
[b] Vaccine Research Institute, Créteil, France

ARTICLE INFO

Article history:
Received 27 April 2016
Received in revised form 7 July 2016
Accepted 12 July 2016
Available online xxxx

Keywords:
HIV
SIV
AIDS
Non-human primates
Animal models

ABSTRACT

An ideal model for HIV-1 research is still unavailable. However, infection of non-human primates (NHP), such as macaques, with Simian Immunodeficiency Virus (SIV) recapitulates most virological, immunological and clinical hallmarks of HIV infection in humans. It has become the most suitable model to study the mechanisms of transmission and physiopathology of HIV/AIDS. On the other hand, natural hosts of SIV, such as African green monkeys and sooty mangabeys that when infected do not progress to AIDS, represent an excellent model to elucidate the mechanisms involved in the capacity of controlling inflammation and disease progression. The use of NHP-SIV models has indeed enriched our knowledge in the fields of: i) viral transmission and viral reservoirs, ii) early immune responses, iii) host cell-virus interactions in tissues, iv) AIDS pathogenesis, v) virulence factors, vi) prevention and vii) drug development. The possibility to control many variables during experimental SIV infection, together with the resemblance between SIV and HIV infections, make the NHP model the most appropriate, so far, for HIV/AIDS research. Nonetheless, some limitations in using these models have to be considered. Alternative models for HIV/AIDS research, such as humanized mice and recombinant forms of HIV-SIV viruses (SHIV) for NHP infection, have been developed. The improvement of SHIV viruses that mimic even better the natural history of HIV infection and of humanized mice that develop a greater variety of human immune cell lineages, is ongoing. None of these models is perfect, but they allow contributing to the progress in managing or preventing HIV infection.

© 2016 Elsevier B.V. All rights reserved.

1. Introduction

HIV/AIDS is still a major public health issue. According to the World Health Organization, HIV infection figures, even today, among the ten major leading causes of death and is the second cause of mortality in adolescents. Since the first report in 1981 and the identification of HIV as a causative agent in 1983 (Barré-Sinoussi et al., 2004), AIDS has claimed for >35 million of lives and only in 2015, 2.1 million of people became newly infected with HIV.

HIV infection is characterized by a slow and progressive loss of $CD4^+$ T cells that, in absence of treatment, generally leads to an immunosuppressive condition. Nowadays, it is admitted that chronic immune activation is the driving force of such immunodeficiency (Paiardini and Müller-Trutwin, 2013). Under successful combined antiretroviral therapy (cART), the virus is controlled up to undetectable level in blood, but a residual chronic inflammation persists and is associated with the morbidity and mortality observed in the antiretroviral-treated patients.

Despite of the great advances obtained in HIV/AIDS knowledge, there are still key problems to solve, in particular the lack of a vaccine and a cure and the absence of treatments for resolution of HIV-induced inflammation. Animal models for HIV have already contributed to answer major questions, but they also have several limitations. The "perfect animal model" for HIV-1 research is indeed still unavailable. However, infection of non-human primates (NHP), such as macaques, with Simian Immunodeficiency Virus (SIV) leads to a disease that is similar to AIDS induced by HIV in humans. So far, this is the most suitable model to study the mechanisms of transmission and physiopathology of the disease. Indeed, SIV infection in macaques fulfills numerous conditions generally requested to constitute a reliable animal model for a human disease:

1. The virus causing disease in the model should cause the same disease in humans;
2. The course of the disease in the animals should resemble that in humans;
3. The range of cells, tissues and organs involved should be similar in humans and in the animal;

* Corresponding author.
E-mail addresses: thalia.garcia-tellez@pasteur.fr (T. Garcia-Tellez), nicolas.huot@pasteur.fr (N. Huot), mickael.ploquin@pasteur.fr (M.J. Ploquin), philippe.rascle@pasteur.fr (P. Rascle), beatrice.jacquelin@pasteur.fr (B. Jacquelin), michaela.muller-trutwin@pasteur.fr (M. Müller-Trutwin).

http://dx.doi.org/10.1016/j.meegid.2016.07.012
1567-1348/© 2016 Elsevier B.V. All rights reserved.

Please cite this article as: Garcia-Tellez, T., et al., Non-human primates in HIV research: Achievements, limits and alternatives, Infection, Genetics and Evolution (2016), http://dx.doi.org/10.1016/j.meegid.2016.07.012

4. Immune responses to infection in the animal model should be similar to those in humans.

These conditions are not fulfilled by other animal models, such as FIV in cats or HIV-1 in humanized mice (see below). Here, we review characteristics of the SIV infection in NHP that have favored its use as a model for HIV/AIDS research and summarize some of the major past and recent advances in the field obtained thanks to the NHP models (Table 1). We will briefly evoke advances in other models, such as humanized mice, in research toward a HIV vaccine and cure. Finally, we will explain the limits of NHP models and discuss how these models could nonetheless help in the global effort to achieve the development of efficient preventive and cure approaches.

2. SIV models and their contributions to research on HIV prevention and treatment

Human AIDS is caused by two types of HIV (HIV-1 and HIV-2). These viruses are subdivided into groups (M, N, O, and P for HIV-1; A to I for HIV-2), subtypes, circulating recombinant forms (CRF) and unique recombinant forms (URF), HIV-1 group M subtype C being the most prevalent in the world (Peeters et al., 2013; Hemelaar, 2012).

Since the first cases of HIV infection, there has been interest in identifying the origin of the epidemic. The first insight came to light when a close relationship between HIV-2 and a virus that infects macaques was found (Chakrabarti et al., 1987). This virus was called SIVmac in analogy to HIV and according to the species from which it was isolated. Thereafter, another phylogenetic association was discovered between HIV-2 and SIVsmm, a virus that infects sooty mangabeys in West Africa (Hirsch et al., 1989). Subsequent studies confirmed that SIVmac and HIV-2 derived both from SIVsmm (Hirsch et al., 1989; Gao et al., 1999; Bailes et al., 2003; Chen et al., 1996).

The origin of HIV-1 was traced on non-human primates, as well. The human virus is closely related to SIVcpz, which infects West-Central Africa chimpanzees (*Pan troglodytes troglodytes*) (Gao et al., 1999; Bailes et al., 2003; Peeters et al., 1989; Simon et al., 1998; Corbet et al., 2000) and from which HIV-1 M and N derived (Simon et al., 1998; Corbet et al., 2000; Müller-Trutwin et al., 2000; Nerrienet et al., 2005; Keele et al., 2006; Peeters and Delaporte, 2012). On the other hand, the analysis of fecal samples from Cameroon gorillas revealed the existence of SIVgor (Van Heuverswyn et al., 2006; Plantier et al., 2009). The latter virus is related to HIV-1 O and P. Phylogenetic analyses indicate that chimpanzees constitute most likely the original reservoir and source of SIVgor as well as of HIV-1 O and P (Plantier et al., 2009; Takehisa et al., 2009; D'arc et al., 2015) (Fig. 1).

Table 1
Examples of major contributions of NHP models to HIV/AIDS research.

- Discovery of initial founder populations of infected cells (foci) (Haase (2010))
- $CD8^+$ T cell response: "too little, too late" to clear infection (Reynolds et al. (2005))
- Short window of opportunity to prevent infection (Sodora et al. (1998))
- $CD8^+$ T cells: impact on viral set-point (Nomura and Matano (2012); Letvin et al. (1999))
- Proof of concept that Nab can protect against infection (Barouch et al. (2015))
- Nef viral protein: necessary for high viral load *in vivo* (Kestler et al. (1991))
- Resting memory T cells: main target of the virus in lymphoid tissues (Mattapallil et al. (2005); Li et al. (2005))
- Rapid and dramatic depletion of $CD4^+$ T cells in gut (Veazey et al. (1998); Li et al. (2005))
- Trafficking of Treg, PDC, NK cells to the gut (Reeves et al. (2010a); Reeves et al. (2010b); Reeves et al. (2012))
- Loss of TCM associated with disease progression (Mattapallil et al. (2005); Picker et al. (2004))
- Events in acute infection determine disease progression (Saez-Cirion et al. (2014))
- TRIM5a alleles restrict viral replication *in vivo* (Reynolds et al. (2005))
- Analyses of the virome and microbiome in tissues (Barbian et al. (2015); Handley et al. (2016); Monaco et al. (2016); Palmer et al. (2016))
- *In vivo* imaging of SIV (Santangelo et al. (2015))

More than 40 NHP species have been found to carry SIV in the wild. Noteworthy, natural carriers of SIV are all African species. In contrast, Asian monkeys, such as macaques, are only infected in captivity.

The first report of AIDS in a NHP was provided by Letvin and cols in 1983 (Letvin et al., 1983), soon after the discovery of HIV. This syndrome was detected in captive macaques (*Macaca cyclopis* and *Macaca mulatta*) that died of lymphomas or opportunistic infections like *Pneumocystis carinii*. The revision of autopsy records and laboratory studies revealed that these animals suffered of anemia, neutropenia and monocytosis before decease. A lymphocyte ratio (CD4/CD8) reversion and a loss of T cell numbers and functionality were observed as well before death. The causes of death included necrotizing gingivitis, *Pneumocystis carinii* and cytomegalovirus infections, as well as three atypical cases of lymphoma.

Macaques infected by SIVmac became the most important animal model for HIV/AIDS research. The disease progression profile during SIV infections in macaques depends both on the macaque species and the SIVmac strain used (Fig. 2). The most frequently used animals are Indian and Chinese rhesus macaques as well as cynomolgus macaques infected by the SIVmac239 molecular clone or the SIVmac251 viral isolate. The most rapid disease progression is generally observed in Indian rhesus macaques infected with SIVmac239. This macaque model revealed the massive $CD4^+$ T cell depletion in the gut in the very early phase of infection (Veazey et al., 1998; Kewenig et al., 1999; Mattapallil et al., 2005). While it was already known that HIV replicates in the gut (Schneider et al., 1995), the macaque model helped to underscore the rapidity of the events in this tissue (within the first 24 h upon infection) and to what extent the degree of T lymphocyte loss in the gut is associated with disease progression. It was subsequently shown that resting memory $CD4^+$ T cells were the most frequently infected cells within the gastrointestinal (GI) tract (Brenchley et al., 2004; Li et al., 2005). These cells can live for decades and are now considered as a major reservoir for HIV-1 (Schmitz et al., 2012; Chomont et al., 2009).

Experimental SIV infections can be performed through the intravenous route. Several additional experimental protocols have been developed for infection through the rectal, vaginal or oral route in order to mimic the predominant routes of transmission encountered in humans, *i.e.* sexual or mother-to-child transmission by breast feeding (D'arc et al., 2015; Veazey et al., 1998; Kewenig et al., 1999; Mattapallil et al., 2005). To better resemble even more what is happening during infection and dissemination of the virus throughout the body in humans, protocols for repetitive low-dose challenges have been set up as well. These models contribute to evaluate vaccine candidates and already lead to the demonstration of two constructions that can confer strong control, *i.e.* SIVΔnef and rhesus cytomegalovirus (CMV)-based vectors. However, the degree of protection correlates inversely with the level of attenuation, the least-attenuated strain giving the greatest protection (Johnson and Desrosiers, 1998; Koff et al., 2006). Vaccine candidates based on CMV-vectors generate very strong and persistent T effector memory responses in half of the animals leading to a controlled infection and an elimination of viral reservoirs (Hansen et al., 2013). While it is at the moment unclear if such constructions can be used as a vaccine, the studies of these vaccine candidates have already and will continue to provide important clues about the correlates of protection against HIV (Daniel et al., 1992; Billingsley et al., 2015).

The macaque/SIVmac models also allow to examine the very first immunological events after viral exposure in relation to the transmission route or to study the selection mechanisms of transmitted/founder virus resulting from the genetic bottleneck that occurs during transmission (Table 1) (Sodora et al., 1998; Milush et al., 2004; Keele et al., 2009a; Tsai et al., 2014; Tully et al., 2016). It was shown for instance in the macaque model, that while in most cases the transmission is based on the selection and persistence of only one viral variant from the donor, the number of transmitted founder variants increases with the viral dose in the challenge (Fennessey and Keele, 2013; Ma et al., 2011; Keele and Estes, 2011; Gambhira et al., 2014).

Please cite this article as: Garcia-Tellez, T., et al., Non-human primates in HIV research: Achievements, limits and alternatives, Infection, Genetics and Evolution (2016), http://dx.doi.org/10.1016/j.meegid.2016.07.012

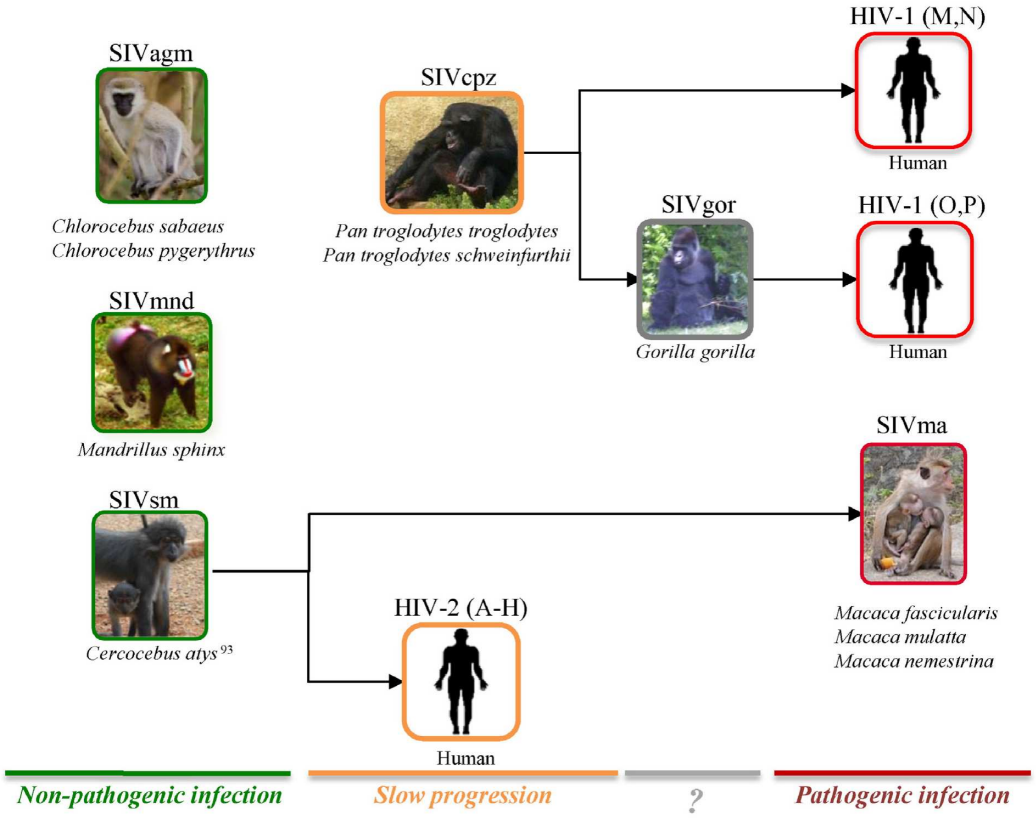


Fig. 1. Non-human primate models for the study of HIV infection. Non-human primates can be divided into pathogenic (macaques) and non-pathogenic (sooty mangabeys, mandrills and African Green Monkeys) models for HIV research. The figure depicts the relationship between the HIV and SIV viruses and the type of infection caused by them.

In the search for a vaccine against HIV-1, there is a need for an animal model that can be infected with the human virus. Such a model would help, for instance, in the study of neutralizing antibodies (Nabs) against HIV-1. Macaques are susceptible to HIV-2 but not to HIV-1 infection. Chimpanzees constitute the original reservoir of HIV-1 and therefore are naturally susceptible to HIV-1 viruses. However, HIV-1 had adapted to the new human host, most likely by circumventing restriction factors, among other reasons. Therefore, the results obtained from HIV-1 infection in these primates have been non conclusive. Some groups have reported the development of AIDS in this model (Novembre et al., 1997; Davis et al., 1998; O'Neil et al., 2000; Ferrari et al., 1993), characterized by marked depletion of $CD4^+$ T cells, sustained viremia, severe CD4:CD8 inversion and increased T cell apoptosis. Others have observed animals that do not or only slowly progress to AIDS, maintaining their normal $CD4^+$ T cell counts and displaying undetectable viremia (Juompan et al., 2008). The scientific limitations of the model, together with the new guidelines for the use of chimpanzees in biomedical research, leaded to the interruption of its use for HIV (Anon, 2011).

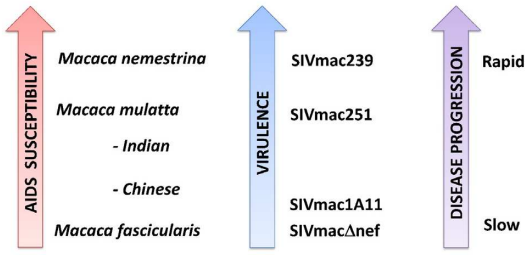


Fig. 2. Host and viral determinants of disease progression rate. The progression of the disease depends on the intrinsic susceptibility of each species to develop AIDS and on the virulence of the SIV strain used.

Infection of macaques with HIV-1 has also revealed to be challenging. Indeed, HIV-1 faces in macaques the existence of cellular proteins that restrict the replication of the human virus, such as TRIM5α (Stremlau et al., 2004), APOBEC3G and Tetherin (Misra et al., 2013). This makes it difficult to infect macaques or their $CD4^+$ T cells by HIV-1 *in vivo* and *in vitro*, but allowed to contribute to the discovery and extensive characterization of restriction factors (Table 1). Several TRIM5α alleles have been identified and characterized in monkeys. It has been clearly shown that the viral replication differs depending on the TRIM5α allele present in the simian host (Wu et al., 2015; Lim et al., 2010). The only macaque susceptible to be infected by HIV-1 is the pig-tailed macaque (*Macaca nemestrina*). This occurs as a result of a 2-nucleotide deletion in the 5′-end of TRIM5α transcript, which impairs the action of this RF (Peeters and Delaporte, 2012). However, the viral replication is not efficient and there is no disease progression.

A recombinant virus has been engineered, which consists of a HIV-1 backbone where target sites of restriction factors were replaced by the corresponding SIVmac sequences (Hatziioannou et al., 2014). While this virus induces persistent viremia, disease progression is only observed after *in vivo* depletion of CD8 + T cells in acute infection. This modified model allows the study of some virus-host interactions, but needs further development for its application in HIV research.

Please cite this article as: Garcia-Tellez, T., et al., Non-human primates in HIV research: Achievements, limits and alternatives, Infection, Genetics and Evolution (2016), http://dx.doi.org/10.1016/j.meegid.2016.07.012

Another attempt to circumvent the lack of a macaque model for HIV-1 consists in the construction of other types of recombinant viruses of HIV and SIV, called SHIV (Thippeshappa et al., 2012). These have been used since many years to overcome the lack of an animal model by constructing for instance SIVmac viruses coding for HIV-1 Env instead of SIVmac Env. Such macaque/SHIV models were essential for providing the proof of concept that antibodies alone can protect against infection by taking advantage of the possibility to passively transfer the antibodies and challenge the animals experimentally (Mascola et al., 2000) (Table 1). However, these types of approaches are challenged by the large diversity of the envelope glycoprotein, their glycan shields and by the high plasma titers of NAbs needed for protection. Lately, the improvement of broadly neutralizing monoclonal antibodies (bNAbs) allowed to enhance their neutralization potency and to protect, for instance, SHIV-challenged macaques with much lower NAbs concentrations (Rudicell et al., 2014). This new generation of very broad and potent Abs might have a potential not only as pre-exposure blocking agents but also in view of a cure or remission of HIV. The treatment with those Abs resulted indeed in control of viremia and reduced proviral DNA in blood and tissues (Barouch et al., 2013; Shingai et al., 2013).

Very early on, SIVs that encode for HIV-1 Pol have also been engineered. Indeed, SIVmac viruses are not susceptible to some drugs used against HIV-1, such as non-nucleoside reverse transcriptase inhibitors (NNRTIs), fusion inhibitors and some integrase inhibitors. The engineering of SHIVs expressing the HIV-1 Pol protein makes them susceptible to such antiretrovirals. They contributed to the development of therapeutic approaches. As an example, NHP infection models have demonstrated the effectiveness of subcutaneous, gel, and oral formulations of tenofovir (PMPA) in preventing transmission of SIV or SHIV viruses, even when applied several hours after viral challenge (Gengiah et al., 2012). Such *in vivo* activity of tenofovir made it a promising agent for prevention of HIV-1 infection.

Most SHIV viruses, however, do not reproduce all characteristics of HIV-1 infection in humans. The first generation of SHIV was composed of X4 viruses and therefore displayed a distinct cellular tropism than primary HIV in early infection. CD8 + T cell depletion in monkeys is still often needed for disease progression to AIDS. Nevertheless, SHIV models have allowed overcoming specific hurdles and cannot be missed so far for pre-clinical trials of vaccine and drug candidates (Hessell and Haigwood, 2015; Veazey, 2013; Wilson and Watkins, 2009; Dezzutti, 2015; Hatziioannou and Evans, 2012).

As we have recapitulated, SIV infection in NHP constitutes a good model, in many aspects, for HIV research. It is, however, not perfect. One cannot ignore that SIV and HIV are close but different viruses, which can lead to differences in certain aspects of their interactions with the host or susceptibility to drugs and vaccine candidates.

3. Models for spontaneous SIV control

The majority of the individuals infected by HIV progresses to AIDS within 7 to 10 years in the absence of cART. There exist, however, a few individuals (<0.2%) known as HIV-controllers who spontaneously and efficiently control viral replication. The deep characterization of these individuals and the factors that are involved in the control of the infection have been the focus of many researches (Policicchio et al., 2016; Passaes and Sáez-Cirión, 2014). Multiple causes are suspected, and are not mutually exclusive. In particular the genetic background of the individuals enriched in MHC alleles such as B27 and/or B57, strong CD8 + T cell responses, reduced susceptibility of $CD4^+$ T cells to HIV infection and early control of viral replication are likely involved (Saez-Cirion et al., 2014; Bruel et al., 2015). All distinct profiles of disease progression in humans are recapitulated by macaques after SIVmac infection, including the occurrence of a spontaneously controlled infection in a minority of macaques that can also be related to a specific MHC background (Anon, 2011; Kirchhoff, 2009). The disease progression rate depends both on the virus and host species (Fig. 2), as well as on individual host features, as in humans. Studies in the macaque model allow deciphering, one by one, the role of each viral gene *in vivo* by infecting macaques with genetically engineered SIVmac clones containing defective or lacked accessory genes. This is how it was discovered that Nef is essential for high viral replication *in vivo*, while *in vitro*, Nef was dispensable (Kestler et al., 1991). Mutations in *Nef* indeed are associated with attenuated HIV-1 infection in humans.

The role of MHC alleles (Mamu alleles in rhesus macaque) has been extensively studied in the spontaneous control in macaques. Some *Mamu* alleles (e.g *Mamu-A*01* (Mothé et al., 2003)) are associated with a better containment of viral replication while others are linked to a faster disease progression (Nomura and Matano, 2012). Furthermore, the combination of *Mamu* alleles and KIR receptors in NK cells increases the complexity of the response (Walter and Ansari, 2015; Albrecht et al., 2014), as showed for example in an epistatic analysis of KIR3DL05, KIR3DS05, and KIR3DL10 in association with *Mamu*-B*012 that contribute to elevate the viral load in rhesus macaques (Albrecht et al., 2014).

The NHP models allow investigators to address not only the very early events that follow SIV exposure, but also to study these events in tissues, such as lymphoid tissues, genital tract, lung, liver, intestine, and central nervous system (CNS) (Santangelo et al., 2015). Latent reservoirs of HIV are located throughout the body and persist during infection even in presence highly efficient cART. NHP models allow to study the establishment of these reservoirs in tissues, which occurs in the first hours and days following infection (Whitney et al., 2014; Sellier et al., 2010; Kader et al., 2008). Advances in our understanding of the role of the different immune cell populations as viral target cells, have been provided by experiments in which these populations are depleted in NHP models. Depletion of $CD4^+$ T-cells in macaques prior to SIV infection was associated with higher viral load, massive activation and infection of macrophages and microglia that become the predominant infected cells (Micci et al., 2014). The SIVmac-infected macaque model was used as a proof-of-concept to demonstrate that CD8 + cells participate in the control of infection, using *in vivo* CD8 + T cell depletion (Table 1) (Schmitz et al., 1999; Matano et al., 1998; Jin et al., 1999). Additionally, this model allowed to demonstrate the presence of a CTL response as soon as 7 days p.i., and helped to understand how quickly HIV/SIV evades this cellular response through the acquisition of mutations very early on in acute infection (O'Connor et al., 2002). The macaque model also provided the concept that $CD8^+$ T cell responses arrive "too little" and "too late" into vaginal mucosa to control viral dissemination and that the "window of opportunity" to prevent infection is very short (Reynolds et al., 2005; Haase, 2011). Furthermore, depletion of NK cells resulted in modest changes in plasma viral load but in a significant increase in the gut (Choi et al., 2008; Takahashi et al., 2013). However, no tools exist so far to specifically deplete NK cells and $CD8^+$ T cells. Noteworthy, cell depletion induce homeostatic proliferations of other cells, this side effect in addition to others need to be taken into consideration in the interpretation of the results.

4. Models for disease control

About 40 distinct African NHP are natural hosts of SIV. Only in a few species though, studies could be conducted to evaluate the natural history of SIV infection and its outcome in these animals. Studies based on non-invasive techniques have shown that SIVcpz infection in wild chimpanzees reduces their lifespan, when compared to non-infected animals in the same habitat (Peeters and Delaporte, 2012; Keele et al., 2009b). One case of AIDS related symptoms was also reported in a naturally infected Central African chimpanzee, which presented lymphopenia, weight loss and opportunistic infections 7 years after SIV positive screening. Efforts should be made to better characterize the pathogenicity of SIV in natural hosts and to find out whether SIV infection also plays a role in ape population decline (Etienne et al., 2011). Other studies in semi-free mandrills infected by SIVmnd in their natural

Please cite this article as: Garcia-Tellez, T., et al., Non-human primates in HIV research: Achievements, limits and alternatives, Infection, Genetics and Evolution (2016), http://dx.doi.org/10.1016/j.meegid.2016.07.012

habitat revealed, in contrast, a strong protection against AIDS. Similarly, other African NHP, such as African Green Monkeys (AGM) and Sooty mangabeys (SM) revealed to be resistant to AIDS (Sodora et al., 2009). The latter serve today as model to study the control of the disease, in particular SM and AGM, and are called the "natural hosts" models. Cross-species transmissions demonstrated that the same SIV strain can cause opposite outcomes of infection, depending of the host species (Fig. 3). On the other hand, not all SIV strains induce AIDS in macaques, some SIV viruses being easily controlled in the animals, while others not. This demonstrates that the outcome of the infection depends on a combination of both viral and host determinants.

Natural hosts of SIV have been used to better understand the mechanisms responsible of disease progression in HIV infection (Sodora et al., 2009; Chahroudi et al., 2012). The most striking difference between non-pathogenic SIV and pathogenic HIV-1/SIVmac infections is the lack of chronic immune activation. Paradoxically, natural hosts of SIV exhibit high titers of virus in plasma, but they do not display chronic activation of the adaptive and innate immune system (Kornfeld et al., 2005; Chakrabarti et al., 2000). This feature resembles the 'viremic non-progressors', very rare human individuals who display elevated viremia but maintain CD4 T + cell counts and avoid disease progression for years (Rotger et al., 2011). Extensive studies are ongoing in order to elucidate the mechanisms involved in the capacity for controlling inflammation and disease progression. Some non-mutually exclusive hypotheses are listed below (Kirchhoff, 2009):

- Intact mucosa barrier, thereby, lack of microbial translocation and lack of microbial products that would drive the continuous stimulation of the immune system (Estes et al., 2010). Experimentally mimicking microbial translocation in these nonpathogenic models provided evidence of the link between this phenomenon and immune activation. LPS administration in AGMs leaded indeed to elevated T cell activation levels (Pandrea et al., 2008a). However, it is unlikely that this is the only event involved in the deleterious chronic inflammation as it has been shown that infection of macaques with a mutated virus still leads to AIDS without acute loss of $CD4^+$ T cells and microbial translocation (Breed et al., 2013).
- Ancient infection that led to an adaptation of the host's immune response responsible for differences in the intensity or nature of SIV sensing. The capacity to produce IFN-I is normal in natural hosts, but other sensing pathways have only poorly been explored in natural hosts so far (Jacquelin et al., 2009; Jochems et al., 2015).
- The ability of the Nef protein to block the activation of infected T cells by downregulation of CD3 (Schindler et al., 2006).

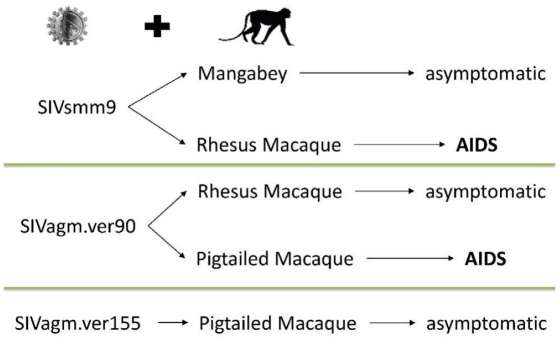


Fig. 3. Cross-species transmissions of SIV and fates of infection. The presence or absence of progression depends on both, viral and host factors; *i.e.* the infection with a given SIV strain will not cause disease in some primates, whereas in others will lead to the development of AIDS. Host and viral determinants interact which each other and a combination of both determines the outcome of infection.

- Natural hosts show low levels of CCR5 surface expression on $CD4^+$ T cells and apparent protection of central memory T cells from SIV infection (Paiardini et al., 2011; Veazey et al., 2003; Pandrea et al., 2008b)
- Controlled viral replication in secondary lymphoid organs (Ploquin et al., 2016). One hallmark of SIV infection in natural hosts is the low viral burden in lymph nodes in the chronic phase of infection in contrast to other tissues (Gueye et al., 2004; Martinot et al., 2013; Brenchley et al., 2012; Diop et al., 2000; Goldstein et al., 2000). This constitutes one of the major differences in lymph nodes of AGMs and SMs. Furthermore, lymph nodes in these natural hosts are characterized by: (i) lack of lymphadenopathy and thus no extensive sequestration of lymphocytes in AGM LNs, (ii) no or less follicular dendritic cell deposition of virus in AGM and SM compared to SIVmac infections (Brenchley et al., 2012; Goldstein et al., 2000; Beer et al., 1996); (iii) more rapid control of interferon-stimulated genes (ISGs) in LNs as compared to blood and gut (Jacquelin et al., 2009; Martinot et al., 2013; Brenchley et al., 2012; Diop et al., 2000). The control of viral replication and immune activation in lymph nodes prevents fibrosis and maintains normal immune function (Gueye et al., 2004; Ploquin et al., 2012; Ploquin et al., 2004) in this organ which is essential for the induction and shaping of adaptive immune responses. Maintenance of normal immune functions might lead to a better control of other infections in the host (*i.e.* CMV, virome) that otherwise could also contribute to immune activation.
- Depletion of $CD4^+$ T cells through apoptosis leading to homeostatic proliferation of T cells (Cumont et al., 2008; Hurtrel et al., 2005)

5. Small animal models for HIV research

Besides NHPs, other animal models have been used for the study of HIV-1. In the past, feline immunodeficiency virus (FIV) infection in cats served as a model of naturally occurring immunodeficiency. During FIV infection, $CD4^+$ T cells are depleted and a chronic inflammatory state is established, such as it happens during HIV/SIV infection (Elder et al., 2010). The FIV model has also been useful in the past to test some antiretroviral drugs (Mohammadi and Bienzle, 2012). Nowadays, however, this model is generally not used any more for HIV research since some important features of the infection are clearly different. For example, FIV is able to infect $CD8^+$ T cells and B cells in addition to $CD4^+$ T cells and macrophages, due to its affinity for CD134 as a receptor. Thus, FIV establishes different viral reservoirs in comparison with the human or primate infection by HIV/SIV.

Other attempts for studying HIV-1 infection in small animals such as rats, mice or rabbits were performed without success. Indeed, rodent cells are refractory to HIV infection. This could not be circumvented by the expression of the human viral receptor on the cell surface. When the murine cells were engineered for allowing HIV to enter, the virus encountered additional problems to effectively replicate, most likely due to restriction factors, among others.

The development of humanized mice arose the possibility to infect them with HIV-1 and answer some specific research questions. Examples of humanized mice used in HIV research comprise, *inter alia*, SCID-hu, SCID-hu-PBL, NOD-SCID, Hu-HSC and BLT mice (Hatziioannou and Evans, 2012; Policicchio et al., 2016; Denton and Garcia, 2011; Garcia, 2016; Legrand et al., 2009). Humanized mice have been used to study punctual aspects of HIV-1 infection, such as T cell exhaustion (Seung et al., 2013), mucosal immunity (Denton and Garcia, 2011; Kovarova et al., 2016; Olesen et al., 2011), viral latency, antiretroviral drug efficacies and infection of macrophages (Kovarova et al., 2016; Sundell et al., 2012; Honeycutt et al., 2016), among others (Table 2). Humanized mice have already contributed to the knowledge of specific aspects of HIV infection. However, their development requires complex surgical engineering. Moreover, they need to be generated *de novo* for each experiment, being tailored according to the immunological requirements of the research, which increases the cost of their establishment and maintenance.

Please cite this article as: Garcia-Tellez, T., et al., Non-human primates in HIV research: Achievements, limits and alternatives, Infection, Genetics and Evolution (2016), http://dx.doi.org/10.1016/j.meegid.2016.07.012

Table 2
Alternative models for HIV research

Model	Characteristics	Examples of utility	Drawbacks
Alternative viruses			
SHIV	Chimeric viruses that express HIV proteins in a SIV backbone to replicate in NHP.	Antiretroviral development Vaccination strategies Study of viral restriction	Variability in the infectivity Lack of AIDS induction Unusual phisiopathology
Alternative hosts			
SCID-hu Namikawa et al. (1988)	Human hematopoietic progenitor stem cells that mature mainly into T cells.	Study of $CD4^+$ T cell loss Test of antiretroviral drugs Sundell et al. (2012)	Absence of innate immunity. Not suitable to study viral transmission.
Hu-HSC	Irradiated non-obese diabetic (NOD) mice injected with human hematopoietic stem cells. Produces human T and B cells.	Neuropathogenesis Viral latency Choudhary et al. (2012)	Absence of innate immune response Not suitable to study primary infection
BLT (Bone-liver-thymus) Wege et al. (2008)	Human T and B lymphocytes, monocytes, macrophages, NK and dendritic cells. Develops mucosal immunity, including GALT.	Antiretroviral treatment tests Kovarova et al. (2016)) Studies of viral transmission and replication in mucosa Kovarova et al. (2016); Olesen et al. (2011); Denton et al. (2008)	Defect in class-switched antibody production. Predominance of pre-mature B cells Karpel et al. (2015)

In addition, there exist anatomical differences, for example, at the level of lymphoid organs that are not fully developed and a lack of several human immune cell lineages, in particular related to innate immune responses. Of note, the field is evolving fast and much effort is put on the improvement of humanized mice models (Garcia, 2016).

6. Limitations, perspectives and conclusions

Despite the numerous advantages that NHP represent, it is important not to forget that choosing the right model for each research question is an essential point. Macaque models of transmission were established very early on as models for HIV (Miller et al., 1989). Animal models offer the possibility to control the viral strain, viral dose and infection route. However, while it is well admitted that rectal SIV infection mimics what is happening in humans, vaginal infections are more difficult to modelize as menstrual cycle variations impact the thickness of the epithelium and the efficacy of infection (Evans and Silvestri, 2013; Veazey et al., 2012). Progesterone is used to control the cycle but to what extent this impacts the relevance of the studies is still under debate.

Also, humans are infected through biological fluids that do not only contain free virus, but also infected cells and other components, such as inflammatory cytokines. Studies are ongoing to evaluate if there are differences depending on the composition of the inoculum (Bernard-Stoecklin et al., 2014; Bernard-Stoecklin et al., 2013).

Natural transmission of SIV in African NHPs is predominantly horizontal and thought to occur through sexual contacts or bite wounds. In contrast to HIV infections, vertical transmission of SIV is extremely rare. The expression of the co-receptor CCR5 on $CD4^+$ T cells in AGMs is low in infants and dramatically increases in adults (Pandrea et al., 2012). Susceptibility to infection through the vaginal and rectal route was linked to the availability of memory $CCR5^+$ $CD4^+$ T cells in the targeted mucosa and it has been suggested that the low rate of vertical SIV infection is associated with the few target cell availability in newborns and infants (Chahroudi et al., 2011; Ma et al., 2014). Thus, while HIV and SIV infections are distinct in the frequency of mother to child transmission, NHP models can be used to better understand the underlying mechanism of this difference (Chahroudi et al., 2011; Marlin et al., 2011; Tripathi et al., 2009).

Once infection takes place at mucosal sites, the virus crosses the epithelial barrier, establishes a first pool of infected cells (foci) and disseminates thereafter in draining lymph nodes (LNs) (Haase, 2010). It is still under debate which cells are the first targets of the virus. It has been suggested that $CD4^+$ $CCR5^+$ T cells are the primary targets of infection in mucosa (Mattapallil et al., 2005; Brenchley et al., 2004; Li et al., 2005; Veazey et al., 2000; Li et al., 2009). Dendritic cells (DCs) might also play a role in the process of viral dissemination. The use of macaque models permitted to analyze their role in virus dissemination during the first hours and days *in vivo* (Reimann et al., 1994). Nonetheless, the events leading to the establishment of infection are still not fully elucidated.

Repeated low-dose viral challenges might provide a benefit for the evaluation of vaccine candidates or the understanding of the establishment of viral reservoirs. The low number of animals for ethical and economic reasons renders interpretation of the results however sometimes difficult. Taken this into account, technical improvements are being made. For instance, novel techniques, such as *in vivo* imaging, are highly promising (Santangelo et al., 2015). It is important to mention that not only the number of specimens allowed for each research is often limited, but the tools are limited as well. Thus, there are still markers for which no monoclonal antibody exists in monkeys. This is the case for example for most of the KIRs.

NHP are the closest animal model for HIV/AIDS research, but an ideal model for HIV-1 is still not available. SIV and HIV are close but distinct

Table 3
NHP use toward a cure for HIV: advantages and applications.

Aim	Advantage of NHP use	Examples of strategies studied
Pharmacological viral suppression and diminution of viral reservoirs Whitney et al. (2014); Shytaj et al. (2012); Del Prete et al. (2016)	Control of viral strain Control of viral dose and nature of inoculum Control of route of administration and timing Control of duration, type and combination of antiretrovirals	Diffusion of antiretroviral drugs in tissues Very early treatment initiation Treatment with IFN-α Treatment with bNabs Treatment with Interleukins (IL-7, IL-15, IL-21)
Restauration and enhancing of immune response O'Connor et al. (2002); Reynolds et al. (2005); Vassena et al. (2012); Xu et al. (2014)	Extensive characterization of viral reservoirs in tissues Analyses of immune responses in tissues including immediately after infection	Treatment with TLR7 agonists Treatment with anti PD-1
Purge latent HIV-reservoir Ling et al. (2014); Del Prete et al. (2014); Trautmann (2016); Datta et al. (2016); Wen et al. (2016)	Intervention in the early stage of primary infection Administration of potentially risky substances	Administration of inhibitors of chromatin-remodeling molecules (SAHA-inhibitors) Gene editing Nanoparticles

Please cite this article as: Garcia-Tellez, T., et al., Non-human primates in HIV research: Achievements, limits and alternatives, Infection, Genetics and Evolution (2016), http://dx.doi.org/10.1016/j.meegid.2016.07.012

viruses, which cause differences in certain aspects of their interactions with the host, vaccines and drugs. To overcome these potential discrepancies between SIV and HIV, recombinant viruses, including SHIVs, have been generated. SHIVs have been and still are particularly useful in the study of humoral responses, vaccine candidates and antiretroviral drugs (Hatziioannou and Evans, 2012). In the future, it would be useful however to dispose of SHIV viruses that mimic even better the natural history of HIV infection. The development of new generations of SHIV strains is already ongoing.

In conclusion, non-human primates infected by SIV represent a model with numerous advantages for the study of HIV infection. Its close resemblance to HIV infection in humans probably makes it the best or at least the most deeply characterized animal model for a human disease. NHP-SIV models have allowed the study of: i) viral transmission, ii) early immune responses, iii) host cell-virus interactions in tissues, iv) prevention and v) drug development (Table 3).

Despite of all the caveats noted and the potential difficulty in translating the findings from primates to humans, these models can be and have been highly instructive in establishing certain basic principles that would have been difficult or impossible to determine by experimentation in humans for safety reasons.

Of note, the suitability of each model depends on the study's specific question, the available tools and appropriate interpretation of the results. Nonetheless, if used correctly, it constitutes an essential model, in many aspects, for HIV research until a vaccine and therapy for HIV cure or HIV remission are discovered.

Funding

TGT is a fellow from the Pasteur Paris University International PhD program and supported by the Institut Carnot Pasteur Maladies Infectieuses. NH and MJP were, respectively, supported by fellowships from the Vaccine Research Institute (VRI) and Sidaction. We thank the French Agency for AIDS Research (ANRS), the Institut Pasteur, Sidaction, the “Investissements d'Avenir” program managed by the ANR grant agreement No. ANR-10-LABX-77 and ANR-11-INBS-0008, as well as L'Oréal in partnership with UNESCO for their support. The funding sources had no influence on our studies or in the writing of this report.

Conflict of interests

The authors declare not to have any conflict of interests.

Acknowledgments

We would like to thank Livia Pedroza-Martins and Pierre Roques for contributing with visual material. Furthermore, we acknowledge the state-of-the-art National Center for Infectious Disease Models and Innovative Therapies (IDMIT).

References

Albrecht, C., et al., 2014. Progression to AIDS in SIV-infected rhesus macaques is associated with distinct KIR and MHC class I polymorphisms and NK cell dysfunction. Front. Immunol. 5, 600.

Anon, 2011. Institute of Medicine (US) and National Research Council (US) Committee on the Use of Chimpanzees in Biomedical and Behavioral Research. Chimpanzees in Biomedical and Behavioral Research: Assessing the Necessity. National Academies Press (US).

Bailes, E., et al., 2003. Hybrid origin of SIV in chimpanzees. Science 300, 1713.

Barbian, H.J., et al., 2015. Destabilization of the gut microbiome marks the end-stage of simian immunodeficiency virus infection in wild chimpanzees. Am. J. Primatol. http://dx.doi.org/10.1002/ajp.22515.

Barouch, D.H., et al., 2013. Therapeutic efficacy of potent neutralizing HIV-1-specific monoclonal antibodies in SHIV-infected rhesus monkeys. Nature 503, 224–228.

Barouch, D.H., et al., 2015. Protective efficacy of adenovirus/protein vaccines against SIV challenges in rhesus monkeys. Science 349, 320–324.

Barré-Sinoussi, F., et al., 2004. Isolation of a T-lymphotropic retrovirus from a patient at risk for acquired immune deficiency syndrome (AIDS). 1983. Rev. Investig. Clín. Organo Hosp. Enferm. Nutr. 56, 126–129.

Beer, B., et al., 1996. Lack of dichotomy between virus load of peripheral blood and lymph nodes during long-term simian immunodeficiency virus infection of African green monkeys. Virology 219, 367–375.

Bernard-Stoecklin, S., et al., 2013. Semen CD4 + T cells and macrophages are productively infected at all stages of SIV infection in macaques. PLoS Pathog. 9.

Bernard-Stoecklin, S., Gommet, C., Cavarelli, M., Grand, R.L., 2014. Nonhuman primate models for cell-associated simian immunodeficiency virus transmission: the need to better understand the complexity of HIV mucosal transmission. J. Infect. Dis. 210, S660–S666.

Billingsley, J.M., et al., 2015. Characterization of $CD8^+$ T cell differentiation following SIVΔnef vaccination by transcription factor expression profiling. PLoS Pathog. 11.

Breed, M.W., et al., 2013. Loss of a tyrosine-dependent trafficking motif in the simian immunodeficiency virus envelope cytoplasmic tail spares mucosal CD4 cells but does not prevent disease progression. J. Virol. 87, 1528–1543.

Brenchley, J.M., et al., 2004. $CD4^+$ T cell depletion during all stages of HIV disease occurs predominantly in the gastrointestinal tract. J. Exp. Med. 200, 749–759.

Brenchley, J.M., et al., 2012. Differential infection patterns of $CD4^+$ T cells and lymphoid tissue viral burden distinguish progressive and nonprogressive lentiviral infections. Blood 120, 4172–4181.

Bruel, T., et al., 2015. Long-term control of Simian Immunodeficiency Virus (SIV) in cynomolgus macaques not associated with efficient SIV-Specific $CD8^+$ T-cell responses. J. Virol. 89, 3542–3556.

Chahroudi, A., et al., 2011. Mother-to-infant transmission of simian immunodeficiency virus is rare in sooty mangabeys and is associated with low viremia▾. J. Virol. 85, 5757–5763.

Chahroudi, A., Bosinger, S.E., Vanderford, T.H., Paiardini, M., Silvestri, G., 2012. Natural SIV hosts: showing AIDS the door. Science 335.

Chakrabarti, L., et al., 1987. Sequence of simian immunodeficiency virus from macaque and its relationship to other human and simian retroviruses. Nature 328, 543–547.

Chakrabarti, L.A., et al., 2000. normal t-cell turnover in sooty mangabeys harboring active simian immunodeficiency virus infection. J. Virol. 74, 1209–1223.

Chen, Z., et al., 1996. Genetic characterization of new West African simian immunodeficiency virus SIVsm: geographic clustering of household-derived SIV strains with human immunodeficiency virus type 2 subtypes and genetically diverse viruses from a single feral sooty mangabey troop. J. Virol. 70, 3617–3627.

Choi, E.I., Reimann, K.A., Letvin, N.L., 2008. In vivo natural killer cell depletion during primary simian immunodeficiency virus infection in rhesus monkeys. J. Virol. 82, 6758–6761.

Chomont, N., et al., 2009. HIV reservoir size and persistence are driven by T cell survival and homeostatic proliferation. Nat. Med. 15, 893–900.

Choudhary, S.K., et al., 2012. Latent HIV-1 infection of resting $CD4^+$ T cells in the humanized $Rag2^{-/-}\gamma c^{-/-}$ mouse. J. Virol. 86, 114–120.

Corbet, S., et al., 2000. env sequences of simian immunodeficiency viruses from chimpanzees in cameroon are strongly related to those of human immunodeficiency virus group N from the same geographic area. J. Virol. 74, 529–534.

Cumont, M.-C., et al., 2008. Early divergence in lymphoid tissue apoptosis between pathogenic and nonpathogenic simian immunodeficiency virus infections of nonhuman primates. J. Virol. 82, 1175–1184.

Daniel, M.D., Kirchhoff, F., Czajak, S.C., Sehgal, P.K., Desrosiers, R.C., 1992. Protective effects of a live attenuated SIV vaccine with a deletion in the nef gene. Science 258, 1938–1941.

D'arc, M., et al., 2015. Origin of the HIV-1 group O epidemic in western lowland gorillas. Proc. Natl. Acad. Sci. U. S. A. 112, E1343–E1352.

Datta, P.K., et al., 2016. HIV-1 Latency and Eradication: Past, Present and Future. Curr. HIV Res. 14, 1–11.

Davis, I.C., Girard, M., Fultz, P.N., 1998. Loss of $CD4^+$ T cells in human immunodeficiency virus type 1-infected chimpanzees is associated with increased lymphocyte apoptosis. J. Virol. 72, 4623–4632.

Del Prete, G.Q., et al., 2014. Effect of suberoylanilide hydroxamic acid (SAHA) administration on the residual virus pool in a model of combination antiretroviral therapy-mediated suppression in SIVmac239-infected Indian rhesus macaques. Antimicrob. Agents Chemother. 58, 6790–6806.

Del Prete, G.Q., et al., 2016. Short communication: comparative evaluation of coformulated injectable combination antiretroviral therapy regimens in simian immunodeficiency virus-infected rhesus macaques. AIDS Res. Hum. Retrovir. 32, 163–168.

Denton, P.W., Garcia, J.V., 2011. Humanized mouse models of HIV infection. AIDS Rev. 13, 135–148.

Denton, P.W., et al., 2008. Antiretroviral pre-exposure prophylaxis prevents vaginal transmission of HIV-1 in humanized BLT mice. PLoS Med. 5.

Dezzutti, C.S., 2015. Animal and human mucosal tissue models to study HIV biomedical interventions: can we predict success? J. Int. AIDS Soc. 18.

Diop, O.M., et al., 2000. High levels of viral replication during primary simian immunodeficiency virus SIVagm infection are rapidly and strongly controlled in African green monkeys. J. Virol. 74, 7538–7547.

Elder, J.H., Lin, Y.-C., Fink, E., Grant, C.K., 2010. Feline immunodeficiency virus (FIV) as a model for study of lentivirus infections: parallels with HIV. Curr. HIV Res. 8, 73–80.

Estes, J.D., et al., 2010. Damaged intestinal epithelial integrity linked to microbial translocation in pathogenic simian immunodeficiency virus infections. PLoS Pathog. 6.

Etienne, L., et al., 2011. Characterization of a new simian immunodeficiency virus strain in a naturally infected *Pan troglodytes troglodytes* chimpanzee with AIDS related symptoms. Retrovirology 8, 4.

Evans, D.T., Silvestri, G., 2013. Non-human primate models in AIDS research. Curr. Opin. HIV AIDS 8, 255–261.

Fennessey, C.M., Keele, B.F., 2013. Using nonhuman primates to model HIV transmission. Curr. Opin. HIV AIDS 8, 280–287.

Ferrari, G., et al., 1993. The impact of HIV-1 infection on phenotypic and functional parameters of cellular immunity in chimpanzees. AIDS Res. Hum. Retrovir. 9, 647–656.

Please cite this article as: Garcia-Tellez, T., et al., Non-human primates in HIV research: Achievements, limits and alternatives, Infection, Genetics and Evolution (2016), http://dx.doi.org/10.1016/j.meegid.2016.07.012

Gambhira, R., et al., 2014. Transmitted/founder simian immunodeficiency virus envelope sequences in vesicular stomatitis and Semliki forest virus vector immunized rhesus macaques. PLoS ONE 9.
Gao, F., et al., 1999. Origin of HIV-1 in the chimpanzee *Pan troglodytes troglodytes*. Nature 397, 436–441.
Garcia, J.V., 2016. In vivo platforms for analysis of HIV persistence and eradication. J. Clin. Invest. 126, 424–431.
Gengiah, T.N., et al., 2012. A drug evaluation of 1% tenofovir gel and tenofovir disoproxil fumarate tablets for the prevention of HIV infection. Expert Opin. Investig. Drugs 21, 695–715.
Goldstein, S., et al., 2000. Wide range of viral load in healthy African green monkeys naturally infected with simian immunodeficiency virus. J. Virol. 74, 11744–11753.
Gueye, A., et al., 2004. Viral load in tissues during the early and chronic phase of non-pathogenic SIVagm infection. J. Med. Primatol. 33, 83–97.
Haase, A.T., 2010. Targeting early infection to prevent HIV-1 mucosal transmission. Nature 464, 217–223.
Haase, A.T., 2011. Early events in sexual transmission of HIV and SIV and opportunities for interventions. Annu. Rev. Med. 62, 127–139.
Handley, S.A., et al., 2016. SIV infection-mediated changes in gastrointestinal bacterial microbiome and virome are associated with immunodeficiency and prevented by vaccination. Cell Host Microbe 19, 323–335.
Hansen, S.G., et al., 2013. Immune clearance of highly pathogenic SIV infection. Nature 502, 100–104.
Hatziioannou, T., Evans, D.T., 2012. Animal models for HIV/AIDS research. Nat. Rev. Microbiol. 10, 852–867.
Hatziioannou, T., et al., 2014. HIV-1-induced AIDS in monkeys. Science 344, 1401–1405.
Hemelaar, J., 2012. The origin and diversity of the HIV-1 pandemic. Trends Mol. Med. 18, 182–192.
Hessell, A.J., Haigwood, N.L., 2015. Animal models in HIV-1 protection and therapy. Curr. Opin. HIV AIDS 10, 170–176.
Hirsch, V.M., Olmsted, R.A., Murphey-Corb, M., Purcell, R.H., Johnson, P.R., 1989. An African primate lentivirus (SIVsm) closely related to HIV-2. Nature 339, 389–392.
Honeycutt, J.B., et al., 2016. Macrophages sustain HIV replication in vivo independently of T cells. J. Clin. Invest. 126, 1353–1366.
Hurtrel, B., et al., 2005. Apoptosis in SIV infection. Cell Death Differ. 12, 979–990.
Jacquelin, B., et al., 2009. Nonpathogenic SIV infection of African green monkeys induces a strong but rapidly controlled type I IFN response. J. Clin. Invest. 119, 3544–3555.
Jin, X., et al., 1999. Dramatic rise in plasma viremia after CD8$^+$ T cell depletion in simian immunodeficiency virus–infected macaques. J. Exp. Med. 189, 991–998.
Jochems, S.P., et al., 2015. Plasmacytoid dendritic cell infection and sensing capacity during pathogenic and nonpathogenic simian immunodeficiency virus infection. J. Virol. 89, 6918–6927.
Johnson, R.P., Desrosiers, R.C., 1998. Protective immunity induced by live attenuated simian immunodeficiency virus. Curr. Opin. Immunol. 10, 436–443.
Juompan, L.Y., et al., 2008. Analysis of the immune responses in chimpanzees infected with HIV type 1 isolates. AIDS Res. Hum. Retrovir. 24, 573–586.
Kader, M., et al., 2008. Antiretroviral therapy prior to acute viral replication preserves CD4 T cells in the periphery but not in rectal mucosa during acute simian immunodeficiency virus infection. J. Virol. 82, 11467–11471.
Karpel, M.E., Boutwell, C.L., Allen, T.M., 2015. BLT humanized mice as a small animal model of HIV infection. Curr. Opin. Virol. 13, 75–80.
Keele, B.F., Estes, J.D., 2011. Barriers to mucosal transmission of immunodeficiency viruses. Blood 118, 839–846.
Keele, B.F., et al., 2006. Chimpanzee reservoirs of pandemic and nonpandemic HIV-1. Science 313, 523–526.
Keele, B.F., et al., 2009a. Low-dose rectal inoculation of rhesus macaques by SIVsmE660 or SIVmac251 recapitulates human mucosal infection by HIV-1. J. Exp. Med. 206, 1117–1134.
Keele, B.F., et al., 2009b. Increased mortality and AIDS-like immunopathology in wild chimpanzees infected with SIVcpz. Nature 460, 515–519.
Kestler, H.W., et al., 1991. Importance of the nef gene for maintenance of high virus loads and for development of AIDS. Cell 65, 651–662.
Kewenig, S., et al., 1999. Rapid mucosal CD4(+) T-cell depletion and enteropathy in simian immunodeficiency virus-infected rhesus macaques. Gastroenterology 116, 1115–1123.
Kirchhoff, F., 2009. Is the high virulence of HIV-1 an unfortunate coincidence of primate lentiviral evolution? Nat. Rev. Microbiol. 7, 467–476.
Koff, W.C., et al., 2006. HIV vaccine design: insights from live attenuated SIV vaccines. Nat. Immunol. 7, 19–23.
Kornfeld, C., et al., 2005. Antiinflammatory profiles during primary SIV infection in African green monkeys are associated with protection against AIDS. J. Clin. Invest. 115, 1082–1091.
Kovarova, M., et al., 2016. A long-acting formulation of the integrase inhibitor raltegravir protects humanized BLT mice from repeated high-dose vaginal HIV challenges. J. Antimicrob. Chemother. http://dx.doi.org/10.1093/jac/dkw042 (dkw042).
Legrand, N., et al., 2009. Humanized mice for modeling human infectious disease: challenges, progress, and outlook. Cell Host Microbe 6, 5–9.
Letvin, N.L., et al., 1983. Acquired immunodeficiency syndrome in a colony of macaque monkeys. Proc. Natl. Acad. Sci. U. S. A. 80, 2718–2722.
Letvin, N.L., et al., 1999. Cytotoxic T lymphocytes specific for the simian immunodeficiency virus. Immunol. Rev. 170, 127–134.
Li, Q., et al., 2005. Peak SIV replication in resting memory CD4$^+$ T cells depletes gut lamina propria CD4$^+$ T cells. Nature 434, 1148–1152.
Li, Q., et al., 2009. Glycerol monolaurate prevents mucosal SIV transmission. Nature 458, 1034–1038.
Lim, S.-Y., et al., 2010. TRIM5α modulates immunodeficiency virus control in rhesus monkeys. PLoS Pathog. 6.
Ling, B., et al., 2014. Effects of treatment with suppressive combination antiretroviral drug therapy and the histone deacetylase inhibitor suberoylanilide hydroxamic acid; (SAHA) on SIV-infected Chinese rhesus macaques. PLoS ONE 9.
Ma, Z.-M., et al., 2011. SIVmac251 is inefficiently transmitted to rhesus macaques by penile inoculation with a single SIVenv variant found in ramp-up phase plasma. AIDS Res. Hum. Retrovir. 27, 1259–1269.
Ma, D., et al., 2014. Factors associated with simian immunodeficiency virus transmission in a natural African nonhuman primate host in the wild. J. Virol. 88, 5687–5705.
Marlin, R., et al., 2011. Decidual soluble factors participate in the control of HIV-1 infection at the maternofetal interface. Retrovirology 8, 58.
Martinot, A.J., et al., 2013. Acute SIV infection in sooty mangabey monkeys is characterized by rapid virus clearance from lymph nodes and absence of productive infection in germinal centers. PLoS ONE 8.
Mascola, J.R., et al., 2000. Protection of macaques against vaginal transmission of a pathogenic HIV-1/SIV chimeric virus by passive infusion of neutralizing antibodies. Nat. Med. 6, 207–210.
Matano, T., et al., 1998. Administration of an anti-CD8 monoclonal antibody interferes with the clearance of chimeric simian/human immunodeficiency virus during primary infections of rhesus macaques. J. Virol. 72, 164–169.
Mattapallil, J.J., et al., 2005. Massive infection and loss of memory CD4$^+$ T cells in multiple tissues during acute SIV infection. Nature 434, 1093–1097.
Micci, L., et al., 2014. CD4 depletion in SIV-infected macaques results in macrophage and microglia infection with rapid turnover of infected cells. PLoS Pathog. 10.
Miller, C.J., et al., 1989. Genital mucosal transmission of simian immunodeficiency virus: animal model for heterosexual transmission of human immunodeficiency virus. J. Virol. 63, 4277–4284.
Milush, J.M., et al., 2004. Rapid dissemination of SIV following oral inoculation. AIDS London, England 18, 2371–2380.
Misra, A., Thippeshappa, R., Kimata, J.T., 2013. Macaques as model hosts for studies of HIV-1 infection. Front. Microbiol. 4, 176.
Mohammadi, H., Bienzle, D., 2012. Pharmacological inhibition of feline immunodeficiency virus (FIV). Viruses 4, 708–724.
Monaco, C.L., et al., 2016. Altered virome and bacterial microbiome in human immunodeficiency virus-associated acquired immunodeficiency syndrome. Cell Host Microbe 19, 311–322.
Mothé, B.R., et al., 2003. Expression of the major histocompatibility complex class I molecule Mamu-A*01 is associated with control of simian immunodeficiency virus SIVmac239 replication. J. Virol. 77, 2736–2740.
Müller-Trutwin, M.C., et al., 2000. SIVcpz from a naturally infected Cameroonian chimpanzee: biological and genetic comparison with HIV-1 N. J. Med. Primatol. 29, 166–172.
Namikawa, R., Kaneshima, H., Lieberman, M., Weissman, I.L., McCune, J.M., 1988. Infection of the SCID-hu mouse by HIV-1. Science.
Nerrienet, E., et al., 2005. Simian immunodeficiency virus infection in wild-caught chimpanzees from Cameroon. J. Virol. 79, 1312–1319.
Nomura, T., Matano, T., 2012. Association of MHC-I genotypes with disease progression in HIV/SIV infections. Front. Microbiol. 3.
Novembre, F.J., et al., 1997. Development of AIDS in a chimpanzee infected with human immunodeficiency virus type 1. J. Virol. 71, 4086–4091.
O'Connor, D.H., et al., 2002. Acute phase cytotoxic T lymphocyte escape is a hallmark of simian immunodeficiency virus infection. Nat. Med. 8, 493–499.
Olesen, R., Wahl, A., Denton, P.W., Garcia, J.V., 2011. Immune reconstitution of the female reproductive tract of humanized BLT mice and their susceptibility to human immunodeficiency virus infection. J. Reprod. Immunol. 88, 195–203.
O'Neil, S.P., et al., 2000. Progressive infection in a subset of HIV-1-positive chimpanzees. J. Infect. Dis. 182, 1051–1062.
Paiardini, M., Müller-Trutwin, M., 2013. HIV-associated chronic immune activation. Immunol. Rev. 254, 78–101.
Paiardini, M., et al., 2011. Low levels of SIV infection in sooty mangabey central-memory CD4$^+$ T-cells is associated with limited CCR5 expression. Nat. Med. 17, 830–836.
Palmer, B.E., Li, S.X., Lozupone, C.A., 2016. The HIV-associated enteric microbiome has gone viral. Cell Host Microbe 19, 270–272.
Pandrea, I., et al., 2008a. Cutting edge: experimentally induced immune activation in natural hosts of simian immunodeficiency virus induces significant increases in viral replication and CD4$^+$ T cell depletion. J. Immunol. 1950 (181), 6687–6691 (Baltim. Md).
Pandrea, I., et al., 2008b. Paucity of CD4$^+$ CCR5$^+$ T cells may prevent transmission of simian immunodeficiency virus in natural nonhuman primate hosts by breast-feeding. J. Virol. 82, 5501–5509.
Pandrea, I., et al., 2012. Mucosal simian immunodeficiency virus transmission in African green monkeys: susceptibility to infection is proportional to target cell availability at mucosal sites. J. Virol. 86, 4158–4168.
Passaes, C.P., Sáez-Cirión, A., 2014. HIV cure research: advances and prospects. Virology 454-455, 340–352.
Peeters, M., Delaporte, E., 2012. Simian retroviruses in African apes. Clin. Microbiol. Infect. Off. Publ. Eur. Soc. Clin. Microbiol. Infect. Dis. 18, 514–520.
Peeters, M., et al., 1989. Isolation and partial characterization of an HIV-related virus occurring naturally in chimpanzees in Gabon. AIDS 3, 625–630.
Peeters, M., Jung, M., Ayouba, A., 2013. The origin and molecular epidemiology of HIV. Expert Rev. Anti-Infect. Ther. 11, 885–896.
Picker, L.J., et al., 2004. Insufficient production and tissue delivery of CD4$^+$ memory T cells in rapidly progressive simian immunodeficiency virus infection. J. Exp. Med. 200, 1299–1314.

Please cite this article as: Garcia-Tellez, T., et al., Non-human primates in HIV research: Achievements, limits and alternatives, Infection, Genetics and Evolution (2016), http://dx.doi.org/10.1016/j.meegid.2016.07.012

Plantier, J.-C., et al., 2009. A new human immunodeficiency virus derived from gorillas. Nat. Med. 15, 871–872.
Ploquin, M.J.-Y., et al., 2004. DC-SIGN from African green monkeys is expressed in lymph nodes and mediates infection in trans of simian immunodeficiency virus SIVagm. J. Virol. 78, 798–810.
Ploquin, M.J.-Y., Jacquelin, B., Jochems, S.P., Barré-Sinoussi, F., Müller-Trutwin, M.C., 2012. Innate immunity in the control of HIV/AIDS: recent advances and open questions. AIDS London England 26, 1269–1279.
Ploquin, M.J., Silvestri, G., Müller-Trutwin, M., 2016. Immune activation in HIV infection: what can the natural hosts of simian immunodeficiency virus teach us? Curr. Opin. HIV AIDS 11, 201–208.
Policicchio, B.B., Pandrea, I., Apetrei, C., 2016. Animal models for HIV cure research. Front. Immunol. 7.
Reeves, R.K., Evans, T.I., Gillis, J., Johnson, R.P., 2010a. Simian immunodeficiency virus infection induces expansion of $\alpha 4\beta 7^+$ and cytotoxic $CD56^+$ NK cells. J. Virol. 84, 8959–8963.
Reeves, R.K., et al., 2010b. CD16-natural killer cells: enrichment in mucosal and secondary lymphoid tissues and altered function during chronic SIV infection. Blood 115, 4439–4446.
Reeves, R.K., et al., 2012. SIV infection induces accumulation of plasmacytoid dendritic cells in the gut mucosa. J. Infect. Dis 206, 1462–1468.
Reimann, K.A., et al., 1994. Immunopathogenic events in acute infection of rhesus monkeys with simian immunodeficiency virus of macaques. J. Virol. 68, 2362–2370.
Reynolds, M.R., et al., 2005. $CD8^+$ T-Lymphocyte response to major immunodominant epitopes after vaginal exposure to simian immunodeficiency virus: too late and too little. J. Virol. 79, 9228–9235.
Rotger, M., et al., 2011. Comparative transcriptomics of extreme phenotypes of human HIV-1 infection and SIV infection in sooty mangabey and rhesus macaque. J. Clin. Invest. 121, 2391–2400.
Rudicell, R.S., et al., 2014. Enhanced potency of a broadly neutralizing HIV-1 antibody in vitro improves protection against lentiviral infection in vivo. J. Virol. 88, 12669–12682.
Saez-Cirion, A., Jacquelin, B., Barré-Sinoussi, F., Müller-Trutwin, M., 2014. Immune responses during spontaneous control of HIV and AIDS: what is the hope for a cure? Philos. Trans. R. Soc. B Biol. Sci. 369.
Santangelo, P.J., et al., 2015. Whole-body immunoPET reveals active SIV dynamics in viremic and antiretroviral therapy-treated macaques. Nat. Methods 12, 427–432.
Schindler, M., et al., 2006. Nef-mediated suppression of T cell activation was lost in a lentiviral lineage that gave rise to HIV-1. Cell 125, 1055–1067.
Schmitz, J.E., et al., 1999. Control of Viremia in simian immunodeficiency virus infection by $CD8^+$ lymphocytes. Science 283, 857–860.
Schmitz, J.E., et al., 2012. Memory $CD4^+$ T lymphocytes in the gastrointestinal tract are a major source of cell-associated simian immunodeficiency virus in chronic nonpathogenic infection of African green monkeys. J. Virol. 86, 11380–11385.
Schneider, T., et al., 1995. Loss of CD4 T lymphocytes in patients infected with human immunodeficiency virus type 1 is more pronounced in the duodenal mucosa than in the peripheral blood. Berlin diarrhea/wasting syndrome study group. Gut 37, 524–529.
Sellier, P., et al., 2010. Antiretroviral treatment start-time during primary SIVmac infection in macaques exerts a different impact on early viral replication and dissemination. PLoS ONE 5.
Seung, E., et al., 2013. PD-1 blockade in chronically HIV-1-infected humanized mice suppresses viral loads. PLoS ONE 8.
Shingai, M., et al., 2013. Antibody mediated immunotherapy of macaques chronically infected with SHIV suppresses. Nature 503, 277–280.
Shytaj, I.L., et al., 2012. A highly intensified ART regimen induces long-term viral suppression and restriction of the viral reservoir in a simian AIDS model. PLoS Pathog. 8.
Simon, F., et al., 1998. Identification of a new human immunodeficiency virus type 1 distinct from group M and group O. Nat. Med. 4, 1032–1037.
Sodora, D.L., Gettie, A., Miller, C.J., Marx, P.A., 1998. Vaginal transmission of SIV: assessing infectivity and hormonal influences in macaques inoculated with cell-free and cell-associated viral stocks. AIDS Res. Hum. Retrovir. 14 (Suppl. 1), S119–S123.
Sodora, D.L., et al., 2009. Toward an AIDS vaccine: lessons from natural simian immunodeficiency virus infections of African nonhuman primate hosts. Nat. Med. 15, 861–865.
Stremlau, M., et al., 2004. The cytoplasmic body component TRIM5alpha restricts HIV-1 infection in Old World monkeys. Nature 427, 848–853.
Sundell, I.B., Cortado, R.V., Koka, P.S., 2012. Sulfatide–a new candidate for ART treatment in HIV-1 infection. J. Stem Cells 7, 61–72.
Takahashi, Y., et al., 2013. In vivo administration of a JAK3 inhibitor to chronically SIV infected rhesus macaques leads to NK cell depletion associated with transient modest increase in viral loads. PLoS ONE 8.
Takehisa, J., et al., 2009. Origin and biology of simian immunodeficiency virus in wild-living western gorillas. J. Virol. 83, 1635–1648.
Thippeshappa, R., Ruan, H., Kimata, J.T., 2012. Breaking barriers to an AIDS model with macaque-tropic HIV-1 derivatives. Biology 1, 134–164.
Trautmann, L., 2016. Kill: boosting HIV-specific immune responses. Curr. Opin. HIV AIDS http://dx.doi.org/10.1097/COH.0000000000000286.
Tripathi, V., et al., 2009. Differential expression of RDC1/CXCR7 in the human placenta. J. Clin. Immunol. 29, 379–386.
Tsai, L., Tasovski, I., Leda, A.R., Chin, M.P., Cheng-Mayer, C., 2014. The number and genetic relatedness of transmitted/founder virus impact clinical outcome in vaginal R5 SHIVSF162P3N infection. Retrovirology 11, 22.
Tully, D.C., et al., 2016. Differences in the selection bottleneck between modes of sexual transmission influence the genetic composition of the HIV-1 founder virus. PLoS Pathog. 12, e1005619.
Van Heuverswyn, F., et al., 2006. Human immunodeficiency viruses: SIV infection in wild gorillas. Nature 444, 164.
Vassena, L., et al., 2012. Treatment with IL-7 prevents the decline of circulating $CD4^+$ T cells during the acute phase of SIV infection in rhesus macaques. PLoS Pathog. 8.
Veazey, R.S., 2013. Animal models for microbicide safety and efficacy testing. Curr. Opin. HIV AIDS 8, 295–303.
Veazey, R.S., et al., 1998. Gastrointestinal tract as a major site of $CD4^+$ T cell depletion and viral replication in SIV infection. Science 280, 427–431.
Veazey, R.S., et al., 2000. Identifying the target cell in primary simian immunodeficiency virus (SIV) infection: highly activated memory $CD4^+$ T cells are rapidly eliminated in early SIV infection in vivo. J. Virol. 74, 57–64.
Veazey, R., et al., 2003. Decreased CCR5 expression on $CD4^+$ T cells of SIV-infected sooty mangabeys. AIDS Res. Hum. Retrovir. 19, 227–233.
Veazey, R.S., Shattock, R.J., Klasse, P.J., Moore, J.P., 2012. Animal models for microbicide studies. Curr. HIV Res. 10, 79–87.
Walter, L., Ansari, A.A., 2015. MHC and KIR polymorphisms in rhesus macaque SIV infection. Front. Immunol. 6, 540.
Wege, A.K., Melkus, M.W., Denton, P.W., Estes, J.D., Garcia, J.V., 2008. Functional and phenotypic characterization of the humanized BLT mouse model. Curr. Top. Microbiol. Immunol. 324, 149–165.
Wen, J., et al., 2016. Specific elimination of latently HIV-1 infected cells using HIV-1 protease-sensitive toxin nanocapsules. PLoS ONE 11, e0151572.
Whitney, J.B., et al., 2014. Rapid seeding of the viral reservoir prior to SIV viremia in rhesus monkeys. Nature 512, 74–77.
Wilson, N.A., Watkins, D.I., 2009. Is an HIV vaccine possible? Braz. J. Infect. Dis. Off. Publ. Braz. Soc. Infect. Dis. 13, 304–310.
Wu, F., et al., 2015. TRIM5α restriction affects clinical outcome and disease progression in simian immunodeficiency virus-infected rhesus macaques. J. Virol. 89, 2233–2240.
Xu, H., Wang, X., Veazey, R.S., 2014. Th17 cells coordinate with Th22 cells in maintaining homeostasis of intestinal tissues and both are depleted in SIV-infected macaques. J. AIDS Clin. Res. 5.

Please cite this article as: Garcia-Tellez, T., et al., Non-human primates in HIV research: Achievements, limits and alternatives, Infection, Genetics and Evolution (2016), http://dx.doi.org/10.1016/j.meegid.2016.07.012

Available online at www.sciencedirect.com

ScienceDirect

Current Opinion in Virology

Innate immune cell responses in non pathogenic *versus* pathogenic SIV infections

Nicolas Huot[1,2,3,4], Philippe Rascle[1,3,4], Thalia Garcia-Tellez[1], Beatrice Jacquelin[1] and Michaela Müller-Trutwin[1,3]

HIV-1/SIVmac infections deeply disturb innate host responses. Most studies have focused on the impact on dendritic cells and NK cells. A few but insufficient data are available on other innate immune cell types, such as neutrophils. It has been shown that innate lymphoid cells are depleted early and irreversibly during SIVmac/HIV-1 infections. Studies in natural hosts of SIV have contributed to pinpoint that early control of inflammation is crucial. In natural hosts, plasmacytoid dendritic cells, myeloid dendritic cells and NK cells are depleted during acute infection but return to normal levels by the end of acute infection. We summarize here the similarities and differences of various types of innate immune responses in natural hosts compared to pathogenic HIV/SIV mac infections.

Addresses
[1] Institut Pasteur, Unité HIV, Inflammation and Persistence, Paris, France
[2] CEA, Division of Immuno-Virology, iMETI, DSV, Fontenay-aux-Roses, France
[3] Vaccine Research Institute, Créteil, France

Corresponding author: Müller-Trutwin, Michaela (michaela.muller-trutwin@pasteur.fr)
[4] Co-first authors.

Current Opinion in Virology 2016, **19**:37–44

This review comes from a themed issue on **Animal models for viral diseases**

Edited by **Mirko Paiardini**

http://dx.doi.org/10.1016/j.coviro.2016.06.011

1879-6257/© 2016 Elsevier B.V. All rights reserved.

Introduction

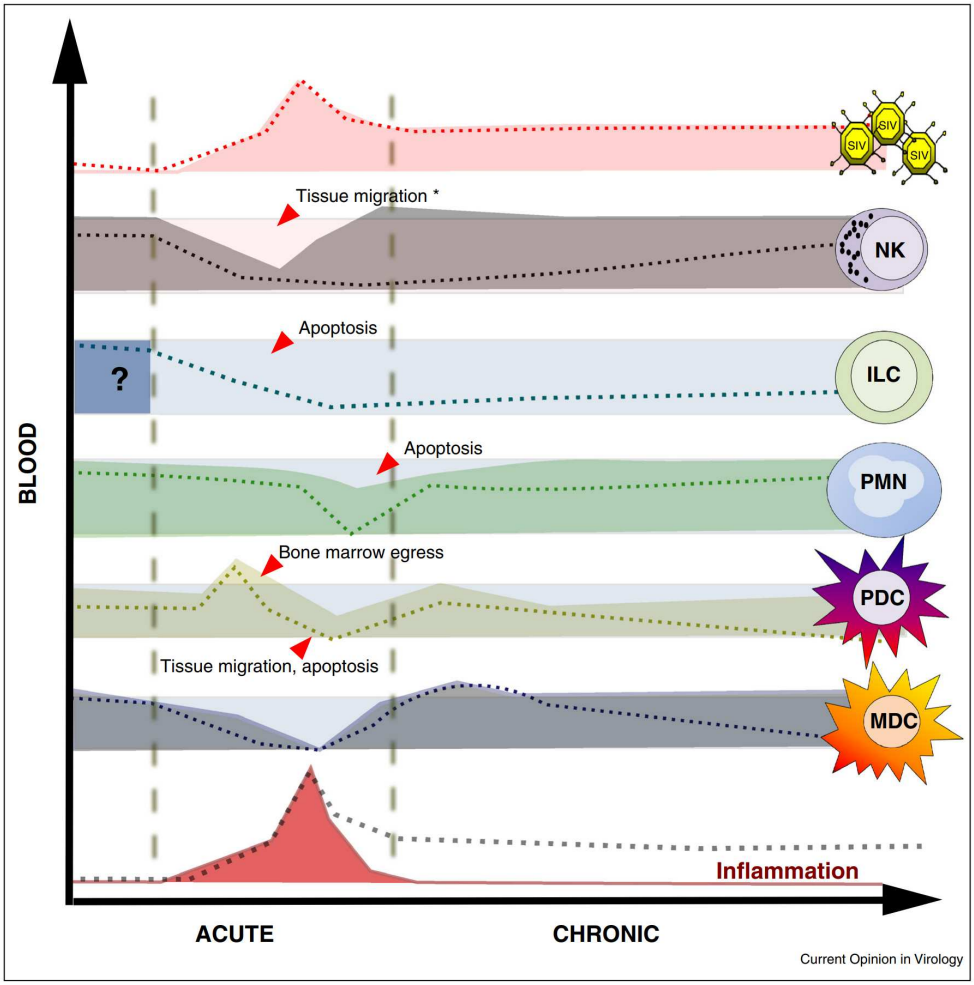
The infection of a host by a virus leads to one of the following three distinct outcomes: clearance of the virus, establishment of a chronic infection and the worst possibility, the death of the host. The quality and the duration of the host response, which may be influenced intrinsically (i.e. genetic background) or extrinsically (i.e. medication) engages the resolution of the infection toward one of those possibilities.

The host response can be divided into two main arms: the innate immune system and its orchestration of cells belonging to the adaptive immune system and the adaptive immune system itself. These different arms are interdependent and their actions are spatially and temporally organized in order to give an optimal response against the pathogen.

HIV infection is disturbing both the innate and adaptive arms of the host response. The introduction of the combined anti-retroviral treatment (cART) allows immune restoration, however to variable degrees. The capacity of the treatment to restore the functionality of the immune system varies depending on several factors, in particular the stage of infection at which the treatment is initiated.

Little is known on the impact of cART on the innate immune system. This lack of knowledge is partly due to the fact that patients were rarely detected for HIV during the acute phase of infection, at the moment where the inflammation and the innate response is the most active. In this context, the study of SIV infection in non human primates (NHP) remains a major model of choice to study the first steps of infection. Indeed, Asian species of NHP, such as rhesus and cynomolgus macaques, experimentally infected by SIV, experience a spectrum of disorders identical to HIV-1 infected humans. NHP models contributed to increase significantly our knowledge on HIV infection, for instance helped to apprehend the early establishment of the viral reservoirs and the immense immunological insult to the gut, as well as other tissues, given by the viral infection [1,2,3•,4]. NHP from Africa, such as African green monkeys (AGM), sooty mangabeys (SM) and mandrills, are natural hosts of SIV. SIV infection in these natural hosts generally does not lead to any signs of disease, even though they carry high plasma and intestinal viral load [5]. One major difference between AIDS progressors and non-progressors is the duration of the inflammation, which is totally resolved in natural hosts by the end of the acute infection, while chronic inflammation persists in AIDS progressors (Figure 1). Inflammation is initially induced by cells that sense the virus. Subsequently, cells of the adaptive immune system, as well as other mechanisms, might contribute to chronic inflammation, for instance microbial translocation which is absent in natural hosts [6–8]. Indeed, natural hosts maintain the integrity of the intestinal barrier and do not loose their Th17 cells [5,8,9]. Another remarkable difference in the natural host is the preservation of the architecture of the secondary lymphoid tissues, the latter being progressively disrupted in HIV and SIVmac infections [10,11]. The preservation of such a structure could

Figure 1



Dynamics of the innate immune cells during pathogenic and non pathogenic SIV infections. The dynamics are indicated for the natural hosts (full) and for the pathogenic models (dotted). The schemes illustrate what is known about innate immune cell population changes during the time of infection. The evolution of the different innate immune cells is compared to the dynamics of viremia (top) and the evolution of inflammation (bottom). The main reason(s) suggested to explain a change in cell subset frequencies are indicated by a red arrow. The asterisk means that the mechanism has only been observed in pathogenic infection. The question mark indicates a population for which the evolution has not been characterized in the natural host.

participate to the better orchestration of immune responses in natural hosts. This review will discuss in particular the hallmarks of innate immune responses in natural hosts. Innate immunity is generally less well explored than T and B cell responses, except for dendritic cells and NK cells. We will here summarize the information that is available on innate immune responses in natural hosts and explain the major differences with respect to pathogenic HIV and SIVmac infections.

Monocyte/macrophages

Monocytes and macrophages possess receptors for entry of HIV/SIV viruses, like dendritic cells and CD4 T cells. While primary monocytes are not susceptible to HIV infection, HIV infection of macrophages in tissues, such as the brain, lung and decidua, has been reported in many studies [12,13]. It has been suggested that this cell population figures among the first target cells to be infected by SIV/HIV in vaginal mucosa [13,14]. PCR

and immunohistochemistry analyses of the central nervous system and lungs of AGM showed that macrophages are also infected in natural hosts [15]. Surprising results were however obtained during *in vivo* depletion studies. Upon depletion of CD4+ T cells in chronically infected SM, viremia declined [16,17]. The latter finding contrasts with macaques in which upon CD4+ T cell depletion viremia increased, followed by quick progression to AIDS [18,19•]. This increase in viral replication in CD4-depleted macaques was due to massive infection of macrophages, suggesting that natural host's macrophages are less susceptible to infection. The potentially lower susceptibility of macrophages to SIV infection has been further shown in monocyte-derived macrophages (MDM) *in vitro* and attributed to a higher expression of IFN-α inducible restriction factors, such as Tetherin and TRIM22 [20]. In line with this, immunohistochemistry of the intestine did not reveal any SIV-infected macrophages in AGM at the stage of peak viral production in early infection [7]. More studies need to be done at distinct stages of infection and in other tissues to better understand the SIV infection pattern of macrophages in natural hosts.

In macaques, AIDS and death can occur in the absence of detectable macrophage infection [21,22]. These results could indicate that it is not the infection of monocyte/macrophages that matters but maybe more their role in inflammation. Soluble markers of inflammation and coagulation but not T-cell activation predict non-AIDS-defining morbid events during treatment [23,24]. Markers of monocyte activation (sCD14, TNF-α, CXCL10/IP-10) and microbial translocation have been shown to be associated with disease progression in HIV infection and a poor CD4+ T cell recovery under ART [25,26]. In treated patients, monocyte activation predicts coronary artery calcium progression [27]. Massive turnover of peripheral monocytes associated with death of tissue macrophages correlates with AIDS progression [28] in the macaque model. Importantly, the level of monocyte turnover was a better predictive marker for AIDS progression than was viral load or lymphocyte activation [29].

In SM, a reduced monocyte TNF-α response was noted as compared to monocytes from humans and macaque [30]. Moreover, since microbial translocation is not occurring in natural hosts, their monocytes/macrophages are not exposed to LPS [31,32••,33•]. In line with this, the monocyte/macrophage activation marker sCD14 is not increased in wild SIV-infected AGMs in contrast to macaques [32••]. Altogether, these findings suggest that monocyte/macrophages are less activated in natural hosts than during HIV/SIVmac infections in human and macaques.

Plasmacytoid dendritic cells

Plasmacytoid dendritic cells (pDC) are rapidly mobilized by day 2 post-infection (p.i.), both in pathogenic and non pathogenic infection (Figure 1) [34••,35,36]. Only in pathogenic infection, there is however a progressive decline of pDC numbers in the blood in chronic infection.

Data on the infection rates of pDC *in vivo* are scarce. One study reported the presence of HIV DNA in circulating pDC of chronically HIV-infected patients [37]. Another study reported high infection levels in lymph node (LN) pDC during acute SIVmac infection [36]. We have reported that AGM pDC express extremely low levels of CD4, unlike MAC and human pDC [38•]. Moreover, both AGM and SM pDC were found to be, in contrast to MAC pDC, predominantly negative for CCR5. Despite such limited CD4 and CCR5 expression, lymphoid tissue pDC were infected to a similar degree as $CD4^+$ T cells, both in MAC and AGM [38•].

pDC form a rare cell population that is however responsible for the vast majority of IFN-I production after HIV/SIVmac encounter. To analyze whether pDC of natural hosts are also the predominant producers of IFN-I in response to SIV, PBMC from healthy AGM were depleted for pDC and stimulated with SIVagm. This led to a 96.7% reduction in IFN-I production upon stimulation with SIVagm, confirming the predominant role of pDC for SIV sensing in natural hosts as well [34••]. pDC from natural hosts are fully functional to sense SIV [34••,39,40]. In line with this, no significant differences are observed between pathogenic and non pathogenic SIV infections regarding the capacity to produce IFN-I *in vivo* [40,41,42••]. The maturation and homing profiles of pDC in response to SIV infection *in vivo* were also similar between AGM and macaques [41,42••]. pDC from AGM even show a higher capacity to sense species-specific viruses (SIVagm) than viruses from experimental hosts (SIVmac), evoking host-virus adaptation and selective pressures to maintain the capacity of SIV sensing in the natural host [38•].

IFN-I produced during acute infection strongly upregulates type I IFN-stimulated genes (ISGs) in both pathogenic and non-pathogenic SIV infection [39,43,44]. ISG expression returns, however, to basal levels after acute infection in natural hosts, while it remains sustained in macaques, as in HIV infection in humans. Since the capacity of IFN-I production is similar between natural hosts and macaques, the sustained ISG response during chronic SIVmac/HIV infections is most likely due to factors distinct from IFN-I, such as translocated microbial products or other factors [39,42••,45].

Myeloid dendritic cells

The kinetics of myeloid dendritic cell (mDC) numbers are similar between non-pathogenic and pathogenic infection during the first year post SIV infection (Figure 1) [42••]. The numbers are sometimes significantly increased in the early stages of infection in both types of

infection. Only in pathogenic infection though, declines of mDC can be observed afterwards.

The infection of mDC by SIV in natural hosts has not been explored. Vpx has been shown to increase the susceptibility of HIV-1 to replicate in myeloid cells [46]. However, while Vpx is present in viruses of some natural hosts (SIVsm), it is absent in others (SIVagm), and its impact in non pathogenic infection is unclear.

HIV-1 is known to activate pDC, which activation is necessary to induce the bystander maturation of mDC, that do not mature if exposed to HIV in the absence of pDC [47]. *In vivo*, mDC show a lower maturation profile in natural hosts than in HIV/SIVmac infections [33•,42••]. After infection, spontaneous production of proinflammatory cytokines by mucosal mDCs increased only in progressor macaques but not in natural hosts. These findings are consistent with a model in which myeloid cells are less activated in natural hosts than during pathogenic infection, although more studies are needed to confirm this hypothesis.

Innate lymphoid cells

Recently discovered innate lymphoid cells (ILC) are composed of three classes with their own specificities [48–49]. These cells are mainly located near the mucosal epithelial barriers. The population of ILC3 (NKp44+ and RORγT+) producing IL-17 is lost during the acute phase of SIV infection in macaques and HIV-1 infection in humans [3•,4,49,50]. IL-17 is essential for the recruitment of neutrophils at the inflammation site [51]. This fact might explain in part the neutropenia observed during acute phase of pathogenic HIV/SIV infections. In addition, it might be associated with the fragility of the intestinal barrier. The absence of bacterial translocation in the natural hosts raises the question about the role of ILCs in this model. ILC have not been characterized yet in the natural hosts.

Polymorphonuclear cells

Neutrophils are commonly known as 'professional' phagocytic cells of the innate immune system [51,52]. They are present in large numbers in the peripheral blood (50–70% of white cells) and are recruited rapidly to peripheral sites of damage, where they can capture and kill microbes efficiently through the production of ROS (such as O_2^-, H_2O_2, HOCl, and $OH^•$) [53].

The role played by neutrophils in HIV/SIV infection has rarely been investigated [53,54]. An increase of PMN apoptosis has been shown in humans, particularly in the later stages of HIV disease [53,55], but the mechanisms have not been identified. In NHP, PMN are identified as CD45+ CD11b^{high}CD14^{lo} [56,57]. Two studies have shown a strong depletion of neutrophils, attributed to an increase of neutrophil apoptosis, during the acute phase of infection in macaques, whereas this depletion was not observed in the natural host (Figure 1) [56,57].

Besides producing cytokines and chemokines, another novel and emerging aspect consists in the ability of neutrophils to interact with, and modulate the activity of different leukocyte types *in vitro* and *in vivo* [58]. Recent studies also highlight a new role for neutrophils as non-redundant regulatory cells ensuring the terminal maturation of NK cells in both humans and mice [58–60]. Future studies in natural hosts will help to decipher to which extent these functions play a role in the pathogenic outcome of HIV/SIV infections.

Invariant natural killer T cells (iNKT)

A small subset of T lymphocytes named NKT cells express surface markers characteristic of both T cells and NK cells. They are known to play an important link between innate and adaptive immune responses [61,62]. Despite the low frequency of the iNKT population in the periphery (<1% of the CD3+ cells), the role iNKT in various pathologies such as allergy, cancer and infectious diseases is well considered.

In humans and NHP models, iNKT cells are characterized by the expression of a TCR comprised Vα24-Jα18 associated with Vβ11 [63]. The majority of iNKT express CD161 and all respond to lipid ligands through CD1d restriction. In Humans and macaques, iNKT express CD4 and CD8α, allowing the iNKT subset to be defined as CD4$^+$, DN (CD4$^-$CD8$^-$), or CD8$^+$ [64–67]. In SM, iNKT cells are either CD8$^+$ or DN, and never CD4$^+$ [68,69]. Studies of iNKT in NHP highlight the importance of iNKT activation during HIV-1 infection. Infection of macaques resulted in peripheral CD4+ iNKT depletion similar to human HIV-1 infection, and was correlated with CD4+ T cell decline. Moreover iNKT numbers were inversely correlated with viral load [67,68].

The macaque model also revealed an early expansion of IL-17 expressing CD4$^+$ NKT cells in peripheral and mesenteric lymph nodes [70]. This could be a compensatory mechanism for the loss of other IL-17 producing cells such as Th17 cells. In contrast, in the nonpathogenic model, no change in the level of IL-17-expressing cells was observed in these tissues by immunohistochemistry. Consistent with the emergence of TGF-β and IL-18 during the acute phase in SIV-infected macaques, but not in SIV-infected AGM, *in vitro* TGF-β and IL-18 induced the differentiation and expansion of IL-17$^+$NKT [70].

SM iNKT have the capacity to produce IL-2, IL-13, and IL-10, which could provide these cells a role in the regulation of inflammation [67]. Indeed in murine models, the production of IL-4 and IL-10 by iNKT can induce

regulatory T cell (Treg) development [71]. Alternately, the data described in SM also raise the possibility that loss of anti-inflammatory NKT function promotes chronic immune activation in pathogenic SIV infection, while intact NKT function helps to protect natural hosts from developing immunodeficiency and aberrant immune activation [68].

Natural killer cells

NK cells were thought to be a primitive cell lineage, which evolved before the development of the adaptive immune system. Recently, however, NK cells have been shown to also possess traits of adaptive immunity and to acquire immunological memory in primates [72••].

Healthy human subjects typically exhibit three distinct NK cell subsets that are defined by the differential expression of CD56 and CD16 within the $CD3^-$ population. Following HIV infection, a significant decline occurs in the cytolytic subset ($CD56^{dim}CD16+$) while an expansion of the otherwise rare population of $CD56^-CD16^+$ NK cells occurs. Alterations in the levels of $CD3^-CD56^{bright}CD16^-$ cells do not appear to be major but reduced cytokine and chemokine production has been reported. These and other data demonstrated that in addition to adversely affecting the adaptive immune response, HIV-infection also results in functional impairment of the NK cell compartment of the innate immune system.

Studies in SIV-infected rhesus macaques also highlight multiple effects on NK-cell function, such as a decreased ability to secrete IFN-γ, TNFα and IL-2. NK cells in SIV infected rhesus macaques with rapid disease progression and high viral load show sustained proliferation but less lytic activity [73•].

In natural hosts, the NK cell responses appear earlier and stronger than in SIVmac-infected macaques during the acute phase [42••,74]. The cytolytic subset is not depleted and sometimes even seems to expand. The rapid and strong increase in NK cell proliferation might be a direct consequence of the early and robust production of IL-15 and IFN-α during primary SIVagm infection [42••]. It has been shown that IFN-α and IL-15 promote NK cell proliferation and survival, while IFN-α is able to increase NK cell cytotoxicity, and IL-15 to augment the secretion of IFN-γ [42••]. In natural hosts, despite the induction of both cytokines (IFN-α, IL-15) during the acute phase of SIV infection, no *ex vivo* production of IFN-γ by NK cells could be observed [42••]. Interestingly though, the expression of CD107a on NK cells was increased in lymph nodes during the acute phase of SIVagm infection. An increase of CD16+CD56+ NK cells, generally considered as the cytolytic subset of NK cells, has also been described in blood of SIV-infected SM [74]. These few studies on NK cells in natural hosts suggest that they display a stronger cytotoxic activity in response to SIV infection than during SIVmac infection.

Conclusions

Many events occur simultaneously after HIV infection with very tightly regulated interactions between the distinct components of the immune system. A better understanding of the cross-talks between these cells and their impact on control of viral replication and disease is needed. For instance, more knowledge is desirable on the contribution of myeloid cells on inflammation during HIV/SIV infections. It is also unclear, to which extent specific cell types of the innate immune system, in particular macrophages or myeloid dendritic cells, are targeted by the virus *in vivo*.

Moreover, several other cells have been understudied so far. For instance, ILCs might play an important role during HIV/SIV infections, particularly in the intestine. An IL-17-mediated crosstalk between ILCs and neutrophils shows another type of possible communication between cells. Other less explored cells, such as iNKT, have the capacity to induce many anti-inflammatory cytokines and have a potential role in regulating locally the immune system. Additional innate cells exist that have been poorly or not at all investigated in HIV/SIV infections [75,76].

NK cells have been largely studied in humans and macaques, but only poorly in natural hosts. NK are the only immune cells, that were stronger activated in natural hosts than in pathogenic infection [42••,74]. Thus, NK cells might play a so far unknown role in the lack of disease progression in natural hosts.

The recent description of the full genome of African green monkeys, as well as future whole genome sequence information from other natural hosts will help to develop more tools to analyze innate immune cells [77,78]. Finally, studies on the metabolic changes due to the stress induced by the viral infection within innate immune cells might reveal new aspects of immune and viral regulation [79,80].

Studies in natural hosts have contributed to pinpoint that early control of infection is crucial. For instance in natural hosts for SIV, the inflammation is rapidly resolved, by the end of acute infection. Some patients showed that receiving a treatment in early HIV infection can lead to control the virus after treatment interruption [81]. A limitation of virus replication in early time points of infection enhances the capacity of the host to control the infection [82]. It will be important to understand to what extent an early antiretroviral treatment impacts the function of the innate immune system and the intercellular communications. Further studies in natural hosts should help to distinguish

those early events which are associated or not with a good outcome of infection [1].

Acknowledgements

We would like to thank the French National Agency for Research on AIDS and Viral Hepatitis (ANRS) Vaccine Research Institute funded by the Investissements d'Avenir program' managed by the ANR under reference ANR-10-LABX-77, as well as the Center for Infectious Disease models and Innovative Therapies (IDMIT) funded by "Programme investissements d'avenir" under grant agreement N° ANR-11-INBS-0008).

References and recommended reading

Papers of particular interest, published within the period of review, have been highlighted as:

- • of special interest
- •• of outstanding interest

1. Micci L, Ryan ES, Fromentin R, Bosinger SE, Harper JL, He T, Paganini S, Easley KA, Chahroudi A, Benne C, Gumber S, McGary CS, Rogers KA, Deleage C, Lucero C, Byrareddy SN, Apetrei C, Estes JD, Lifson JD, Piatak M, Chomont N, Villinger F, Silvestri G, Brenchley JM, Paiardini M: **Interleukin-21 combined with ART reduces inflammation and viral reservoir in SIV-infected macaques**. *J Clin Invest* 2015, **125**:4497-4513.

2. Whitney JB, Hill AL, Sanisetty S, Penaloza-MacMaster P, Liu J, Shetty M, Parenteau L, Cabral C, Shields J, Blackmore S, Smith JY, Brinkman AL, Peter LE, Mathew SI, Smith KM, Borducchi EN, Rosenbloom DIS, Lewis MG, Hattersley J, Li B, Hesselgesser J, Geleziunas R, Robb ML, Kim JH, Michael NL, Barouch DH: **Rapid seeding of the viral reservoir prior to SIV viraemia in rhesus monkeys**. *Nature* 2014, **512**:74-77.

3. • Li H, Richert-Spuhler LE, Evans TI, Gillis J, Connole M, Estes JD, Keele BF, Klatt NR, Reeves RK: **Hypercytotoxicity and rapid loss of NKp44+ innate lymphoid cells during acute SIV infection**. *PLoS Pathogens* 2014, **10**:e1004551.

The article reports first evidence for acute, systemic, and permanent loss of mucosal ILCs during SIV infection, that was associated with reduction of IL-17 expression.

4. Xu H, Wang X, Lackner AA, Veazey RS: **Type 3 innate lymphoid cell depletion is mediated by TLRs in lymphoid tissues of simian immunodeficiency virus-infected macaques**. *FASEB J* 2015, **29**:5072-5080.

5. Ploquin MJ, Silvestri G, Müller-Trutwin M: **Immune activation in HIV infection: what can the natural hosts of simian immunodeficiency virus teach us?** *Curr Opin HIV AIDS* 2016, **11**:201-208.

6. Gordon SN, Klatt NR, Bosinger SE, Brenchley JM, Milush JM, Engram JC, Dunham RM, Paiardini M, Klucking S, Danesh A, Strobert EA, Apetrei C, Pandrea IV, Kelvin D, Douek DC, Staprans SI, Sodora DL, Silvestri G: **Severe depletion of mucosal CD4+ T cells in AIDS-free simian immunodeficiency virus-infected sooty mangabeys**. *J Immunol* 2007, **179**:3026-3034.

7. Pandrea IV, Gautam R, Ribeiro RM, Brenchley JM, Butler IF, Pattison M, Rasmussen T, Marx PA, Silvestri G, Lackner AA, Perelson AS, Douek DC, Veazey RS, Apetrei C: **Acute loss of intestinal CD4+ T cells is not predictive of simian immunodeficiency virus virulence**. *J Immunol* 2007, **179**:3035-3046.

8. Estes JD, Harris LD, Klatt NR, Tabb B, Pittaluga S, Paiardini M, Barclay GR, Smedley J, Pung R, Oliveira KM, Hirsch VM, Silvestri G, Douek DC, Miller CJ, Haase AT, Lifson J, Brenchley JM: **Damaged intestinal epithelial integrity linked to microbial translocation in pathogenic simian immunodeficiency virus infections**. *PLoS Pathog* 2010, **6**:e1001052.

9. Brenchley JM, Paiardini M, Knox KS, Asher AI, Cervasi B, Asher TE, Scheinberg P, Price DA, Hage CA, Kholi LM, Khoruts A, Frank I, Else J, Schacker T, Silvestri G, Douek DC: **Differential Th17 CD4 T-cell depletion in pathogenic and nonpathogenic lentiviral infections**. *Blood* 2008, **112**:2826-2835.

10. Diop OM, Gueye A, Dias-Tavares M, Kornfeld C, Faye A, Ave P, Huerre M, Corbet S, Barre-Sinoussi F, Müller-Trutwin MC: **High levels of viral replication during primary simian immunodeficiency virus SIVagm infection are rapidly and strongly controlled in African green monkeys**. *J Virol* 2000, **74**:7538-7547.

11. Estes JD, Haase AT, Schacker TW: **The role of collagen deposition in depleting CD4+ T cells and limiting reconstitution in HIV-1 and SIV infections through damage to the secondary lymphoid organ niche**. *Semin Immunol* 2008, **20**:181-186.

12. Li Y, Kang G, Duan L, Lu W, Katze MG, Lewis MG, Haase AT, Li Q: **SIV infection of lung macrophages**. *PLOS ONE* 2015, **10**:e0125500.

13. El Costa H, Quillay H, Marlin R, Cannou C, Duriez M, Benjelloun F, de Truchis C, Rahmati M, Ighil J, Barré-Sinoussi F, Nugeyre MT, Menu E: **The local environment orchestrates mucosal decidual macrophage differentiation and substantially inhibits HIV-1 replication**. *Mucosal Immunol* 2016, **9**:634-646.

14. Arrildt KT, LaBranche CC, Joseph SB, Dukhovlinova EN, Graham WD, Ping L-H, Schnell G, Sturdevant CB, Kincer LP, Mallewa M, Heyderman RS, Van Rie A, Cohen MS, Spudich S, Price RW, Montefiori DC, Swanstrom R: **Phenotypic correlates of HIV-1 macrophage tropism**. *J Virol* 2015, **89**:11294-11311.

15. Goldstein S, Ourmanov I, Brown CR, Beer BE, Elkins WR, Plishka R, Buckler-White A, Hirsch VM: **Wide range of viral load in healthy African green monkeys naturally infected with simian immunodeficiency virus**. *J Virol* 2000, **74**:11744-11753.

16. Milush JM, Mir KD, Sundaravaradan V, Gordon SN, Engram J, Cano CA, Reeves JD, Anton E, O'Neill E, Butler E, Hancock K, Cole KS, Brenchley JM, Else JG, Silvestri G, Sodora DL: **Lack of clinical AIDS in SIV-infected sooty mangabeys with significant CD4+ T cell loss is associated with double-negative T cells**. *J Clin Invest* 2011, **121**:1102-1110.

17. Klatt NR, Villinger F, Bostik P, Gordon SN, Pereira L, Engram JC, Mayne A, Dunham RM, Lawson B, Ratcliffe SJ, Sodora DL, Else J, Reimann K, Staprans SI, Haase AT, Estes JD, Silvestri G, Ansari AA: **Availability of activated CD4+ T cells dictates the level of viremia in naturally SIV-infected sooty mangabeys**. *J Clin Invest* 2008, **118**:2039-2049.

18. Ortiz AM, Klatt NR, Li B, Yi Y, Tabb B, Hao XP, Sternberg L, Lawson B, Carnathan PM, Cramer EM, Engram JC, Little DM, Ryzhova E, Gonzalez-Scarano F, Paiardini M, Ansari AA, Ratcliffe S, Else JG, Brenchley JM, Collman RG, Estes JD, Derdeyn CA, Silvestri G: **Depletion of CD4+ T cells abrogates post-peak decline of viremia in SIV-infected rhesus macaques**. *J Clin Invest* 2011, **121**:4433-4445.

19. • Micci L, Alvarez X, Iriele RI, Ortiz AM, Ryan ES, McGary CS, Deleage C, McAtee BB, He T, Apetrei C, Easley K, Pahwa S, Collman RG, Derdeyn CA, Davenport MP, Estes JD, Silvestri G, Lackner AA, Paiardini M: **CD4 depletion in SIV-infected macaques results in macrophage and microglia infection with rapid turnover of infected cells**. *PLoS Pathog* 2014, **10**:e1004467.

CD4-depleted animals showed macrophages constituting 80% of all SIV vRNA+ cells in lymph node and mucosal tissues; substantial expansion of pro-inflammatory monocytes and aberrant activation of microglial cells; and lifespan of productively infected macrophages shorter than previously estimated.

20. Mir KD, Mavigner M, Wang C, Paiardini M, Sodora DL, Chahroudi AM, Bosinger SE, Silvestri G: **Reduced simian immunodeficiency virus replication in macrophages of sooty mangabeys is associated with increased expression of host restriction factors**. *J Virol* 2015, **89**:10136-10144.

21. Sandler NG, Douek DC: **Microbial translocation in HIV infection: causes, consequences and treatment opportunities**. *Nat Rev Microbiol* 2012, **10**:655-666.

22. Westmoreland SV, Converse AP, Hrecka K, Hurley M, Knight H, Piatak M, Lifson J, Mansfield KG, Skowronski J, Desrosiers RC: **SIV vpx is essential for macrophage infection but not for development of AIDS**. *PLOS ONE* 2014, **9**:e84463.

23. Kuller LH, Tracy R, Belloso W, De Wit S, Drummond F, Lane HC, Ledergerber B, Lundgren J, Neuhaus J, Nixon D, Paton NI, Neaton JD, INSIGHT SMART Study Group: **Inflammatory and**

coagulation biomarkers and mortality in patients with HIV infection. *PLoS Med* 2008, **5**:e203.

24. Tenorio AR, Zheng Y, Bosch RJ, Krishnan S, Rodriguez B, Hunt PW, Plants J, Seth A, Wilson CC, Deeks SG, Lederman MM, Landay AL: **Soluble markers of inflammation and coagulation but not T-cell activation predict non-AIDS-defining morbid events during suppressive antiretroviral treatment**. *J Infect Dis* 2014, **210**:1248-1259.

25. León A, Leal L, Torres B, Lucero C, Inciarte A, Arnedo M, Plana M, Vila J, Gatell JM, García F: **Association of microbial translocation biomarkers with clinical outcome in controllers HIV-infected patients**. *AIDS* 2015, **29**:675-681.

26. Brenchley JM: **Mucosal immunity in human and simian immunodeficiency lentivirus infections**. *Mucosal Immunol* 2013, **6**:657-665.

27. Baker JV, Hullsiek KH, Singh A, Wilson E, Henry K, Lichtenstein K, Onen N, Kojic E, Patel P, Brooks JT, Hodis HN, Budoff M, Sereti I, CDC SUN Study Investigators: **Immunologic predictors of coronary artery calcium progression in a contemporary HIV cohort**. *AIDS* 2014, **28**:831-840.

28. Hasegawa A, Liu H, Ling B, Borda JT, Alvarez X, Sugimoto C, Vinet-Oliphant H, Kim W-K, Williams KC, Ribeiro RM, Lackner AA, Veazey RS, Kuroda MJ: **The level of monocyte turnover predicts disease progression in the macaque model of AIDS**. *Blood* 2009, **114**:2917-2925.

29. Burdo TH, Soulas C, Orzechowski K, Button J, Krishnan A, Sugimoto C, Alvarez X, Kuroda MJ, Williams KC: **Increased monocyte turnover from bone marrow correlates with severity of SIV encephalitis and CD163 levels in plasma**. *PLoS Pathog* 2010, **6**:e1000842.

30. Mir KD, Bosinger SE, Gasper M, Ho O, Else JG, Brenchley JM, Kelvin DJ, Silvestri G, Hu S-L, Sodora DL: **Simian immunodeficiency virus-induced alterations in monocyte production of tumor necrosis factor alpha contribute to reduced immune activation in sooty mangabeys**. *J Virol* 2012, **86**:7605-7615.

31. **Into the wild: simian immunodeficiency virus (SIV) infection in natural hosts — PubMed — NCBI**. *Trends Immunol* 2008. Available from: http://www.ncbi.nlm.nih.gov/pubmed/18676179 [accessed 17.05.16] [online].

32. •• Ma D, Jasinska A, Kristoff J, Grobler JP, Turner T, Jung Y, Schmitt C, Raehtz K, Feyertag F, Martinez Sosa N, Wijewardana V, Burke DS, Robertson DL, Tracy R, Pandrea I, Freimer N, Apetrei C, International Vervet Research Consortium: **SIVagm infection in wild African green monkeys from South Africa: epidemiology, natural history, and evolutionary considerations**. *PLoS Pathog* 2013, **9**:e1003011.
Here, the authors assessed, for the first time in a natural host, immune activation markers during SIV infection in wild monkeys.

33. • Wijewardana V, Kristoff J, Xu C, Ma D, Haret-Richter G, Stock JL, Policicchio BB, Mobley AD, Nusbaum R, Aamer H, Trichel A, Ribeiro RM, Apetrei C, Pandrea I: **Kinetics of myeloid dendritic cell trafficking and activation: impact on progressive, nonprogressive and controlled SIV infections**. *PLoS Pathog* 2013, **9**:e1003600.
This is the first study that investigated mDC in natural hosts. Sustained mDC immune activation and loss of mucosal mDCs was associated with pathogenic SIV infection, while mDC activation occurred only during acute infection in natural hosts.

34. •• Jochems SP, Petitjean G, Kunkel D, Liovat A-S, Ploquin MJ, Barré-Sinoussi F, Lebon P, Jacquelin B, Müller-Trutwin MC: **Modulation of type I interferon-associated viral sensing during acute simian immunodeficiency virus infection in African green monkeys**. *J Virol* 2015, **89**:751-762.
This study revealed that cells other than pDCs increase their abilities for viral sensing during acute infection. The results suggest that pDC-produced IFN-I upregulates viral sensors in bystander cells, the latter gaining the capacity to produce IFN-I in response to viruses other than SIV.

35. Bruel T, Dupuy S, Démoulins T, Rogez-Kreuz C, Dutrieux J, Corneau A, Cosma A, Cheynier R, Dereuddre-Bosquet N, Le Grand R, Vaslin B: **Plasmacytoid dendritic cell dynamics tune interferon-alfa production in SIV-infected cynomolgus macaques**. *PLoS Pathog* 2014, **10**:e1003915.

36. Brown KN, Wijewardana V, Liu X, Barratt-Boyes SM: **Rapid influx and death of plasmacytoid dendritic cells in lymph nodes mediate depletion in acute simian immunodeficiency virus infection**. *PLoS Pathog* 2009, **5**:e1000413.

37. Donaghy H, Gazzard B, Gotch F, Patterson S: **Dysfunction and infection of freshly isolated blood myeloid and plasmacytoid dendritic cells in patients infected with HIV-1**. *Blood* 2003, **101**:4505-4511.

38. • Jochems SP, Jacquelin B, Chauveau L, Huot N, Petitjean G, Lepelley A, Liovat A-S, Ploquin MJ, Cartwright EK, Bosinger SE, Silvestri G, Barré-Sinoussi F, Lebon P, Schwartz O, Müller-Trutwin MC: **Plasmacytoid dendritic cell infection and sensing capacity during pathogenic and nonpathogenic simian immunodeficiency virus infection**. *J Virol* 2015, **89**:6918-6927.
The author show that PDC from AGM display reduced CD4 and CCR5 expressions. Nonetheless, infection levels in vivo were similar to MAC PDC. AGM pDC efficiently sensed species-specific SIVagm isolates, but only weakly SIVmac/HIV-1 viruses, showing that viral determinants play a role in PDC-mediated sensing of SIV and suggesting a host-virus adaptation in natural hosts.

39. Jacquelin B, Mayau V, Targat B, Liovat A-S, Kunkel D, Petitjean G, Dillies M-A, Roques P, Butor C, Silvestri G, Giavedoni LD, Lebon P, Barré-Sinoussi F, Benecke A, Müller-Trutwin MC: **Nonpathogenic SIV infection of African green monkeys induces a strong but rapidly controlled type I IFN response**. *J Clin Invest* 2009, **119**:3544-3555.

40. Bosinger SE, Johnson ZP, Folkner KA, Patel N, Hashempour T, Jochems SP, Del Rio Estrada PM, Paiardini M, Lin R, Vanderford TH, Hiscott J, Silvestri G: **Intact type I interferon production and IRF7 function in sooty mangabeys**. *PLoS Pathog* 2013, **9**:e1003597.

41. Diop OM, Ploquin MJ-Y, Mortara L, Faye A, Jacquelin B, Kunkel D, Lebon P, Butor C, Hosmalin A, Barré-Sinoussi F, Müller-Trutwin MC: **Plasmacytoid dendritic cell dynamics and alpha interferon production during Simian immunodeficiency virus infection with a nonpathogenic outcome**. *J Virol* 2008, **82**:5145-5152.

42. •• Jacquelin B, Petitjean G, Kunkel D, Liovat A-S, Jochems SP, Rogers KA, Ploquin MJ, Madec Y, Barré-Sinoussi F, Dereuddre-Bosquet N, Lebon P, Le Grand R, Villinger F, Müller-Trutwin M: **Innate immune responses and rapid control of inflammation in African green monkeys treated or not with interferon-alpha during primary SIVagm infection**. *PLoS Pathog* 2014, **10**:e1004241.
The study reveals that natural hosts of SIV infection were still able to control inflammation, even in the presence of high IFN-α levels during acute infection.

43. Sandler NG, Bosinger SE, Estes JD, Zhu RTR, Tharp GK, Boritz E, Levin D, Wijeyesinghe S, Makamdop KN, del Prete GQ, Hill BJ, Timmer JK, Reiss E, Yarden G, Darko S, Contijoch E, Todd JP, Silvestri G, Nason M, Norgren RB, Keele BF, Rao S, Langer JA, Lifson JD, Schreiber G, Douek DC: **Type I interferon responses in rhesus macaques prevent SIV infection and slow disease progression**. *Nature* 2014, **511**:601-605.

44. Bosinger SE, Li Q, Gordon SN, Klatt NR, Duan L, Xu L, Francella N, Sidahmed A, Smith AJ, Cramer EM, Zeng M, Masopust D, Carlis JV, Ran L, Vanderford TH, Paiardini M, Isett RB, Baldwin DA, Else JG, Staprans SI, Silvestri G, Haase AT, Kelvin DJ: **Global genomic analysis reveals rapid control of a robust innate response in SIV-infected sooty mangabeys**. *J Clin Invest* 2009, **119**:3556-3572.

45. Manches O, Bhardwaj N: **Resolution of immune activation defines nonpathogenic SIV infection**. *J Clin Invest* 2009, **119**:3512-3515.

46. Laguette N, Sobhian B, Casartelli N, Ringeard M, Chable-Bessia C, Ségéral E, Yatim A, Emiliani S, Schwartz O, Benkirane M: **SAMHD1 is the dendritic- and myeloid-cell-specific HIV-1 restriction factor counteracted by Vpx**. *Nature* 2011, **474**:654-657.

47. Fonteneau J-F, Larsson M, Beignon A-S, McKenna K, Dasilva I, Amara A, Liu Y-J, Lifson JD, Littman DR, Bhardwaj N: **Human immunodeficiency virus type 1 activates plasmacytoid dendritic cells and concomitantly induces the bystander maturation of myeloid dendritic cells**. *J Virol* 2004, **78**:5223-5232.

48. Eberl G, Colonna M, Di Santo JP, McKenzie ANJ: **Innate lymphoid cells: a new paradigm in immunology**. *Science* 2015, **348** aaa6566.

49. Yang Q, Bhandoola A: **The development of adult innate lymphoid cells**. *Curr Opin Immunol* 2016, **39**:114-120.

50. Walker JA, Barlow JL, McKenzie ANJ: **Innate lymphoid cells — how did we miss them?** *Nat Rev Immunol* 2013, **13**:75-87.

51. Németh T, Mócsai A: **Feedback amplification of neutrophil function**. *Trends Immunol* 2016.

52. Tecchio C, Cassatella MA: **Neutrophil-derived chemokines on the road to immunity**. *Semin Immunol* 2016.

53. Elbim C, Pillet S, Prevost MH, Preira A, Girard PM, Rogine N, Hakim J, Israel N, Gougerot-Pocidalo MA: **The role of phagocytes in HIV-related oxidative stress**. *J Clin Virol* 2001, **20**:99-109.

54. Casulli S, Elbim C: **Interactions between human immunodeficiency virus type 1 and polymorphonuclear neutrophils**. *J Innate Immun* 2014, **6**:13-20.

55. Elbim C, Katsikis PD, Estaquier J: **Neutrophil apoptosis during viral infections**. *Open Virol J* 2009, **3**:52-59.

56. Elbim C, Monceaux V, Mueller YM, Lewis MG, François S, Diop O, Akarid K, Hurtrel B, Gougerot-Pocidalo M-A, Lévy Y, Katsikis PD, Estaquier J: **Early divergence in neutrophil apoptosis between pathogenic and nonpathogenic simian immunodeficiency virus infections of nonhuman primates**. *J Immunol* 2008, **181**:8613-8623.

57. Elbim C, Monceaux V, François S, Hurtrel B, Gougerot-Pocidalo M-A, Estaquier J: **Increased neutrophil apoptosis in chronically SIV-infected macaques**. *Retrovirology* 2009, **6**:29.

58. Amano K, Hirayama M, Azuma E, Iwamoto S, Keida Y, Komada Y: **Neutrophils induced licensing of natural killer cells**. *Mediators Inflamm* 2015, **2015**:747680.

59. Costantini C, Cassatella MA: **The defensive alliance between neutrophils and NK cells as a novel arm of innate immunity**. *J Leukoc Biol* 2011, **89**:221-233.

60. Jaeger BN, Donadieu J, Cognet C, Bernat C, Ordoñez-Rueda D, Barlogis V, Mahlaoui N, Fenis A, Narni-Mancinelli E, Beaupain B, Bellanné-Chantelot C, Bajénoff M, Malissen B, Malissen M, Vivier E, Ugolini S: **Neutrophil depletion impairs natural killer cell maturation, function, and homeostasis**. *J Exp Med* 2012, **209**:565-580.

61. Bandyopadhyay K, Marrero I, Kumar V: **NKT cell subsets as key participants in liver physiology and pathology**. *Cell Mol Immunol* 2016, **13**:337-346.

62. Gapin L: **Development of invariant natural killer T cells**. *Curr Opin Immunol* 2016, **39**:68-74.

63. Matsuda JL, Gapin L, Fazilleau N, Warren K, Naidenko OV, Kronenberg M: **Natural killer T cells reactive to a single glycolipid exhibit a highly diverse T cell receptor beta repertoire and small clone size**. *Proc Natl Acad Sci U S A* 2001, **98**:12636-12641.

64. Lee PT, Benlagha K, Teyton L, Bendelac A: **Distinct functional lineages of human V(alpha)24 natural killer T cells**. *J Exp Med* 2002, **195**:637-641.

65. Takahashi T, Chiba S, Nieda M, Azuma T, Ishihara S, Shibata Y, Juji T, Hirai H: **Cutting edge: analysis of human V alpha 24+CD8+ NK T cells activated by alpha-galactosylceramide-pulsed monocyte-derived dendritic cells**. *J Immunol* 2002, **168**:3140-3144.

66. Ishihara S, Nieda M, Kitayama J, Osada T, Yabe T, Ishikawa Y, Nagawa H, Muto T, Juji T: **CD8(+)NKR-P1A (+)T cells preferentially accumulate in human liver**. *Eur J Immunol* 1999, **29**:2406-2413.

67. Fernandez CS, Chan AC, Kyparissoudis K, De Rose R, Godfrey DI, Kent SJ: **Peripheral NKT cells in simian immunodeficiency virus-infected macaques**. *J Virol* 2009, **83**:1617-1624.

68. Rout N, Else JG, Yue S, Connole M, Exley MA, Kaur A: **Paucity of CD4+ natural killer T (NKT) lymphocytes in sooty mangabeys is associated with lack of NKT cell depletion after SIV infection**. *PLoS ONE* 2010, **5**:e9787.

69. Rout N, Greene J, Yue S, O'Connor D, Johnson RP, Else JG, Exley MA, Kaur A: **Loss of effector and anti-inflammatory natural killer T lymphocyte function in pathogenic simian immunodeficiency virus infection**. *PLoS Pathog* 2012, **8**:e1002928.

70. Campillo-Gimenez L, Cumont M-C, Fay M, Kared H, Monceaux V, Diop O, Müller-Trutwin M, Hurtrel B, Lévy Y, Zaunders J, Dy M, Leite-de-Moraes MC, Elbim C, Estaquier J: **AIDS progression is associated with the emergence of IL-17-producing cells early after simian immunodeficiency virus infection**. *J Immunol* 2010, **184**:984-992.

71. Hirai T, Ishii R, Miyairi S, Ikemiyagi M, Omoto K, Ishii Y, Tanabe K: **Clonal deletion established via invariant NKT cell activation and costimulatory blockade requires in vivo expansion of regulatory T cells**. *Am J Transplant* 2016, **16**:426-439.

72. •• Reeves RK, Li H, Jost S, Blass E, Li H, Schafer JL, Varner V, Manickam C, Eslamizar L, Altfeld M, von Andrian UH, Barouch DH: **Antigen-specific NK cell memory in rhesus macaques**. *Nat Immunol* 2015, **16**:927-932.

The author show for the first time, that antigen-specific NK cell memory can be induced in primates following both infection and vaccination. These findings could impact the role of NK cells in vaccination strategies against viral infections.

73. • Schafer JL, Li H, Evans TI, Estes JD, Reeves RK: **Accumulation of cytotoxic CD16+ NK cells in simian immunodeficiency virus-infected lymph nodes associated with in situ differentiation and functional anergy**. *J Virol* 2015, **89**:6887-6894.

NK cells did not appear to be trafficking to lymph nodes (LN) during SIVmac infection. The cytotoxic subset of NK cells was increased in LN but not the cytolytic function, while Tim-3 was upregulated, indicative of an exhausted phenotype of LN NK cells in chronically infected animals.

74. Pereira LE, Johnson RP, Ansari AA: **Sooty mangabeys and rhesus macaques exhibit significant divergent natural killer cell responses during both acute and chronic phases of SIV infection**. *Cell Immunol* 2008, **254**:10-19.

75. Baumgarth N: **The double life of a B-1 cell: self-reactivity selects for protective effector functions**. *Nat Rev Immunol* 2011, **11**:34-46.

76. Mucida D, Husain MM, Muroi S, van Wijk F, Shinnakasu R, Naoe Y, Reis BS, Huang Y, Lambolez F, Docherty M, Attinger A, Shui J-W, Kim G, Lena CJ, Sakaguchi S, Miyamoto C, Wang P, Atarashi K, Park Y, Nakayama T, Honda K, Ellmeier W, Kronenberg M, Taniuchi I, Cheroutre H: **Transcriptional reprogramming of mature CD4$^+$ helper T cells generates distinct MHC class II-restricted cytotoxic T lymphocytes**. *Nat Immunol* 2013, **14**:281-289.

77. Warren WC, Jasinska AJ, García-Pérez R, Svardal H, Tomlinson C, Rocchi M, Archidiacono N, Capozzi O, Minx P, Montague MJ, Kyung K, Hillier LW, Kremitzki M, Graves T, Chiang C, Hughes J, Tran N, Huang Y, Ramensky V, Choi O-W, Jung YJ, Schmitt CA, Juretic N, Wasserscheid J, Turner TR, Wiseman RW, Tuscher JJ, Karl JA, Schmitz JE, Zahn R, O'Connor DH, Redmond E, Nisbett A, Jacquelin B, Müller-Trutwin MC, Brenchley JM, Dione M, Antonio M, Schroth GP, Kaplan JR, Jorgensen MJ, Thomas GWC, Hahn MW, Raney BJ, Aken B, Nag R, Schmitz J, Churakov G, Noll A, Stanyon R, Webb D, Thibaud-Nissen F, Nordborg M, Marques-Bonet T, Dewar K, Weinstock GM, Wilson RK, Freimer NB: **The genome of the vervet (*Chlorocebus aethiops* sabaeus)**. *Genome Res* 2015, **25**:1921-1933.

78. Bosinger SE, Jacquelin B, Benecke A, Silvestri G, Müller-Trutwin M: **Systems biology of natural simian immunodeficiency virus infections**. *Curr Opin HIV AIDS* 2012, **7**:71-78.

79. Galván-Peña S, O'Neill LAJ: **Metabolic reprograming in macrophage polarization**. *Front Immunol* 2014, **5**:420.

80. El Kasmi KC, Stenmark KR: **Contribution of metabolic reprogramming to macrophage plasticity and function**. *Semin Immunol* 2015, **27**:267-275.

81. Saez-Cirion A, Jacquelin B, Barré-Sinoussi F, Müller-Trutwin M: **Immune responses during spontaneous control of HIV and AIDS: what is the hope for a cure?** *Philos Trans R Soc Lond B Biol Sci* 2014, **369**:20130436.

82. Passaes CP, Sáez-Cirión A: **HIV cure research: advances and prospects**. *Virology* 2014, **454–455**:340-352.

Revue

Virologie

Virologie 2019, 23 (4) : 229-40

Apport des modèles animaux dans la recherche sur le VIH

Contribution of animal models to HIV research

Nicolas Huot[1]
Philippe Rascle[1,2]
Michaela Müller-Trutwin[1]

[1] Institut Pasteur,
Unité VIH, inflammation,
Institut Pasteur,
28 rue du Docteur Roux,
75015, Paris, France
<mmuller@pasteur.fr>
[2] Université Paris Diderot,
École doctorale
Bio Sorbonne Paris Cité
Paris, France

Résumé. Encore aujourd'hui, en dépit des trithérapies, l'épidémie du virus de l'immunodéficience humaine (VIH) représente un problème de santé publique majeur. Dans cette optique, la recherche reste essentielle dans la mise au point d'approches curatives et vaccinales. Les modèles animaux contribuent à la mise en place de nouvelles stratégies thérapeutiques et préventives. Nous présentons ici les caractéristiques et avancées des modèles animaux du VIH, qui sont principalement les primates non humains (macaques infectés par SIV ou SHIV et hôtes naturels du SIV), ainsi que les souris humanisées. Nous énumérerons également comment ils ont déjà permis, et permettent encore aujourd'hui, d'élargir nos connaissances sur la physiopathologie de l'infection par le VIH, la distribution tissulaire du virus, le réservoir viral, les réponses immunitaires contre le virus dans les phases très précoces de l'infection et au niveau tissulaire, tout comme dans le développement de vaccins candidats (RhCMV, anticorps à large spectre...) et essais cliniques en vue d'une guérison. Les avantages et limites des différents modèles animaux seront décrits. Tout en continuant la recherche sur des méthodes de remplacement, raffinement ou réduction du modèle animal, une bonne connaissance des spécificités de chaque modèle animal permet une utilisation adéquate par rapport aux questions scientifiques posées.

Mots clés : VIH, SIV, primates, pathogénèse, vaccins, rémission, souris humanisées

Abstract. Even today, despite triple therapy, the epidemic of the human immunodeficiency virus (HIV) is a major public health problem. In this perspective, continuous research is essential for the development of curative and vaccinal approaches. Animal models contribute to the implementation of new therapeutic and preventive strategies. We present here the characteristics of major animal models of HIV, which are non-human primates (SIV or SHIV-infected macaques and natural hosts of SIV), as well as different humanized mouse models and their advances. We will also list how they have already allowed, and still allow today, to broaden our knowledge on the physiopathology of HIV infection, tissue distribution of the virus, viral reservoirs, immunological responses against the virus in the very early infection stages and at the tissue level, but also in the development of vaccine candidates (RhCMV, broad-spectrum antibodies, etc...) and clinical trials for a cure. The advantages and limitations of the different animal models will be described. While continuing research on alternative methods, refinement or reduction of the animal model, a good knowledge of the specificities of each animal model allows an adequate use in relation to the scientific questions addressed.

Key words: HIV, SIV, primates, pathogenesis, vaccines, remission, cure, humanized mice

Correspondance : M. Müller-Trutwin
<mmuller@pasteur.fr>

Copyright © 2020 John Libbey Eurotext. Téléchargé par INSTITUT PASTEUR le 09/08/2020.

doi:10.1684/vir.2019.0783

Pour citer cet article : Huot N, Rascle P, Müller-Trutwin M. Apport des modèles animaux dans la recherche sur le VIH. *Virologie* 2019; 23(4) : 229-40 doi:10.1684/vir.2019.0783

Introduction

Trente-six ans après sa découverte, l'épidémie du virus de l'immunodéficience humaine (VIH) continue à poser un problème de santé publique. Par conséquent, réduire le nombre de nouvelles infections *via* la mise au point de nouveaux outils et stratégies de prévention reste une priorité. L'introduction de la combinaison d'antirétroviraux efficace (cARV) a été un élément clé pour allonger l'espérance de vie des personnes séropositives et transformer une maladie jadis mortelle en une infection chronique. Le traitement cARV devrait au-delà contribuer à diminuer le nombre de nouvelles infections [1]. Toutefois, l'action de cette thérapie cARV ne permet pas d'éradiquer le réservoir viral faisant de celui-ci un obstacle majeur à la guérison du VIH [2]. L'étude de nouvelles approches thérapeutiques et préventives des infections humaines par le VIH passe, entre autres, par le développement de modèles animaux permettant aux études pharmacologiques et pré-cliniques d'évaluer la pertinence de la stratégie choisie. Après plus de 30 ans d'intenses investigations, nous manquons encore de connaissances nécessaires au développement d'un vaccin contre le VIH sûr et efficace. La lente évolution clinique de l'infection par le VIH, la complexité des interactions entre le virus et son hôte, le nombre considérable de dysfonctionnements immunitaires engendrés directement ou indirectement par la réplication virale, l'établissement de réservoirs viraux dans les tissus, ainsi que l'atteinte du système nerveux central rendent impossible toute approche exclusivement *in vitro*. La mise en place d'outils pour l'étude des réponses immunitaires et du génome chez les primates non humains (PNH), le développement de meilleurs modèles murins humanisés [3] ainsi que de nouveaux virus recombinants ont augmenté la pertinence des modèles disponibles [4]. Il est cependant essentiel d'en définir les avantages et limites dans le cadre du développement de vaccins et de nouvelles stratégies curatives du VIH, mais également de continuer les efforts de diminution du nombre d'animaux et de méthodes de remplacement.

L'apport des primates non humains dans la recherche sur le VIH

La mise en place de modèles animaux ayant pour but de mieux comprendre la maladie a été une des difficultés rencontrées après la découverte du VIH. Cette difficulté tient au fait que le VIH-1 possède un tropisme strictement limité aux humains et aux chimpanzés. C'est pourquoi les premiers modèles animaux utilisés pour lutter contre le VIH furent les chimpanzés, modèles qui aujourd'hui ont été abandonnés pour des raisons éthiques évidentes [5].

Le premier lentivirus simien fut isolé en 1985 chez des macaques détenus en captivité et nommé SIVmac (*Simian Immunodeficiency Virus* [SIV]) [6]. Ces singes présentaient des symptômes cliniques identiques au syndrome d'immunodéficience acquise (sida) chez l'homme. Cependant, l'infection par le SIV n'existe pas chez les macaques sauvages, ni chez d'autres singes asiatiques dans leur habitat naturel. Seuls les primates d'Afrique sont porteurs du lentivirus à l'état sauvage. La première espèce de primate d'Afrique identifiée comme porteur naturel de ce lentivirus fut le mangabey enfumé (« *sooty mangabey* » en anglais). Cette espèce est porteuse du virus SIVsm [7]. Par la suite, il a été montré que l'infection SIV chez les macaques résultait de transmissions expérimentales de tissus provenant de mangabeys enfumés infectés par le SIVsm et maintenus en captivité dans les mêmes centres de primatologie.

Les similitudes frappantes, qui existent entre le sida induit chez l'homme infecté par le VIH-1 et la maladie induite par le SIVmac chez les macaques, ont fait de ces derniers un modèle très important pour l'étude de la pathogénie de ces virus. Les études chez les primates PNH ont contribué à définir et mieux caractériser les principaux paradigmes de la pathogenèse de l'infection par le VIH. Les modèles PNH sont utilisés pour tester divers traitements et sont essentiels dans la recherche d'un vaccin contre le VIH [8].

Modélisation de l'infection par le VIH chez le modèle macaque

Les PNH présentent certains avantages dans l'étude de l'infection au VIH, car ils permettent de contrôler le moment, la dose et la voie d'inoculation du virus. Ces modèles permettent l'étude des premières heures de l'infection, ainsi que de prélever des échantillons de tissus qui, pour des raisons éthiques et logistiques, sont difficiles à prélever chez l'homme (par exemples, les muqueuses vaginale et rectale, les ganglions lymphatiques, la rate, les poumons, le foie ou le cerveau...) [9].

Les macaques peuvent être infectés par voie vaginale ou rectale pour modéliser la transmission sexuelle du VIH-1, par inoculation orale pour modéliser la transmission du lait maternel de la mère à l'enfant et par inoculation intraveineuse. De plus, les macaques infectés et traités avec les antirétroviraux permettent de modéliser l'infection par le VIH-1 chez des patients sous trithérapie [10].

Une des questions posées lorsque l'on utilise un modèle animal pour des études de vaccins candidats, consiste à déterminer si la dose et le mode d'administration de l'agent pathogène inoculé correspond à une réalité biologique. Les premières études menées chez les PNH utilisaient des doses suffisamment élevées de virus injectées par voie

Copyright © 2020 John Libbey Eurotext. Téléchargé par INSTITUT PASTEUR le 09/08/2020.

intraveineuse pour obtenir un taux d'infection égale ou supérieur à 100 %. Cependant, la relevance de ce choix a été questionnée dans le cadre d'études sur l'efficacité de candidats vaccins ou de microbicides étant donné la quantité de virus généralement plus faible présente lors d'une infection par le VIH pendant un rapport sexuel. De plus, l'injection de virus par voie intraveineuse ne permet pas d'étudier les premières étapes de la dissémination du virus au sein des muqueuses génitales [11, 12]. Afin de répondre à ces questions, des modèles d'exposition répétée à faible dose de virus par voie mucosale ont été développés [13-16]. Ces expériences ont des conséquences importantes sur le coût et la gestion des protocoles expérimentaux. En effet, ce type d'expérimentation nécessite la production d'une plus grande quantité de stock viral. Surtout, en raison de la faible fréquence d'infection, cela oblige à augmenter le nombre d'animaux de l'étude. En dépit de cela, les infections par voie mucosale à forte dose ont été d'un apport considérable dans la compréhension de la physiopathologie des premiers jours de l'infection et ont contribué à comprendre comment le virus pénètre et se dissémine au travers des muqueuses.

Diversité des modèles de pathogenèse

L'infection du macaque par le SIV entraîne une infection persistante dans laquelle la progression vers le sida se produit généralement de manière similaire à celle chez les individus infectés par le VIH [17]. Parmi l'ensemble des PNH, trois espèces sont principalement utilisées dans la recherche sur le VIH. Il s'agit du macaque rhésus (*Macaca mulatta*), du cynomolgus macaque (*Macaca fascicularis*) et du macaque à queue de cochon (*Macaca nemestrina*). Chacune de ces espèces montre des susceptibilités distinctes au sida et qui varient selon le SIV *(figure 1)*.

Les macaques rhésus (RM) d'origine indienne sont souvent infectés soit par l'isolat SIVmac251, soit par le clone moléculaire dérivé du SIVmac251, le SIVmac239. Ces deux virus reproduisent la physiopathologie de l'infection VIH-1, ce qui comprend une charge virale plasmatique souvent élevée, une déplétion immédiate et durable des cellules T $CD4^+$ au sein des muqueuses, ainsi qu'une activation chronique du système immunitaire [18, 19]. Les RM d'origine chinoise infectés par le SIVmac239/251 représentent un autre modèle d'intérêt pour la recherche sur le VIH. Comparativement aux RM indiens, les RM chinois infectés par le SIVmac239 ont une charge virale plasmatique moins élevée et une dynamique des marqueurs immunologiques plus proche de celle observée chez l'homme [20]. En revanche, le macaque à queue de cochon infecté par le SIV représente un modèle de progression rapide, pour lequel la progression vers l'état sida se fait souvent en trois mois. Dans ce modèle, la plupart des animaux développent une inflammation intestinale importante et des maladies du système nerveux central [21]. Le modèle de neuro-sida chez le macaque a beaucoup été utilisé pour étudier par exemple le rôle des macrophages dans l'inflammation et le réservoir viral au niveau du cerveau [21, 22]. Enfin, les macaques cynomolgus infectés par le SIVmac présentent des niveaux de virémie et de progression variables selon la dose virale et la voie d'infection. Ils ont été utilisés notamment pour étudier des mécanismes de contrôle de la réplication virale [23-26].

Apport des modèles PNH pour la compréhension de la physiopathologie de l'infection par le VIH

De manière tout à fait remarquable, ces animaux peuvent reproduire, une fois infectés, tous les profils d'évolution distincte de l'infection observés chez l'homme. Ainsi, certains animaux peuvent progresser rapidement (quelques mois) vers un état sida, alors que la majorité développera un état sida après une période d'infection chronique s'étalant sur plusieurs mois/années, et enfin une minorité d'entre eux contrôleront l'infection spontanément, mimant les contrôleurs du VIH (« *elite controllers* » ou « *HIV controllers* » en anglais) [27]. Ces différences sur le devenir de l'infection sont dépendantes d'une combinaison de facteurs entre le virus et son hôte, tels que l'espèce de singe étudié (les macaques rhésus progressant généralement plus vite que les macaques cynomolgus), la souche virale inoculée (le clone SIVmac239 étant plus virulent que l'isolat SIVmac251), ainsi que le fond génétique des animaux infectés. En effet, comme chez l'homme, où certains haplotypes, tels que HLA (*human leukocyte antigen*)-B*27/57 sont protecteurs, la charge virale peut varier selon des facteurs génétiques chez les PNH, notamment les complexes majeurs d'histocompatibilité (CMH)-I et TRIM5α [28-30]. Le choix du modèle d'études dépendra donc grandement de la question qui sera posée. Cependant, et en partie à cause du coût élevé et de la logistique considérable nécessaire, seul un nombre limité d'études a été réalisé pour clairement comparer la physiopathologie de l'infection par les lentivirus de primates dans différentes espèces de macaques. De plus, la variabilité des paramètres utilisés entre les laboratoires, rend parfois difficile la comparaison des résultats obtenus dans les différents modèles.

En plus de ces différents modèles de macaque, la recherche fait également recours à des PNH d'origine africaine comme le singe vert d'Afrique (AGMs) (genre *Chlorocebus*), le mangabey enfumé (SM) (*Cercocebus atys*) et le mandrill (*Mandrillus sphinx*) [31]. Ces trois espèces simiennes sont nommées les porteurs naturels de virus SIV.

Copyright © 2020 John Libbey Eurotext. Téléchargé par INSTITUT PASTEUR le 09/08/2020.

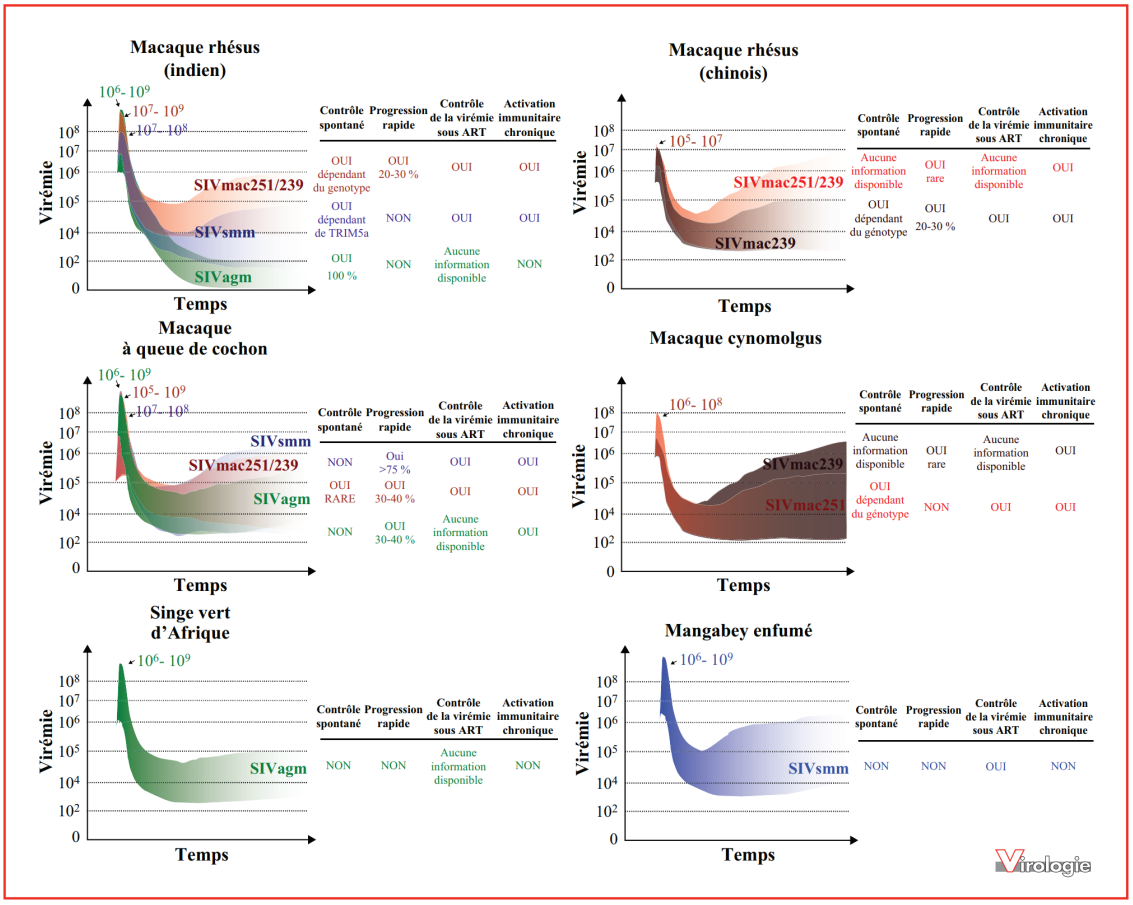


Figure 1. Principaux modèles d'infection par le SIV chez les primates non humains utilisés dans la recherche sur le VIH. Représentation non exhaustive des différents modèles de primate non humain utilisés le plus fréquemment dans la recherche sur le VIH. Les espèces simiennes sont indiquées. Les courbes de couleurs représentent la variation de la charge virale plasmatique pour un virus donné en fonction du temps. Les principales caractéristiques de chaque modèle sont indiquées dans les tableaux adjacents au graphique. Les études qui ont été réalisées avec le SIVmac239/251 chez le macaque rhésus chinois et macaque cynomolgus sont moins fréquentes que celles chez les singes macaques rhésus indiens. Or la charge virale mesurée peut grandement varier selon plusieurs paramètres comme l'espèce et le fond génétique de l'hôte, son âge, la souche virale, les techniques du laboratoire pour ne citer qu'eux.

Ces hôtes naturels du SIV ne développent généralement pas de sida, contrairement aux macaques, et cela malgré une charge virale plasmatique très élevée. Il est à noter que l'infection de SIVsm chez le macaque ou l'infection de certains isolats SIVagm chez le macaque à queue de cochon aboutit à un sida *(figure 1)*.

Les hôtes naturels ont été utilisés pour définir des corrélats de protection et servent à comprendre quels mécanismes sont impliqués pour éviter la progression vers l'état sida. Des études comparatives entre les infections SIV pathogènes chez les macaques et les infections SIV non pathogènes chez l'hôte naturel ont montré que le niveau de virémie n'est pas le facteur déterminant de la progression vers la maladie. Elles ont été essentielles à mieux appréhender le rôle clé de l'inflammation chronique dans la progression vers la maladie [32]. L'étude des modèles d'infection non pathogène a participé aux changements du paradigme de la pathogenèse du VIH, une charge virale élevée n'étant plus le déterminant unique de la progression vers le sida. Ces travaux ont contribué à attirer l'attention sur l'inflammation résiduelle qui persiste même chez des individus avirémiques et à mieux appréhender l'importance de contrôler l'infection dès les phases précoces de l'infection [33]. L'inflammation est résolue rapidement et efficace-

Copyright © 2020 John Libbey Eurotext. Téléchargé par INSTITUT PASTEUR le 09/08/2020.

ment chez l'hôte naturel. Les mécanismes à l'origine de ce contrôle efficace de l'inflammation ne sont pas encore totalement élucidés [32].

Les PNH ont grandement participé à notre compréhension d'autres éléments de la physiopathologie de l'infection par le VIH. À titre d'exemple, l'infection de macaques permet l'étude des mécanismes mis en jeu dans la destruction de l'intégrité de la barrière intestinale et des réseaux des cellules dendritiques folliculaires aux niveaux des follicules dans les organes lymphoïdes secondaires [34-36]. Ces études ont ainsi dévoilé le rôle joué par les cellules T régulatrices et le TGF-β dans les étapes conduisant à la fibrose au sein des ganglions lymphatiques de macaques chroniquement infectés [37-39]. Ces dommages ne sont que partiellement réversibles après la mise sous traitement cARV [40]. Contrairement aux modèles macaques, les hôtes naturels ne montrent pas de dommages tissulaires en phase chronique de l'infection. L'étude de l'hôte naturel pourrait donc dans le futur apporter des connaissances sur les mécanismes de protection de ces tissus en dépit de l'infection [32].

Les modèles de PNH pour l'étude du réservoir viral

L'introduction de protocoles permettant de traiter les macaques infectés par SIVmac par cART a profondément impliqué le modèle PNH dans l'étude du réservoir viral [41]. Un des obstacles majeurs rencontré pour établir une guérison totale de l'infection par le VIH tient au fait que le virus se dissémine rapidement après la primo-infection et établit des réservoirs viraux persistants dans de nombreux tissus [42, 43]. Les travaux chez le macaque ont permis de démontrer que l'ensemencement du réservoir est un événement extrêmement rapide qui se produit avant que la virémie plasmatique ne soit détectable [41, 44, 45].

Après avoir atteint les organes lymphoïdes secondaires, véhiculé entre autres par les cellules dendritiques, le virus s'y réplique massivement où il finit par gagner les centres germinatifs [46]. Dans les centres germinatifs, le virus infecte les cellules T auxiliaires folliculaires (TFH) [47]. L'utilisation des modèles PNH a contribué à mettre en évidence que les cellules TFH infectées constituent un des réservoirs cellulaires majeurs chez des sujets ayant une virémie indétectable [48, 49]. En effet, il a été montré que les animaux contrôleurs du SIVmac ont une réplication virale qui persiste à bas bruit dans les cellules TFH des centres germinatifs [50]. Cette persistance du virus est principalement attribuée à l'incapacité des cellules T $CD8^+$ cytotoxiques à migrer dans les centres germinatifs pour éliminer le virus, ce qui fait de ce compartiment un sanctuaire pour le SIV/VIH [51]. Cette même observation a ensuite été réalisée chez l'homme et chez des animaux traités par des antirétroviraux. Dans ce contexte, il est important de garder en mémoire que la diffusion des antirétroviraux dans ces tissus est peu efficace [52]. Le modèle primate joue un rôle important pour étudier la biodisponibilité tissulaire des drogues dirigées contre le VIH/SIV [53].

L'étude des organes lymphoïdes secondaires chez l'hôte naturel a mis en évidence une réplication virale élevée lors du pic de virémie, mais qui est ensuite fortement contrôlée jusqu'à devenir indétectable chez certains animaux [54]. L'infection par le SIV est par ailleurs généralement absente au sein des TFH de l'AGM et faible chez le SM. Ainsi, l'hôte naturel semble tolérer la virémie élevée dans le sang et les muqueuses, mais a développé des mécanismes de protection des organes lymphoïdes secondaires. Cette distribution tissulaire pourrait expliquer en partie le ratio plus faible d'infection de cellules T auxiliaires mémoires, et un ratio plus élevée de cellules T auxiliaires effectrices chez l'hôte naturel comparativement au modèle pathogène [55-57].

Vers une stratégie curative de l'infection par le VIH-1 : l'apport des modèles de PNH

Le traitement par trithérapie seul n'est pas suffisant pour éliminer le VIH de l'organisme. Il est nécessaire d'intensifier la recherche vers de nouvelles stratégies ayant pour but une élimination du réservoir viral. Cependant, de telles études ne peuvent pas toujours être menées chez l'homme. Les modèles animaux contribuent à l'étude de la réponse immunitaire au niveau des tissus. Grâce à des approches de déplétion *in vivo* de certains types de cellules immunes, il est par exemple possible de comprendre, si ceux-ci sont susceptibles d'affecter la réplication virale. Ce type d'approche a formellement démontré le rôle des cellules T $CD8^+$ dans le contrôle de la réplication virale chez le macaque ainsi que le rôle des cellules *natural killer* (NK) dans le contrôle de la réplication virale au sein des ganglions lymphatiques chez des hôtes naturels. Il a ainsi été montré que les singes verts d'Afrique infectés par le SIVagm, les cellules NK sont capables de pénétrer à l'intérieur des centres germinatifs en augmentant l'expression à leur surface du récepteur CXCR5 et de supprimer la réplication virale au sein des cellules $CD4^+$ TFH [55]. Ceci questionne le rôle sous-estimé des cellules NK dans la régulation des réservoirs viraux et ouvre la piste à de nouvelles stratégies thérapeutiques et vaccinales ciblant ces cellules.

Un autre aspect intéressant des VIH et SIV est qu'ils partagent les mêmes mécanismes aboutissant à la persistance virale. Le génome du VIH/SIV s'intègre dans le génome de la cellule cible [58, 59], avec selon certaines études des sites d'intégration préférentiels communs entre les deux

Copyright © 2020 John Libbey Eurotext. Téléchargé par INSTITUT PASTEUR le 09/08/2020.

virus [60]. La réponse interféron est capable de favoriser la persistance de l'ADN viral dans les cellules infectées simiennes et humaines en jouant sur les mécanismes épigénétiques (désacétylation des histones) [61]. L'entrée en latence du virus peut se faire sans co-stimulation du T-*cell receptor* (TCR) [62]. La distribution des cellules contenant du génome viral intégré au sein des différents tissus (sang, organes lymphoïdes secondaires, intestin. . .) a été rapporté être similaire entre l'homme et les PNH [63-65]. Ainsi, ces observations suggèrent que la dynamique du réservoir viral est identique à ce que l'on retrouve chez l'homme. Des différences existeront néanmoins toujours entre l'infection SIV chez le singe et l'infection VIH chez l'homme. Notamment, chez les PNH, la durée du traitement est généralement de plusieurs années plus courte que chez l'homme, ce qui peut influencer les données observées. En absence d'autres modèles aussi puissants, le modèle singe reste toutefois un outil important pour étudier des stratégies curatives contre le VIH.

De nombreuses approches curatives sont actuellement en cours d'étude. Ces modèles permettent par exemple d'évaluer la biosécurité et l'efficacité d'agents révertants de la latence virale. Il a ainsi été montré que l'administration d'un inhibiteur d'histone désacétylase (HDAC), chez des macaques infectés et placés sous trithérapie, ne permet pas de mettre en évidence une augmentation significative de la réactivation virale [66]. De plus, le mode d'action de ce type de molécules semble affecter négativement les réponses des lymphocytes T $CD8^+$ contre le virus et plus particulièrement leurs capacités à produire de l'interféron-γ [66]. Plus récemment, l'administration de l'auranofine, qui est un complexe d'or organique utilisé comme traitement contre la polyarthrite rhumatoïde, a mis en avant une réduction significative du réservoir viral chez des macaques rhésus infectés sous trithérapie, et un délai accru du rebond viral après cessation de tout traitement [67]. Ces animaux permettent aussi d'étudier l'action de ces molécules dans différents contextes. L'administration d'agents révertants de la latence peut être réalisée par exemple chez des animaux contrôleurs naturels ou sous traitement antirétroviraux et à l'inverse chez des animaux où la réplication virale n'est pas contrôlée. Réaliser de telles études en absence de cARV chez l'homme ne serait éthiquement pas possible. Beaucoup d'autres approches sont en cours d'étude en utilisant différentes stratégies, y compris des vaccins candidats, ciblant soit les réservoirs viraux, les cellules immunes ou de facteurs cellulaires [37, 68-71].

Globalement, l'utilisation de modèles animaux est pour l'instant, en absence d'autres modèles physiopathologiques meilleurs, indispensable pour aborder certaines questions dans le domaine des mécanismes d'établissement des réservoirs viraux tissulaires et de leur régulation.

Vers une stratégie vaccinale de l'infection par le VIH : l'apport des modèles de PNH

Malgré d'intensives recherches, un vaccin contre le VIH n'existe toujours pas. Afin de contrôler au mieux l'épidémie, la mise au point d'un vaccin contre le VIH reste une des priorités majeures dans le domaine [72]. Dans ce contexte, les modèles PNH sont d'une utilité incontestable. Tout en sachant qu'il n'est pas toujours possible de transposer les données obtenues chez le singe à l'homme, ceux-ci permettent de tester des stratégies qui pourraient s'avérer risquées si elles étaient testées chez l'homme [73]. De plus, les PNH sont indispensables pour évaluer la dissémination du virus et les réponses immunitaires dans les tissus. Les modèles primates ont contribué à mieux comprendre les mécanismes d'échappement du virus aux cellules T CD8 cytotoxiques [74, 75]. C'est dans le modèle macaque que la preuve du concept que d'administration d'anticorps neutralisants à large spectre (bNAbs) confère une protection contre l'infection a été obtenue. Ceci a été réalisé avec des SIV chimériques exprimant la glycoprotéine d'enveloppe (Env) du VIH-1 (SHIV) [76]. Les anticorps neutralisants à large spectre se sont révélés difficiles à obtenir par immunisation. Afin de permettre leur induction, des vecteurs du virus adéno-associé recombinant (AAVs) ont été développés pour permettre la délivrance directe de gènes d'immunoglobuline de spécificité prédéterminée. Dans ce contexte, il a pu être montré chez des macaques rhésus qu'une seule inoculation intramusculaire d'AAV exprimant un bNAb spécifique pour l'enveloppe du virus, était suffisante pour obtenir des anticorps neutralisants circulants et permettant une protection des animaux contre une inoculation du virus par voie intraveineuse [77]. D'autres approches sont en cours et consistent par exemple dans des immunisations répétitives avec des antigènes évolutifs.

Des stratégies vaccinales visant à induire les réponses T $CD8^+$ anti-VIH sont également sous étude. À titre d'exemple, des études réalisées à l'aide de vecteurs vaccinaux à base de virus herpès recombinants ont montré des résultats intéressants. Ainsi, l'immunisation de macaques rhésus avec des vecteurs de cytomégalovirus de rhésus (RhCMV) exprimant des antigènes du SIV permet l'éradication du SIV chez environ 50 % des animaux immunisés [78]. Des lymphocytes T mémoires effecteurs spécifiques du SIV sont retrouvés abondamment aux sites connus de réplication du SIV et l'induction de ces cellules T $CD8^+$ effectrices semble pérenne. Ce modèle de protection se distingue par différents aspects, comme l'absence d'anticorps spécifiques à l'enveloppe virale (malgré l'inclusion d'un vecteur exprimant Env) et des réponses T $CD8^+$ HLA-E dépendantes.

Copyright © 2020 John Libbey Eurotext. Téléchargé par INSTITUT PASTEUR le 09/08/2020.

Copyright © 2020 John Libbey Eurotext. Téléchargé par INSTITUT PASTEUR le 09/08/2020.

En conclusion, le PNH est un modèle d'étude important pour la compréhension de la physiopathologie du VIH et les études curatives et vaccinales. L'étude des macaques a apporté une meilleure connaissance sur les interactions virus-hôte très précoces, la dissémination virale, les réservoirs viraux ou encore les réponses immunes tissulaires [79]. De plus, les modèles macaques peuvent être utiles pour l'étude des traitements antirétroviraux, comme dans le cas de suivis pharmacocinétiques au niveau tissulaire. Ils ont contribué au développement de ce que l'on connaît aujourd'hui sous le nom de la prophylaxie préexposition [80]. Dans le futur, ils pourront peut-être aider à développer un vaccin efficace et à expliquer les mécanismes présents chez les rares personnes qui ont contrôlé la charge virale après l'arrêt du traitement antirétroviral. En outre, tout comme les macaques, les hôtes naturels du SIV ont apporté de nouvelles connaissances. Ce modèle a souvent poussé les dogmes et l'idée de ce que pouvait être le contrôle de l'infection chez un individu, promulguant ainsi de nouveaux concepts qui pourront éventuellement être traduits un jour par des immunothérapies pouvant contribuer à une rémission durable du VIH.

Vue d'ensemble des modèles murins utilisés dans la recherche sur le VIH

Les cellules murines sont résistantes à l'infection par le VIH. Des souris humanisées ont alors été développées pour étudier l'infection par le VIH, afin de remplacer en partie le modèle PNH dans un modèle animal plus petit. La notion de souris humanisée se rapporte à toute modification génétique d'une souche murine permettant l'expression de gènes humains. Cette notion englobe une vaste étendue de modifications génétiques allant du simple ajout de transgènes jusqu'à l'implantation de cellules souches dans des souris immunodéprimées facilitant ainsi la reconstitution d'un système immunitaire humanisé. Ce chapitre va décrire les principaux modèles murins ainsi que les découvertes récentes dans le domaine de la recherche sur le VIH réalisées grâce à leurs utilisations.

Le début des modèles murins humanisées

Afin de limiter le rejet des cellules humaines transplantées par le système immunitaire de la souris receveuse, des souris immunodéficientes ont dû être utilisées. Ainsi, des souches murines arborant diverses mutations conduisant à une diminution, voire une abrogation de leur système immunitaire ont été sélectionnées. C'est en 1966 que la première souche murine ne possédant pas de cellules T $CD4^+$ et $CD8^+$ matures fut décrite. Cette absence de maturation est le résultat d'une mutation dans le gène *Foxn1mu* qui conduit à une absence de maturation des cellules T dans le thymus. Cette mutation entraîne aussi une diminution de la pilosité, ce qui a conduit à baptiser cette souche de souris, les souris *nude* athymiques.

En 1983, les souris CB17-SCID (*severe combined immunodeficiency*) ont été obtenues [81]. Elles se caractérisent par une mutation autosomale récessive du gène *prkdc* (*protein kinase DNA activated catalytic polypeptide*). Celui-ci code une protéine jouant un rôle dans les mécanismes de réparation de l'ADN, et dont l'action est indispensable aux recombinaisons V(D)J nécessaires aux réarrangements des récepteurs des cellules T et B.

Afin d'accentuer l'immunodéficience des souches murines, des souris ont été mutées pour les gènes *RAG1* et *RAG2* ($RAG1^{-/-}$ et $RAG2^{-/-}$) *(tableau 1)*. Les gènes *RAG1* et *RAG2* codent des protéines indispensables au réarrangement des TCR et B-*cell receptor* (BCR) présents sur les cellules T et B respectivement. En les bloquant, la réponse immunitaire spécifique dans ces souris est perdue [82]. Ainsi, grâce à une plus faible activité résiduelle du système immunitaire, ces souches murines ont historiquement beaucoup été utilisées pour mener des études de transplantation de tissus humains et d'infusion de cellules humaines. Cependant, des limites majeures sont très vite apparues. En effet dans ces modèles, la forte activité du système immunitaire innée et notamment celle des cellules NK limite la prise de greffe de cellules humaines provenant de tissus hématopoïétiques fœtaux (foie, thymus) et/ou celle de cellules progénitrices hématopoïétiques (CPH) $CD34^+$, empêchant ainsi le développement d'un système immunitaire humanisée complet.

Une avancée majeure fut faite à partir de souris portant une mutation dans la chaîne gamma du récepteur à l'interleukine-2 (*IL2rg ou IL2*γ_c), perturbant ainsi l'activité des cytokines IL-2, IL-4, IL-7, IL-9, IL-15 et IL-21, qui sont indispensables pour le fonctionnement du système immunitaire, et notamment pour les cellules NK, qui sont complètement absentes chez cette souche murine. Avec l'objectif de perfectionner le blocage du système immunitaire de la souris receveuse, des croisements ont alors été entrepris entre les différentes souches précédemment décrites et la souche murine NOD-SCID. Le croisement entre des souches murines *IL-2*γ_c et des souris NOD-SCID a permis de générer des souris NOD-SCID-$\gamma c^{-/-}$ appelées souris (NSG), et le croisement entre des souches murines *IL-2*γ_c avec les souris BALB/c-$Rag2^{-/-}$ de générer les souris dites BRG.

Tableau 1 Principaux modèles de souris humanisées utilisés dans la recherche sur le VIH-1.

	HIV-SCID-hu	HIV/hu-HSC	HIV/BLT
Méthode d'obtention	Souris SCID transplantée avec du thymus et du foie d'embryon humain	Souris NOD/NSG, irradiée et transplantée avec des cellules souches humaines	Souris NOD/NSG, irradiée et transplantée avec des cellules souches humaines et du thymus / foie d'embryon humain
Délai nécessaire pour leur obtention (à partir de leur naissance)	5-7 mois	2-3 mois	5-7 mois
Cellules du système immunitaire humain reconstituées	Cellules T	Cellules T, cellules B, cellules dendritiques	Cellules T, cellules B, cellules dendritiques, cellules NK, monocytes, macrophages
Distribution des cellules reconstituées	Limité à l'implant thymus et foie	Moelle osseuse, structures lymphoïdes secondaires	Moelle osseuse, organes lymphoïdes secondaires, muqueuses (intestin, appareil reproductif)
Durée de l'infection par le VIH-1	Environ 1 an (dépend du greffon)	6-7 mois	Plus d'un an
Charge virale plasmatique (copies/mL)	10^4-10^5	10^7	10^4-10^5

Les modèles de souris humanisées dans la recherche sur le VIH

C'est à partir de ces premières souris mutantes que la première expérience d'infection par le VIH a été menée. Ces modèles étaient limités, car les cellules immunitaires ne maturent pas chez ces souris, mais proviennent comme mentionné ci-dessus, de transfusions de cellules humaines isolées à partir du sang, donc sans renouvellement possible. Mener des études sur une longue période de temps est presque impossible à réaliser pour les mêmes raisons.

C'est alors qu'il a été entrepris de générer des souris dans lesquelles une hématopoïèse complète pourrait avoir lieu. C'est à partir des souches NSG et BRG que les processus d'humanisation plus complexes ont principalement été effectués, car celles-ci sont dépourvues de cellules T, B, NK, ne développent pas spontanément de tumeurs et sont génétiquement très stables. Afin d'obtenir des souris avec un système immunitaire complet aux propriétés humaines, il est important de garder en mémoire que la procédure d'humanisation chez ces souris mutantes est difficile. Il existe, à ce jour, quatre approches expérimentales permettant de réaliser cette tâche avec des ajustements de procédure pouvant varier d'une expérience et d'un laboratoire à l'autre et qui ne seront pas détaillées dans cette revue.

À ce jour, trois modèles sont principalement utilisés dans la recherche sur le VIH. Ces modèles sont capables de générer une réponse adaptative complète ou partielle et permettent la dissémination du virus à partir de différentes voies d'inoculation.

Le premier modèle utilisé est le modèle de souris SCID-thymus/foie humanisées (SCID-hu-thy/liv), dans lesquelles des cellules du thymus et du foie humains sont implantées sous la capsule rénale. Cette implantation permet aux cellules souches du foie ($CD34^+$) de générer à travers le thymus des cellules T $CD4^+$ et $CD8^+$ naïves [83]. Une des limites de ce modèle est le faible niveau de cellules T humaines systémiques. Le second modèle murin humanisé utilisé dans la recherche sur le VIH est le modèle de moelle osseuse/foie/thymus (BLT). Celui-ci a été obtenu par transplantation de cellules progénitrices de l'hématopoïèse $CD34^+$ humaines dans des souris NSG préalablement implantées avec du thymus et du foie [84-86]. Ce modèle permet une éducation active des lymphocytes T humains par une thymopoïèse proche de celle observée chez l'homme, ce qui aboutit à des réponses T humaines restreintes par le CMH de classe I. Cependant, bien que le modèle BLT soit une avancée majeure, celui-ci reste coûteux et lourd à développer, principalement en raison des procédures chirurgicales compliquées (co-implantation de fragments de tissus multiples sous la capsule rénale) et un accès au matériel limité (thymus et tissu hépatique humain), limitant son utilisation pour la recherche. Une alternative à ce modèle est la souris *human hematopoietic stem cell* (Hu-HSC) [87]. Celui-ci est obtenu par seule transplantation de cellules souches humaines dans des souris BRG ou

Copyright © 2020 John Libbey Eurotext. Téléchargé par INSTITUT PASTEUR le 09/08/2020.

Copyright © 2020 John Libbey Eurotext. Téléchargé par INSTITUT PASTEUR le 09/08/2020.

NSG préalablement conditionnées par radiation. Comme pour le modèle BLT, une distribution systémique des cellules B, des cellules T, des monocytes/macrophages, des cellules NK et des cellules dendritiques est observée. Mais contrairement au modèle BLT, la maturation des cellules T se fait dans le thymus murin empêchant ainsi une réponse adaptative dépendante du CMH-I. Dans chacun des modèles BLT ou Hu-HSC, les souris sont capables d'une forte production d'anticorps (IgG) après leur immunisation avec des antigènes T-dépendants *in vivo* [88]. Elles produisent aussi des cytokines pro-inflammatoires en réponse au LPS [89]. De plus, ces souris sont sensibles à l'infection par le VIH et au traitement antirétroviral. Dans le modèle BLT, les cellules T $CD4^+$ non activées ($CD4^+$ $CD27^+$ $CCR7^+$) infectées de manière latente sont présentes à des niveaux comparables à ceux présents chez les patients humains soumis à un traitement antirétroviral [86, 90].

Les récentes avancées dans la recherche sur le VIH : apport des modèles murins

Dans ce chapitre, nous allons développer les avancées récentes faites dans la compréhension de la physiopathologie de l'infection par le VIH et comment ces modèles sont utilisés pour développer de nouvelles stratégies antivirales.

Il est communément admis que, dans les premiers jours de l'infection, l'établissement du VIH est partiellement conditionné par des facteurs produits par l'hôte. Un de ces facteurs est l'interféron de type I qui, *via* l'induction de chimiokines, permet le recrutement de nouvelles cibles pour le virus [32, 91]. Cependant, l'interféron de type I peut aussi jouer un rôle important pour contenir la dissémination du virus. Des études réalisées chez les primates non humains a montré qu'une neutralisation du récepteur à l'interféron de type I accélère la progression de l'infection vers un état sida [92]. En revanche, la production constante d'interféron observée durant la phase chronique, même chez des personnes sous antirétroviraux, pourrait participer à l'exacerbation et à l'épuisement du système immunitaire facilitant ainsi la persistance du virus. C'est afin de mieux comprendre le rôle joué par l'interféron de type I dans l'infection par le VIH que des études ont été réalisées dans des souris humanisées. Récemment, deux études ont montré que bloquer les récepteurs à l'interféron de type 2 (IFNAR2), ou la voie de signalisation des récepteurs à l'interféron de type α/β (IFNAR1) à l'aide d'anticorps neutralisants chez des souris (BLT, hu-HSC ou NRG) chroniquement infectées par le VIH, permettait de diminuer l'épuisement du système immunitaire (diminution de l'expression de TIM-3 et PD-1 à la surface des cellules T), ainsi que la réplication virale [93]. De plus, en combinant ce traitement aux antirétroviraux, il a été montré une diminution des réservoirs viraux dans les organes lymphoïdes secondaires, permettant d'augmenter le délai du rebond viral lors de l'arrêt du traitement.

Afin de déterminer quel sous-type d'interféron participe au contrôle de la réplication virale *in vivo*, des souris $Rag2^{-/-}\gamma c^{-/-}CD47^{-/-}$-BLT ont été infectées par le VIH [94]. Cette étude montre une forte capacité antivirale du sous-type d'interféron α14 sur la réplication virale lorsque celui-ci est administré en prophylaxie ou pendant la phase aiguë. Cet effet était plus fort que celui du sous-type d'interféron α2, qui est le principal interféron utilisé dans les études menées chez l'homme et le singe.

Les souris humanisées permettent aussi l'étude des réservoirs cellulaires du virus. En effet, bien que les cellules T $CD4^+$ soient la cible majeure du VIH, il reste à ce jour des zones d'ombres concernant l'apport des macrophages dans la physiopathologie de l'infection. Il est évident que les macrophages sont infectés *in vivo* par le VIH, particulièrement dans le cerveau, cependant leur contribution au réservoir viral chez des patients sous traitement antirétroviraux reste toujours controversée. Cela tient, entre autres, au fait qu'il est difficile *in vivo* de différencier l'ADN viral d'un macrophage infecté de façon latente, de celui d'un macrophage ayant phagocyté une cellule T $CD4^+$ infectée de manière latente. C'est pour répondre à cette question que des souris humanisées NOD/SCID-hu-HSC ne pouvant générer de cellules de la lignée lymphocytaire ont été infectées. Ainsi en absence de cellules T, une réplication virale a pu être obtenue chez ses souris dans de multiples organes, démontrant ainsi que les macrophages sont capables, à eux seuls, de supporter une forte réplication virale dans différents tissus [95]. Une autre étude conduite chez des souris NSG-hu-HSC a permis de mettre en évidence que des provirus intégrés pouvaient se trouver dans des monocytes/macrophages (définis par l'expression $CD14^+$ $CD16^+$). Ces résultats confirment l'hypothèse que les macrophages provenant des tissus participent aussi à la composition du réservoir viral [96].

Les modèles de souris humanisées permettent aussi de mieux étudier et définir de nouvelles stratégies d'éradication des réservoirs viraux [89, 97]. Une des stratégies, qui a été le plus étudiée pour éliminer le réservoir viral, est celle du « *shock and kill* ». Cela consiste à stimuler la réplication du virus latent dans les cellules réservoirs (le « *shock* »). Ainsi, ces cellules réservoirs deviennent sensibles aux antirétroviraux et aux réponses immunitaires, les cellules infectées sont alors détruites par cette action conjuguée (le « *kill* »). Dans ce contexte, une étude menée sur des souris NSG-BLT traitées par antirétroviraux a montré que l'action d'un agent révertant de la latence, le panobinostat, ne permettait pas de diminuer le réservoir viral malgré une

forte capacité de cette molécule à modifier l'acétylation de l'ADN à un niveau systémique [98]. Une seconde étude menée chez ces mêmes souris a montré le rôle joué par la protéine chaperonne HSP90 dans l'établissement de la latence, et comment celle-ci affecte le rebond viral lors de l'arrêt du traitement [99]. Cette étude a pu montrer que la protéine HSP90 joue un rôle clé dans la réactivation du virus en modulant l'activité de certaines protéines comme NF-κB, STAT5 et NFAT.

Le modèle de souris humanisées est aussi utilisé pour étudier l'impact des bNAbs sur le virus. Ainsi, des études ont montré que le transfert passif de bNAbs dans des souris NOD *RAG1*$^{-/-}$ *IL2rg*^{null} permettait de réduire la charge virale plasmatique en dessous du seuil de détection [100].

Conclusion

La recherche utilisant des animaux comme modèles d'infection par le VIH a permis d'énormes progrès sur nos connaissances de l'infection par le VIH. Les modèles de souris humanisées infectées par le VIH-1 permettent l'étude du VIH et également d'éviter dans certains cas le modèle PNH tout en offrant un modèle d'infection qui est plus complexe et plus informatif que les infections *in vitro* de cellules ou explants tissulaires, et où les réponses immunitaires sont en partie semblables à l'homme. Néanmoins, ce modèle est difficile à mettre en place. Il n'existe pas d'élevage de ce type de souris, les infections par le VIH à long terme sont rares, la reconstitution des organes lymphoïdes est incomplète et la taille des animaux limite les études tissulaires. L'infection par le *feline immunodeficiency* (FIV) des chats n'a qu'une applicabilité limitée dans la recherche d'une stratégie curative contre le VIH-1, en raison des différences dans la nature du réservoir. Les singes infectés par le SIV offrent un modèle d'infection où la physiologie et la progression de la maladie sont très similaires à celles des humains infectés par le VIH-1. Cependant, leur utilisation est complexe, aussi du point de vue éthique, les « challenges » viraux lors d'études vaccinales ne peuvent être réalisés qu'avec un virus SHIV, le coût de maintenance est plus élevé et l'utilisation du modèle primate nécessite des structures plus grandes.

Toutefois, les modèles animaux, les PNH inclus, offrent un potentiel unique en matière de découvertes qui pourront contribuer au développement de vaccins et nouveaux traitements contre le VIH, et également apporter des connaissances sur les interactions virus-hôte en général au-delà du VIH. Les récents progrès technologiques dans la recherche, comme en imagerie, devraient accélérer les connaissances tout en diminuant le nombre d'animaux nécessaires dans le futur.

Remerciements. Nous remercions l'Agence nationale de recherche sur le VIH et les hépatites (ANRS), ainsi que le Centre pour modèles de maladies infectieuses et thérapies innovantes (IDMIT) soutenu par l'ANR (10-INSB-04-01).

Liens d'intérêts : les auteurs déclarent ne pas avoir de lien d'intérêt en rapport avec cet article.

Références

1. Antiretroviral Therapy Cohort Collaboration. Life expectancy of individuals on combination antiretroviral therapy in high-income countries: a collaborative analysis of 14 cohort studies. *Lancet Lond Engl* 2008 ; 372 : 293-9.

2. Shen L, Siliciano RF. Viral reservoirs, residual viremia, and the potential of highly active antiretroviral therapy to eradicate HIV infection. *J Allergy Clin Immunol* 2008 ; 122(1) : 22-8.

3. Walsh NC, Kenney LL, Jangalwe S, *et al*. Humanized mouse models of clinical disease. *Annu Rev Pathol* 2017 ; 12 : 187-215.

4. Policicchio BB, Pandrea I, Apetrei C. Animal models for HIV cure research. *Front Immunol* 2016 ; 7 : 12.

5. Nath BM, Schumann KE, Boyer JD. The chimpanzee and other non-human-primate models in HIV-1 vaccine research. *Trends Microbiol* 2000 ; 8(9) : 426-31.

6. Weiss RA. Special anniversary review: twenty-five years of human immunodeficiency virus research: successes and challenges. *Clin Exp Immunol* 2008 ; 152(2) : 201-10.

7. Silvestri G, Paiardini M, Pandrea I, Lederman MM, Sodora DL. Understanding the benign nature of SIV infection in natural hosts. *J Clin Invest* 2007 ; 117(11) : 3148-54.

8. Hatziioannou T, Evans DT. Animal models for HIV/AIDS research. *Nat Rev Microbiol* 2012 ; 10(12) : 852-67.

9. Gardner MB, Luciw PA. Macaque models of human infectious disease. *ILAR J* 2008 ; 49(2) : 220-55.

10. Del Prete GQ, Lifson JD. Considerations in the development of non-human primate models of combination antiretroviral therapy for studies of AIDS virus suppression, residual virus, and curative strategies. *Curr Opin HIV AIDS* 2013 ; 8(4) : 262-72.

11. Del Prete GQ, Lifson JD, Keele BF, *et al*. Nonhuman primate models for evaluation of HIV-1 preventative vaccine strategies: model parameter considerations and consequences. *Curr Opin HIV AIDS* 2016 ; 11(6) : 546-54.

12. Trivedi P, Horejsh D, Hinds SB, *et al*. Intrarectal transmission of Simian immunodeficiency virus in rhesus macaques: selective amplification and host responses to transient or persistent viremia. *J Virol* 1996 ; 70(10) : 6876-83.

13. Hansen SG, Vieville C, Whizin N, *et al*. Effector-memory T cell responses are associated with protection of rhesus monkeys from mucosal SIV challenge. *Nat Med* 2009 ; 15(3) : 293-9.

14. Demberg T, Robert-Guroff M. Mucosal immunity and protection against HIV/SIV infection: strategies and challenges for vaccine design. *Int Rev Immunol* 2009 ; 28(1) : 20-48.

15. Marthas ML, Miller CJ. Developing a neonatal HIV vaccine: insights from macaque models of pediatric HIV/AIDS. *Curr Opin HIV AIDS* 2007 ; 2(5) : 367-74.

16. Moreau M, Le Tortorec A, Deleage C, *et al*. Impact of short-term HAART initiated during the chronic stage or shortly post-exposure on SIV infection of male genital organs. *PLoS One* 2012 ; 7(5) : e37348.

17. Fauci AS, Desrosiers RC. Pathogenesis of HIV and SIV. In : Coffin JM, Hughes SH, Varmus HE, eds. *Retroviruses*. Cold Spring Harbor (NY) : Cold Spring Harbor Laboratory Press, 1997.

Copyright © 2020 John Libbey Eurotext. Téléchargé par INSTITUT PASTEUR le 09/08/2020.

Copyright © 2020 John Libbey Eurotext. Téléchargé par INSTITUT PASTEUR le 09/08/2020.

18. Haase AT. Early events in sexual transmission of HIV and SIV and opportunities for interventions. *Annu Rev Med* 2011 ; 62 : 127-39.

19. Lackner AA, Veazey RS. Current concepts in AIDS pathogenesis: insights from the SIV/macaque model. *Annu Rev Med* 2007 ; 58 : 461-76.

20. Monceaux V, Viollet L, Petit F, *et al.* CD4+ CCR5+ T-cell dynamics during Simian immunodeficiency virus infection of Chinese rhesus macaques. *J Virol* 2007 ; 81(24) : 13865-75.

21. Zink MC, Suryanarayana K, Mankowski JL, *et al.* High viral load in the cerebrospinal fluid and brain correlates with severity of Simian immunodeficiency virus encephalitis. *J Virol* 1999 ; 73(12) : 10480-8.

22. Chrétien F, Vallat-Decouvelaere AV, Bossuet C, *et al.* Expression of excitatory amino acid transporter-2 (EAAT-2) and glutamine synthetase (GS) in brain macrophages and microglia of SIVmac251-infected macaques. *Neuropathol Appl Neurobiol* 2002 ; 28(5) : 410-7.

23. Greene JM, Weiler AM, Reynolds MR, *et al.* Rapid, repeated, low-dose challenges with SIVmac239 infect animals in a condensed challenge window. *Retrovirology* 2014 ; 11(1) : 66.

24. Willer DO, Guan Y, Luscher MA, *et al.* Multi-low-dose mucosal Simian immunodeficiency virus SIVmac239 challenge of cynomolgus macaques immunized with "hyperattenuated" SIV constructs. *J Virol* 2010 ; 84(5) : 2304-17.

25. Bruel T, Hamimi C, Dereuddre-Bosquet N, *et al.* Long-term control of Simian immunodeficiency virus (SIV) in cynomolgus macaques not associated with efficient SIV-specific CD8+ T-cell responses. *J Virol* 2015 ; 89(7) : 3542-56.

26. Böttiger D, Vrang L, Öberg B. Influence of the infectious dose of Simian immunodeficiency virus on the acute infection in cynomolgus monkeys and on the effect of treatment with 3′-fluorothymidine. *Antivir Chem Chemother* 1992 ; 3(5) : 267-71.

27. Loffredo JT, Maxwell J, Qi Y, *et al.* Mamu-B*08-positive macaques control Simian immunodeficiency virus replication. *J Virol* 2007 ; 81(16) : 8827-32.

28. Nakayama EE, Shioda T. TRIM5α and species tropism of HIV/SIV. *Front Microbiol* 2012 ; 3 : 13.

29. Mee ET, Berry N, Ham C, *et al.* Mhc haplotype H6 is associated with sustained control of SIVmac251 infection in Mauritian cynomolgus macaques. *Immunogenetics* 2009 ; 61(5) : 327-39.

30. Aarnink A, Dereuddre-Bosquet N, Vaslin B, *et al.* Influence of theMHCgenotype on the progression of experimental SIV infection in the Mauritian cynomolgus macaque. *Immunogenetics* 2011 ; 63(5) : 267-74. doi: 10.1007/s00251-010-0504-6 [Epub 2011 Jan 14].

31. Sodora DL, Allan JS, Apetrei C, *et al.* Toward an AIDS vaccine: lessons from natural Simian immunodeficiency virus infections of African nonhuman primate hosts. *Nat Med* 2009 ; 15(8) : 861-5.

32. Paiardini M, Müller-Trutwin M. HIV-associated chronic immune activation. *Immunol Rev* 2013 ; 254(1) : 78-101.

33. Plaeger SF, Collins BS, Musib R, Deeks SG, Read S, Embry A. Immune activation in the pathogenesis of treated chronic HIV disease: a workshop summary. *AIDS Res Hum Retroviruses* 2012 ; 28(5) : 469-77.

34. Estes JD. Pathobiology of HIV/SIV-associated changes in secondary lymphoid tissues. *Immunol Rev* 2013 ; 254(1) : 65-77.

35. Hong JJ, Silveira ELV, Amancha PK, *et al.* Early initiation of antiretroviral treatment post-SIV infection does not resolve lymphoid tissue activation. *AIDS Lond Engl* 2017 ; 31(13) : 1819-24.

36. Dimopoulos Y, Moysi E, Petrovas C. The lymph node in HIV pathogenesis. *Curr HIV/AIDS Rep* 2017 ; 14(4) : 133-40.

37. Estes JD, Wietgrefe S, Schacker T, *et al.* Simian immunodeficiency virus-induced lymphatic tissue fibrosis is mediated by transforming growth factor β1-positive regulatory T cells and begins in early infection. *J Infect Dis* 2007 ; 195(4) : 551-61.

38. Lei Huang, Jianning Deng, Wen Xu, *et al.* CD8+ T cells with high TGF-β1 expression cause lymph node fibrosis following HIV infection. *Mol Med Rep* 2018 ; 18(1) : 77-86.

39. Cumont MC, Monceaux V, Viollet L, *et al.* TGF-beta in intestinal lymphoid organs contributes to the death of armed effector CD8 T cells and is associated with the absence of virus containment in rhesus macaques infected with the Simian immunodeficiency virus. *Cell Death Differ* 2007 ; 14(10) : 1747-58.

40. Sanchez JL, Hunt PW, Reilly CS, *et al.* Lymphoid fibrosis occurs in long-term nonprogressors and persists with antiretroviral therapy but may be reversible with curative interventions. *J Infect Dis* 2015 ; 211(7) : 1068-75.

41. Okoye AA, Hansen SG, Vaidya M, *et al.* Early antiretroviral therapy limits SIV reservoir establishment to delay or prevent post-treatment viral rebound. *Nat Med* 2018 ; 24(9) : 1430.

42. Estes JD, Kityo C, Ssali F, *et al.* Defining total-body AIDS-virus burden with implications for curative strategies. *Nat Med* 2017 ; 23(11) : 1271-6.

43. Damouche A, Lazure T, Avettand-Fènoël V, *et al.* Adipose tissue is a neglected viral reservoir and an inflammatory site during chronic HIV and SIV infection. *PLoS Pathog* 2015 ; 11 : e1005153.

44. Whitney JB, Hill AL, Sanisetty S, *et al.* Rapid seeding of the viral reservoir prior to SIV viraemia in rhesus monkeys. *Nature* 2014 ; 512(7512) : 74-7.

45. Bourry O, Mannioui A, Sellier P, *et al.* Effect of a short-term HAART on SIV load in macaque tissues is dependent on time of initiation and antiviral diffusion. *Retrovirology* 2010 ; 7 : 78.

46. Chakrabarti L, Cumont M-C, Montagnier L, Hurtrel B. Kinetics of primary SIV infection in lymph nodes. *J Med Primatol* 1994 ; 23(2-3) : 117-24.

47. Hong JJ, Chang K-T, Villinger F. The dynamics of T and B cells in lymph node during chronic HIV infection: TFH and HIV, unhappy dance partners? *Front Immunol* 2016 ; 7 : 522.

48. Moukambi F, Rodrigues V, Fortier Y, *et al.* CD4 T follicular helper cells and HIV infection: friends or enemies? *Front Immunol* 2017 ; 8 : 135.

49. Xu H, Wang X, Malam M, *et al.* Persistent Simian immunodeficiency virus infection drives differentiation, aberrant accumulation, and latent infection of germinal center follicular T helper cells. *J Virol* 2016 ; 90(3) : 1578-87.

50. Fukazawa Y, Lum R, Okoye AA, *et al.* B cell follicle sanctuary permits persistent productive Simian immunodeficiency virus infection in elite controllers. *Nat Med* 2015 ; 21(2) : 132-9.

51. Bronnimann MP, Skinner PJ, Connick E. The B-cell follicle in HIV infection: barrier to a cure. *Front Immunol* 2018 ; 9 : 20.

52. Rothenberger M, Nganou-Makamdop K, Kityo C, *et al.* Impact of integrase inhibition compared with nonnucleoside inhibition on HIV reservoirs in lymphoid tissues. *J Acquir Immune Defic Syndr* 2019 ; 81(3) : 355-60.

53. Thompson CG, Rosen EP, Prince HMA, *et al.* Heterogeneous antiretroviral drug distribution and HIV/SHIV detection in the gut of three species. *Sci Transl Med* 2019 ; 11 : 499.

54. Diop OM, Gueye A, Dias-Tavares M, *et al.* High levels of viral replication during primary Simian immunodeficiency virus SIVagm infection are rapidly and strongly controlled in African green monkeys. *J Virol* 2000 ; 74(16) : 7538-47.

55. Huot N, Jacquelin B, Garcia-Tellez T, *et al.* Natural killer cells migrate into and control Simian immunodeficiency virus replication in lymph node follicles in African green monkeys. *Nat Med* 2017 ; 23(11) : 1277-86.

56. Paiardini M, Lichterfeld M. Follicular T helper cells: hotspots for HIV-1 persistence. *Nat Med* 2016 ; 22(7) : 711-2.

57. Paiardini M, Cervasi B, Reyes-Aviles E, *et al.* Low levels of SIV infection in sooty mangabey central memory $CD4^+$ T cells are associated with limited CCR5 expression. *Nat Med* 2011 ; 17(7) : 830-6.

58. Nishimura Y, Sadjadpour R, Mattapallil JJ, *et al.* High frequencies of resting CD4+ T cells containing integrated viral DNA are found in rhesus macaques during acute lentivirus infections. *Proc Natl Acad Sci U S A* 2009 ; 106(19) : 8015-20.

59. Shen A, Zinkl MC, Mankowski JL, *et al*. Resting CD4+ T Lymphocytes but not thymocytes provide a latent viral reservoir in a Simian immunodeficiency virus-Macaca nemestrina model of human immunodeficiency virus type 1-infected patients on highly active antiretroviral therapy. *J Virol* 2003 ; 77(8) : 4938-49.

60. Crise B, Li Y, Yuan C, *et al*. Simian immunodeficiency virus integration preference is similar to that of human immunodeficiency virus type 1. *J Virol* 2005 ; 79(19) : 12199-204.

61. Barber SA, Gama L, Dudaronek JM, Voelker T, Tarwater PM, Clements JE. Mechanism for the establishment of transcriptional HIV latency in the brain in a Simian immunodeficiency virus-Macaque model. *J Infect Dis* 2006 ; 193(7) : 963-70.

62. Shen A, Yang HC, Zhou Y, *et al*. Novel pathway for induction of latent virus from resting CD4+ T cells in the Simian immunodeficiency virus/Macaque model of human immunodeficiency virus type 1 Latency. *J Virol* 2007 ; 81(4) : 1660-70.

63. Mannioui A, Bourry O, Sellier P, *et al*. Dynamics of viral replication in blood and lymphoid tissues during SIVmac251 infection of macaques. *Retrovirology* 2009 ; 6 : 106.

64. Sellier P, Mannioui A, Bourry O, *et al*. Antiretroviral treatment start-time during primary SIV(mac) infection in macaques exerts a different impact on early viral replication and dissemination. *PLoS One* 2010 ; 5(5) : e10570.

65. Budde ML, Greene JM, Chin EN, *et al*. Specific CD8+ T cell responses correlate with control of Simian immunodeficiency virus replication in Mauritian cynomolgus macaques. *J Virol* 2012 ; 86(14) : 7596-604.

66. Jones RB, O'Connor R, Mueller S, *et al*. Histone deacetylase inhibitors impair the elimination of HIV-infected cells by cytotoxic T-lymphocytes. *PLoS Pathog* 2014 ; 10(8) : e1004287.

67. Lewis MG, DaFonseca V, Chomont N, *et al*. Gold drug auranofin restricts the viral reservoir in the monkey AIDS model and induces containment of viral load following ART suspension. *AIDS Lond Engl* 2011 ; 25(11) : 1347-56.

68. Nishimura Y, Gautam R, Chun TW, *et al*. Early antibody therapy can induce long-lasting immunity to SHIV. *Nature* 2017 ; 543(7646) : 559-63.

69. Laforge M, Silvstre R, Rodrigues V, *et al*. The anti-caspase inhibitor Q-VD-OPH prevents AIDS disease progression in SIV-infected rhesus macaques. *J Clin Invest* 2018 ; 128(4) : 1627-40.

70. Del Prete GQ, Alvord WG, Li W, *et al*. TLR7 agonist administration to SIV-infected macaques receiving earlyinitiated cART does not induce plasma viremia. *JCI Insight* 2019 ; 4(11) : 127717.

71. Micci L, Ryan ES, Fromentin R, *et al*. Interleukin-21 combined with ART reduces inflammation and viral reservoir in SIV-infected macaques. *J Clin Invest* 2015 ; 125(12) : 4497-513.

72. Trovato M, D'Apice L, Prisco A, De Berardinis P. HIV Vaccination : A Roadmap among Advancements and Concerns. *Int J Mol Sci* 2018 ; 19 : E1241.

73. Amara RR, Robinson HL. A new generation of HIV vaccines. *Trends Mol Med* 2002 ; 8(10) : 489-95.

74. Goulder PJR, Watkins DI. HIV and SIV CTL escape: implications for vaccine design. *Nat Rev Immunol* 2004 ; 4(8) : 630-40.

75. Chen ZW, Craiu A, Shen L, *et al*. Simian immunodeficiency virus evades a dominant epitope-specific cytotoxic T lymphocyte response through a mutation resulting in the accelerated dissociation of viral peptide and MHC class I. *J Immunol* 2000 ; 164(12) : 6474-9.

76. Julg B, Sok D, Schmidt SD, *et al*. Protective efficacy of broadly neutralizing antibodies with incomplete neutralization activity against simian-human immunodeficiency virus in rhesus monkeys. *J Virol* 2017 ; 91 : e01187-17.

77. Johnson PR, Schnepp BC, Zhang J, *et al*. Vector-mediated gene transfer engenders long-lived neutralizing activity and protection against SIV infection in monkeys. *Nat Med* 2009 ; 15(8) : 901-6.

78. Hansen SG, Ford JC, Lewis MS, *et al*. Profound early control of highly pathogenic SIV by an effector memory T-cell vaccine. *Nature* 2011 ; 473(7348) : 523-7.

79. Garcia-Tellez T, Huot N, Ploquin MJ, Rascle P, Jacquelin B, Müller-Trutwin M. Non-human primates in HIV research: achievements, limits and alternatives. *Infect Genet Evol* 2016 ; 46 : 324-32.

80. García-Lerma JG, Cong ME, Mitchell J, *et al*. Intermittent prophylaxis with oral truvada protects macaques from rectal SHIV infection. *Sci Transl Med* 2010 ; 2(14) : 14ra4.

81. Pearson T, Greiner DL, Shultz LD. Humanized SCID mouse models for biomedical research. *Curr Top Microbiol Immunol* 2008 ; 324 : 25-51.

82. Traggiai E, Chicha L, Mazzucchelli L, *et al*. Development of a human adaptive immune system in cord blood cell-transplanted mice. *Science* 2004 ; 304(5667) : 104-7.

83. Bonyhadi ML, Kaneshima H. The SCID-hu mouse: an *in vivo* model for HIV-1 infection in humans. *Mol Med Today* 1997 ; 3(6) : 246-53.

84. Baenziger S, Tussiwand R, Schlaepfer E, *et al*. Disseminated and sustained HIV infection in CD34+ cord blood cell-transplanted Rag2$^{-/-}\gamma c^{-/-}$ mice. *Proc Natl Acad Sci* 2006 ; 103(43) : 15951-6.

85. Berges BK, Akkina SR, Remling L, Akkina R. Humanized Rag2$^{-/-}\gamma c^{-/-}$ (RAG-hu) mice can sustain long-term chronic HIV-1 infection lasting more than a year. *Virology* 2010 ; 397(1) : 100-3.

86. Karpel ME, Boutwell CL, Allen TM. BLT humanized mice as a small animal model of HIV infection. *Curr Opin Virol* 2015 ; 13 : 75-80.

87. Akkina R. New generation humanized mice for virus research: comparative aspects and future prospects. *Virology* 2013 ; 435(1) : 14-28.

88. Seung E, Tager AM. Humoral immunity in humanized mice: a work in progress. *J Infect Dis* 2013 ; 208(Suppl. 2) : S155-9.

89. Shultz LD, Brehm MA, Garcia JV, Greiner DL. Humanized mice for immune system investigation: progress, promise and challenges. *Nat Rev Immunol* 2012 ; 12(11) : 786-98.

90. Marsden MD, Kovochich M, Suree N, *et al*. HIV latency in the humanized BLT mouse. *J Virol* 2012 ; 86(1) : 339-47.

91. Borrow P. Innate immunity in acute HIV-1 infection. *Curr Opin HIV AIDS* 2011 ; 6(5) : 353-63.

92. Sandler NG, Bosinger SE, Estes JD, *et al*. Type I interferon responses in rhesus macaques prevent SIV infection and slow disease progression. *Nature* 2014 ; 511(7511) : 601-5.

93. Cheng L, Ma J, Li J, *et al*. Blocking type I interferon signaling enhances T cell recovery and reduces HIV-1 reservoirs. *J Clin Invest* 2017 ; 127 (1) : 269-79.

94. Lavender KJ, Gibbert K, Peterson KE, *et al*. Interferon alpha subtype-specific suppression of HIV-1 infection *in vivo*. *J Virol* 2016 ; 90(13) : 6001-13.

95. Honeycutt JB, Wahl A, Baker C, *et al*. Macrophages sustain HIV replication *in vivo* independently of T cells. *J Clin Invest* 2016 ; 126(4) : 1353-66.

96. Arainga M, Su H, Poluektova LY, Gorantla S & Gendelman HE. HIV-1 cellular and tissue replication patterns in infected humanized mice. *Sci Rep* 2016 ; 6 : 23513.

97. Lavender KJ, Pace C, Sutter K, *et al*. An advanced BLT-humanized mouse model for extended HIV-1 cure studies. *AIDS* 2018 ; 32(1) : 1-10.

98. Tsai P, Wu G, Baker CE, *et al*. *In vivo* analysis of the effect of panobinostat on cell-associated HIV RNA and DNA levels and latent HIV infection. *Retrovirology* 2016 ; 13(1) : 36.

99. Joshi P, Maidji E, Stoddart CA. Inhibition of heat shock protein 90 prevents HIV rebound. *J Biol Chem* 2016 ; 291(19) : 10332-46.

100. Klein F, Halper-Stromberg A, Horwitz JA, *et al*. HIV therapy by a combination of broadly neutralizing antibodies in humanized mice. *Nature* 2012 ; 492 : 7427.

Copyright © 2020 John Libbey Eurotext. Téléchargé par INSTITUT PASTEUR le 09/08/2020.

Part VIII: Substantial Summary

A ce jour, l'infection du VIH reste un grand problème de santé publique. Alors que, le traitement antirétroviral développé à la fin des années 90, a permis d'améliorer l'espérance de vie des personnes vivantes avec le VIH, l'activation immunitaire chronique est toujours présent et le virus persistant. Cette activation chronique dû à la persistance du virus est un problème important car augmentant, pour les personnes vivantes avec le VIH, le risque de comorbidités non liées au SIDA. La persistance virale est donc associée à plusieurs dérégulations immunitaires telles que l'inflammation chronique résiduelle, l'hypergammaglobulinémie et la désorganisation du réseau cellulaire dendritique du follicule. Ainsi il est aujourd'hui clair que le traitement antirétroviral ne parvient pas à éliminer le virus dans tout l'organisme et que la non résolution de l'inflammation durant le traitement favorise des comorbidités tel que des maladies cardiovasculaires et cancers.
La production virale majoritairement non détectable dans le sang chez les personnes vivantes avec le VIH sous traitement est bien détectable dans certains tissus. Ces réservoirs productifs du VIH se présente comme des sanctuaires anatomiques où le traitement inefficace pour contrôler la production virale. Les principaux réservoirs productifs sont localisés dans les ganglions lymphatiques et l'intestin. Plus précisément, le VIH persiste dans des cellules réservoirs, tels que les lymphocytes T auxiliaires folliculaires (T_{FH}) dans les follicules des cellules B des ganglions lymphatiques pendant le traitement antirétroviral.

À l'aide de modèles animaux, nous recherchons des mécanismes de protection contre ces dérégulations. L'infection par SIVmac chez le macaque (*Macaca fascicularis*, *Macaca mulatatta*, MAC) reproduit la physiopathologie de l'infection par le VIH-1 chez l'homme. En revanche, l'infection à SIVagm chez le singe vert africain (*Chlorocebus sabaeus*, AGM) n'est pas pathogène. Les AGM infectés par le SIVagm sont dépourvues d'inflammation chronique, malgré une forte virémie persistante. Ainsi les AGM infectés par le SIV ne progressent pas vers un état SIDA. SIVagm se réplique dans l'intestin, où il n'y a pas de lésion tissulaire. En effet, malgré la production virale présent dans l'intestin, les cellules T CD4+ mucosale se rétablissent partiellement. Cela contribuerait en partie au contrôle de l'inflammation local malgré la présence du virus. De plus et contrairement à l'intestin, la réplication du SIVagm est fortement contrôlée dans les ganglions lymphatiques. Les AGM contrôlent les réservoirs productifs dans les follicules B (BCF) des ganglions lymphatiques périphériques.

Par la suite, nous avons découvert que les cellules Natural Killer (NK) migrent au sein des BCF chez les AGM infectés par le SIVagm. Grâce à l'expression du CXCR5 à la surface des cellules NK celle-ci acquièrent la capacité de migré dans le BCF, ici montré en phase chronique de l'infection. D'ailleurs, nous avons remarqué qu'à ce moment de l'infection les NK s'accumulent dans ces BCF. Nous avons montré *in situ* une forte expression d'ARNm IL-15 et d'IL-15 protéique dans les BCF de l'AGM lors la phase chronique de l'infection chez l'AGM contrairement au MAC. En outre, nous avons également noté que l'IL-15 protéique était présenté à la surface des cellules dendritiques folliculaires chez l'AGM lors la phase chronique de l'infection chez l'AGM contrairement au MAC. La production d'IL-15 favorise entre autres, la survie et la différentiation des cellules NK vers un phénotype cytotoxique. Lors de la réduction de la fréquence de cellules NK chez l'AGM chroniquement infecté par le SIV via un anti-IL-15. Nous avons montré que la présence de ces cellules NK dans les BCF des ganglions périphériques permettaient le contrôle de la production virale dans ce sanctuaire anatomique. Ce mécanisme supposé cytotoxique serait à l'origine de l'absence de réservoir virale dans les BCF des ganglions périphériques chez l'AGM chroniquement infecté par le SIV.

Suite à ces observations, il nous a semblé important d'étudier le mécanisme permettant aux cellules NK d'acquérir la capacité de migrer dans les follicules mais également le mécanisme de reconnaissance des cellules infectés par les cellules NK.
Nous avons commencé par rechercher à identifier le ou les facteurs importants pour la migration des cellules NK dans l'infection SIV chez l'AGM. Par immunohistochimie, nous avons observé la présence de cellules NK dans les follicules uniquement lorsque les BCF étaient activés. En observant une proximité *in situ* entre les cellules NK et les cellules B, nous avons entrepris des co-cultures entre ces deux types cellulaires autologues. Nous avons observé d'important changements phénotypiques et fonctionnels sur ces cellules qui s'influençaient mutuellement. Dans ces changements phénotypiques nous nous sommes particulièrement intéressés à l'augmentation significative de CXCR5 sur les cellules NK. Or, cette augmentation n'a été observée qu'en condition de co-culture entre les cellules NK et les cellules B mais séparés par une membrane perméable aux facteurs sécrétés. Ainsi, après avoir récupéré le surnageant de cette condition de culture. Nous avons montré une induction du CXCR5 sur les cellules NK. Une analyse de profilage transcriptionnel des cellules CXCR5 + NK a révélé l'expression de *bcl-6*, connu pour étant un facteur de transcription important dans la lignée de différenciation T_{FH} avec un rôle majeur dans l'expression de CXCR5. De plus, cette analyse transcriptionnelle nous a montré une forte expression du récepteur à IL-6 (*IL6R*). Or l'IL-6 est impliqué dans l'induction du CXCR5 comme IL-21 et IL-27. Cependant, il a été noté que les cellules B étaient seulement capables de produire IL-6. Nous avons relevé que durant nos conditions de culture la production de l'IL-6 était stimulée chez les cellules B. Dans la continuité de cette observation nous avons ajouté à différentes doses de l'IL-6 sur des cultures de NK seul. Nous avons relevé que l'IL-6 induisait l'expression de CXCR5 sur les cellules NK d'AGM et d'humains, mais curieusement pas chez le macaque. En suivant au cours de l'infection SIV chez l'AGM et le MAC (non infecté, phase aiguë et phase chronique) la production de l'IL-6 protéique dans les ganglions nous n'avons relever aucune variation en comparant le moment où les singes étaient non infectés à la phase aigüe ou chronique. Dans la suite de cette idée, nous avons également démontré des foyers d'expression d'ARNm de l'*IL-6* dans le cortex et la zone interfolliculaire des ganglions lymphatiques dans la phase aigüe de l'infection SIVagm. A contrario il a été relevé que peu de production d'ARNm de l'*IL-6* dans les ganglions des macaques infectés par le SIV en phase aigüe. Ainsi peut-être que la détection de l'IL-6 protéique chez le singe affiche une certaine limite.

Ensuite, nous avons analysé comment les cellules NK contrôlent la réplication du SIVagm dans les ganglions lymphatiques. La fonction cytotoxique de la cellule NK s'applique selon un équilibre entre la force des signaux inhibiteur et activateur. Il y a plein de récepteurs et ligands capable d'être reconnu et présent à la surface des cellules. Nous nous sommes particulièrement intéressés par le CMH-E car dans l'infection au VIH la fréquence de cellules T CD4+ CMH-E+ augmentait. De plus, le CMH-E reconnu par le couple activateur NKG2C/CD94, peut également être reconnu par le couple inhibiteur NKG2A/CD94 qui a été mis en relation dans l'infection au VIH avec la perte de fonction effectrice des cellules NK face aux cellules cibles. Nous avons donc exploré les peptides viraux pouvant être lié au CMH-E. Or, nous avons identifié une nouvelle région composée de peptides dérivés de SIV ENV qui se lient au CMH-E. Lors d'expériences réalisées *in vitro*, nous avons démontré une inhibition des cellules NK provenant du sang et la rate macaque et de l'AGM non infectés ; par le CMH-E présentant le peptide dérivé de SIVagm ENV. Tandis que le peptide dérivé de SIVmac ENV présenté par le CMH-E inhibait fortement les cellules NK provenant du sang et la rate macaque et de l'AGM non infectés. Lorsque le peptide dérivé de SIVagm ENV et SIVmac ENV sont présentés par le CMH-E et reconnus par les cellules NK d'AGM SIV infectés provenant du sang et de la rate ; nous avons pu observer une forte activité cytotoxique de ces cellules NK. Cependant, sur les cellules NK de macaques infectés par le SIV, nous avons pu observer une inhibition de l'activité cytotoxique face à la présentation du peptide SIVagm ENV mais également pour le peptide SIVmac ENV qui sont présentés par le CMH-E. Dans la continuité de cette expérience, nous avons remplacé la région qui concerne le peptide identifié sur la souche virale SIVagm.sab92018 par le peptide

identifié dans la même région chez le SIVmac, cette souche virale sera appelée SIVagm.sab92018 muté. Après avoir infecté des cellules T CD4+, provenant d'AGM non infectés, avec le SIVagm.sab92018 sauvage ; nous avons observé que la concentration de protéines virales (p27) diminuait après avoir ajouté les cellules NK autologue. Ensuite nous avons répété la même expérience mais avec le SIVagm.sab92018 muté. Or nous n'avons pas noté de différences au niveau de la concentration p27 lorsque nous comparons la condition de cellules T CD4+ infectés avec la co-culture cellules T CD4+ infectés et cellules NK autologues.

Les cellules NK sont impactées de manière différente dans les infections SIVagm par rapport à l'infection SIVmac. Pour cela, nous avons donc analysé longitudinalement le phénotype et le génotype des cellules NK NKG2A^{fort} et NKG2A^{faible} lors d'une infection au SIVagm et SIVmac dans le sang et les tissus. En analysant des sous-ensembles distincts de cellules NK d'AGM et de MAC au niveau transcriptomique et protéique, nous avons démontré ici que NKG2A combiné avec CD16 définit des étapes distinctes de la différenciation des cellules NK chez les singes. Or cette étude a montré que l'infection par le SIV chez l'hôte naturel induisait des cellules NK NKG2A^{faible}CD16^{+} fortement différenciées dans les ganglions et présentant une forte activité de dégranulation et un profil transcriptionnel des cellules NK adaptatives. En revanche, le processus de différenciation des cellules NK a été bloqué dans les ganglions pendant l'infection SIVmac de MAC après le deuxième jour après infection, malgré la génération d'un ensemble de cellules NK très diversifiées. Les cellules NK dans l'infection SIVmac présentaient un profil moins différencié et pro-inflammatoire (IFN-g), ce qui rejoint les précédentes études sur le sujet. Nos résultats révèlent également que les cellules NK sont éduquées pour tuer efficacement les cellules infectées par le SIV dans une infection SIVagm non pathogène alors que cette éducation ne se produit pas dans une infection SIV pathogène. Nous avons également observé une activité cytotoxique pour les cellules NK NKG2A^{faible}CD16^{-} et les cellules NK CXCR5$_{+}$ présente dans le ganglion.
Les raisons pour lesquelles les cellules NK NKG2A^{faible} se sont développées après l'infection SIVagm mais pas pendant l'infection SIVmac ne sont pas encore claires. L'idée que la différenciation des cellules NK est le résultat d'un processus continu et qui peut s'adapter en réponse à une infection virale, peut être une solution. Ce mécanisme conduirait ainsi les cellules NK vers un phénotype cytotoxique terminal différencié dans l'infection SIVagm, cela permettrait la présence de cellules NK avec la capacité de tuer les cellules infectées dans le ganglion. Tout en évitant l'inflammation associée à la production d'IFN-g médiée par les cellules NK qui se produit dans l'infection SIVmac.

Pour faire suite à cette étude, nous avons étudier les NK dans différent tissus afin de mieux comprendre leur différent rôle, contrôle de la production virale ou contrôle de l'inflammation dans l'infection SIVagm. Le phénotype et la fonction des cellules NK dans l'intestin d'AGM et de macaques sains et infectés par le SIV. Pour cela, nous avons analysé les marqueurs de résidence tissulaire combinés à la fonction à l'intérieur des tissus (ganglion et intestin).
Immédiatement après l'infection par le SIV, des changements se produisent dans les populations de cellules NK de l'intestin. Nos données chez le macaque montrent une diminution des cellules NK dans les ganglions et une augmentation de ces niveaux dans l'intestin. Ces données relevées sont cohérentes avec les précédentes études. De manière frappante, nous avons observé une dynamique tissulaire opposée chez le modèle pathogène et le modèle non pathogène du SIV. Chez le modèle non pathogène, les cellules NK n'étaient pas dirigées vers l'intestin et les fréquences des cellules NK totales dans l'intestin étaient diminuées dans l'infection à SIVagm contrairement à l'infection à SIVmac. Cela pourrait expliquer le manque de contrôle viral médié par les cellules NK dans l'intestin des AGM infectés par SIVagm.

Nos données démontrent aussi que les cellules NK de macaques étaient rarement CD8+ dans les tissus. Aussi la fréquence des cellules CD69 dans les tissus lors d'une infection pathogène était relativement faible. Alors que chez le modèle non pathogène la fréquence élevée de cellules NK CD69+ ont été observées dans les tissus. De

plus, l'analyse combinée de CD69 avec la granzyme B et l'IFN-g indique que la plupart des cellules NK résidentes avaient un profil cytotoxique, tandis que les cellules NK (CD69-) potentiellement infiltrées exprimaient également la cytokine IFN-g pro-inflammatoire. Cependant, il n'est pas clair si ces changements sont le résultat d'une infiltration de cellules NK sanguines ou s'il y a des changements phénotypiques dans les populations de cellules NK résidentes au cours d'une infection par le SIV.
Ces distributions tissulaires distinctes des cellules NK étaient associées à l'expression de CXCR3 et de α4β7. Soutenant ainsi et entre-autre, des précédentes données relevant des niveaux plus élevés du ligand CXCR3 dans l'intestin des macaques infectés par SIVmac par rapport aux AGM infectés par SIVagm. Et nous montrons que le CXCR5 est exprimé à haute fréquence par les cellules NK de l'iléon macaques et AGM sains. Cette fréquence élevée de cellules NK CXCR5+ a également été observée dans le jéjunum et le côlon de macaques sains. De façon frappante, après l'infection SIVmac, la fréquence des cellules NK CXCR5+ a fortement diminué dans l'intestin de macaques. Sachant que le CXCR5 est connu pour soutenir la formation de follicules B intestinaux solitaires qui est lui-même responsable du contrôle du microbiote. Il pourrait être intéressant d'étudier si cette diminution de cellules NK CXCR5 + dans l'intestin au cours de l'infection SIVmac est également lié à l'apparition de la translocation bactérienne durant l'infection.

Nous avons ensuite approfondi la question de savoir comment l'AGM protège les tissus intestinaux malgré l'absence de contrôle viral efficace. Nous nous sommes donc intéressés aux différents compartiments de l'intestin et aux ganglions mésentériques qui drainent les intestins et ont un grand rôle dans le contrôle de l'inflammation dans ce tissu. Or notre étude révèle des différences majeures concernant la réponse IgA dans le mLN et l'intestin entre le SIVagm non pathogène et l'infection SIVmac pathogène. En effet, nous démontrons que les cellules NK migrent rapidement dans le BCF de ganglions mésentériques au cours d'une infection à SIVagm où elles contrôlent la réplication virale. Nous montrons que les cellules B IgA+ mémoires étaient augmentées dans les ganglions mésentériques au cours d'une infection à SIVagm contrairement à une infection à SIVmac. Les niveaux de cellules CXCR5+ NK et de cellules B IgA+ mémoires dans les ganglions mésentériques étaient fortement corrélés. Ainsi, notre étude souligne que contrairement aux infections pathogènes, les réponses IgA dans les ganglions mésentériques sont protégées lors de l'infection SIVagm en AGM.

De plus, les taux normaux d'IgA intestinales (jéjunum, iléon et côlon) ont été maintenus pendant l'infection aiguë et chronique du SIVagm, alors qu'ils ont fortement diminué chez les macaques infectés de façon chronique par le SIVmac. Ces données dans le modèle SIV pathogène sont conformes aux rapports sur l'infection par le VIH-1 chez l'Homme. La diminution de la production d'IgA était due à une forte perte de signal dans la lumière, et non dans la lamina propria, cela signifie que les IgA sécrétés (SIgA) a été perdue alors que les cellules IgA+ étaient encore présentes. Une différence majeure entre l'infection à SIVagm non pathogène et pathogène était donc ici noté qui est le maintien sélectif de SIgA dans l'infection à SIVagm. Or les SIgA sont connu pour jouer un rôle crucial dans le maintien de l'intégrité de la barrière muqueuse. L'IgA totale était négativement corrélée avec le sCD14 dans l'infection SIVmac, tandis que les IgA spécifiques à ENV n'ont pas montré de corrélations. Cela suggère que le contrôle inflammatoire de l'infection par le SIV dans l'intestin est plus associé au maintien des réponses IgA non spécifiques qu'aux réponses IgA spécifiques du SIV. Les réponses IgA non spécifiques totales dans l'intestin au cours d'une infection à SIVagm pourraient fortement contribuer à protéger contre la translocation des bactéries ainsi que les autres mécanismes proposés protégeant la barrière épithéliale. Nous avons également observé une augmentation de cellules B spécifique au SIV dans les différents compartiments de l'intestin chez l'AGM infectés alors que cette population est totalement absente chez les macaques infectés par le SIV. Il est donc possible qu'une contribution partielle des cellules B soit à l'origine du contrôle de l'inflammation via un contrôle de la réplication virale dans l'intestin au cours d'une infection par SIVagm.

Dans la recherche de facteurs immunitaires liés au contrôle de l'inflammation dans l'intestin chez les AGM infectés par le SIV. Pour cela, nous nous sommes intéressés aux cellules T CD8+ exprimant NKG2A. Cette population ayant déjà été observées au cours d'une infection par le VIH-1 a rapporté une forte diminution au cours de l'infection. De plus, le rôle de cette population noté dans les maladies auto-immunitaires chronique de l'intestin tel que la maladie de Crohn, nous a amenés à suivre cette population dans l'infection SIV chez l'AGM et en étudier s'il existe un potentiel rôle dans le contrôle de l'inflammation dans ce modèle.

Après des mesures dans le sang, le ganglion et l'intestin. Nous avons identifié une expansion des cellules T NKG2A+CD8+ dans l'intestin au cours d'une infection à SIVagm, tandis que les cellules NK étaient diminuées chez les macaques infectés par le SIV. Pour mieux définir ces cellules, des analyses du transcriptome chez l'AGM ont montré que les cellules T CD8+ NKG2A+ exprimaient également l'ARNm de NKG2C. Les niveaux d'expression de NKG2C n'étaient cependant pas plus élevés que ceux de NKG2A. Ensuite il a été relevé que lors des infections au SIVagm et SIVmac, l'expression du marqueur cytotoxique (perforine) était augmentée comparé à l'IFN-g. Cependant, les fréquences globales des cellules T CD8+ NKG2A+ dans l'intestin ont augmenté pendant une période plus longue dans SIVagm que dans l'infection SIVmac. En effectuant des études longitudinales simultanément dans des tissus distincts, nous montrons une expansion plus intense des cellules T CD8+ NKG2A+ dans le sang et l'intestin en réponse au SIVagm dans l'AGM par rapport à l'infection SIVmac. Les expansions étaient associées à des niveaux de virémie suggérant que la stimulation antigénique est à l'origine des expansions.

Le CMH-E reconnu par le NKG2A et NKG2C comme précédemment cité, est exprimé sur la plupart des cellules, y compris sur les cellules T CD4+ et également à des niveaux élevés sur les cellules épithéliales intestinales. La présentation de peptides par le CMH-E d'une cellule non infecté est lié à son environnement et son état de stress. Et parmi le petit nombre d'autres peptides cellulaires qui ont été identifiés pour se lier au CMH-E, il y a été découvert un peptide dérivé de la protéine de stress Hsp60. Dans les conditions de stress de l'infection SIV, le peptide dérivé de la protéine Hsp60 pourrait être suffisamment importante pour entrer en compétition avec les peptides dérivés du CMH-I pour la présentation par le CMH-E. Nous rapportons ici des niveaux accrus de protéine HSP60 dans l'intestin de MAC infectés par SIVmac, alors qu'ils n'étaient pas augmentés dans l'infection SIVagm. Par conséquent, soit il y a des cellules moins stressées dans l'infection à SIVagm et donc moins de cellules non infectées seraient tuées par ce mécanisme, soit les cellules stressées sont tuées par ce mécanisme et donc moins présentes.

Ainsi, chez les modèle non pathogène, l'environnement intestinal avec une charge antigénique élevée pourrait permettre aux lymphocytes T CD8+ NKG2A+ de répondre initialement aux antigènes du SIV. Mais plus tard avec la diminution de l'inflammation et l'échappement du virus, cela conduirait les cellules T CD8+ NKG2A+ a ne répondre qu'aux antigène de stress cellulaire et ainsi participer à un contrôle de l'inflammation et de préservation des tissus sur le long terme.

Pour continuer, nous avons également détecté une corrélation négative entre les niveaux d'IL-23 (cytokine impliquée dans l'homéostasie intestinal) dans l'intestin et les cellules T CD8+ NKG2A+ intestinaux au cours d'une infection pathogène. Alors qu'un faible niveau d'IL-23 a été observé de manière concomitante à une fréquence élevée de lymphocytes T CD8+ NKG2A+ dans l'intestin lors de l'infection chez le modèle non pathogène. Ces résultats suggèrent bien que ces cellules pourraient plutôt contribuer au contrôle inflammatoire dans l'intestin plutôt qu'au contrôle de la réplication virale dans l'infection du SIV.

Dans l'ensemble, nos études ont fourni de nouveaux mécanismes liés au contrôle du réservoir virale et de l'inflammation, une nouvelle approche pour mieux étudier les cellules NK dans les modèles primates, mais aussi pour mieux comprendre l'infection SIV chez le modèle non pathogène. En participant à la protection efficace des structures tissulaires via le contrôle local du virus et de l'inflammation ou seulement de l'inflammation locale. L'infection SIV chez le modèle non pathogène nous fournit une nouvelle réflexion et approche pour le contrôle de infections virales chez l'Homme. De plus, nous proposons ici de nouveaux mécanismes qui pourraient être intéressants également nécessiteux dans le cadre d'autres maladies auto-immunitaires ou infectieuses.